SAPIENZA
UNIVERSITÀ DI ROMA

SCUOLA DI DOTTORATO "VITO VOLTERRA"

Dottorato di Ricerca in Scienze Chimiche - XXIX Ciclo

New Organocatalytic Strategies in Asymmetric Synthesis

Thesis submitted to obtain the degree of
Dottore di Ricerca - Philosophiae Doctor
Ph.D. in Chemical Sciences - XXIX Cycle

Mauro Moliterno

Thesis Supervisor: Prof. Marco Bella

Ph.D. Program Coordinator: Prof. Osvaldo Lanzalunga

Academic Year: 2015-2016

Table of Contents

List of Abbreviations

BET	back electron transfer
BINAM	2,2'-diamino-1,1'-binaphthyl
BINAP	2,2'-bis(diphenylphosphino)-1,1'-binaphthyl
BINOL	2,2'-dihydroxy-1,1'-binaphthyl
Boc	*tert*-butyloxycarbonyl
CAN	diammonium cerium(IV) nitrate
CD	cinchonidine
CFL	compact fluorescent lamp
CN	cinchonine
CSP	chiral stationary phase
Cy	cyclohexyl
DABCO	1,4-diazabicyclo[2.2.2]octane
DCC	*N*,*N'*-dicyclohexylcarbodiimide
DCE	1,2-dichloroethane
DCM	dichloromethane
DFT	density functional theory
DHQ	hydroquinine
DHQD	hydroquinidine
DIAD	diisopropyl azodicarboxylate
DKR	dynamic kinetic resolution
DME	1,2-dimethoxyethane
DMF	*N*,*N*-dimethylformamide
DMSO	dimethyl sulfoxide
DPPA	diphenylphosphoryl azide
ESI	electrospray ionization
FG	fragmenting group

HMBC	heteronuclear multiple bond correlation
HOMO	highest occupied molecular orbital
HPLC	high-performance liquid chromatography
HPNP	2-hydroxypropyl *p*-nitrophenyl phosphate
HRMS	high-resolution mass spectrometry
HSQC	heteronuclear single quantum coherence
LDA	lithium diisopropylamide
LED	light-emitting diode
LiHDMS	lithium bis(trimethylsilyl)amide
LUMO	lowest unoccupied molecular orbital
MOP	2-methoxy-2'-(diphenylphosphino)-1,1'-binaphthyl
MTBE	methyl *tert*-butyl ether
NBP	*N*-bromophthalimide
NMR	nuclear magnetic resonance
NOBIN	2-amino-2'-hydroxy-1,1'-binaphthyl
PG	protecting group
QD	quinidine
QN	quinine
QUINAP	1-(2-diphenylphosphino-1-naphthyl)isoquinoline
RT	room temperature
SET	single electron transfer
SOMO	singly occupied molecular orbital
TBS	*tert*-butyldimethylsilyl
TDMS	thexyldimethylsilyl
TFA	trifluoroacetic acid
THF	tetrahydrofuran
VAR	vinylogous aldol reaction

1. State of the Art

1.1. Asymmetric Synthesis by Means of Organocatalysis: an Outlook

Asymmetric synthesis is an important and challenging area of synthetic organic chemistry and its aim is to produce chiral, enantiomerically pure compounds, starting from achiral substrates and exploiting the presence of chiral reagents. The role of the latter is to generate diastereomorphic transition states leading to the two enantiomers, so that one of them is preferentially formed. The dependence of the biological properties of organic molecules on their absolute configuration is one of the main reasons explaining the major need for enantiopure compounds. Since the '80s international legislation has been introduced which requires any company wishing to produce a new drug as a racemic mixture to investigate the activity of both enantiomers separately.[1] Therefore, in the case of couples of enantiomers in which only one of the two is pharmaceutically active, it is convenient to produce it as a single stereoisomer.

Enantioselective synthesis can be accomplished by the use of chiral reagents, chiral auxiliaries or chiral catalysts. The catalytic approach is the most advantageous, as sub-stoichiometric amounts of enantiomerically pure material can produce large quantities of enantioenriched product. Enantioselective catalysis may employ enzymes, chiral metal complexes or small chiral organic molecules as catalysts. The exploitation of these latter is what organocatalysis deals with. In the last 16 years, that is since the reports of List's[2a] and MacMillan's2[b] groups on enamine and iminium ion catalysis respectively, organocatalysis has experienced an impressive growth, establishing itself as a fundamental tool for asymmetric synthesis. It is now recognized as a versatile and convenient method both in academia and in industry thanks to its potential for saving in cost, time and energy due to easier experimental procedure and reduction in waste. In fact, the organic molecules used as catalysts are usually scarcely sensitive to air and moisture, therefore there is no need for anhydrous reaction and storage conditions. In addition, many organic molecules are available from natural sources as single enantiomers and can be used as chiral scaffolds for organocatalysts,

[1] Stinson, S. C. *Chem. Eng. News* **1992**, *39*, 46.
[2] a) List, B.; Lerner, R. A.; Barbas, C. F. III *J. Am. Chem. Soc.* **2000**, *122*, 2395; b) Ahrendt, K. A., Borths, C. J.; MacMillan, D. W. C. *J. Am. Chem. Soc.* **2000**, *122*, 4243.

which are thus cheap and readily accessible. Finally, small organic molecules, especially natural ones, are typically non-toxic.[3]

Organocatalysis offers the possibility to activate the substrates through different interactions, which can be divided into covalent and non-covalent activation modes. The former include (but are not limited to) aminocatalysis, whose rise on the dawn of the third millennium has been defined as a "gold rush" in organic chemistry.[4] An example is given in *Figure 1*: the enamine **A** is a common covalent intermediate in aminocatalysis. Covalent organocatalysis offers the advantage of forming covalent intermediates whose conformation depends almost only on the catalyst scaffold and it is observed a little effect of solvent or other experimental conditions on the stereochemical outcome. Still, the substrates must possess a functional group which can react reversibly with the catalyst. On the other hand, non-covalent organocatalysis exploits electrostatic (**B**, *Figure 1*), hydrogen-bonding (**C**, *Figure 1*) or van der Waals interactions between the catalyst and the substrate(s).[5] The main benefit of this approach is that virtually all organic reactive species can interact in such a way with a chiral catalyst.

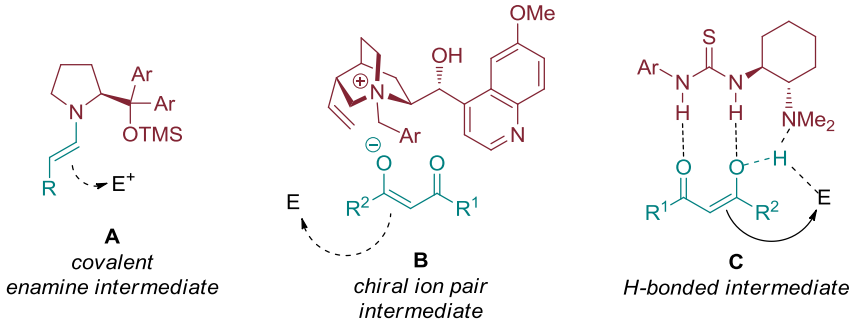

Figure 1: Examples of chiral intermediates arising from the interaction of a chiral organocatalyst with an achiral nucleophilic substrate.

Despite impressive advancement, the search for new asymmetric catalyzed reactions is still an evergreen in organic chemistry, since only some of the known chemical transformations have been already developed in an asymmetric fashion showing wide substrate generality. Moreover, recent results have shown that organocatalytic strategies can be also applied to

[3] MacMillan, D. W. C. *Nature* **2008**, *455*, 304.
[4] Melchiorre, P.; Marigo, M.; Carlone, A.; Bartoli, G. *Angew. Chem. Int. Ed.* **2008**, *47*, 6138.
[5] Doyle, A. G.; Jacobsen, E. N. *Chem. Rev.* **2007**, *107*, 5713.

photo-induced reactions. This opens up new horizons concerning the chemical reactions accessible to organocatalysis, as light-promoted reactive pathways go way beyond the classical ground-state reactivity. Photo-organocatalysis is still in its infancy, but it already possesses promising potentials to become a well-established strategy for the exploitation in asymmetric synthesis of a virtually endless source, that is light.

The aim of this Ph.D. thesis has been the development of new strategies in the field of asymmetric organocatalysis. Three main works will be herein presented. The first one, discussed in *Chapter 2*, deals with the application of the simple and well-known natural organocatalyst quinine to a novel transformation leading to enantioenriched biaryl compounds, by atroposelective direct C-C coupling. This approach represents one of the few and current strategies for the asymmetric synthesis of biaryls without the employment of transition metal-based catalysts.
Within the second work (*Chapter 3*), the design and application of a new class of organocatalysts will be presented. The guanidine moiety has been attached to the *Cinchona* alkaloid scaffold to obtain bifunctional catalysts. Their efficiency has been tested on the intramolecular transesterification of RNA model compound 2-hydroxypropyl *p*-nitrophenyl phosphate (HPNP) and on a new vinylogous aldol reaction.
Finally, as discussed in *Chapter 4*, covalent organocatalysis has been merged with photochemistry. I carried out this work during a six month-period of study abroad at Institut Català d'Investigació Quimica (ICIQ) in Tarragona (Spain), under the supervision of Prof. Paolo Melchiorre. Exploiting for the first time in enantioselective catalysis the ability of ene-iminium ions to absorb visible light and access a highly reactive excited state, we were able to accomplish the asymmetric β-alkylation of enals. To the best of my knowledge, this is the first organocatalytic method for the enantioselective β-functionalization of carbonyl compounds with simple alkyl groups.

2. A New Organocatalyzed Atroposelective Biaryl Coupling

2.1. Introduction

2.1.1. Axial chirality: general features

Axial chirality leading to optical activity is known since the beginning of 20th century and was first correctly described in 1922 by Christie and Kenner studying polinitrobenzoic acids.[6]

There are three stereogenic elements responsible for chirality: stereogenic centers, axes or planes. An axially chiral molecule is such by virtue of the arrangement of atoms or groups about a stereogenic axis.

The most important classes of axially chiral compounds are allenes, methylenecyclohexanes and hindered biaryls. In the latter case, chirality arises from restricted rotation along a C-C single bond: the enantiomers can in principle be interconverted without breaking any covalent bond. For this reason, this type of chirality is also referred to as *atropisomerism*, from the ancient Greek α- = "without" and τροπή = "turn".

In order for a biaryl to be chiral, two conditions are required (*Figure 2*):

a) the *ortho*-substituents must be large enough (usually different from H) to make the axis rotationally hindered;
b) on each aromatic ring the two *ortho*-substituents must be different from one another, i.e. A ≠ A' and B ≠ B'.

Molecules such as the biorcinol **2**, in which A = B and A' = B', have a C_2 symmetry axis, but still are not superimposable with their mirror image and therefore they are chiral. Furthermore, the difference between the groups can arise also from the *meta* substitution pattern, as in the bimesityl **3**.

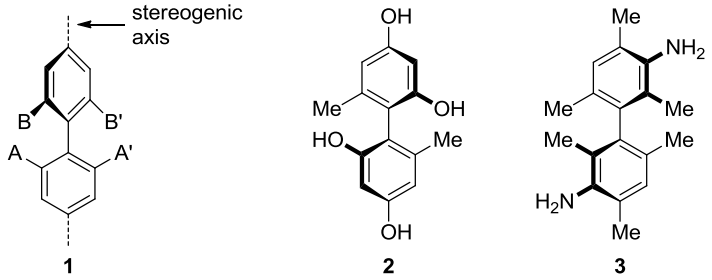

1 **2** **3**

Figure 2: Examples of hindered biaryls showing atropisomerism.

[6] Christie, C. H.; Kenner, J. *J. Chem. Soc., Trans.* **1922**, *121*, 614.

Concerning the rotational stability of atropisomers, the temperature plays a crucial role in overcoming the energy barrier which prevents free rotation. For example, biaryls which are conformationally stable at room temperature, could start to rotate freely upon heating, resulting in loss of stereochemical information. It has been proposed that in order to consider two atropisomers as physically separable species, they must have a half-life of at least 1000 s. This results in a minimum free energy barrier at room temperature of $\Delta G^{\neq}_{300\,\mathrm{K}} \approx 22$ kcal/mol.[7]

Besides temperature, other factors may lead to atropisomerization. For example, chemical processes such as keto-enol tautomerism in biphenols or binaphthols can make them racemize[8] or even photoracemization can occur in atropisomers in the excited state.[9]

2.1.2. Axially chiral biaryls: presence in nature and applications in catalysis

Biaryl moieties bearing chiral axis are widespread in nature and their configuration may influence their bioactivity.[10] Knipholone (**4**, *Figure 3*), a 1-phenylanthraquinone found in the roots of the Ethiopian herb *Kniphofia foliosa*, is used in local traditional medicine for the treatment of abdominal cramps.[11] Knipholone possesses a chiral axis and has been shown to have antimalarial and antitumoral properties. Increasingly complex molecules can be found, such as the nerve-growth stimulating agent mastigophorene A (**5**),[12] which exhibits both central and axial chirality, all the way to the antibiotic vancomycin (**6**). This compound bears all the three types of stereogenic elements: many chiral centers, two chiral planes (corresponding to the macrocycles containing the chlorophenyl rings) and one chiral biaryl

[7] "*Recent Advances in atropisomerism"* Öki, M. in *Topics in Stereochemistry, Vol. 14* (Eds. Allinger, N. L.; Eliel, E. L.; Wilen, S. H.), Wiley, 1984.

[8] Racemization of BINOL in acidic media: Kyba, E. P.; Gokel, G. W.; de Jong, F.; Koga, K.; Sousa, L. R.; Siegel, M. G.; Kaplan, L.; Sogah, G. D. Y., Cram, D. J. *J. Org. Chem.* **1977**, *42*, 4173.

[9] Racemization of 1,1'-binaphthyl in the triplet state: Irie, M.; Yoshida, K.; Hayashi, K. *J. Phys. Chem.* **1977**, *81*, 969.

[10] For a review on axially chiral biaryl natural products, see: Bringmann, G.; Gulder, T.; Gulder, T. A. M.; Breuning, M. *Chem. Rev.* **2011**, *111*, 563.

[11] Dagne, E.; Steglich, W. *Phytochemistry* **1984**, *23*, 1729.

[12] Fukuyama, Y.; Asakawa, Y. *J. Chem. Soc., Perkin Trans. 1* **1991**, 2737.

axis. All these features confer to vancomycin the appropriate three-dimensional structure that makes it able to efficiently block the biosynthesis of bacterial cell wall.[13] Since 1954, this antibiotic has been being used in the treatment of severe infections by gram-positive bacteria unresponsive to other drugs.

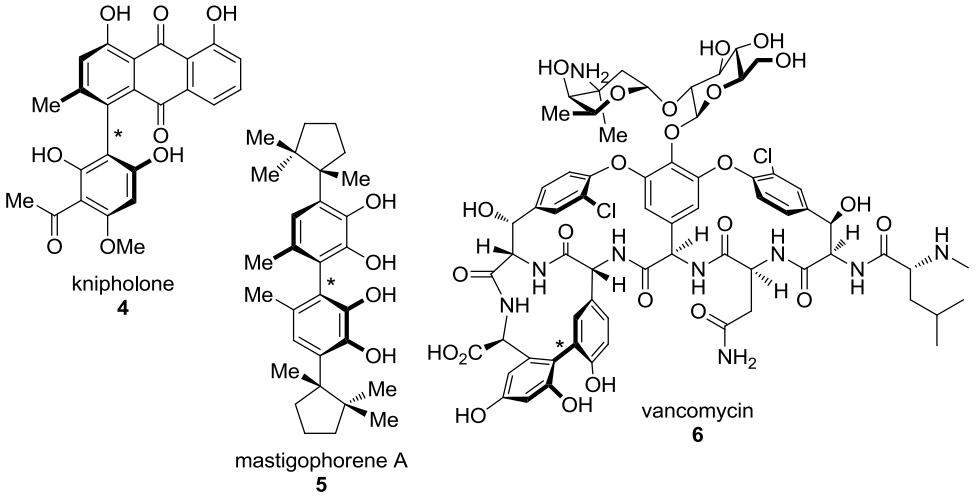

Figure 3: Selected examples of axially chiral natural compounds.

Major interest in axially chiral biaryls has been aroused since the first synthesis and resolution of enantiomerically pure 2,2'-bis(diphenyl-phosphino)-1,1'-binaphthyl (BINAP, **7**) was accomplished by the groups of Tayaka and Noyori. They showed that the rhodium complexes of either (+)-BINAP or (-)-BINAP are effective catalysts for the asymmetric hydrogenation of acrylic acids.[14] From then on, numerous atropisomeric biaryl compounds have been developed in order to be employed as chiral ligands in asymmetric metal catalysis. Most of them (*Figure 4*), including BINAP, are derived from the privileged framework of 1,1'-binaphthyl-2,2'-diol **8** (BINOL), such as the diamine BINAM (**9**). All these ligands are employed in a variety of transition metal-catalyzed reactions. As a remarkable example, in 1987 Noyori reported the first BINAP-Ru complex catalyzed asymmetric hydrogenation of carbonyl compounds.[15] Thanks also

[13] Sheldrick, G. M.; Jones, P. G.; Kennard, O.; Williams, D. H.; Smith, G. A. *Nature* **1978**, *271*, 223.
[14] Miyashita, A.; Yasuda, A.; Takaya, H.; Toriumi, K.; Ito, T.; Souchi, T.; Noyori, R. *J. Am. Chem. Soc.* **1980**, *102*, 7932.
[15] Noyori, R.; Ohkuma, T.; Kitamura, M.; Takaya, H.; Sayo, N.; Kumobayashi, H.; Akutagawa, S. *J. Am. Chem. Soc.* **1987**, *109*, 5856.

to this study, he was awarded the Nobel Prize in Chemistry in 2001, together with Sharpless and Knowles. BINOL itself can serve as a chiral ligand in many metal-catalyzed processes, including reductions, oxidations, aldol reactions and cycloadditions.[16]

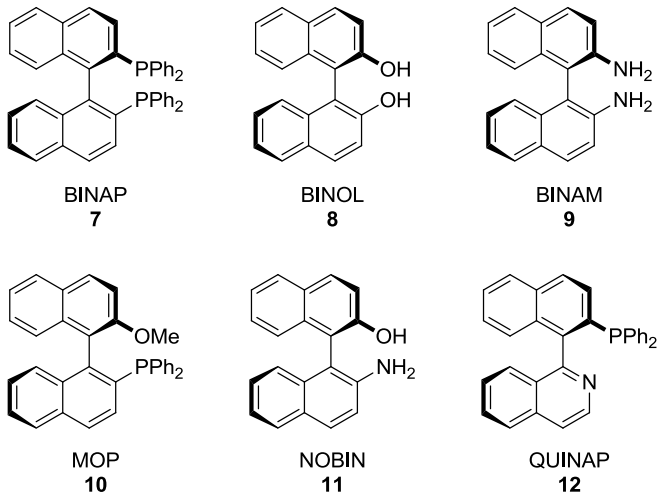

Figure 4: Examples of C_2-symmetrical (**7**, **8** and **9**) and non-C_2-symmetrical (**10**, **11** and **12**) axially chiral biaryls employed as ligands in metal-catalyzed asymmetric reactions.

Until the early '90s it was thought that only C_2-symmetrical homo-bidentate biaryls were efficient chiral ligands for metal catalysis. However, the group of Hayashi in 1991 synthesized the non-C_2-symmetrical methoxyphosphine MOP (**10**),[17] immediately followed by Kočovský's amino naphthol NOBIN (**11**).[18] These compounds work well as ligands for asymmetric reductions, aldol and hydrosilylation reactions.[19] In addition, axially chiral heteroaromatic biaryls were developed: the isoquinoline-containing phosphine QUINAP (**12**)[20] has been used as a ligand in asymmetric hydroboration and allylic alkylation reactions.

Besides being used as chiral ligands, in the last ten years axially chiral biaryl compounds have been employed in a new field of catalysis, namely organocatalysis. Following the blossoming in the employment of chiral

[16] For a comprehensive review on BINOL-metal catalyzed reactions: Brunel, J. M. *Chem. Rev.* **2007**, *107*, PR1.
[17] Uozumi, Y.; Hayashi, T. *J. Am. Chem. Soc.***1991**, *113*, 9887.
[18] Smrčina, M.; Lorenc, M.; Hanuš, V.; Kočovský, P. *Synlett* **1991**, 231.
[19] For a comprehensive review on non-C_2-symmetrical binaphthyls: Kočovský, P.; Vyskočil, Š.; Smrčina, M. *Chem. Rev.* **2003**, *103*, 3213-3245.
[20] Brown, J. M.; Hulmes, D. I.; Layzell, T. P. *J. Chem. Soc., Chem. Commun.* **1993**, 1673.

organic molecules as catalysts, in 2004 the groups of Akiyama and Terada independently developed chiral phosphoric acids derived from BINOL[21]. This new class of compounds responded to the problem presented by Brønsted acid asymmetric catalysis. In fact, protonation of a substrate is the most straightforward and classical approach to promote a reaction, but the nearly proton-like character of the catalyst barely provide a chiral environment to the reactive intermediate. However, in chiral phosphoric acids such as TRIP (**13**, *Figure 5*) the proton is surrounded by bulky substituents and hence asymmetric induction is possible. This, coupled with their intrinsic high acidity, resulted in the fortune of these organocatalysts. Soon after, many research groups started to develop their own axially chiral Brønsted acids. *N*-Triflyl phosphoric amides, bis(sulfonyl)imides and, finally, bis(sulfuryl)imides like **14** were reported to act as excellent acidic organocatalysts, reaching pK_a values as low as 5.2 in acetonitrile (as a comparison, the pK_a of HCl in acetonitrile is 10.3).[22] A number of asymmetric reactions have been developed using these chiral acids, including Mannich-type, Friedel-Crafts, cycloaddition and oxidation reactions.[23]

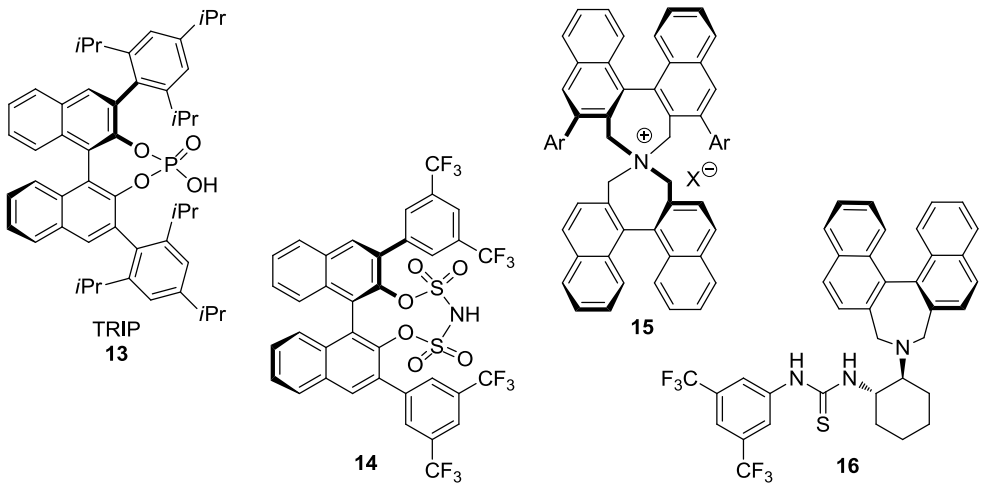

Figure 5: Selected examples of axially chiral organocatalysts.

[21] a) Akiyama, T.; Itoh, J.; Yokota, K.; Fuchibe, K. *Angew. Chem. Int. Ed.* **2004**, *43*, 1566; b) Uraguchi, D.; Terada, M. *J. Am. Chem. Soc.* **2004**, *126*, 5356.

[22] a) Nakashima, D.; Yamamoto, H. *J. Am. Chem. Soc.* **2006**, *128*, 9626; b) García-García, P.; Lay, F.; García-García, P.; Rabalakos, C.; List, B. *Angew. Chem. Int. Ed.* **2009**, *48*, 4363; c) Berkessel, A.; Christ, P.; Leconte, N.; Neudörfl, J.-M.; Schäfer, M. *Eur. J. Org. Chem.* **2010**, 5165; d) acidity scale of chiral acids: Kaupmees, K.; Tolstoluzhsky, N; Raja, S.; Rueping, M.; Leito, I. *Angew. Chem. Int. Ed.* **2013**, *52*, 11569.

[23] For a review: Terada, M. *Synthesis* **2010**, 1929.

There are also other remarkable applications of axially chiral molecules as organocatalysts. One of most relevant is the development of a series of C_2-symmetric quaternary ammonium salts **15**, reported by Maruoka and co-workers.[24] These BINOL-derived, structurally rigid spiro compounds are efficient phase-transfer catalysts and represent an alternative to *Cinchona* alkaloid-based quaternary ammonium salts. They are commercially available and have been applied to this day to perform various bond-forming transformations under mild phase-transfer conditions.[25]

Bifunctional catalysts have also been synthesized based on BINOL skeleton. The bridged amine-thiourea **16**, developed by Shao and co-workers,[26] has been recently applied to the atroposelective synthesis of new axially chiral urazoles **17**, as reported in a paper appeared in March 2016 on *Nature Communications*.[27] This transformation, outlined in *Scheme 1*, defined as an "asymmetric tyrosine click-like reaction" proceeds under mild conditions and with high yield and excellent enantioselectivity. Furthermore, it represents a convenient method for the synthesis of a new class of "non-conventional" axially chiral compounds with potential biological activity and suitable properties as organocatalysts or ligands.

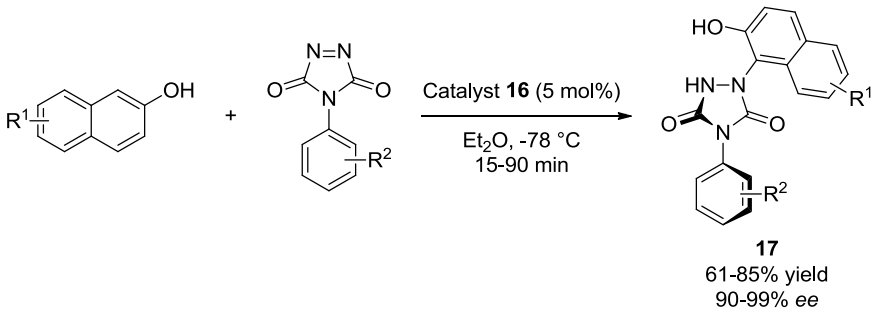

Scheme 1: Atroposelective tyrosine click-like reaction leading to chiral urazoles **17**.

In the next section the main available methodologies for the synthesis of axially chiral biaryls will be presented.

[24] OOi, T.; Kameda, M.; Maruoka, K. *J. Am. Chem. Soc.* **1999**, *121*, 6519.
[25] Hashimoto, T.; Maruoka, K. *Chem. Rev.* **2007**, *107*, 5656.
[26] Peng, F.-Z.; Shao, Z.-H.; Fan, B.-M.; Song, H.; Li, G.-P.; Zhang, H.-B. *J. Org. Chem.* **2008**, *73*, 5202.
[27] Zhang, J.-W.; Xu, J.-H.; Cheng, D.-J.; Shi, C.; Liu, X.-Y.; Tan, B. *Nat. Commun.* **2016**, *7*, 10677.

2.1.3. Atroposelective synthesis of axially chiral biaryl compounds

Owing to the role that axially chiral biaryl compounds play both in biology and in asymmetric catalysis, a number of strategies for their atroposelective synthesis have been developed. In this section, the three main approaches to this problem will be discussed:

A. aromatic ring construction: the chiral axis is generated starting from a C-C bond between an arene and an appropriate substituent;
B. desymmetrization of a prochiral biaryl system;
C. direct biaryl formation by C-C coupling.

Each of these strategies relies on different concepts and has got its own points of strength and limitations, on which we will focus here.

Strategy A: aromatic ring construction

The *de novo* construction of an aromatic ring starting from a simple arene and leading to the atroposelective formation of a stereogenic axis is a quite recent strategy and results in methodologies which are often suitable only for specific substrates. The asymmetric induction of the processes derives either from a stereogenic center already present in the substrate (central-to-axial chirality transfer) or from the employment of a chiral catalyst, most often a transition metal-based one.
One of the first examples of central-to-axial chirality transfer is represented by the work of Nishi and Tanabe[28] who reported the benzannulation of enantiomerically pure cyclopropylmethanols **18** to give enantiopure biaryl products **19** (*Scheme 2*). The reaction is mediated by $TiCl_4$, whose coordination to the hydroxyl group makes the *ortho* substituent R_1 to orient itself at the backside of the chelation face. In this way, the ring-opening and subsequent Friedel-Crafts-type cyclization occur to deliver only one atropisomer.

[28] Nishii, Y.; Wakasugi, K.; Koga, K.; Tanabe, Y. *J. Am. Chem. Soc.* **2004**, *126*, 5358.

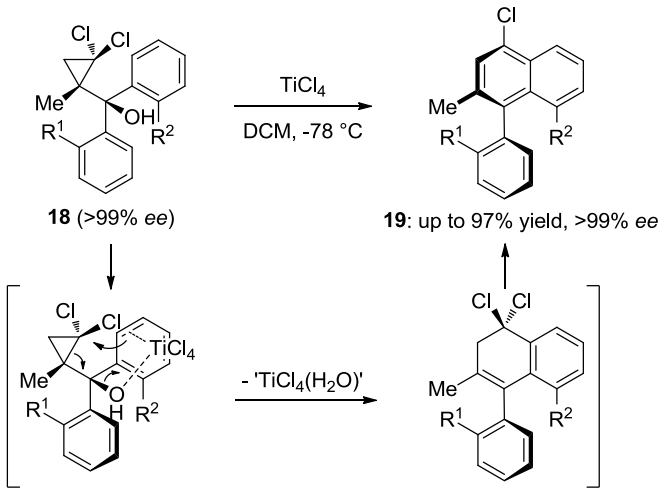

Scheme 2: Atroposelective benzannulation of optically active cyclopropylmethanols **18**.

In 2011 Thomson and co-workers[29] reported a stereochemical exchange for the synthesis of biaryldiols **21**. It is a two-step process in which enantiomerically enriched dimethylketal quinones **19** are, at first, subjected to oxidative dimerization to give intermediates **20** as single diastereoisomers in nearly enantiopure form. *Scheme 3* depicts the structure of diones **20**, highlighting that all the substituents are equatorially disposed. The restricted rotation along the central C-C bond due to steric hindrance accounts for the stereochemical outcome of the $BF_3{\cdot}Et_2O$-promoted aromatization step. The value of this work resides in the importance of being able to prepare, with simple operations, enantiomerically pure biaryldiols, even though with moderate yields and limited substrate scope.

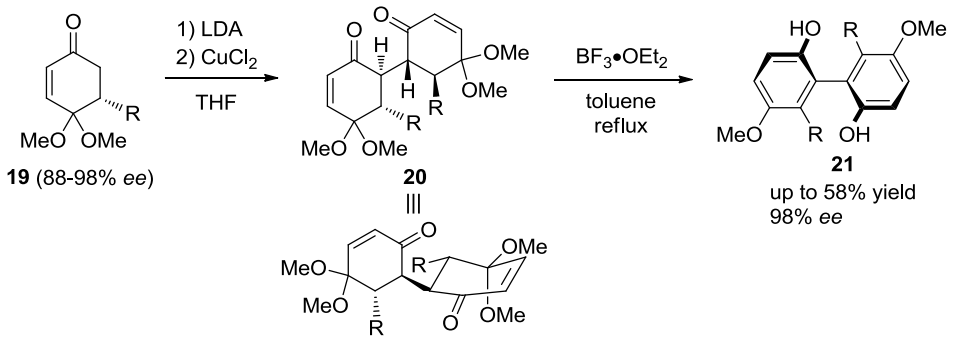

Scheme 3: Atroposelective synthesis of biaryldiols **21** from 1,4-diketones.

[29] Guo, F.; Konkol, L. C.; Thomson, R. J. *J. Am. Chem. Soc.* **2011**, *133*, 18.

In parallel to the central-to-axial chirality transfer approach, studies have been conducted to perform atroposelective aromatic ring formation by means of asymmetric catalysis. The pioneering work in this field is the [2+2+2] cycloaddition reported by the group of Gutnov and Heller in 2004.[30] The reaction, outlined in *Scheme 4*, is catalyzed by chiral cobalt(I)/cyclopentadiene complex **24**, in THF under light irradiation. In these conditions, aryl-substituted 1,7-diyne **22** is reacted with various nitriles, leading to enantioenriched biaryl pyridines **23**. Interestingly, products can be recrystallized to near enantiopurity and with overall yields up to 57%.

Improvements of metal-catalyzed cycloadditions for this purpose have been achieved moving to iridium, rhodium and nickel based catalysts, which are often commercially available and feature broader generality.[31]

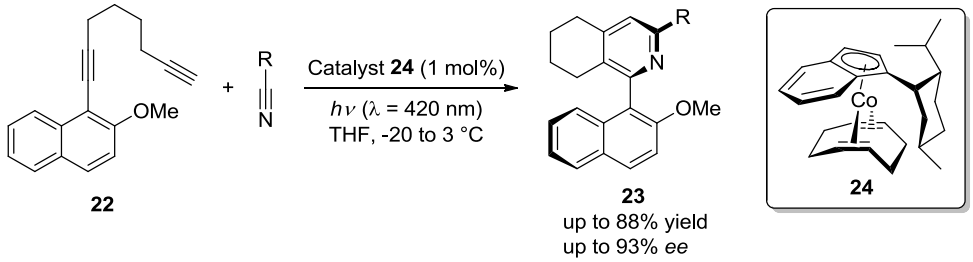

Scheme 4: Chiral cobalt(I)/cyclopentadiene complex-catalyzed atroposelective [2+2+2] cycloaddition between 1,7-diyne **22** and nitriles.

To conclude this brief overview on the "aromatic ring construction" strategy, an organocatalytic method is presented. In the work of Sparr,[32] an intramolecular aldol condensation, catalyzed by pyrrolidinyl-tetrazole **26** allows to get 1,1'-binaphthyl-2-carbaldehydes **27** in good yield and excellent enantioselectivity (*Scheme 5*). The stereochemical outcome is explained considering that the substrate **25** is activated by dienamine formation (intermediate **28**). Its conformation is determined by coordination of the ketone by the NH-group of the tetrazole moiety and by the *Z* geometry of the olefin: in this way the activated α-carbon of the aldehyde is positioned exactly over the ketone. Therefore, the nucleophilic attack and subsequent

[30] Gutnov, A.; Heller, B.; Fischer, C.; Drexler, H.-J.; Spannenberg, A.; Sundermann, B.; Sundermann, C. *Angew. Chem. Int. Ed.* **2004**, *43*, 3795.
[31] For a review on cycloadditions for atroposelective synthesis: Tanaka, K. *Chem. Asian J.* **2009**, *4*, 508.
[32] Link, A.; Sparr, C. *Angew. Chem. Int. Ed.* **2014**, *53*, 5458.

dehydration-aromatization step occur with efficient transfer of stereochemical information from the catalyst to the newly formed chiral axis. A limitation of this methodology is the instability of substrates **25**, which must be prepared *in situ* by oxidation of the corresponding 1,7-diols.

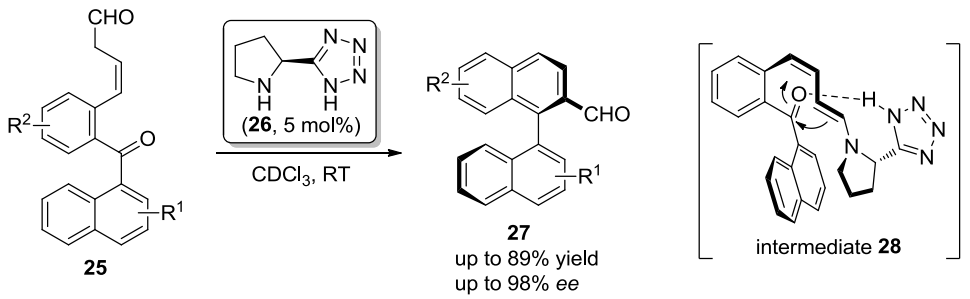

Scheme 5: Organocatalytic atroposelective intramolecular aldol condensation.

Strategy B: desymmetrization of prochiral biaryls

Prochiral biaryl systems can be grouped in two categories: rotationally hindered molecules in which at least one of the two aromatic portions is symmetric, thus resulting in an achiral *meso* form, and chiral but conformationally unstable compounds. To achieve desymmetrization of biaryls belonging to the first category, the enantiotopos-differentiating transformation of one of the identical substituents is employed. On the other hand, for coonformationally unstable biaryls, a dynamic kinetic resolution can be implemented with simultaneous introduction of some steric hindrance about the axis.

An early example of desymmetrization of rotationally hindered achiral biaryls is represented by the work of Hayashi *et al.*,[33] who reported the enantioposition-selective cross-coupling between symmetric biaryl triflates **29** and Grignard reagents (*Scheme 6, A*). The reaction is mediated by chiral palladium complex **31**, which is capable of differentiating the two enantiotopic triflate groups on the substrate, making the coupling to proceed on only one of them. Enantiomeric excesses of up to 99% are thus observed.

[33] a) Hayashi, T.; Niizuma, S.; Kamikawa, T:; Suzuki, N.; Uozumi, Y. *J. Am. Chem. Soc.* **1995**, *117*, 9101; b) Kamikawa, T.; Uozumi, Y.; Hayashi, T. *Tetrahedron Lett.* **1996**, *37*, 3161.

Moving to organocatalytic approaches, the axially chiral phosphoric acid **34** has been employed for an elegant asymmetric electrophilic aromatic bromination on achiral biphenols **32** (*Scheme 6, B*).[34] This transformation actually consists of two distinct steps: a desymmetrization followed by a kinetic resolution. In fact, in the presence of an excess of *N*-bromophthalimide, a first bromination occurs leading to **33** in 81-93% *ee*. However, under the reaction conditions, *ent*-**33** is immediately subjected to a faster second bromination giving a dibrominated achiral byproduct: this results in a significant enantioenrichment of **33**, with only slight sacrifice of chemical yield. The highly functionalized products are valuable because they can potentially be subjected to other transformations. However, a drawback is the high loading of a such expensive catalyst, which could make this procedure disadvantageous for many applications.

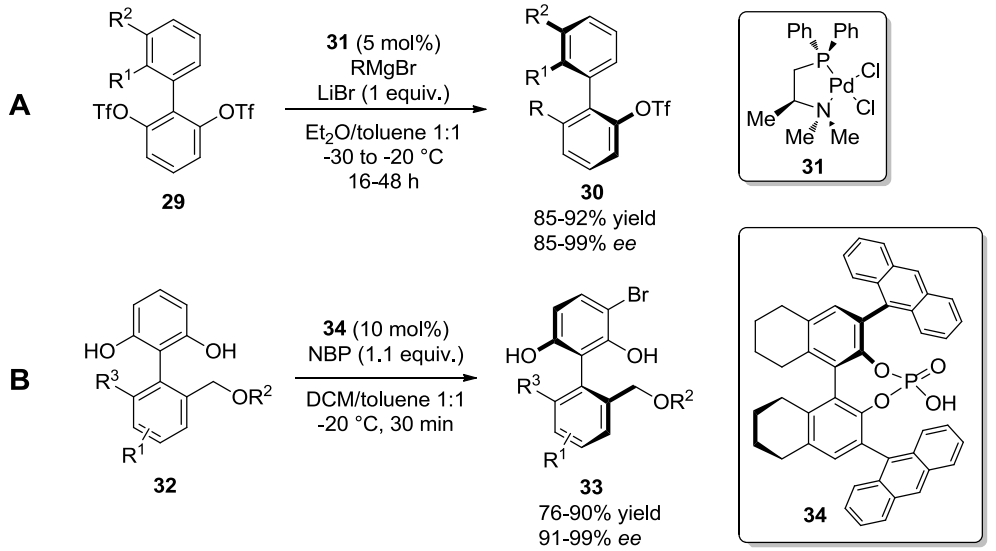

Scheme 6: Selected examples of metal- (**A**) and organo-catalyzed (**B**) desymmetrizations.

Dynamic kinetic resolution (DKR) is a process in which two configurationally unstable enantiomers are subjected to a transformation which is selective for only one of them. Unlike "ordinary" racemate resolution, including simple kinetic resolution, the enantiomeric excess of the product depends only on the enantioselectivity of the process and there is

[34] Mori, K.; Ichikawa, Y.; Kobayashi, M.; Shibata, Y.; Yamanaka, M.; Akiyama, T. *J. Am. Chem. Soc.* **2013**, *135*, 3964.

not the limit of 50% yield, as the slowly reacting enantiomer continuously interconverts in the one which is consumed faster.

This concept was successfully applied to rotationally non-restricted biaryls by the group of Miller.[35] In his work, which first appeared on *Science* in 2010, peptide **37** mediates the asymmetric bromination of biaryl benzoic acids **35** with good yields and enantioselectivity. The catalyst is able to chelate the substrate, giving to the biaryl C-C bond the conformation which is then blocked by introduction of bulky bromo substituents, as depicted in *Scheme 7*.

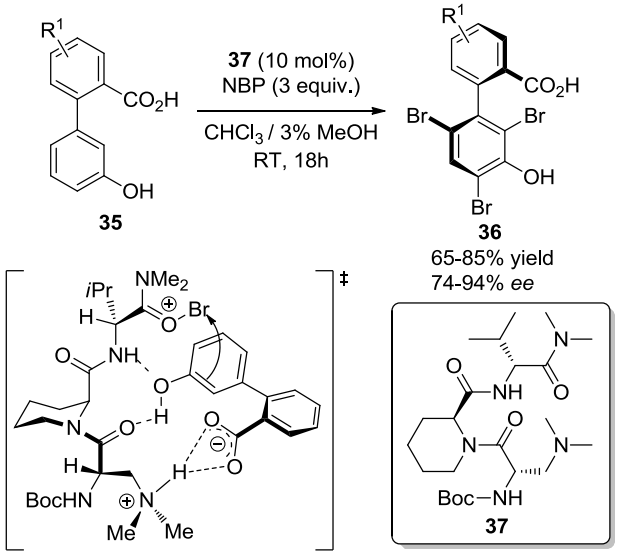

Scheme 7: DKR of atropisomers **35** via peptide-catalyzed asymmetric bromination.

A similar reaction, catalyzed by a *Cinchona* alkaloid-based urea and leading to axially chiral isoquinoline *N*-oxide, has been developed by Matsubara and co-workers.[36] Both these strategies to get axially chiral biaryls are intellectually valuable, but afford very specific products and do not take into account the synthetic issues of the substrate preparation.

[35] Gustafson, J. L.; Lim, D.; Miller, S. J. *Science* **2010**, *328*, 1251.
[36] Miyaji, R.; Asano, K.; Matsubara, S. *J. Am. Chem. Soc.* **2015**, *137*, 6766.

Concerning DKR of biaryls, a number of methodologies involving transition metal-based catalysts have been developed, but they go beyond the scope of this thesis.[37]

Strategy C: direct biaryl formation via asymmetric C-C coupling

The most straightforward strategy to prepare enantioenriched biaryl systems is the direct C-C coupling reaction: the aryl-aryl axis is formed with contextual chiral induction. This approach has to face two opposite features. On the one hand, the construction of a conformationally stable biaryl compound is an inherently hindered reaction, thus requiring "forced" reaction conditions to occur in good yield. On the other hand, the desired atroposelective induction most often needs mild conditions not to overcome the rotational barrier.

Several methods have been developed for the asymmetric biaryl coupling reaction. Early examples include protocols which may be classified as first and second generation methods for asymmetric synthesis. In these cases, asymmetric induction is due to chiral starting materials (e.g. aryl moieties linked by a chiral bridge,[38] aryl groups substituted with chiral *ortho* substituents[39]) or chiral auxiliaries which are removed during the coupling reaction.[40] Despite further studies in this field and considerable improvements in efficiency, these approaches have been overcome by fourth generation methods, i.e. asymmetric catalysis, with two major advantages: substoichiometric quantities of chiral materials are employed and there is no need to dedicate extra steps for installation and removal of chiral auxiliaries. Time and cost of the synthesis are thus reduced.

C_2-symmetrical biaryls can be obtained by oxidative homocoupling of phenols. Due to its operational simplicity and good availability of the substrates, it is largely employed to get racemic biaryls, followed by resolution of the enantiomers. Also the large scale preparation of BINOL (**8**)

[37] For selected examples of metal-catalyzed DKRs: Bringmann, G.; Price Mortimer, A. J.; Keller, P. A.; Gresser, M. J.; Garner, J.; Breuning, M. *Angew. Chem. Int. Ed.* **2005**, *44*, 5384.
[38] Miyano, S.; Tobita, M.; Hashimoto, H. *Bull. Chem. Soc. Jpn.* **1981**, *54*, 3522.
[39] Meyers, A. I.; Lutomski, K. A. *J. Am. Chem. Soc.* **1982**, *104*, 879.
[40] Wilson, J. M.; Cram, D. J. *J. Am. Chem. Soc.* **1982**, *104*, 881.

relies on this strategy. For this purpose, a stoichiometric amount of oxidant is needed, most often a transition metal-based one (Fe, Mn, Cu or Ti). A mechanistic rationale for the oxidative homocoupling of 2-naphthols with Fe(III) is depicted in *Scheme 8*.[41] A one-electron oxidation of naphthol **38a** with Fe^{3+} results in the radical species **39**, which adds to another neutral molecule of **38a**. Further oxidation of adduct **40** by O_2 and release of a proton lead to the product in racemic form (*rac*-**8**).

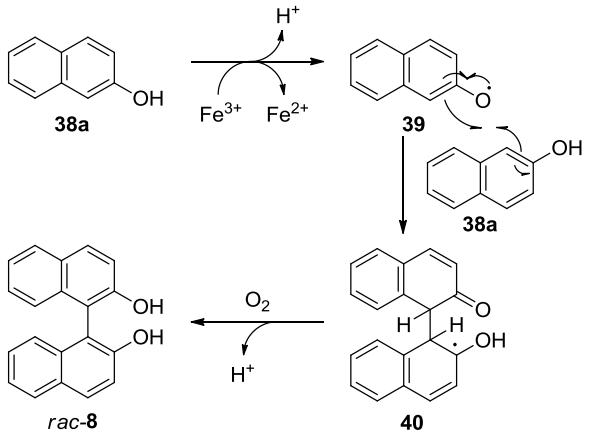

Scheme 8: Mechanistic rationale for the oxidative homocoupling leading to *rac*-BINOL.

Asymmetric versions of oxidative homocoupling reactions have been implemented resorting to chiral additives in combination with transition metal oxidants or to chiral transition metal-based complexes. Despite the extensive efforts put in this field and the number of reports published in the literature, almost all the methods seem to be really efficient (good yield and *ee* > 90%) only for a specific substrate or, despite being general, they require large amounts of chiral additives (up to 8 equivalents).[16, 42]

In order to get a biaryl compound consisting of two different aryl moieties, a cross-coupling approach is necessary. This is the most widely used method in non-stereoselective synthesis and relies on the separate activation of the coupling partners as different reactive species. Belonging to this category, Kumada, Negishi and Suzuki biaryl couplings are nowadays recognized as fundamental transformations for organic synthesis. Indeed, the Nobel Prize for Chemistry was awarded in 2010 to Negishi and Suzuki, together with

[41] Ding, K.; Wang, Y.; Zhang, L.; Wu, Y. *Tetrahedron* **1996**, *52*, 1005.
[42] Kozlowski, M. C.; Morgan, B. J.; Linton, E. C. *Chem. Soc. Rev.* **2009**, *38*, 3193.

Heck, for their studies on palladium-catalyzed cross-couplings. Increasing attention has been paid to the development of asymmetric versions of these reactions focusing on the search for suitable chiral ligands, with interesting results.

Atroposelective versions of both Kumada[43] and Negishi[44] biaryl couplings have been implemented. However, they employ unstable organometallic species which are not compatible with a number of functional groups and so they are less attractive then Suzuki coupling. The latter makes use of aryl boronic acids or boronates, which are air stable, less reactive and more tolerant of various functionalities. A quite recent example of enantioselective Suzuki coupling is the one reported by Buchwald and co-workers,[45] who for the first time expanded the scope of the reaction to compounds other than binaphthyls. Naphthyl boronic acids **41** can be coupled with halogenated benzamides **42**, employing an *in situ* generated chiral palladium catalyst (*Scheme 9*). The chiral ligand is (*S*)-KenPhos (**44**), an axially chiral aminophosphine. To achieve high asymmetric induction and good yields, protection of **42** with a cumyl group is necessary. This protecting group can be easily removed via acidic hydrolysis with trifluoroacetic acid and the resulting free amide recrystallized to enantiopurity.

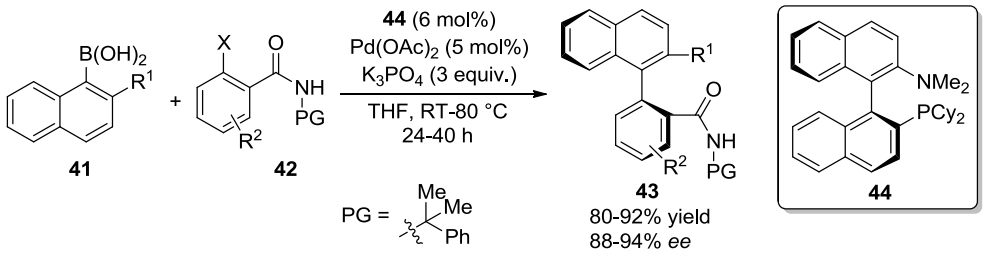

Scheme 9: Atroposelective Suzuki coupling using axially chiral ligand **44**.

Organocatalytic attempts to perform atroposelective direct biaryl couplings can be counted on the finger of one hand and they are discussed in the next section.

[43] Hayashi, T.; Hayashizaki, K.; Kiyoi, T.; Ito, Y. *J. Am. Chem. Soc.* **1988**, *110*, 8153.
[44] Genov, M.; Fuentes, B.; Espinet, P.; Pelaz, B. *Tetrahedron: Asymmetry* **2006**, *17*, 2593.
[45] A) Yin, J.; Buchwald, S. L. *J. Am. Chem. Soc.* **2000**, *122*, 12051; b) Shen, X.; Jones, G. O.; Watson, D. A.; Bhayana, B.; Buchwald, S. L. *J. Am. Chem. Soc.* **2010**, *132*, 11278.

2.1.4. Organocatalytic biaryl coupling: recent advances and aim of this work

The possibility of performing a C-C biaryl coupling without transition metal-based catalysts has attracted much interest over the years. In fact, despite their synthetic power, the use of transition metals presents some critical points, especially for industrial applications. Waste disposal, products and reaction vessels contamination are some of the issues that a manufacturer has to face in such processes.[46] Moreover, most of the asymmetric strategies presented in the previous section have not yet been proven to be scalable. Therefore, for the large scale synthesis of axially chiral biaryl compounds, a transition metal-catalyzed racemic coupling is usually employed, followed by chiral resolution, with a maximum theoretical yield of 50%.[47]

An important step in this direction seemed to have been taken in 2003, when Leadbeater reported the first transition metal-free Suzuki coupling, catalyzed by simple Na_2CO_3 and tetrabutylammonium bromide, under microwave irradiation.[48] Although it afforded racemic products, it could have paved the way to an asymmetric version. However, the enthusiasm was reduced a year later, when a revision of the study explained that the reaction worked only because part-per-billion traces of palladium were present in the sodium carbonate employed.[49]

The first "real" reports of a fully organocatalytic atroposelective synthesis of axially chiral biaryl compounds via direct C-C coupling, albeit in an intramolecular fashion, appeared in 2013 by the group of Kürti[50] and List.[51] They independently developed the Brønsted acid-catalyzed enantioselective rearrangement of *N,N'*-dinaphthylhydrazines **45** leading to 1,1'-binaphthyl diamine (BINAM) derivatives **46**. The reaction is depicted in *Scheme 10*,

---

[46] a) Blaser, H. U.; Federsel, U.-J. *Asymmetric Catalysis On Industrial Scale: Challenges, Approaches, and Solutions, 2nd ed.*, Wiley-VCH, Weinheim, 2010; b) Berkessel, A.; Gröger, H. *Asymmetric Organocatalysis: From Biomimetic Concepts to Applications in Asymmetric Synthesis*, Wiley-VCH, Weinheim, 2005, Chap. 14.

[47] See, for example, Monsanto and Merck synthesis of BINAP: Berthod, M.; Mignani, G.; Woodward, G.; Lemaire, M. *Chem. Rev.* **2005**, *105*, 1801.

[48] Leadbeater, N. E.; Marco, M. *Angew. Chem. Int. Ed.* **2003**, *42*, 1407.

[49] Arvela, R. K.; Leadbeater, N. E., Sangi, M. S.; Williams, V. A., Granados, P.; Singer, R. D. *J. Org. Chem.* **2005**, *70*, 161.

[50] Li, G.-Q.; Gao, H.; Keene, C.; Devonas, M.; Ess, D. H.; Kürti, L. *J. Am. Chem. Soc.* **2013**, *135*, 7414.

[51] De, C. K.; Pesciaioli, F.; List, B. *Angew. Chem. Int. Ed.* **2013**, *52*, 9293.

under List's conditions, which are the most efficient (Kürti used the same catalyst, but with different solvent and additives). The catalyst employed is the chiral phosphoric acid **47**, together with an acidic resin as an additive.

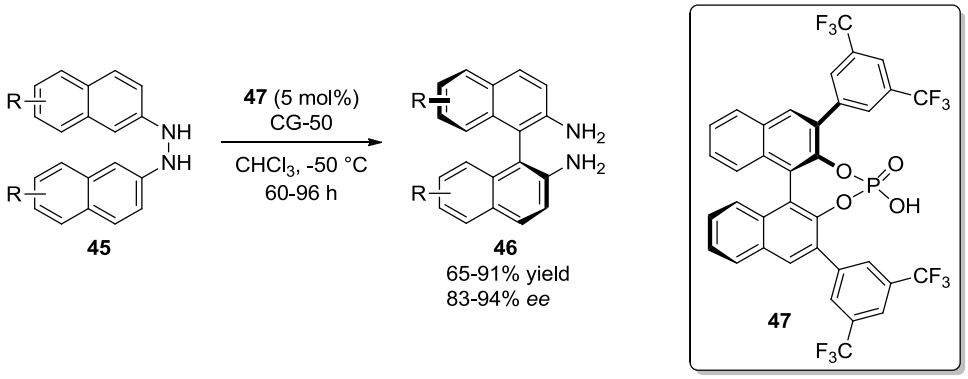

Scheme 10: List's organocatalytic rearrangement of hydrazines **45** leading to enantioenriched BINAM derivatives **46**.

Being the first example of its kind, the yield and enantioselectivity of this reaction were excellent. However, some issues needed to be fixed. First, as it is a benzidine rearrangement, it is applicable only to hydrazines, which are oxygen and light sensitive and whose preparation requires anyway some transition metal-catalyzed step. Second, compound **47** is quite expensive and an organocatalytic process could yearn for a more affordable catalyst. Moreover, an intermolecular reaction would be amenable to introduce chemical diversity in the products.

With this in mind, we started to develop a new atroposelective organocatalyzed biaryl coupling. We were inspired by the work of Bella, Jørgensen and co-workers[52] who reported that *Cinchona* alkaloid-derived chiral bases could activate 2-naphthols **38**, which would add to azodicarboxylates **48**, producing C-N axially chiral compounds **49** (*Scheme 11*). We exploited this information to develop a $C(sp^2)$-$C(sp^2)$ coupling between activated aromatic compounds and 1,4-benzoquinones **52**, as electrophiles. Indeed, 1,4-benzoquinones have been already proven to act as good agents for the asymmetric arylation of nucleophiles such as β-keto

[52] Brandes, S.; Bella, M.; Kjærsgaard, A.; Jørgensen, K. A. *Angew. Chem. Int. Ed.* **2006**, *45*, 1147.

esters and aldehydes.[53] Our approach would deliver C-C axially chiral molecules **52** which closely resemble the skeleton of BINOLs.

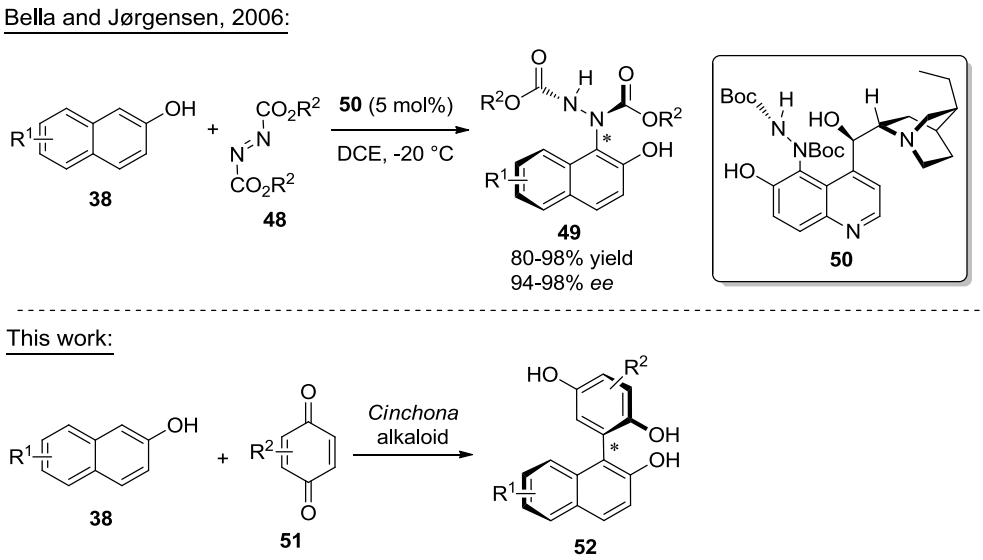

Scheme 11: Aim of this work and background.

The aim of this work was therefore the study of the new transformation reported in *Scheme 11*, the optimization of the asymmetric procedure in terms of yield and enantioselectivity and its implementation on a large scale, thus demonstrating the potential application in an industrial process.[54]

While this work was ongoing and the related manuscript was in preparation, three reports were published which used 2-naphthols as nucleophiles in organocatalytic biaryl couplings, both in racemic[55] and asymmetric[56] fashion. The atroposelective reactions were catalyzed by chiral phosphoric acids like **13**. Therefore, our strategy, besides being in some ways complementary to those, also offers the opportunity to use a much cheaper and widely available catalyst, the *Cinchona* alkaloid quinine.

---

[53] a) Alemán, J.; Richter, B.; Jørgensen, K. A. *Angew. Chem. Int. Ed.* **2007**, *46*, 5515; b) Alemán, J.; Cabrera, S..; Maerten, E.; Overgaard, J.; Jørgensen, K. A. *Angew. Chem. Int. Ed.* **2007**, *46*, 5520.

[54] Moliterno, M.; Cari, R.; Puglisi, A.; Antenucci, A.; Sperandio, C.; Moretti, E.; Di Sabato, A.; Salvio, R.; Bella, M. *Angew. Chem. Int. Ed.* **2016**, *55*, 6252.

[55] Gao, H.; Xu, Q.-L.; Keene, C.; Yousufuddin, M.; Ess, D. H.; Kürti, L. *Angew. Chem. Int. Ed.* **2016**, *55*, 566.

[56] a) Chen, Y.-H.; Cheng, D.-J.; Zhang, J.; Wang, Y.; Liu, X.-Y.; Tan. B. *J. Am. Chem. Soc.* **2015**, *137*, 15062; b) Wang, J.-Z.; Zhou, J.; Xu, C.; Sun, H.; Kürti, L.; Xu, Q.-L. *J. Am. Chem. Soc.* **2016**, *138*, 5202.

2.2. Results and Discussion

2.2.1. Preliminary investigations and determination of the rotational barriers

We started our preliminary investigations studying the addition of 2-phenylindole (**53**) to 1,4-benzoquinone (**51a**) in the presence of the *Cinchona* alkaloid quinine (**I**) as the chiral base catalyst. Based on the work of Prakash's group,[57] we believed that indoles could be significantly more activated than naphthols. Unfortunately, we could only isolate traces of the desired product **54a** which could not be separated in two enantiomers on any of the conditions we tested. Repeating the reaction with the more activated 2,5-dibromo-1,4-benzoquinone (**51b**) we obtained the desired compound **54b**, along with its oxidized form **54b'** as the main product. The latter could be reduced to **54b** by treatment with $NaBH_4$ in methanol.

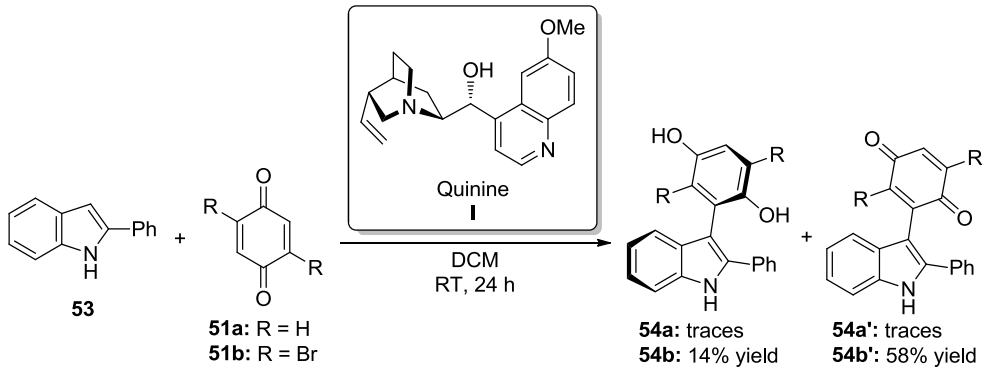

Scheme 12: Preliminary study on the addition of phenylindole **53** to benzoquinones **51a-b**.

Biaryl **54b** could be separated on chiral HPLC into two enantiomers, with baseline peak separation. We therefore screened several reaction conditions and catalysts to get some chiral induction, but we were unable to obtain products with any optical activity. We then calculated the rotational barrier between the two atropisomers of **54b** and of **54b'**. As shown in *Table 1*, we found a high barrier for compound **54b**, which indicates that its two enantiomers should not interconvert by rotation around the $C(sp^2)$-$C(sp^2)$. On the other hand, the quinonic form **54b'** possesses a low barrier (racemization

[57] Török, B.; Abid, M.; London, G.; Esquibel, J.; Török, M.; Mhadgut, S. C.; Yan, P.; Prakash, G. K. S. *Angew. Chem. Int. Ed.* **2005**, *44*, 3086.

half-life is less than a minute), accounting for the fact that we were not able to resolve it into two enantiomers by HPLC.

We then separated the two enantiomers of compound **54b** by preparative HPLC and we observed a rapid racemization, which was not compatible with their high rotational barrier. Therefore, we hypothesized that racemization might occur by a different mechanism: the internal disproportion between the quinone (**54b'**) and its reduced form (**54b**). This limitation prompted us to move directly to the investigation of the behavior of naphthol-derived biaryls.

	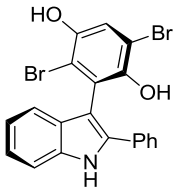 **54b**	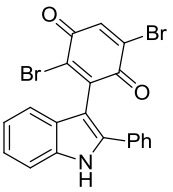 **54b'**	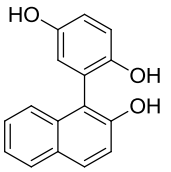 **52a**	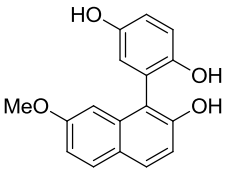 **52b**
Calculated				
$\Delta G^{\ddagger}$ (kcal/mol)	34.6	19.9	22.9	22.1
$t_{1/2}$ rac (s)	3.2×10^{12}	49	7800	2000
Experimental				
$\Delta G^{\ddagger}$ (kcal/mol)	-	-	22.0 ± 0.1	21.3 ± 0.1
$t_{1/2}$ rac (s)	-	-	1650 ± 250	510 ± 80
	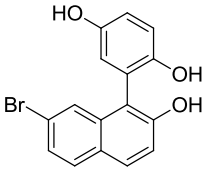 **52c**	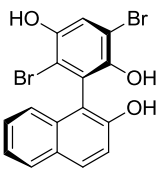 **52d**	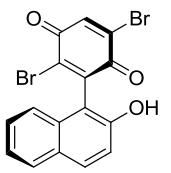 **52d'**	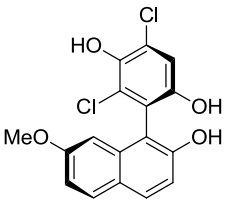 **52e**
Calculated				
$\Delta G^{\ddagger}$ (kcal/mol)	22.8	45.8	32.4	40.2
$t_{1/2}$ rac (s)	6600	5.5×10^{20}	7.6×10^{10}	4.2×10^{16}
Experimental				
$\Delta G^{\ddagger}$ (kcal/mol)	21.9 ± 0.1	-	-	-
$t_{1/2}$ rac (s)	1340 ± 270	-	-	-

Table 1: Energies of the rotational barriers calculated by DFT[58] and experimentally determined by HPLC.

[58] (b3lyp/6-311 +g(d,p) // b3lyp/6-311 +g(d,p)) using Gaussian09 (Revision D.01), > M. J. Frisch *et. al.*, Gaussian, Inc., Wallingford CT, **2010**.

The first question we raised about our target compounds (**52**) was about their conformational stability. The rotational restriction of BINOLs (whose energy barriers are known) stems from the presence of the hydroxy groups (in the 2,2'-positions) and of the *peri* protons (in the 8,8'-positions). Since our compounds were missing this feature and no data about them could be found in the literature, a preliminary aspect to be investigated was the substitution pattern allowing a sufficient rotational barrier along the newly formed chiral axis to obtain conformationally stable atropisomers.

We prepared a first series of biaryls **52a-e**, reacting 2-naphthols **38a-c** with 1,4-benzoquinones **51a-c**, in the presence of an equimolar mixture of *pseudo*enantiomers quinine (**I**) and quinidine (**II**) (*Scheme 13*). This strategy is commonly employed in *Cinchona* alkaloid catalysis to obtain nearly racemic mixtures and it is preferred to the use of an achiral base to avoid possibly different interactions or reactive pathways. Although these first conditions were not the optimal ones, large enough amounts of the products were isolated in order to evaluate their conformational stability.

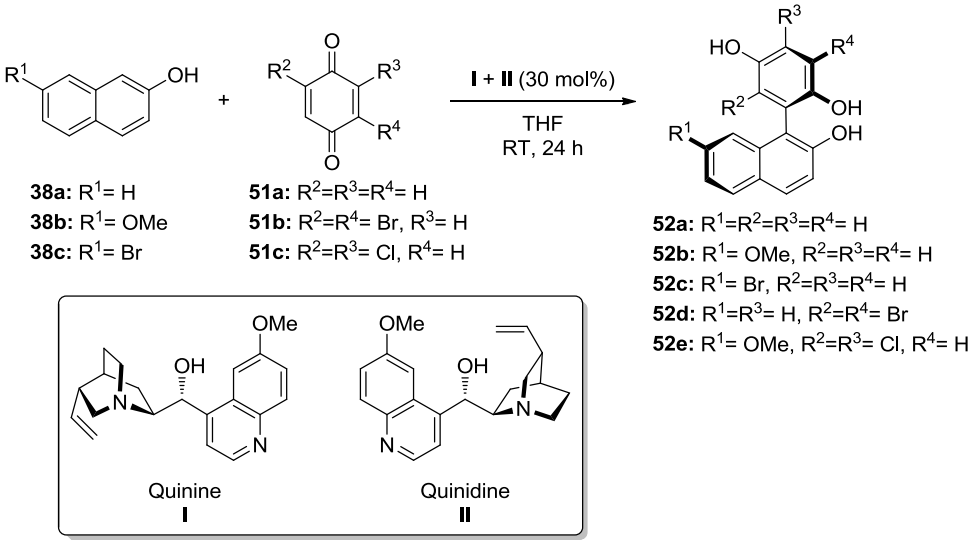

Scheme 13: First attempts to the organocatalyzed addition of 2-naphthols **38a-c** to 1,4-benzoquinones **51a-c**.

Compound **52a** was separated into two enantiomers by HPLC using a chiral stationary phase, but the shape of the trace is anomalous because of the appearance of peaks with a plateau between them. This characteristic profile

is also known as a "Batman" profile.[59] Such peaks can be observed in the case of atropisomers with hindered rotation, which are interconverting on a time-scale comparable to the retention time of the HPLC run. Indeed, analytical chiral separations can be used to determine the rotational barriers of racemization, following the method described by Dalla Cort, Gasparrini and co-workers.[60]

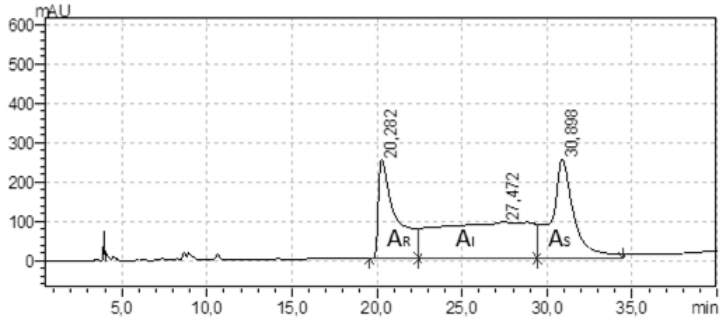

Figure 6: HPLC trace of biaryl **52a**, showing a "Batman" profile

Given the "Batman" profile (*Figure 6*), three different areas can be identified and integrated: the two outer peaks (A_R and A_S) and the in-between plateau (A_I). If t^* is defined as the average retention time of the entire profile, the areas A_R and A_S represent the amount of molecules which had not racemized in t^*. Conversely, A_I represents the amount of molecule which had changed their conformation during the time t^*. With a first-order isomerization kinetics, it can be written:

$$[B]_t = [B]_0 \, e^{-kt}$$

where $[B]_t$ is the amount of molecules which did not racemize at the time t;
$[B]_0$ is the total amount of molecules at the time t_0;
k is the racemization rate constant.

As concentrations and areas of the peaks in the chromatogram are directly proportional, for $t = t^*$ the previous equation can be written as follows:

$$A_R + A_S = (A_R + A_S + A_I) \, e^{-kt^*}$$

from which the kinetic constant k can be calculated. Using this value of k, the activation energy $\Delta G^{\ddagger}$ of the racemization process is given by the Eyring equation:

$$\Delta G^{\ddagger} = RT \ln \frac{k_B T}{kh}$$

[59] Stalcup, A. M. *Annu. Rev. Anal. Chem.* **2010**, *3*, 341.
[60] Ciogli, A.; Dalla Cort, A.; Gasparrini, F.; Lunazzi, L.; Mandolini, L.; Mazzanti, A.; Pasquini, C; Pierini, M; Schiaffino, L; Mihan, F. Y. *J. Org. Chem.* **2008**, *73*, 6108.

where R is the gas constant

T is the absolute temperature

k_B is the Boltzmann constant

h is the Planck constant.

Employing once again the rate constant k, the racemization half-time is

$$t_{1/2}\, rac = \frac{\ln 2}{k}$$

The rotational energy barrier (22 kcal/mol) and the racemization half-time of some minutes experimentally determined in this way for compound **52a** are in good agreement with the *ab initio* calculations (see *Table 1*). These data clearly indicates a non-conformationally stable biaryl system.

We then prepared **52b** and **52c**, bearing a methoxy and a bromo substituent, respectively, at the 7-position and the rotational barrier, both calculated and experimentally determined, still remained similar to that of **52a**. We thus tried to add some bulky groups on the quinone moiety, at the *ortho* position with respect to the biaryl axis, in order to restrict the rotation. We tested the same reaction starting from 2,5-dibromo-1,4-benzoquinone (**51b**), thus obtaining a mixture of **52d** and its oxidized form **52d'**. Both *in silico* and experimental data indicated that the two compounds have a high rotational barrier and consequently are conformationally stable: in particular, compound **52d** has a racemization half-time of thousand billions years (*Table 1*). Also the presence of a chloro substituent on quinone **51c** results in a significant rotational barrier (**52e**).

From these preliminary experiments we could drew the following conclusions. First, given the agreement between *ab initio* and experimental data, DFT calculations turned out to be useful to predict whether the enantiomers can have an interconversion rate comparable to the HPLC timescale and therefore whether a plateau between the peaks of the enantiomers can be observed. Second, to obtain conformationally stable atropisomers, it is necessary to employ substituted quinones, such as the halogenated **51a** and **51b**. Finally, in the case of compounds **52**, the energy of rotational barriers are high enough both in the reduced and the oxidized form of the compounds. It is therefore possible to develop an atroposelective synthesis of conformationally stable atropisomers starting from 2-naphthols, without running into racemization due to internal disproportion.

2.2.2. Optimization of the reaction conditions

We chose as a model reaction the addition of 7-methoxy-2-naphthol (**38b**) to 2,6-dichloro-1,4-benzoquinone (**51c**) to investigate which reaction conditions could afford the highest yield and stereoselectivity. We started screening several organocatalysts, based on the *Cinchona* alkaloid scaffold (*Figure 7*). *Cinchona* alkaloids are known to be privileged structures for the design of organocatalysts, given their highly pre-organized chiral skeleton and the possibility to functionalize them in several positions.[61]

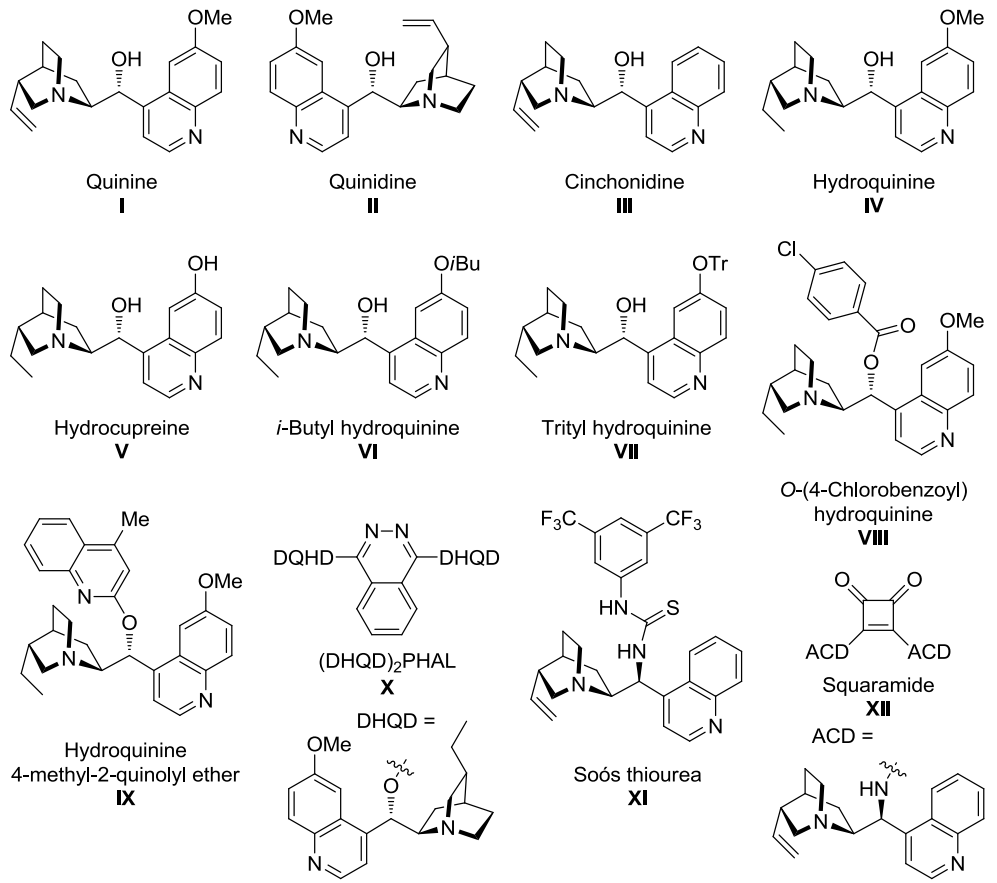

Figure 7: *Cinchona* alkaloid-derived catalyst tested for the model reaction.

The results of this first screening are summarized in *Table 2*. In any case, the reaction produced a mixture of the desired **52e** and its oxidized form. Attempts to run the reaction under argon did not solve the issue. This oxidation process might be due to the presence of **51c** as it can act as an

[61] Marcelli, T.; Hiemstra, H. *Synthesis* **2010**, 1229.

oxidant towards the product. To get reproducible results in term of yield and a simpler purification step, a reduction of the crude reaction mixture after completion of the transformation was necessary. We therefore added sodium borohydride and methanol to the reaction mixture to reduce any oxidized quinone compound and then trifluoroacetic acid (TFA) to reprotonate the naphthol sodium salts. We concentrated the resulting mixture over silica gel and a quick filtration afforded a substantially pure sample of **52e**. This process did not affect the enantiomeric excess of the product and also served to quench the reaction.

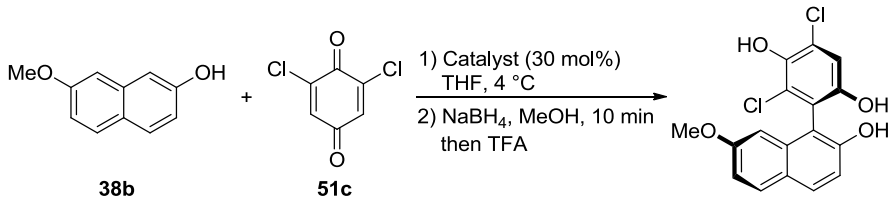

38b + **51c** → **52e**

Entry[a]	Catalyst	Time (h)	Yield (%)[b]	*ee* (%)[c]
1	**I**	24	98	66
2	**II**	48	99	-58
3	**III**	85	99	64
4	**IV**	4	50	66
5	**V**	72	<10	0
6	**VI**	24	99	70
7[d]	**VII**	72	99	12
8	**VIII**	48	60	18
9	**IX**	48	57	10
10	**X**	100	no conversion	-
11	**XI**	85	10	6
12	**XII**	48	98	34

Table 2: Catalyst screening for the organocatalyzed addition of **38b** to **51c** to afford axially chiral **52e**. [a] Reaction performed employing 40 mg (0.23 mmol, 1 equiv) of **38b** and 50 mg (0.28 mmol, 1.2 equiv) of **51c**, in 4 mL THF (concentration: 0.057 M). [b] Yield of isolated product. [c] The *ee* was determined by HPLC on CSP using Chiralpack ID column and *n*-hexane/*i*-propanol 88:12 (flow 0.9 mL/min). [d] Reaction performed in toluene.

The first catalyst tested was simple quinine (**I**) (*Table 2*, entry 1), which afforded **52e** in nearly quantitative yield and with 66% enantiomeric excess. The pseudoenantiomer quinidine (**II**) behaved similarly, albeit with opposite stereocontrol, as expected (entry 2). Neither cinchonidine (**III**) nor

hydroquinine (**IV**) performed better (entries 3 and 4). Hydrocupreine (**V**), which usually gives the best results in polar solvents, such as THF, in this case afforded a racemic product with a yield lower than 10% (entry 5). We then tried to introduce bulkier substituents on the quinoline ring of hydroquinine, without any significant improvement on the enantioselectivity (entry 6 and 7). Interestingly any modifications involving the alcohol group of the quinine led to detrimental effects on the stereocontrol. For example if the hydroxyl group was protected as an ester, like in catalyst **VIII**, or as an ether, like in catalyst **IX**, the enantiomeric excess dropped to 18% and 10% respectively, with negative effects also on the yield (entries 8 and 9). Even worse is the case of the ether dimer $(DHQD)_2PHAL$ (**X**), which after 100 hours did not catalyze any conversion at all. These observations strongly suggest that the hydroxyl function of quinine plays a crucial role both in the catalysis and in transferring the chiral information to the reactive species. This could be due to hydrogen-bonding activation of the electrophile **51c**. We therefore tested the bifunctional catalysts **XI** and **XII**, capable of a similar activation mode. However, none of the two gave satisfactory results in term of yield and enantioselectivity (entries 11 and 12).

At this point we recognized that simple quinine (**I**) was the most effective catalyst, at least in our hand, as all the other natural and synthetic *Cinchona* alkaloid derivates did not perform significantly better.
We therefore went on optimizing the other reaction conditions, using **I** as the catalyst. Among the solvents tested, chloroform or toluene, which are commonly employed in *Cinchona* alkaloid-derivatives catalysis, were not as effective as THF (*Table 3*, entries 2 and 3). The temperature of 4 °C, which can be conveniently achieved, appeared ideal so as to maximize the enantiomeric excess; the reaction run at -20 °C did not increase enantioselectivity (entry 5) and the one conducted at room temperature produced the product in less satisfactory enantiomeric excess (entry 4). A fewer amount of catalyst (lowered to 15 mol%) and higher dilution were instead beneficial and when we combined these findings we achieved 72% *ee* (entry 6). In these optimal conditions of dilution and catalyst loading, we tested two different solvent mixture of tetrahydrofuran and toluene, with an increasing in enantioselectivity along with a little erosion in the yield (entries 7 and 8). Finally, employing 2 equivalents of quinone **51c**, the reaction resulted faster and with the highest enantioselectivity: quantitative yield was achieved after 4 h, with 74% *ee* (entry 9 versus entry 6).

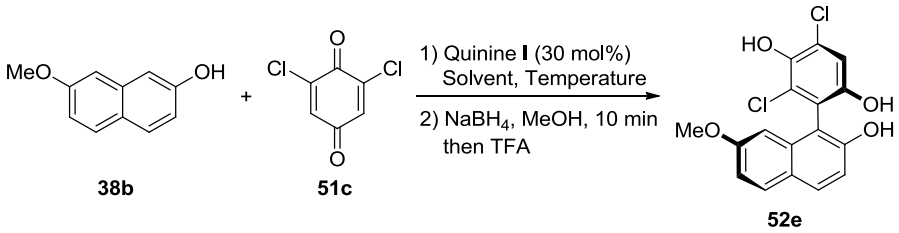

38b + **51c** → **52e**

Entry[a]	Solvent	T (°C)	Time (h)	Yield (%)[b]	*ee* (%)[c]
1	THF	4	24	98	66
2	$CHCl_3$	4	18	65	26
3	PhMe	4	18	99	26
4	THF	RT	24	90	58
5	THF	-20	3	-20	66
6[d,e]	THF	4	48	99	72
7[d]	THF/PhMe 1:1	4	48	93	74
8[d]	THF/PhMe 20:1	4	48	81	74
9[d,e,f]	THF	4	5	99	74

Table 3: Optimization of the reaction conditions for the organocatalyzed addition of **38b** to **51c** to afford axially chiral **52e**. [a] Reaction performed employing 40 mg (0.23 mmol, 1 equiv) of **38b** and 50 mg (0.28 mmol, 1.2 equiv) of **51c**, in 4 mL THF (concentration: 0.057 M). [b] Yield of isolated product. [c] The *ee* was determined by HPLC on CSP using Chiralpack ID column and *n*-hexane/*i*-propanol 88:12 (flow 0.9 mL/min). [d] Concentration of 0.0275 M. [e] 15 mol% catalyst. [f] 2 equiv of **51c**.

We also investigated the conformational stability of compound **52e** in the reaction environment. Two reactions run at 4 °C and room temperature were monitored over 150 hours and samples were taken at regular intervals: no change in the enantiomeric excess was observed.

Although the enantioselectivity was not excellent, the experience of our research group regarding an asymmetric reaction which became a large-scale industrial process[62] suggested that for the wide applicability of a novel process this was not a major issue. Specifically, mild reaction conditions (RT or 4 °C), high yield (over 95%), cheap and commercially available catalyst (quinine) and reagents, plus the potential to avoid chromatography to purify the products are aspects which are more important than finding a catalyst which would afford a higher enantiomeric excess.

[62] a) Bella, M; Scarpino Shietroma, D. M.; Cusella, P. P.; Gasperi, T.; Visca, V. *Chem. Commun.* **2009**, 597; b) Abele, S.; Inauen, R.; Spielvogel, D.; Moessner, C. *J. Org. Chem.* **2012**, *77*, 4765.

2.2.3. Scope of the reaction and scale-up to grams

With the optimized reaction conditions in hand, we explored the scope of our reaction by testing several combinations of 2-naphthols **38** and 1,4-benzoquinones **51**, using a catalyst loading of 15 mol%, as reported in *Scheme 14*. To maximize the enantiomeric excess, we ran the reactions at high dilution and at 4 °C, when compatible with reasonable reaction time. Most of the reactions were run employing 2 equivalents of quinone, but in some cases only a slight excess was needed to ensure a good adjustment of yield and enantioselectivity.

2,5-dibromo-1,4-benzoquinone (**51b**) afforded the biaryls **52d,g** in good yield and moderate stereoselectivity (up to 63% *ee*). The benzoquinone substituted in the same positions with chlorine atoms (2,5-dichloro-1,4-benzoquinone **51e**) performed similarly (**52h**, quantitative yield, 59% *ee*). The use of 2,6-dibromo- (**51d**) and 2,6-dichloro- (**51c**) benzoquinones resulted in a considerable improvement in the enantioselectivity (**52f**, **52i-l**): surprisingly, the naphthols bearing substituents away from the chiral axis (6-bromo **38d** and 6-methoxy **38e**) or unsubstituted (**38a**) afforded the biaryls **52i,k-l** with higher enantiomeric excess (76-78%). This observation suggests that the steric hindrance at the 7-position of naphthol is not beneficial to the stereocontrol, possibly interfering in the interactions between the catalyst and the reactive species.
Also a reduction in the symmetry of the quinone substrate seemed to help its enantiotopic faces discrimination by the catalyst, thus resulting in superior performances. 2-Chloro-1,4-benzoquinone (**51f**), despite being less reactive (longer reaction times or room temperature were necessary for full substrate consumption), led to the biaryl products **52m-r** with enantiomeric excesses between 77% and 84%. The best results in term of enantioselectivity, albeit with slightly lower yield, were shown by 2-bromo-1,4-benzoquinone (**51g**), which afforded biaryls **53s** and **52t** with 81 and 93% yield and 86 and 85% *ee*, respectively.

We tested also the highly activated 2-carbomethoxy-1,4-benzoquinone (**51h**, not shown in the scheme), which was the most reactive quinone, but it produced the corresponding biaryl (**52u**) only as a racemic mixture. The lack of stereocontrol might be due to the fast, nonselective reaction.

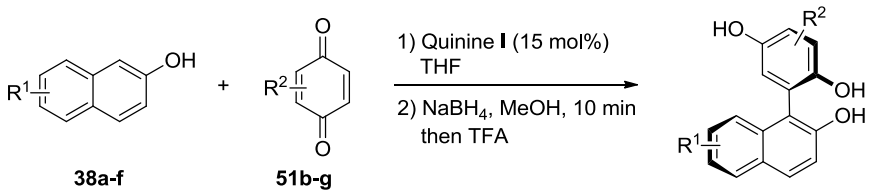

38a-f + **51b-g** → **52d,52f-t**

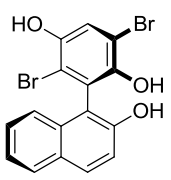

52d
(3d, 4 °C)[c]
82% yield
60% *ee*

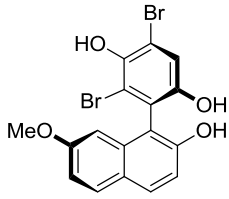

52f
(5d, 4 °C)
92% yield
70% *ee*

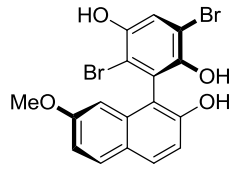

52g
(2d, RT)
99% yield
63% *ee*

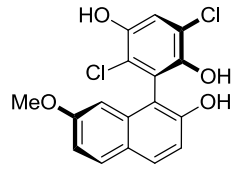

52h
(2d, RT)
99% yield
59% *ee*

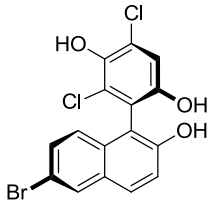

52i
(4d, 4 °C)
99% yield
77% *ee*

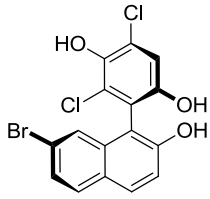

52j
(4d, 4 °C)
99% yield
70% *ee*

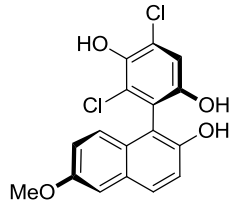

52k
(2d, RT)
99% yield
78% *ee*

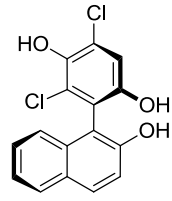

52l
(2d, RT)
99% yield
76% *ee*

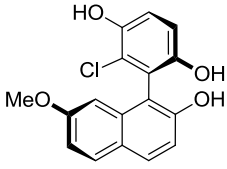

52m
(3d, RT)
99% yield
77% *ee*

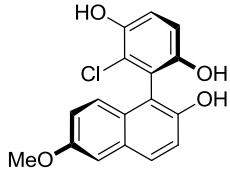

52n
(4d, 4 °C)
84% yield
84% *ee*

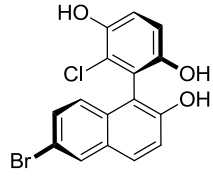

52o
(3d, RT)
95% yield
82% *ee*

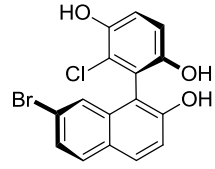

52p
(3d, RT)
60% yield
82% *ee*

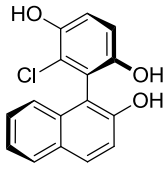

52q
(3d, RT)
99% yield
78% *ee*

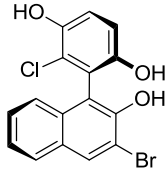

52r
(2d, 4 °C)[c]
70% yield
80% *ee*

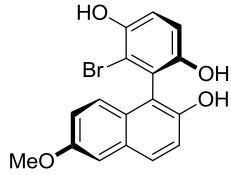

52s
(5d, 4 °C)[c]
81% yield
86% *ee*

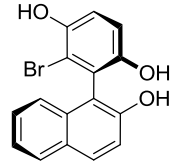

52t
(4d, RT)
93% yield
85% *ee*

Scheme 14: Scope of the quinine-catalyzed addition reaction of naphthols (**38**) to quinones (**51**) to produce enantioenriched axially chiral compounds (**52**). [a] Reaction performed employing 1.0 equiv of naphthol **38** (0.15 mmol), 2.0 equiv of **51**, 0.15 equiv. of **I** and with 5.5 mL of solvent. [b] Values in brackets are reaction time in days. [c] Used 1.2 equiv of **51**.

To show the preparative usefulness of our transformation, we performed two reactions on gram scale, reacting 8 mmol of 2-naphthols **38d** and **38e** with 1.5 and 2 equivalents of 2,6-dichloro-1,4-benzoquinone (**51c**), respectively. The reactions were run at room temperature and at higher concentration of reagents. The products **52i** and **52k** were obtained in high yield and with minimal erosion of stereoselectivity. Recrystallization from toluene afforded the biaryls in high enantiomeric excess: 98% in the case of **52i** and 94% in the case of **52k** (*Scheme 15*).

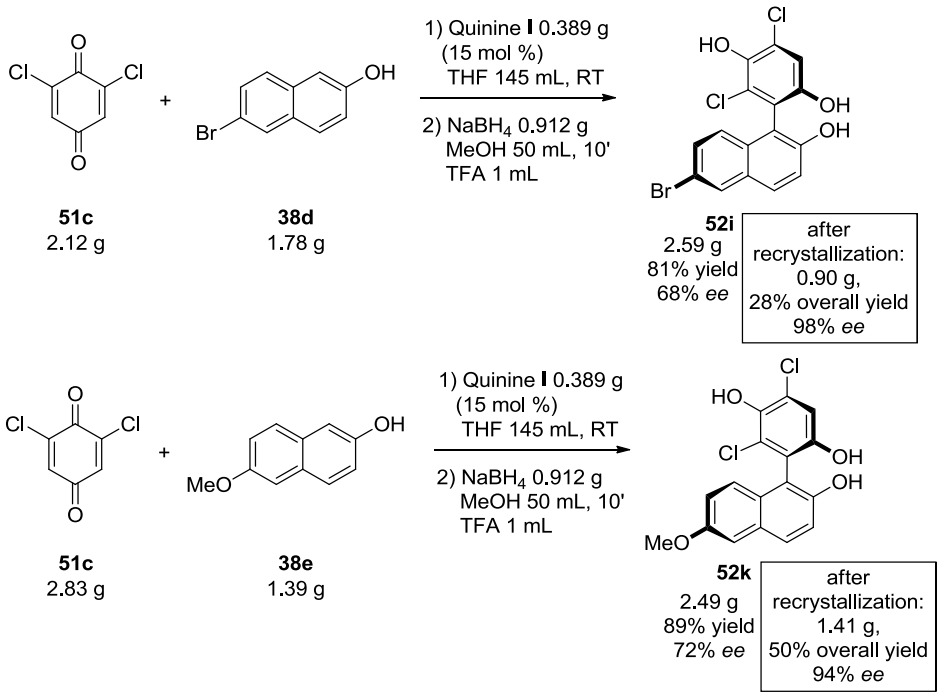

Scheme 15: Preparative large-scale reactions for **52i** and **52k**.

2.2.4. Determination of the absolute configuration and stereochemical rationale

The absolute configuration of compound **52m** was determined based on what reported by Tan *et al.*[56a] We analyzed the biaryl **52m** by HPLC on chiral stationary phase, in the same conditions used by them (Chiralpak AS-H column, eluent *n*-hexane/*i*-propanol 80/20, flow 1.0 mL/min). They reported the following retention times: τ_1 (*R* isomer) = 13.6 min; τ_2 (*S* isomer) = 21.3 min. The HPLC traces we got for the racemic mixture and the enantioenriched sample are reported in *Figure 8*.

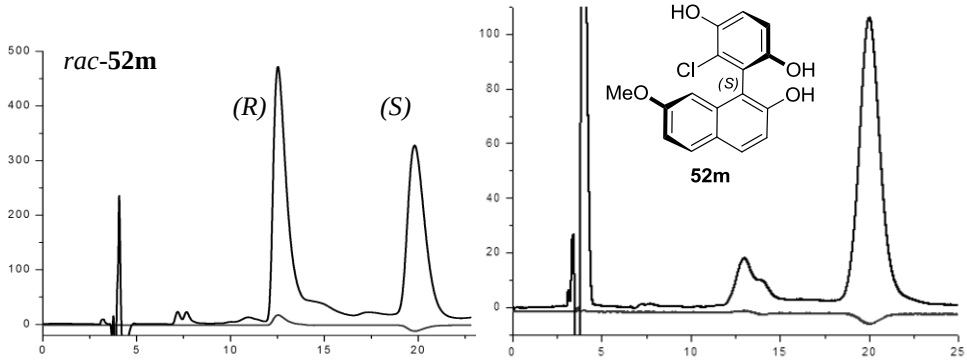

Figure 8: HPLC traces of *rac*-**52m** (left) and of an enantioenriched sample of **52m** (right) for the determination of the absolute configuration.

Based on the retention times, the absolute configuration of compound **52m** was determined to be *S*. The absolute configuration of all the other compounds was assigned by analogy.

Compound **52m** was fully characterized, as all the other products, but also subjected to in-depth analysis with NMR techniques. In particular HSQC (Heteronuclear Single Quantum Coherence) and HMBC (Heteronuclear Multiple Bond Correlation) spectroscopies were useful to assign every peak of the ^{1}H and ^{13}C NMR spectra (*Figure 9*) to its corresponding nucleus in the compound. The proton spectrum shows one resolved signal for each hydrogen atom present in **52m**, with the only exception of the systems centered at 7.68 ppm and at 6.90 ppm. The former results from the overlap of two distinct doublets, while the latter is due to a doublet overlapped to a double doublet.

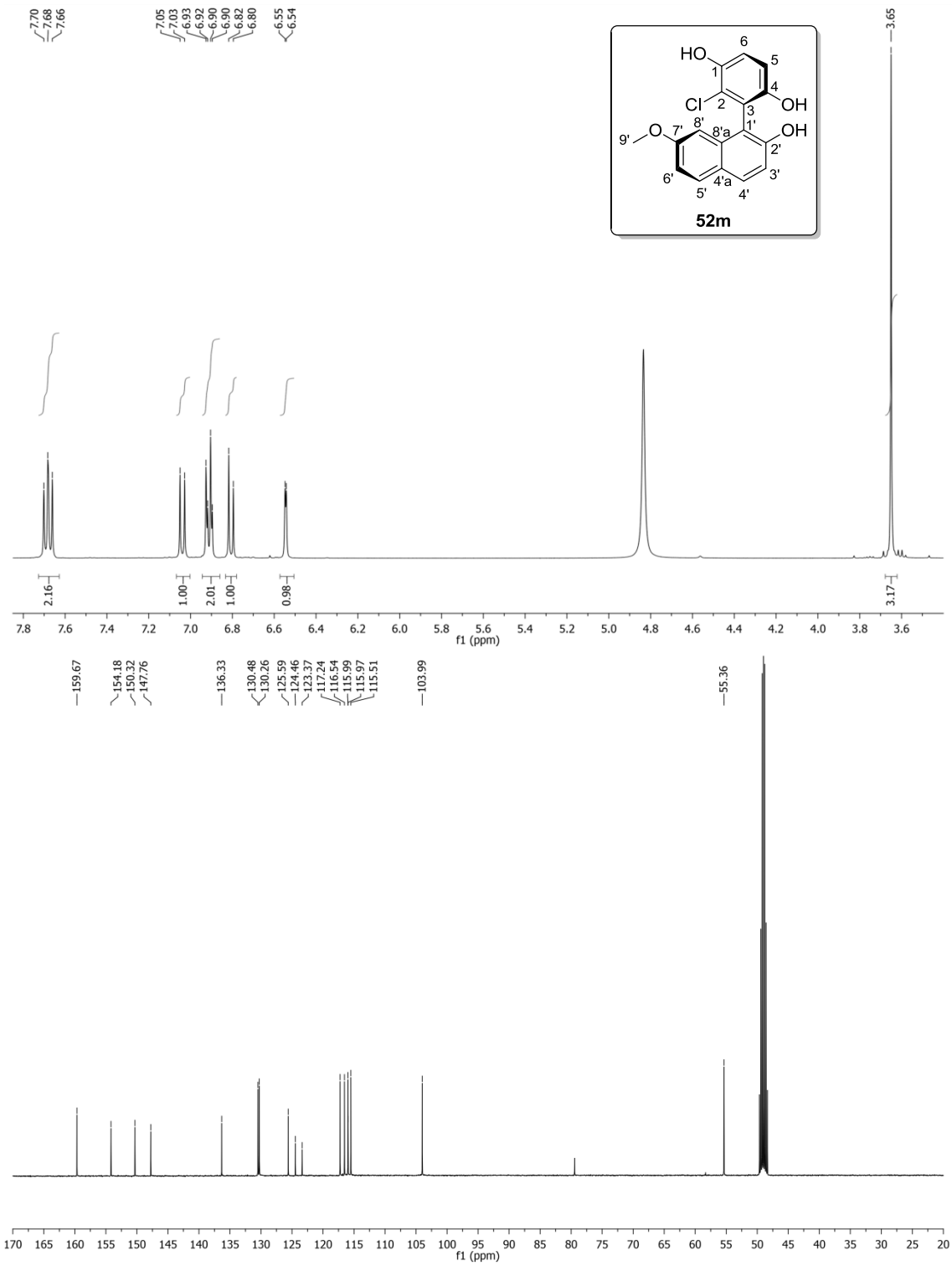

Figure 9: ^{1}H and ^{13}C NMR spectra of compound **52m** (400 MHz, CD_3OD).

Exploiting the correlation spots visible in the HSQC spectrum (*Figure 10*), each proton was matched with the carbon atom directly connected. Indeed, HSQC allows to see all the correlations between carbon-13 nuclei and the protons one-bond away from them. Quaternary carbons do not show any correlation in this spectroscopy.

With this information in hand, the assignment of some signals could be made. It was trivial to attribute the signals at 3.65 ppm (^{1}H) and 54.4 ppm (^{13}C) to the methyl group, as it is the only alkyl group in **52m**. Also the doublet at 6.55 ppm and its related ^{13}C signal at 104.0 ppm was attributed to the position 8', because the little value of its coupling constant is typical of ^{meta}Js. Similarly, the double doublet at 6.91 ppm is due to proton H6', the only one to have both *ortho* and *meta* coupling.

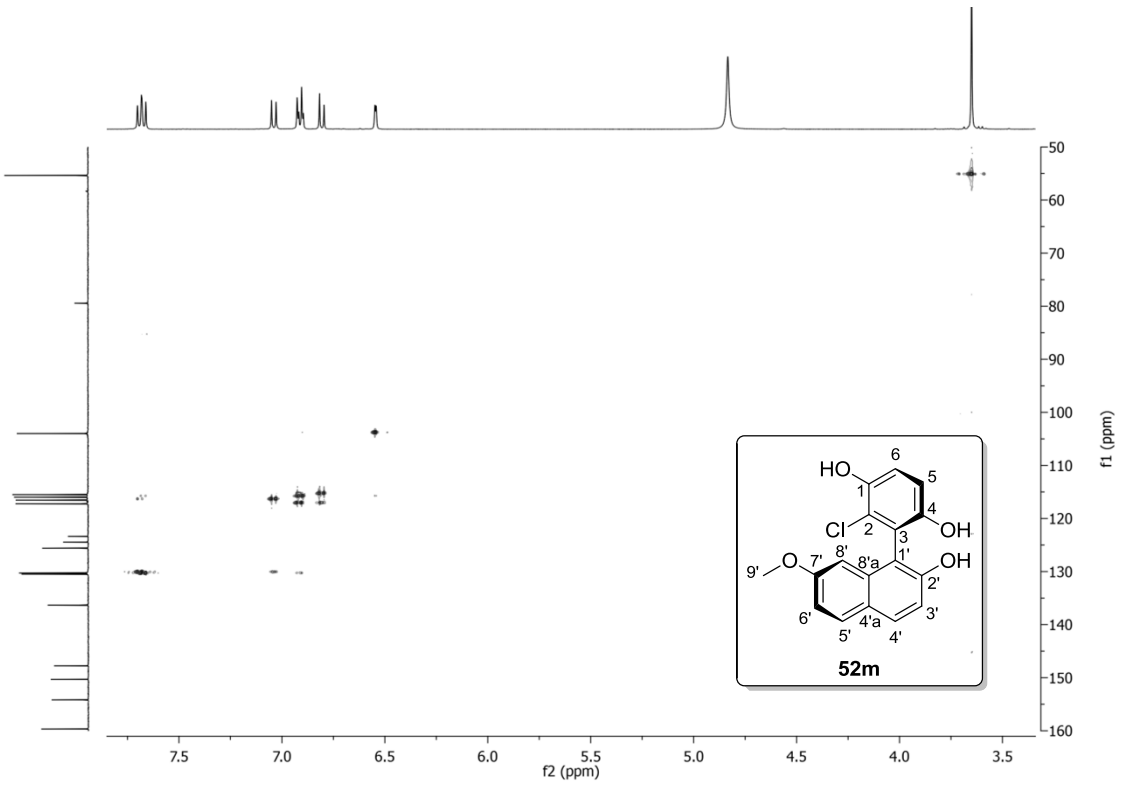

Figure 10: HSQC spectrum of compound **52m** (400 MHz, CD_3OD).

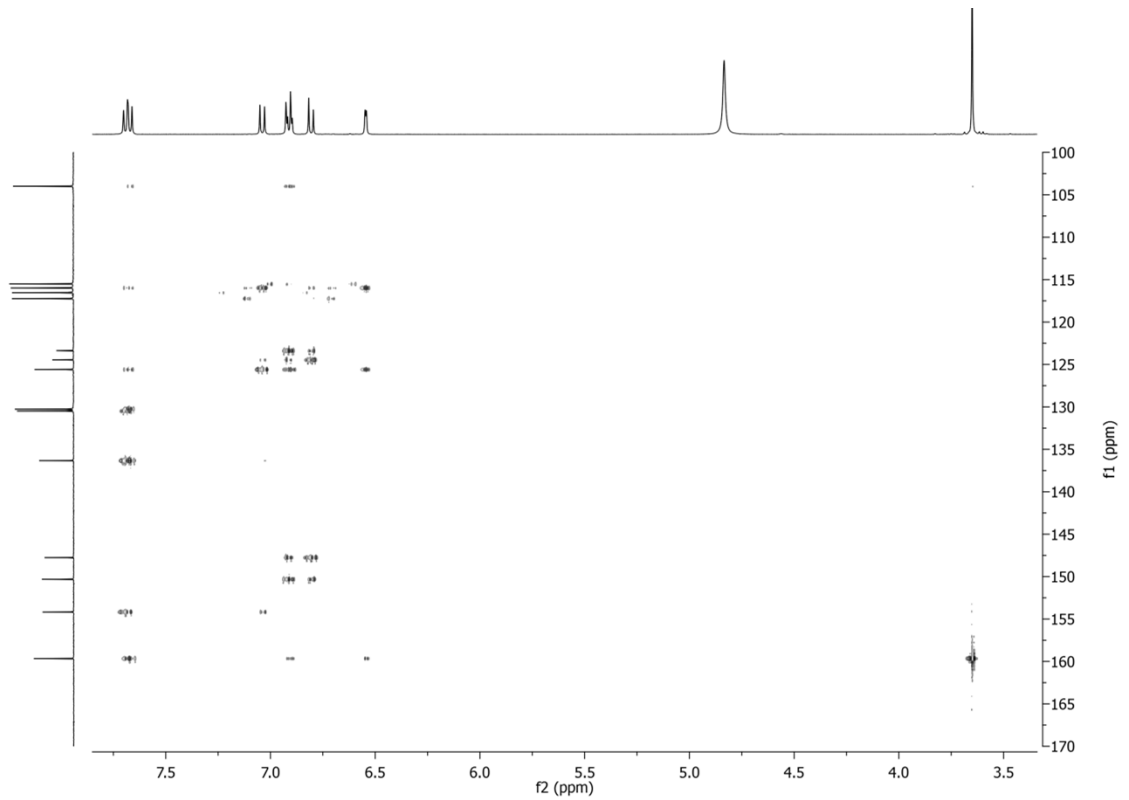

Figure 11: HMBC spectrum of compound **52m** (400 MHz, CD_3OD).

To solve the rest of the structure, HMBC spectrum (*Figure 11*) was crucial. In this type of spectroscopy, correlations between carbon-13 nuclei and two or three bonds away protons are visible. More-than-three-bond correlations are detected only in conjugated system, such as an aromatic ring. Moreover, three-bond correlations are often more intense than two-bond ones.

Starting from the already assigned signals, all the other can be found. For example, the carbon at 159.7 ppm shows a strong correlation with the methyl protons signal, so that it can be assigned to carbon 7', but also with one of the doublets at 7.68 ppm, which can be attributed to the H5' proton (three bonds away). Weak correlations (two bonds) are detected with H6' and H8' protons, which were already assigned based on the multiplicity.

There are only three other carbon signals which can be assigned, based on their chemical shifts, to aromatic carbons bearing an oxygen substituent (154.2, 150.3, 147.8 ppm). Given that two of them (150.3 and 147.8 ppm) show correlations with protons coupled with each other (two doublets with the same *J* and strong roof effect at 6.91 and 6.81 ppm), they must be

attributed to C1 and C4. The remaining one (154.2 ppm) must be the 2' carbon. The latter shows two HMBC correlations: a strong one with the 7.68 ppm doublet and a weaker one with the 7.04 ppm doublet, which must belong to H4' and H3' respectively. This is in line with the fact the position 3' is more shielded because of mesomeric effects of the electron-donating OH group and with the observation that three-bond correlations are often stronger than two-bond ones.

Following this "dominoes" method, all the NMR signals could be attributed to the right nucleus, as tabulated in *Table 4*.

ID	δ (^{1}H)	Multiplicity	δ (^{13}C)	HMBC correlations
1	-	-	147.8	H6 (s), H5 (w)
2	-	-	123.4	H6 (s), H5 (w)
3	-	-	124.5	H5 (s), H6,3' (w)
4	-	-	150.3	H6 (s), H5 (w)
5	6.81	d (*J* = 8.8 Hz)	115.5	n.d.
6	6.91	d (*J* = 8.8 Hz)	117.2	n.d.
1'	-	-	116.0	H3',8' (s), H5,4',5' (w)
2'	-	-	154.2	H4' (s), H3' (w)
3'	7.04	d (*J* = 8.8 Hz)	116.5	n.d.
4'	7.68	d (not resolved)	130.3	H5' (s)
4'a	-	-	125.6	H3',6',8' (s), H4',5' (w)
5'	7.68	d (not resolved)	130.5	H4' (s)
6'	6.91	dd (not resolved)	116.0	H8' (s)
7'	-	-	159.7	H5',9' (s), H6',8' (w)
8'	6.55	d (*J* = 2.3 Hz)	104.0	H6' (s), H4',5' (w)
8'a	-	-	136.3	H4',5' (s)
9'	3.65	S	55.4	n.d.

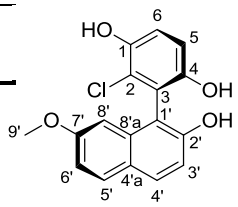

52m

Table 4: Attribution of chemical shifts to the nuclei of **52m** (s= strong, w= weak).

Concerning the stereochemical outcome of the reaction, a possible rationalization regarding the formation of the major enantiomer is depicted in *Figure 12*, for the quinine-catalyzed addition of 7-methoxy-2-naphthol (**38b**) to 2,6-dichloro-1,4-benzoquinone (**51c**) leading to the model biaryl **52e**. According to this scenario, the deprotonated hydroxy function on the naphthol unit would interact with the protonated nitrogen of the quinuclidine basic unit of quinine. At the same time, the quinone reagent would be activated towards nucleophilic attack by hydrogen-bonding at the 9-hydroxy functionality of the catalyst. With this interactions, the catalyst both activates the reagents and orients their mutual disposition, thus transferring the chiral

information to the product. The central role played by the OH group of the catalyst is also confirmed by the enantioselectivity shown by the catalysts lacking this feature, as already discussed in *Section 2.2.2*. By converse, the π-π staking between the aromatic moieties of the reagents and the quinoline ring of the catalyst does not seem to play any major role. DFT calculations support these hypotheses.[63]

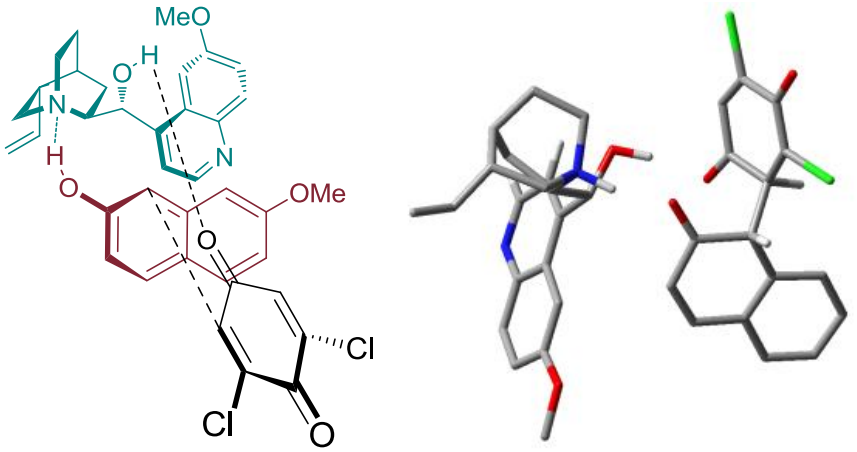

Figure 12: Proposed transition state leading to the major enantiomer and corresponding DFT optimized structure (some atoms are omitted for clarity).

[63] (b3lyp/6-31g* // b3lyp/6-31g*) using Gaussian09 (see ref. 58).

2.3. Summary of the Chapter

In this chapter, a new organocatalyzed synthesis for a class of novel axially chiral biaryl compounds (**52**) has been presented. The reaction is catalyzed under mild reaction conditions by the *Cinchona* alkaloid quinine (**I**), which is a cheap and commercially available natural compound. Excellent yield and enantioselectivity were achieved for almost all the substrates tested. We have also demonstrated the feasibility of the reaction on gram-scale for the preparation of compounds **52i** and **52k**, with the possibility to recrystallize them to near enantiopurity.
These features should render this process attractive for the large scale preparation of these important compounds, at the very least in a research laboratory.

In addition, the structural requirements to prepare conformationally stable atropisomers have been discussed.

The importance of this class of axially chiral molecules and of their atroposelective synthesis have been presented in *Section 2.1*. Furthermore, the presence of several halogens on the products synthesized with our strategy offers the possibility to functionalize them via several transformations.

Future development of this project may involve the following studies:

- application of biaryls **52** as ligands or catalysts for new asymmetric transformations;[64]
- development of a derivatization procedure of biaryls **52** to get already known powerful ligands or catalysts, such as chiral phosphoric acids, using this simple organocatalyzed reaction;
- expansion of the reaction scope to phenols, which would give access to axially chiral biphenyls.

[64] The effectiveness of the biaryl diols as chiral ligands in the asymmetric addition of diethyl zinc to aldehydes, with performances better than C_2-symmetrical BINOL, has been demonstrated in a preliminary experiment by Tan *et al.*[56a]

3. Novel Chiral Guanidines as Bifunctional Catalysts

3.1. Introduction

3.1.1. Bifunctional catalysis

Bifunctional catalysis involves the employment of small structurally defined molecules which possess two distinct functional groups. The usage of these moieties opens up new reactive pathways with defined stereochemistry. These processes are typically polar addition reactions of pronucleophiles and electrophiles which are simultaneously activated by bifunctional catalysts. In fact, these catalysts bear either a Lewis or Brønsted basic functionality and a hydrogen-bond donor group suitably positioned over a chiral scaffold. The cooperative effect of the two functional groups can lead to new reactivity and high stereocontrol in reactions that were challenging or unprecedented with the use of single functional group catalysts. Furthermore, both the functional groups and the chiral scaffold can be readily tuned to optimize reactivity of substrates and selectivity of reactions. Moreover, the number of available pronucleophiles and electrophiles is vast and therefore a whole variety of polar additions are amenable to bifunctional catalysis. This field is continually expanding and a lot of interesting reports can be found in the literature.

It is important to stress that this is exactly how Nature brings about its extraordinary transformations in living organisms, through enzymes whose active sites are designed to behave as bi- or multifunctional catalysts. A well known example is the enzymatic hydrolysis of peptide bonds carried out by serine proteases.[65] Their tasks are performed mainly by the so-called "catalytic triad", a coordinated structure of three amino acid residues, namely histidine-57, aspartate-102 and serine-195 (*Figure 13, left*). After the binding of the peptide to the active site of the enzyme, serine is responsible for the nucleophilic attack onto the carbonyl carbon. In this step, it is assisted by the histidine, which takes the proton from the hydroxyl group of serine and by aspartic acid, which hydrogen-bonds the histidine itself, thus adjusting its pK_a. Moreover, the resulting tetrahedral intermediate of the peptide is stabilized by the amino acid residues of the "oxyanion hole", a structure capable of coordinating negative charged species by means of hydrogen-bonding of the amide NH groups of glycine-193 and serine-195.

[65] Voet, D.; Voet, J. G; Pratt, C. W. *Fundamentals of Biochemistry: Life at the Molecular Level, 3rd ed*., Wiley, 2008.

The last steps of the catalytic cycle, involving breakage of the peptide bond and hydrolysis of the resulting acyl-enzyme intermediate, occur in a very similar fashion, in which the hydrogen bonds of the "catalytic triad" play a crucial role.

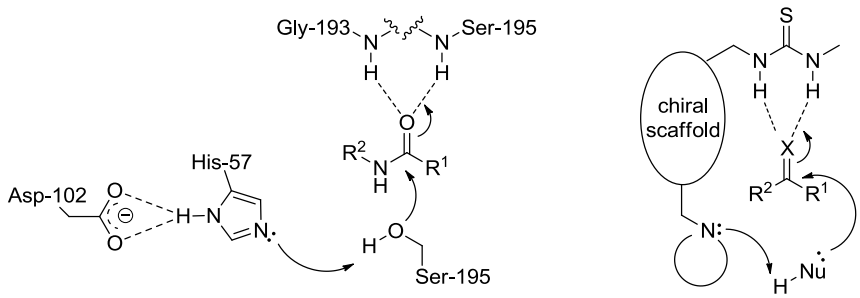

Figure 13: H-bond biocatalysis (left) and bifunctional catalysis (right).

The development of synthetic bifunctional catalysts able to mimic the action of enzymes is a field which have been extensively studied in the last decades. Before the blossoming of organocatalysis, mainly metal-based catalysts had been extensively investigated.[66] Actually, an early study on organic bifunctional catalysis appeared in 1981, when Wynberg reported the *Cinchona* alkaloid-catalyzed addition of thiophenols to cyclic enones, in moderate enantioselectivity.[67] The screening of several modified *Cinchona* alkaloids showed that both the basic tertiary amine moiety of the quinuclidine ring (capable of deprotonating the thiol pronucleophile) and the hydroxy function (capable of activating the enone electrophile via hydrogen bonding) were essential for the catalytic activity: the first bifunctional organocatalyst had been recognized. The authors also concluded that a catalyst containing a stronger base or a better hydrogen bond donor could extend the field of application of these new concept. Unfortunately, no significant improvement of *Cinchona* alkaloids as bifunctional catalysts would have been achieved for more than twenty years and, during that time, they were employed almost only as "simple" chiral β-amino alcohols.[68]

[66] For a review on metallic bifunctional catalysts: Shibasaki, M.; Sasai, H.; Arai, T. *Angew. Chem. Int. Ed.* **1997**, *36*, 1236.
[67] Hiemstra, H.; Wynberg, H. *J. Am. Chem. Soc.* **1981**, *103*, 417.
[68] a) France, S.; Guerin, D. J.; Miller, S. J.; Lectka, T. *Chem. Rev.* **2003**, *103*, 2985; b) Della Sala, G.; Russo, A.; Lattanzi, A. *Curr. Org. Chem.* **2011**, *15*, 2147.

One of the first efficient bifunctional organocatalysts was developed by Takemoto and co-workers[69] in 2003. At that time, it was known that chiral ureas and thioureas could act as acid catalysts for the enantioselective addition of cyanides and ketene silyl acetals to carbonyl and related compounds. For example the group of Jacobsen reported the asymmetric synthesis of quaternary amino acids, catalyzed by chiral ureas.[70] In fact, hydrogen bond donors are able to activate electrophiles through LUMO-lowering interactions. Takemoto foresaw that the introduction of an additional basic group on the acidic catalyst could facilitate the activation of a number of nucleophiles, thus expanding the scope of urea derivative-catalyzed asymmetric reactions. Therefore, catalysts bearing a hydrogen bond donor, acidic thiourea functionality linked, through a chiral scaffold, to a basic tertiary amine were developed. *Figure 13* shows the analogy in the mode of action between this class of catalysts (right) and hydrogen bond-based catalysis of serine proteases (left).

Takemoto's amine-thiourea catalyst (**58**) was first applied to the asymmetric addition of malonates **56** to nitroolefins like **55**. *Scheme 16* depicts the general reaction together with the proposed mechanism for the addition of diethyl malonate (**56a**). The tertiary amine of catalyst **58** first deprotonates the acidic **56a**, generating the complex **A**, in which the substrate and the catalyst are kept together by both ion-pairing and hydrogen-bonding. Then, nitrostyrene (**55**) is coordinated via hydrogen bonding by the acidic moiety of the catalyst, *i.e.* the thiourea function, thus leading to ternary complex **B**. The favored conformation of the double bond of the nitro compound in the transition state (**B**), with the phenyl group away from the cyclohexane ring of the catalyst, accounts for the observed stereoselectivity. Nucleophilic attack in this highly stereodefined environment and reprotonation of the adduct (**C**) lead to the product **57a** and to the free catalyst.

[69] Okino, T.; Hoashi, Y.; Takemoto, Y. *J. Am. Chem. Soc.* **2003**, *125*, 12672.
[70] Vachal, P.; Jacobsen, E. N. *Org. Lett.* **2000**, *2*, 867.

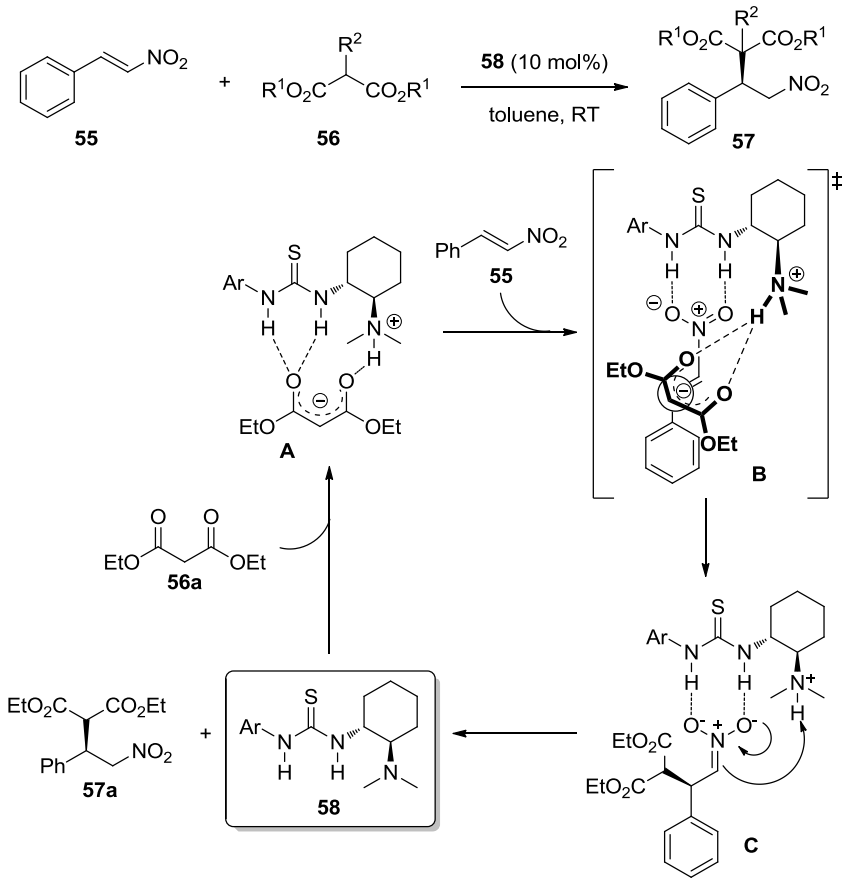

Scheme 16: Bifunctional amine-thiourea (**58**) catalyzed asymmetric addition of malonates **56** to nitrostyrene (**56**) and proposed reaction mechanism.[71]

Mindful of Wynberg pioneering studies and expanding Takemoto's achievement, new *Cinchona* alkaloid-based amine thioureas seemed to be the next advancement in bifunctional catalysis. It is no coincidence that in 2005 four different research groups independently reported the development of what would have been called the "Soós thiourea".[72] *Cinchona* alkaloid-derived thioureas (*Figure 14*) offer a number of advantages. The alkaloids are cheap natural compounds, available in both *pseudo*enantiomeric forms. Their secondary alcohol function at the C-9 position can be readily

[71] b) Okino, T.; Hoashi, Y.; Furukawa, T.; Xu, X.; Takemoto, Y. *J. Am. Chem. Soc.* **2005**, *127*, 119; b) Mechanism elucidation: Hamza, A.; Schubert, G.; Soós, T.; Pápai, I. *J. Am. Chem. Soc.* **2006**, *128*, 13151.

[72] a) Li, B.-J.; Jiang, L.; Liu, M.; Chen, Y.-C.; Ding, L.-S.; Wu, Y. *Synlett* **2005**, 603; b) Vakulya, B.; Varga, S.; Csámpai, S.; Soós, T. *Org. Lett.* **2005**, *7*, 1967; c) McCooey, S. H.; Connon, S. J. *Angew. Chem. Int. Ed.* **2005**, *44*, 6367; d) Ye, J.; Dixon, D. J.; Hynes, P. S. *Chem. Commun.* **2005**, 4481.

converted into an amino group, with either retention or inversion of configuration, thus accessing both the epimers of ureas and thioureas. For example thiourea **62** was prepared from quinine, with inversion of configuration at C-9, while *epi*-**62** has retained the original configuration. Concerning the quinuclidine ring, it is naturally available with two different absolute configurations at C-8 position, possesses a tertiary amine capable to act as a general base for the activation of pronucleophiles and is located in close proximity to the thiourea moiety. The latter can stabilize developing negative charges in the transition state of polar additions and can be substituted with a number of other groups: the 3,5-bis(trifluoromethyl)phenyl has proved to be most effective for the catalytic activity. Moreover, another point of variability is the substitution at the C-6' position on the quinoline ring (see **59** vs. **62**; **60** vs. **63**) and the possibility to hydrogenate the C10-C11 double bond (**61** vs. **62**).

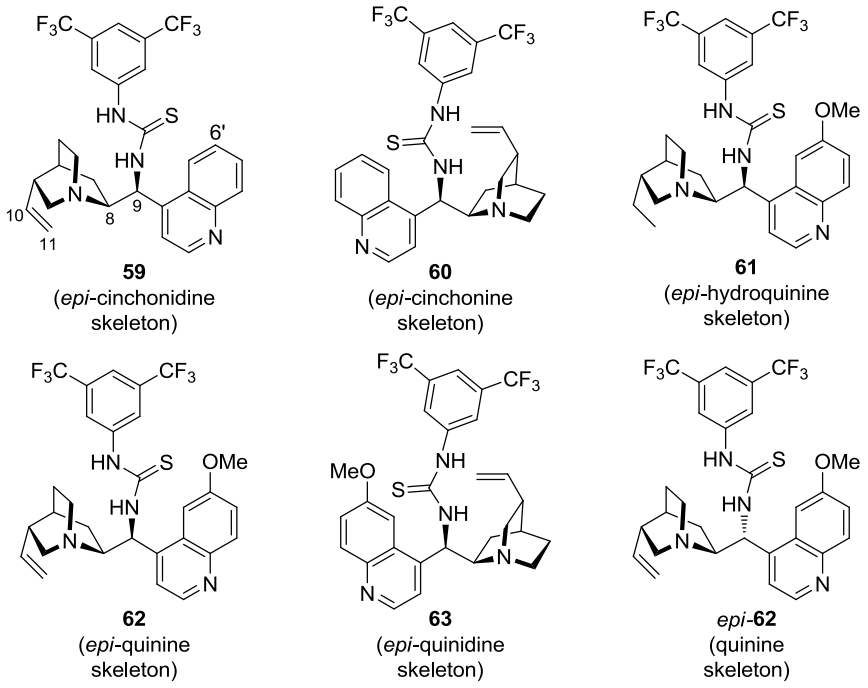

Figure 14: Thioureas derived from natural *Cinchona* alkaloids.

The first report was that of Chen and co-workers,[72a] who observed that cinchonidine- and cinchonine-derived thioureas **59** and **60** were very active catalysts for a sulfa-Michael reaction, albeit with low enantioselectivity. Soon after, the group of Soós[72b] found that *epi*-quinine and *epi*-quinidine

derivatives **62** and **63** were efficient catalysts for the asymmetric addition of nitromethane to chalchones. Interestingly, the quinine-thiourea *epi*-**62** showed no activity, thus strongly suggesting a bifunctional activation mode. In fact, the relative configuration of C-8 and C-9 in *epi*-**62** probably leads to a favored conformation of the catalyst in solution in which the complementary Brønsted-basic and Lewis-acidic functions are in close contact and can quench each other. This observations were confirmed, by means of molecular dynamics calculations, in the work of Connon,[72c] who applied catalyst **61** to the asymmetric Michael addition of malonates to nitroolefins. Very similar results were independently obtained by the group of Dixon.[72d]
In all cases the mechanism of action of these catalysts is analogous to that discussed for Takemoto's catalyst.

A further advancement in the field of bifunctional organocatalysis came from the design of hydrogen bonding moieties with higher acidity, for example the bis-amides of squaric acid. Rawal and co-workers[73] were the first to connect this functionality to an amine group through a chiral scaffold, based once again on *Cinchona* alkaloid cinchonine. Catalyst **64** (*Figure 15*) efficiently promotes, at a very low loading (0.5 mol%), the conjugate addition of malonates to nitroalkenes, showing generally better performances, in terms of yield and enantioselectivity, compared to the already known amine-thiourea catalysts.

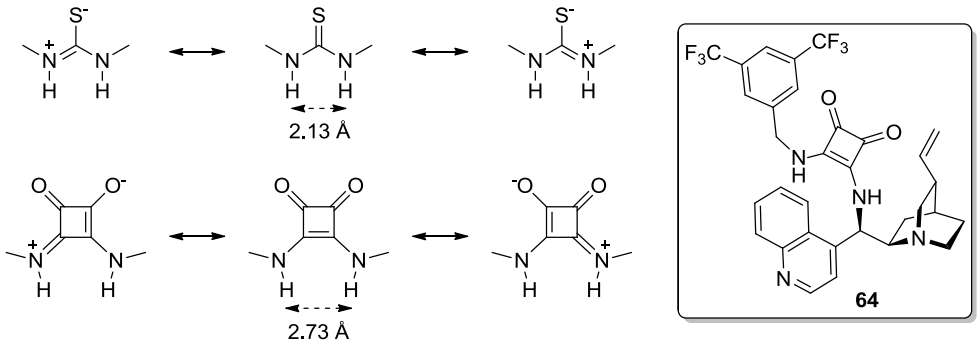

Figure 15: Left: Comparison between thiourea and squaramide units. Right: Rawal's first amine-squaramide bifunctional catalyst (**64**).

Figure 15 shows the differences between a thiourea and a squaramide moiety. The success of thioureas in catalysis is due to their ability to form

[73] Malerich, J. P.; Hagihara, K.; Rawal, V. H. *J. Am. Chem. Soc.* **2008**, *130*, 14416.

two H-bonds to a reactant, providing high activation and constraining it to a defined orientation, which is essential for asymmetric induction. The same task can be accomplished by a squaramide. However, the two acidic protons of thioureas are about 2.13 Å apart, while this distance is lengthened to 2.73 Å in squaramides. This feature has been called upon to suggest a higher versatility of squaramides as double H-bond activators. Furthermore, the lone pairs on the nitrogen atoms of both these functional groups is delocalized, thus restricting rotation of the C-N bond and increasing the acidity of the protons, *i.e.* the hydrogen bond donor capability. In squaramide the nitrogen lone pair delocalization occurs also through the cyclobutenedione ring, which accounts for a lower pK_a.

Over the years, several amine-thioureas and amine-squaramides were developed, including axially chiral, modified *Cinchona* alkaloid or Takemoto-like derivatives. They have proven to be efficient catalysts for a number of asymmetric transformations, such as 1,2- and 1,4-additions to carbonyl compounds and their *aza*-analogues, cycloadditions, Friedel-Crafts and cascade reactions.[74]

An important aspect to take into account is that bifunctional catalysts, bearing complementary functions, are prone to self-association in certain conditions. For this reason, a strong dependence on concentration and temperature is often observed in reactions which are catalyzed by these systems, with reactivity and enantioselectivity erosion either at higher concentration or at lower temperature. To face this problem, dimers of bifunctional catalysts have been designed, for example squaramide **67**.

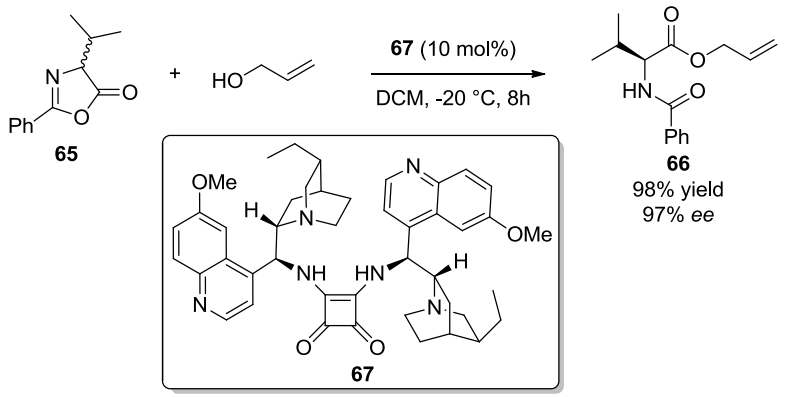

Scheme 17: Dynamic kinetic resolution of **65**, catalyzed by dimeric squaramide **67**.

[74] a) Siau, W.-Y.; Wang, J. *Adv. Synth. Catal.* **2011**, *1*, 1298; b) Alemán, J.; Parra, A.; Jiang, H.; Jørgensen, K. A. *Chem. Eur. J.* **2011**, *17*, 6890.

The dimeric squaramide **67**, which is readily prepared reacting *epi*-aminohydroquinine with dimethylsquarate in 2:1 molar ratio, was reported to catalyze the dynamic kinetic resolution of configurationally unstable azlactones **65**.[75] In this reaction dimeric squaramides turned out to be superior to monomeric bifunctional catalysts. Actually, they have a different application scope and often the latter are still more competent for polar addition reactions.

3.1.2. Chiral guanidines as bifunctional catalysts

Another important class of bifunctional organocatalysts includes chiral guanidines. They are neutral nitrogen compounds widely exploited as strong bases in organic synthesis. Due to the stabilization by resonance of their conjugated acid, the guanidine unit can be considered an organic "superbase". The basicity of unsubstituted guanidine and of its alkyl derivative in solution (in water pK_a > 13.5) is comparable to that of the hydroxyl ion (pK_a = 15.7).[76] *Figure 16* depicts all the chemical functionalities of guanidines and guanidiniums. The free guanidine presents, as already said, a strong Brønsted basicity, but can also act as a Lewis base and accept or donate hydrogen bonds. By converse, guanidinium salts are weak Brønsted acids, but highly active bidentate hydrogen bond donors.

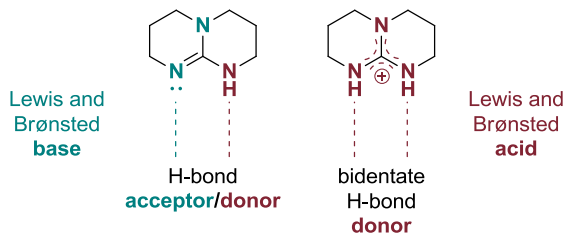

Figure 16: Functionalities of a free guanidine (left) and of its conjugate acid (right).

The active site of many enzymes contains the amino acid arginine, whose side chain is provided with a guanidinium functional group. Its pK_a is so high that arginine stays protonated over a wide range of pH, including physiological conditions. This amino acid is known to contribute to the

[75] Lee, J. W.; Ryu, T. H.; Oh, J. S.; Bae, H. Y.; Jang, H. B.; Song, C. E. *Chem. Commun.* **2009**, 7224.
[76] Raczyńska, E. D.; Maria, P.-C.; Gal, J.-F.; Decouzon, M. *J. Phys. Org. Chem.* **1994**, *7*, 725.

stabilization of anionic reaction intermediates through electrostatic interactions, to the substrate recognition at the active site through hydrogen bonding and to the stabilization of the protein tertiary structure via salt bridges with carboxylate groups. Indeed, both electrostatic interactions and the two parallel hydrogen bonds contribute to the high affinity of guanidinium functionalities and bidentate anions, such as carboxylates, phosphates or sulfates.[77]

Despite all these features, the application of guanidine-based organocatalysts has not been as extensively explored as other basic or hydrogen bond donor catalysts. This could be due to their high polarity and basicity itself, that often make challenging the synthesis and purification of guanidine compounds. Nevertheless, several noteworthy reports in this field can be found in the literature.[78] Herein the main examples in which guanidines act as both basic and hydrogen-bonding catalysts will be discussed. In these cases the guanidine generally initiates a reaction by abstracting an acidic proton to form its conjugated acid, the guanidinium, which in turn participates to the reaction via ion-pairing and hydrogen-bonding interactions, thus accelerating the reaction rate and providing chiral induction. There are two possible way of interaction of the guanidinium: it can activate only the nucleophile (*Scheme 18*, right equation) or both the electrophile and nucleophile in a bifunctional mode (*Scheme 18*, left equation), in a similar fashion to thioureas and squaramides.

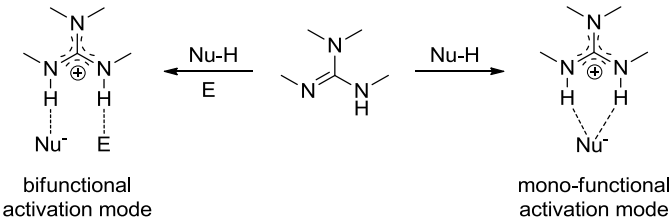

Scheme 18: Mono-functional (right) and bifunctional (left) activation modes in a guanidine-guanidinium catalyzed reaction.

As an example of mono-functional activation mode, we report the reaction developed by Terada and co-workers, involving axially chiral guanidine **70** as the catalyst of the stereoselective α-hydrazination of 1,3-dicarbonyl compounds **68** (*Scheme 19*).[79] Products **69** are obtained in excellent yield

[77] Schug, K. A:, Lindner, W. *Chem. Rev.* **2005**, *105*, 67.
[78] a) Leow, D.; Tan, C.-H. *Chem. Asian J.* **2009**, *4*, 488. b) Selig, P. *Synthesis* **2013**, *45*, 703.
[79] Terada, M.; Nakano, M.; Ube, H. *J. Am. Chem. Soc.* **2006**, *128*, 16044.

and enantioselectivity, the catalyst loading being low (2 mol%). The authors proposed a mechanism in which substrate **68** is first deprotonated by the catalyst and then coordinated via three hydrogen bonds, as showed in *Scheme 19*. The fact that one of the guanidinium acidic N-H groups interacts with both oxygen atoms of the enolate results in an "unparallel" chelation and accounts for the stereochemical outcome.

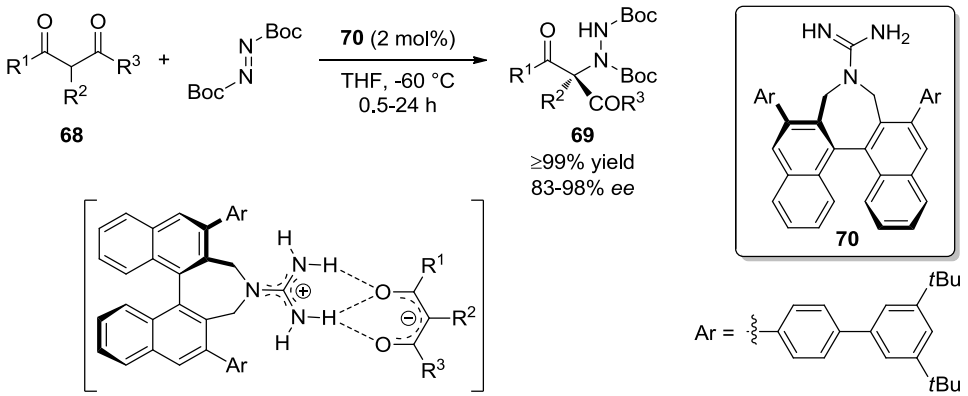

Scheme 19: Guanidine-catalyzed asymmetric amination of 1,3-dicarbony compounds **68**.

By contrast, bicyclic guanidine catalyst **73** was shown to act in a bifunctional fashion in the enantioselective addition of fluoro-β-ketoesters **71** to *N*-ethyl maleimide.[80] The reaction is diastereospecific and highly enantioselective.

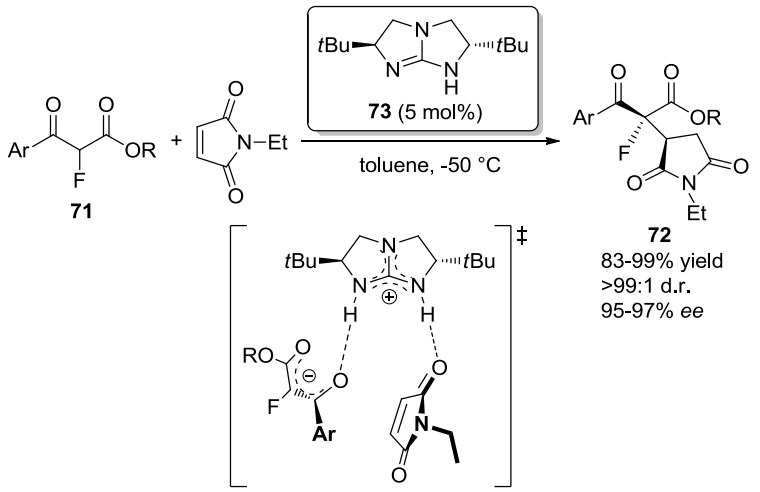

Scheme 20: Bifunctional guanidine-catalyzed highly stereoselective addition of fluoroketoesters to *N*-ethyl maleimide.

[80] Jiang, Z.; Pan, Y.; Zhao, Y.; Ma, T.; Lee, R.; Yang, Y.; Huang, K.-W.; Wong, M. W.; Tan, C.-H. *Angew. Chem. Int. Ed.* **2009**, *48*, 3627.

DFT calculations suggested that, upon deprotonation of the dicarbonyl compound by the catalyst, the guanidinium interacts with both substrates via two hydrogen bonding, thus taking advantage of a considerable stabilization. This calculated pre-transition state, depicted in *Scheme 20*, is supported also by the absolute configuration of the products **72**.

In 2010 Lu *et al.*[81] introduced the quinidine-derived guanidine **74**, which is an efficient catalyst for the enantioselective amination of fluoro-β-ketoesters (*Scheme 21*). The mode of activation seems similar to the mono-functional way described for the reaction in *Scheme 19*.
This is one of the few examples of an efficient organocatalyst bearing both a guanidine and a tertiary amine functionality. Yet, the possible interactions between these two units has not been highlighted and, actually, this is a field of interests which has remained quite unexplored.

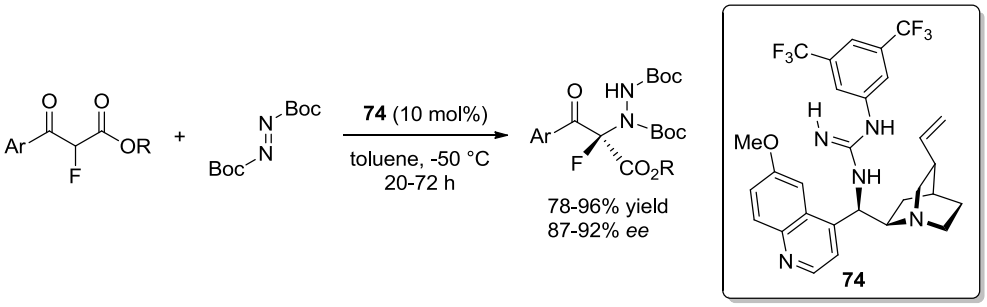

Scheme 21: Asymmetric amination of fluoro-β-ketoesters catalyzed by quinidine-derived guanidine **74**.

[81] Han, X.; Zhong, F; Lu, Y. *Adv. Synth. Catal.* **2010**, *352*, 2778.

3.1.3. Aim of this work

In the previous section the potentiality of chiral guanidines as organocatalysts, in terms of their versatile mode of action has been discussed. In addition, it has been highlighted that introduction of new functional groups on the *Cinchona* alkaloid scaffold has often led to the development of new classes of highly efficient organocatalysts.

We thought to design new bifunctional organocatalysts combining the potentialities of guanidines and *Cinchona* alkaloids and expanding the findings of Lu.[81] In fact we recognized that special attention had still to be paid to the possible interactions between the guanidine unit and the tertiary amine of the *Cinchona* alkaloids quinuclidine ring. Based on the observation of Soós and Connon,[72b,c] a cooperative behavior could not be excluded which would lead to an enhancement in basicity and to peculiar catalytic properties. Moreover, guanidine substituents with different electronic features result in effects on the catalyst activity which would deserve to be investigated.

The aim of this work can be therefore summarized as follows:

- design and preparation of new chiral guanidines, based on the framework of *Cinchona* alkaloids;
- study of the possible interactions between the guanidine unit and the tertiary amine of the quinuclidine moiety, with particular regard to the effects of different relative configurations of the chiral scaffold and of the guanidine substituents nature;
- application of these new catalysts to the development of novel asymmetric reactions.

3.2. Synthesis of Novel Chiral Guanidines

Guanidines can be conveniently prepared by reacting amines with guanidinating reagents, which include the commercially available *N*,*N'*-bis(*tert*-butyloxycarbonyl)thiourea (**79**)[82] and *N*,*N'*-bis(*tert*-butyloxycarbonyl)-*N''*-triflylguanidine (**80**).[83]

We took the first steps synthesizing a series of primary amines derived from *Cinchona* alkaloids. This task could be accomplished by application of the Mitsunobu-Staudinger protocol, which allowed to convert the secondary alcohol of **I**-**IV** and **XIII** into an amine group with complete inversion of the absolute configuration.[84] The 9-amino(9-deoxy)*epi*-derivatives **75a**-**e** were thus obtained (*Scheme 22*).

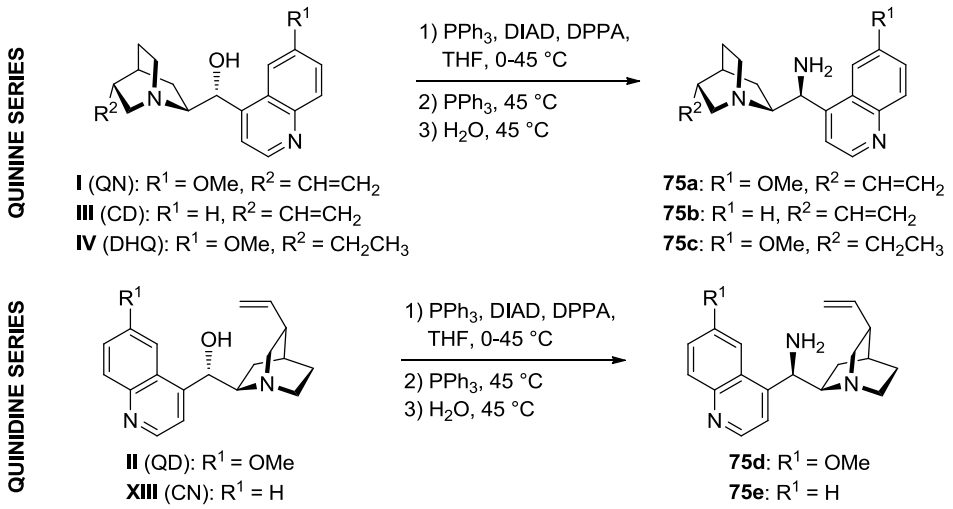

Scheme 22: Mitsunobu-Staudinger reaction to get the *epi*-amino derivatives **75a**-**e**.

We also prepared the epimer of amine **75a**. In principle, *epi*-**75a** derives from quinine **I** via conversion of the hydroxyl group into an amine group with retention of absolute configuration at the C9 position. However, such a transformation is not available and the retention of configuration must be accomplished through a double inversion. We therefore had to prepare first *epi*-quinine (*epi*-**I**) through a Mitsunobu reaction leading to nitrobenzoyl-*epi*-

[82] Yong, Y. F.; Kowalski, J. A.; Lipton, M. A. *J. Org. Chem.* **1997**, *62*, 1540.
[83] Feichtinger, K.; Zaph, C.; Sings, H. L.; Goodman, M. *J. Org. Chem.* **1998**, *63*, 3804.
[84] Cassani, C.; Martín-Rapún, R.; Arceo, E.; Bravo, F.; Melchiorre, P. *Nat. Protoc.* **2013**, *8*, 325.

quinine followed by hydrolysis[85] (*Scheme 23*). At this point we tried a Mitsunobu-Staudinger reaction protocol on *epi*-**I**, but the desired compound was obtained in low yield. Following a stepwise synthesis, through the mesylate **76** and the azide **77**, we could finally get 9-amino(9-deoxy)quinine (*epi*-**75**). In *Scheme 23* the preparation of the 5'-amino derivative **75f** is also depicted. It was prepared by nitration of hydroquinine (**III**) and reduction of the adduct **78** following a literature procedure.[86]

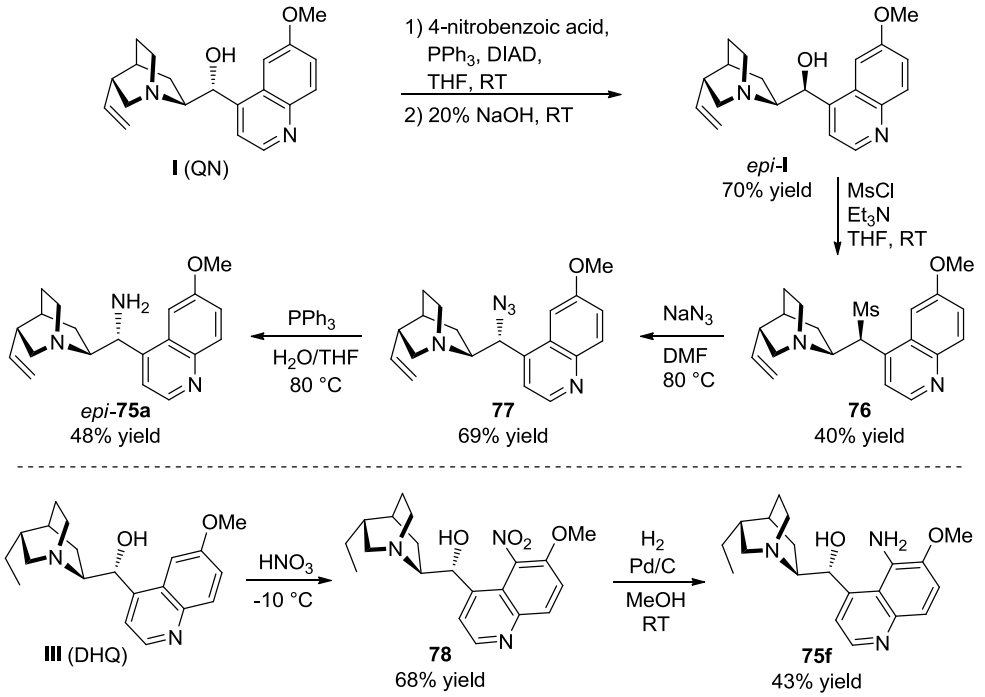

Scheme 23: Synthesis of 9-amino(9-deoxy)quinine *epi*-**75** and of 5'-aminohydroquinine **83**.

We then subjected **75a-f** and *epi*-**75a** to the guanidination reaction. For this purpose, two different procedures were employed. The first one (procedure A) makes use of thiourea **79** together with a large excess of mercury(II) chloride. The reaction proceeds through mercury-mediated conversion of **79** into the corresponding carbodiimide and subsequent addition of the primary amines **75a-f**. By contrast, the second procedure (B) employs the triflate **80** in milder and preferable conditions, as a simple nucleophilic substitution takes place. In some cases, for example for the synthesis of **XIVf**, only

[85] Taggi, A. E.; Hafez, A. M.; Wack, H.; Young, B.; Ferraris, D.; Lectka, T. *J. Am. Chem. Soc.* **2002**, *124*, 6626.
[86] Palacio, C.; Connon, S. J. *Org. Lett.* **2011**, *13*, 1298.

procedure A gave satisfactory results. The general transformations are outlined in *Scheme 24*, together with the products obtained.

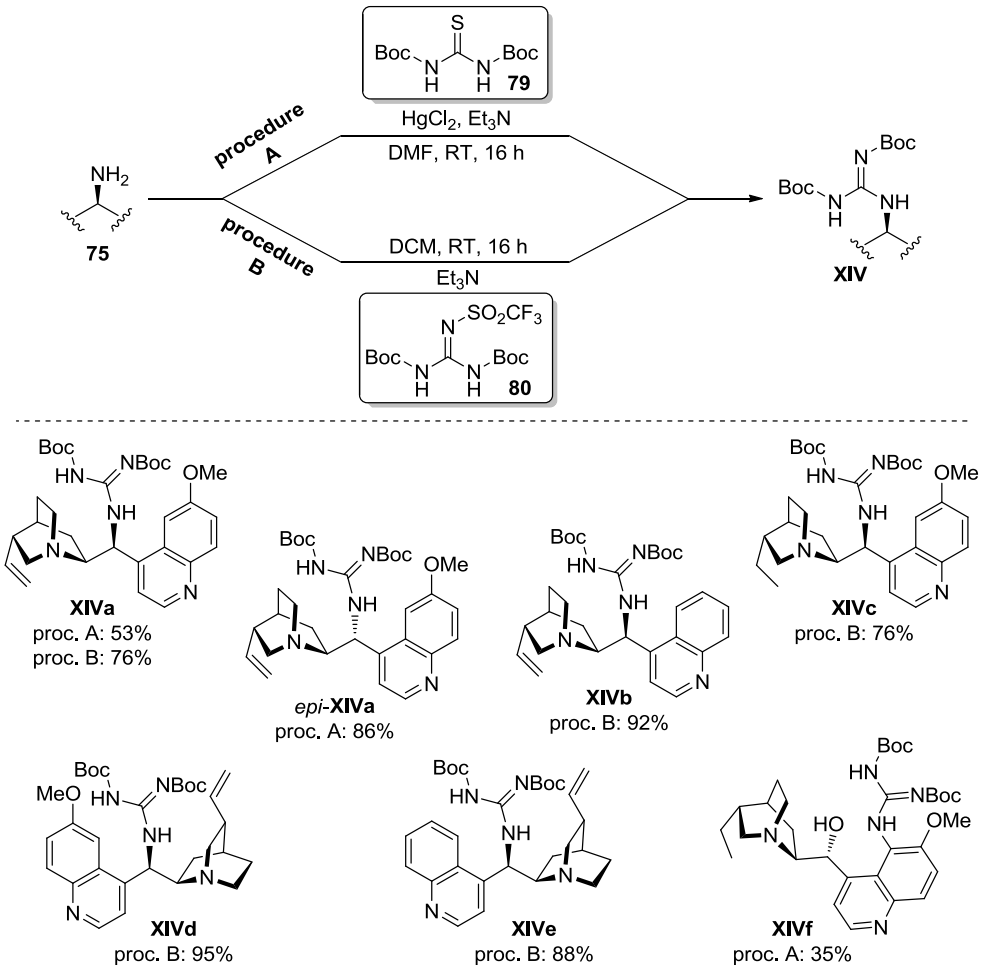

Scheme 24: Guanidination of amino compounds **75a-f** to afford di-Boc-guanidines **XIVa-f** (yields are reported under the products, according to the procedure used).

Di-Boc-guanidines **XIVa-f** were ready to be tested as organocatalysts. However, our aim was to prepare also more basic compounds, in which the guanidine unit was not substituted with an electron-withdrawing group. Moreover, it is known that the *tert*-butyloxycarbonyl protecting group can be easily removed via acidic hydrolysis. We therefore subjected **XIVa-f** to hydrolysis with hydrochloric or trifluoroacetic acid and, after basic work-up, we could get the free guanidines **XVa-f**. The reaction proceeds at room temperature with good to excellent yields (*Scheme 25*).

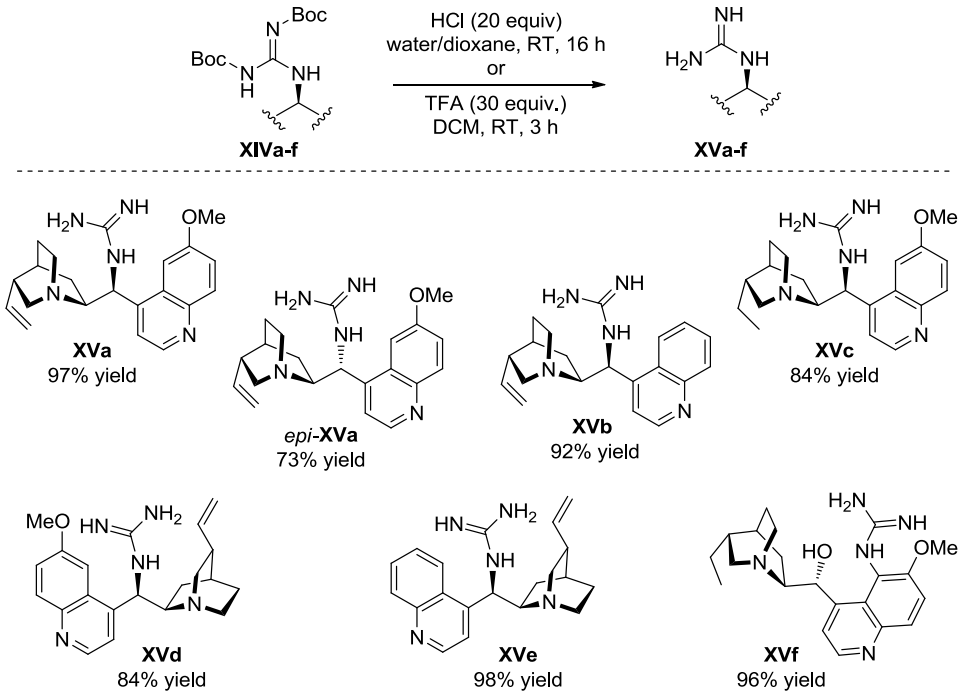

Scheme 25: Acidic hydrolysis of **XIVa-f** to get the free guanidines **XVa-f**.

We went on trying to prepare alkyl and aryl substituted *Cinchona* alkaloid-based guanidines. It is known that a straightforward route to guanidines is the addition of amines (hydroamination) to carbodiimides. The latter can be in turn readily prepared by the corresponding thioureas. This atom economic transformation is attractive, but it requires harsh conditions and complex catalytic systems.[87] Most of them are organometallic compounds based on transition metals or rare earths and are sensitive to air and moisture, thus requiring the reactions to be run under an inert atmosphere. Zinc trifluoromethanesulfonate has been reported to catalyzed the addition of amines and anilines to carbodiimides, in refluxing benzene.[88] Looking for an alternative reagent, we found that also zirconium tetrachloride, which is a cheap and green catalyst often employed for electrophiles activation,[89] could catalyze the reaction in refluxing toluene. It was not necessary to take particular precautions to keep air or moisture away from the reaction

[87] Many papers report that the addition of primary alkyl amines to carbodiimides proceeds without catalyst at high temperature, based on what stated by Richeson *et al.* (*J. Chem. Soc., Dalton Trans.* **1999**, 2947), who still does not give details on the procedure used. We observed no conversion reacting **75b** with DCC (**81a**) in refluxing toluene.
[88] Li, D.; Guang, J.; Zhang, W.-X.; Wang, Y.; Xi, Z. *Org. Biomol. Chem.* **2010**, *8*, 1816.
[89] Mo, L.-P.; Zhang, Z.-H. *Curr. Org. Chem.* **2011**, *15*, 3800.

environment in order to achieve good product yields. To the best of our knowledge no such specific application of $ZrCl_4$ has been reported yet. Under this conditions, we reacted **75a-b**,**e** with carbodiimides **81a-c** (*Scheme 26*). The hydroamination of dicyclohexylcarbodiimide (DCC, **81a**) proceeded with good to excellent yields (**XVIa-c**). Similar results were obtained employing unsymmetrical substituted carbodiimides **81b-c**, which bore both a phenyl and a cycloalkyl group.

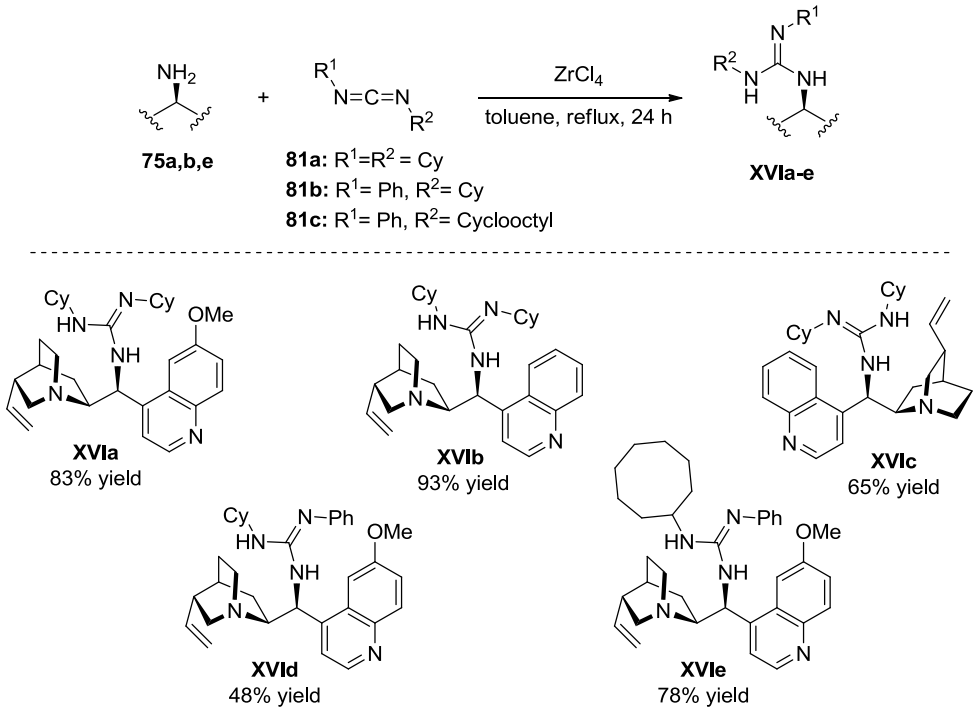

Scheme 26: Zirconium tetrachloride-catalyzed addition of **75a-b**,**e** to carbodiimides **81a-c** to get alkyl and aryl substituted guanidines **XVIa-e**.

Substituted guanidines **XVIa-e** showed unresolved broad signals in the ^{1}H NMR spectrum and we could not register acceptable ^{13}C NMR spectra. This is because this guanidines can exist as different isomers rapidly interconverting due to tautomerism (1,3-proton shift), *E*/*Z* isomerization of the C-N double bond and conformational isomerism.[90a] The phenomenon concerns di-Boc-substituted guanidines **XIVa-f** to a minor extent, probably because of intramolecular hydrogen bonds which determine a preferential

[90] a) O'Donovan, D. H.; Kelly, B.; Diez-Cecilia, E.; Kitson, M.; Rozas, I. *New J. Chem.* **2013**, *37*, 2408; b) Kelly, B.; O'Donovan, D. H.; O'Brien, J.; McCabe, T.; Blanco, F.; Rozas, I. *J. Org. Chem.* **2011**, *76*, 9216.

isomer.[90b] An exemplification of possible equilibria involving **XIV** and **XVI**, together with stabilizing intramolecular hydrogen bonds, is depicted in *Scheme 27*.

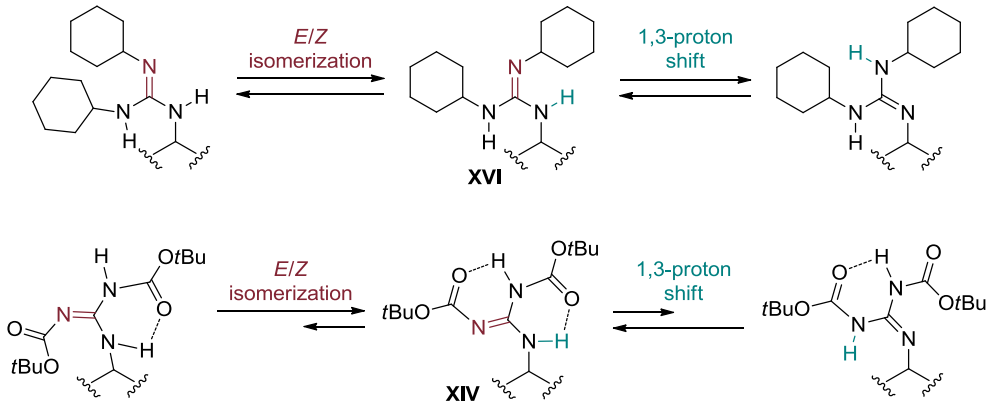

Scheme 27: Examples of some possible equilibria involving guanidines **XIV** and **XVI**.

No such phenomena can be observed for the symmetrically pentasubstituted guanidine **XVII**. It was synthesized by reaction with chloroamidinium salt **83**, which can be prepared from urea **82** and oxalyl chloride.[91]

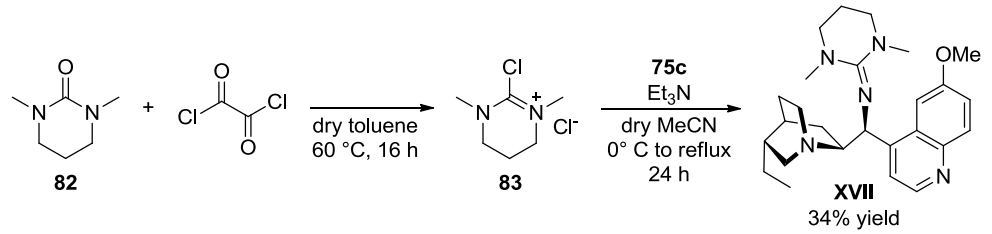

Scheme 28: Synthesis of guanidine **XVII** from chloroamidinium salt **83**.

[91] Kremzow, D.; Seidel, G.; Lehmann, C. W.; Fürstner, A. *Chem. Eur. J.* **2005**, *11*, 1833.

3.3. Evaluation of Catalytic Efficiency of New Guanidines

The first investigations on the catalytic efficiency of the novel *Cinchona* alkaloid-based chiral guanidines, whose preparation has been presented in the previous section, were carried out on compounds **XVa**, *epi*-**XVa** and **XVf**. In particular, their activity in the transesterification of the RNA model compound 2-hydroxypropyl *p*-nitrophenyl phosphate (HPNP, **84**) was studied. The results obtained in terms of potentiometric, kinetic and DFT-calculation evidences are discussed in the present section.[92]

The importance of phosphodiester bonds in biology and chemistry and their reluctance towards hydrolysis have encouraged many scientists to design and synthesize artificial catalysts able to cleave DNA, RNA and their model compounds with the idea of using these systems in health-related targets.[93] Most artificial enzyme-mimics are bifunctional catalysts whose activity is strictly related to their scaffold which must feature both preorganization and flexibility, keeping the active functions at the proper distance and in a favorable orientation. We thought that our guanidine catalysts could serve the purpose and we tested them in the model reaction outlined in *Scheme 29*, with a particular attention to their ability to accomplish a kinetic resolution of the substrate **84**.

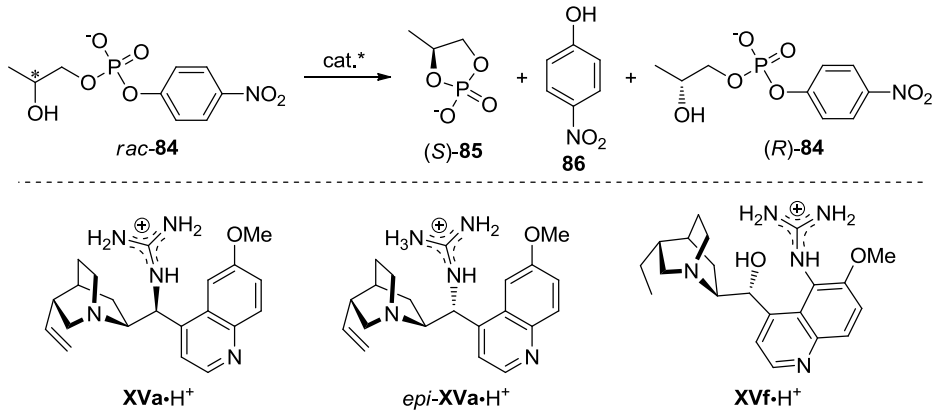

Scheme 29: Intramolecular transesterification of HPNP (**84**) catalyzed by chiral guanidiniums **XVa,f**•H^+ and *epi*-**XVa**•H^+

[92] Salvio, R.; Moliterno, M.; Caramelli, D.; Pisciottani, L.; Antenucci, A.; D'Amico, M.; Bella, M. *Catal. Sci. Technol.* **2016**, *6*, 2280.
[93] Salvio, R. *Chem. Eur. J.* **2015**, *21*, 10960.

The acidity constants determination of the investigated compounds was a prerequisite for the kinetic study of their catalytic properties. Compound **XVa**,**f** and *epi*-**XVa** were thus subjected to potentiometric titration in 80:20 DMSO:H_2O solvent mixture. Also the 9-amino(9-deoxy)*epi*-quinine (**75a**), 9-amino(9-deoxy)quinine (*epi*-**75a**) and simple quinine (**I**) were titrated for comparison. All these compounds possess three basic functionalities, except for **I** which has only two of them, and therefore, in their protonated forms they showed as many titratable protons. The results of the elaboration of the titration plots are summarized in *Table 5*.

Entry[a]	Compound	pK_1	pK_2	pK_3
1	**XVa**·$3H^+$	< 2	8.7	13.5
2	*epi*-**XVa**·$3H^+$	< 2	8.9	13.7
3	**XVf**·$3H^+$	< 2	8.4	11.6
4	**75a**·$3H^+$	2.1[b]	7.9	9.0
5	*epi*-**75a**·$3H^+$	2.2[b]	8.0	8.9
6	**I**·$2H^+$	3.5	8.6	-

Table 5: Acidity constants of *Cinchona* alkaloid derivatives in 80% DMSO at 25 °C. [a] The titrations were carried out on 6 mL of 2 mM solutions in the presence of NMe_4ClO_4. Experimental error = ±0.1 p*K* units. [b] Experimental error = ±0.3 p*K* units.

The most acidic proton of each compound can be attributed to nitrogen atom of the quinoline unit. They show very low pK_1, which cannot be accurately determined for titrations carried out at millimolar concentration. However, it can be said that this high acidity compared to quinolinium ion (pK_a= 4.90) is probably due to the marked electrostatic repulsion between the positively charged units, which facilitates the departure of a proton from the quinoline moiety. Indeed the effect is more dramatic in the compounds bearing three positive charges (p$K_1 \leq 2$), compared to the dication **I**·$2H^+$ (pK_1= 3.5). pK_2 is similar for guanidines **XVa**,**f** and *epi*-**XVa**, ranging from 8.4 to 8.9 and can be attributed to the quinuclidine moiety. These values are comparable to pK_2 of quinine (**I**), which possesses only this basic functionality, and to pK_3 values of amino-derivatives **75a** and *epi*-**75a**, whose most basic functionality is the tertiary amine and whose pK_2 must be attributed to the less basic primary amine.

The least acidic protons in entries 1-3 belong to the guanidinium units. The pK_3 of 5′-guanidine derivative **XVf** (entry 3) reveals a significantly lower basicity compared to the other two guanidine-substituted compounds (entry

2-3). This is a common observation when aromatic and aliphatic guanidines are compared.[94] The essentially identical value of pK_3 values of **XVa** and *epi*-**XVa** allowed us to exclude an enhancement in basicity due to relative stereochemistry-dependent cooperation between the guanidine and the quinuclidine units of our compounds. We had envisaged this possibility based on the catalytic behavior reported for *Cinchona* alkaloid-derived epimeric (thio)ureas (see *Section 3.1.1.* and ref. 72b,c).

The catalytic activity of **XVa**,**f** and *epi*-**XVa** in the transesterification of the RNA model compound HPNP **84** (*Scheme 29*) was investigated in the same solvent mixture and conditions used for the titrations (80% DMSO, 10 mM Me_4NClO_4, 25.0 °C). A first set of kinetic experiments were carried out to evaluate the best pH value to carry out the measurements. The trihydrochloride salt of **XVa** was prepared and several solutions at 5.0 mM concentration in the solvent mixture were set up. Partial neutralization of this solutions with different amounts of Me_4NOH afforded a number of buffer solutions with pH values in the range of around 8-12. They were used for catalytic rate measurements of HPNP (**84**) transesterification using the initial rate method. The pseudo-first-order law employed is the following:

$$\boldsymbol{r = k_{obs}[84]} \qquad (1)$$

Applying the initial rate method, for each solution at different pH, k_{obs} was calculated from equation (2):

$$r_0 = k_{obs}[\mathbf{84}]_0 \qquad (2)$$

where r_0 is the initial formation rate of *p*-nitrophenol (**86**, *Scheme 29*) which was spectrophotometrically determined. The rate constants k_{obs} as function of pH are reported in *Figure 17*. The pH rate profile shows a maximum of activity around pH 10-12. If we assume that **XVa**·H^+, the monoprotonated form of the catalyst, is the only catalytically active species, equation (1) can be written as follows:

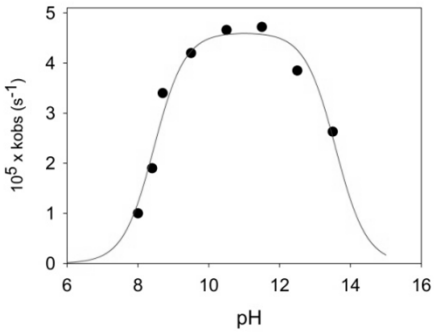

Figure 17: k_{obs} versus pH for the cleavage of **84** catalyzed by **XVa**.

[94] Corona-Martinez, D. O.; Taran, O.; Yatsimirsky, A. K. *Org. Biomol. Chem.* **2010**, *8*, 873.

$$r = k_{obs}[\mathbf{84}] = k_{\text{cat}}[\mathbf{XVa} \cdot \text{H}^+][\mathbf{84}] \qquad (3)$$

and therefore k_{obs} can be given by equation (4), where K_2 and K_3 are the acidity constant of **XVa**, as defined in *Table 5*, and C_{cat} is the total catalyst concentration.

$$k_{\text{obs}} = \frac{k_{\text{cat}}\, C_{\text{cat}}}{\frac{K_3}{[\text{H}^+]} + \frac{[\text{H}^+]}{K_2} + 1} \qquad (4)$$

The data in *Figure 17* can be fitted to a good precision to equation (4). The acidity constants (K_2, K_3) and k_{cat} were treated as adjustable parameters in a nonlinear least-squares fitting procedure. The following values of best fit parameters were obtained: pK_2 = 8.45 ± 0.12, pK_3 = 13.58 ± 0.13 and k_{cat} = (9.2 ± 0.4)×10^{-3} M^{-1} s^{-1}. The nice fit of data points to equation (4) and the good agreement of the kinetically determined acidity constant values with the potentiometrically determined ones (*Table 5*, entry 1) are clearly consistent with the idea that **XVa**·H^+ is the sole active species and suggest the operation of a bifunctional mechanism in which the guanidinium is acting as an electrophilic activator and the quinuclidine moiety is acting as a general base.

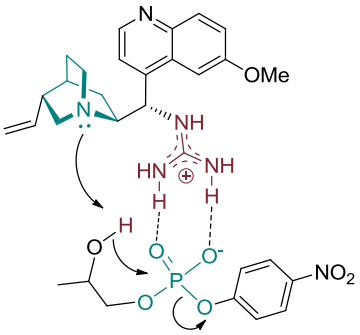

Figure 18: Proposed bifunctional mechanism for the guanidine **XVa**-catalyzed cleavage of HPNP.

In a second set of kinetic experiments 5.0 mM solutions in 80% DMSO of the hydrochloride salts of guanidines **XVa**,**f** and *epi*-**XVa**, of amines **75a** and *epi*-**75a** and of simple quinine (**I**) were prepared and partially neutralized with Me_4NOH. In the resulting buffer solutions the predominant species are the di- and mono-protonated forms of the catalysts, based on their pK_a values. These buffer solutions were employed for the measurement of k_{obs} of the transesterification of HPNP (**84**) using the initial rate method (equations (1) and (2)). The observed constants for each catalyst are reported in *Table 6* and are compared to the rate constants of background reaction (k_{bg}), that is the spontaneous transesterification of **84** taking place without the catalyst. k_{gb} values were

calculated following a literature method.[95] HPNP transesterification in the presence of the catalysts was in all cases faster than the background reaction. However, only in the guanidine-equipped *Cinchona* alkaloids the rate enhancements (k_{obs}/k_{bg}) cluster around 5×10^3-fold (*Table 6*, entries 1-3) and reach four orders of magnitude in the case of catalyst **XVa**. Comparison between the activity of **XVa** and *epi*-**XVa** (entries 2-3) indicates that the absolute configuration at C9 plays a crucial role in modulating the activity of the catalyst. Moreover, the compounds which are not provided with the guanidinium unit exhibit a sensibly lower activity (entries 4-6). This experimental evidence proves that the presence of the guanidinium unit is a key requisite to obtain high catalytic efficiency and confirms the postulated mechanism depicted in *Figure 18*.

Entry	Precat.[a]	pH	k_{obs}[b] (10^{-6} s^{-1})	k_{bg}[c] (10^{10} s^{-1})	$\frac{k_{obs}}{k_{bg}}$	k^R_{obs}[d] (10^{-6} s^{-1})	k^S_{obs}[d] (10^{-6} s^{-1})	$\frac{k^S_{obs}}{k^R_{obs}}$
1	**XVa**	8.7	34	32	10600	62	11.6	5.2
2	*epi*-**XVa**	8.9	12	50	2400	18.3	6.0	3.0
3	**XVf**	8.4	8.7	16	5400	13.5	3.9	2.4
4	**75a**	7.9	0.08	5.0	160	-	-	-
5	*epi*-**75a**	8.0	0.12	6.3	190	-	-	-
6	**I**	8.6	0.10	25	40	-	-	-

Table 6: Rate constants for the transesterification of HPNP (**84**) catalyzed by *Cinchona* alkaloid derivatives (80% DMSO, 25 °C). [a] The trihydrochloride (dihydrochloride for **I**) of the precatalysts at 5 mM concentration were used, $[\mathbf{84}]_i$ = 0.1 mM, 10 mM NMe_4ClO_4. [b] Error limit = ±5%. [c] The spontaneous transesterification rate was calculated according to literature equation. [d] Error limit = ±12%.

The three guanidine catalysts also exhibit a different catalytic activity towards the two enantiomers of HPNP. For the general case in which a kinetic resolution occurs, the pseudo-first-order rate constants relative to the reaction of each of the two enantiomers, k^R_{obs} and k^S_{obs}, are different. Therefore the rate law must take in account this contributions separately. The integrated kinetic equation for the formation of *p*-nitrophenol (**86**) would thus be given by (5).[96]

$$[\mathbf{86}] = [\mathbf{84}]_0\left(1 - \frac{e^{-k^R_{obs}\,t} + e^{-k^S_{obs}\,t}}{2}\right) \qquad (5)$$

[95] Baldini, L.; Cacciapaglia, R.; Casnati, A.; Mandolini, L.; Salvio, R.; Sansone, F.; Ungaro, R. *J. Org. Chem.* **2012**, *77*, 3381.
[96] Keith, J. M.; Larrof, J. F.; Jacobsen, E. N. *Adv. Synth. Catal.* **2001**, *343*, 5.

If there was no kinetic resolution ($k_{obs}^{R} = k_{obs}^{S} = k_{obs}$) the concentration of *p*-nitrophenol (**86**) would be given by the well-known simpler equation (6).

$$[\mathbf{86}] = [\mathbf{84}]_0\left(1 - e^{-k_{obs}\,t}\right) \qquad (6)$$

Figure 19 shows the full time-course profile of HPNP transesterification in the presence of catalyst **XVa**, as the increasing concentration of product **86** versus time. It can be fitted (red line) to good precision to equation (5) and deviates from simple first-order (black line) of equation (6). In the fitting procedure, the k_{obs}^{R} and k_{obs}^{S} were treated as adjustable parameters obtaining the values reported in *Table 6*. The same experiments were conducted employing catalysts *epi*-**XVa** and **XVf**.

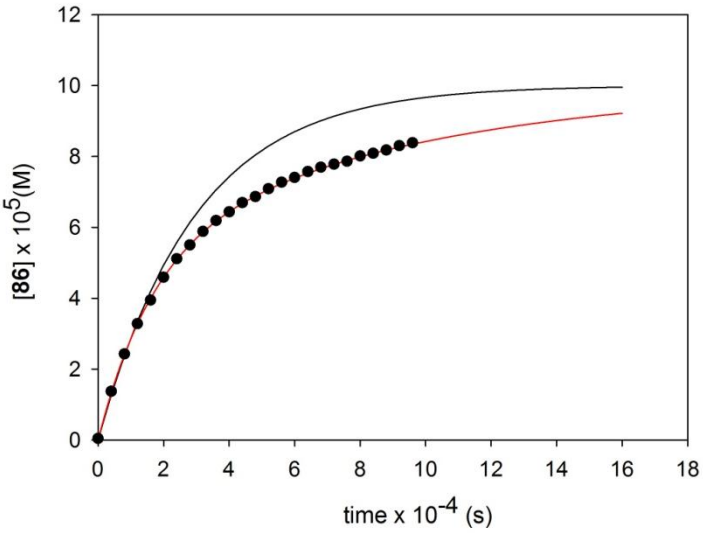

Figure 19: Data points (black dots) for the transesterification of **84** catalyzed by **XVa** and liberating *p*-nitrophenol (**86**). Data points are fitted to equation 5 (red line). Equation 6 (black line) does not fit the data points.

Data about the kinetic resolution were confirmed by chiral HPLC chromatography. Reaction mixtures were quenched with acidic solutions at proper time intervals and the unreacted substrate **84** was subjected to determination of enantiomeric excess, from which k_{obs}^{R}/k_{obs}^{S} can be calculated.[96] Values were in accordance to that reported in *Table 6*.

The values of k_{obs}^{R} and k_{obs}^{S} show that our guanidine catalysts are able of discriminating the two enantiomers of HPNP **84** and performing a kinetic resolution. Catalyst **XVa** is the most selective, with five-fold higher preference for (*S*)-**84** over (*R*)-**84**.

DFT calculations[97] were carried out to predict the transition state structure of the catalysts **XVa**,**f** and *epi*-**XVa** and each of the two enantiomers of the substrate **84**. *Figure 20* reports as an example the transition state structure involving **XVa**·H^+ and (*R*)-**84**. The geometry of the guanidinium-phosphate group and the distances H_2-O_3 and H_3-O_4 (average value = 1.72 Å) indicate the presence of a chelate hydrogen bonding and not only a mere electrostatic interaction. The bond between the hydrogen atom H_1 of the hydroxyl group of **84** and the oxygen atom O_1 is breaking (1.42 Å) and a new bond is forming between the hydrogen and the quinuclidine nitrogen N_1 (1.15 Å). The distances O_1-P (2.08 Å) and O_2-P (1.86 Å), if compared with the average P-O distance of phosphodiesters, indicate the forthcoming formation of a σ-bond and the breaking of the oxygen-phosphorous bond of the leaving group. These findings suggest the operation of a concerted mechanism rather than a stepwise one and are in accordance to the mechanism proposed on the basis of the kinetic measurements and schematically depicted in *Figure 18*.

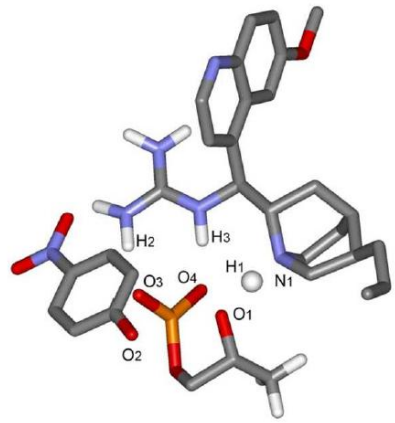

Figure 20: DFT calculated TS structure for the transesterification of (*R*)-HPNP catalized by **XVa**·H^+.

Moreover, the transition state involving **XVa**·H^+ and (*S*)-**84** has a significantly lower energy compared to the TS involving (*R*)-**84**, as expected from the selectivity observed in the kinetic resolution. This is probably due to the repulsive interaction of the (*R*)-**84** methyl group with the bulky quinuclidine moiety of the scaffold (*Figure 20*).

The content of this section has represented an important result in the investigation of the activity of our new *Cinchona* alkaloid-based guanidine catalysts, giving insights in their possible mode of action and in the difference in the catalytic activity of C9-epimers.

The next section will deal with a novel reaction and to the application of our guanidine catalysts for the development of its asymmetric version.

[97] b3lyp/6-31g(d,p)//b3lyp/6-31g(d,p) using Gaussian09 (see ref. 58).

3.4. A Highly Diastereoselective Vinylogous Aldol Reaction

3.4.1. Vinylogous aldol reactions: a brief overview

The aldol reaction is a fundamental transformation in synthetic organic chemistry for the construction of new carbon-carbon bonds. Thanks to the phenomenon of vinylogy, which involves transmission of electronic effects through a conjugate π-system, also α,β-unsaturated carbonyl compounds can be employed as the nucleophilic components in aldol reactions (*Scheme 30*). The resulting transformation is then called vinylogous aldol reaction (VAR). The structural motives arising from vinylogous reactions are usually more complex than their classical counterparts, because of extended carbon skeletons, additional functionalities and increasing stereochemical complexity. All these features render VARs useful transformations in modern organic synthesis and account for the terrific efforts that chemists have been putting into studying them and their asymmetric versions.

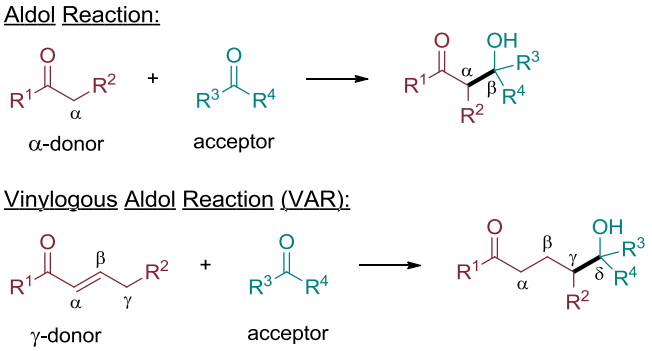

Scheme 30: Comparison between a general aldol reaction and its vinylogous extension.

Vinylogous aldol reactions occur via the formation of extended enolates of the donors, which present some issues in terms of chemo- and regio-selectivity. To overcome this problem, synthetic equivalents of the donors can be employed, such as the silyloxydienes in the Mukayama VAR. Despite the fact that the majority of reports dealing with vinylogous aldol reactions are actually Mukayama variants and many catalytic systems have been developed to perform highly diastereo- and enantioselective transformations, a direct VAR is still more desirable. In fact the preparation and purification of silyloxydienes adds at least one step to the synthesis and they often have a limited shelf life.

The direct VAR has found significant application to α,β-unsaturated esters, in particular cyclic systems such as 2-(5*H*)-furanones (γ-butenolides). In fact these compounds can be readily deprotonated at the γ-position, because it leads to the formation of aromatic anions (furanolates).

One of the first examples of organocatalytic vinylogous aldol reaction involving 2-(5*H*)-furanones came from Zhang and co-workers, based at Pfizer corporation. They were looking for a mild transformation not involving strong bases (such as LiHMDS), extremely low temperatures or stoichiometric additives, which are often employed for this purpose and unsuitable for scale up.[98] They found that mucochloric acid (**87a**) could be deprotonated by triethylamine and added to aldehydes under mild conditions. The racemic products are formed in moderate to good yields with *syn*/*anti* diastereomeric ratios clustering around 2:1 (*Scheme 31*).

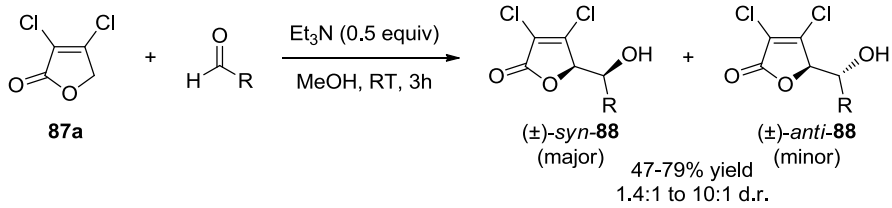

Scheme 31: Non-asymmetric organocatalytic vinylogous aldol addition of mucochloric acid (**87a**) to aldehydes.

Concerning asymmetric organocatalyzed direct VARs of γ-butenolides, a few examples have been reported. An interesting work came from Terada and co-workers,[99] who developed the guanidine catalyst **90**, which is able to catalyze the direct vinylogous addition of mucochloric and mucobromic acids (**87a,b**) to benzaldehydes (*Scheme 32*). The reaction proceeds with excellent enantioselectivity and good diastereoselectivity. The catalyst was not equally efficient with mono- or unsubstituted furanones substrates. Other similar examples are often limited to aromatic aldehydes as electrophiles and show high enantioselectivity but moderate diastereoselectivity. An exception is represented by the reaction developed by Lu and co-workers,[100] who employed α-keto esters as electrophiles in an amine thiourea-catalyzed asymmetric addition of mucochloric acid (**87a**).

[98] Das Sarma, K.; Zhang, J.; Curran, T. T. *J. Org. Chem.* **2007**, *72*, 3311.
[99] Ube, H.; Shimada, N.; Terada, M. *Angew. Chem. Int. Ed.* **2010**, *49*, 1858.
[100] Luo, J.; Wang, H.; Han, X.; Xu, L.-W.; Kwiatwoski, J.; Huang, K.-W.; Lu, Y. *Angew. Chem. Int. Ed.* **2011**, *50*, 1861.

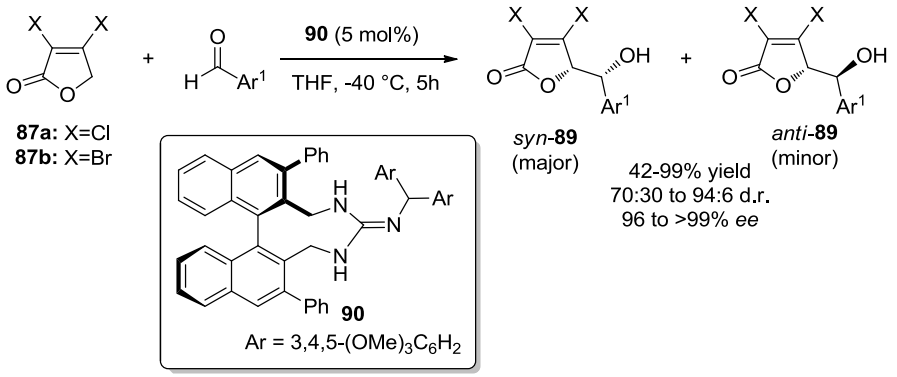

Scheme 32: Asymmetric VAR catalyzed by chiral guanidine **90**.

It is worth noting that the 5-(1'-hydroxy)-γ-butyrolactone moiety is an important component of many naturally occurring and biologically active compounds. Some examples of small molecules belonging to this class are showed in *Figure 21*. *Iso*-cladospolide B (**91**) has been found to be a root growth stimulator in plants[101a] and sapinofuranone B (**92**) is a phytotoxic metabolite of a pathogenic fungus of pine.[101b] Cardiobutanolide (**93**) was isolated from a plant of the *Annonaceae* family, whose products are known to have several activities, such as antitumor, teratogenic, pesticidal, cytotoxic and embryotoxic effects.[101c] Due to its peculiar structure and activity, several total syntheses of **93** have been reported.

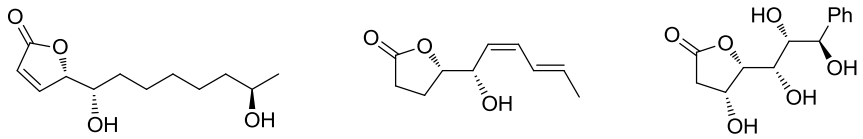

Figure 21: Selected example of naturally occurring, biologically active γ-butyrolactones.

The valuable products achievable through asymmetric vinylogous aldol additions of γ-butenolides account for the efforts put in the development of new and more efficient applications of this synthetic strategy. In the next section a new organocatalyzed highly diastereoselective vinylogous aldol reaction will be presented.

[101] a) Hirota, A.; Sakai, H.; Isogai, A. *Agric. Biol. Chem.* **1985**, *49*, 731; b) Cabras, A.; Mannoni, M. A.; Serra, S.; Andolfi, A.; Fiore, M.; Evidente, A. *Eur. J. Plant. Pathol.* **2006**, *115*, 187; c) Blázquez, M. A.; Bermejo, A.; Zafra-Polo, M. C.; Cortes, D. *Phytochem. Anal.* **1999**, *10*, 161.

3.4.2. Reaction and scope

We decided to use α-substituted γ-butenolides (like **94a**) as nucleophiles in a novel vinylogous aldol reaction. These compounds can be easily prepared starting from commercially available 2,5-dihydro-2,5-dimethoxy furan. In addition, the double bond can be readily reduced to saturated γ-butyrolactones[102] similar to the above mentioned **92** or **93**.

The electrophilic partners that we have investigated are β,γ-unsaturated α-keto esters (like **95a**), which can be synthesized by aldol condensation of pyruvate with arylaldehydes and subsequent esterification.[103] We considered them interesting candidates for a new VAR for two main reasons. First, they are electrophilic carbonyl compounds without enolizable protons, thus avoiding undesired side reactions or autocondensation. Second, upon addition on their ketone functionality, a quaternary stereogenic center would be formed. Therefore, the products obtained would be valuable, highly functionalized compounds. However, forging quaternary stereocenters is a challenging task in organic synthesis, because of intrinsic lower reactivity due to steric reasons and because of the difficulty to control the stereochemical outcome.[104]

Moreover, the reaction of α-substituted butenolides with α-keto esters affords products with two stereogenic centers, which are both formed during the transformation. This reaction could thus lead to four possible stereoisomer, as two couple of enantiomers. Therefore, to perform a highly stereoselective transformation both diastereo- and enantiocontrol must be exerted by the catalyst.

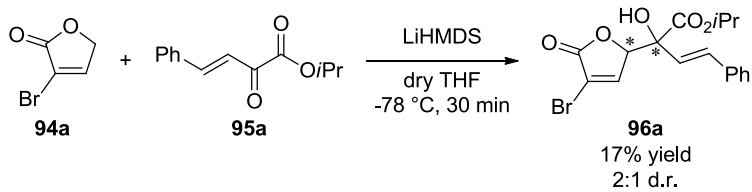

Scheme 33: Preliminary attempt to get **96a** through a vinylogous aldol reaction.

We started our preliminary investigations quantitatively generating the extended enolate of bromofuranone **94a** with the strong base lithium

[102] Bella, M.; Piancatelli, G.; Squarcia, A. *Tetrahedron* **2001**, *57*, 4429.
[103] Belmessieri, D.; Morrill, L. C.; Simal, C.; Slawin, A. M. Z.; Smith, A. D. *J. Am. Chem. Soc.* **2011**, *133*, 2714.
[104] Bella, M.; Gasperi, T. *Synthesis*, **2009**, 1583.

bis(trimethylsilyl)amide (LiHMDS) and reacting it with α-keto ester **95a**, as outlined in *Scheme 33*. After 30 minutes the reaction was quenched and product **96a** could be isolated in low yield together with the unreacted substrates. The NMR spectrum of the crude reaction mixture showed that **96a** was formed as a mixture of two diastereoisomers in 2:1 ratio. Each of them could be separated into two enantiomers using HPLC on chiral stationary phase.

Moving to an organocatalytic mode of activation, we ran the same reaction using triethylamine as the base to catalytically generate the enolate of **94a**. Performing the reaction in toluene at -20 °C for 20 hours, the product **96a** was obtained in 39% yield and as a single diastereoisomer (d.r. > 99:1). A possible explanation of the dramatic difference in the stereochemical outcome of these first two reactions may be the role played by the countercation of the enolate. The lithium cation of LiHMDS and the triethylammonium ion may exert a different steric effect for the discrimination of the *syn* and *anti* conformations of the transition state, although the *syn* or *anti* configuration of the product has not been established yet. Interestingly, running the reaction at room temperature resulted in complete loss of diastereoselectivity.

With these first conditions in hand, we explored the scope of the reaction preparing racemic samples of adducts **96b-i** (*Scheme 34*) with the intention to subsequently develop an efficient protocol for their asymmetric synthesis. The yield of the process does not seem to be affected on the nature of the aryl group of the keto ester. Electron-rich phenyl (**96c**) or an heteroaromatic moiety (**96e**) afforded the products in similar yield. The reaction performed on the butadienylphenyl keto ester was significantly less efficient (**96d**, 10% yield).

Moving from isopropyl to methyl esters (**96f,g**), improved the reactivity, with an excellent yield in the case of **96g**. The reaction could be performed also with chloro- (**94b**) and phenylselenyl- (**94c**) substituted nucleophiles, affording products **96h** and **96i** in 39% and 54% yield, respectively.

All these diverse substitution patterns did not affect the diastereoselectivity of the process, as every product was obtained as a single diastereoisomer.

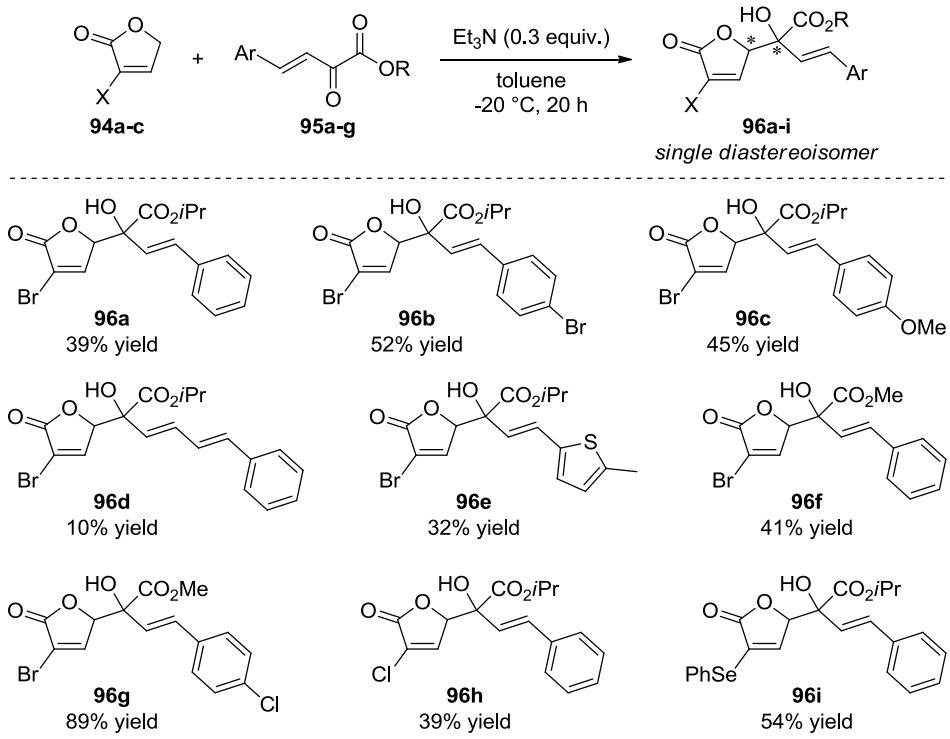

Scheme 34: Diastereoselective synthesis of **96a-i** through the vinylogous aldol addition of γ-butenolides **94a-c** to β,γ-unsaturated α-keto esters **95a-g**. [a] Reaction performed employing 1.0 equiv of **94** (0.64 mmol), 1.0 equiv of **95**,0.3 equiv of Et_3N in 3 mL toluene. All products were obtained as single diastereoisomer. Isolated yields are reported.

3.4.3. Application of Cinchona alkaloid-based guanidines as organocatalysts

We chose as a model the reaction between bromofuranone **94a** and α-keto ester **95a** in order to find the best conditions to perform our diastereoselective VAR in an enantioselective fashion.

The first catalyst tested, in toluene at -20 °C, was the simple quinine (**I**) which smoothly delivered product **96a** as a single diastereoisomer, but as a racemic mixture (*Table 7*, entry 1). The reactivity was determined by measuring the substrate conversion by means of HPLC analysis of the crude reaction mixture. Moving to the bifunctional catalyst **62** (Soós thiourea) we observed an increase in the reactivity and a modest enantiomeric excess of 16% (entry 2). The dimeric squaramide **XIX** afforded the product with little higher enantioselectivity, but with a conversion of only 9% after 21h (entry 4). The thiourea **XVIII**, which had been developed in our group and successfully applied as a complementary alternative to Soós-type thioureas,[105] performed significantly better yielding the opposite enantiomer with 41% *ee* (entry 3).
We then started to screen our new guanidine catalysts, beginning with the unsubstituted ones (**XVa-f**). None of them proved to be highly enantioselective (up to 25% *ee*, entry 10) and in two cases the product was obtained as a racemic mixture (entries 6 and 11). Moreover, opposite enantioselection was observed in the case of *pseudo*enantiomeric catalysts (entries 5, 7 and 8 versus 9 and 10), as expected.
Given these not exciting results for series **XV** catalysts, we thought to investigate the behavior of catalysts of type **XIV**, from which the former derive. In fact the substitution on the guanidine moiety with two electron-withdrawing groups (*tert*-butyloxycarbonyl) should make the guanidinium, resulting from deprotonation of the substrate, a better hydrogen bond donor. Therefore, hypothesizing a bifunctional mode of activation, it might result in a more stereochemically defined transition state and hence in higher enantioselectivity. Actually, di-Boc substituted catalysts **XIVa-f** (entries 12-18) were generally more efficient then the unsubstituted ones. In particular,

[105] Silvi, M.; Renzi, P.; Rosato, D.; Margarita, M.; Vecchioni, A.; Bordacchini, I.; Morra, D.; Nicolosi, A.; Cari, R.; Sciubba, F.; Scarpino Schietroma, D. M.; Bella, M. *Chem. Eur. J.* **2013**, *19*, 9973.

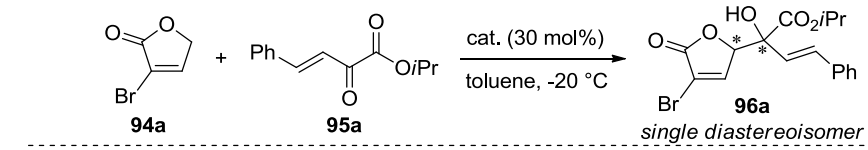

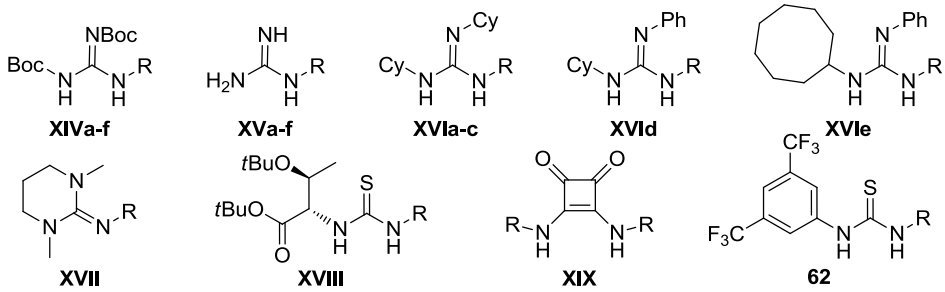

Entry[a]	-R	Catalyst	Time (h)	Conv. (%)[b]	*ee* (%)[c]
1	-	quinine (**I**)	20	80	< 5
2	*epi*QN	**62**	23	91	16
3	*epi*QN	**XVIII**	16	87	-41
4	*epi*QN	**XIX**	21	9	21
5	*epi*QN	**XVa**	69	72	14
6	QN	*epi*-**XVa**	66	26	< 5
7	*epi*CD	**XVb**	24	68	21
8	*epi*DHQ	**XVc**	66	68	16
9	*epi*QD	**XVd**	21	88	-12
10	*epi*CN	**XVe**	64	43	-25
11	-5'-(*epi*DHQ)	**XVf**	68	66	< 5
12	*epi*QN	**XIVa**	66	44	60
13	QN	*epi*-**XIVa**	66	67	< 5
14	*epi*CD	**XIVb**	22	20	69
15	*epi*DHQ	**XIVc**	65	66	61
16	*epi*QD	**XIVd**	20	46	-41
17	*epi*CN	**XIVe**	66	44	-59
18	-5'-(*epi*DHQ)	**XIVf**	68	14	-32
19	*epi*QN	**XVIa**	25	20	48
20	*epi*CD	**XVIb**	22	16	47
21	*epi*CN	**XVIc**	23	41	-19
22	*epi*QN	**XVId**	48	68	43
23	*epi*QN	**XVIe**	86	87	38
24	*epi*DHQ	**XVII**	22	18	-18

Table 7: Catalyst screening for the organocatalyzed vinylogous aldol addition of **941** to **95a** to afford enantioenriched **96a** as a single diastereoisomer. [a] Reaction performed employing 25 mg (0.15 mmol, 1 equiv) of **94a** and 34 mg (0.15 mmol, 1 equiv) of **95a**, in 0.4 mL toluene (concentration: 0.37 M). [b] Conversion of substrate **95a** determined by HPLC analysis at λ= 272 nm. [c] The *ee* was determined by HPLC on CSP using Chiralpack IC column and *n*-hexane/*i*-propanol 85:15 (flow 0.9 mL/min).

the cinchonidine-derived catalyst **XIVb** yielded the product with 69% *ee* (entry 14), which is the best results we obtained in terms of enantioselectivity. It is worth noting that the *pseudo*enantiomeric behavior of these catalysts was once again observed (entries 12, 14 and 15 versus 16 and 17) and that the epimeric catalysts **XIVa** and *epi*-**XIVa** performed in a sensibly different way.

In order to get insights into the electronic and steric role of the guanidine group substituents, we tested the alkyl and aryl substituted catalysts **XVIa-e**, which all showed similar reactivity and enantioselectivity (19-48% *ee*, entries 19-23), always lower than that of the di-Boc substituted **XIV**. Moreover, catalyst **XVII**, who lacks hydrogens on the guanidine unit, afforded the product in low enantiomeric excess (entry 24) and, interestingly, as the opposite enantiomer with respect to that obtained by catalysts **XVc** and **XIVc** (entries 8-15). All these three catalysts (**XIVc**, **XVc** and **XVII**) are based on the skeleton of *epi*-hydroquinine, therefore an opposite stereochemical outcome may indicate a different mechanism of action. In fact, catalyst **XVII** does not have the possibility to chelate the electrophile through a double hydrogen bond, as in its protonated form it possesses only one acidic hydrogen. This observations suggest that in all the other cases (catalysts of series **XIV**, **XV** and **XVI**) the hydrogen bonding capability of the guanidinium groups plays a crucial role in the catalysis.

The catalyst screening showed that di-Boc substituted guanidines of type **XIV** were the best catalysts among the ones tested. Changing the solvent (dichloromethane, veratrole, THF or benzonitrile, which are common solvents for guanidine-catalysis) was not beneficial for the enantioselectivity of the process. Similarly, trying to accelerate the reaction running it at room temperature, resulted once again in loss of diastereoselectivity.

We believe that our new *Cinchona* alkaloid-based guanidines are promising catalysts for this or other similar reactions, even though studies are still ongoing to finely tune the substitution pattern on the guanidine unit in order to increase both reactivity and enantioselectivity.

3.5. Summary of the Chapter

In this chapter the development of new chiral guanidines based on *Cinchona* alkaloids has been presented. Different synthetic approaches were followed to prepare a small library of potential guanidine-based catalysts.

Potentiometric and kinetic experiments, as well as *ab initio* calculations, were employed to investigate the catalytic activity of some of our novel guanidine compounds, with particular attention on the relative configuration of their chiral centers. They were shown to catalyze the intramolecular transesterification of RNA model compound 2-hydroxypropyl *p*-nitrophenyl phosphate (HPNP), performing a kinetic resolution of the substrate. Experimental data also indicates the operation of a bifunctional mechanism in which both the tertiary amine of the *Cinchona* alkaloid quinuclidine ring and the guanidine moiety are involved.

The novel guanidines were also employed to develop a new highly diastereoselective organocatalytic vinylogous aldol reaction. The transformation leads to valuable 5-(1'-hydroxy)-γ-butyrolactones, with the formation of a quaternary stereogenic center. The novel *Cinchona* alkaloid-based di-Boc substituted guanidines were the best catalysts among the ones tested and experimental observations suggest that they act as bifunctional catalysts.

Future development of this project may involve the fine tuning of the structure of these guanidine catalysts, in order to make completely efficient our new vinylogous aldol reaction. Moreover, application of these novel catalysts to asymmetric reactions which could benefit from a bifunctional activation mode could break new grounds in synthetic organic chemistry.

4. Asymmetric β-Alkylation of Enals through Photo-Organocatalysis

4.1. Introduction

4.1.1. Merging photoredox catalysis with organocatalysis

Nature continuously brings about its transformations exploiting an endless resource coming from the sun: the light. An amazing example is the photosynthesis, through which solar energy is converted into chemical energy to be stored and exploited by living organisms.

Such a capability and the power held by light have always attracted chemists. Moreover, it has been known for a long time that some reactions can occur only upon irradiation of the reagents. This is because light absorption generates high-energy intermediates with electron properties much different from those of the ground state. For example, considering an electron transfer reaction, an excited species is both a better oxidant and a better reductant than the ground state species. The reason for this is schematically depicted in *Scheme 35* employing the frontier orbitals descriptors. Let us consider species **A**, whose HOMO (Highest Occupied Molecular Orbital) and LUMO (Lowest Unoccupied Molecular Orbital) are drawn. **A** can act as an oxidant, receiving one electron into its LUMO from a reductant species (**Red**) which has an occupied orbital at higher energy: the energy gain of the process is related to the difference in energy of the two orbitals (ΔE_{red}). Similarly, **A** can act as a reductant, donating one electron from its HOMO to an oxidant species (**Ox**) which has an unoccupied orbital at lower energy: the energy gain of the process is related to the difference in energy of the two orbitals (ΔE_{ox}).

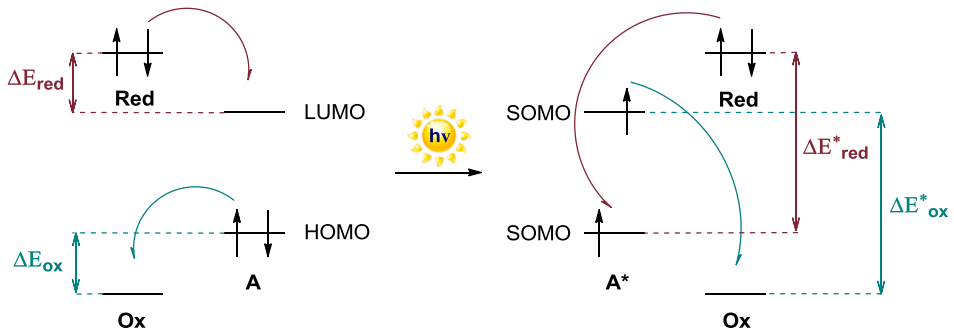

Scheme 35: Frontier orbitals rationalization of the different redox potentials in ground and excited states.

If **A** absorbs a photon which promotes one of its electron of the HOMO to

the LUMO, the excited $\mathbf{A}^*$ will possess two SOMOs (Singly Occupied Molecular Orbitals). $\mathbf{A}^*$ can thus be either reduced by **Red** accepting one electron in its own lower SOMO or oxidized by **Ox** donating the electron of its own higher SOMO. The potentials of these two reactions are now ΔE^*_{red} and ΔE^*_{ox} respectively, which are both greater than ΔE_{red} and ΔE_{ox}, i.e. the electron transfers are more energetically favorable in the excited state.

Although photochemistry was extensively studied in the last century, its applications were limited to artificial photosynthesis studies, material sciences and organic reactions with very little regard to asymmetric synthesis.[106] This may be explained considering that developing enantioselective light-driven transformations is a challenging task due to the high reactivity and fleeting nature of the radical photo-generated intermediates. Therefore an enantioselective photocatalytic system should provide the right activation of the substrates, which would lead to a non-dispersive reaction, and ensure that they react in a chiral environment.

Asymmetric photocatalysis reached the turning point in 2008, when the group of MacMillan[107] published a report on *Science*, with the same title as the present section, showing that highly efficient and enantioselective light-driven transformations could be developed. The direct coupling between aldehydes **97** and α-bromo carbonyl compounds **98** leading to enantioenriched α-functionalized products **99** (*Scheme 36*) is thought to proceed through the interaction of two catalytic cycles. In the organocatalytic one, chiral secondary amine **XX** condenses with the aldehyde substrate giving enamine **102**. At the same time, the main actor of the photoredox cycle is tris(bipyridine)ruthenium(II) complex **XXI**, which upon irradiation with a compact fluorescent lamp (CFL) can absorb a photon producing high-energy excited intermediate **101**. In the initiation step (not shown in the scheme), **100** oxidizes a sacrificial amount of enamine **102**, reducing itself to species **101**. Another single electron transfer (SET) towards bromoderivative **98** regenerates the photocatalyst **XXI** and the electrophilic radical **103**. The latter then enters the organocatalytic cycle, undergoing enantioselective nucleophilic attack by chiral enamine **102**. The resulting α-amino radical **104** is then oxidized by **100** affording the iminium ion **105**, which hydrolyzes to give the free amine catalyst and the

[106] Wessig, P. *Angew. Chem. Int. Ed.* **2006**, *45*, 2168.
[107] Nicewicz, D. A.; MacMillan, D. W. C. *Science* **2008**, *322*, 77.

enantioenriched product **99**. This type of "dual catalysis" is based on the fine tuning of reduction potentials of all the species involved, in order to make all the electron transfers to be energetically favored and to happen in an clockwork-like fashion.

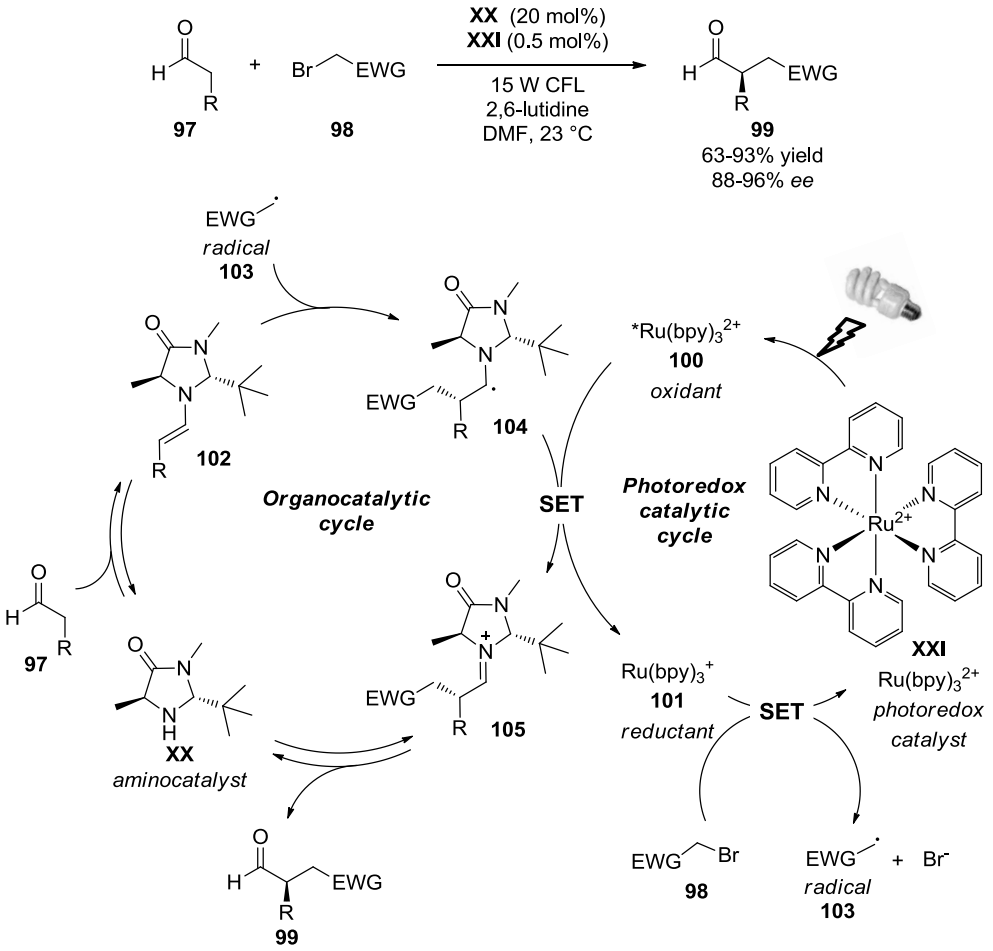

Scheme 36: The first photo-organocatalytic asymmetric α-alkylation of aldehydes and proposed mechanism.

Since the pioneering work of MacMillan, many other "dual" photoredox processes with transition metal complexes have been developed to perform a number of reactions.[108] The common feature of these processes is that the photochemical activation of substrates, which furnishes reactive radical species under the action of a visible light-active photoredox catalyst, is differentiated from the stereoselective ground state process, controlled by a distinct chiral catalyst.

[108] Prier, C. K.; Rankic, D. A.; MacMillan, D. W.C. *Chem. Rev.* **2013**, *113*, 5322.

An alternative approach consists in the photoexcitation of substrates which already reside in a chiral environment. This is generally more challenging because most organic molecules cannot absorb light in the visible spectrum. However, the possibility to perform photocatalytic asymmetric reactions without the employment of a metal-based catalyst is attractive and the study of photo-active organic intermediates to be exploited for this purpose is a growing field of research.

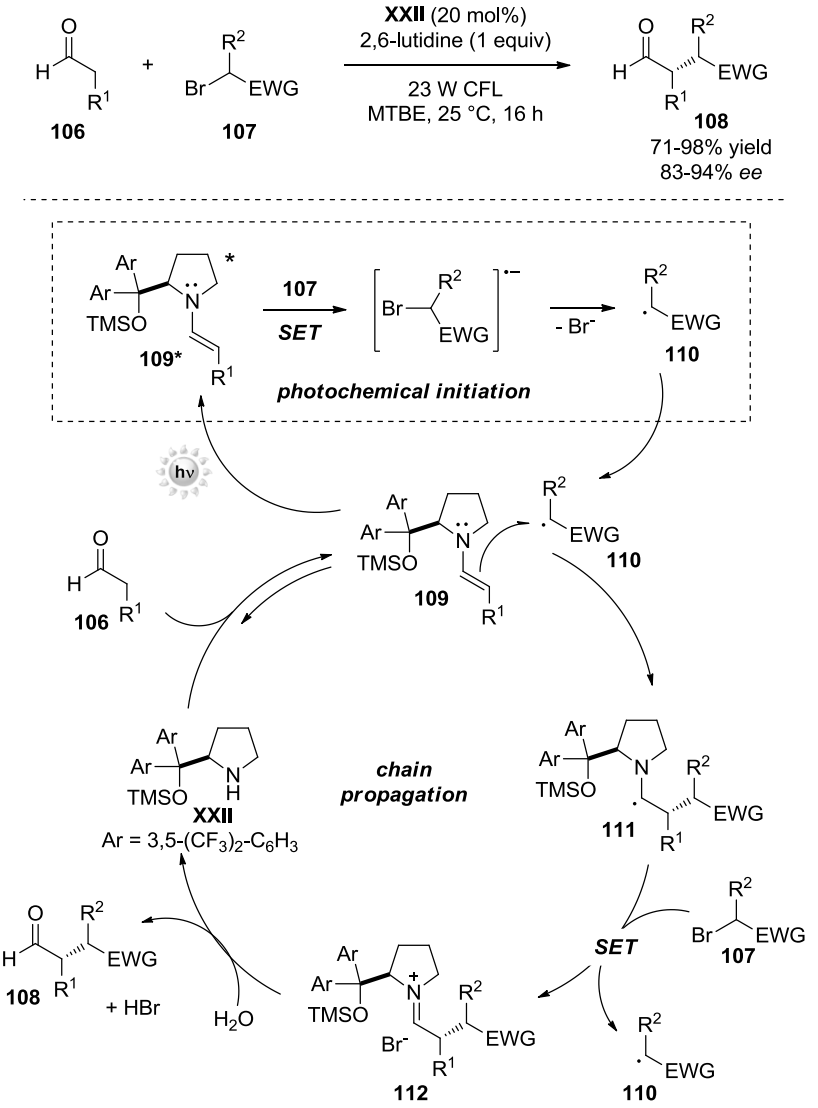

Scheme 37: Enantioselective organocatalytic α-alkylation of aldehydes driven by the direct photoexcitation of enamines and proposed mechanism.

An example of pure photo-organocatalysis is the α-functionalization of aldehydes developed by Melchiorre and co-workers. After having shown that enamines and electron-deficient benzyl bromides could form an electron donor-acceptor complex capable of absorbing visible light and triggering a photocatalytic reaction,[109a] they demonstrated that enamines themselves can undergo photoexcitation.[109b] In this transformation, depicted in *Scheme 37*, the chiral secondary amine **XXII** is employed as the catalyst to form, together with the aldehyde substrate, the enamine intermediate **109**. In the photochemical initiation step, a sacrificial amount of enamine **109** absorbs a visible photon giving rise to excited **109***. This species has a reduction potential low enough to reduce one molecule of the bromo derivative **107** to the corresponding radical anion, which upon fragmentation produces the electron-deficient radical **110**. The latter enters the chain propagation cycle and is attacked by electron-rich enamine **109** in the stereo-determining C-C bond forming step. The resulting α-amino radical **111** has the right reduction potential to reduce another molecule of **107** in a single electron transfer which allows to propagate the chain and delivers the iminium ion **112**. Hydrolysis of this intermediate affords the enantioenriched products **108** and the free catalyst **XXII**.

The studies on the capability of enamines to act as photosensitizers under visible light irradiation has played a fundamental role in the design of new photo-catalytic strategies. To date, this approach offers the possibility to carry out transformations which are not accessible to ground-state reactivity and without the employment of expensive transition metal-based catalysts.[110]

4.1.2. Asymmetric β-alkylation of carbonyl compounds

Carbonyl compounds are fundamental intermediates in organic synthesis due to their peculiar reactivity and to the transformations they can undergo to accomplish functional group interconversion. This is why many strategies for the functionalization of aldehydes and ketones have been developed,

[109] a) Arceo, E.; Jurberg, I. D.; Álvarez-Fernández, A.; Melchiorre, P. *Nat. Chem.* **2013**, *5*, 750; b) Silvi, M.; Arceo, E.; Jurberg, I. D.; Cassani, C.; Melchiorre, P. *J. Am. Chem. Soc.* **2015**, *137*, 6120.
[110] Brimioulle, R.; Lenhart, D.; Maturi, M. M.; Bach, T. *Angew. Chem. Int. Ed.* **2015**, *54*, 3872.

including enantioselective ones. In particular, the functionalization of the carbon atom at the β-position with respect to the carbonyl group requires special approaches, since that is not an activated position under ordinary conditions.

The most widely explored reaction for this purpose is the conjugate addition to α,β-unsaturated carbonyl compounds. Both transition metal-based and organocatalytic methods have been designed for asymmetric Michael additions. Among the organocatalytic ones, employment of basic or bifunctional catalysts can be mentioned together with covalent catalysis. The latter employs chiral amines as catalysts, which can form iminium ions with lowered LUMO, thus facilitating the functionalization with a nucleophile at the β-position.[111] The 1,4-addition to unsaturated carbonyl compounds can be performed with a variety of nucleophiles, including 1,3-dicarbonyl (or generally methylene-active) compounds, silyl enol ethers or hetero-atom nucleophiles (N, O, P, S).[112] To the best of my knowledge, no methodologies are available for the functionalization of α,β-unsaturated carbonyl compounds with simple alkyl groups without the employment of transition metals or organometallic reactant.

More recently, the possibility to achieve a direct β-functionalization of saturated carbonyl compounds have been investigated. This strategy, developed by Li, Wang and co-workers[113] is outlined in *Scheme 38* and relies upon the formation of an enamine intermediate thanks to the presence of a chiral amine catalyst. The enamine is then oxidized *in situ* to the corresponding iminium ion, which reacts in the classical way to afford enantioenriched β-substituted aldehydes. The reaction potentially works with the same type of nucleophiles employed for iminium-catalyzed Michael additions.

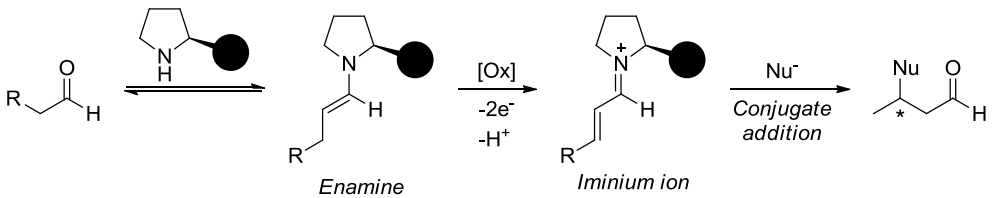

Scheme 38: Organocatalytic asymmetric β-functionalization of aldehydes by oxidation of enamines.

[111] List, B. *Chem. Commun.* **2006**, 819.
[112] Vicario, J. L.; Badía, D.; Carrillo, L. *Synthesis* **2007**, 2065.
[113] Zhang, S.-L.; Xie, H.-X.; Zhu, J.; Li, H.; Zhang, X.-S.; Li, J.; Wang, W. *Nat. Commun.* **2011**, *2*, 211.

The enamine oxidation strategy allows to circumvent the synthesis of unsaturated carbonyl compounds. However, some drawbacks must be noted. For example, a stoichiometric amount of oxidant (*o*-iodoxybenzoic acid, IBX) is needed in addition to the chiral catalyst. Moreover, a high loading (30 mol%) of amine catalyst is necessary because it is partially deactivated by its undesired oxidation operated by IBX. Again, functionalization with simple alkyl groups is not achievable through this process.

A breakthrough in the β-functionalization of aldehydes came in 2013 from MacMillan and co-workers, who exploited photoredox catalysis to perform a direct β-arylation of aldehydes.[114a] Soon after, the β-alkylation of the same substrates was also reported[114b] (*Scheme 39*). The reaction works thanks to the interconnection of two catalytic cycles (dual catalysis). The photoredox cycle involves excitation of iridium(III) catalyst **XXIII** to produce an oxidant excited species ($^*Ir^{III}$), which reduces itself to an Ir^{II} species taking an electron from the enamine **115**, formed from the condensation of the aldehyde substrate **106** and the secondary amine catalyst. The resulting nitrogen-centered radical cation **116** shows enhanced acidity at the γ-amino position which results in deprotonation and formation of radical **117**. This is the key-step in which the β-position of the aldehyde is activated. In fact, the nucleophilic radical **117** is prone to addition to the electron-deficient acceptor **113**. This carbon-carbon bond forming reaction leads to carbon-centered radical **118**, which is reduced by the Ir^{II} species via single electron transfer. This SET restores the photoredox catalyst **XXIII** and delivers the enamine of the product, which is hydrolyzed to afford the β-alkylated product **114** and the free amine catalyst. The reaction works in mild conditions, with very low photoredox catalyst loading, at room temperature and using a blue light; the alkylated products are obtained in 50-83% yield. Despite being an attractive method to get a direct β-alkylation of aldehydes, no asymmetric version of this transformation has been reported to date.

To conclude this section, we can point out that although many methods have been developed for the β-functionalization of aldehydes and ketones, at the time being there is not any organocatalytic strategy to perform an enantioselective β-alkylation of carbonyl compounds.

[114] a) Pirnot, M. T.; Rankic, D. A.; Martin, D. B. C.; MacMillan, D. W. C. *Science* **2013**, 1593; b) Terrett, J. A.; Clift, M. D.; MacMillan, D. W. C. *J. Am. Chem. Soc.* **2014**, *136*, 6858.

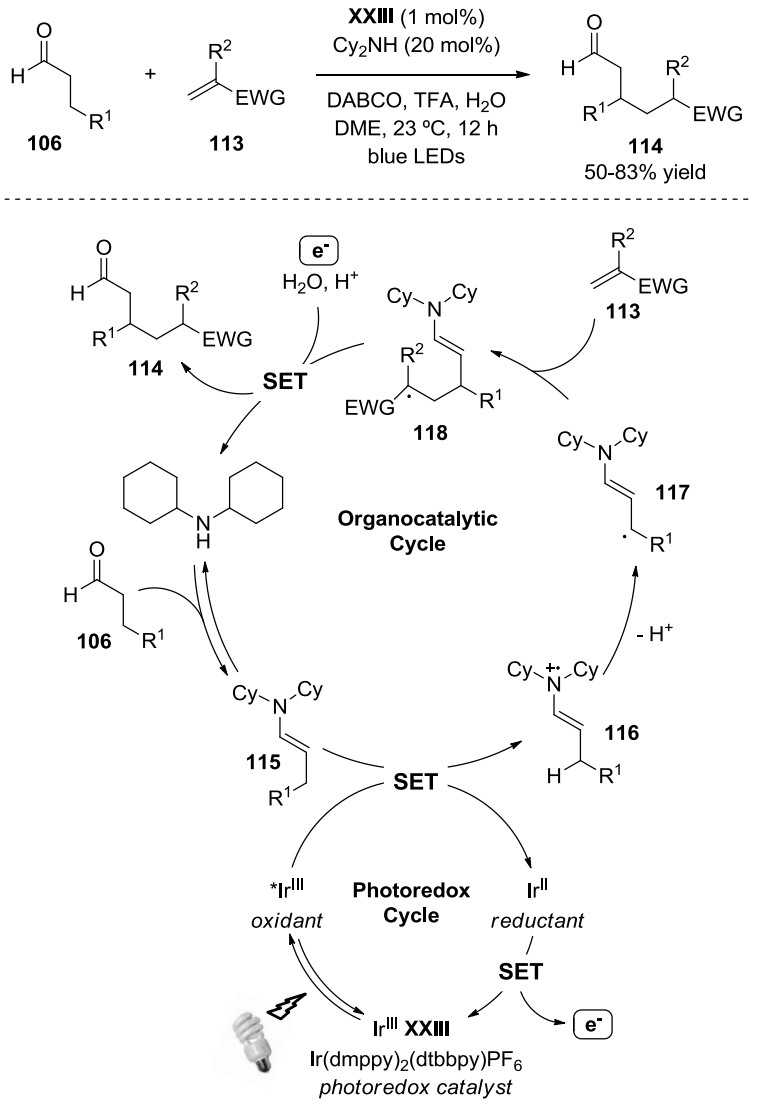

Scheme 39: Direct β-alkylation of aldehydes via photoredox organocatalysis.

4.1.3. Aim of this work

The aim of this work was the development of a new photo-organocatalytic process able to accomplish the asymmetric β-functionalization of aldehydes with simple alkyl groups. In particular we thought that iminium ions, catalytically generated by reaction of a chiral secondary amine with α,β-unsaturated aldehydes, could serve as chromophores to trigger a photochemical process which would open up reactive pathways not accessible to the ground state.

Actually, the ability of iminium ions to absorb visible light is used by Nature. In fact the excitation of the iminium ion of retinal in the photoreceptor rhodopsin, leading to *cis*/*trans* isomerization, constitutes the primary photochemical event in vision.[115] By contrast, the photo-excitation of iminium ions has found very limited application in synthetic organic chemistry and, to the best of my knowledge, it has been never applied to enantioselective catalysis. Yet, the studies of Mariano and co-workers unveiled interesting details on the photochemical properties of iminium ions.[116] For example it has been reported that they can undergo π-π* electronic transitions upon absorption of light in the near UV spectrum, at higher wavelengths with respect to the corresponding alkenes. In the case of conjugated ene-iminium ions, such as those derived from enals, a further bathochromic shift is observed and visible light can be used for the excitation of these species. Moreover, excited iminium ions possess high reduction potentials ($E_{1/2}^{\mathrm{red}}$ = 2.5-3.0 V) and therefore they are strong oxidants, prone to single electron transfer, which generates long-living (*ca* 100 ms) α-amino radicals. When excited ene-iminium ions are oxidized, the resulting γ-amino radicals are the reactive species.

Based on this, we designed the strategy outlined in *Scheme 40*. Enal **119** in the presence of a chiral secondary amine forms an iminium ion (**120**) which could be excited by visible light. In the presence of a suitable electron-donor, single electron transfer should occur to form the long-living γ-amino radical and the radical cation of the donor. If the latter is provided with a fragmenting group (FG), back electron transfer (BET) is avoided and

[115] Ernst, O. P.; Lodowski, D. T.; Elstner, M.; Hegemann, P.; Brown, L. S.; Kandori, H. *Chem. Rev.* **2014**, *114*, 126.
[116] Mariano, P. S. *Tetrahedron* **1983**, *39*, 3845.

fragmentation would lead to an alkyl radical, which would couple enantioselectively to the chiral γ-amino radical. The resulting enamine can be hydrolyzed to deliver enantioenriched β-alkylated aldehyde **121**.

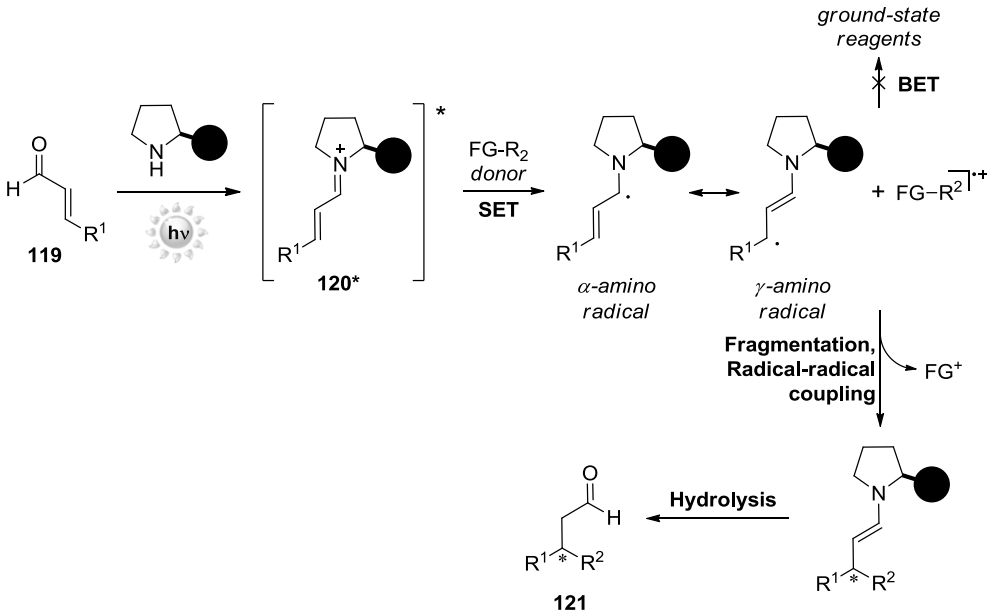

Scheme 40: Photo-organocatalytic β-alkylation of enals **119** via photoexcited ene-iminium ion **120***.

The present project involved the following:

- choice of the suitable substrates to accomplish the novel transformation depicted in *Scheme 40*;
- search for the best reaction conditions which would lead to the desired reaction;
- screening of aminocatalysts to optimize yield and enantioselectivity of the process;
- preliminary investigations of the scope of the reaction.

4.2. Results and Discussion

4.2.1. Choice of model reaction and catalyst screening

We decided to begin our investigation employing cinnamaldehyde (**119a**) as the substrate, envisioning that extended conjugation of the resulting iminium ion would lead to absorption of visible light.

As coupling partners potassium organotrifluoroborate salts (**122**) appeared to be a suitable choice. In fact, they have been reported to be excellent radical precursors in photoredox processes.[117] Upon single electron transfer, in which they act as reductants, organotrifluoroborates loose the BF_3 fragmenting group leading to carbon-centered radicals. The more stable is the resulting radical, the lower is its reduction potential, i.e. the more favored is the SET. For example potassium benzyltrifluoroborate has a reduction potential of $E_{1/2}^{\mathrm{red}}$ = 1.07 V, while potassium cyclohexyltrifluoro-borate has a reduction potential of $E_{1/2}^{\mathrm{red}}$ = 1.50 V, as the benzyl radical is more stable than the cyclohexyl one. A similar trend can be observed for tertiary, secondary and primary alkyltrifluoroborate, which possess increasing reduction potentials. Moreover, the SET rate is related to the strength of the carbon-boron bond, being the higher for C(sp^3)-B and slowing down for C(sp^2)-B and C(sp)-B species.
Potassium alkyltrifluoroborates can be easily prepared by reaction of the corresponding alkyl-Grignard reagent with trimethylborate and treatment of the resulting adduct with potassium bifluoride.[118] The products are air, moisture and shelf-stable.

We thought that a secondary alkyltrifluoroborate such as **122a** would feature intermediate properties for the study and optimization of the novel β-alkylation of enals. The model reaction, depicted in *Scheme 41*, was performed reacting cinnamaldehyde (**119a**) with potassium isopropyltrifluoroborate (**122a**) in acetonitrile, in the presence of trifluoroacetic acid and of an amine catalyst. The mixture was kept under an argon atmosphere and light was shined on the reaction vessel. In order to

[117] a) Yasu, Y.; Koike, T.; Akita, M. *Adv. Synth. Catal.* **2012**, *354*, 3414; b) Tellis, J. C.; Primer, D. N.; Molander, G. A. *Science* **2014**, *435*, 433.
[118] Sorin, G.; Martinez Mallorquin, R.; Contie, Y.; Baralle, A.; Malacria, M.; Goddard, J.-P.; Fensterbank, L. *Angew. Chem. Int. Ed.* **2010**, *49*, 8721-8723.

explore the effect of light and ensure homogeneous irradiation, monochromatic LEDs (405 nm) arranged on a flexible strip were employed. Moreover, a fan or a flux of air directed onto the sealed reaction vessel was needed to avoid overheating of the reaction environment.

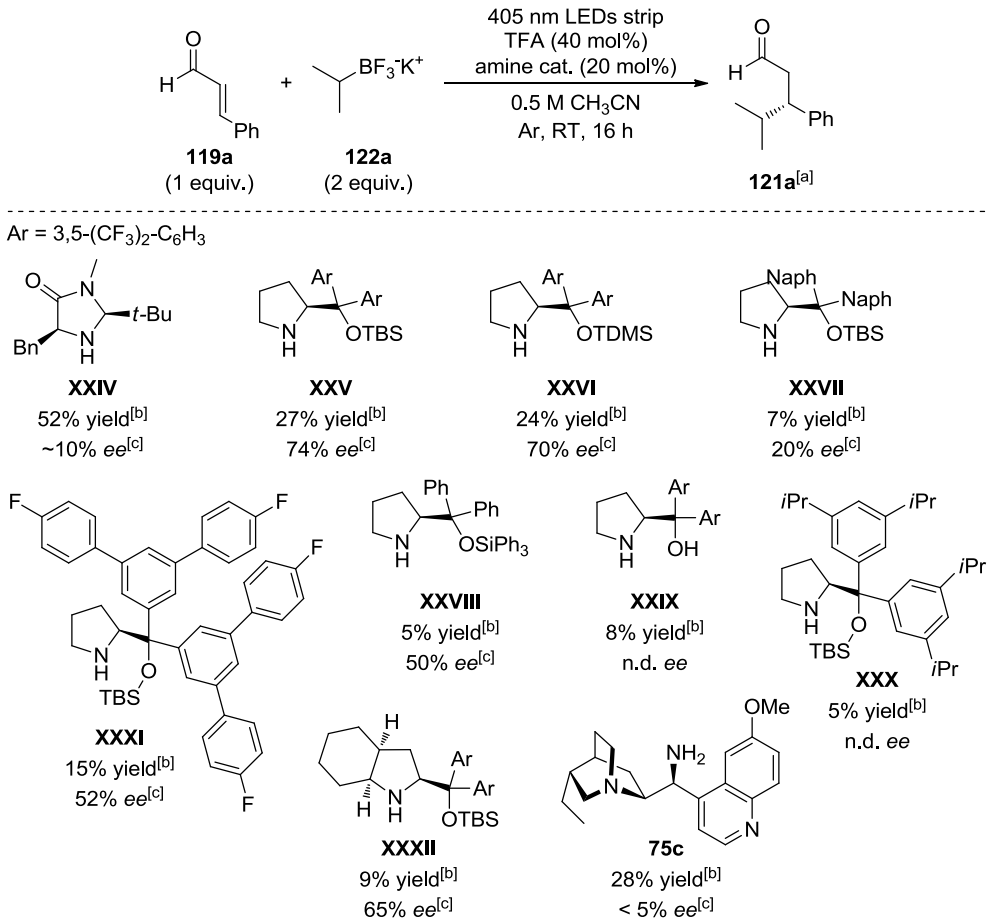

Scheme 41: Catalyst screening for the photo-organocatalytic alkylation of **119a** with **122a**. [a] Reaction performed employing 13 mg (0.10 mmol, 1 equiv) of **119a**, 30 mg (0.20 mmol, 2 equiv) of **122a** in 200 μL acetonitrile. [b] Yield was determined by ^{1}H NMR spectroscopy, by addition of trichloroethylene to the crude reaction mixture as an internal standard. [c] The *ee* of **121a** was determined on the corresponding primary alcohol obtained by reduction with $NaBH_4$. HPLC on CSP was employed, using Chiralpack IC column and *n*-hexane/*i*-propanol 97:3 (flow 0.8 mL/min).

The reaction run in the presence of imidazolidinone catalyst **XXIV** afforded the product **121a** in 52% yield after 16 h and 10% enantiomeric excess, the latter being measured on the primary alcohol derived from reduction of the product with sodium borohydride. Moving to the *tert*-butyldimethylsilyl

(TBS) diaryl prolinol catalyst **XXV** resulted in lower yield but sensibly higher enantiomeric excess (74%). We tried to improve the enantioselectivity with catalyst **XXVI**, which is provided with a bulkier *O*-protecting group (TDMS = thexyldimethylsilyl), but a worse performance was observed. Both changing the bis(trifluoromethyl)phenyl groups with naphthyl (**XXVII**) or simple phenyl (**XXVIII**) groups and deprotection of the hydroxyl functionality (**XXIX**) resulted in low yield (< 10%) and low enantiomeric excess (≤ 50%). We prepared and tested the new catalysts **XXX** and **XXXI**: the former showed very low reactivity and the latter did not lead to any improvement. These observations suggest that substitution of the aryl rings with electron-withdrawing groups and protection of the hydroxyl moiety both play a crucial role in determining the activity of the catalyst. We tried to replace the pyrrolidine ring with a perhydroindole (catalyst **XXXII**), but this resulted in formation of the product in low yield (9%). Finally we observed that primary amines, such as **75a**, despite catalyzing the reaction (up to 28% yield) were not able to exert stereochemical control.

After this screening we identified TBS-protected diaryl prolinol **XXV** as the best catalyst and we used it for the optimization of the other reaction parameters.

4.2.2. Optimization of the reaction conditions

The first parameter we considered in order to optimize the outcome of our reaction was the solvent. Since the chiral aminocatalyst covalently binds to the substrate, a minor effect of the solvent was expected on the stereoselectivity of the process and indeed the yield was the most affected variable. As reported in *Table 8*, acetonitrile, which is commonly employed in photochemical reactions, was the best solvent (entry 1) with 27% yield and 74% *ee*. Adding water to the reaction mixture resulted in higher yield (entry 3) but considerably lower enantioselectivity. The enhanced reactivity could be explained considering the capability of water to act as a nucleophile towards the trifluoroborate radical catalyzing its fragmentation; this kind of effect has been described for the fragmentation of silane radical cations.[119] None of the other solvent tested performed better, with apolar solvents such

[119] Dockery, K. P.; Dinnocenzo, J. P.; Farid, S.; Goodman, J. L.; Gould, I. R.; Todd, W. P. *J. Am. Chem. Soc.* **1997**, *119*, 1876.

as dichloromethane (entry 4), toluene (entry 6) and methyl-*tert*-butyl ether (entry 7) standing out for the low yield afforded. The very viscous ethylene glycol in combination with acetonitrile led to formation of the product in only 3% yield (entry 9).

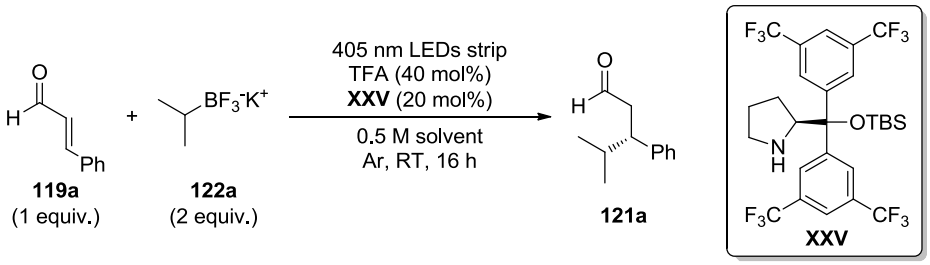

Entry[a]	Solvent	Yield (%)[b]	*ee* (%)[c]
1	MeCN	27	74
2	MeCN/water 3:1	26	64
3	MeCN/water 1:1	33	64
4	DCM	6	n.d.
5	Dioxane	11	63
6	Toluene	7	n.d.
7	MTBE	6	61
8	THF	20	62
9	MeCN/$HO(CH_2)_2OH$ 1:1	3	n.d.

Table 8: Solvent screening for the photo-organocatalytic alkylation of **119a** with **122a**. [a], [b], [c]: see notes to *Scheme 41*.

We then investigated the effect of the acid cocatalyst on the yield and enantioselectivity of the reaction (*Table 9*). The acid is necessary in this reaction to catalyze the formation of the iminium ion, which is the photoactive species. In the absence of an acidic cocatalyst (*Table 9*, entry 9), no reaction took place. Trifluoroacetic acid is commonly employed in iminium ion catalysis and we screened the effect of different amounts with respect to the limiting reagent (entries 1-4). The best results were obtained with an amount of acid which was twice the catalyst loading (40 mol%, entry 2). We then observed that the conversion of cinnamaldehyde **119a**, observed with ^{1}H NMR spectroscopy of the crude reaction mixture, was often higher than the yield of product **121a**. We therefore inverted the stoichiometric ratio of the two reactants. In the presence of an excess of cinnamaldehyde, the yield almost doubled (45%, entry 6) with no effect on the enantiomeric excess. In these new conditions, we tested some inorganic acids such as perchloric or phosphoric acid (entries 7-8), which always had a detrimental

effect on the enantioselectivity. It is worth noting that running the reaction in the absence either of light (entry 10) or of the amine catalyst (entry 11) did not yield the product, strongly indicating that the photoexcitation of the catalytically generated iminium ion is the key event to trigger the reaction.

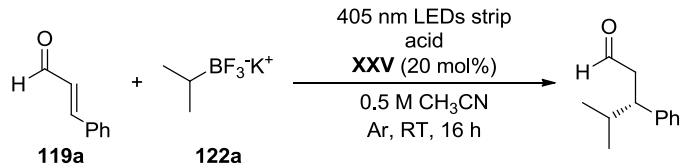

Entry[a]	Stoichiometry (119a:122a)	Acid (mol%)	Yield (%)[b]	*ee* (%)[c]
1	1:2	TFA (20)	24	74
2	1:2	TFA (40)	27	74
3	1:2	TFA (60)	19	72
4	1:2	TFA (100)	15	71
5	2:1	TFA (40)	44	74
6	3:1	TFA (40)	45[d]	74
7	3:1	$HClO_4$ (40)	20	29
8	3:1	H_3PO_4 (40)	22	67
9	1:2	None	0	-
10[e]	3:1	TFA (40)	0	-
11[f]	3:1	TFA (40)	0	-

Table 9: Effect of acid and reagents stoichiometry on the photo-organocatalytic alkylation of **119a** with **122a**. [a], [b], [c]: see notes to *Scheme 41*. [d] Isolated yield. [e] Reaction performed in the dark. [f] Reaction performed without amine catalyst **XXV**.

Despite the efforts to increase the efficiency of the reaction, we could not obtain the product with yield higher than 45% overnight. Longer reaction times resulted in slightly higher yield, but with erosion of enantiomeric excess. Moreover, formation of by-products and degradation of the aldehyde substrate was observed. We therefore examined in depth the possible reactive pathways which would lead to degradation of the substrates or deactivation of the catalyst. In order to isolate the by-products, we ran the reaction depicted in *Scheme 42*, employing an excess of cinnamaldehyde **119a**, 1 equivalent of amine catalyst **XXV** and 2 equivalents of trifluoroacetic acid. The desired product **121a** was isolated in 32% yield. We also isolated the addition by-product **123** and the benzophenone **124**.

Moreover, a complex mixture of inseparable compounds, probably derived from degradation of cinnamaldehyde **119a** was obtained.

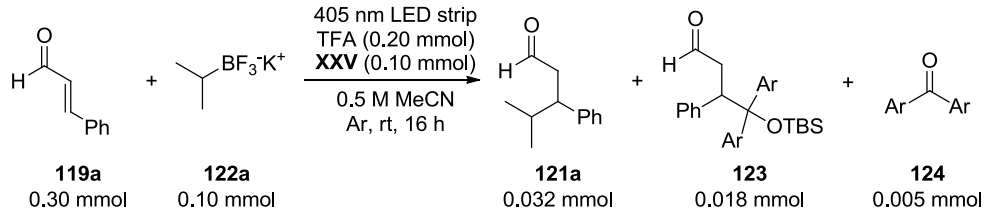

Scheme 42: Isolation of by-products of the photo-organocatalytic isopropylation of **119a**.

The possible reaction pathways leading to by-products **123** and **124** are depicted in *Scheme 43*. As already said, the photoexcited iminium ion **120*** can act as a strong oxidant. In the desired reactivity (reported in black) it oxidizes the trifluoroborate **122a** forming the alkyl radical **125**, which upon coupling delivers the product **121a**. However, **123** and **124** clearly derive from fragmentation of the catalyst. One possible explanation is the oxidation of the free catalyst **XXV** (red pathway), leading to amino radical cation **XXV**$^{+\cdot}$, which could fragment and produce either the addition by-product **123**, upon radical-radical coupling, or benzophenone **124**, upon desilylation. This process is thermodynamically allowed, as the catalyst **XXV** has a reduction potential[109b] similar to that of the alkyltrifluoroborate.[117a]

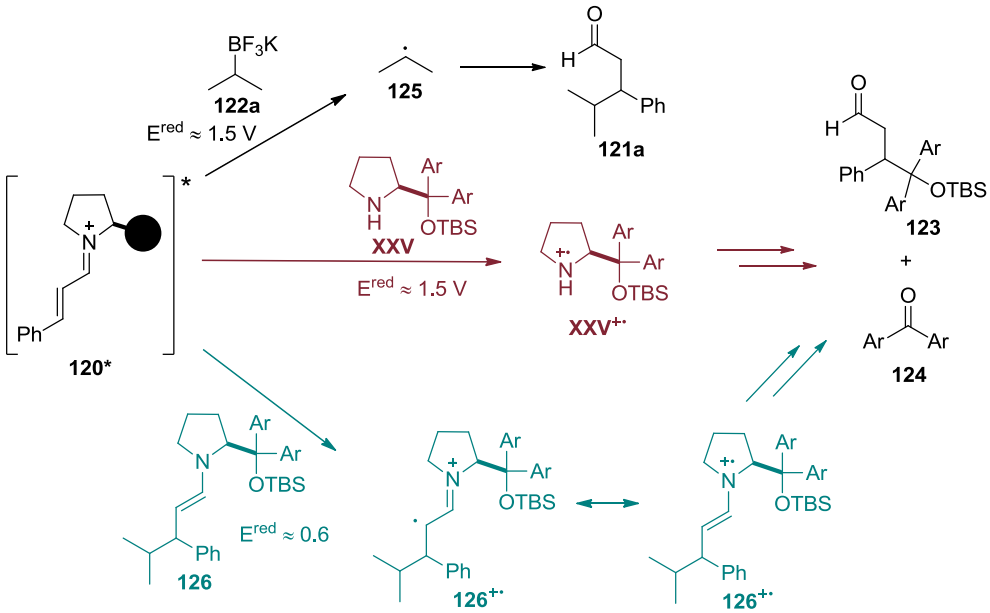

Scheme 43: Possible reactive pathways leading to by-products **123** and **124**.

However, it should be noted that the presence of an excess of trifluoroacetic acid in the reaction mixture, should make the amine catalyst to be fully protonated and this would result in an increase of its reduction potential, favoring the reduction of the trifluoroborate instead. Therefore, a more plausible mechanism would be that outlined in blue in *Scheme 43*. In fact, at the end of the catalytic cycle, the enamine of the product (**126**) is formed and it is known that this electron-rich species has a low reduction potential,[109b] which would account for its oxidation by the excited iminium ion **120***. Moreover, it has been reported that branched iminyl radicals like **126**$^{+\cdot}$ can fragment in several ways, including at the α-position with respect to the nitrogen atom.[120] This would lead to the reactive species generating **123** and **124** and to an achiral pyrrolidine moiety. If the latter can enter the catalytic cycle, it would result in a non-stereoselective reaction: this hypothesis is in line with the observed erosion of enantioselectivity for longer reaction times.

Having fully characterized the main by-products of the reaction, it was possible to easily estimate their presence from the ^{1}H NMR spectra of the crude reaction mixtures. Selected results, for different reaction conditions are reported in *Table 10*. When the limiting reagent was cinnamaldehyde (entries 1-2) the degradation of the catalyst was quite slow: after 16 hours all the catalyst **XXV** was still present and after 63 hours 12 mol% of catalyst was there. However, the degradation of cinnamaldehyde limits the yield: after 63 hours only 2% of **119a** was still present in the reaction mixture and the yield of the product **121a** is 45% (entry 2). Reverting the stoichiometry (3 equiv of cinnamaldehyde and 1 equiv of trifluoroborate **122a**) led to a much faster degradation of the catalyst. After 16 hours it was possible to obtain a yield of 45% of **121a**, but only 12 mol% of catalyst left, the rest having degraded into by-product **123** (entry 3). After more than 60 hours almost all the catalyst was destroyed and converted into by-product **123** and the yield of product **121a** was 53% (entry 4). In this case, the enantiomeric excess of the product was only 69%, probably because of the aforementioned non-stereoselective reaction arising from catalyst degradation. Employing light of higher wavelength (blue LEDs or white LEDs) made the catalyst degradation slower, although the yield of **121a** was very low: after 63 hours 17 mol% of the catalyst was still there and 10-13% of product was obtained

[120] Jakobsen, H. J.; Lawesson, S.-O.; Marshall, J. T. B.; Schroll, G.; Williams, D. H. *J. Chem. Soc. B* **1966**, 940.

(entries 5-6). Finally, running the reaction in the absence of the trifluoroborate **122a** (entry 7), the reaction between the catalyst **XXV** and cinnamaldehyde was observed with half the catalyst converted into by-product **123**.

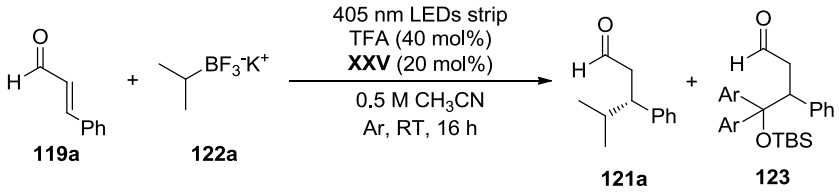

119a **122a** **121a** **123**

Entry	Time (h)	Yield of 121a (%)[c]	*ee* of 121a (%)[d]	Yield of 123 (%)[c]	XXV left (mol%)[c]
1[a]	16	27	74	0	20
2[a]	63	45	74	6	12
3[b]	16	45[e]	74	8	12
4[b]	68	53[e]	69	15	3
5[b,f]	63	10	75	2	17
6[b,g]	63	13	75	2	17
7[b,h]	16	-	-	10	10

Table 10: Catalyst degradation in various reaction conditions. [a] Reaction performed employing 13 mg (0.10 mmol, 1 equiv) of **119a**, 30 mg (0.20 mmol, 2 equiv) of **122a** in 200 μL acetonitrile. [b] Reaction performed employing 40 mg (0.30 mmol, 3 equiv) of **119a**, 19 mg (0.10 mmol, 1 equiv) of **122a** in 200 μL acetonitrile. [c] Determined by ^{1}H NMR spectroscopy, see note b to *Scheme 41*. [d] See note c to *Scheme 41*. [e] Isolated yield. [f] Blue LEDs strip (465 nm) was employed. [g] White LEDs strip (5000 K) was employed. [h] Reaction performed without the trifluoroborate **122a**.

On the basis of these observations we can conclude that the excess of trifluoroborate **122a** delays catalyst degradation, probably due to the higher probability of the oxidation of the trifluoroborate instead of the catalyst **XXV** or the enamine **126**. However, the degradation of cinnamaldehyde (that would be the limiting reagent) has to be solved: substituted cinnamaldehydes could act in a different way thus leading to higher yields. Moreover, higher wavelengths delay catalyst and cinnamaldehyde degradation, although with lower yields, due to minor absorption of the iminium ion. However, high power LEDs could be able to exploit efficiently this little absorption of the iminium ion leading to the product and avoiding side-reactions. Also the design of new chiral catalysts could help in tuning the reduction potentials of the species involved in the reaction, suppressing undesired reactivity.

Studies are still ongoing to completely optimize the reaction conditions in order to obtain higher yields and improve the enantioselectivity of the process.

4.2.3. Preliminary reaction scope

While going on with the optimization studies, we started to preliminary explore the scope of our new asymmetric photo-organocatalytic alkylation of enals. As depicted in *Scheme 44*, cinnamaldehyde (**119a**) was reacted with potassium alkyltrifluoroborates **122a-h**, in the presence of the chiral amine catalyst **XXV** and trifluoroacetic acid as cocatalyst. The light source employed was a strip of LEDs with emission centered at 405 nm.

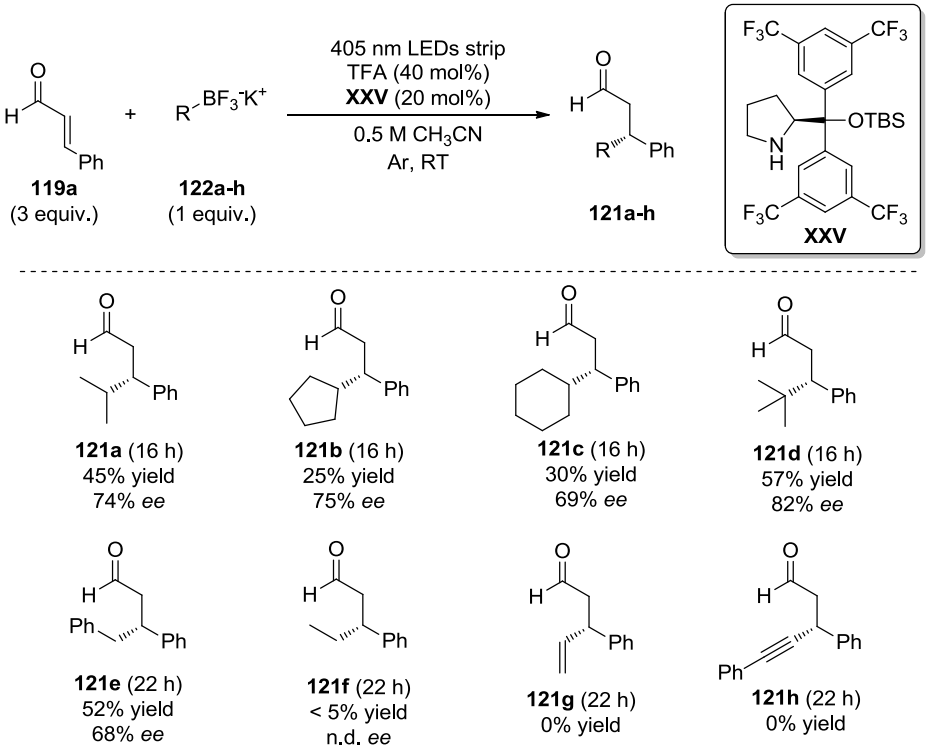

Scheme 44: Preliminary scope of the asymmetric photo-organocatalytic alkylation of cinnamaldehyde (**119a**) with potassium alkyltrifluoroborates **122a-h**. [a] Reactions performed employing 1.0 equiv of **122a-h** (0.10 mmol), 3.0 equiv of **119a** (0.30 mmol, 40 mg), 0.20 equiv of **XXV** (0.020 mmol, 12 mg), 0.40 equiv of TFA (0.040 mmol, 5 mg) and 200 μL of acetonitrile.

The reaction works very similarly for secondary alkyltrifluoroborates **122a-c**, allowing to functionalize cinnamaldehyde with a cyclopentyl and a cyclohexyl group, in addition to isopropyl (25-45% yield, 69-75% *ee*). The higher stability of tertiary *tert*-butyl radical accounts for the higher yield observed for **121d**: in this case the enantiomeric excess was also higher (82%), which is consistent with the greater steric hindrance of this group. A similar reactivity was shown by benzyltrifluoroborate **122e**, which readily produces the stabilized benzyl radical and afforded product **121e** in 52% yield and 68% *ee*.[121] Under the conditions so far developed, it was not possible to get significant reactivity with primary alkyl-, alkenyl- and alkynyltrifluoroborates, which yielded little or nothing of products **121f-h**. This is in accordance with low stability of primary alkyl radicals and with the low single electron transfer rate expected for C(sp^2)-B and C(sp)-B species, as discussed in *Section 4.2.1*.

The absolute configuration of the products was determined by comparison of the optical activity shown by compounds **121a**,**c-d** with literature reported data (see experimental section for details).

[121] Functionalization of cinnamaldehyde with "stabilized" alkyl groups have been accomplished in Melchiorre's group employing silanes (including benzyltrimethylsilane) as reaction partners: Buzzetti, L.; Silvi, M.; Verrier, C.; Melchiorre, P., *submitted*.

4.3. Summary of the Chapter

In this work a new photo-organocatalytic reaction has been developed in order to accomplish the first asymmetric β-functionalization of aldehydes with simple alkyl groups without the employment of metals. In particular the ene-iminium ion catalytically generated by reaction of a proline-derived catalyst with cinnamaldehyde has been shown to act as a chromophore. It can absorb visible light, accessing an excited state in which it can oxidize, via single electron transfer, potassium alkyltrifluoroborates, which are radical precursors. Subsequent radical-radical coupling leads to stereoselective alkylation of the aldehyde.

The model reaction between cinnamaldehyde (**119a**) and potassium isoporpyltrifluoroborate (**122a**) was extensively studied. The best reaction conditions, in terms of the amine catalyst and the acidic cocatalyst employed, the solvent, the reaction time and the light source were identified. Under these conditions, the asymmetric alkylation of cinnamaldehyde was accomplished with several secondary alkyl groups and with a tertiary alkyl and a benzyl group (25-57% yield, 68-82% *ee*).

Moreover, the main issues for the development of a fully efficient process, in terms of yield and enantioselectivity, were pointed out, isolating the main by-products of the reaction and quantifying their presence in diverse reaction conditions. Studies are still ongoing in Prof. Melchiorre's group in order to overcome these problems.

Future developments of this project may include:

- extension of the reaction to the functionalization of enals with primary alkyl, alkenyl and alkynyl groups;
- study of the reaction with different enals, including β-branched enals, which would lead to the formation of a quaternary stereogenic center;
- application of this strategy to the direct excitation of ketone-derived iminium ions: a specifically designed catalytic system could allow the first asymmetric photo-organocatalytic β-alkyaltion of α,β-unsaturated ketones.

5. Other Publications during the Ph.D.

5.1. Focus Review: Alkynes in Organocatalysis

During my Ph.D. work I contributed to the writing of a focus review presenting the employment of alkynes as substrates in organocatalyzed transformations.[122]

Alkynes are organic moieties with a wide diffusion in nature; over the last two centuries more than a thousand naturally occurring acetylenes have been reported. Moreover, alkynes can be employed in several useful synthetic transformations. Besides the capability of terminal acetylenes, thanks to their acidity, of being converted into metal acetylides to be used for electrophiles functionalization, alkynes can undergo most of the typical transformations of alkenes. Addition of hydrogen, halogens and related reagents, or cycloadditions and oxidations reactions are some examples of possible modifications involving both double and triple bonds.

Despite the enhanced reactivity of alkynes with respect to alkenes, the latter still find wider application in organic chemistry, as testified by the number of reports dealing with them. Two main reasons may be given to explain this. The first one is related to the fact that only few alkynes are currently commercially available and a quick search on a chemicals supplier's catalogue shows that triple-bond containing molecules are far more expensive than their olefin analogues. The second reason may be the high reactivity of alkynes itself, as it could represent a potential issue for their use and storage. This is why they have found also limited application as active pharmaceutical ingredients, with some noteworthy exceptions, such as the contraceptive norethynodrel, the antiretroviral efavirenz or the antitumor calicheamicin.

On the other hand, it should be considered that the high reactivity of alkynes could be also a great advantage, especially in asymmetric synthesis, where higher stereocontrol is achieved lowering the reaction temperature. Moreover, it is worth noting that the carbon-carbon triple bond can be easily converted into other functionalities. Therefore exploitation of alkynes reactivity and subsequent removal of this moiety could be a convenient strategy, also in the preparation of a drug.

[122] Salvio, R.; Moliterno, M.; Bella, M. *Asian J. Org. Chem.* **2014**, *3*, 340.

Many authors have already reported promising results exploiting the reactivity of alkynes and we believe that in the future their synthetic potential will be further and successfully exploited in a growing number of transformations. Moreover, if the demand of alkynes increases their availability will increase consequently and their price will decrease, thus overcoming one of the limiting reasons for their application.

Considering these aspect, we felt it was useful to present a critical selection of applications of alkynes as nucleophiles or electrophiles in the growing field of organocatalyzed asymmetric reactions. We therefore wrote the focus review "Alkynes in Organocatalysis", which can be found herein among the articles reprint, with the hope that it could be informative and inspiring for the development of novel transformations and research lines. In this review, the reaction discussed are classified on the basis of the kind of catalysis employed. Both non-covalent strategies, including base, phase-transfer and bifunctional catalysis, and covalent approaches, including enamine, iminium ion, carbene and phosphine catalysis, are presented in the review. Two special sections also deal with non-asymmetric organocatalytic reactions, given that chiral compounds are not the only valuable ones which can be conveniently prepared employing organocatalysis, and with multiple catalysis, in which at least two catalysts with different operating mechanisms are used to accomplish one reaction in a synergistic way.

5.2. Book Chapter: Organocatalyzed Addition to Activated C=C Bonds

During my Ph.D. work I contributed to the writing of a chapter for Science of Synthesis Reference Library, a collection of volumes edited by Thieme which covers special topics of organic chemistry. The work presented in the present section was published in the volume "Applications of Domino Transformations in Organic Synthesis 2".[123]

Domino reactions are chemical transformations in which two or more consecutive transformations take place in the same reaction conditions,

[123] Renzi, P.; Moliterno, M.; Salvio, R.; Bella, M. "Organocatalyzed addition to activated C=C bonds" in *Applications of domino transformations in organic synthesis 2*, Science of Synthesis, Georg Thieme Verlag KG, Stuttgart, **2016**, 337-386.

without addition of reagents. Each subsequent reaction step occurs thanks to the functionalities formed in the previous step(s). These cascade processes are advantageous because complex products can be obtained from simple starting material, with no need for isolation of reaction intermediates and for additional operations before the final work-up. Organocatalytic strategies have been developed to carry out domino transformations, so that highly functionalized, enantioenriched compounds can be easily prepared in mild operational conditions and with the already discussed advantages of organocatalysis.

This book chapter highlights and critically discusses some selected examples of organocatalyzed domino reactions involving activated carbon-carbon double bonds. A review of the first ground-breaking examples is presented, concerning processes with consecutive enamine-iminium ion catalytic cycles on α,β-unsaturated carbonyl compounds. Subsequently more specific applications from the chemistry of oxindoles are discussed together with large-scale domino transformations. The latter include the syntheses of (-)-oseltamivir, a neuroamidase inhibitor commercialized under the name of Tamiflu for the treatment of type A and B human influenza, and ABT-341, a drug applied in the therapy of type-2 diabetes, and industrial-scale processes for the synthesis of chiral diene ligands.

6. Conclusions

In this thesis three works have been presented dealing with new strategies in organocatalyzed asymmetric synthesis.

The first work reported is the quinine-catalyzed atroposelective coupling between 2-naphthols **38a-f** and 1,4-benzoquinones **51b-g**, affording enantiomerically enriched biaryl compounds **52d-t** (*Scheme 45*). This transformation is one of the very few available strategies for the asymmetric synthesis of biaryls through a direct coupling without the employment of transition metals. We have demonstrated the feasibility of the reaction on gram-scale, obtaining the products in near enantiopurity upon recrystallization. Moreover, the rotational barrier required to have two stable atropisomers was investigated by means of *ab initio* calculations and HPLC analysis on chiral stationary phase

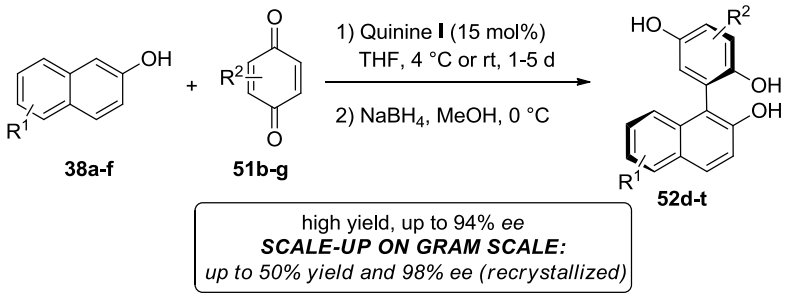

Scheme 45: Summary of quinine-catalyzed atroposelective biaryl coupling.

The second project dealt with the development and application of a new class of bifunctional organocatalysts based on the versatile *Cinchona* alkaloid scaffold; their general structures are shown in *Figure 22*. The presence of both a tertiary amine in the quinuclidine ring and a guanidine group can give rise to a bifunctional mode of activation.

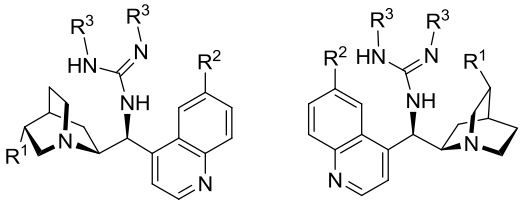

Figure 22: Novel *Cinchona* alkaloid-based guanidines.

These novel guanidines were tested in potentiometric, kinetic and *ab initio* experiments as catalysts in the intramolecular transesterification of 2-hydroxypropyl *p*-nitrophenyl phosphate (HPNP). Results indicate that our guanidines can catalyze the reaction performing a kinetic resolution of the substrate, via a bifunctional activation mode. Moreover these guanidine catalysts have been being

applied to a new enantioselective and highly diastereoselective vinylogous aldol reaction between α-keto esters and γ-butenolides. At the time being, moderate yields and enantiomeric excess have been achieved, but the far better performances of the new guanidines with respect to already available catalysts are encouraging for further developments.

Finally, working for six months in the group of Prof. Paolo Melchiorre at Institut Català d'Investigació Quimica in Tarragona (Spain), I had the opportunity to investigate a new photo-organocatalytic process. We have used catalytically generated iminium ions as chromophores to trigger the photochemical β-alkylation of cinnamaldehyde (*Scheme 46*). This transformation cannot be achieved through the classical thermal reactivity of iminium ions. We have demonstrated that under visible light irradiation, the radical precursors trifluoroborates **122a-e** can act as donors towards the excited iminium ion (**119a** + chiral amine catalyst) in a single electron transfer process. The resulting alkyl and α-amino radicals then couple in an enantioselective fashion to afford the products **121a-e**. I have extensively studied the reaction conditions in order to optimize yield and enantioselectivity. The main by-products of the reaction have been isolated and identified and a rationale for their formation together with possible strategies to avoid it have been formulated. Work is still ongoing in Melchiorre's group to optimize the yield and the stereochemical outcome of this new reaction.

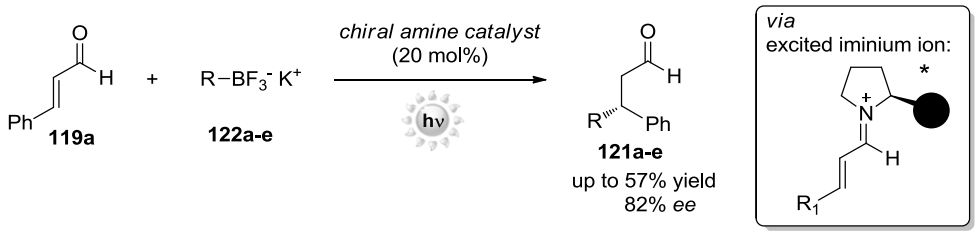

Scheme 46: Photo-organocatalyzed asymmetric β-alkylation of cinnamaldehyde.

Moreover, I contributed to the writing of a focus review about alkynes in organocatalysis, which is herein reproduced, and of a book chapter about domino organocatalyzed additions to activated double bonds.

7. Experimental Section

7.1. General methods

^{1}H NMR and ^{13}C NMR spectra were recorded at 300 MHz and 75 MHz (Varian spectrometer), at 400 MHz and 100 MHz (Bruker spectrometer) or at 500 MHz and 125 MHz (Bruker spectrometer) respectively. Chemical shifts are reported in ppm relative to the resonance of $CDCl_3$ (δ= 7.26), CD_3OD (δ= 3.31) or DMSO-d_6 (δ= 2.50) for ^{1}H NMR and to the central peak of $CDCl_3$ (δ= 77.5), CD_3OD (δ= 49.0) or DMSO-d_6 (δ= 39.5) for ^{13}C NMR. Signal multiplicity is indicated by the following symbols: s (singlet), d (doublet), t (triplet), q (quartet), dd (double doublet), dt (double triplet), ddd (double doublet of doublets), tt (triple triplet), hept (heptuplet), m (multiplet), bs (broad singlet), br (broad signal).
Flash chromatography (FC) was carried out using Merck silica gel 60 (230-400 mesh).
Enantiomeric excess (*ee*) of the products was determined by HPLC employing a Daicel CHIRALPAK IA, IB, IC, ID, IF or AS-H column, mixtures of *n*-hexane/*i*-propanol as eluent and PDA (photo diode array) or single wavelength UV detector.
HRMS analyses were carried out with a Micromass ESI Q-TOF insturment.

All analytical grade solvents were used as received. All commercially available reagents and catalysts were used as received.

7.2. Preparation of the Organocatalysts

Organocatalysts **I-IV**, **VIII-X**, **XIII** and **XXIV** are commercially available and were used as received. Organocatalysts **V-VII**, **XII** and **XIX** were used as received from Prof. Bella's collection. Organocatalysts **XXVI-XXVIII** and **XXII** were used as received from Prof. Melchiorre's collection.

7.2.1. Amino derivatives of Cinchona alkaloids 75a-f and epi-75a

7.2.1.a. Synthesis and characterization of 9-amino(9-deoxy)*epi*-*Cinchona* alkaloids 75a-e

Amino derivatives **75a-e** were prepared following the procedure reported by Melchiorre *et al.*,[84] as outlined in *Scheme 22*.

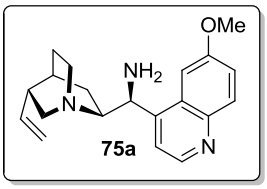

***epi*-aminoquinine (75a).** Amber-colored viscous oil; 4.8 g, 96% yield (reaction performed on 5.0 g of quinine **I**).

^{1}H NMR (300 MHz, $CDCl_3$): δ 8.70 (d, 1H; *J* = 5.0 Hz), 8.00 (d, 1H; *J* = 9.0 Hz), 7.60 (bs, 1H), 7.38-7.45 (m, 1H), 7.34 (dd, 1H; *J* = 9.0, 6.0 Hz), 5.75 (ddd, 1H; *J* = 17.0, 10.0, 7.5 Hz), 4.50-4.60 (m, 1H), 3.90 (s, 3H), 2.95-3.20 (m, 3H), 2.60-2.90 (m, 2H), 2.17-2.30 (m, 1H), 2.40 (bs, 2H), 1.30-1.62 (m, 4H), 0.65-0.80 (m, 1H).

^{13}C NMR (75 MHz, $CDCl_3$): δ 157.5, 147.7, 146.7, 144.6, 141.4, 131.7, 128.5, 121.1, 119.8, 114.4, 101.8, 61.7, 56.0, 55.4, 52.4, 40.8, 39.5, 27.9, 27.4, 25.8.

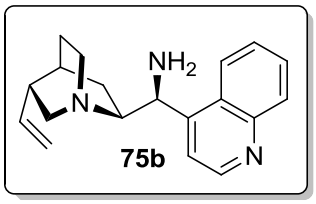

***epi*-aminocinchonidine (75b).** Amber-colored viscous oil; 4.8 g, 96% yield (reaction performed on 5.0 g of cinchonidine **III**).

^{1}H NMR (300 MHz, $CDCl_3$): δ 8.84 (d, 1H; *J* = 4.4 Hz), 8.29 (bs, 1H), 8.06 (d, 1H; *J* = 8.2 Hz), 7.63 (t, 1H; *J* = 7.6 Hz), 7.55-7.44 (m, 2H), 5.71 (ddd, 1H; *J* = 17.6, 9.8, 8.1 Hz), 5.02-4.84 (m, 2H), 4.64 (d, 1H; *J* = 9.1 Hz), 3.34-2.94 (m, 3H); 2.87-2.63 (m, 2H), 2.41 (s, 2H), 2.20 (bs, 1H), 1.53-1.46 (m, 3H), 1.34 (t, 1H; *J* = 11.1 Hz), 0.67 (dd, 1H; *J* = 13.3, 7.5 Hz).

^{13}C NMR (75 MHz, $CDCl_3$): δ 150.3 (2C), 148.5, 141.5, 130.4, 128.9, 127.7, 126.4, 123.3, 119.6, 114.4, 61.8, 56.1, 40.9, 39.6, 27.9, 27.5, 25.9.

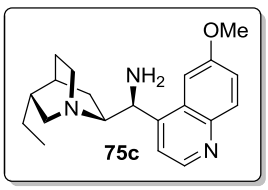

***epi*-aminohydroquinine (75c).** Amber-colored viscous oil; 1.1 g, 73% yield (reaction performed on 1.5 g of hydroquinine **IV**).

^{1}H NMR (300 MHz, $CDCl_3$): δ 8.72 (d, 1H; *J* = 4.4 Hz), 8.01 (d, 1H; *J* = 9.2 Hz), 7.64 (bs, 1H), 7.45 (d, 1H; *J* = 3.8 Hz), 7.36 (dd, 1H; *J* = 9.1, 2.3 Hz), 4.57 (d, 1H; *J*= 9.5 Hz), 3.95 (s, 3H), 3.28-3.15 (m, 2H), 3.09-3.00 (m, 1H), 2.80-2.72 (m, 2H), 2.60-2.48 (m, 3H), 1.57-1.24 (m, 8H), 0.80 (t, 3H; *J* = 7.3 Hz).

^{13}C-NMR (75 MHz, $CDCl_3$): δ 157.7, 147.9, 147.3, 144.8, 131.9, 128.9, 121.3, 120.0, 102.2, 61.9, 58.0, 55.7, 41.2, 37.6, 28.9, 27.7, 25.9, 25.3, 12.1.

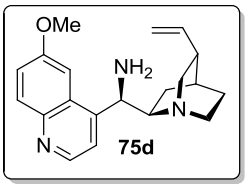

***epi*-aminoquinidine (75d).** Amber-colored viscous oil; 0.81 g, 41% yield (reaction performed on 2.0 g of quinidine **II**).

^{1}H NMR (300 MHz, $CDCl_3$): δ 8.73 (d, 1H; *J* = 4.6 Hz), 8.00 (d, 1H; *J* = 9.2 Hz), 7.58-7.51 (m, 2H), 7.36 (dd, 1H; *J* = 9.2, 2.6 Hz), 5.87 (ddd, 1H; *J* = 17.1, 10.7, 6.5 Hz), 5.07 (d, 1H; *J* = 7.3 Hz), 5.02 (s, 1H), 4.66 (d, 1H; *J*= 9.7 Hz), 3.95 (s, 3H), 3.07-2.89 (m, 5H), 2.30-2.15 (m, 3H), 1.59-1.50 (m, 3H), 1.16-1.09 (m, 1H), 0.98-0.83 (m, 1H).

^{13}C NMR (75 MHz, $CDCl_3$): δ 157.8, 147.9, 147.6, 144.9, 140.9, 131.9, 128.8, 121.7, 120.1, 114.6, 101.7, 62.5, 55.6, 49.7, 47.6, 39.6, 27.7, 26.8, 25.1.

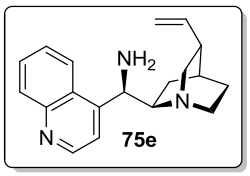

***epi*-aminocinchonine (75e).** Amber-colored viscous oil; 3.6 g, 72% yield (reaction performed on 5.0 g of cinchonine **XIII**).

^{1}H NMR (300 MHz, $CDCl_3$): δ 8.87 (d, 1H; *J* = 4.5 Hz), 8.32 (bs, 1H), 8.11 (d, 1H; *J* = 8.4 Hz), 7.70 (d, 1H; *J* = 8.0 Hz), 7.58-7.53 (m, 2H), 6.10-5.47 (ddd, 1H), 5.07 (s, 1H), 5.02 (d, 1H; *J* = 8.1 Hz), 4.73 (d, 1H; *J* = 9.5 Hz), 3.07-2.83 (m, 6H); 2.36-2.20 (m, 3H), 1.56-1.49 (m, 3H), 1.12-1.05 (m, 1H), 0.94-0.82 (m, 1H).

^{13}C NMR (75 MHz, $CDCl_3$): δ 150.4, 149.1, 148.7, 140.6, 130.5, 129.0, 127.9, 126.4, 123.5, 119.8, 114.6, 62.4, 49.6, 49.4, 47.5, 39.7, 27.8, 26.8, 25.1.

5′-aminohydroquinine 75f

Amino derivative **75f** was prepared following the procedure reported by Connon *et al.*,[86] as outlined in *Scheme 23*.

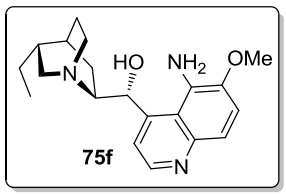

5’-aminohydroquinine (**75f**). Yellow solid; 0.917 g, 29% yield (over two steps, starting from 3.00 g of hydroquinine **III**).

^{1}H NMR (300 MHz, $CDCl_3$): δ 8.49 (d, 1H; *J* = 4.4 Hz), 7.53 (d, 1H; *J* = 9.2 Hz), 7.33 (d, 1H; *J* = 9.2 Hz), 7.19 (d, 1H; *J* = 4.4 Hz), 5.85 (vbs, 2H), 5.32 (bs, 1H), 3.94 (s, 3H), 3.47-3.39 (m, 1H), 2.97 (dd, 1H; *J* = 13.5, 9.2 Hz), 2.89-2.77 (m, 1H), 2.48-

2.39 (m, 2H), 1.85-1.74 (m, 2H), 1.67-1.52 (m, 2H), 1.44-1.32 (m, 4H), 0.85 (t, 3H; J = 7.1 Hz).
^{13}C NMR (75 MHz, $CDCl_3$): δ 147.3, 146.7 (2C), 144.6, 144.3, 130.2, 120.2, 119.2, 114.5, 75.3, 61.4, 56.7, 56.0, 41.9, 37.2, 28.1, 27.9, 24.9, 23.2, 11.5.

7.2.1.b. Synthesis and characterization of aminoquinine *epi*-75a

Aminoderivative *epi*-**75a** was prepared starting from *epi*-quinine (*epi*-**I**), as outlined in *Scheme 23*. *Epi*-**I** was prepared following the procedure reported by Lectka *et al.*[85]

9-Methanesulfonate(9-deoxy)*epi*-quinine (76). 2.71 g of *epi*-**I** (8.35 mmol) and 4.6 ml of triethylamine were dissolved in dry THF under nitrogen atmosphere. The reaction flask was cooled down to 0 °C and mesyl chloride (1.33 ml, 17.2 mmol) was added dropwise to the solution. The mixture was stirred for 30 minutes at 0°C, then 3.5 hours at room temperature. After that the solvent was evaporated under reduced pressure. The residue was dissolved in dichloromethane (400 mL) and washed with a 3.5% $NaHCO_3$ aqueous solution (3 x 200 mL). The organic phase was dried over Na_2SO_4 and concentrated. The crude material was purified by flash chromatography on silica gel, with DCM/MeOH 14:1 elution, giving **76** as a pale yellow amorphous solid (1.35 g, 3.36 mmol, 40% yield). **^{1}H NMR** (300 MHz, $CDCl_3$): δ 0.63-0.75 (m, 1H), 1.27-1.48 (m, 1H), 1.49-1.58 (m, 2H), 1.60-1.67 (m, 1H), 2.20-2.32 (bs, 1H), 2.72-2.85 (m, 2H), 2.88-3.07 (bs, 3H), 3.15-3.28 (m,1H), 3.25-3.50 (br, 2H), 3.94 (s, 3H), 4.90-5.05 (m, 2H), 5.62-5.87 (m, 1H), 6.30 (bs, 1H), 7.37 (d, 1H; J = 3 Hz), 7.40 (d, 1H; J = 3 Hz), 7.46 (m, 1H), 8.03 (d, 1H; J = 9 Hz), 8.76 (s, 1H). **^{13}C NMR** (75 MHz, $CDCl_3$): δ 24.9, 27.2, 27.6, 39.0, 39.2, 41.0, 55.5, 59.6, 76.6, 100.4, 114.5, 119.6, 122.1, 127.2, 131.9, 139.6, 141.2, 144.8, 147.3, 158.3. **HRMS (ESI)**: calcd for $C_{21}H_{27}N_2O_4S$ $[M+H]^+$: 403.1692, found 403.1685.
9-Azido(9-deoxy)quinine (77). 1.35 g of 9-methanesulfonate(9-deoxy)*epi*-quinine (**76**, 3.36 mmol) were dissolved in DMF under nitrogen atmosphere. Sodium azide (0.813 g, 12.5 mmol) was added to the solution. The mixture was stirred for 3 hours at 80°C and then one night at room temperature. After that, the mixture was evaporated under reduced pressure. 400 mL of a 1M NaOH aqueous solution and DCM (400 mL) were added to the residue. The

organic phase was separated, washed with a 1M NaOH aqueous solution (3 x 200 mL), and dried over Na_2SO_4. The solvent was evaporated and the crude material was purified by flash chromatography on silica gel, with DCM/MeOH 100:1 elution. Compound **77** was obtained as white amorphous solid (0.813 g, 2.33 mmol, 69% yield). **^{1}H NMR** (300 MHz, $CDCl_3$): δ 1.45-1.80 (m, 3H), 1.80-1.99 (m, 2H), 2.23-2.37 (m, 1H), 2.57-2.75 (m, 2H), 3.01-3.35 (m, 3H), 3.97 (s, 3H), 4.96-5.05 (m, 2H), 5.17-5.37 (bs, 1H), 5.70-5.89 (m, 1H), 7.30-7.36 (m, 1H), 7.36-7.43 (m, 2H), 8.06 (d, 1H; *J* = 9 Hz), 8.79 (d, 1H; *J* = 3 Hz). **^{13}C NMR** (75 MHz, $CDCl_3$): δ 24.7, 27.2, 27.5, 39.4, 42.1, 55.8, 56.5, 58.4, 65.0, 101.0, 114.7, 119.5, 121.8, 127.0, 132.0, 141.3, 141.7, 144.9, 147.5, 158.2. **HRMS (ESI)**: calcd for $C_{20}H_{24}N_5O$ $[M+H]^+$: 350.1981, found 350.1992.

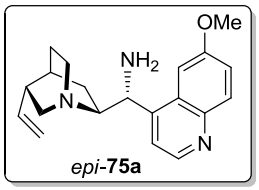

epi-**75a**

9-amino(9-deoxy)quinine (*epi*-75a). 2.46 g of 9-azido(9-deoxy)*epi*-quinine (**77**, 7.04 mmol) and triphenylphosphine (4.14 mg, 15.8 mmol) were dissolved in dry THF under nitrogen atmosphere. The mixture was stirred for 3 hours at 80°C. After cooling, 1 mL of water was added and the reaction mixture was stirred for 12 h at room temperature. Afterward the solvent was evaporated under reduced pressure and the residue dissolved in 10% aqueous HCl (400 mL) and washed with DCM (3 x 200 mL). 1M NaOH aqueous solution was added to the water phase until alkaline pH was reached. The mixture was extracted with DCM and the organic phase was dried over Na_2SO_4. The crude material was purified by flash chromatography on silica gel, with DCM/MeOH 30:1 elution. Compound *epi*-**75a** was obtained as a pale yellow oil (1.10 g, 3.41 mmol; 48% yield).

^{1}H NMR (300 MHz, $CDCl_3$): δ 1.45-1.63 (m, 2H), 1.64-1.78 (m, 2H), 1.83-1.95 (m, 2H), 2.08-2.21 (m, 1H), 2.24-2.35 (m, 1H), 2.47-2.75 (m, 2H), 2.95-3.12 (m, 2H), 3.13-3.26 (m, 1H), 3.96 (s, 3H), 4.65 (d, 1H; *J* = 9 Hz), 5.00-5.13 (m, 2H), 5.84-6.00 (m, 1H), 7.32-7.39 (m, 2H), 7.43 (d, 1H; *J* = 3 Hz), 8.02 (d, 1H; *J* = 12 Hz), 8.73 (d, 1H; *J* = 3 Hz).

^{13}C NMR (75 MHz, $CDCl_3$): δ 26.3, 27.7, 39.6, 41.9, 53.6, 55.6, 56.1, 60.5, 101.1, 114.4, 118.2, 121.1, 127.6, 131.9, 141.7, 144.7, 147.8, 149.1, 157.7.

HRMS (ESI): calcd for $C_{20}H_{26}N_3O$ $[M+H]^+$: 324.2076, found 324.2089.

7.2.2. Thiourea catalysts XI and XVIII

Thiourea **XI** was prepared starting from *epi*-aminocinchonidine **75b** following the procedure reported by Soós *at al.*[72b]

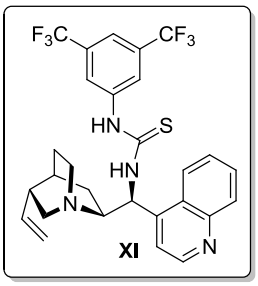

XI. Off-white solid; 1.6 g, 82% yield (reaction performed on 1.0 g of **75b**).

^{1}H-NMR (300 MHz, $CDCl_3$): δ 8.60 (bs, 1H), 8.43 (bs, 1H), 8.04 (d, 1H; *J* = 8.20 Hz), 7.80 (s, 2H), 7.69-7.57 (m, 3H), 7.13 (bs, 1H), 5.93 (bs, 1H), 5.64 (ddd, 1H; *J*= 17.0, 14.2, 9.17), 4.98-4.91 (m, 2H), 3.39-2.99 (m, 3H), 2.79-2.61 (m, 2H), 2.34-2.21 (m, 1H), 1.74-1.53 (m, 3H), 1.37-1.27 (m, 1H), 0.98-0.85 (m, 1H).

^{13}C-NMR (75 MHz, $CDCl_3$): δ 180.9, 150.0 (2C), 148.5, 140.7 (2C), 140.0, 132.6 (q, 2C; *J* = 33.8 Hz), 130.3, 129.6, 127.1, 123.8 (2C), 123.0 (q, 2C; *J* = 272.8 Hz), 118.9, 115.1, 55.0, 41.3, 39.2, 27.6, 27.2, 25.7, 21.1, 14.3.

Thiourea **XVIII** was prepared starting from *epi*-aminoquinine **75a** following the procedure reported by Bella *at al.*[105]

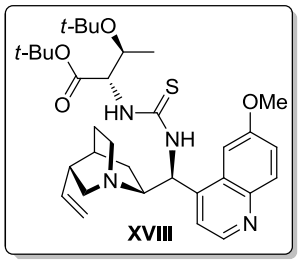

XVIII. White solid; 1.1 g, 61% yield (reaction performed on 0.99 g of **75a**).

^{1}H-NMR (300 MHz, $CDCl_3$): δ 8.74 (d, 1H; *J* = 4.4 Hz), 8.02 (s, 1H; *J* = 9.4 Hz), 7.68 (bs, 2H), 7.45 (bs, 1H), 7.38 (dd, 1H; *J* = 9.2, 1.9 Hz), 6.28 (d, 1H, *J* = 8.8 Hz), 5.69-5.58 (m, 1H), 4.97-4.88 (m, 2H), 4.75 (d, 1H; *J* = 6.8 Hz), 3.97 (s, 3H), 3.26 (dd, 1H; *J* = 13.91, 10.1 Hz), 3.09 (bs, 2H), 2.84-2.67 (m, 2H), 2.29 (s, 1H), 1.69-1.61 (m, 3H), 1.40 (s, 9H), 1.34-0.98 (m, 4H), 0.89 (s, 9H), 0.46 (bs, 3H).

^{13}C-NMR (75 MHz, $CDCl_3$): δ 180.5, 169.8, 158.2, 147.8, 146.7, 145.2, 141.2, 132.2, 129.6, 122.4, 120.9, 114.9, 101.6, 81.8, 73.7, 67.2, 64.6, 56-0, 55.8, 40.83, 39.71, 28.7, 28.3, 28.1, 28.1, 27.6, 20.1.

7.2.3. Proline derived aminocatalysts XXV, XXIX-XXXI

7.2.3.a. Synthesis and characterization of catalysts XXV and XXIX

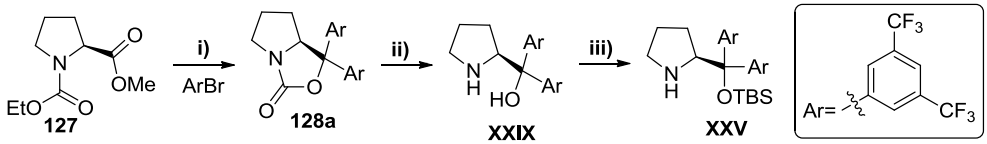

(*S*)-1,1-Bis[3,5-bis(trifluoromethyl)phenyl]tetrahydropyrrolo[1,2-*c*]oxazol-3(1*H*)-one (128a). To a stirred solution of 3,5-bis(trifluoromethyl)bromobenzene (7.62 mL, 13.2 g, 45.0 mmol) in anhydrous THF (37 mL) was added a solution 2.0 M of isopropylmagnesium chloride in anhydrous THF (23.6 mL) dropwise at 0 °C. The resulting mixture was stirred at 0 °C for 1 hour before being treated with a solution of 1-ethyl 2-methyl (*S*)-pyrrolidine-1,2-dicarboxylate (**127**, 3.02 g, 15.0 mmol) in anhydrous THF (11 mL) dropwise at 0 °C. After the addition, the ice bath was removed and the reaction mixture was heated to 65 °C and stirred at this temperature for 5 hours. The reaction was then quenched with saturated aqueous NH_4Cl solution (90 mL) and extracted with EtOAc (2 x 75 mL). The combined organic layers were washed with brine, dried over $MgSO_4$, filtered and concentrated under reduced pressure to afford the crude **128** as a viscous oil, which was directly used in the following step without further purification.

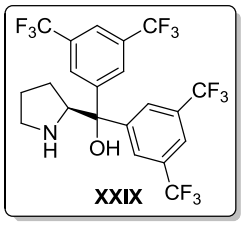

(*S*)-Bis[3,5-bis(trifluoromethyl)phenyl](pyrrolidin-2-yl)methanol (XXIX). To a stirred solution of the crude **128** (8.27 g, 15.0 mmol) in methanol (MeOH, 60 mL) was added solid potassium hydroxide (KOH, 8.40 g, 150 mmol) at room temperature. The resulting dark reaction mixture was heated to 65 °C and stirred at this temperature for 22 hours. The mixture was then cooled to room temperature. The solvent was evaporated under reduced pressure and the residue was diluted with water (75 mL) and extracted with EtOAc (2 x 75 mL). The combined organic layers were washed with brine, dried over $MgSO_4$, filtered and concentrated under reduced pressure. The residue was then purified by flash chromatography on silica gel with 0-30% EtOAc/hexane gradient elution to afford pure **XXIX** (3.69 g, 7.02 mmol, 47% yield over 2 steps) as an off-white solid.

^{1}H-NMR (400 MHz, $CDCl_3$): δ 8.04 (s, 2H), 7.96 (s, 2H), 7.76 (d, 2H; *J* = 4.4 Hz), 5.06 (bs, 1H), 4.34 (t, 1H; *J* = 7.7 Hz), 3.11-3.01 (m, 2H), 1.83-1.74 (m, 2H), 1.63-1.48 (m, 4H).

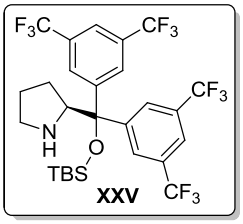

XXV

(*S*)-2-(Bis[3,5-bis(trifluoromethyl)phenyl][*tert*-butyl (dimethyl)silyl]-oxymethyl)pyrrolidine (XXV). To a stirred solution of **XXIX** (1.20 g, 2.28 mmol) in anhydrous THF (20 mL) at 0 °C was added NaH (0.274 g, 6.85 mmol). *Tert*-butyldimethylsilyl trifluoromethanesulfonate (0.787 mL, 0.906 g, 3.43 mmol) was then added dropwise over 10 minutes. The reaction mixture was stirred at room temperature for 16 h, after which time a saturated aqueous solution of potassium sodium tartrate (45 mL) was added. The mixture was extracted with EtOAc (3 x 60 mL). The combined organic phases were dried over Na_2SO_4, filtrated and concentrated under reduced pressure. The crude residue was purified by flash chromatography on silica gel, eluting with hexane/Et_2O 20:1. Pure catalyst **XXV** was obtained as a colorless viscous oil (1.20 g, 82% yield).

^{1}H-NMR (400 MHz, $CDCl_3$): δ 8.09 (s, 2H), 7.85 (s, 2H), 7.74 (s, 2H), 4.23 (dd, 1H; *J* = 7.9, 6.1 Hz), 2.90 (dt, 1H; *J* = 10.2, 6.9 Hz), 2.56-2.50 (m, 1H), 1.82-1.73 (m, 2H), 1.51-1.45 (m, 2H), 0.94-0.86 (m, 10H), -0.21 (s, 3H), -0.47 (s, 3H).

^{13}C-NMR (100 MHz, $CDCl_3$): δ 147.9, 146.3, 131.7 (q, 2C; *J* = 33.7 Hz), 130.8 (q, 2C; *J* = 33.3 Hz), 129.3 (m, 2C), 128.9 (m, 2C), 122.0 (m), 121.6 (m), 123.4 (q, 4C; *J* = 247.9 Hz), 82.5, 64.2, 47.4, 28.0, 26.0, 25.4, 19.0, -2.6, -3.2.

7.2.3.b. Synthesis and characterization of catalysts XXX and XXXI

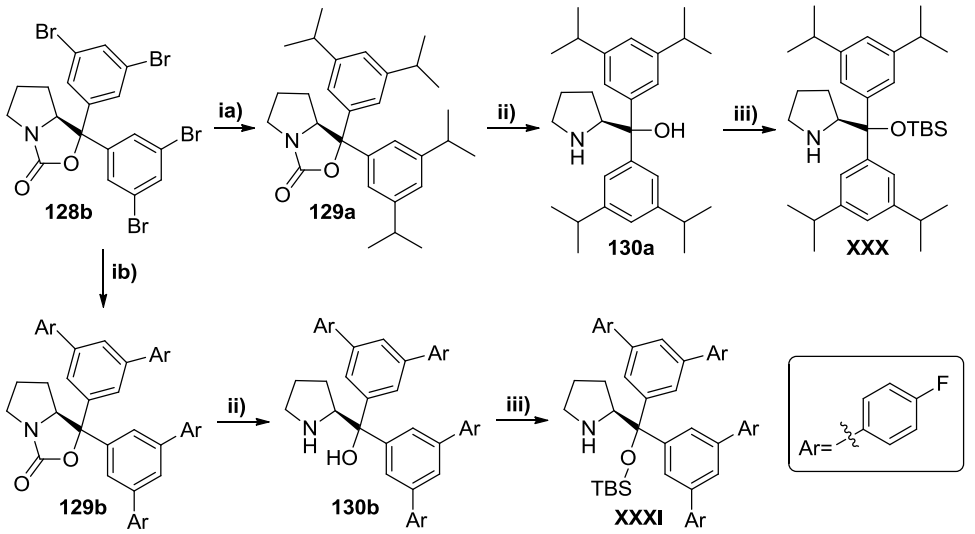

Compound **128b** was prepared following the procedure described for **128a** and employing 1,3,5-tribromobenzene as the aryl bromide.

(*S*)-1,1-Bis[3,5-di(isopropyl)phenyl]tetrahydropyrrolo[1,2-*c*]oxazol-3(1*H*)-one (129a). To a stirred suspension of $ZnCl_2$ (1.09 g, 8.00 mmol) in anhydrous THF (3.5 mL) was added a solution 2.0 M of isopropylmagnesium chloride in anhydrous THF (4.00 mL, 8.00 mmol) dropwise at 0 °C. (*S*)-1,1-bis[3,5-dibromophenyl]tetrahydropyrrolo[1,2-*c*]oxazol-3(1*H*)-one **128b** (0.595 g, 1.00 mmol) dissolved in anhydrous THF (2.5 mL) and [1,1'-bis(diphenylphosphino)ferrocene] dichloropalladium (0.082 g, 0.100 mmol) were then added. The reaction mixture was stirred at reflux for 24 h, after which time it was cooled to room temperature and quenched with H_2O (15 mL). The mixture was extracted with EtOAc (3 x 15 mL). The combined organic phases were dried over Na_2SO_4, filtered and concentrated under reduced pressure. The crude product was purified by flash chromatography on silica gel, with hexane/DCM 5:1 to 2:1 gradient elution. **129a** was obtained as a white solid (0.400 g, 89% yield). **^{1}H-NMR** (500 MHz, $CDCl_3$): δ 7.20 (d, 2H; *J* = 1.7 Hz), 7.07 (d, 2H; *J* = 1.7 Hz), 7.01 (bt, 1H; *J* = 1.5 Hz), 6.96 (bt, 1H, *J* = 1.6 Hz), 4.49 (dd, 1H; *J* = 10.5, 5.4 Hz), 3.79 (dt, 1H; *J* = 11.4, 8.3 Hz), 3.24 (ddd, 1H; *J* = 11.4, 9.5, 3.7 Hz), 2.91-2.83 (m, 4 H), 2.01-1.94 (m, 1H), 1.91-1.81 (m, 1H), 1.76-1.71 (m, 1H), 1.63-1.56 (m, 1H), 1.22-1.20 (m, 24H).

(*S*)-1,1-Bis[3,5-di(4-fluorophenyl)phenyl]tetrahydropyrrolo[1,2-*c*] oxazol-3(1*H*)-one (129b). to a stirred solution of (*S*)-1,1-bis[3,5-dibromo-

phenyl]tetrahydropyrrolo[1,2-*c*]oxazol-3(1*H*)-one **128b** (0.200 g, 0.336 mmol) in toluene (1.20 mL) were added EtOH (0.80 mL), H_2O (0.80 mL), (4-fluorophenyl)boronic acid (0.282 g, 2.02 mmol), Cs_2CO_3 (0.657 g, 2.02 mmol) and tetrakis(triphenylphosphine)palladium(0) (0.194 g, 0.168 mmol). The reaction was stirred at 100 °C for 16 h, after which time it was cooled to room temperature. H_2O (10 mL) was added and the mixture was extracted with EtOAc (3 x 10 mL). The combined organic layers were dried over Na_2SO_4, filtered and concentrated under reduced pressure. The crude product was purified by flash chromatography on silica gel, with hexane/DCM 5:1 to 1:4 gradient elution. **129b** was obtained as a yellowish solid (0.215 g, 98% yield). **^{1}H-NMR** (300 MHz, $CDCl_3$): δ 7.73 (d, 2H; *J* = 1.6 Hz), 7.65-7.53 (m, 12H), 7.17-7.11 (m, 8H), 4.71 (dd, 1H; *J* = 10.7, 5.1 Hz), 3.80 (dt, 1H; *J* = 11.6, 8.0 Hz), 3.36-3.28 (m, 1H), 2.14-1.84 (m, 3H), 1.34-1.24 (m, 1H).

130a and **130b** were prepared from **129a** and **129b**, respectively, following the same procedure employed for **XXIX**.

(*S*)-Bis[3,5-di(isopropyl)phenyl](pyrrolidin-2-yl)methanol (130a). White solid, 0.284 g, 75% yield. **^{1}H-NMR** (400 MHz, $CDCl_3$): δ 7.27 (d, 2H; *J* = 1.6 Hz), 7.19 (d, 2H; *J* = 1.6 Hz), 6.87-6.86 (m, 2H), 4.23 (t, 1H; *J* = 7.7 Hz), 3.05-3.00 (m, 1H), 2.97-2.80 (m, 7 H), 1.74-1.53 (m, 2H), 1.23-1.20 (m, 24H).

(*S*)-Bis[3,5-di(4-fluorophenyl)phenyl](pyrrolidin-2-yl)methanol (130b). White solid, 0.073 g, 67% yield. **^{1}H-NMR** (400 MHz, $CDCl_3$): δ 7.27 (d, 2H; *J* = 1.6 Hz), 7.19 (d, 2H; *J* = 1.6 Hz), 6.87-6.86 (m, 2H), 4.23 (t, 1H; *J* = 7.7 Hz), 3.05-3.00 (m, 1H), 2.97-2.80 (m, 7 H), 1.74-1.53 (m, 2H), 1.23-1.20 (m, 24H).

XXX and **XXXI** were prepared from **130a** and **130b**, respectively, following the same procedure employed for **XXV**.

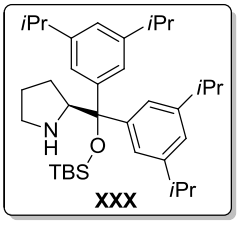

xxx

(*S*)-2-(Bis[3,5-di(isopropyl)phenyl][*tert*-butyl(dimethyl) silyl]oxymethyl)pyrrolidine (XXX). Yellowish oil; 0.097 g, 57% yield.
^{1}H-NMR (500 MHz, $CDCl_3$): δ 7.16 (bs, 2H), 7.07 (d, 2H; *J* = 1.7 Hz), 6.95 (bs, 2H), 4.14-4.10 (m, 1H), 2.89-2.80 (m, 4H), 2.75-2.69 (m, 1H), 2.41-2.36 (m, 1H), 1.71-1.66 (m, 4H), 1.21-1.18 (m, 24H), 0.94 (s, 9H), -0.36 (s, 3H), -0.47 (s, 3H).

^{13}C-NMR (126 MHz, $CDCl_3$): δ 147.9 (4C), 147.4 (2C), 125.2 (2C), 124.9 (2C), 123.4, 123.3, 83.8, 65.5, 47.0, 34.5 (2C), 34.4 (2C), 27.8, 26.4, 25.1, 24.5 (2C), 24.3 (2C), 24.2 (2C), 24.1 (2C), 19.1, -3.1, -3.4.

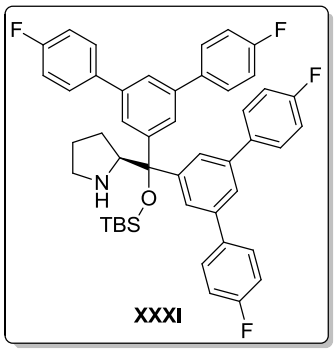

XXXI

(*S*)-2-(Bis[3,5-di(4-fluorophenyl)phenyl][*tert*-butyl(dimethyl)silyl]oxymethyl)pyrrolidine (XXXI). Yellowish oil; 0.076 g, 43% yield.
^{1}H-NMR (500 MHz, $CDCl_3$): δ 7.82 (d, 2H; *J* = 1.6 Hz), 7.63 (t, 1H; *J* = 1.7 Hz), 7.61-7.49 (m, 11H), 7.11 (td, 8H; *J* = 8.7, 1.5 Hz), 4.25 (t, 1H; *J* = 7.2 Hz), 2.91-2.85 (m, 1H), 2.73-2.67 (m, 1H), 1.79-1.67 (m, 3H), 1.00 (s, 9H), 0.93-0.84 (m, 1H), -0.13 (s, 3H), -0.34 (s, 3H).

7.2.4. Cinchona alkaloid-derived di-Boc-substituted guanidines XIVa-f

Guanidines **XIVa-f** were prepared following two different typical procedures, as outlined in *Scheme 24*.
Typical procedure A. 507 mg of 9-amino(9-deoxy)*epi*-quinine (**75a**, 1.57 mmol), *N*,*N'*-di-Boc-thiourea (**79**, 362 mg, 1.31 mmol) and 0.50 mL of triethylamine were dissolved in dry DMF under argon atmosphere. The reaction flask was cooled down to 0 °C and $HgCl_2$ (354 mg, 1.31 mmol) was added to the solution. The mixture was stirred for 12 hours at room temperature. Then 10 mL of EtOAc were added and the HgS black precipitate was eliminated by filtration through a pad of celite. The filtrate was concentrated under reduced pressure and the crude material was purified by flash chromatography on silica gel, eluting with AcOEt/hexane 3:2, to obtain pure **XIVa** as a white solid (395 mg, 53% yield).
Typical procedure B. 532 mg of 9-amino(9-deoxy)*epi*-quinine (**75a**, 1.65 mmol) were dissolved in DCM (16 mL). *N*,*N'*-bis(*tert*-butyloxycarbonyl)-*N''*-triflylguanidine (**80**, 710 mg, 1.82 mmol) and 0.92 mL of triethylamine were then added and the reaction mixture was stirred at room temperature for 16 h, after which time it was concentrated under reduced pressure. The crude residue was purified by flash chromatography on silica gel, with petroleum ether/EtOAc 6:1 to 1:1 gradient elution. Pure compound **XIV** was obtained as a white solid (712 mg, 76% yield).

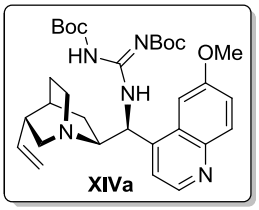

[*N,N′*-bis(*tert*-butyloxycarbonyl)-*N′′*-(9-deoxy)*epi*-quinine]guanidine (XIVa).

^{1}H NMR (300 MHz, $CDCl_3$): δ 0.73-0.84 (m, 1H), 1.37 (s, 9H), 1.44 (s, 9H), 1.58-1.66 (m, 3H), 2.31 (br, 1H), 2.71-2.84 (m, 2H), 3.28-3.47 (m, 3H), 3.99 (s, 3H), 4.98-5.05 (m, 2H), 5.75-5.86 (m, 2H), 7.32-7.38 (m, 2H), 7.85 (s, 1H), 7.99 (d, 1H; *J* = 9.1 Hz), 8.73 (d, 1H; *J* = 4.7 Hz), 8.81 (br, 1H), 11.28 (s, 1H).

^{13}C NMR (75 MHz, $CDCl_3$): δ 27.1, 27.7, 28.0, 28.2, 28.4, 39.7, 41.5, 56.0, 59.6, 78.6, 83.1, 102.4, 114.6, 119.9, 122.4, 128.7, 131.6, 141.7, 144.5, 145.1, 147.6, 153.0, 155.7, 158.1, 163.5.

HRMS (ESI): calcd for $C_{31}H_{44}N_5O_5$ $[M+H]^+$: 566.3342, found 566.3336.

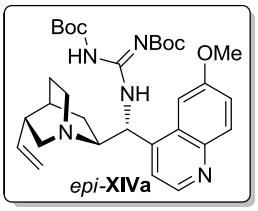

[*N,N′*-bis(*tert*-butyloxycarbonyl)-*N′′*-(9-deoxy)-quinine]guanidine (*epi*-XIVa). Procedure A: white solid; 904 mg, 86% yield (reaction performed on 600 mg of *epi*-**75a**).

^{1}H NMR (300 MHz, $CDCl_3$): δ 1.10-1.30 (m, 1H), 1.45 (s, 9H), 1.47 (s, 9H), 1.65-2.05 (m, 3H), 2.21-2.41 (m, 1H), 2.55-2.88 (m, 3H), 2.90-3.15 (m, 2H), 3.40-3.58 (m, 1H), 3.99 (s, 3H), 4.98-5.14 (m, 2H), 5.81-6.05 (m, 1H), 6.21-6.35 (m, 1H), 7.32-7.43 (m, 2H), 7.81 (s, 1H), 8.98 (d, 1H; *J* = 9 Hz), 8.71 (bs, 1H), 8.75 (d, 1H; *J* = 6 Hz), 11.43 (bs, 1H).

^{13}C NMR (75 MHz, $CDCl_3$): δ 25.1, 27.6, 28.0, 28.2, 39.5, 42.1, 46.1, 51.0, 56.1, 56.4, 58.3, 79.3, 83.7, 101.8, 114.6, 118.8, 122.4, 128.1, 131.5, 141.6, 144.3, 145.0, 147.5, 153.1, 156.3, 158.1, 163.3.

HRMS (ESI): calcd for $C_{31}H_{44}N_5O_5$ $[M+H]^+$: 566.3342, found 566.3329.

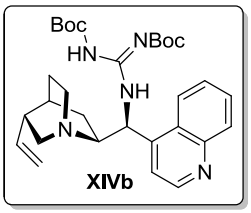

[*N,N′*-bis(*tert*-butyloxycarbonyl)-*N′′*-(9-deoxy)*epi*-cinchonidine]guanidine (XIVb). Procedure B: white solid; 809 mg, 92% yield (reaction performed on 480 mg of **75b**).

^{1}H NMR (300 MHz, $CDCl_3$): δ 0.84-0.91 (m, 1H), 1.33 (s, 9H), 1.46 (s, 9H), 1.65-1.76 (m, 3H), 2.39 (br, 1H), 2.84-2.93 (m, 2H), 3.38-3.50 (m, 3H), 5.00-5.06 (m, 2H), 5.74 (ddd, 1H; *J* = 17.3, 10.3, 7.3 Hz), 5.90 (br d, 1H; *J* = 10.0 Hz), 7.44 (d, 1H; *J* = 4.4 Hz), 7.62 (t, 1H; *J* = 7.3 Hz), 7.74 (t, 1H; *J* = 7.5 Hz), 8.12 (d, 1H; *J* = 8.5 Hz), 8.54 (d, 1H; *J* = 8.2 Hz), 8.90 (d, 1H; *J* = 4.7 Hz).

^{13}C NMR (75 MHz, $CDCl_3$): δ 26.4, 27.7, 28.0, 28.2, 28.3, 39.8, 41.3, 56.2, 60.2, 78.6, 83.0, 114.5, 119.7, 124.6, 126.5, 127.7, 129.1, 130.1, 141.8, 147.5, 148.7, 150.1, 152.9, 155.2, 163.1.

HRMS (ESI): calcd for $C_{30}H_{42}N_5O_4$ $[M+H]^+$: 536.3237, found 536.3221.

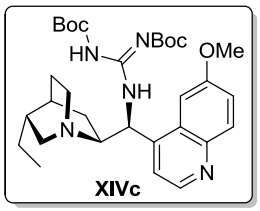

[*N*,*N'*-bis(*tert*-butyloxycarbonyl)-*N''*-(9-deoxy)*epi*-hydroquinine]guanidine (XIVc). Procedure B: white solid; 796 mg, 76% yield (reaction performed on 600 mg of **75c**).

^{1}H NMR (400 MHz, $CDCl_3$): δ 0.73-0.82 (m, 1H), 0.83 (t, 3H; *J* = 7.3 Hz), 1.19-1.34 (m, 3H), 1.37 (s, 9H), 1.43 (s, 9H), 1.47-1.51 (m, 3H), 2.53 (ddd, 1H; *J* = 13.6, 4.8, 2.1 Hz), 2.74-2.82 (m, 1H), 3.33-3.47 (m, 3H), 3.99 (s, 3H), 5.89 (bs, 1H), 7.32-7.38 (m, 2H), 7.84 (s, 1H), 7.99 (d, 1H; *J* = 9.2 Hz), 8.73 (d, 1H; *J* = 4.6 Hz).

^{13}C NMR (100 MHz, $CDCl_3$): δ 12.1, 25.3, 26.7, 27.6, 28.2, 28.3, 37.1, 41.4, 56.0, 57.7, 59.4, 78.7, 83.2, 102.2, 119.8, 122.5, 128.6, 131.5, 144.4, 145.0, 147.5, 153.1, 155.6, 158.2, 163.4.

HRMS (ESI): calcd for $C_{31}H_{46}N_5O_5$ $[M+H]^+$: 568.3499, found 568.3522.

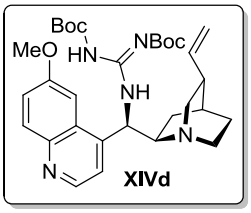

[*N*,*N'*-bis(*tert*-butyloxycarbonyl)-*N''*-(9-deoxy)*epi*-quinidine]guanidine (XIVd). Procedure B: white solid; 938 mg, 95% yield (reaction performed on 560 mg of **75d**).

^{1}H NMR (300 MHz, $CDCl_3$): δ 0.97-1.33 (m, 2 H), 1.42 (s, 18H), 1.78 (br, 3H), 2.47 (br, 1H), 3.12-3.36 (m, 3H), 3.61 (dd, 1H; *J* = 18.3, 9.7 Hz), 3.86-3.93 (m, 1H), 3.98 (s, 3H), 5.21 (d, 1H; *J* = 10.6 Hz), 5.56 (d, 1H; *J* = 17.5 Hz), 5.76-5.85 (m, 1H), 6.24 (br d, 1H; *J* = 11.0 Hz), 7.35-7.39 (m, 2H), 7.77 (s, 1H), 8.00 (d, 1H; *J* = 9.1 Hz), 8.74 (d, 1H; *J* = 4.5 Hz).

^{13}C NMR (75 MHz, $CDCl_3$): δ 25.8, 26.2, 27.1, 28.0, 28.1, 28.3, 38.0, 45.7, 49.4, 55.9, 55.5, 79.0, 83.8, 101.8, 115.7, 123.1, 128.6, 131.4, 139.5, 143.5, 145.0, 145.0, 147.5, 153.2, 155.7, 158.6, 163.1.

HRMS (ESI): calcd for $C_{31}H_{46}N_5O_5$ $[M+H]^+$: 566.3342, found 566.3317.

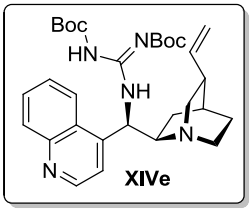

[*N,N′*-bis(*tert*-butyloxycarbonyl)-*N′′*-(9-deoxy)*epi*-cinchonine]guanidine (XIVe). Procedure B: white solid; 847 mg, 88% yield (reaction performed on 530 mg of **75e**).

^{1}H NMR (300 MHz, $CDCl_3$): δ 1.19-1.22 (m, 2H), 1.40 (s, 9H), 1.44 (s, 9H), 1.73-1.76 (m, 3H), 2.44-2.51 (m, 1H), 3.13-3.28 (m, 3H), 3.55 (dd, 1H; *J* = 19.2, 9.2 Hz), 3.75 (dd, 1H; *J* = 14.1, 7.0 Hz), 5.25 (d, 1H; *J* = 10.5 Hz), 5.47 (d, 1H; *J* = 17.3 Hz), 5.75-5.86 (m, 1H), 6.15 (br d, 1H; *J* = 10.5 Hz), 7.44 (d, 1H; *J* = 4.7 Hz), 7.64 (t, 1H; *J* = 7.8 Hz), 7.75 (t, 1H; *J* = 7.5 Hz), 8.13 (d, 1H; *J* = 8.2 Hz), 8.41 (d, 1H; *J* = 8.5 Hz), 8.89 (d, 1H; *J* = 4.7 Hz).

^{13}C NMR (75 MHz, $CDCl_3$): δ 25.3, 25.5, 27.1, 28.1, 28.2, 37.9, 46.0, 49.2, 60.3, 79.1, 83.8, 116.0, 122.6, 124.2, 127.2, 127.3, 129.9, 130.1, 138.8, 145.4, 148.5, 150.1, 153.2, 155.4, 162.8.

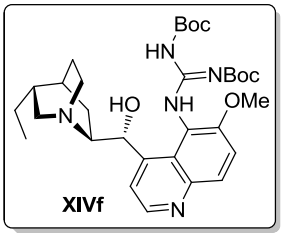

[*N,N′*-bis(*tert*-butyloxycarbonyl)-*N′′*-(5'-hydroquinine)]guanidine (XIVf). Procedure A: yellow sticky solid; 151 mg, 35% yield (reaction performed on 252 mg of **75f**).

^{1}H NMR (300 MHz, $CDCl_3$): δ 0.87 (t, 3H; *J* = 6 Hz), 1.34-1.48 (m, 4H), 1.53 (s, 18H), 1.58-1.75 (m, 2H), 1.77-1.87 (bs, 1H), 2.05-2.21 (m, 1H), 2.41 (d, 1H; *J* = 15 Hz), 2.57-2.72 (m, 1H), 2.91-3.13 (m, 2H), 3.47-3.67 (m, 1H), 4.08 (s, 3H), 5.49 (d, 1H; *J* = 9 Hz), 7.39 (d, 1H; *J* = 3Hz), 7.51 (d, 1H; *J* = 9 Hz), 7.90 (d, 1H; *J* = 9 Hz), 8.71 (d, 1H; *J* = 3 Hz), 12.09 (bs, 1H).

^{13}C NMR (75 MHz, $CDCl_3$): δ 12.8, 25.4, 26.2, 28.8, 29.0, 38.1, 42.5, 57.9, 58.1, 58.5, 80.9, 82.6, 116.3, 119.5, 120.6, 121.5, 121.8, 127.0, 142.6, 144.7, 146.1, 149.2.

HRMS (ESI): calcd for $C_{31}H_{46}N_5O_6$ $[M+H]^+$: 584.3448, found 584.3474.

7.2.5. NMR spectra of di-Boc-substituted guanidines XIVa-f

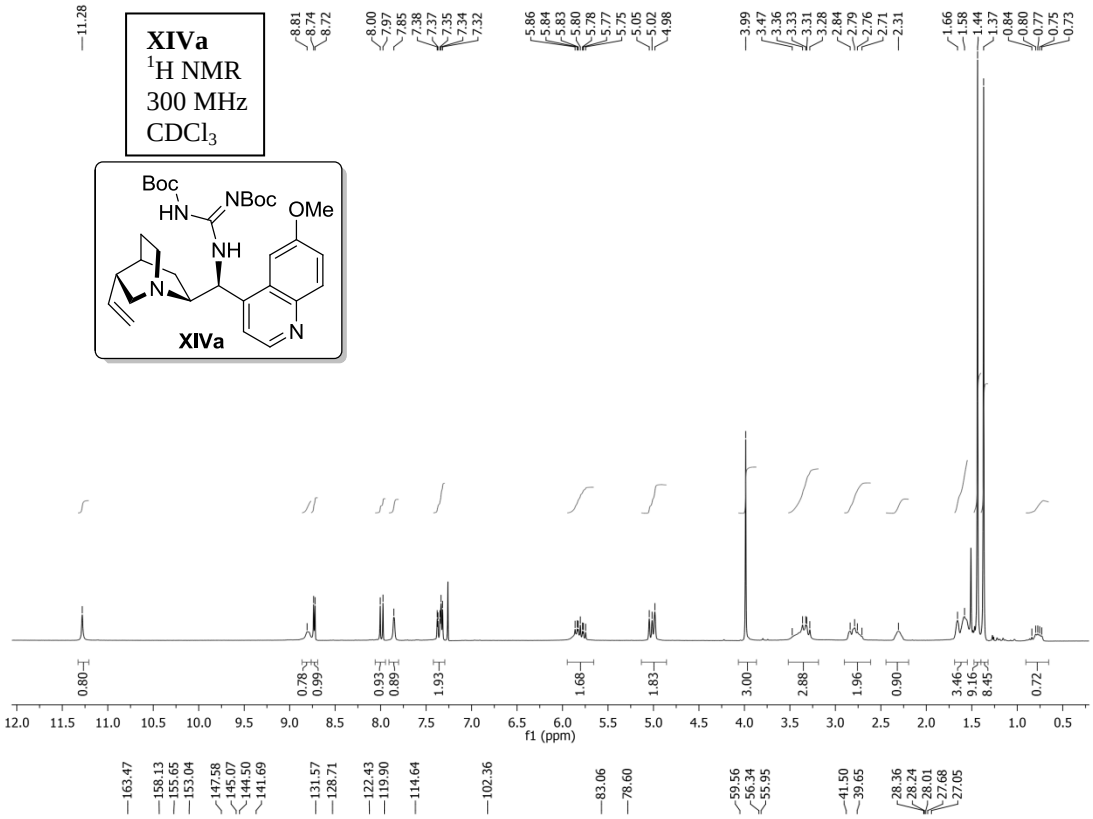

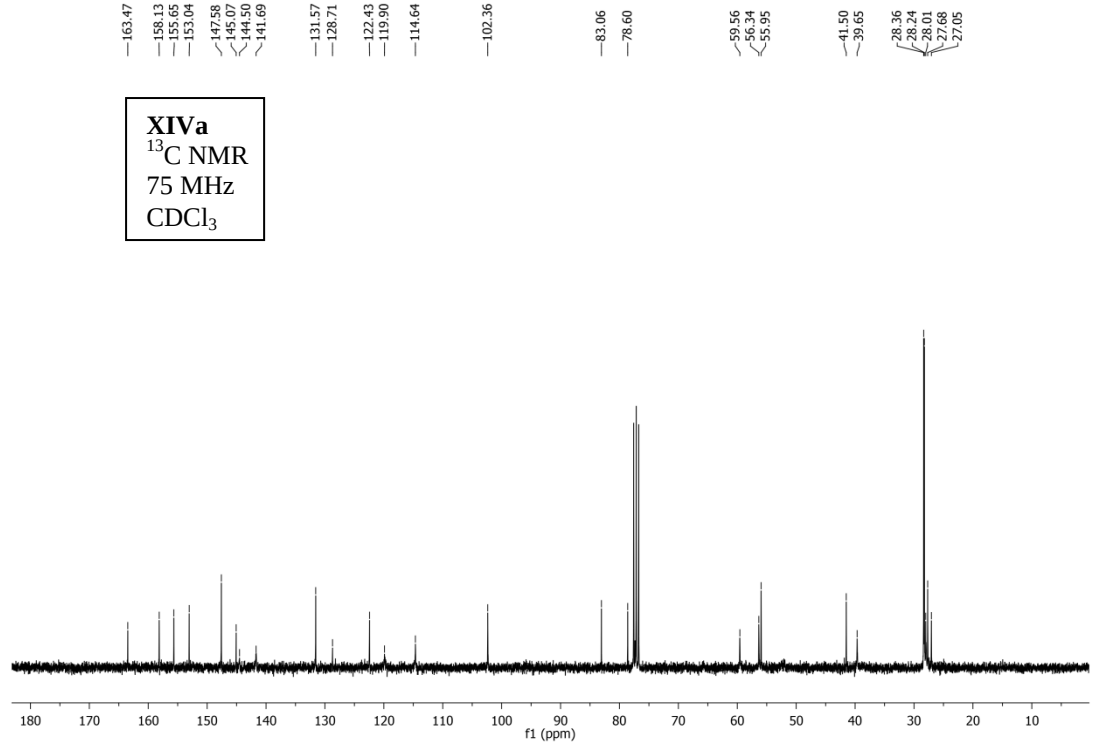

epi-**XIVa**
^{1}H NMR
300 MHz
$CDCl_3$

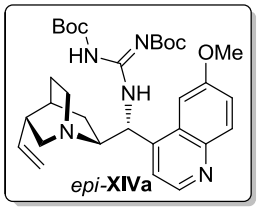

epi-**XIVa**
^{13}C NMR
75 MHz
$CDCl_3$

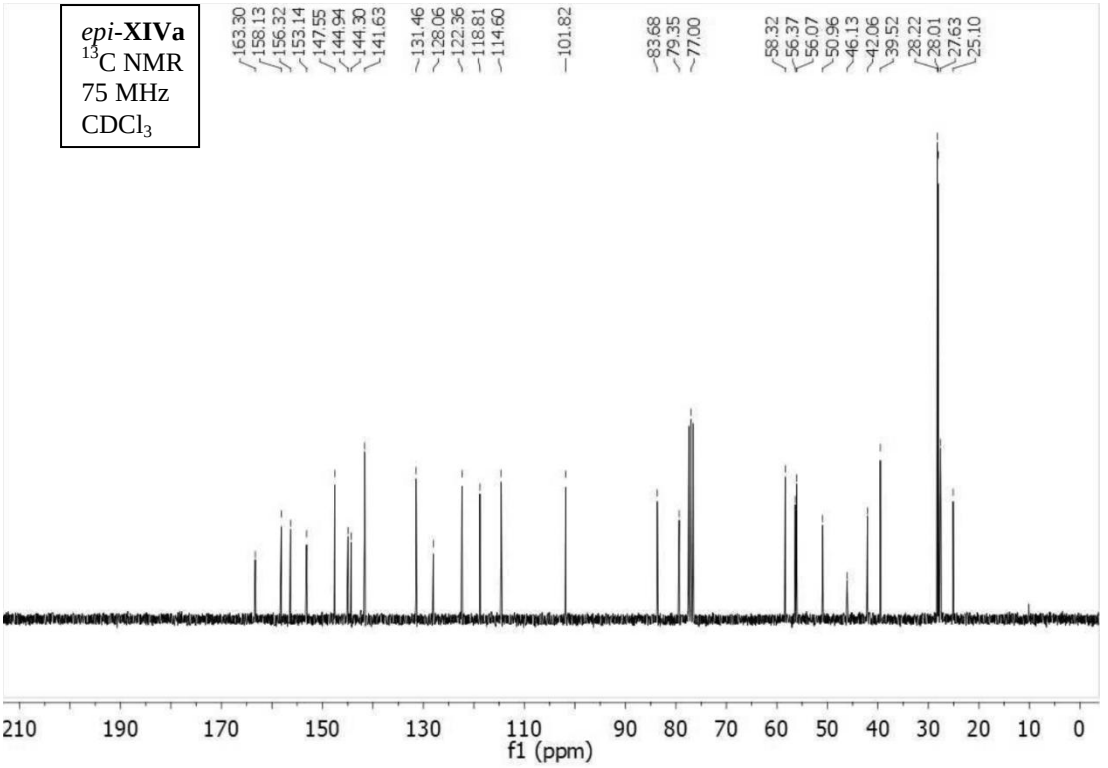

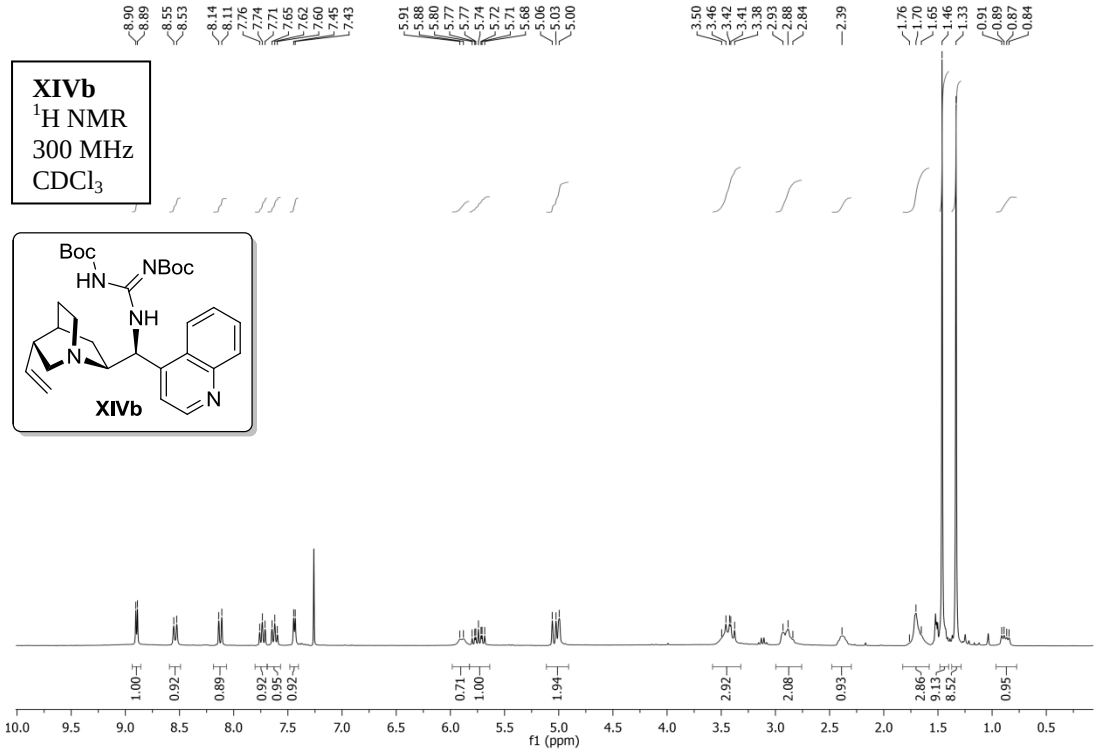
XIVb
1H NMR
300 MHz
CDCl3
Boc
HN
NBoc
NH
N
N
XIVb
f1 (ppm)

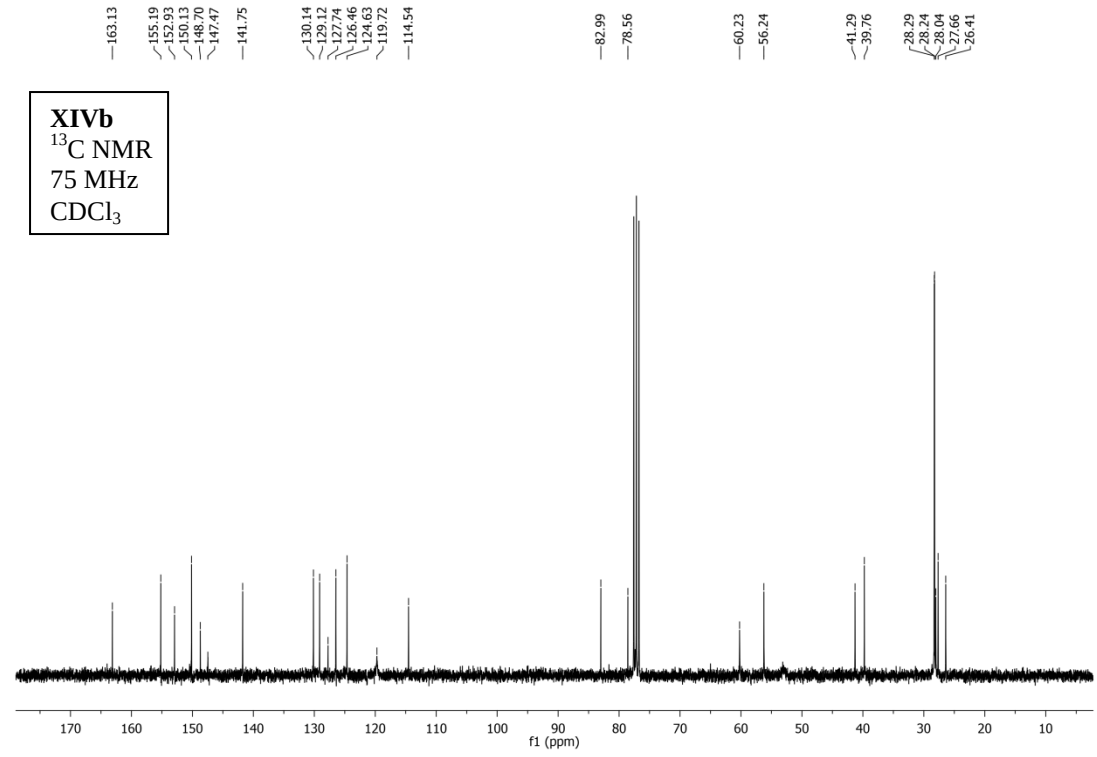
XIVb
13C NMR
75 MHz
CDCl3
f1 (ppm)

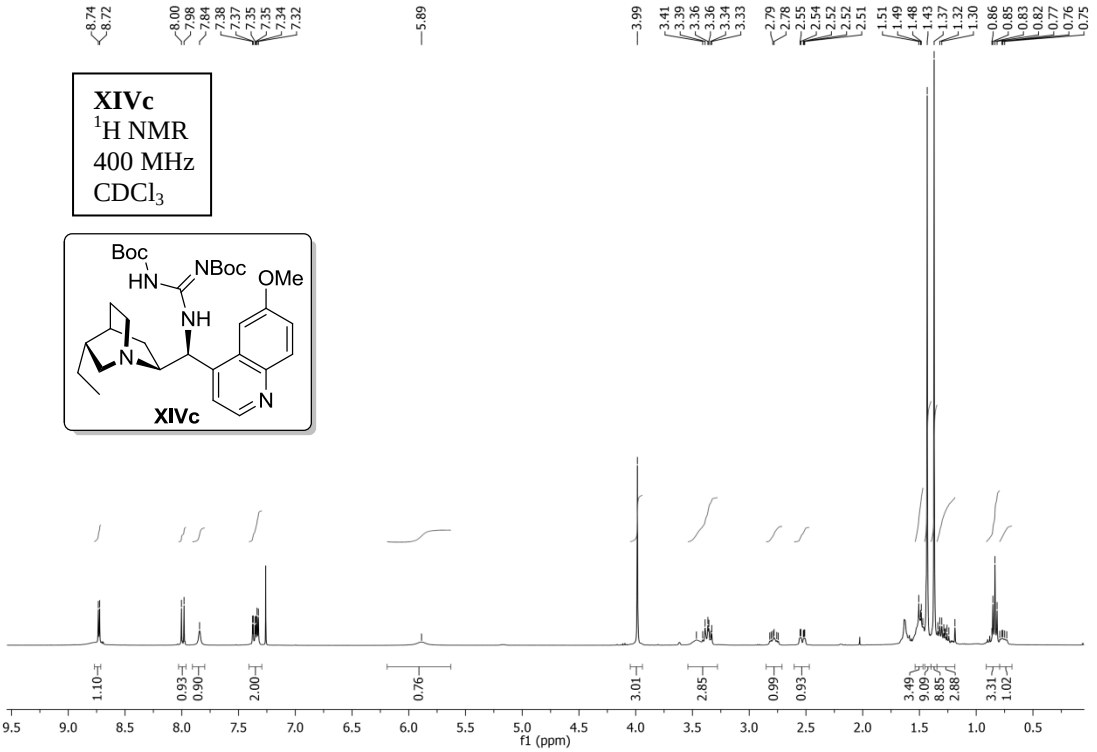
8.74
8.72
8.00
7.98
7.84
7.38
7.37
7.35
7.35
7.34
7.32
5.89
3.99
3.41
3.39
3.36
3.36
3.34
3.33
2.79
2.78
2.55
2.54
2.52
2.52
2.51
1.51
1.49
1.48
1.43
1.37
1.32
1.30
0.86
0.85
0.83
0.82
0.77
0.76
0.75
XIVc
1H NMR
400 MHz
CDCl3
Boc
HN
NBoc
OMe
NH
N
N
XIVc
1.10
0.93
0.90
2.00
0.76
3.01
2.85
0.99
0.93
3.49
9.09
8.85
2.88
3.31
1.02
f1 (ppm)

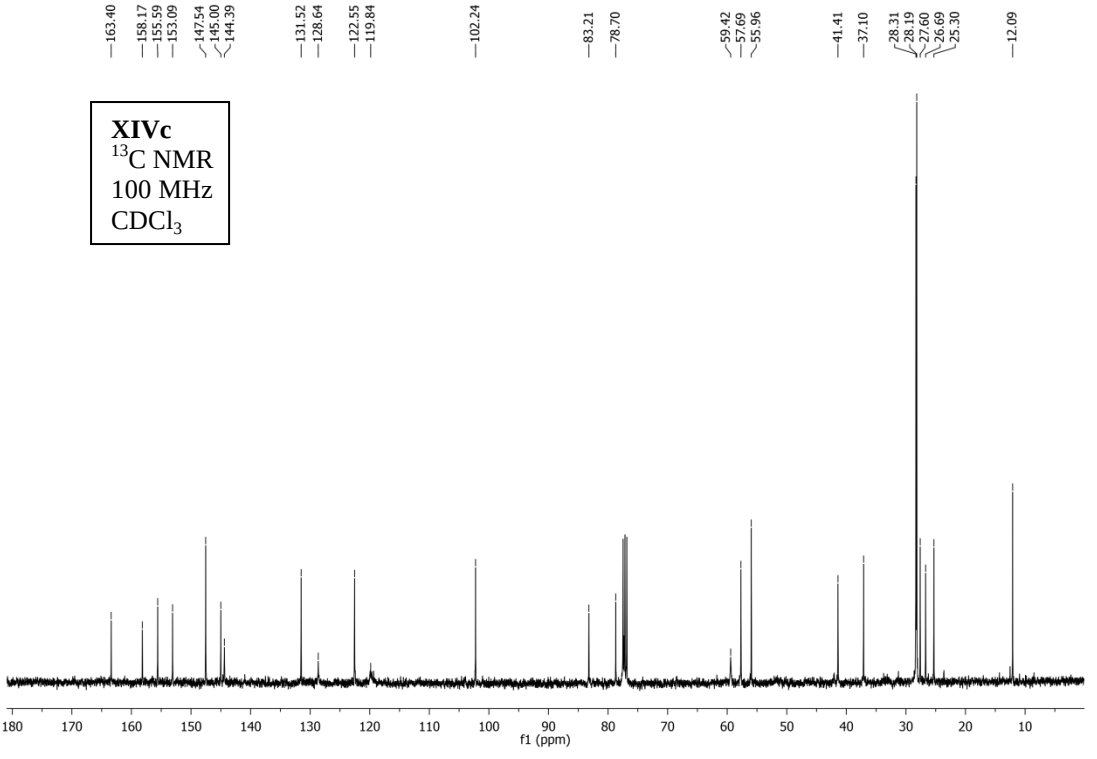
163.40
158.17
155.59
153.09
147.54
145.00
144.39
131.52
128.64
122.55
119.84
102.24
83.21
78.70
59.42
57.69
55.96
41.41
37.10
28.31
28.19
27.60
26.69
25.30
12.09
XIVc
13C NMR
100 MHz
CDCl3
f1 (ppm)

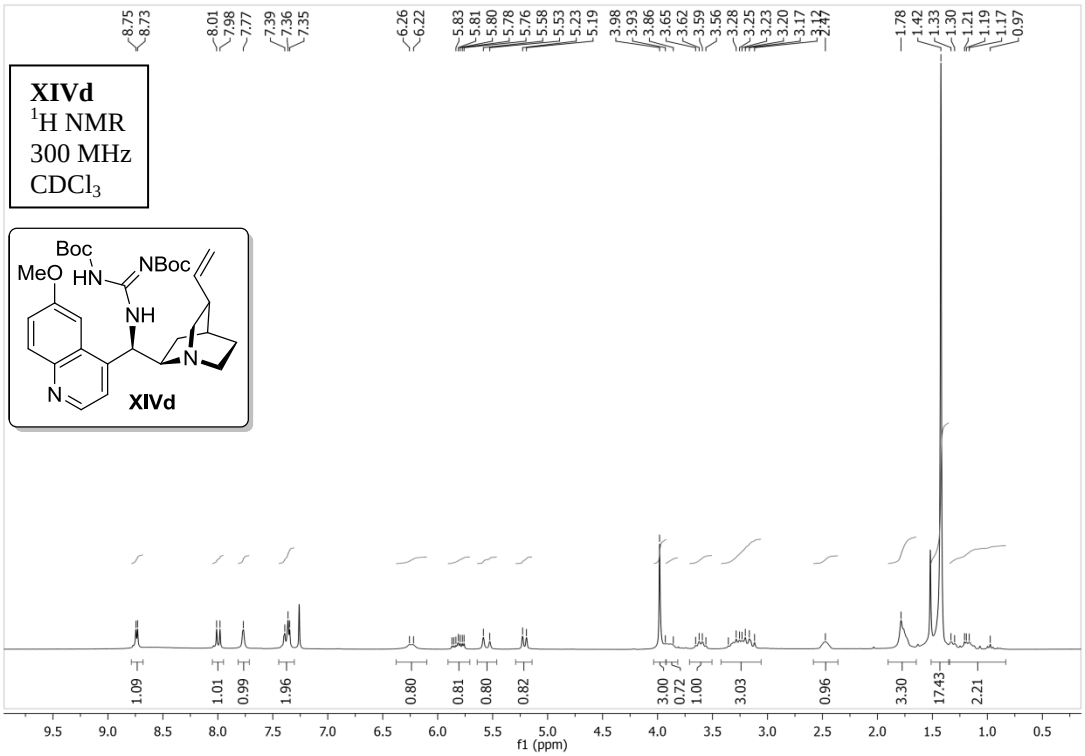
XIVd
1H NMR
300 MHz
CDCl3
Boc
MeO
HN
NBoc
NH
N
N
XIVd
8.75
8.73
8.01
7.98
7.77
7.39
7.36
7.35
6.26
6.22
5.83
5.81
5.80
5.78
5.76
5.58
5.53
5.23
5.19
3.98
3.93
3.86
3.65
3.62
3.59
3.56
3.28
3.25
3.23
3.20
3.17
2.47
1.78
1.42
1.33
1.30
1.21
1.19
1.17
0.97
1.09
1.01
0.99
1.96
0.80
0.81
0.80
0.82
3.00
0.72
1.00
3.03
0.96
3.30
17.43
2.21
f1 (ppm)

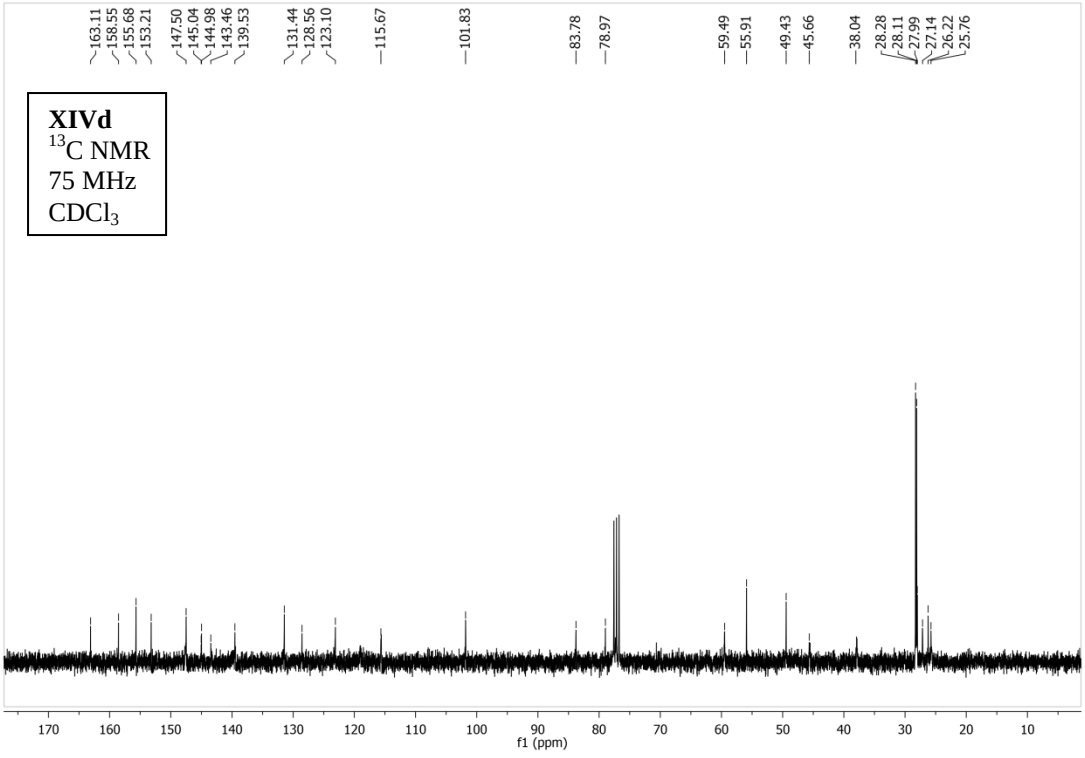
XIVd
13C NMR
75 MHz
CDCl3
163.11
158.55
155.68
153.21
147.50
145.04
144.98
143.46
139.53
131.44
128.56
123.10
115.67
101.83
83.78
78.97
59.49
55.91
49.43
45.66
38.04
28.28
28.11
27.99
27.14
26.22
25.76
f1 (ppm)

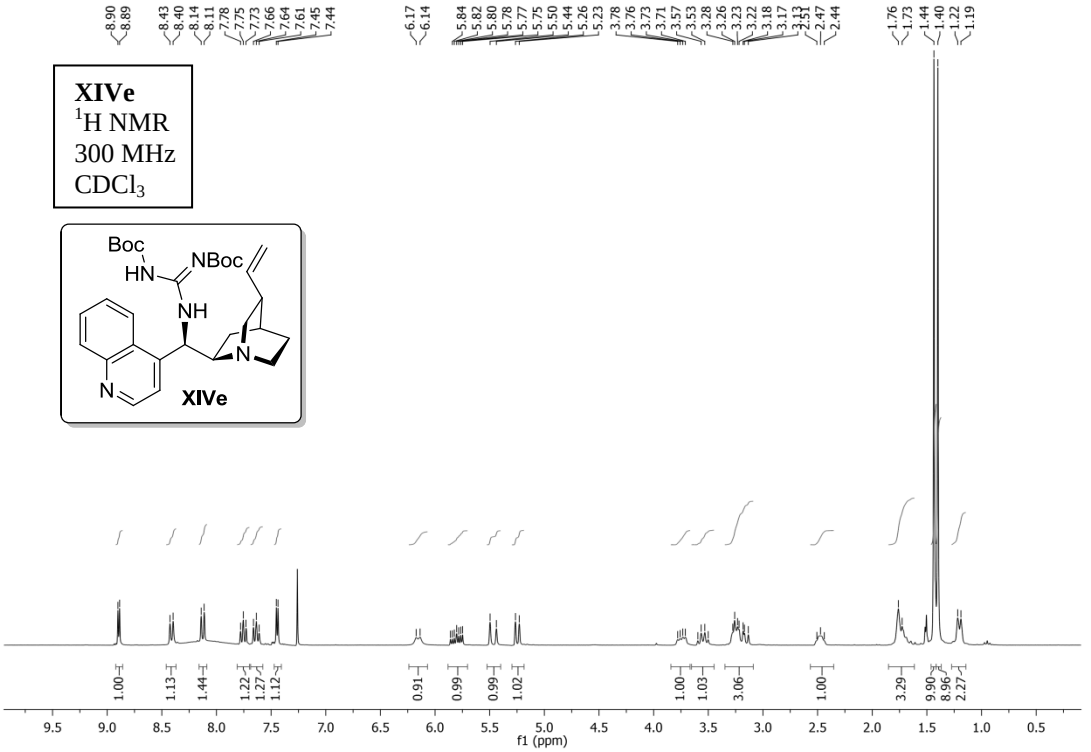
XIVe
^{1}H NMR
300 MHz
$CDCl_3$
Boc
HN
NBoc
NH
N
N
XIVe
f1 (ppm)

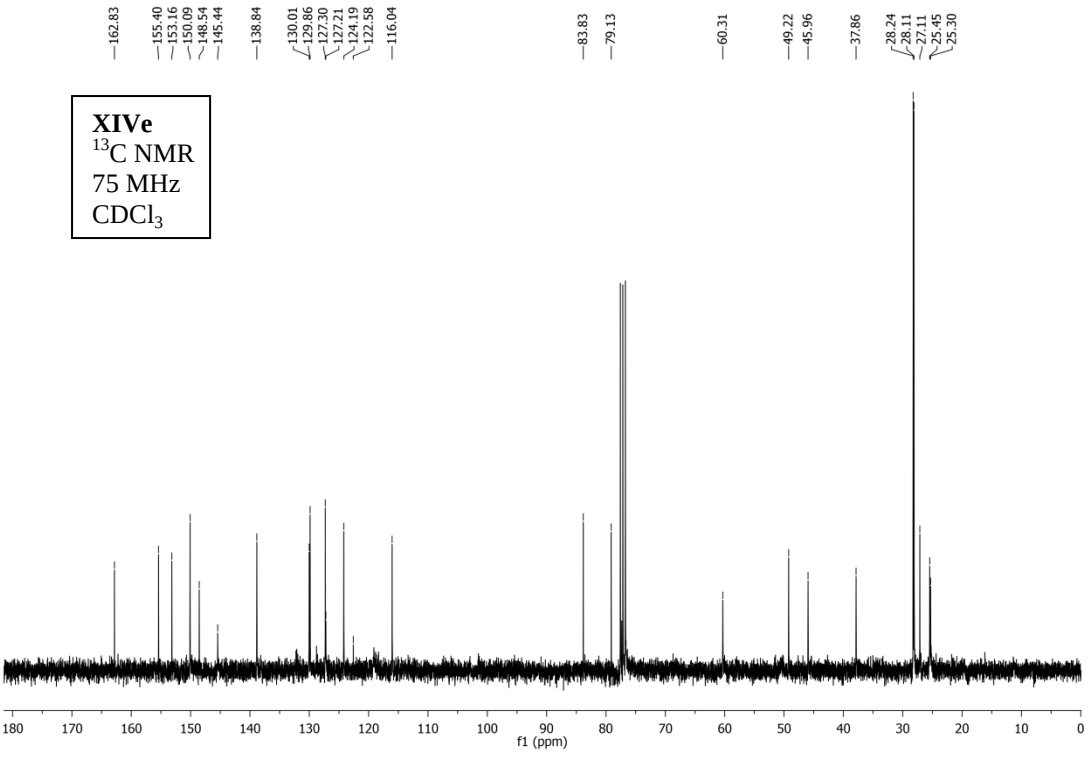
XIVe
^{13}C NMR
75 MHz
$CDCl_3$
f1 (ppm)

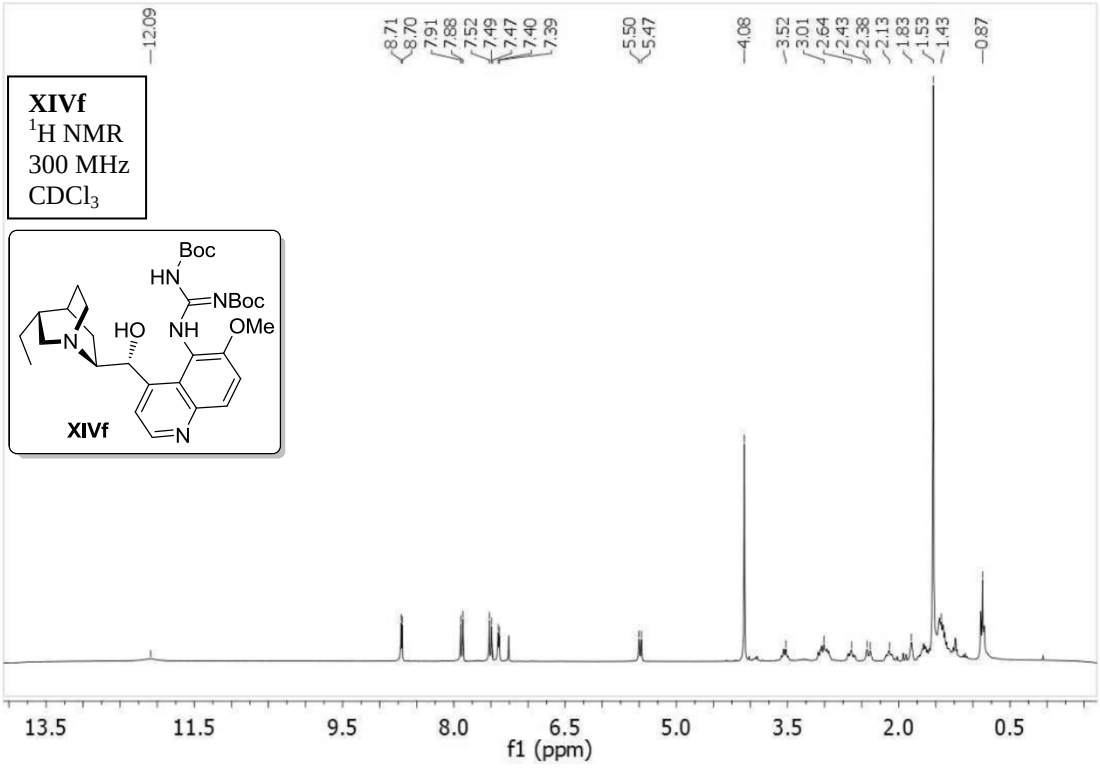
XIVf
1H NMR
300 MHz
CDCl3
Boc
HN
NBoc
HO
NH
OMe
N
XIVf
12.09
8.71
8.70
7.91
7.88
7.52
7.49
7.47
7.40
7.39
5.50
5.47
4.08
3.52
3.01
2.64
2.43
2.38
2.13
1.83
1.53
1.43
0.87
13.5
11.5
9.5
8.0
6.5
5.0
3.5
2.0
0.5
f1 (ppm)

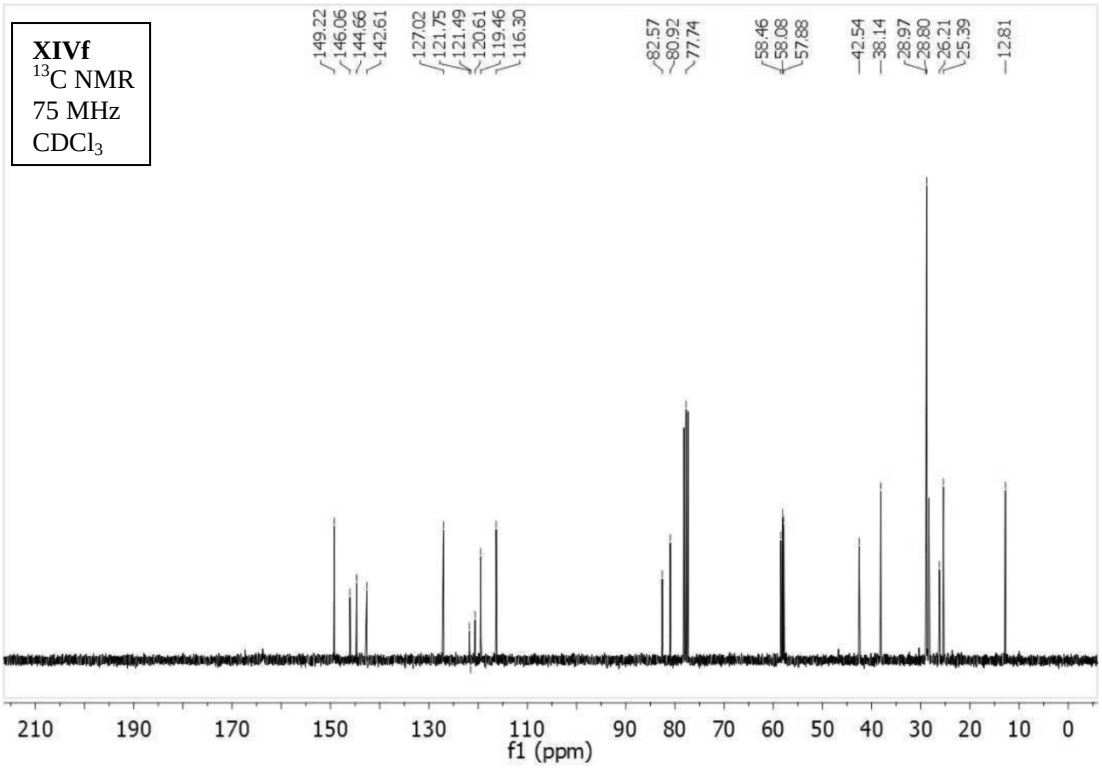
XIVf
13C NMR
75 MHz
CDCl3
149.22
146.06
144.66
142.61
127.02
121.75
121.49
120.61
119.46
116.30
82.57
80.92
77.74
58.46
58.08
57.88
42.54
38.14
28.97
28.80
26.21
25.39
12.81
210
190
170
150
130
110
90
80
70
60
50
40
30
20
10
0
f1 (ppm)

7.2.6. Cinchona alkaloid-derived guanidines XVa-f

Guanidines **XVa-f** were prepared following two different typical procedures, as outlined in *Scheme 25*.

Typical procedure A. A solution of di-Boc guanidine **XIVa** (136 mg, 0.240 mmol) in 20 mL of a 1:1 v/v mixture of dioxane and 0.5 M hydrochloric acid was stirred for 16 hours at room temperature. Evaporation of the solvent gave compound **XVa**·3HCl as a white sticky solid. This residue was dissolved in NaOH 0.5 M (5 mL) and extracted with $CHCl_3$ (3 x 5 mL). The combined organic layers were dried over Na_2SO_4 and concentrated under reduced pressure, to afford free guanidine **XVa** as a white solid (111 mg, 97% yield).

Typical procedure B. To a stirred solution of di-Boc guanidine **XIVa** (105 mg, 0.190 mmol) in DCM (1 mL) was added dropwise trifluoroacetic acid (430 μL, 5.60 mmol). The resulting mixture was stirred for 3 hours at room temperature. The solvent was the evaporated under reduced pressure. The residue was dissolved in NaOH 0.5 M (5 mL) and extracted with $CHCl_3$ (3 x 5 mL). The combined organic layers were dried over Na_2SO_4 and concentrated under reduced pressure, to afford free guanidine **XVa** as a white solid (65 mg, 94% yield).

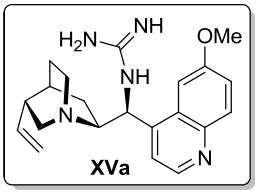

9-Guanidine(9-deoxy)*epi*-quinine (XVa).

^{1}H NMR (300 MHz, CD_3OD): δ 0.89-0.96 (m, 1H), 1.22-1.29 (m, 1H), 1.62 (br, 3 H), 2.28 (br, 1H), 2.75-2.87 (m, 2H), 3.12-3.24 (m, 3H), 4.00 (s, 3H), 4.95-5.01 (m, 2H), 5.21 (br d, 1H; *J* = 9.5 Hz), 5.75 (ddd, 1H; *J* = 17.6, 10.5, 7.3 Hz), 7.48 (dd, 1H; *J* = 9.2, 2.5 Hz), 7.61 (d, 1H; *J* = 1.8 Hz), 7.66 (d, 1H; *J* = 4.7 Hz), 7.99 (d, 1H; *J* = 9.4 Hz), 8.68 (d, 1H; *J* = 4.4 Hz).

^{13}C NMR (75 MHz, CD_3OD): δ 26.4, 28.6, 28.8, 40.7, 40.9, 41.7, 56.2, 56.6, 61.8, 103.2, 115.0, 122.5, 123.5, 129.0, 132.0, 142.6, 144.5, 145.3, 148.5, 158.9, 160.0.

HRMS (ESI): calcd for $C_{21}H_{28}N_5O$ $[M+H]^+$: 366.2294, found 366.2292.

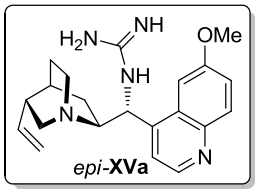

9-Guanidine(9-deoxy)-quinine (*epi*-XVa). Procedure A: white solid; 142 mg, 73% yield (reaction performed on 100 mg of *epi*-**XIVa**).

^{1}H NMR (300 MHz, D_2O): 1.91-2.49 (m, 4H), 2.65-2.75 (m, 1H), 2.80-2.98 (m,1H), 3.05-3.55 (m, 3H), 3.58-3.78 (m, 1H), 4.11 (s, 3H), 4.28-4.48 (m, 1H), 5.15-5.38 (m, 2H), 5.85-5.95 (m, 1H), 5.95-6.10 (m, 1H), 7.83 (d, 1H; *J* = 12 Hz), 7.90-8.00 (m, 1H), 8.15-8.35 (m, 2H), 9.00-9.15 (m, 1H).

^{13}C NMR (75 MHz, D_2O): δ 23.7, 24.3, 25.9, 36.3, 43.5, 54.8, 57.4, 60.3, 63.1, 67.2, 102.6, 117.8, 121.6, 124.9, 128.7, 129.3, 137.7, 142.1, 150.7, 162.4.

HRMS (ESI): calcd for $C_{21}H_{28}N_5O$ $[M+H]^+$: 366.2294, found 366.2286.

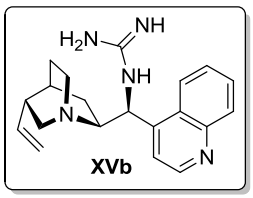

9-Guanidine(9-deoxy)*epi*-cinchonidine (XVb). Procedure B: white solid; 104 mg, 92% yield (reaction performed on 180 mg of **XIVb**).

^{1}H NMR (300 MHz, CD_3OD): δ 0.89-0.96 (m, 1H), 1.25-1.33 (m, 1H), 1.61-1.73 (m, 3H), 2.34 (br, 1H), 2.82-2.90 (m, 2H), 3.23-3.40 (m, 3H), 4.93-5.05 (m, 2H), 5.30 (br d, 1H; *J* = 9.3 Hz), 5.79 (d, 1H; *J* = 17.6, 10.3, 7.3 Hz), 7.67 (d, 1H; *J* = 4.4 Hz), 7.76 (t, 1H; *J* = 7.6 Hz), 7.86 (t, 1H; *J* = 7.6 Hz), 8.13 (d, 1H; *J* = 8.2 Hz), 8.44 (d, 1H; *J* = 8.5 Hz), 8.90 (d, 1H; *J* = 4.7 Hz).

^{13}C NMR (75 MHz, CD_3OD): δ 26.6, 28.5, 28.8, 40.8, 41.7, 56.3, 61.9, 79.4, 115.1, 120.2, 122.1, 124.5, 127.8, 128.9, 130.7, 131.3, 142.5, 149.4, 151.1, 158.9.

HRMS (ESI): calcd for $C_{20}H_{26}N_5$ $[M+H]^+$: 336.2188, found 336.2182.

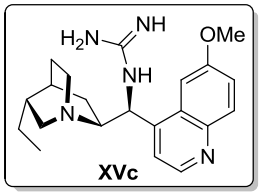

9-Guanidine(9-deoxy)*epi*-hydroquinine (XVc). Procedure B: white solid; 108 mg, 84% yield (reaction performed on 200 mg of **XIVc**).

^{1}H NMR (300 MHz, CD_3OD): δ 0.78 (t, 3H; *J* = 7.2 Hz), 0.94 (dd, 1H; *J* = 12.9, 7.9 Hz), 1.21-1.27 (m, 3H), 1.46-1.73 (m, 4H), 2.55-2.60 (m, 1H), 2-76-2.85 (m, 1H), 3.16-3.33 (m, 3H), 4.00 (s, 3H), 5.25 (br d, 1H; *J* = 8.0 Hz), 7.49 (dd, 1H; *J* = 9.1, 2.3 Hz), 7.63-7.66 (m, 2H), 7.99 (d, 1H; *J* = 9.1 Hz), 8.70 (d, 1H; *J* = 4.7 Hz).

^{13}C NMR (75 MHz, CD_3OD): δ 12.3, 26.1, 26.4, 28.5, 29.1, 38.5, 40.6, 41.8, 56.6, 58.0, 61.8, 103.2, 122.5, 123.5, 129.0, 132.1, 144.5, 145.4, 148.5, 158.9, 160.1.

HRMS (ESI): calcd for $C_{21}H_{30}N_5O$ $[M+H]^+$: 368.2450, found 368.2434.

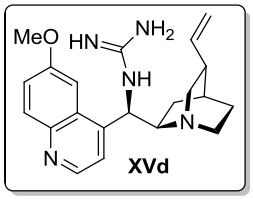

9-Guanidine(9-deoxy)*epi*-quinidine (XVd).
Procedure B: white solid; 434 mg, 84% yield (reaction performed on 800 mg of **XIVd**).
^{1}H NMR (300 MHz, CD_3OD): δ 0.85-0.94 (m, 1H), 1.23-1.31 (m, 1H), 1.55-1.61 (m, 3H), 2.31-2.39 (m, 1H), 2.90-3.10 (m, 4H), 3.18-3.28 (m, 1H), 4.02 (s, 3H), 5.07-5.16 (m, 2H), 5.24 (d, 1H; *J* = 10.0 Hz), 5.93 (ddd, 1H; *J* = 17.3, 10.5, 6.4 Hz), 7.47 (dd, 1H; *J* = 9.4, 2.6 Hz), 7.61 (d, 1H; *J* = 4.7 Hz), 7.66 (d, 1H; *J* = 2.3 Hz), 7.98 (d, 1H; *J* = 9.1 Hz), 8.69 (d, 1H; *J* = 4.7 Hz).
^{13}C NMR (75 MHz, CD_3OD): δ 25.8, 27.1, 29.0, 40.4, 48.2, 49.8, 56.5, 62.5, 76.2, 103.0, 115.4, 121.8, 123.6, 129.4, 131.9, 141.3, 145.3, 146.3, 148.4, 159.9, 159.9.
HRMS (ESI): calcd for $C_{21}H_{28}N_5O$ $[M+H]^+$: 366.2294, found 366.2283.

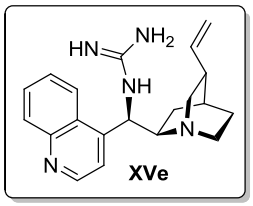

9-Guanidine(9-deoxy)*epi*-cinchonine (XVe).
Procedure B: white solid; 69 mg, 98% yield (reaction performed on 111 mg of **XIVe**).
^{1}H NMR (300 MHz, CD_3OD): δ 0.64-0.70 (m, 1H), 1.0.5-1.16 (m, 1H), 1.37-1.46 (m, 3H), 2.17-2.25 (m, 1H), 2.77-2.93 (m, 4H), 3.00-3.10 (m, 1H), 4.99-5.05 (m, 2H), 5.15 (d, 1H; *J* = 10.0 Hz), 5.82 (ddd, 1H; *J* = 17.3, 10.4, 6.7 Hz), 7.56-7.60 (m, 2H), 7.69 (t, 1H; *J* = 7.6 Hz), 7.96 (d, 1H; *J* = 8.2 Hz), 8.45 (d, 1H; *J* = 8.5 Hz), 8.71 (d, 1H; *J* = 4.4 Hz).
^{13}C NMR (75 MHz, CD_3OD): δ 25.9, 27.2, 28.7, 29.2, 40.7, 48.3, 50.0, 62.5, 115.3, 121.6, 125.1, 128.1, 128.7, 130.2, 130.9, 141.4, 149.0, 150.4, 151.0, 160.6.
HRMS (ESI): calcd for $C_{20}H_{26}N_5$ $[M+H]^+$: 336.2188, found 336.2183.

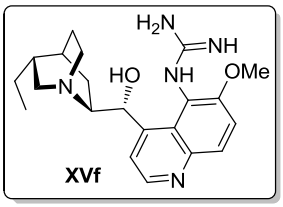

5'-Guanidine-hydroquinine (XVf).
Procedure A: white solid; 16 mg, 96% yield (reaction performed on 26 mg of **XIVf**).
^{1}H NMR (300 MHz, D_2O): δ 0.87 (t, 3H; *J* = 9 Hz), 1.25-1.43 (m,1H), 1.50-1.78 (m, 3H), 1.95-2.17 (m, 3H), 2.81-2.96 (m, 1H), 3.39-3.64 (m, 3H), 3.65-3.80 (m, 1H), 3.88-4.03 (m, 1H), 4.08 (s, 3H), 5.04 (d, 1H; *J* = 9 Hz), 7.65

(d, 1H; *J* = 9 Hz), 7.83 (d, 1H; *J* = 6 Hz), 8.42 (d, 1H; *J* = 9Hz), 8.97 (d, 1H; *J* = 6 Hz).

^{13}C NMR (75 MHz, D_2O): δ 10.8, 22.6 24.1, 26.3, 26.9, 36.1, 41.3, 55.9, 56.7, 58.2, 69.6, 114.0, 117.8, 121.2, 113.3, 133.4, 142.1, 143.9, 148.0, 155.1, 157.1.

HRMS (ESI): calcd for $C_{11}H_{30}N_5O_2$ $[M+H]^+$: 384.2394, found 584.2403.

7.2.7. NMR spectra of guanidines XVa-f

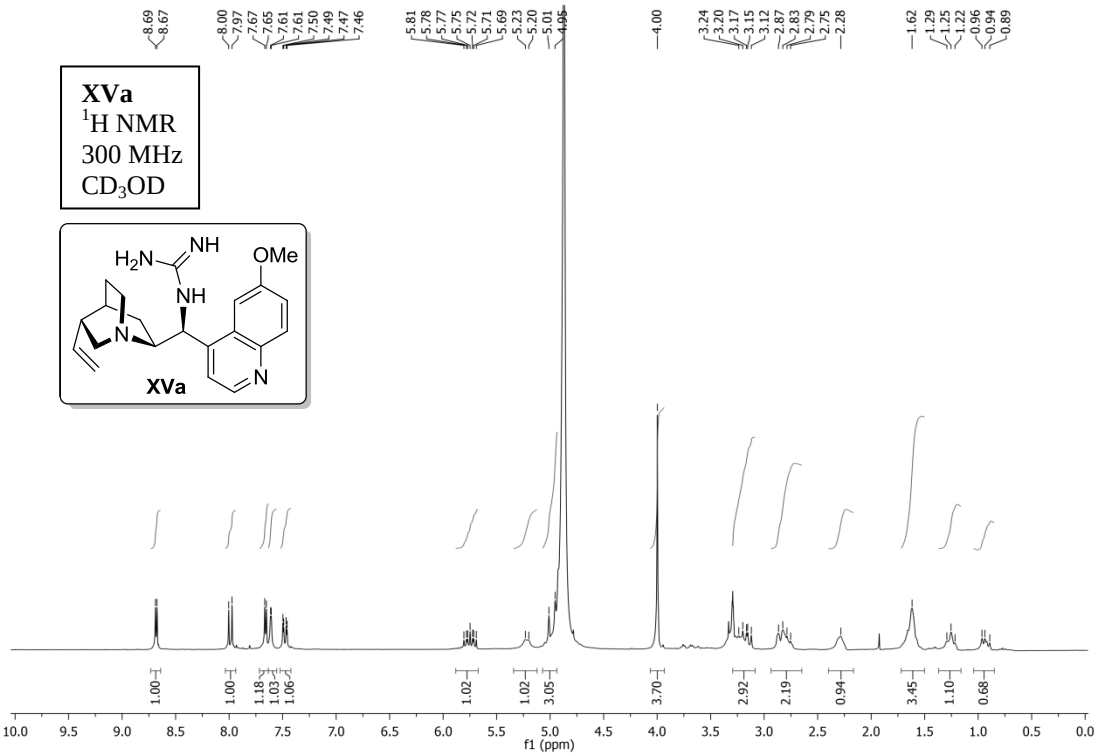

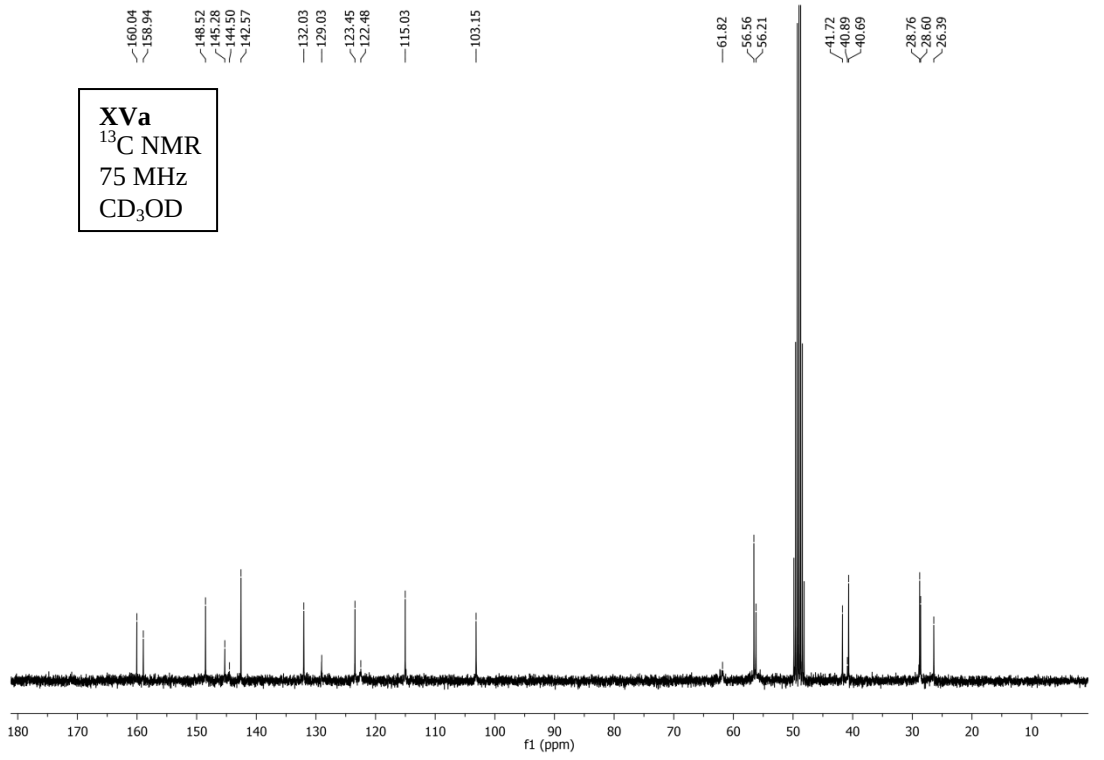

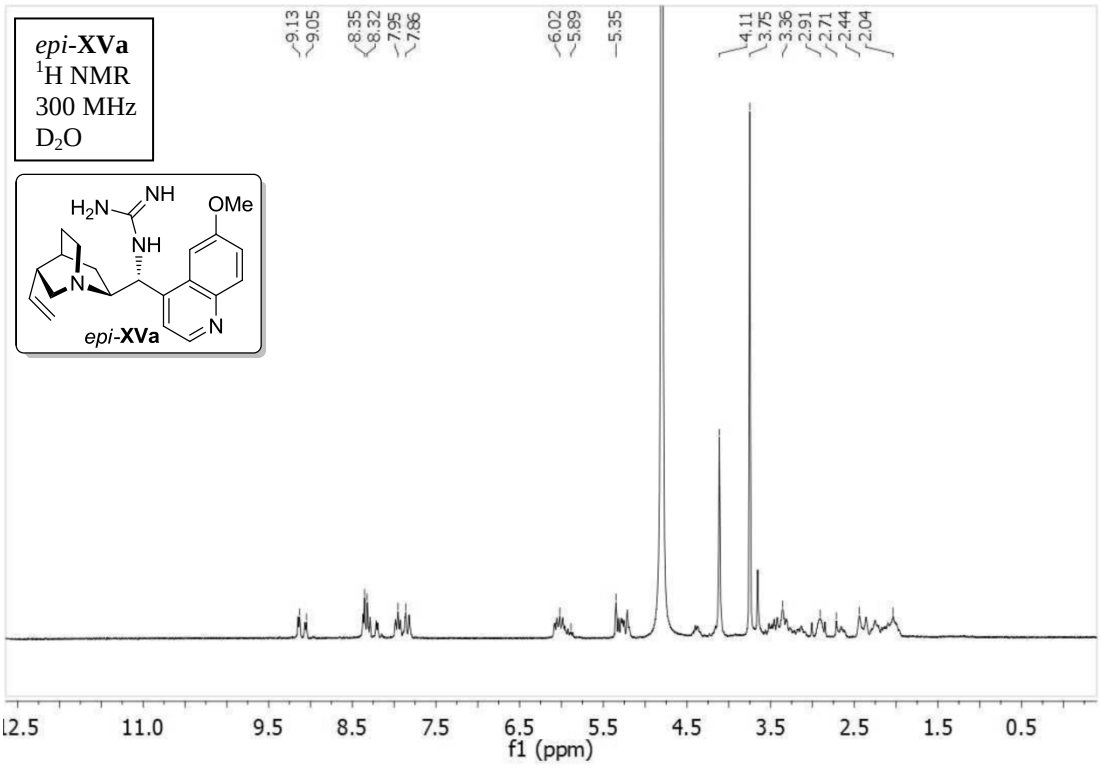
epi-XVa
1H NMR
300 MHz
D2O
9.13
9.05
8.35
8.32
7.95
7.86
6.02
5.89
5.35
4.11
3.75
3.36
2.91
2.71
2.44
2.04
epi-XVa
f1 (ppm)

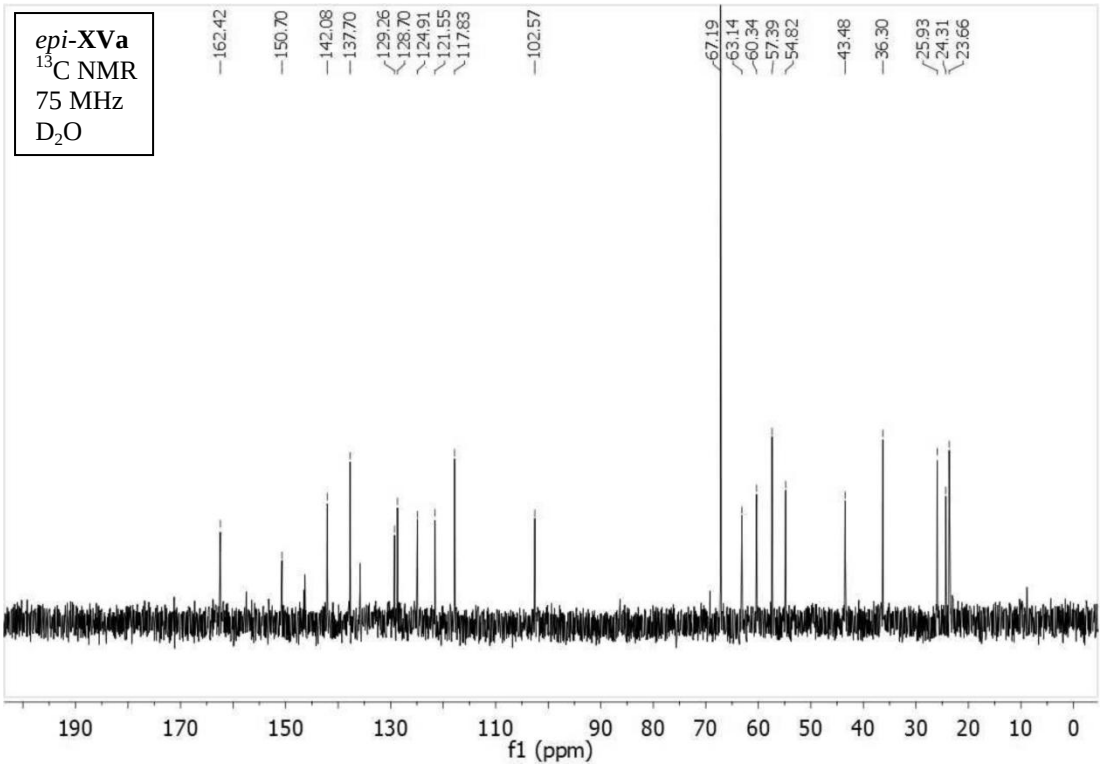
epi-XVa
13C NMR
75 MHz
D2O
162.42
150.70
142.08
137.70
129.26
128.70
124.91
121.55
117.83
102.57
67.19
63.14
60.34
57.39
54.82
43.48
36.30
25.93
24.31
23.66
f1 (ppm)

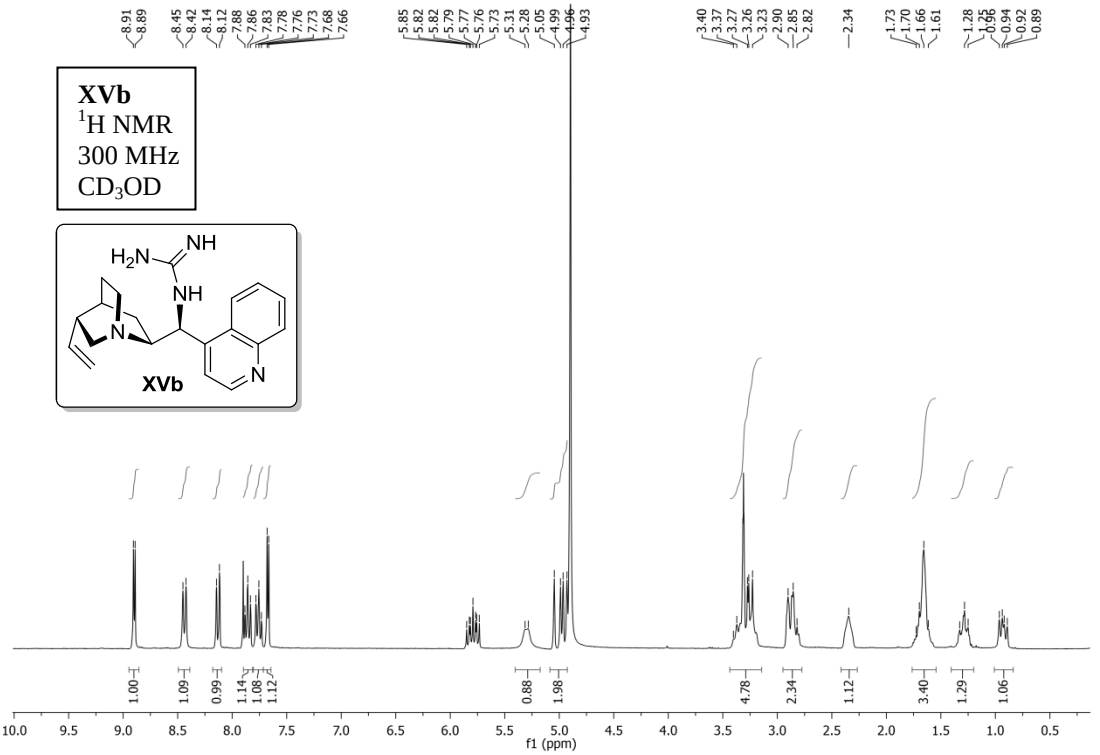
XVb
1H NMR
300 MHz
CD3OD
XVb
f1 (ppm)

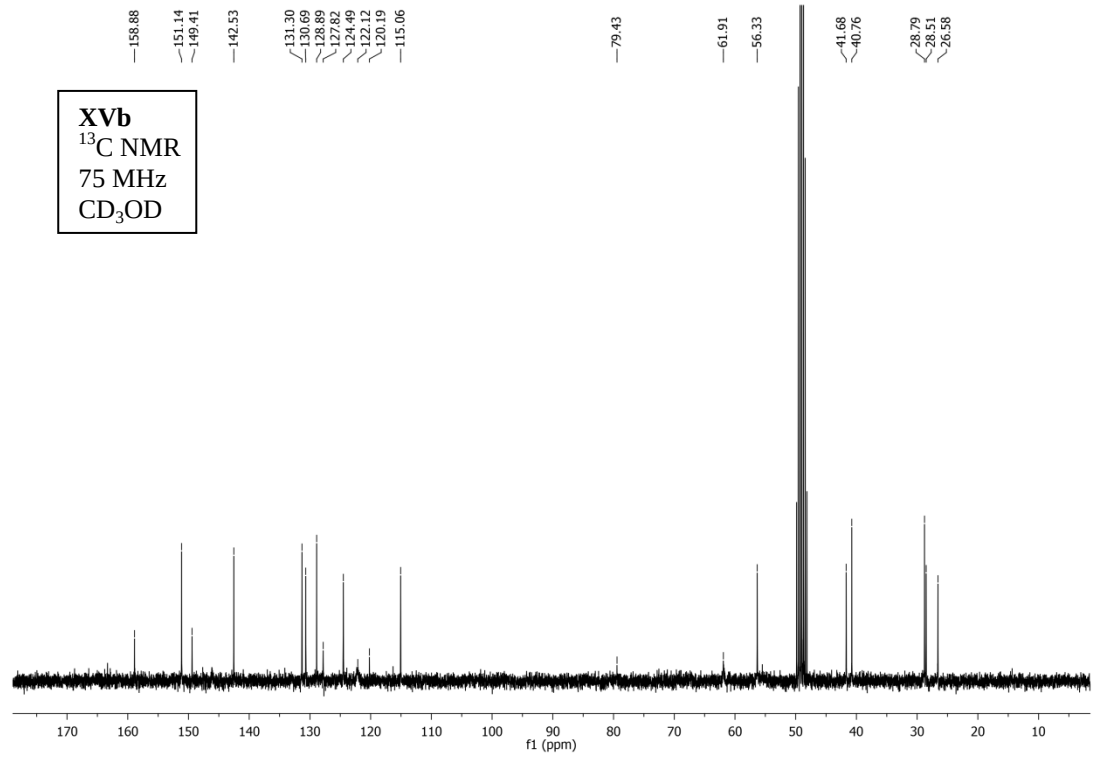
XVb
13C NMR
75 MHz
CD3OD
f1 (ppm)

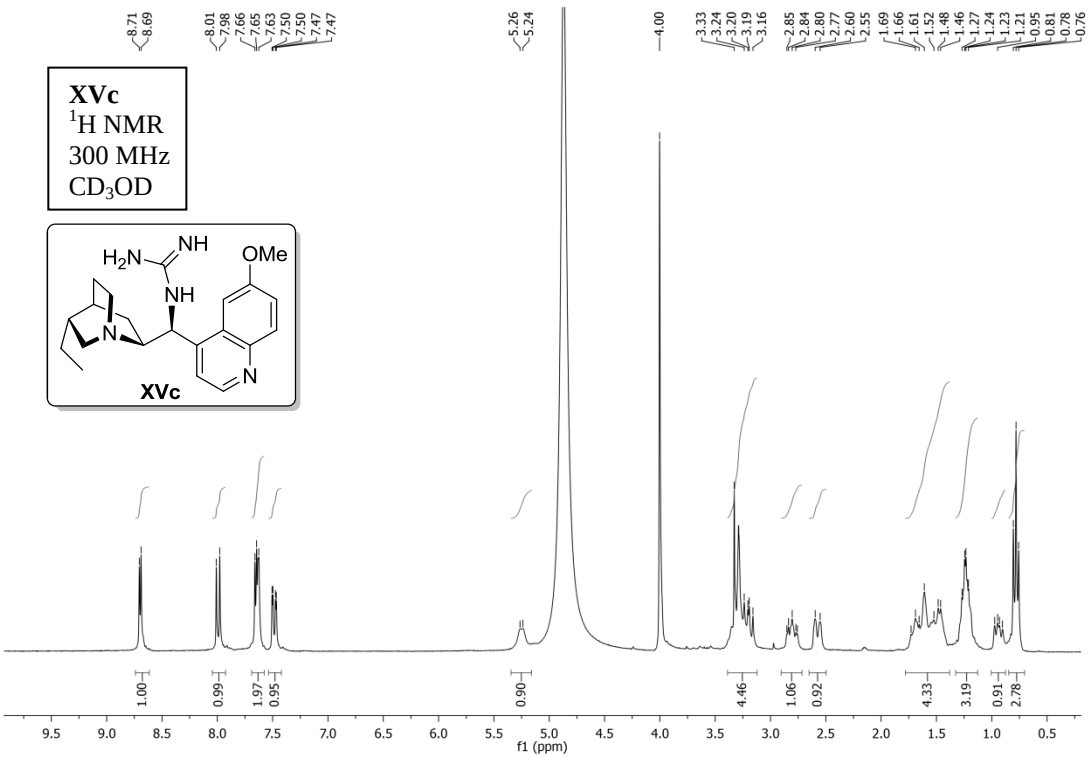
XVc
1H NMR
300 MHz
CD3OD
XVc
f1 (ppm)

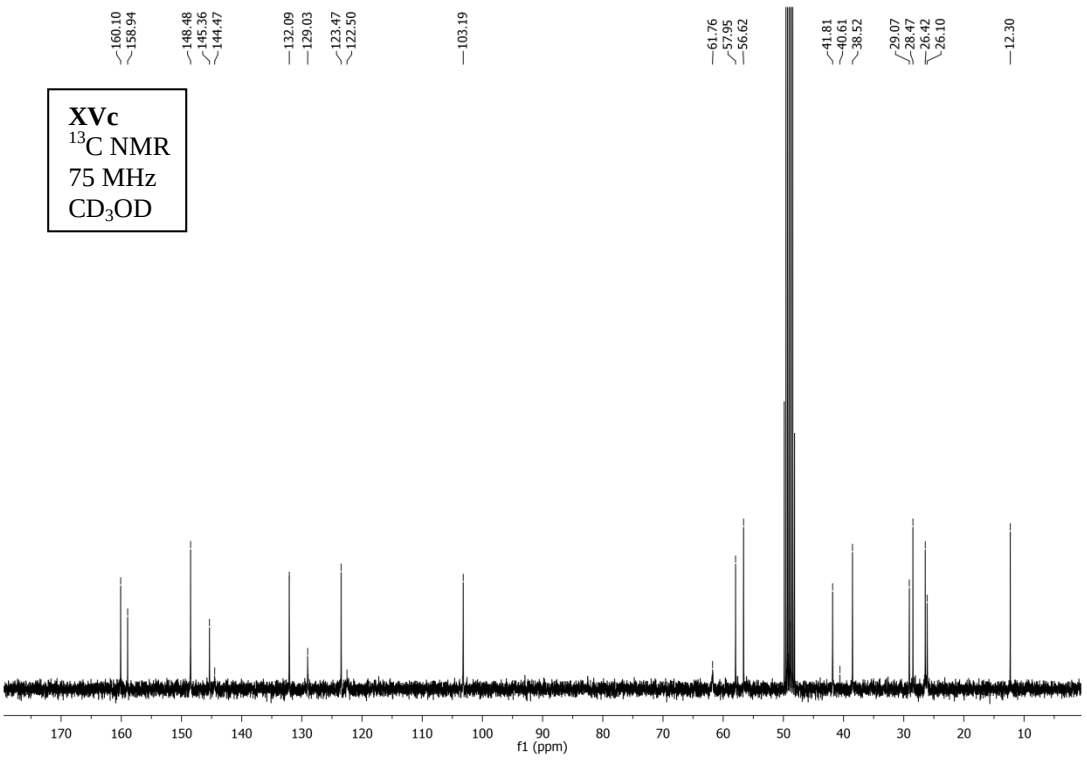
XVc
13C NMR
75 MHz
CD3OD
f1 (ppm)

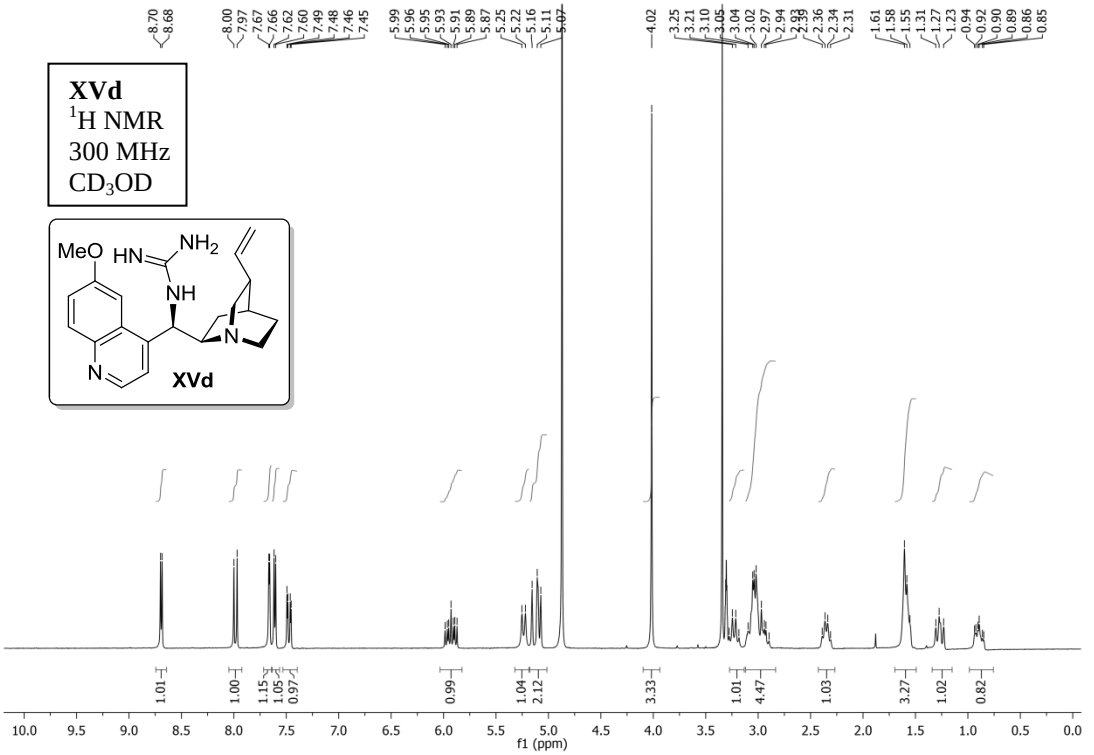
XVd
1H NMR
300 MHz
CD3OD
MeO
HN
NH2
NH
N
N
XVd
f1 (ppm)

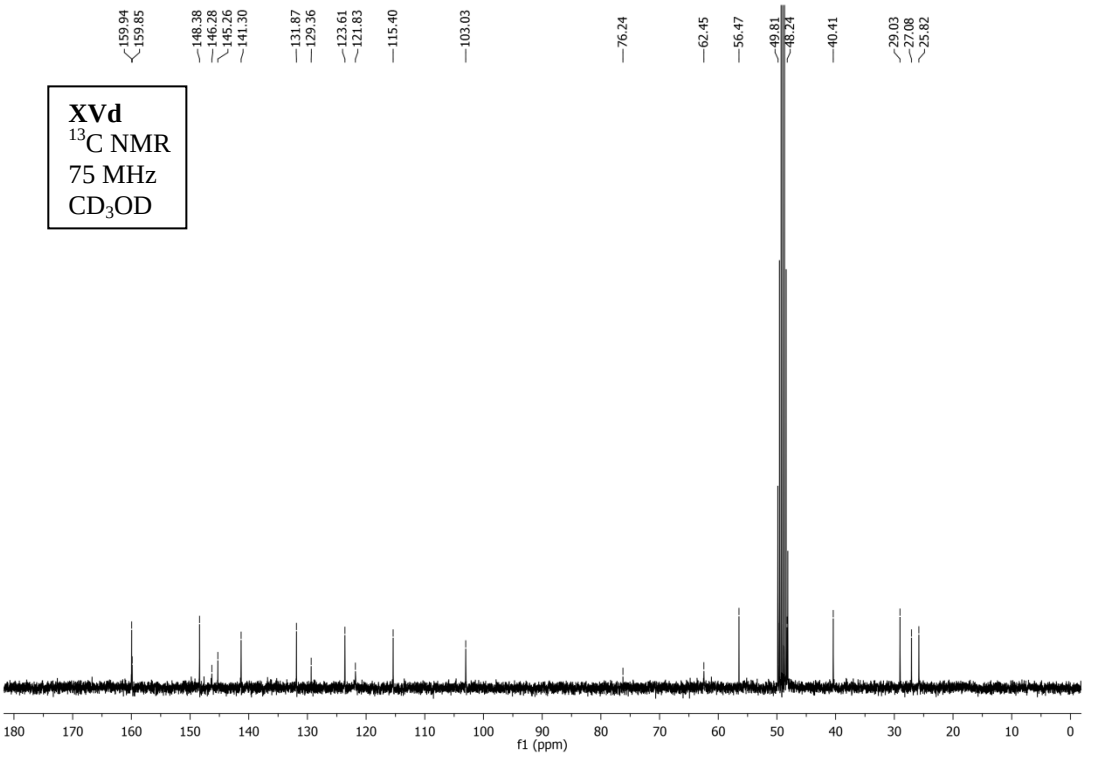
XVd
13C NMR
75 MHz
CD3OD
f1 (ppm)

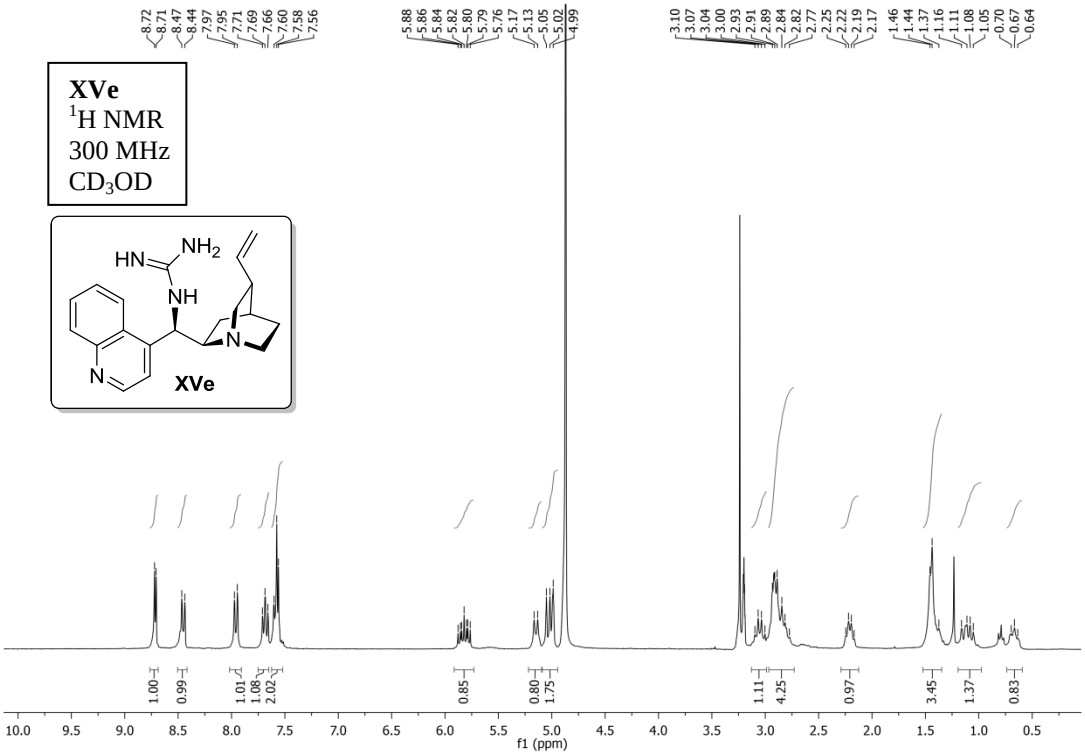
XVe
1H NMR
300 MHz
CD3OD
XVe
f1 (ppm)

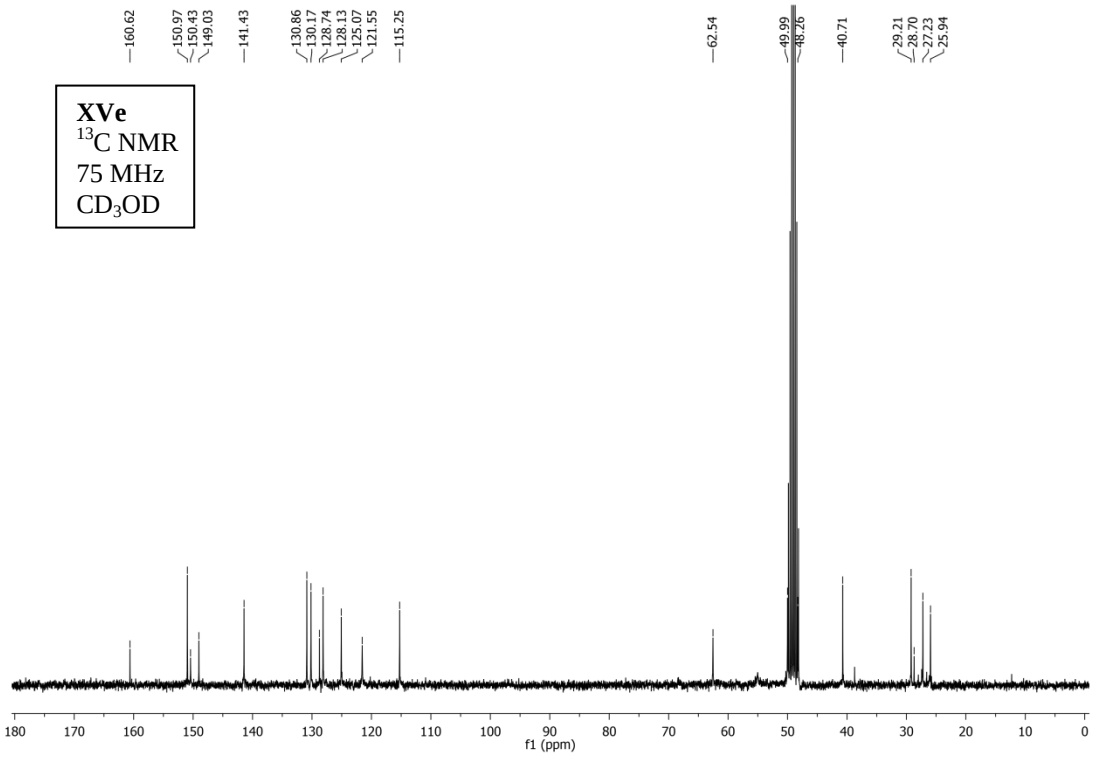
XVe
13C NMR
75 MHz
CD3OD
f1 (ppm)

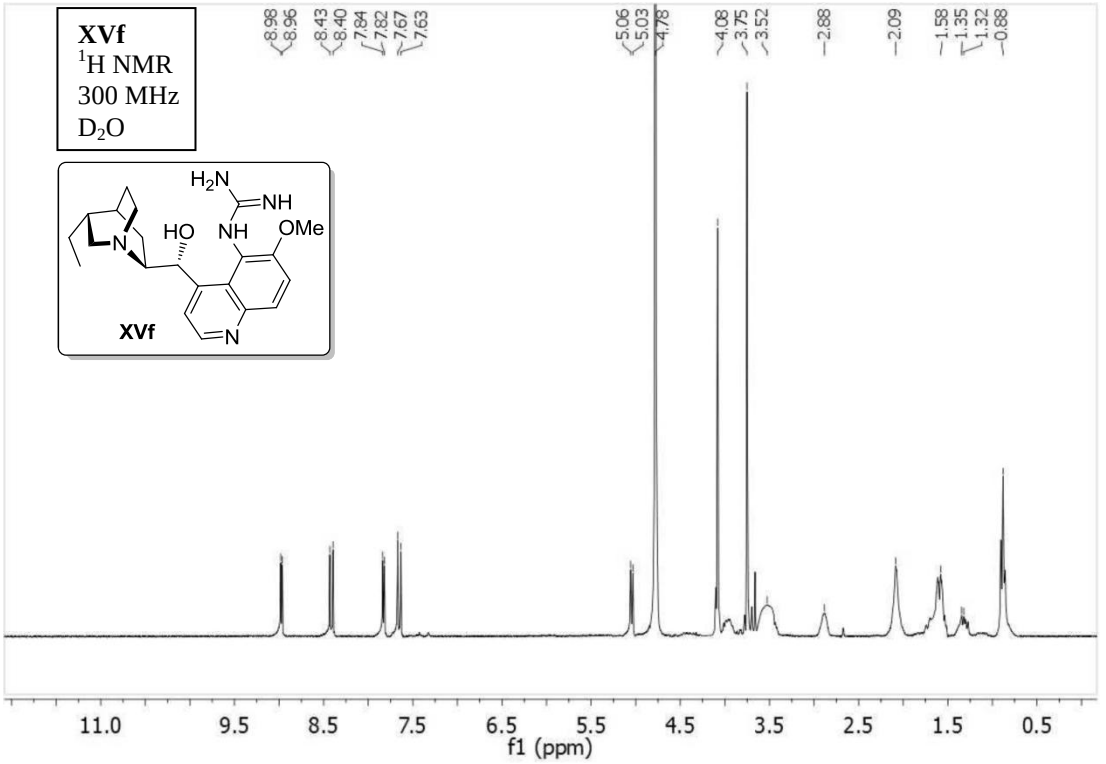
XVf
^{1}H NMR
300 MHz
D_2O
8.98
8.96
8.43
8.40
7.84
7.82
7.67
7.63
5.06
5.03
4.78
4.08
3.75
3.52
2.88
2.09
1.58
1.35
1.32
0.88
H_2N
NH
HO
NH
OMe
N
N
XVf
11.0
9.5
8.5
7.5
6.5
5.5
4.5
3.5
2.5
1.5
0.5
f1 (ppm)

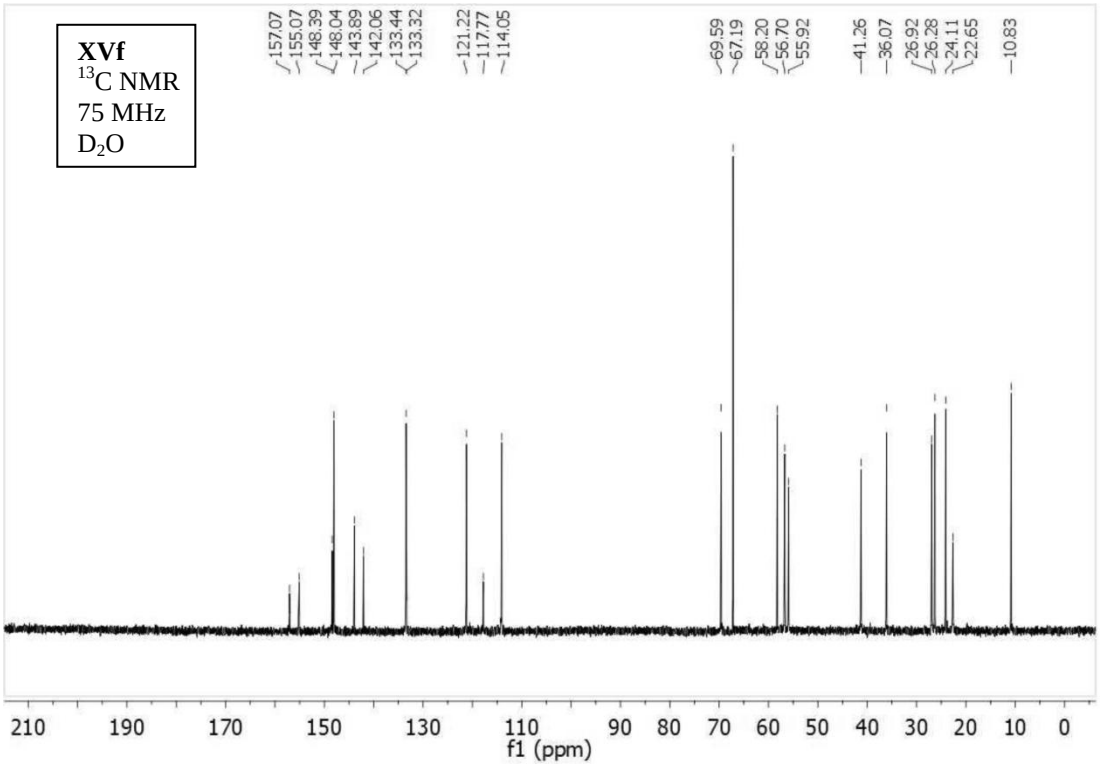
XVf
^{13}C NMR
75 MHz
D_2O
157.07
155.07
148.39
148.04
143.89
142.06
133.44
133.32
121.22
117.77
114.05
69.59
67.19
58.20
56.70
55.92
41.26
36.07
26.92
26.28
24.11
22.65
10.83
210
190
170
150
130
110
90
80
70
60
50
40
30
20
10
0
f1 (ppm)

7.2.8. Cinchona alkaloid-derived alkyl-substituted guanidines XVIa-e and XVII

Typical procedure for the synthesis of XVIa-e. To a stirred solution of 9-amino(9-deoxy)*epi*-quinine (**75a**, 238 mg, 0.74 mmol) in toluene (12 mL) were added DCC (**81a**, 183 mg, 0.89 mmol) and $ZrCl_4$ (86 mg, 0.37 mmol). The reaction mixture was stirred at reflux for 24 h, after which time the solvent was removed under reduced pressure. The crude material was purified by flash chromatography on silica gel, with DCM/MeOH 40:1 to 5:1 gradient elution. The pure product **XVIa** was obtained as a white solid (323 mg, 83% yield).

The NMR spectra of compounds **XIVa-e** show broad, unresolved signals, which in most cases make it difficult to detect all the ^{13}C carbon resonances (see discussion in *Section 3.2.*).

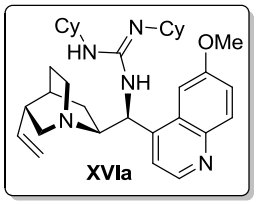

XVIa

[*N,N′*-dicyclohexyl-*N′′*-(9-deoxy)*epi*-quinine] guanidine (XVIa).

^{1}H NMR (300 MHz, $CDCl_3$): δ 0.82-1.95 (m, 26H), 2.30-2.62 (m, 2H), 2.94-3.15 (m, 2H), 3.39-3.59 (m, 4H), 4.06-4.37 (m, 4H), 5.02-5.08 (m, 2H), 5.64 (ddd, 1H; *J* = 17.3, 10.1, 6.9 Hz), 6.49 (br d, 1H; *J* = 8.8 Hz), 7.38-7.60 (m, 3H), 7.99 (d, 1H; *J* = 9.1 Hz), 8.20-8.26 (m, 1H), 8.75 (d, 1H; *J* = 4.1 Hz).

^{13}C NMR (75 MHz, $CDCl_3$): δ 24.1, 24.4, 14.5, 14.9, 15.8, 16.9, 31.3, 32.7, 33.3, 37.7, 42.4, 52.5, 53.4, 54.8, 57.7, 61.9, 102.2, 116.7, 119.3, 123.7, 129.2, 131.6, 138.3, 144.0, 144.8, 147.4, 154.0, 159.5.

HRMS (ESI): calcd for $C_{33}H_{48}N_5O$ $[M+H]^+$: 530.3859, found 530.3846.

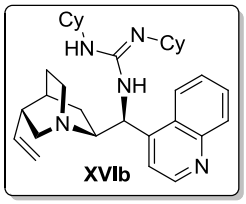

XVIb

[*N,N′*-dicyclohexyl-*N′′*-(9-deoxy)*epi*-cinchonidine] guanidine (XVIb). White solid; 474 mg, 93% yield (reaction performed on 300 mg of **75b** and 252 mg of **81a**).

^{1}H NMR (300 MHz, $CDCl_3$): δ 0.90-1.72 (m, 26H), 2.072.37 (m, 2H), 2.85-3.02 (m, 2H), 3.32-3.68 (m, 4H), 4.88-4.98 (m, 2H), 5.55-5.65 (m, 1H), 6.02 (bs, 1H), 7.62-7.75 (m, 5H), 8.06-8.38 (m, 2 H), 8.85 (bs, 1H).

^{13}C NMR (75 MHz, $CDCl_3$): δ 24.4, 24.6, 25.0, 26.5, 27.1, 31.3, 32.6, 38.3, 38.8, 41.6, 52.5, 55.2, 115.8, 119.2, 124.0, 127.7, 129.9, 130.6, 139.8, 150.3, 153.9.

HRMS (ESI): calcd for $C_{32}H_{46}N_5$ $[M+H]^+$: 500.3753, found 500.3755.

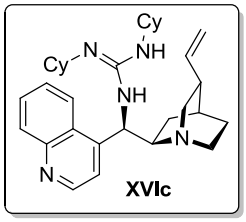

XVIc

[*N*,*N′*-dicyclohexyl-*N′′*-(9-deoxy)*epi*-cinchonine] guanidine (XVIc). White solid; 292 mg; 65% yield (reaction performed on 265 mg of **75e** and 225 mg of **81a**).

^{1}H NMR (300 MHz, $CDCl_3$): δ 0.92-1.91 (m, 26H), 2.40-2.42 (m, 1H), 3.00-3.17 (m, 2H), 3.38-3.47 (m, 5H), 5.13-5.21 (m, 2H), 5.76-5.92 (br, 2H), 7.67-7.85 (m, 5H), 8.18 (d, 1H; *J* = 7.9 Hz), 8.39 (br d, 1H; *J* = 6.2 Hz), 8.98 (d, 1H; *J* = 4.1 Hz).

^{13}C NMR (75 MHz, $CDCl_3$): δ 25.6, 24.8, 25.0, 25.0, 25.2, 25.4, 25.6, 27.9, 32.8, 33.0, 33.3, 36.7, 39.0, 47.6, 49.0, 52.8, 53.5, 116.4, 123.0, 127.6, 129.8, 131.0, 138.6, 150.6.

HRMS (ESI): calcd for $C_{32}H_{46}N_5$ $[M+H]^+$: 500.3753, found 500.3736.

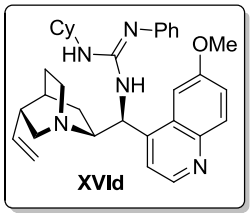

XVId

[*N*-cyclohexyl-*N′*-phenyl-*N′′*-(9-deoxy)*epi*-quinine] guanidine (XVId). White solid; 207 mg, 48% yield (reaction performed on 267 mg of **75a** and 170 mg of **81b**).

^{1}H NMR (300 MHz, $CDCl_3$): δ 0.80-1.94 (m, 16H), 240 (bs, 1H), 2.83-3.46 (m, 5H), 3.88-3.99 (m, 4H), 4.97-5.03 (m, 2H), 5.58-5.69 (m, 1H), 6.08 (bs, 1H), 6.83 (d, 2H; *J* = 6.6 Hz), 7.05-7.14 (m, 3H), 7.33 (bs, 1H), 7.67 (bs, 2H), 7.94 (bs, 1H), 8.75 (bs, 1H).

^{13}C NMR (75 MHz, $CDCl_3$): δ 24.3, 24.4, 24.7, 24.9, 27.0, 32.4, 33.1, 38.5, 41.8, 52.6, 54.9, 56.9, 62.5, 101.9, 116.0, 120.0, 122.9, 126.3, 129.7, 131.7, 131.8, 139.5, 147.6, 154.8, 158.8.

MS (ESI): calcd for $C_{33}H_{42}N_5O$ $[M+H]^+$: 524.3, found 524.4.

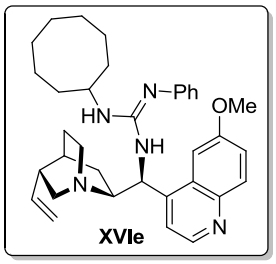

[*N*-cyclooctyl-*N′*-phenyl-*N″*-(9-deoxy)*epi*-quinine] guanidine (XVIe). White solid; 430 mg, 78% yield (reaction performed on 321 mg of **75a** and 271 mg of **81c**).

^{1}H NMR (300 MHz, $CDCl_3$): δ 1.09-1.35 (m, 16H), 1.71-1.77 (m, 3H), 2.00 (bs, 1H), 2.45 (bs, 1H), 2.87-3.50 (m, 3H), 3.94-4.02 (m, 4H), 5.02-5.08 (m, 2H), 5.68 (ddd, 1H; *J* = 17.3, 10.4, 6.9 Hz), 6.13 (bs, 1H), 6.84 (d, 2H; *J*= 6.7 Hz), 7.09-7.20 (m, 3 H), 7.37 (m, 1H), 7.66 (m, 2H), 8.00 (bs, 1H), 8.82 (bs, 1H).

^{13}C NMR (75 MHz, $CDCl_3$): δ 23.0, 23.2, 25.3, 26.2, 26.3, 26.8, 31.3, 32.5, 38.3, 41.6, 53.4, 56.5, 62.2, 101.6, 115.4, 119.5, 122.3, 125.6, 128.2, 129.3, 131.2, 136.4, 139.5, 143.4, 144.2, 147.4, 154.5, 158.3.

HRMS (ESI): calcd for $C_{35}H_{46}N_5O$ $[M+H]^+$: 552.3702, found 552.3709.

Procedure for the synthesis of XVII

2-Chloro-1,3-dimethyl-3,4,5,6-tetrahydropyrimidin-1-ium chloride (83)[91]**.** To a stirred solution of 1,3-dimethyltetrahydropyrimidin-2(1*H*)-one (**82**, 564 mg, 5.00 mmol) in anhydrous toluene (5.0 mL) was added oxalyl chloride (751 mg, 6.00 mmol). The resulting bright yellow solution was stirred for 16 h at 60 °C under argon, causing the precipitation of a white solid. This precipitate was allowed to settle, the solution was removed and the solid was repeatedly washed with Et_2O. Product **83** was obtained as a white solid (435 mg, 48% yield), which was used in the subsequent step without further purification. **^{1}H NMR** (300 MHz, $CDCl_3$): δ 2.04-2.08 (m, 2H), 3.23 (s, 6H), 3.65 (t, 4H; *J* = 5.5 Hz). **^{13}C NMR** (75 MHz, $CDCl_3$): δ 19.0, 43.0, 50.6, 152.3.

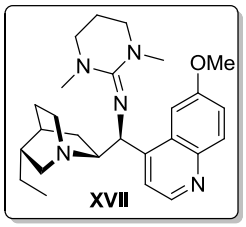

***N*-(1,3-dimethyltetrahydropyrimidin-2(1*H*)-ylidene)-9-amino(9-deoxy) *epi*-hydroquinine (XVII).** To a stirred solution of *epi*-aminohydroquinine (**75c**, 218 mg, 0.670 mmol) in anhydrous MeCN (3.0 mL) was added Et_3N (186 mg, 1.84 mmol). The reaction mixture was cooled to 0 °C, **83** (180 mg, 1.01 mmol) was slowly added and the mixture was allowed to reach room temperature. After that, it was stirred at reflux for 24h hours. 0.5 M NaOH (10 mL) were then added and the mixture was extracted with MeCN (3 x 10 mL). The

combined extracts were dried over Na_2SO_4 and concentrated under reduced pressure. The crude material was purified by flash chromatography on silica gel, with DCM/MeOH 20:1 to 1:1 elution. Pure **XVII** was obtained as a white solid (99 mg, 34% yield).

^{1}H NMR (300 MHz, $CDCl_3$): δ 0.59-0.77 (m, 4H), 1.04-1.45 (m, 7H), 1.84-1.87 (m, 2H), 2.59-2.72 (m, 2H), 2.94-3.15 (m, 12H), 3.26-3.31 (m, 2H), 3.59-3.64 (m, 2H), 3.88 (s, 3H), 4.96 (d, 1H; *J* = 10.0 Hz), 7.26-7.29 (m, 2H), 7.92 (d, 1H; *J* = 9.1 Hz), 8.62 (d, 1H; *J* = 3.7 Hz), 8.74 (d, 1H; *J* = 4.0 Hz).

^{13}C NMR (75 MHz, $CDCl_3$): δ 11.9, 21.7, 24.5, 25.1, 27.2, 28.5, 37.2, 41.1, 41.6, 48.7, 55.8, 56.0, 56.9, 62.3, 101.5, 120.5, 122.3, 127.6, 132.3, 142.7, 144.1, 148.7, 158.1, 158.9.

HRMS (ESI): calcd for $C_{26}H_{38}N_5O$ $[M+H]^+$: 436.3076, found 436.3056.

7.2.9. NMR spectra of alkyl-substituted guanidines XVIa-e and XVII

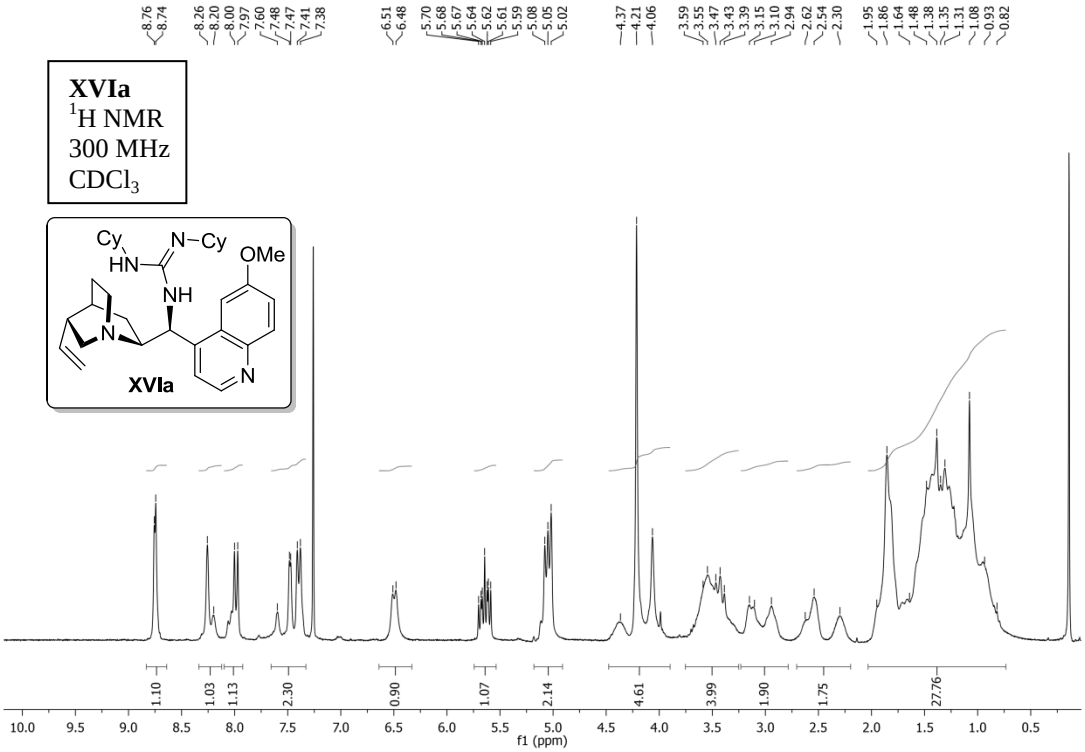

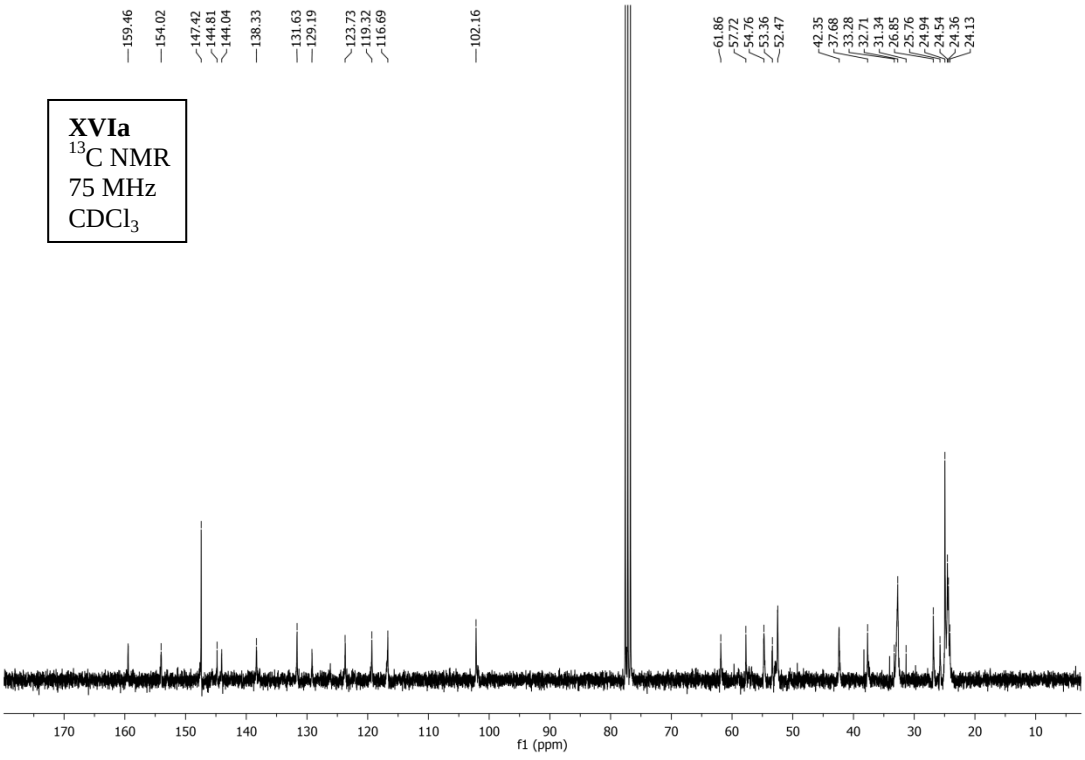

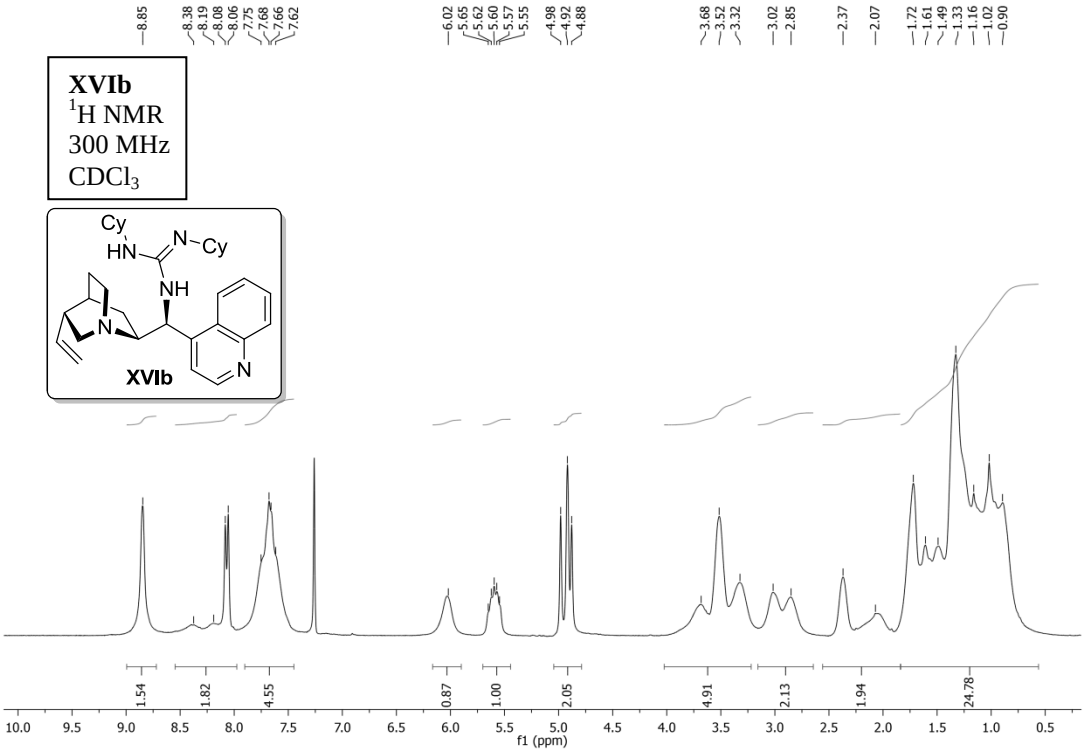
8.85
8.38
8.19
8.08
8.06
7.75
7.68
7.66
7.62
6.02
5.65
5.62
5.60
5.57
5.55
4.98
4.92
4.88
3.68
3.52
3.32
3.02
2.85
2.37
2.07
1.72
1.61
1.49
1.33
1.16
1.02
0.90
XVIb
1H NMR
300 MHz
CDCl3
Cy
HN
N
Cy
NH
N
N
XVIb
1.54
1.82
4.55
0.87
1.00
2.05
4.91
2.13
1.94
24.78
f1 (ppm)

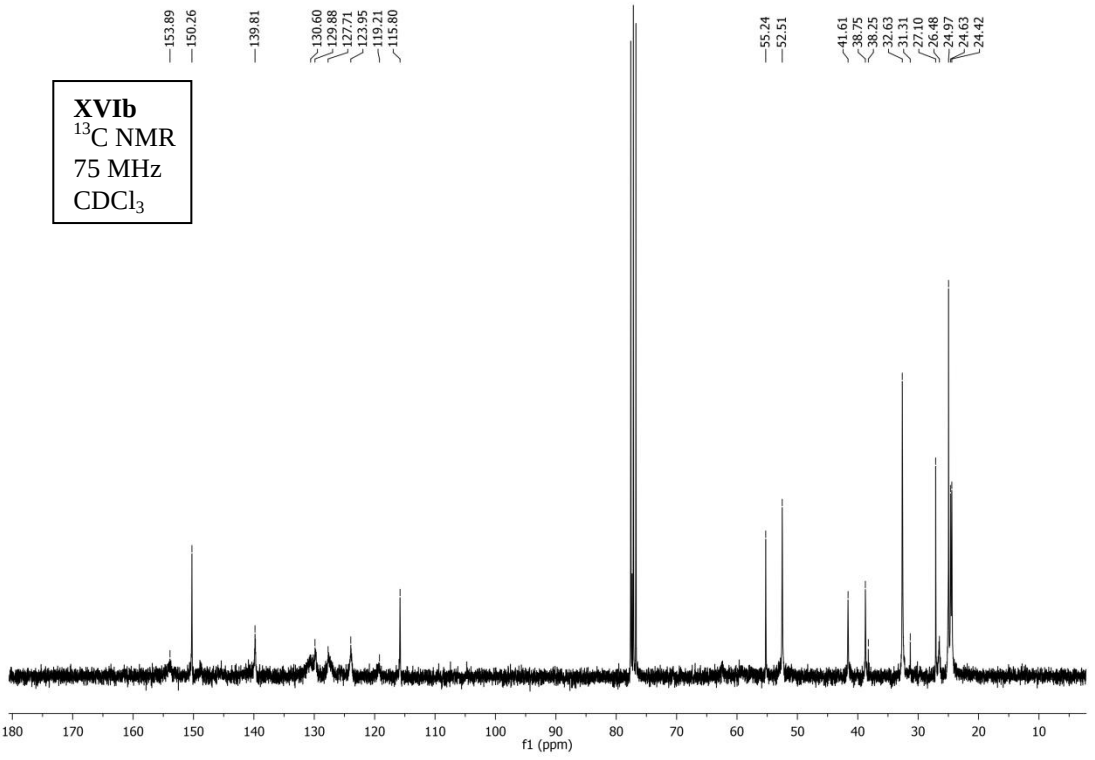
153.89
150.26
139.81
130.60
129.88
127.71
123.95
119.21
115.80
55.24
52.51
41.61
38.75
38.25
32.63
31.31
27.10
26.48
24.97
24.63
24.42
XVIb
13C NMR
75 MHz
CDCl3
f1 (ppm)

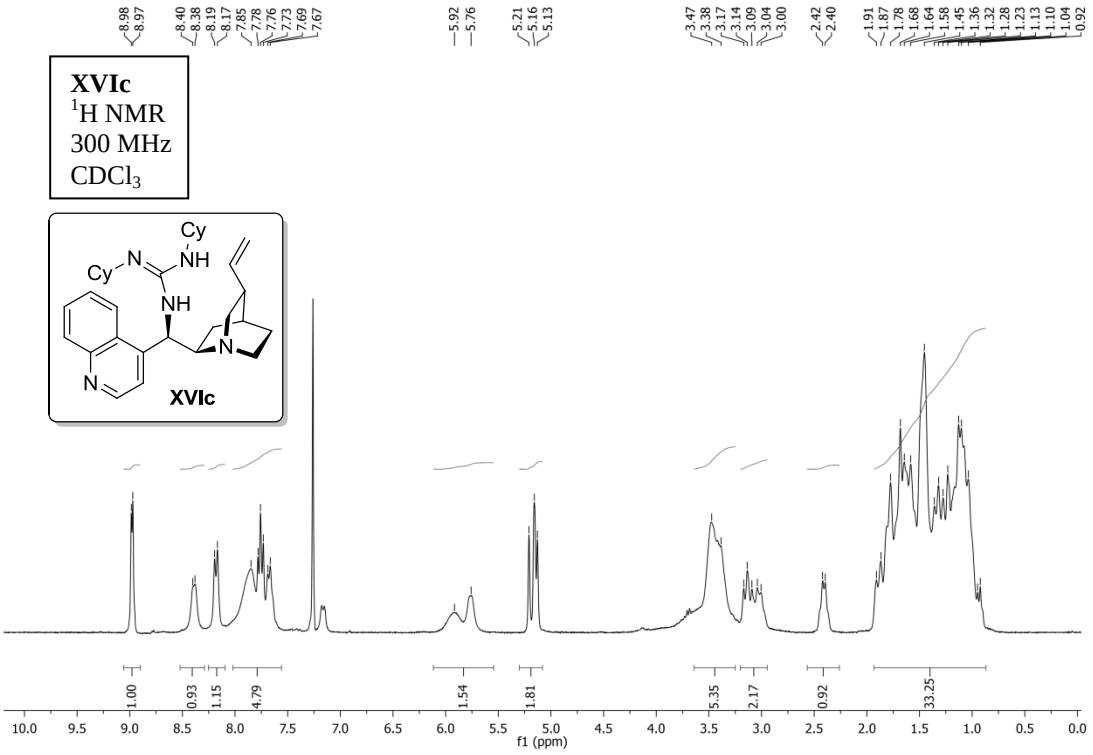
XVIc
1H NMR
300 MHz
CDCl3
XVIc
f1 (ppm)

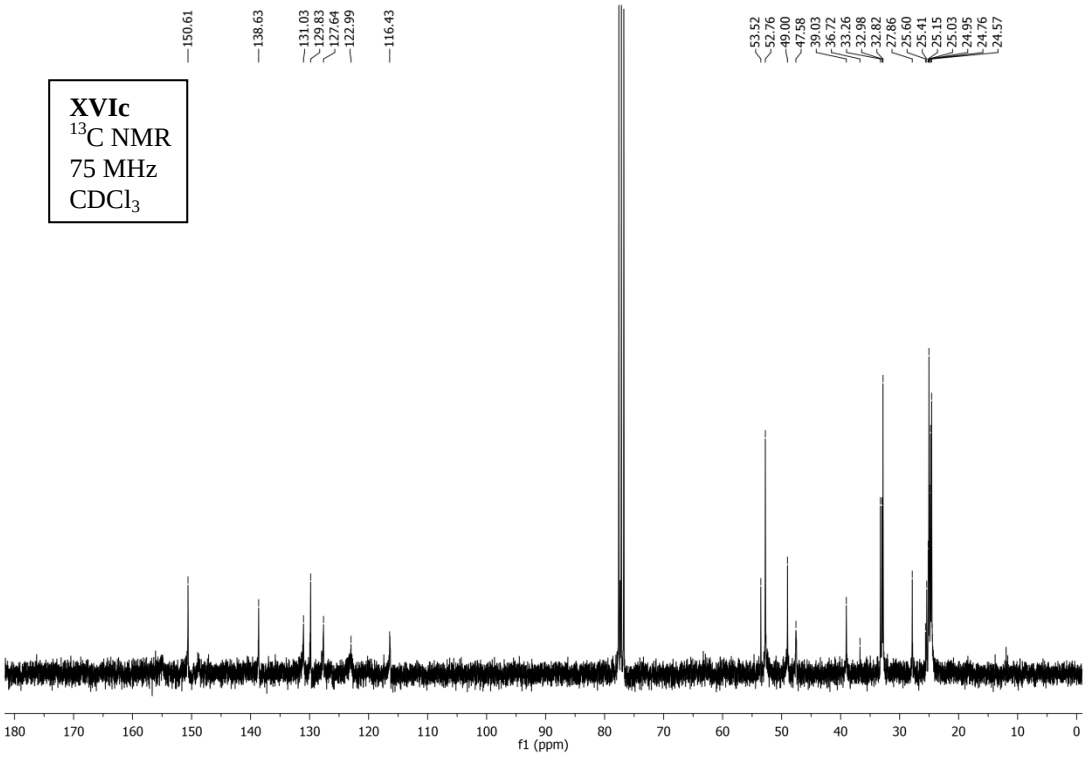
XVIc
13C NMR
75 MHz
CDCl3
f1 (ppm)

XVId
^{1}H NMR
300 MHz
$CDCl_3$

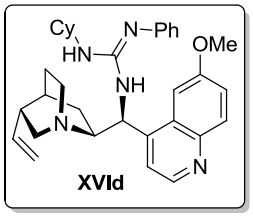

XVId
^{13}C NMR
75 MHz
$CDCl_3$

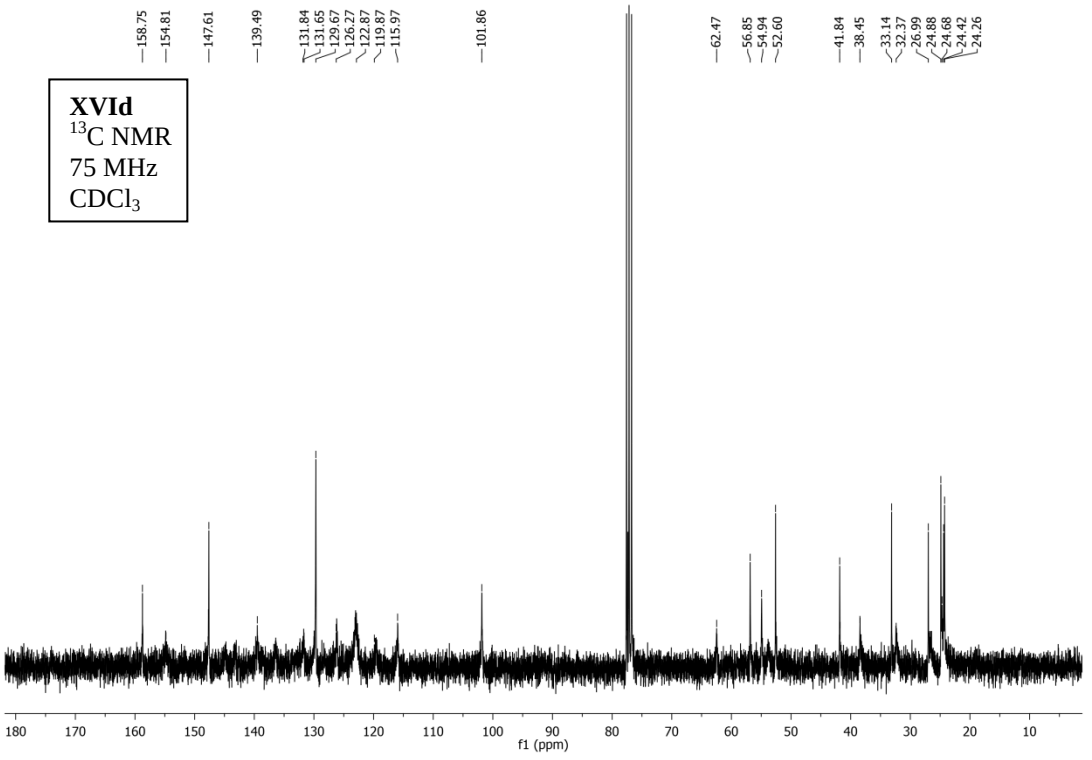

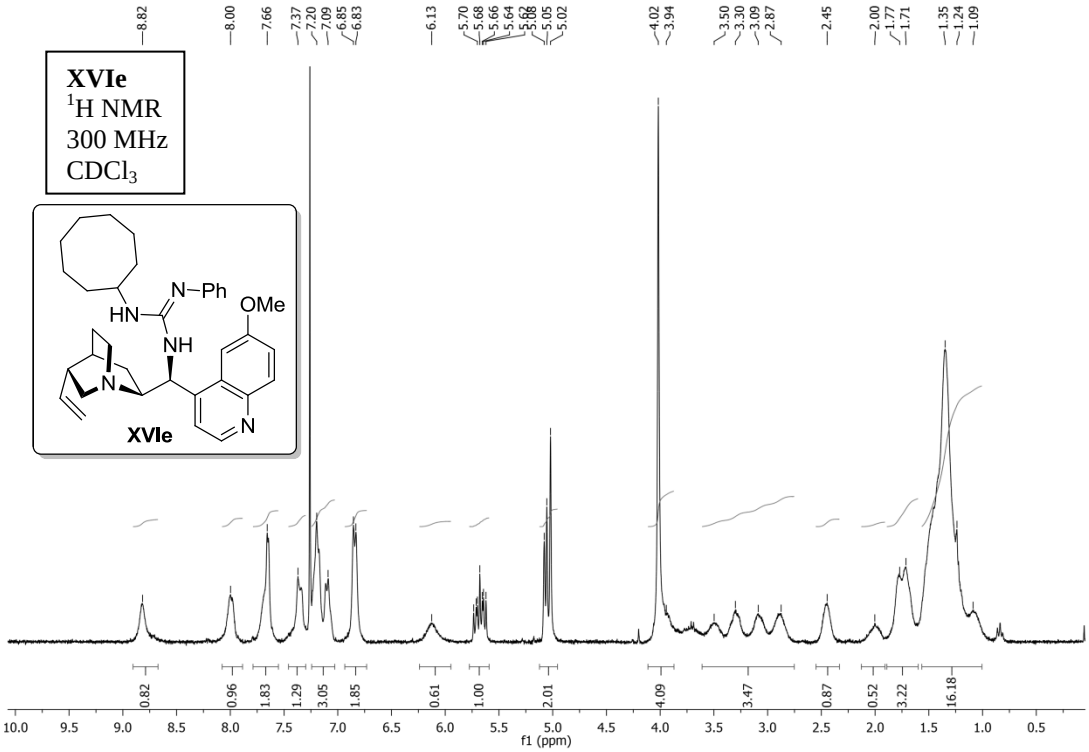
XVIe
^{1}H NMR
300 MHz
$CDCl_3$
XVIe
f1 (ppm)

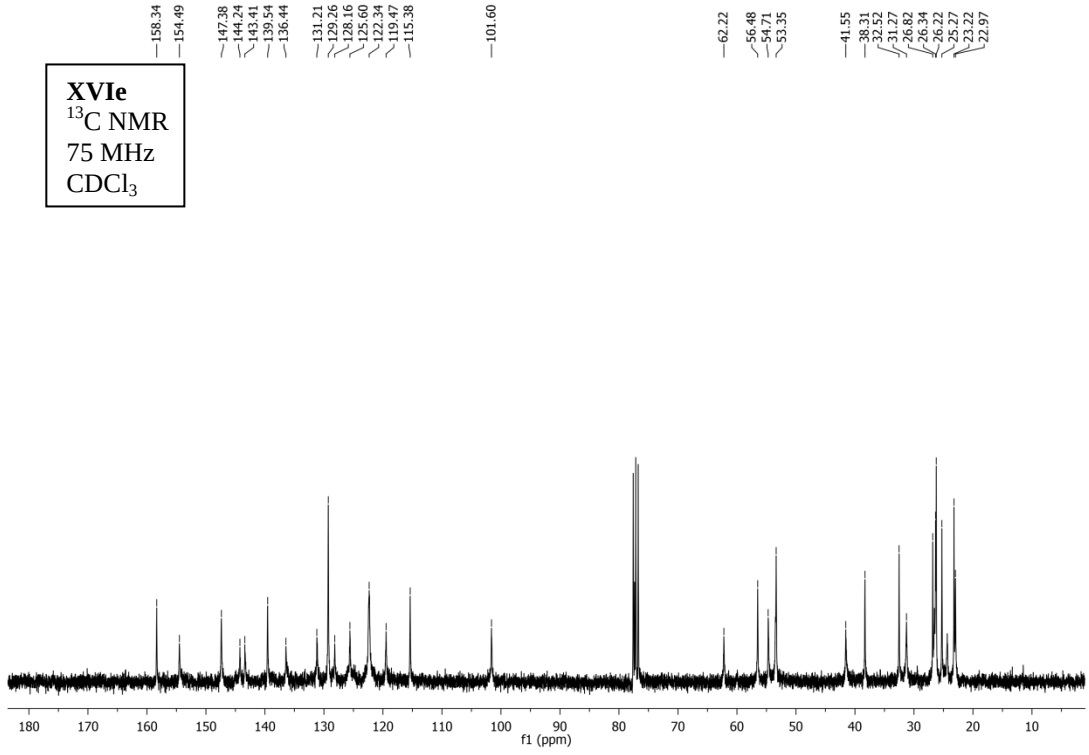
XVIe
^{13}C NMR
75 MHz
$CDCl_3$
f1 (ppm)

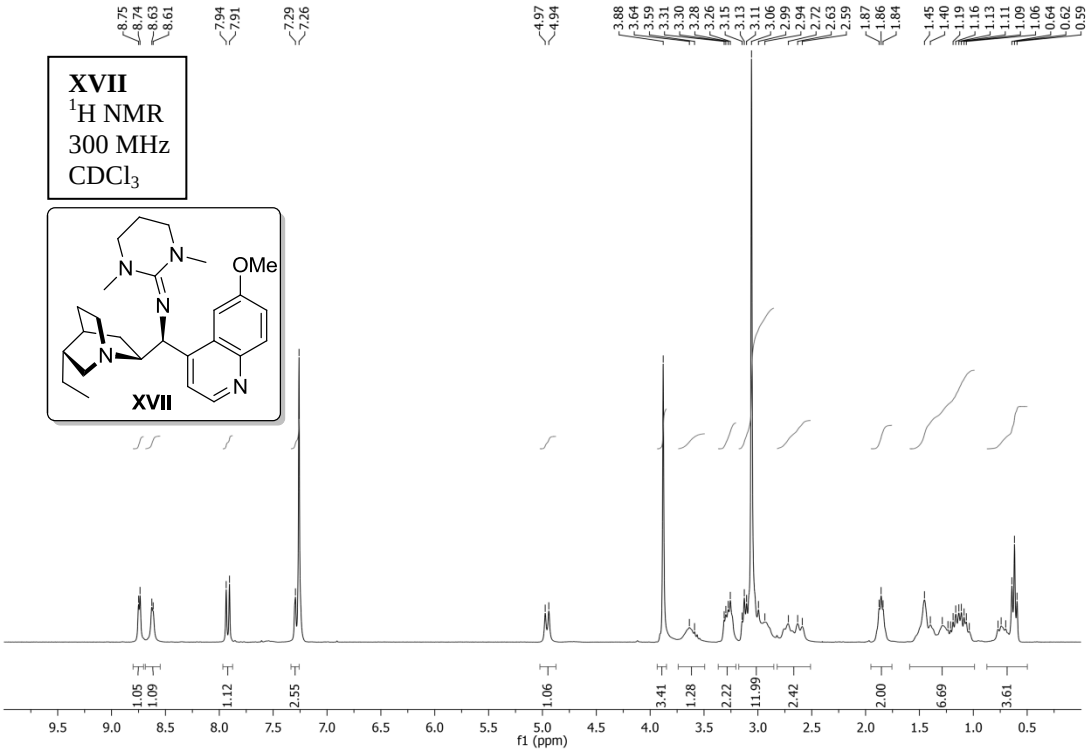
XVII
1H NMR
300 MHz
CDCl3
OMe
XVII
f1 (ppm)

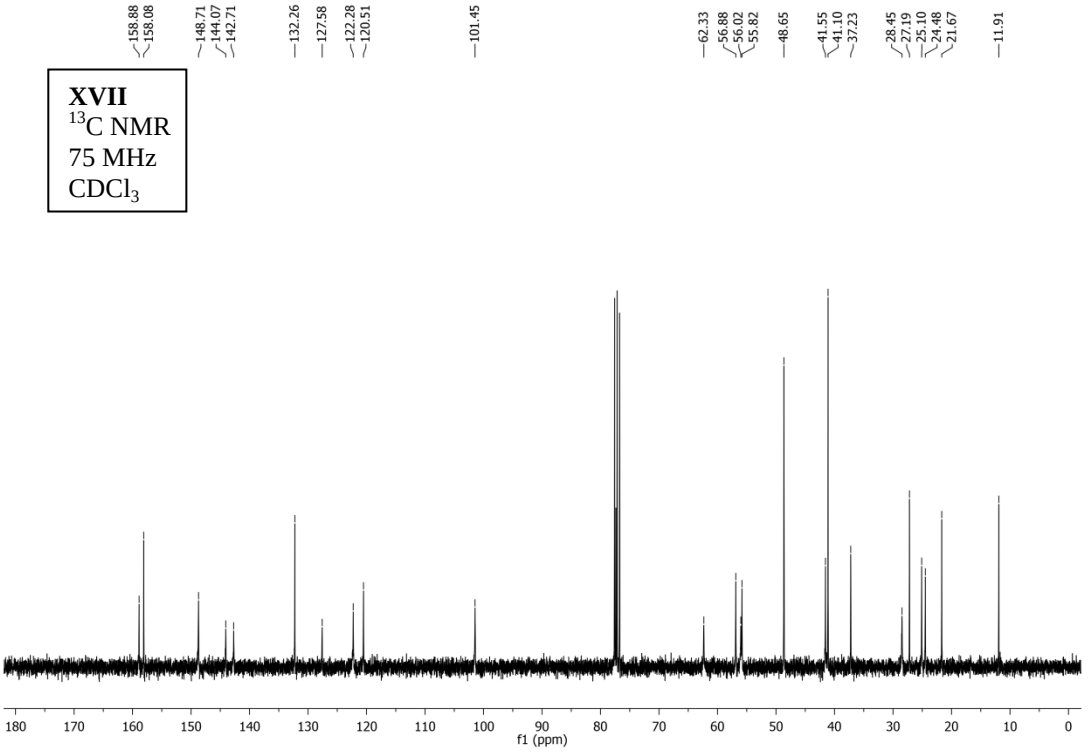
XVII
13C NMR
75 MHz
CDCl3
f1 (ppm)

7.3. Experimental Data for the Atroposelective Biaryl Synthesis

2-Naphthols **38a-f** and 1,4-benzoquinones **51a-c,e** are commercially available and were used as received.

7.3.1. Preparation of substituted 1,4-benzoquinones 51d,f-h

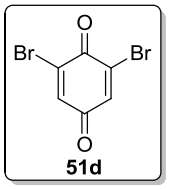

51d

2,6-dibromo-1,4-benzoquinone (51d).[124] A solution of 2,4,6-tribromophenol (6.0 g, 18 mmol) in AcOH (45 mL) was slowly added to a stirred mixture of MnO_2 (3.0 g, 36 mmol) in 70% $HClO_4$ (12 mL) and AcOH (36 mL). The resulting mixture was stirred at room temperature for 30 minutes, after which time it was filtered into a flask containing H_2O (ca. 200 mL). The filter cake was washed with Et_2O into the same flask. The content of this flask was then extracted with Et_2O. The organic extracts were dried over Na_2SO_4 and concentrated under reduced pressure. The resulting residue was purified by flash chromatography on silica gel, eluting with a mixture of petroleum ether/Et_2O 20:1. 2,6-dibromo-1,4-benzoquinone **51d** was obtained as yellow solid (3.4 g, 71% yield). **^{1}H NMR** (300 MHz, $CDCl_3$): δ 7.33 (s, 2H). **^{13}C NMR** (75 MHz, $CDCl_3$): δ 135.8, 138.4, 182.5.

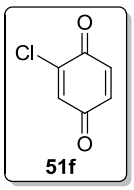

51f

2-Chloro-1,4-benzoquinone (51f).[125] To a stirred solution of chlorohydroquinone (2.0 g, 14 mmol) in Et_2O (20 mL) was added Mn_2O (1.8 g, 21 mmol) and the resulting mixture was stirred at room temperature for 3 hours. The reaction mixture was then filtered through celite and the filtrate was concentrated under reduced pressure. The residue was purified by flash chromatography on silica gel with petroleum ether/Et_2O 20:1 to 5:1 gradient elution. Chloro-1,4-benzoquinone was obtained as a yellow solid (0.89 g, 45% yield). **^{1}H NMR** (300 MHz, $CDCl_3$): δ 6.81 (dd, 1H; J = 10.1, 2.5 Hz), 6.92 (d, 1H; J = 10.3 Hz), 7.01 (d, 1H; J = 2.3 Hz). **^{13}C NMR** (75 MHz, $CDCl_3$): δ 133.9, 136.2, 136.9, 144.3, 179.4, 185.1.

2-Bromo-1,4-benzoquinone (51g). A stirred solution of 4-methoxyphenol (5.00 g, 40.3 mmol) in DCM (150 mL) was cooled to 0 °C followed by

[124] Modified procedure from: Omura, K. *Synthesis* **1998**, 1145.
[125] Hirano, M; Yakabe, S.; Chikamori, H.; Clark, J. H.; Morimoto, T. *J. Chem. Res. (S)* **1998**, 770.

dropwise addition of Br_2 (2.2 mL, 6.84 g, 42.8 mmol). The reaction mixture was stirred for 15 minutes at 0 °C, allowed to reach RT and stirred for 75 minutes. The reaction was quenched by addition of sat. aq. $Na_2S_2O_3$ (40 mL) and H_2O (25 mL). The phases were separated and the aqueous layer was extracted with DCM (3 x 50 mL). The combined organic phases were dried over Na_2SO_4 and concentrated under reduced pressure. Crude 2-bromo-4-methoxyphenol was obtained as an orange solid (8.78 g) and used in the following step without further purification. ^{1}H NMR (300 MHz, $CDCl_3$): δ 3.75 (s, 3H), 6.80 (dd, 1H; *J* = 8.9, 2.8 Hz), 6.94 (d, 1H; *J* = 8.8 Hz), 7.01 (d, 1H; *J* = 2.9 Hz). ^{13}C NMR (75 MHz, $CDCl_3$): δ 56.1, 110.0, 115.5, 116.4, 116.9, 146.6, 153.9.

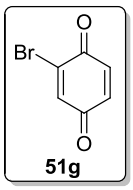

51g

To a stirred mixture of CAN (41 g, 74 mmol) and silica gel (80 g) in H_2O (37 mL) and DCM (350 mL) was added a solution of 2-bromo-4-methoxyphenol (8.8 g, 43 mmol) in DCM (50 mL). The reaction mixture was stirred for 1 hour at RT and then filtered under reduced pressure. The filtrate was washed with brine and concentrated under reduced pressure. The residue was purified by flash chromatography on silica gel with petroleum ether/Et_2O 5:1 to 3:1 gradient elution. 2-Bromo-1,4-benzoquinone **51g** was obtained as a yellow solid (4.34 g, 58% overall yield). **^{1}H NMR** (300 MHz, $CDCl_3$): δ = 6.83 (dd, 1H; *J* = 10.0, 2.3 Hz), 6.97 (d, 1H; *J* = 10.0 Hz), 7.30 (d, 1H; *J* = 2.3 Hz). **^{13}C NMR** (75 MHz, $CDCl_3$): δ = 135.9, 136.8, 137.7, 138.3, 179.3, 184.7.

2-Carbomethoxy-1,4-benzoquinone (51h).[126] To a stirred solution of 2,5-dihydroxybenzoic acid (2.0 g, 13 mmol) in MeOH (20 mL) was added concentrated H_2SO_4 (0.70 mL, 1.3 g, 13 mmol). The reaction mixture was stirred at reflux for 16 h, after which time it was allowed to cool down at RT. The solvent was removed under reduced pressure, the residue was dissolved in DCM (50 mL) and washed with saturated aqueous $NaHCO_3$ (3 x 30 mL). The organic phase was dried over Na_2SO_4 and concentrated under reduced pressure. The crude product was purified by flash chromatography on silica gel with petroleum ether/Et_2O 3:1 to 2:1 gradient elution. Methyl 2,5-dihydroxybenzoate was obtained as a white solid (2.0 g, 92% yield). ^{1}H NMR (300 MHz, $CDCl_3$): δ = 3.92 (s, 3H), 5.34 (brs, 1H), 6.87 (d, 1H; *J* = 8.8 Hz), 7.01 (dd, 1H; *J* = 8.9, 3.1 Hz), 7.27 (d, 1H; *J* = 2.9 Hz), 10.39 (s,

[126] Nakazaki, M.; Naemura, K. *J. Org. Chem.* **1981**, *46*, 106.

1H). ^{13}C NMR (75 MHz, $CDCl_3$): δ = 52.6, 112.3, 114.9, 118.6, 124.3, 147.9, 155.7, 170.3.

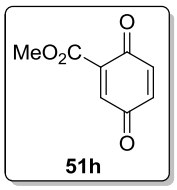

51h

To a mixture of methyl 2,5-dihydroxybenzoate (2.0 g, 12 mmol), Na_2SO_4 (5.0 g) and Et_2O (40 mL) was added Ag_2O (8.3 g, 36 mmol). The reaction mixture was stirred for 3 hours at room temperature, after which time it was filtered through celite and the solvent was evaporated under reduced pressure. Carbomethoxy-1,4-benzoquinone was obtained as an orange solid (1.8 g, 92% yield), which was used without further purification. **^{1}H-NMR** (300 MHz, $CDCl_3$): δ = 3.89 (s, 3H), 6.81 (s, 2H), 7.10 (s, 1H). **^{13}C-NMR** (75 MHz, $CDCl_3$): δ = 53.2, 136.2, 136.6, 137.0, 137.1, 163.2, 183.1, 186.9.

7.3.2. General procedure for the synthesis of biaryls 52a-u

To a cooled (4 °C) solution of the naphthol **2** (0.15 mmol) and quinine (**I**, 7 mg, 0.0225 mmol) in THF (4.5 mL) was added a cooled (4 °C) solution of the 1,4 benzoquinone **1** (0.30 mmol) in THF (1.0 mL). The reaction mixture was stirred at 4 °C for time indicated in *Scheme 14* and then the resulting dark solution was cooled to 0 °C (ice bath) and $NaBH_4$ (17 mg, 0.45 mmol) was added, followed by the dropwise addition of MeOH (1.0 mL). After 5 minutes, to the solution was added trifluoroacetic acid (0.10 mL) and 1.0 g of silica gel and the solvent was removed by rotary evaporation. The resulting white solid was loaded on the top of a column and quickly filtered over a pad of silica gel (20 g) using DCM/Et_2O (20:1) as the eluent. The solvent of the fraction containing the desired compound **3** was evaporated, to give the pure product.

7.3.3. Characterization of biaryls 52a-u

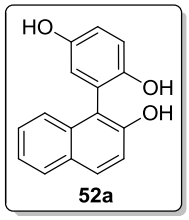

52a

52a. 13 mg, 23% yield (after 24 h). TLC (DCM/Et_2O 10/1): Rf = 0.12. HPLC conditions: CHIRALPAK IA column, eluent *n*-hexane/*i*-propanol 85/15, flow 0.9 mL/min, τ_1= 20.3 min, τ_2= 30.9 min.

^{1}H NMR (400 MHz, CD_3OD): δ 6.77 (d, 1H; *J* = 3.0, 8.6 Hz), 6.85 (d, 1H; *J* = 8.6 Hz), 7.19 (d, 1H; *J* = 8.9 Hz),

7.22-7.30 (m, 2H), 7.41-7.38 (m, 2H), 7.73-7.81 (m, 2H).
Data are in accordance with that previously reported.[127]

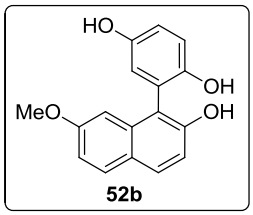

52b

52b. 32 mg, 50% yield (after 24 h). TLC (DCM/Et_2O 10/1): Rf = 0.06. HPLC conditions: CHIRALPAK ID column, eluent *n*-hexane/*i*-propanol 85/15, flow 0.9 mL/min, τ_1= 13.0 min, τ_2= 19.7 min.
^{1}H NMR (400 MHz, CD_3OD): δ 3.67 (s, 3H), 6.64 (d, 1H; *J* = 2.9 Hz), 6.76-6.77 (m, 2H), 6.86 (d, 1H; *J* = 8.7 Hz), 6.91 (dd, 1H; *J* = 2.5, 8.9 Hz), 7.03 (d, 1H; *J* = 8.8 Hz), 7.65 (d, 2H; *J* = 8.8 Hz).
^{13}C NMR (100 MHz, CD_3OD): δ 54.4, 103.8, 115.2, 115.7, 115.8, 117.0 (2C), 118.9, 124.1, 124.8, 128.9, 129.5, 135.7, 148.4, 150.6, 152.7, 158.6.
HRMS (ESI): calcd for $C_{17}H_{13}O_4^-$ [M-H]$^-$ 281.0814; found 281.0809.

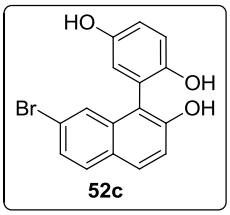

52c

52c. 15 mg, 20% yield (after 24 h). TLC (DCM/Et_2O 10/1): Rf = 0.06. HPLC conditions: CHIRALPAK ID column, eluent n-hexane/i-propanol 85/15, flow 0.9 mL/min, τ_1= 9.5 min, τ_2= 12.5 min.
^{1}H NMR (400 MHz, CD_3OD): δ 6.61 (d, 1H; *J* = 3.0 Hz), 6.80 (dd, 1H; *J* = 3.0, 8.7 Hz), 6.87 (d, 1H; *J* = 8.7 Hz), 7.21 (d, 1H; *J* = 8.9 Hz), 7.33 (dd, 1H; *J* = 2.0, 8.7 Hz), 7.50 (d, 1H; *J* = 1.8 Hz), 7.67 (d, 1H; *J* = 8.7 Hz), 7.73 (d, 1H; *J* = 8.8 Hz).
^{13}C NMR (100 MHz, CD_3OD): δ 115.9, 116.2, 117.0, 117.9, 118.9, 120.5, 123.2, 126.0, 127.1, 127.6, 129.2, 129.9, 135.8, 148.5, 150.5, 153.2.
HRMS (ESI): calcd for $C_{16}H_{10}BrO_3$ [M-H]$^-$ 328.9813; found 328.9815.

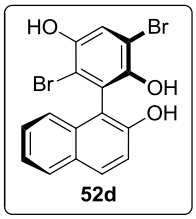

52d

52d. 82% yield, 60% *ee*. TLC (DCM/Et_2O 10/1): Rf = 0.45. HPLC conditions: CHIRALPAK ID column, eluent *n*-hexane/*i*-propanol 88/12, flow 0.9 mL/min, retention times: τ_1 (major)= 28.9 min, τ_2 (minor)= 12.9 min.
^{1}H NMR (300 MHz, DMSO-d_6): δ 7.02 (d, 1H; *J*= 8.2 Hz), 7.19-7.33 (m, 4H), 7.79-7.82 (m, 2H), 8.19 (s, 1H), 9.55 (s, 1H), 9.90 (s, 1H).
^{13}C NMR (75 MHz, DMSO-d_6): δ 109.8, 113.0, 116.7, 118.0, 118.6, 122.4, 123.4, 126.2, 127.9. 128.0 (2C), 129.3, 133.0, 145.4, 148.1, 152.5.

[127] Sartori, G.; Maggi, R.; Bigi, F.; Arienti, A.; Casnati, G. *J. Chem. Soc., Perkin Trans. 1* **1993**, 39-42.

HRMS (ESI): calcd for $C_{16}H_9Br_2O_3$ $[M-H]^-$ 406.8918; found 406.8906.

$[\alpha]_D$ = +28.0° (c 3.9, MeOH, 60% *ee*).

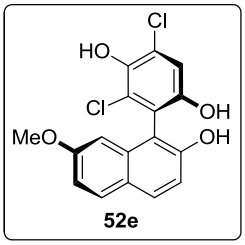

52e

52e. 81 mg, 99% yield, 74% *ee*. TLC (DCM/Et_2O 10/1): Rf = 0.41. HPLC conditions: CHIRALPAK ID column, eluent *n*-hexane/*i*-propanol 88/12, flow 0.9 mL/min, retention times: τ_1(major)= 18.4 min, τ_2(minor)= 14.8 min.

^{1}H NMR (400 MHz, $CDCl_3$): δ 3.74 (s, 3H), 4.78 (br, 2H), 5.65 (br, 1H), 6.50 (d, 1H; *J* = 2.4 Hz), 7.05 (dd, 1H; *J* = 2.5, 8.9 Hz), 7.10-7.13 (m, 2H), 7.75 (d, 1H; *J* = 8.9 Hz), 7.83 (d, 1H; *J* = 8.8 Hz).

^{13}C NMR (100 MHz, $CDCl_3$): δ 55.7, 102.7, 109.8, 115.4, 116.1, 116.6, 118.8, 122.4, 122.7, 124.9, 130.5, 132.0, 134.2, 143.2, 148.5, 153.0, 159.7.

HRMS (ESI): calcd for $C_{17}H_{11}Cl_2O_4$ $[M-H]^-$ 349.0034; found 349.0032.

$[\alpha]_D$ = +20.9° (c 9.0, MeOH, 68% *ee*).

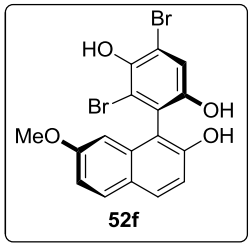

52f

52f. 61 mg. 92% yield, 70% *ee*. TLC (DCM/Et_2O 10/1): Rf = 0.32. HPLC conditions: CHIRALPAK ID column, eluent *n*-hexane/*i*-propanol 85/15, flow 0.9 mL/min, retention times: τ_1 (major)= 19.6 min, τ_2 (minor)= 14.2 min.

^{1}H NMR (400 MHz, $CDCl_3$): δ 3.73 (s, 3H), 4.35-5.25 (br, 2H), 5.73 (br, 1H), 6.49 (s, 1H), 7.03-7.10 (m, 2H), 7.33 (s, 1H), 7.74 (d, 1H, *J* = 8.9 Hz), 7.80 (d, 1H, *J* = 9.0 Hz).

^{13}C NMR (100 MHz, $CDCl_3$): δ 55.7, 102.7, 111.3, 112.0, 113.4, 115.5, 116.7, 119.8, 121.5, 124.9, 130.4, 132.0, 134.0, 144.9, 149.0, 152.7. 159.7.

HRMS (ESI): calcd for $C_{17}H_{11}Br_2O_4$ $[M-H]^-$436.9024; found 436.9022.

$[\alpha]_D$ = +10.3° (c 3.8, MeOH, 70% *ee*).

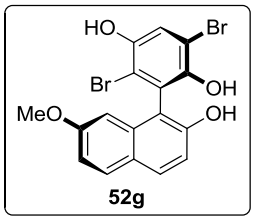

52g

52g. 66 mg. 99% yield, 63% *ee*. TLC (DCM/Et_2O 10/1): Rf = 0.34. HPLC conditions: CHIRALPAK IB column, eluent *n*-hexane/*i*-propanol 85/15, flow 0.9 mL/min, retention times: τ_1(major)= 15.8 min, τ_2(minor)= 20.4 min.

^{1}H NMR (400 MHz, DMSO-d_6): δ 3.61 (s, 3H), 6.33 (d, 1H; *J* = 2.4 Hz), 6.94 (dd, 1H, *J* = 2.5, 8.8 Hz), 7.05 (d, 1H; *J* = 8.8 Hz), 7.17 (s, 1H), 7.69-7.74 (m, 2H), 8.12 (s, 1H), 9.46 (s, 1H), 9.86 (s, 1H).

^{13}C NMR (100 MHz, DMSO-d_6): δ 55.6, 103.7, 110.6, 113.8, 114.4, 116.7, 116.7, 118.8, 124.2, 128.8, 129.9, 130.4, 135.1, 146.1, 148.8, 153.8, 158.4.
HRMS (ESI): calcd for $C_{17}H_{12}Br_2NaO_4$ $[M+Na]^+$ 460.9000; found 460.9007.
$[\alpha]_D$ = -16.1° (c 4.3, MeOH, 46% *ee*).

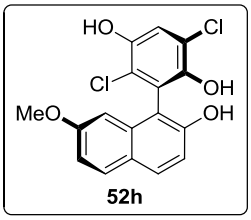

52h

52h. 52 mg. 99% yield, 59% *ee*. TLC (DCM/Et_2O 10/1): Rf = 0.45. HPLC conditions: CHIRALPAK IB column, eluent *n*-hexane/*i*-propanol 85/15, flow 0.9 mL/min, retention times: τ_1(major)= 17.4 min, τ_2(minor)= 24.0 min.
^{1}H NMR (400 MHz, CD_3OD): δ 3.66 (s, 3H), 6.48 (d, 1H; *J* = 2.5 Hz), 6.93 (dd, 1H; *J* = 2.5, 8.9 Hz), 7.03-7.05 (m, 2H), 7.67-7.71 (m, 2H).
^{13}C NMR (100 MHz, CD_3OD): δ 54.5, 102.7, 114.4, 115.2, 115.6, 116.3, 120.0, 121.6, 124.6, 125.8, 129.7, 129.8, 135.2, 145.2, 147.2, 153.5, 158.9.
HRMS (ESI): calcd for $C_{17}H_{12}Cl_2NaO_4$ $[M+Na]^+$ 373.0010; found 373.0005.
$[\alpha]_D$ = +26.8° (c 3.8, MeOH, 58% *ee*)

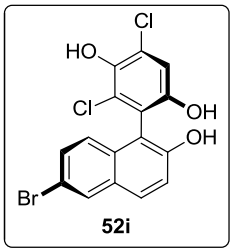

52i

52i. 60 mg. 99% yield, 77% *ee*. TLC (DCM/Et_2O 10/1): Rf = 0.23. HPLC conditions: CHIRALPAK IF column, eluent *n*-hexane/*i*-propanol 90/10, flow 0.9 mL/min, retention times: τ_1(major)= 19.2 min, τ_2(minor)= 24.4 min.
^{1}H NMR (400 MHz, $CDCl_3$): δ 4.54 (br, 1H), 5.12 (br, 1H), 5.64 (br, 1H), 7.10-7.14 (m, 2H), 7.31 (d, 1H; *J* = 9.0 Hz), 7.48 (dd, 1H; *J* = 2.0, 8.9 Hz), 7.83 (d, 1H; *J* = 8.9 Hz), 8.01 (d, 1H; *J* = 2.0 Hz).
^{13}C NMR (100 MHz, $CDCl_3$): δ 107.8, 111.3, 116.5, 118.3, 118.6, 119.5, 122.2, 122.6, 123.3, 125.7, 131.0, 131.5, 131.6, 143.5, 148.7, 152.7.
HRMS (ESI): calcd for $C_{16}H_8BrCl_2O_3$ $[M-H]^-$396.9034; found 396.9052.
$[\alpha]_D$ = +20.7° (c 12.8, MeOH, 98% *ee*).

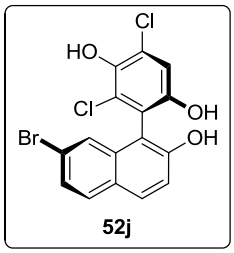

52j

52j. 60 mg. 99% yield, 70% *ee*. TLC (DCM/Et_2O 10/1): Rf = 0.09. HPLC conditions: CHIRALPAK ID column, eluent *n*-hexane/*i*-propanol 92/8, flow 0.9 mL/min, retention times: τ_1(major)= 16.0 min, τ_2(minor)= 14.1 min.

^{1}H NMR (400 MHz, CD_3OD): δ 6.95 (s, 1H), 7.21 (d, 1H; *J* = 8.9 Hz), 7.27 (d, 1H; *J* = 1.9 Hz), 7.33 (dd, 1H; *J* = 1.9, 8.6 Hz), 7.69 (d, 1H; *J* = 8.6 Hz), 7.77 (d, 1H, *J* = 8.9 Hz).

^{13}C NMR (100 MHz, CD_3OD): δ 114.6, 115.0, 118.7, 120.6, 121.9, 122.1, 124.5, 125.8, 125.9, 127.4, 129.6, 129.9, 135.1, 143.0, 149.5, 153.6.

HRMS (ESI): calcd for $C_{16}H_8BrCl_2O_3$ $[M-H]^-$ 396.9034; found 396.9036.

$[\alpha]_D$ = +11.5° (c 2.0, CD_3OD, 80% *ee*).

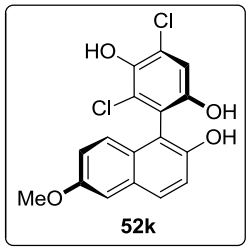

52k

52k. 52 mg. 99% yield, 78% *ee*. TLC (DCM/Et_2O 10/1): Rf = 0.23. HPLC conditions: CHIRALPAK IF column, eluent *n*-hexane/*i*-propanol 88/12, flow 0.9 mL/min, retention times: τ_1(major)= 23.7 min, τ_2(minor)= 30.2 min.

^{1}H NMR (400 MHz, $CDCl_3$/DMSO-d_6): δ 3.83 (s, 3H), 6.11 (br, 3H), 6.96-7.00 (m, 2H), 7.07-7.13 (m, 2H), 7.20 (d, 1H, *J* = 8.88 Hz), 7.64 (d, 1H, *J* = 8.84 Hz).

^{13}C NMR (100 MHz, $CDCl_3$/DMSO-d_6): δ 55.7, 107.1, 114.2, 115.9, 119.4, 119.6, 121.8, 122.0, 123.8, 125.9, 128.7, 129.4, 130.0, 142.9, 149.2, 151.2, 156.2.

HRMS (ESI): calcd for $C_{17}H_{11}Cl_2O_4$ $[M-H]^-$349.0034; found 349.0020.

$[\alpha]_D$ = +28.0° (c 13.9, MeOH, 96% *ee*).

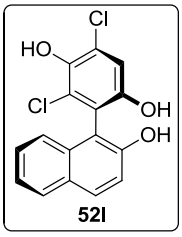

52l

52l. 48 mg. 99% yield, 76% *ee*. TLC (DCM/Et_2O 10/1): Rf = 0.30. HPLC conditions: CHIRALPAK ID column, eluent *n*-hexane/*i*-propanol 88/12, flow 0.9 mL/min, retention times: τ_1(major)= 17.5 min, τ_2(minor)= 14.8 min.

^{1}H NMR (400 MHz, $CDCl_3$): δ 4.64 (br, 1H), 5.12 (br, 1H), 5.66 (br, 1H), 7.13 (s, 1H), 7.26-7.28 (m, 2H), 7.41-7.43 (m, 2H), 7.84-7.87 (m, 1H), 7.91 (d, 1H; *J* = 8.9 Hz).

^{13}C NMR (100 MHz, $CDCl_3$): δ 110.9, 116.3, 118.3, 118.8, 122.7, 123.0, 123.8, 124.8, 128.4, 129.0, 129.8, 132.5, 132.8, 143.4 148.7, 152.5.

HRMS (ESI): calcd for $C_{16}H_9Cl_2O_3^-$ $[M-H]^-$ 318.9934; found 318.9931.

$[\alpha]_D$ = -2.5° (c 3.4, $CDCl_3$, 76% *ee*).

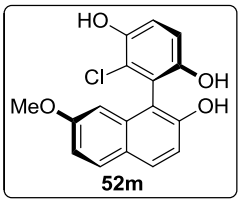

52m. 47 mg. 99% yield, 77% *ee*. TLC (DCM/Et_2O 10/1): Rf = 0.22. HPLC conditions: CHIRALPAK ID column, eluent *n*-hexane/*i*-propanol 85/15, flow 0.9 mL/min, retention times: τ_1(major)= 16.7 min, τ_2(minor)= 11.4 min.

HPLC conditions for determination of the absolute configuration (see *Section 2.2.4*): CHIRALPAK AS-H column, eluent *n*-hexane/*i*-propanol 80/20, flow 1.0 mL/min, retention times: τ_1 (minor) = 13.6 min, τ_2 (major) = 21.3 min.

^{1}H NMR (400 MHz, CD_3OD): δ 3.65 (s, 3H), 6.55 (d, 1H, *J* =2.3 Hz), 6.81 (d, 1H, *J* = 8.8 Hz), 6.87-6.92 (m, 2H), 7.04 (d, 1H, *J* = 8.8 Hz), 7.65-7.70 (m, 2H).

^{13}C NMR (100 MHz, CD_3OD): δ 55.4, 104.0, 115.5, 116.0, 116.0, 116.5, 117.2, 123.4, 124.5, 125.6, 130.3, 130.5, 136.3, 147.8, 150.3, 154.2, 159.7.

HRMS (ESI): calcd for $C_{17}H_{12}ClO_4$ $[M-H]^-$ 315.0424; found 315.0423.

$[\alpha]_D$ = -21.0° (c 1.2, $CDCl_3$, 78% *ee*).

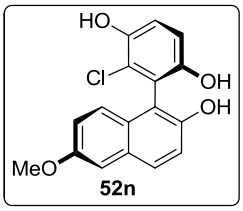

52n. 40 mg. 84% yield, 84% *ee*. TLC (DCM/Et_2O 10/1): Rf = 0.11. HPLC conditions: CHIRALPAK ID column, eluent *n*-hexane/*i*-propanol 85/15, flow 0.9 mL/min, retention times: τ_1(major)= 22.9 min, τ_2(minor)= 17.3 min.

^{1}H NMR (400 MHz, $CDCl_3$): δ 3.90 (s, 3H), 4.56 (br, 1H), 5.97 (br, 1H), 5.32 (br, 1H), 7.00 (d, 1H; *J* = 9.0 Hz), 7.09 (dd, 1H; *J* = 2.5, 9.2 Hz), 7.13 (d, 1H; *J* = 9.0 Hz), 7.15-7.32 (m, 2H), 7.27 (d, 1H; *J* = 9.0 Hz), 7.81 (d, 1H; *J* = 8.9 Hz).

^{13}C NMR (100 MHz, $CDCl_3$): δ 55.7, 107.3, 111.6, 116.1, 118.1, 118.5, 118.7, 120.4, 121.0, 125.4, 127.9, 130.6, 130.7, 146.5, 148.9, 150.6, 156.8.

HRMS (ESI): calcd for $C_{17}H_{12}ClO_4$ $[M-H]^-$ 315.0424; found 315.0429.

$[\alpha]_D$ = -13.6° (c 1.8, $CDCl_3$, 86% *ee*).

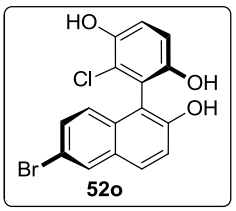

52o. 52 mg. 95% yield, 82% *ee*. TLC (DCM/Et_2O 10/1): Rf = 0.14. HPLC conditions: CHIRALPAK ID column, eluent *n*-hexane/*i*-propanol 90/10, flow 0.9 mL/min, retention times: τ_1(major)= 17.8 min, τ_2(minor)= 14.4 min.

^{1}H NMR (400 MHz, $CDCl_3$): δ 4.47 (br, 1H), 5.16 (br, 1H), 5.33 (br, 1H), 7.01 (d, 1H, *J* = 9.0 Hz), 7.11-7.17 (m, 2H), 7.33 (d, 1H,

J = 9.0 Hz), 7.47 (d, 1H, *J* = 9.0 Hz, 2.0 Hz), 7.83 (d, 1H, *J* = 9.0 Hz), 8.01 (d, 1H, *J* = 1.9 Hz).

^{13}C NMR (100 MHz, $CDCl_3$): δ 111.7, 116.3, 118.0, 118.3, 118.4, 119.3, 121.0, 125.7, 130.7, 130.8, 131.1, 131.2, 131.4, 146.7, 148.9, 152.6.

HRMS (ESI): calcd for $C_{16}H_9BrClO_3$ $[M-H]^-$362.9424; found 362.9437.

$[\alpha]_D$ = -1.6° (c 3.0, CD_3OD, 88% *ee*).

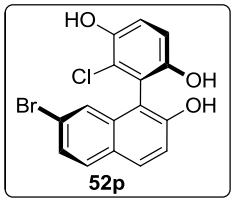

52p

52p. 33 mg. 60% yield, 82% *ee*. TLC (DCM/Et_2O 10/1): Rf = 0.09. HPLC conditions: CHIRALPAK ID column, eluent *n*-hexane/*i*-propanol 92/8, flow 0.9 mL/min, retention times: τ_1(major)= 26.1 min, τ_2(minor)= 19.6 min.

^{1}H NMR (300 MHz, $CDCl_3$): δ 4.49 (br, 1H), 5.16 (br, 1H), 5.36 (br, 1H), 7.03 (d, 1H; *J* = 8.8 Hz), 7.18 (d, 1H; *J* = 9.1 Hz), 7.32 (d, 1H, *J* = 9.1 Hz), 7.37 (s, 1H), 7.47 (dd, 1H; *J* = 1.8, 8.5 Hz), 7.72 (d, 1H; *J* = 8.8 Hz), 7.89 (d, 1H; *J* = 8.8 Hz).

^{13}C NMR (100 MHz, $CDCl_3$): δ 111.1, 116.6, 117.9, 118.7, 121.2, 122.9, 126.2 (2C), 128.2, 128.2, 130.6, 132.1, 134.4, 146.9, 149.1, 153.3.

HRMS (ESI): calcd for $C_{16}H_9BrClO_3$ $[M-H]^-$362.9424; found 362.9413.

$[\alpha]_D$ = -14.3° (c 2.6, MeOH, 90% *ee*).

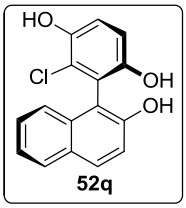

52q

52q. 43 mg. 99% yield, 78% *ee*. TLC (DCM/Et_2O 10/1): Rf = 0.16. HPLC conditions: CHIRALPAK ID column, eluent *n*-hexane/*i*-propanol 85/15, flow 0.9 mL/min, retention times: τ_1(major)= 16.2 min, τ_2(minor)= 10.3 min.

^{1}H NMR (400 MHz, CD_3OD): δ 6.79 (d, 1H; *J* = 8.8 Hz), 6.91 (d, 1H; *J* = 8.8 Hz), 7.16-7.20 (m, 2H), 7.23-7.27 (m, 2H), 7.75-7.78 (m, 2H).

^{13}C NMR (100 MHz, CD_3OD): δ 114.4, 114.7, 116.2, 118.1, 122.7, 123.2, 124.1, 126.1, 127.8, 129.1, 129.4, 133.1, 133.9, 146.6, 149.3, 152.5.

HRMS (ESI): calcd for $C_{16}H_{10}ClO_3$ $[M-H]^-$285.0318; found 285.0331.

$[\alpha]_D$ = +14.7° (c 3.4, MeOH, 82% *ee*)

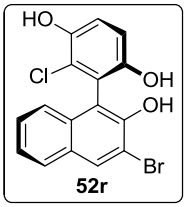

52r

52r. 38 mg. 70% yield, 80% *ee*. TLC (DCM/Et_2O 10/1): Rf = 0.26. HPLC conditions: CHIRALPAK ID column, eluent *n*-hexane/*i*-propanol 85/15, flow 0.9 mL/min, retention times: τ_1(major)= 19.2 min, τ_2(minor)= 15.9 min.

^{1}H NMR (400 MHz, CD_3OD): δ 6.81 (d, 1H; *J* = 8.8 Hz),

6.94 (d,1H; *J* = 8.8 Hz), 7.12-7.15 (m, 1H), 7.28-7.30 (m, 2H), 7.72-7.74 (m, 1H), 8.13 (s, 1H).

^{13}C NMR (100 MHz, CD_3OD): δ 113.5, 114.8, 117.0, 118.3, 122.4, 124.0, 124.6, 126.6 (2C), 127.2, 129.9, 132.0, 133.1, 146.9, 149.0, 149.7.

HRMS (ESI): calcd for $C_{16}H_9BrClO_3$ $[M-H]^-$362.9424; found 362.9420.

$[\alpha]_D$ = -6.0° (c 0.4, MeOH, 80% *ee*).

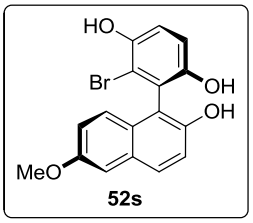

52s

52s. 44 mg. 81% yield, 86% *ee*. TLC (DCM/Et_2O 10/1): rf = 0.16.HPLC conditions: CHIRALPAK ID column, eluent *n*-hexane/*i*-propanol 80/20, flow 0.9 mL/min, retention times: τ_1 (major)= 17.0 min, τ_2 (minor)= 12.5 min.

^{1}H NMR (400 MHz, $CDCl_3$): δ 3.91 (s, 3H), 4.48 (br, 1H), 4.92 (br, 1H), 5.30 (br, 1H), 7.04 (d, 1H, *J* = 9.0 Hz), 7.08 (dd, 1H, *J* = 8.9 Hz, 2.5 Hz), 7.14 (s, 1H), 7.14-7.19 (m, 2H), 7.28 (d, 1H, *J* = 8.9 Hz), 7.82 (d, 1H, *J* = 8.9 Hz).

^{13}C NMR (100 MHz, $CDCl_3$): δ 55.9, 107.5, 113.2, 113.7, 117.0, 118.2, 118.7, 120.6, 120.7, 125.5, 127.9, 130.8, 130.9, 147.9, 149.2, 150.6, 157.1.

HRMS (ESI): calcd for $C_{17}H_{12}BrO_4$ $[M-H]^-$ 358.9919; found 358.9923.

$[\alpha]_D$ = +19.4° (c 1.6, MeOH, 88%*ee*).

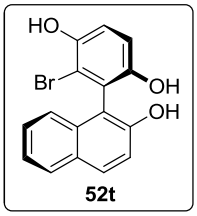

52t

52t. 46 mg. 93% yield, 85% *ee*. TLC (DCM/Et_2O 10/1): Rf = 0.12. HPLC conditions: CHIRALPAK ID column, eluent *n*-hexane/*i*-propanol 85/15, flow 0.9 mL/min, retention times: τ_1 (major)= 16.8 min, τ_2 (minor)= 10.6 min.

^{1}H NMR (400 MHz, $CDCl_3$): δ 5.27 (br, 3H), 7.05 (d, 1H, *J* = 9.0 Hz), 7.16 (d, 1H, *J* = 9.0 Hz), 7.23-7.26 (m, 1H), 7.31 (d, 1H, *J* = 9.0 Hz), 7.39-7.42(m, 2H), 7.87 (dd, 1H, *J* = 6.2 Hz, 2.0 Hz), 7.93 (d, 1H, *J* = 9.0 Hz).

^{13}C NMR (100 MHz, $CDCl_3$): δ 113.1, 113.3, 116.9, 118.0, 118.1, 120.3, 123.8, 124.5, 128.1, 128.8, 129.6, 132.1, 132.7, 147.7, 149.1, 152.2.

HRMS (ESI): calcd for $C_{16}H_{10}BrO_3$ $[M-H]^-$328.9813; found 328.9817.

$[\alpha]_D$ = +13.8° (c 4.0, MeOH, 85% *ee*).

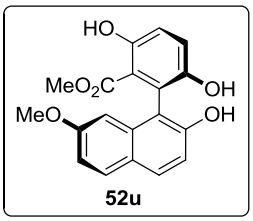

52u

52u. 51 mg. 99% yield, 2% *ee*. TLC (DCM/Et_2O 10/1): Rf = 0.11. HPLC conditions: CHIRALPAK ID column, eluent *n*-hexane/*i*-propanol 90/10, flow 0.9 mL/min, retention times: τ_1(major)= 18.6 min, τ_2(minor)= 27.0 min.

^{1}H NMR (400 MHz, $CDCl_3$): δ 3.25 (s, 3H), 3.69 (s, 3H), 4.68 (br, 1H), 4.99 (br, 1H), 6.44 (d, 1H; *J* = 2.1 Hz), 7.01 (dd, 1H, *J* = 2.5, 8.9 Hz), 7.09-7.16 (m, 2H), 7.31 (d, 1H, *J* = 9.1 Hz), 7.71-7.79 (m, 2H), 10.80 (s, 1H).

^{13}C NMR (400 MHz, $CDCl_3$): δ 52.6, 55.7, 103.2, 113.0, 114.0, 115.3, 116.7, 118.8, 122.6, 124.1, 125.1, 130.0, 131.0, 134.7, 147.8, 152.3, 157.5, 159.7, 171.2.

HRMS (ESI):calcd for $C_{19}H_{16}NaO_6$ $[M+Na]^+$ 363.0845; found 363.0847.

7.3.4. Large scale reactions

7.3.4.a. Large scale preparation of compound 52i

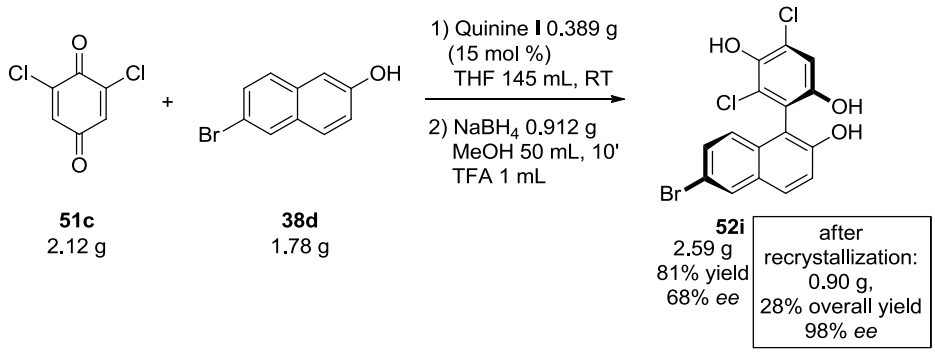

To a solution of naphthol **38d** (1.78 g, 8.00 mmol) and quinine (**I**, 389 mg, 1.20 mmol, 0.15 equiv) in THF (125 mL) was added at room temperature a solution of 2,6-dichloro 1,4-benzoquinone **51c** (2.12 g, 12.0 mmol) dissolved in 20 mL of THF. The reaction mixture was stirred at room temperature for 48 h. The resulting dark solution was then cooled to 0° C (ice bath) and $NaBH_4$ (912 mg, 24.0 mmol) was added, followed by the dropwise addition of 50 mL of MeOH. After 5 min to the solution was added trifluoroacetic acid (1.0 mL) and 7.0 g of silica gel, and the solvent was removed by rotavapor. The resulting white solid was loaded on the top of a column, and quickly filtered over a pad of silica gel (150 g) using as eluent diethyl ether:

DCM in the ratio 1:20. The solvent of the fraction containing the desired product was evaporated, to give chemically pure compound **52i** (2.59 g, 6.48 mmol, 81% yield).

The enantiomeric excess of compound **52i** was determined to be 68% by HPLC on CSP using Chiralpack IF column and hexane: *i*-propanol 90:10 as eluent, flow 0.9 mL min.

Crystallization of product **52i**:

In a 100 mL Erlenmeyer flask, 2.13 g of compound **52i** were dissolved in 30 mL of boiling toluene. The solution was allowed to rest at room temperature for 72 h, in which time a white crystalline solid formed. The supernatant solution was then removed and the crystals were washed with cold toluene (2 x 2 mL) and cold chloroform (1 x 2 mL). The crystals were collected and dried under reduced pressure to give 0.902 g of compound **52i** (98% *ee*).

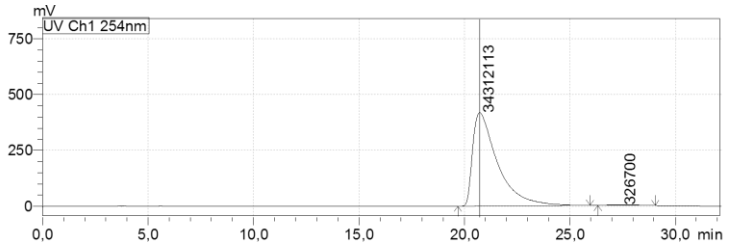

Peak#	Ret. Time	Area	Height	Conc.	Area%
1	20.731	34312113	418602	99.057	99.057
2	27.432	326700	3501	0.943	0.943
Total		34638813	422102	100.000	100.000

7.3.4.b. Large Scale preparation of compound 52k

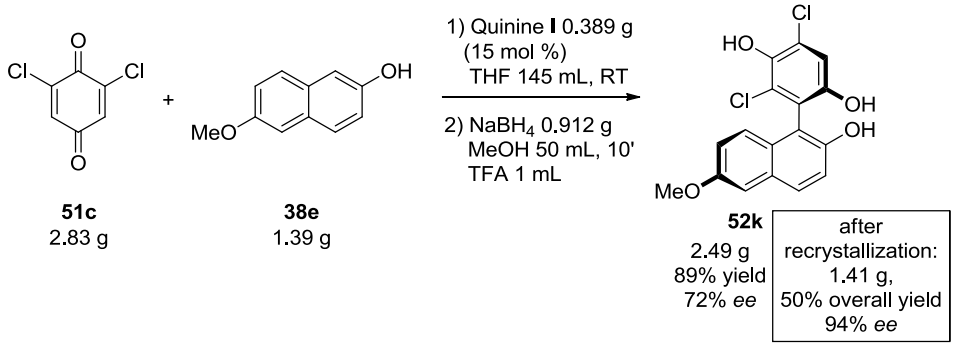

To a solution of naphthol **38e** (1.39 g, 8.00 mmol) and quinine (**I**, 389 mg, 1.20 mmol) in THF (170 mL) was added at room temperature a solution of

2,6-dichloro 1,4-benzoquinone **51c** (2.83 g, 16.0 mmol) dissolved in 30 mL of THF. The reaction mixture was stirred at room temperature for 24h. The resulting dark solution was then cooled to 0° C (ice bath) and $NaBH_4$ (912 mg, 24.0 mmol) was added, followed by the dropwise addition of 50 mL of MeOH. After 5 min to the solution was added trifluoroacetic acid (1.0 mL) and 7.0 g of silica gel, and the solvent was removed by rotavapor. The resulting white solid was loaded on the top of a column, and quickly filtered over a pad of silica gel (150 g) using as eluant diethyl ether: DCM in the ratio 1:20. The solvent of the fraction containing the desired product was evaporated, to give chemically pure compound **52k** (2.49 g, 7.10 mmol, 89% yield).

The enantiomeric excess of compound **52k** was determined to be 72% by HPLC on CSP using Chiralpack IF column and hexane: *i*-propanol 88:12 as eluent, flow 0.9 mL min.

Crystallization of product **52k**:

In a 100 mL Erlenmeyer flask, 2.49 g of compound **52k** were dissolved in 40 mL of boiling toluene. The solution was allowed to rest at room temperature for 72 h, in which time a white crystalline solid formed. The supernatant solution was then removed and the crystals were washed with cold toluene (2 x 2 mL) and cold chloroform (1 x 2 mL). The crystals were collected and dried under reduced pressure to give 1.41 g of compound **52k** (94% *ee*).

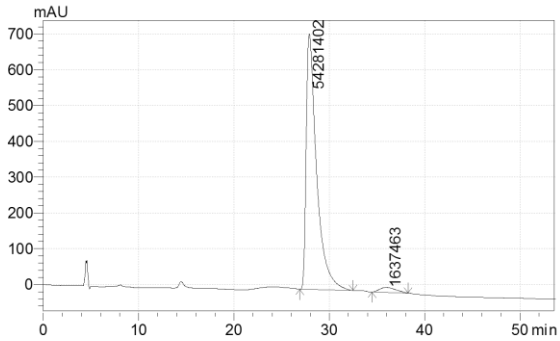

Peak#	Ret. Time	Area	Height	Conc.	Area%
1	27.903	54281402	713885	97.072	97.072
2	35.967	1637463	13831	2.928	2.928
Total		55918865	727716	100.000	100.000

7.3.5. NMR spectra of biaryls 52b-u

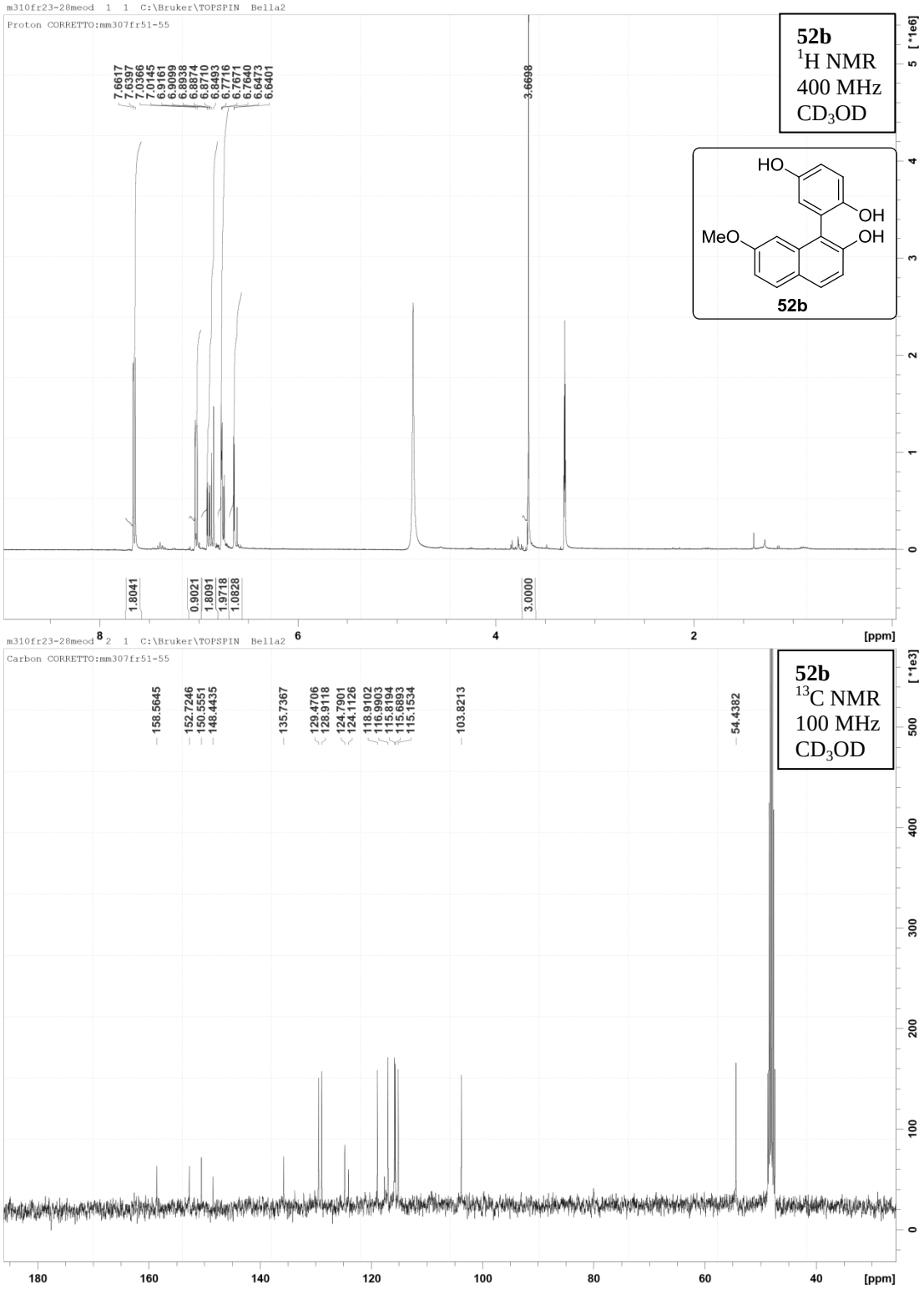

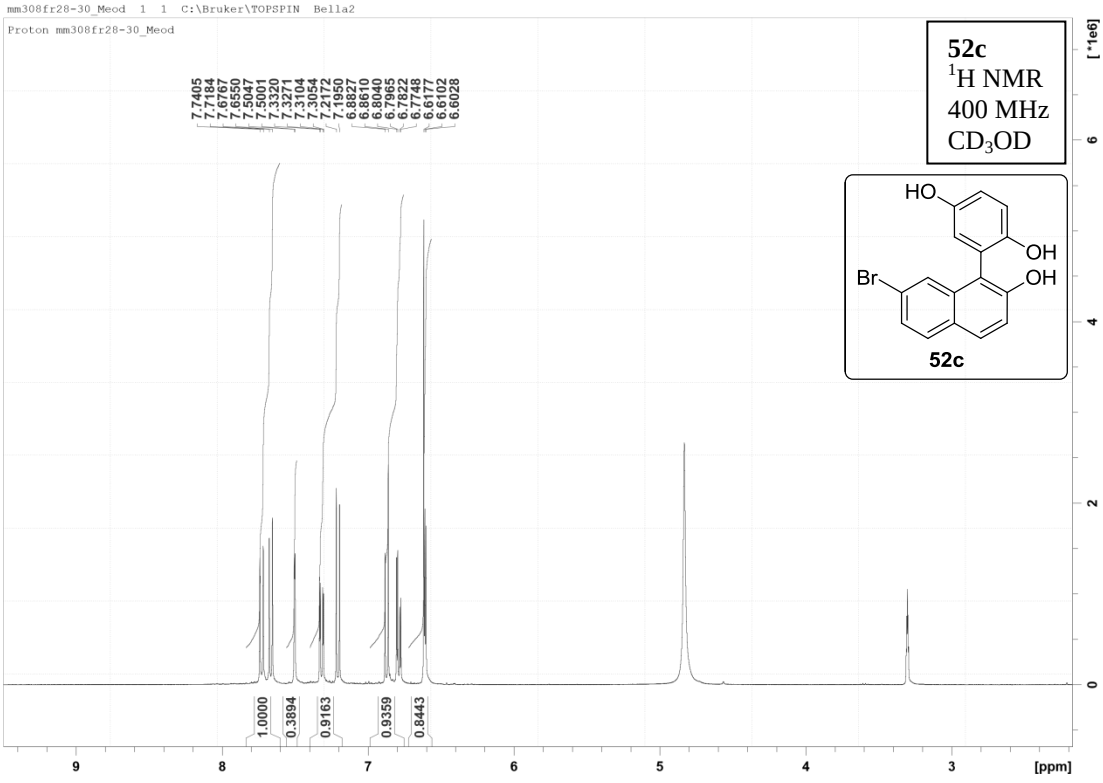
mm308fr28-30_Meod 1 1 C:\Bruker\TOPSPIN Bella2
Proton mm308fr28-30_Meod
7.7405
7.7184
7.6767
7.6550
7.5047
7.5001
7.3320
7.3271
7.3104
7.3054
7.2172
7.1950
6.8827
6.8610
6.8040
6.7965
6.7822
6.7748
6.6177
6.6102
6.6028
1.0000
0.3894
0.9163
0.9359
0.8443
9
8
7
6
5
4
3
[ppm]
[*1e6]
52c
1H NMR
400 MHz
CD3OD
HO
OH
Br
OH
52c

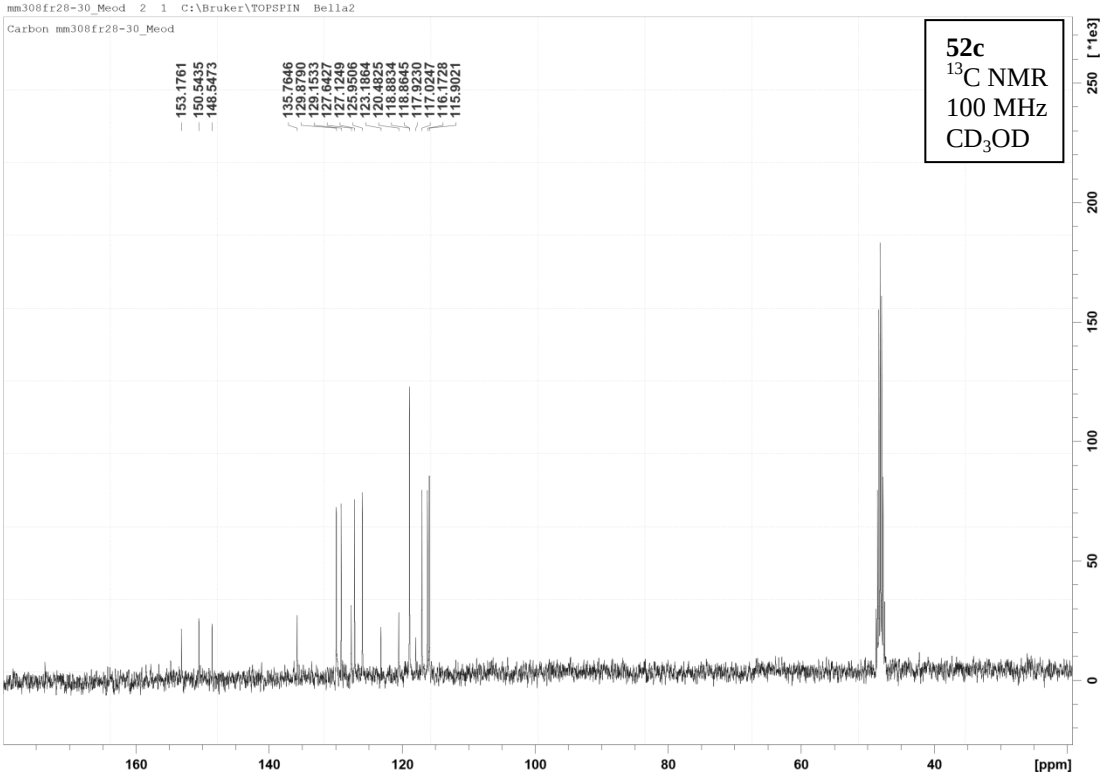
mm308fr28-30_Meod 2 1 C:\Bruker\TOPSPIN Bella2
Carbon mm308fr28-30_Meod
153.1761
150.5435
148.5473
135.7646
129.8790
129.1533
127.6427
127.1249
125.9506
123.1864
120.4825
118.8834
118.8645
117.9230
117.0247
116.1728
115.9021
160
140
120
100
80
60
40
[ppm]
[*1e3]
52c
13C NMR
100 MHz
CD3OD

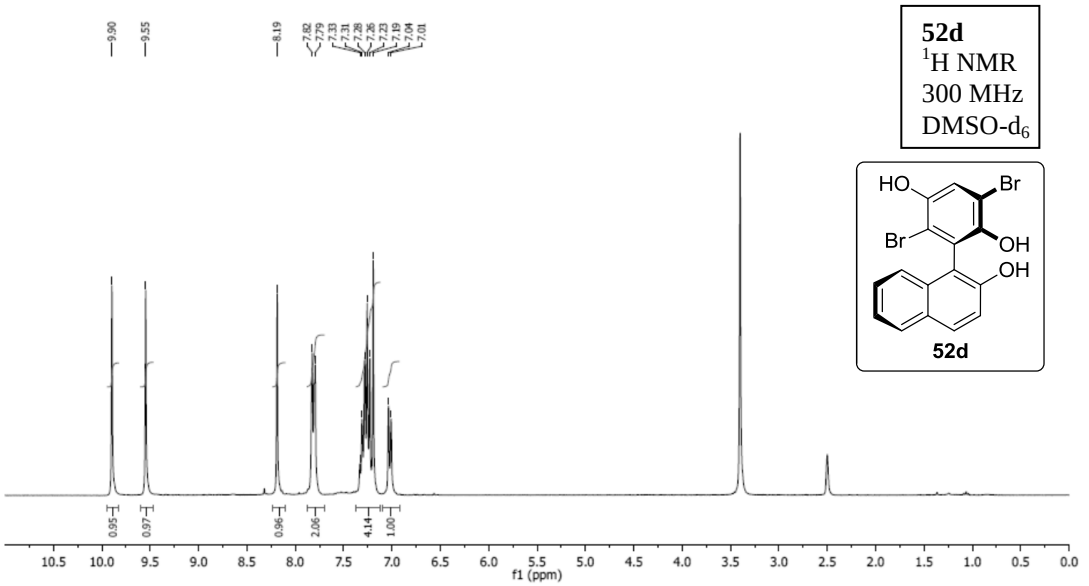
9.90
9.55
8.19
7.82
7.79
7.33
7.31
7.28
7.26
7.23
7.19
7.04
7.01
0.95
0.97
0.96
2.06
4.14
1.00
10.5 10.0 9.5 9.0 8.5 8.0 7.5 7.0 6.5 6.0 5.5 5.0 4.5 4.0 3.5 3.0 2.5 2.0 1.5 1.0 0.5 0.0
f1 (ppm)
52d
1H NMR
300 MHz
DMSO-d6
HO
Br
Br
OH
OH
52d

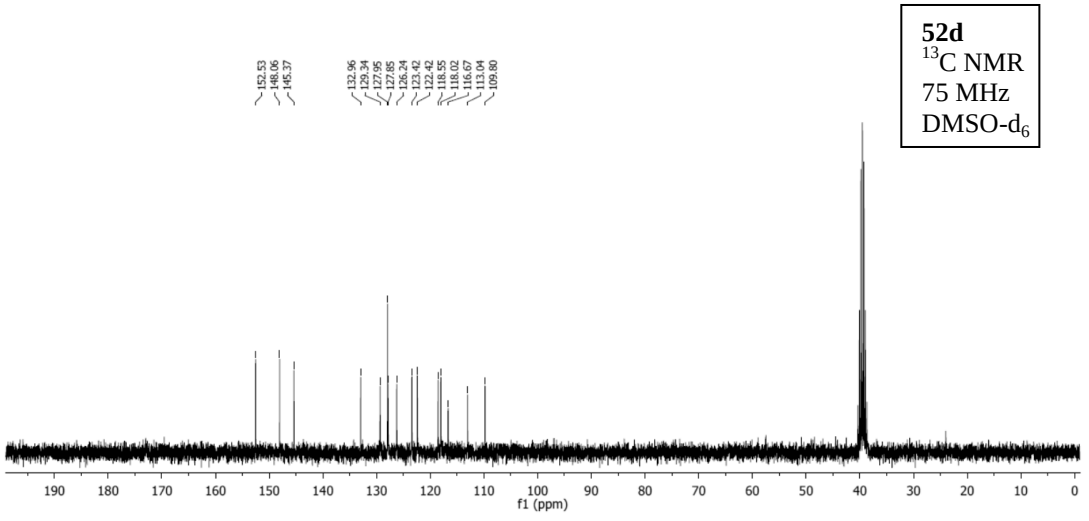
152.53
148.06
145.37
132.96
129.34
127.95
127.85
126.24
123.42
122.42
118.55
118.02
116.67
113.04
109.80
190 180 170 160 150 140 130 120 110 100 90 80 70 60 50 40 30 20 10 0
f1 (ppm)
52d
13C NMR
75 MHz
DMSO-d6

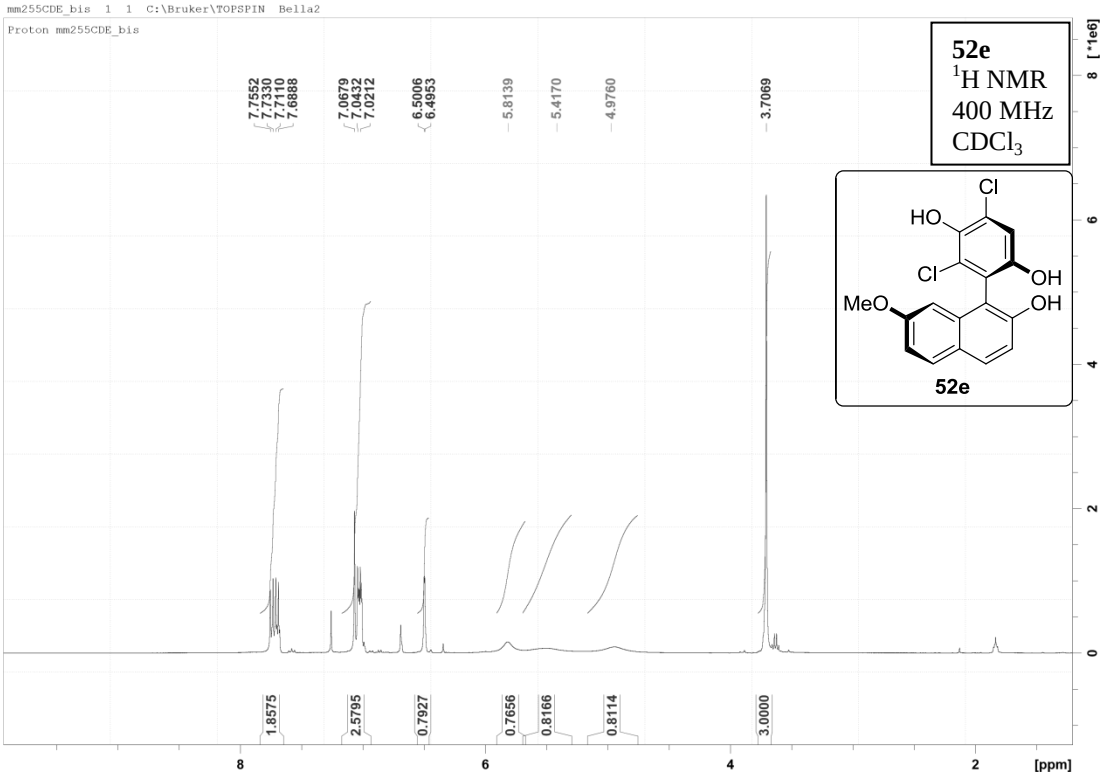
mm255CDE_bis 1 1 C:\Bruker\TOPSPIN Bella2
Proton mm255CDE_bis
52e
1H NMR
400 MHz
CDCl3
7.7552
7.7330
7.7110
7.6888
7.0679
7.0432
7.0212
6.5006
6.4953
5.8139
5.4170
4.9760
3.7069
1.8575
2.5795
0.7927
0.7656
0.8166
0.8114
3.0000
[ppm]

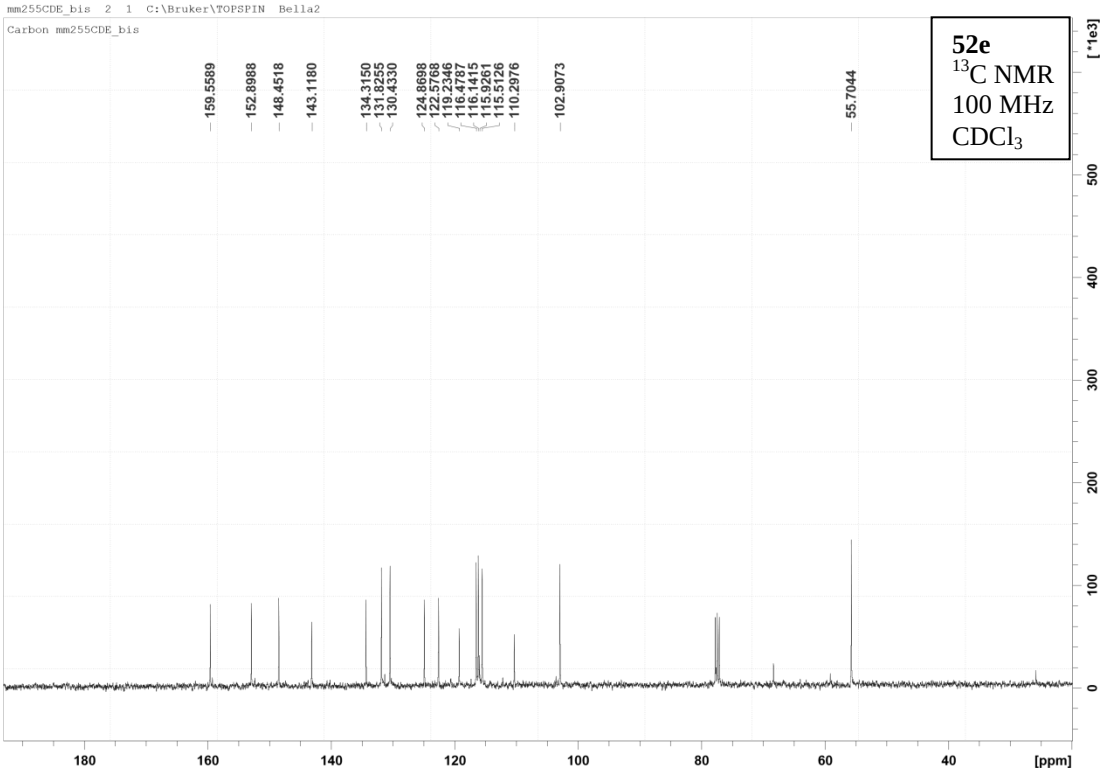
mm255CDE_bis 2 1 C:\Bruker\TOPSPIN Bella2
Carbon mm255CDE_bis
52e
13C NMR
100 MHz
CDCl3
159.5589
152.8988
148.4518
143.1180
134.3150
131.8255
130.4330
124.8698
122.5768
119.2346
116.4787
116.1415
115.9261
115.5126
110.2976
102.9073
55.7044
[ppm]

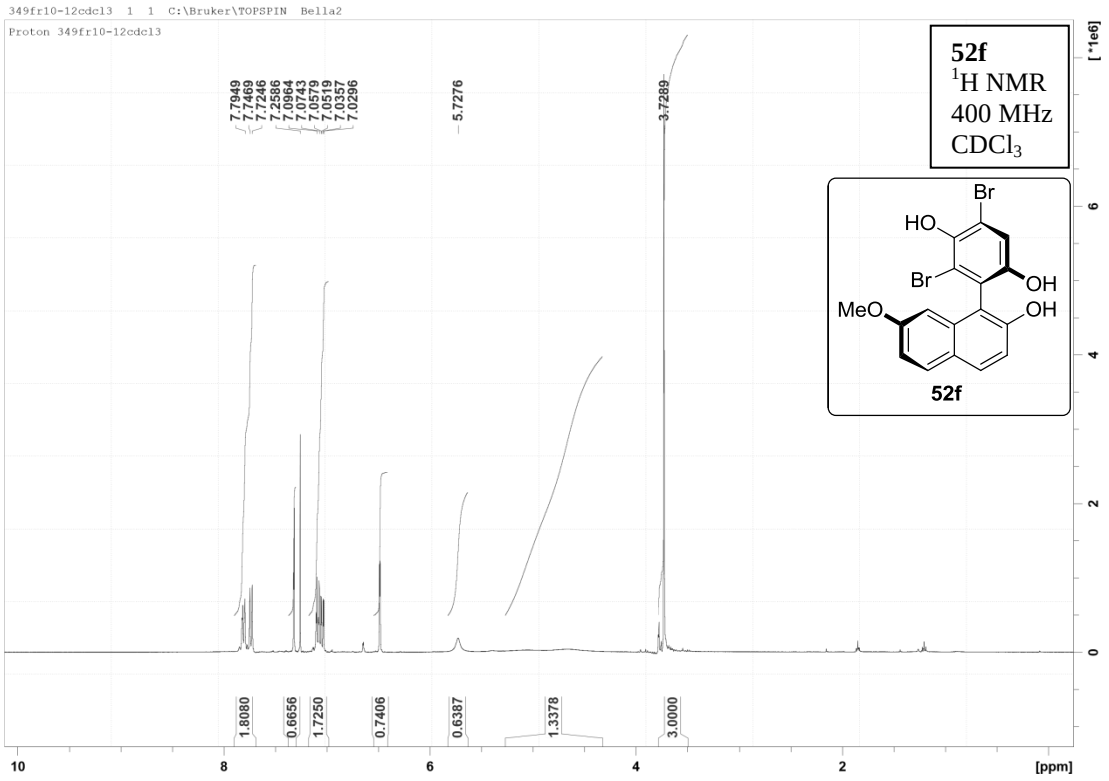
349fr10-12cdcl3 1 1 C:\Bruker\TOPSPIN Bella2
Proton 349fr10-12cdcl3
7.7949
7.7469
7.7246
7.2586
7.0964
7.0743
7.0579
7.0519
7.0357
7.0296
5.7276
3.7289
1.8080
0.6656
1.7250
0.7406
0.6387
1.3378
3.0000
10
8
6
4
2
[ppm]
[*1e6]
52f
^{1}H NMR
400 MHz
$CDCl_3$
Br
HO
Br
OH
MeO
OH
52f

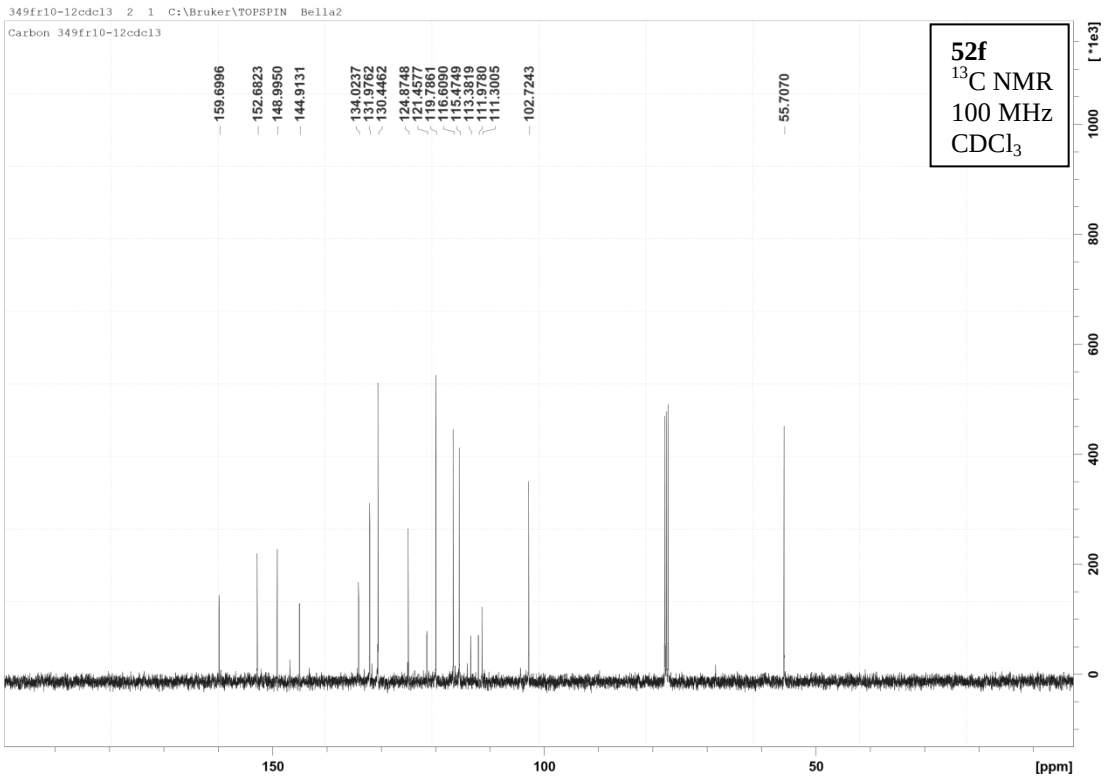
349fr10-12cdcl3 2 1 C:\Bruker\TOPSPIN Bella2
Carbon 349fr10-12cdcl3
159.6996
152.6823
148.9950
144.9131
134.0237
131.9762
130.4462
124.8748
121.4577
119.7861
116.6090
115.4749
113.3819
111.9780
111.3005
102.7243
55.7070
150
100
50
[ppm]
[*1e3]
52f
^{13}C NMR
100 MHz
$CDCl_3$

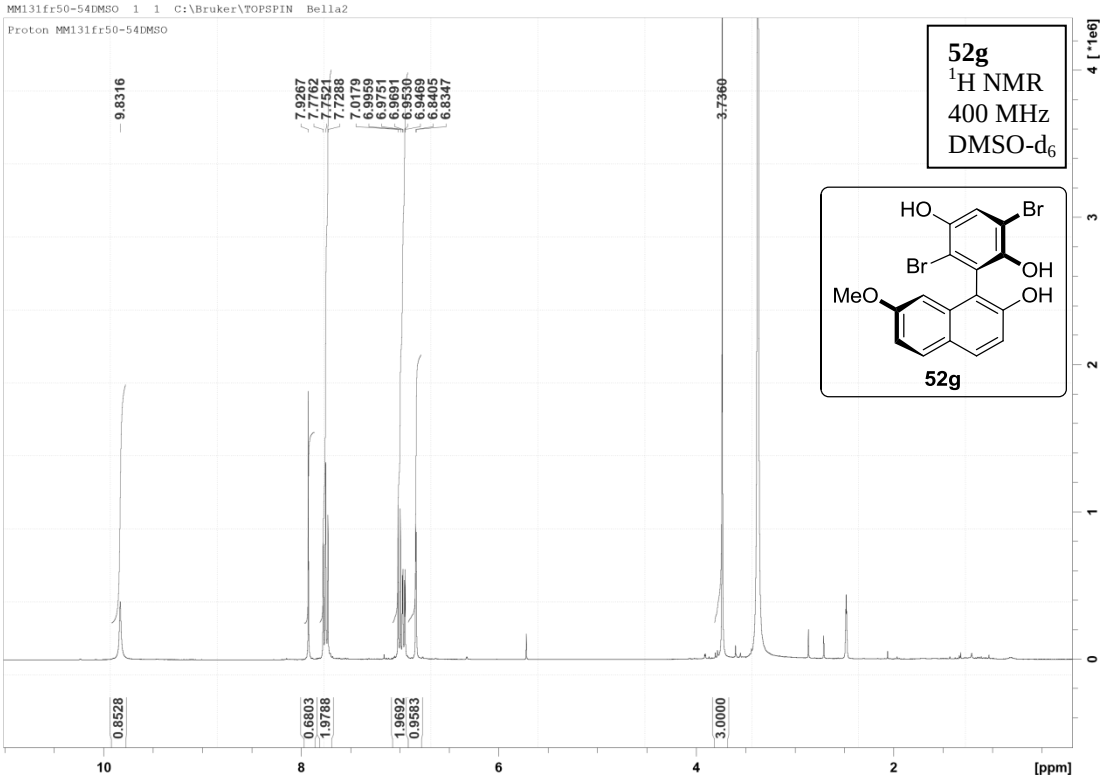
MM131fr50-54DMSO 1 1 C:\Bruker\TOPSPIN Bella2
Proton MM131fr50-54DMSO
9.8316
7.9267
7.7762
7.7521
7.7288
7.0179
6.9959
6.9751
6.9691
6.9530
6.9469
6.8405
6.8347
3.7360
0.8528
0.6803
1.9788
1.9692
0.9583
3.0000
10
8
6
4
2
[ppm]
52g
1H NMR
400 MHz
DMSO-d6
HO
Br
Br
OH
MeO
OH
52g

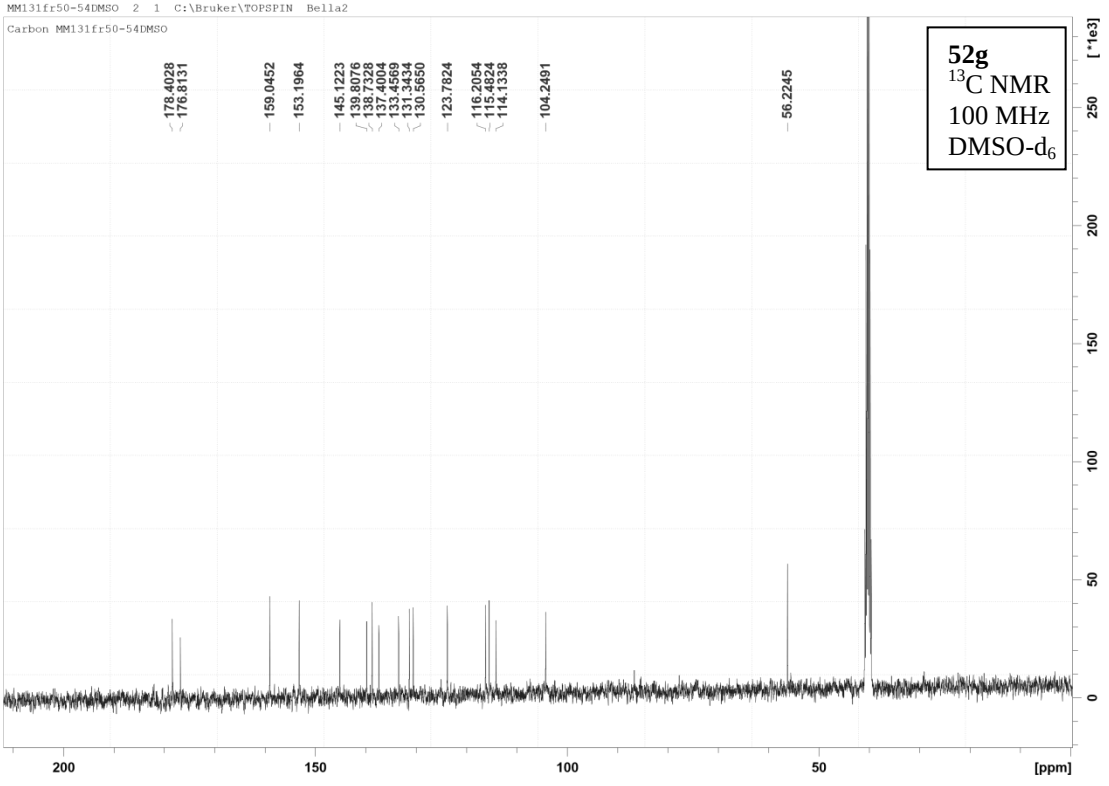
MM131fr50-54DMSO 2 1 C:\Bruker\TOPSPIN Bella2
Carbon MM131fr50-54DMSO
178.4028
176.8131
159.0452
153.1964
145.1223
139.8076
138.7328
137.4004
133.4569
131.3434
130.5650
123.7824
116.2054
115.4824
114.1338
104.2491
56.2245
200
150
100
50
[ppm]
52g
13C NMR
100 MHz
DMSO-d6

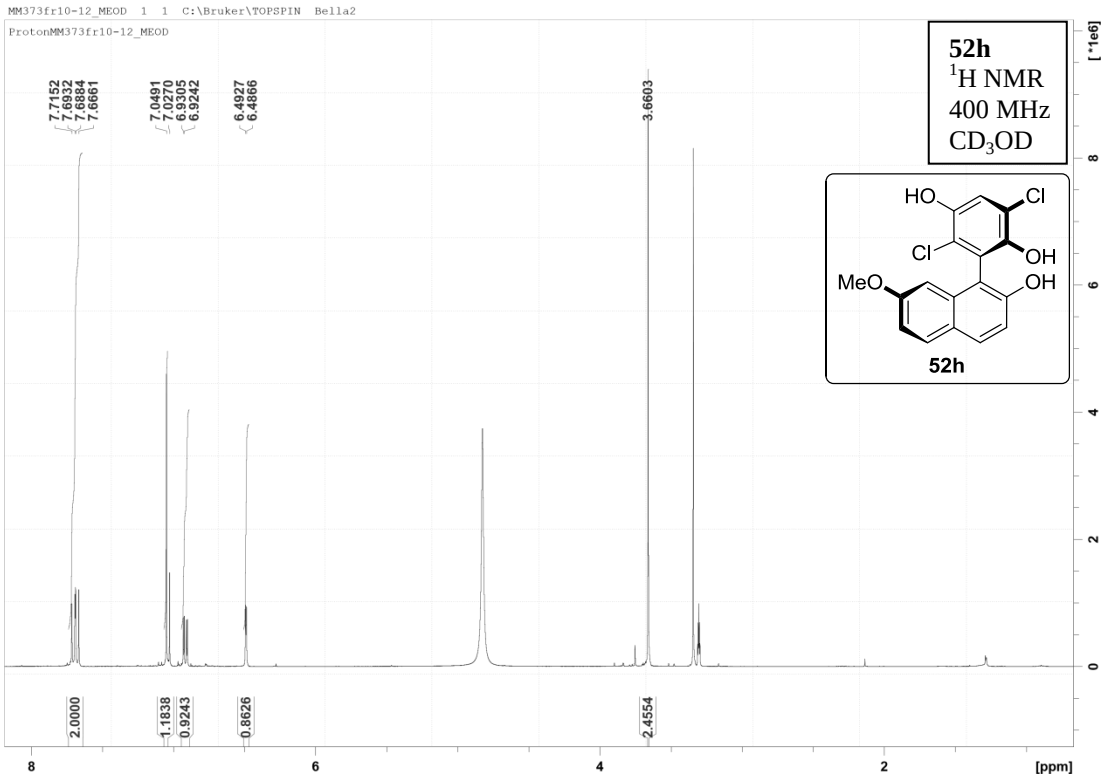
MM373fr10-12_MEOD 1 1 C:\Bruker\TOPSPIN Bella2
ProtonMM373fr10-12_MEOD
7.7152
7.6932
7.6884
7.6661
7.0491
7.0270
6.9305
6.9242
6.4927
6.4866
3.6603
2.0000
1.1838
0.9243
0.8626
2.4554
8
6
4
2
[ppm]
[*1e6]
52h
1H NMR
400 MHz
CD3OD
HO
Cl
Cl
OH
MeO
OH
52h

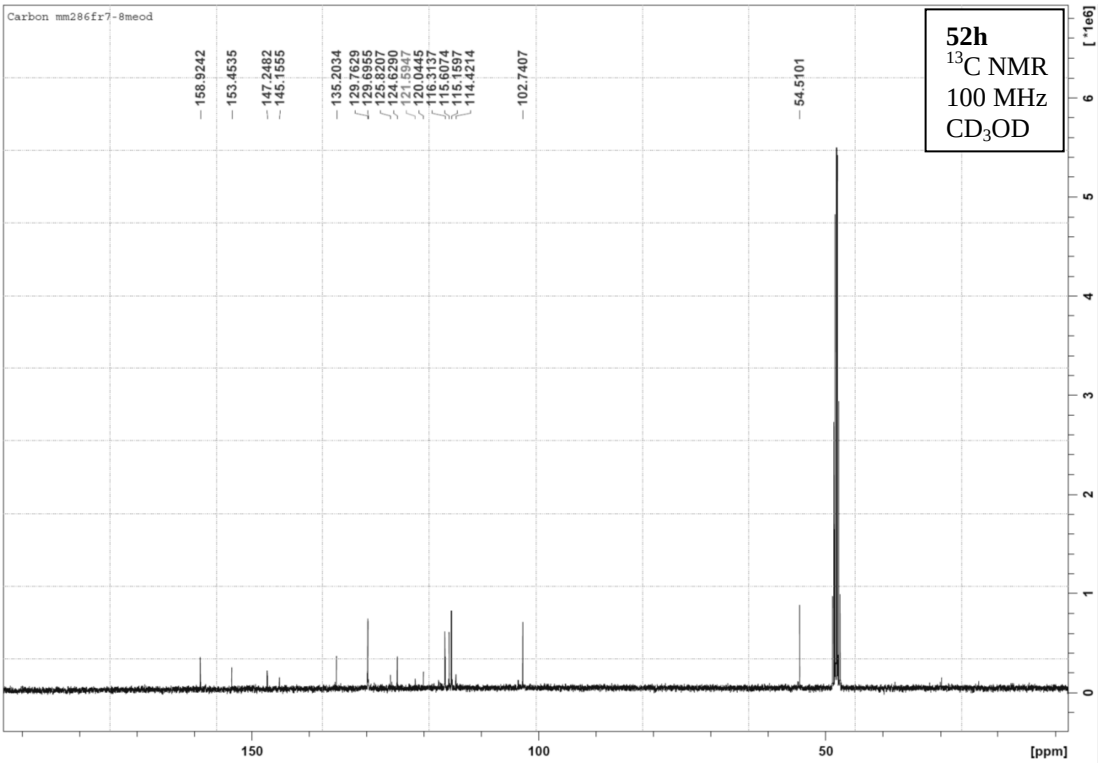
Carbon mm286fr7-8meod
158.9242
153.4535
147.2482
145.1555
135.2034
129.7629
129.6955
125.8207
124.6290
123.1647
120.0445
116.3137
115.6074
115.1597
114.4214
102.7407
54.5101
150
100
50
[ppm]
[*1e6]
52h
13C NMR
100 MHz
CD3OD

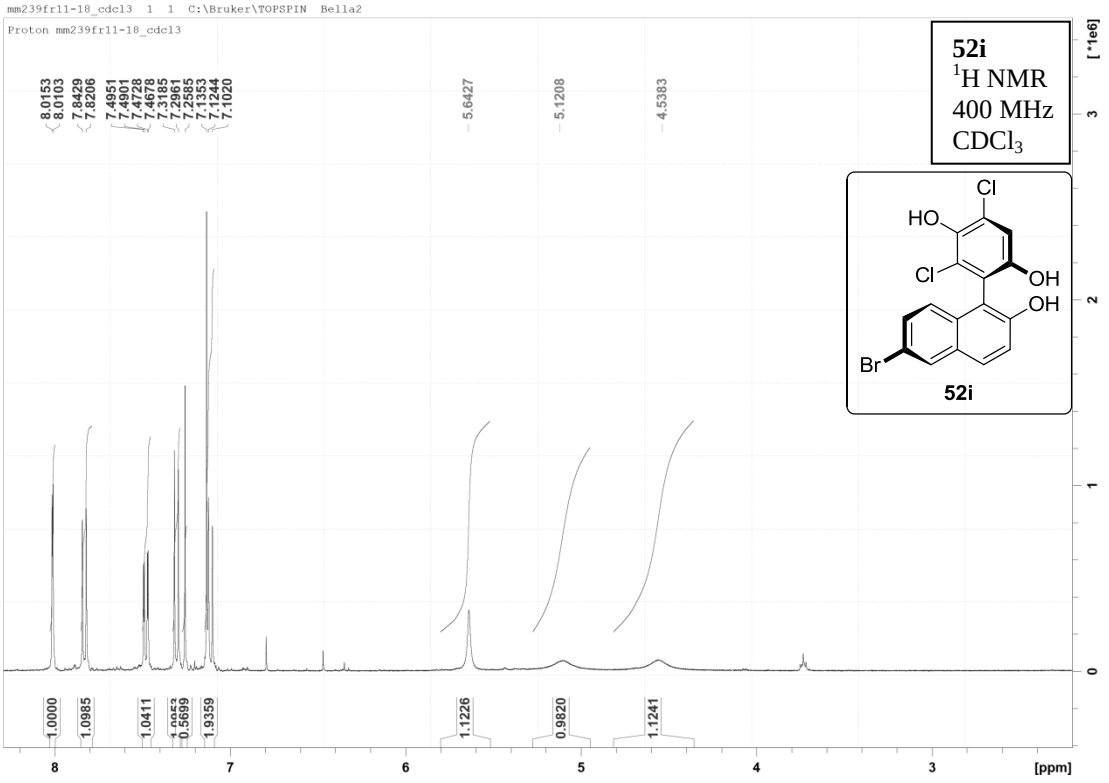
mm239fr11-18_cdcl3 1 1 C:\Bruker\TOPSPIN Bella2
Proton mm239fr11-18_cdcl3
8.0153
8.0103
7.8429
7.8206
7.4951
7.4901
7.4728
7.4678
7.3185
7.2961
7.2865
7.1353
7.1244
7.1020
5.6427
5.1208
4.5383
1.0000
1.0985
1.0411
1.0053
0.5699
1.9359
1.1226
0.9820
1.1241
8
7
6
5
4
3
[ppm]
[*1e6]
52i
1H NMR
400 MHz
CDCl3
Cl
HO
Cl
OH
OH
Br
52i

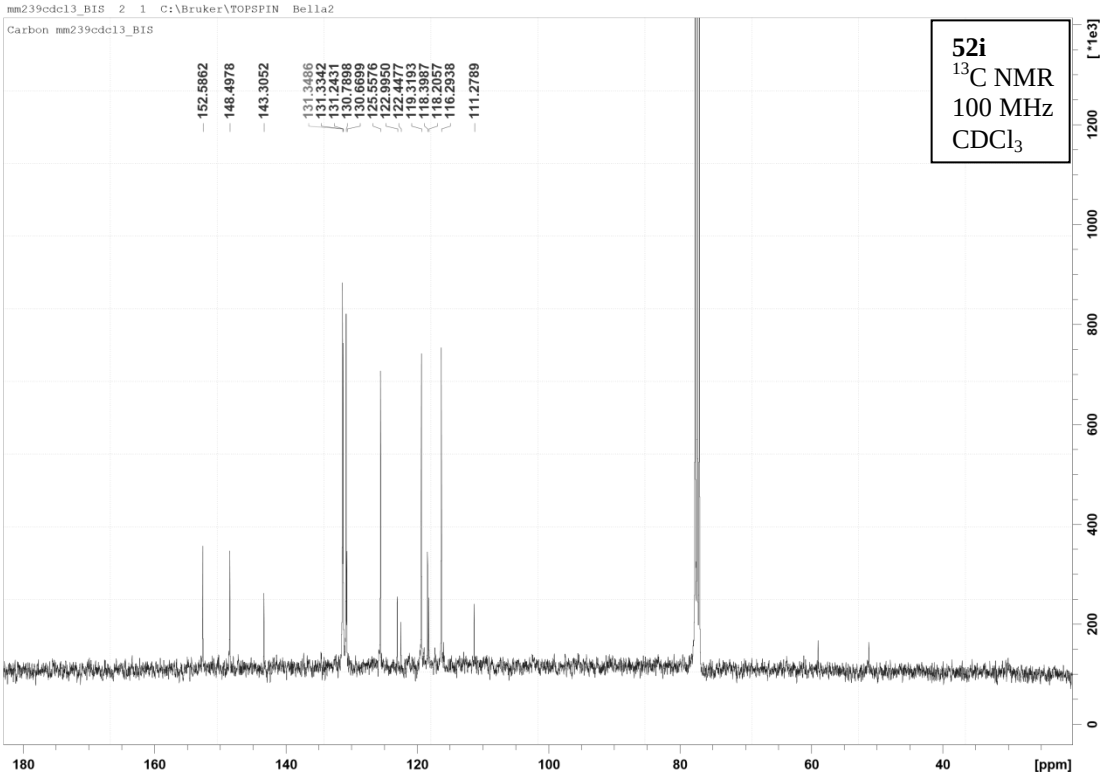
mm239cdcl3_BIS 2 1 C:\Bruker\TOPSPIN Bella2
Carbon mm239cdcl3_BIS
152.5862
148.4978
143.3052
131.3486
131.3342
131.2431
130.7898
130.6699
125.5576
125.3950
122.4477
119.3193
118.3987
118.2057
116.2938
111.2789
180
160
140
120
100
80
60
40
[ppm]
[*1e3]
52i
13C NMR
100 MHz
CDCl3

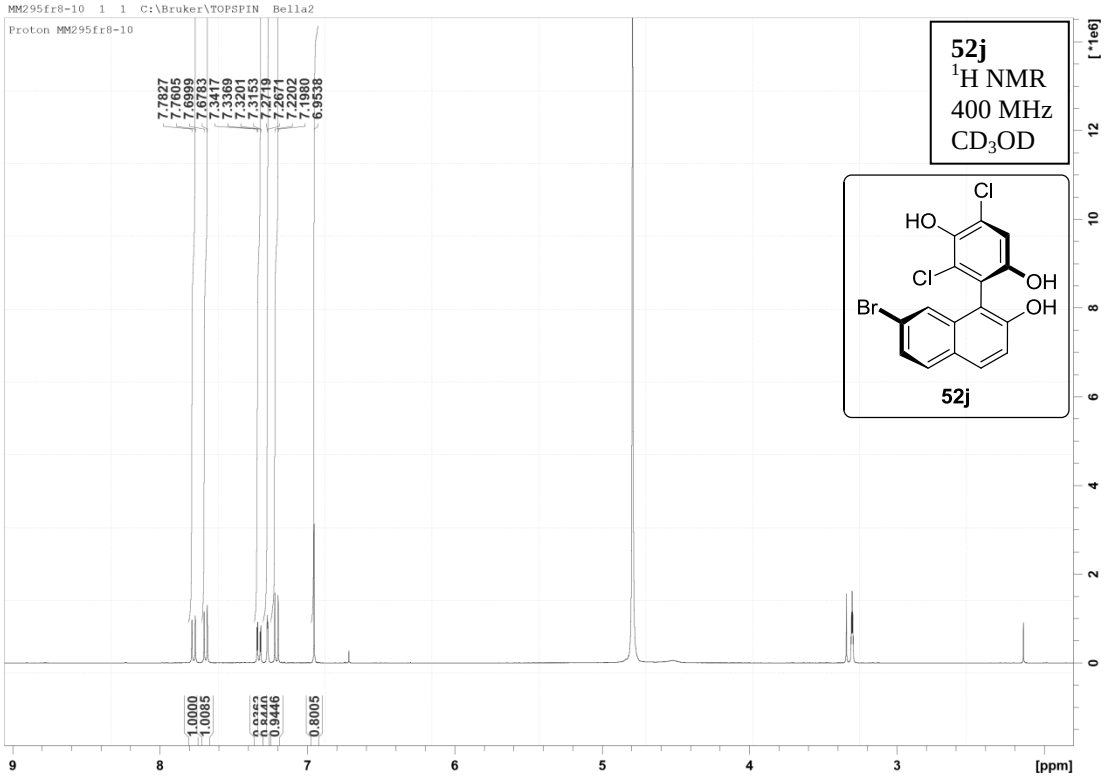
MM295fr8-10 1 1 C:\Bruker\TOPSPIN Bella2
Proton MM295fr8-10
7.7827
7.7605
7.6999
7.6783
7.3467
7.3369
7.3201
7.3153
7.2719
7.2671
7.2202
7.1980
6.9538
1.0000
1.0085
0.8005
52j
^{1}H NMR
400 MHz
CD_3OD
Cl
HO
Cl
OH
Br
OH
52j
[ppm]

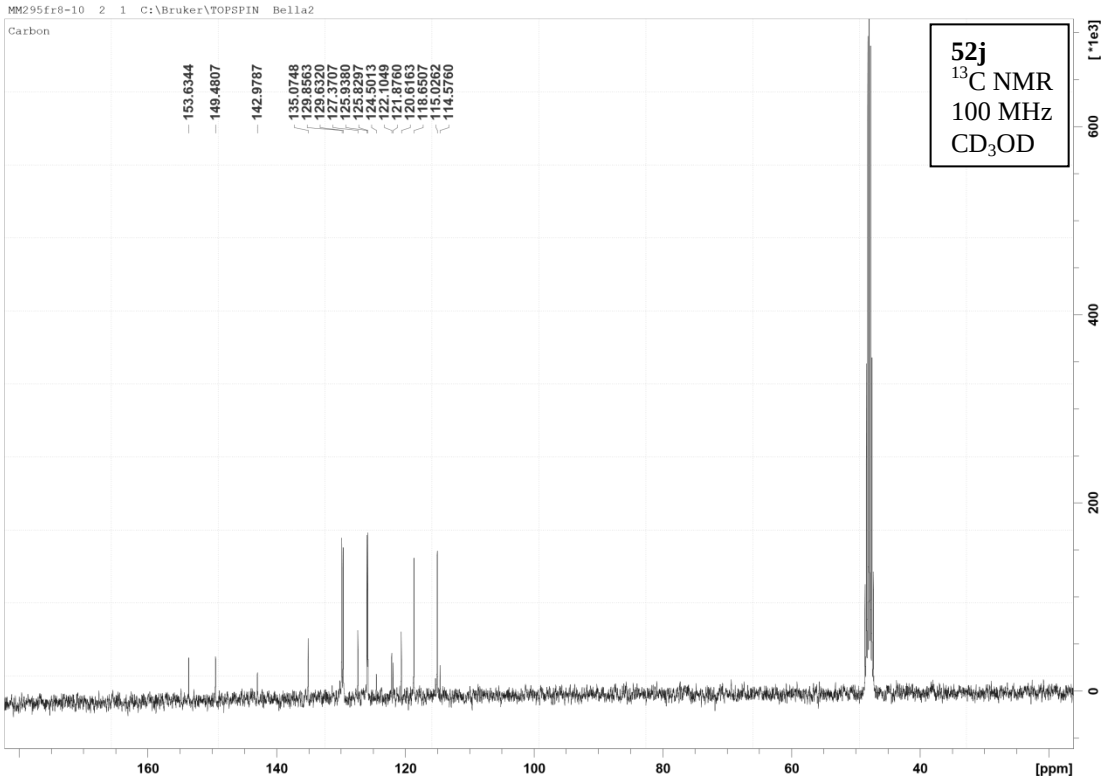
MM295fr8-10 2 1 C:\Bruker\TOPSPIN Bella2
Carbon
153.6344
149.4807
142.9787
135.0748
129.8563
129.6320
127.3707
125.9380
125.8297
124.5013
122.1049
121.8760
120.1653
118.6507
115.0262
114.5760
52j
^{13}C NMR
100 MHz
CD_3OD
[ppm]

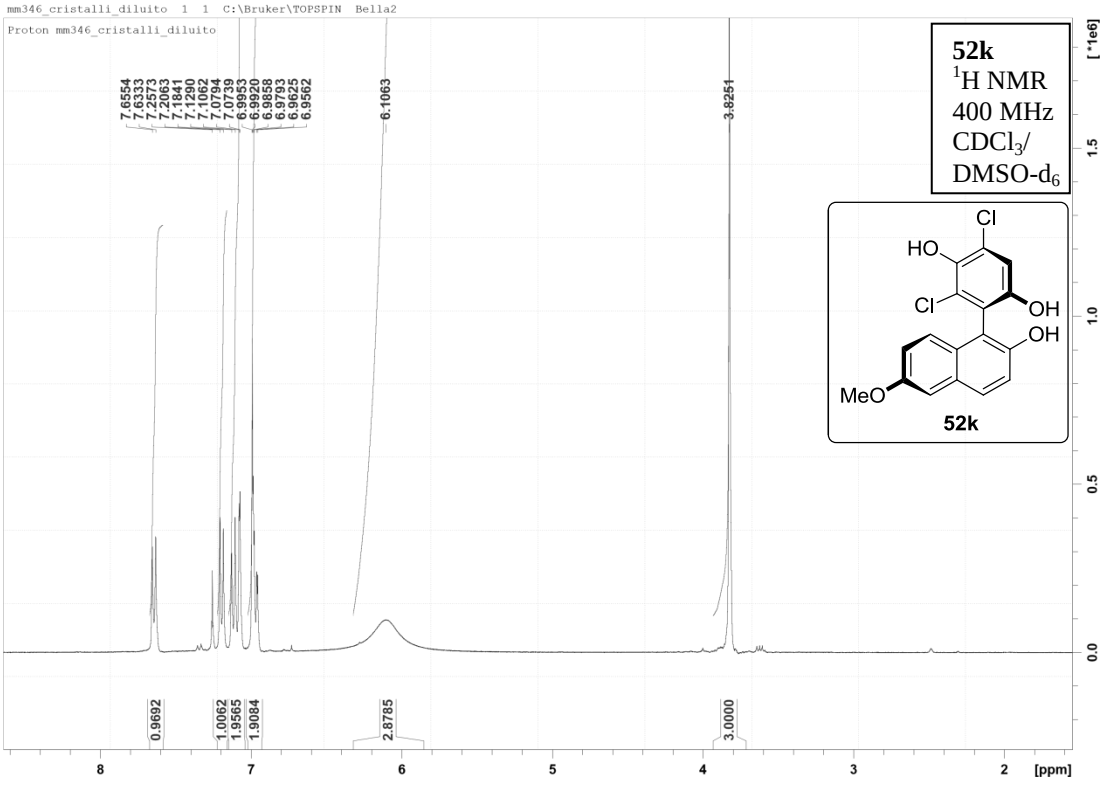
mm346_cristalli_diluito 1 1 C:\Bruker\TOPSPIN Bella2
Proton mm346_cristalli_diluito
7.6554
7.6333
7.2573
7.2063
7.1841
7.1290
7.1092
7.0784
7.0739
6.9953
6.9920
6.9858
6.9793
6.9625
6.9562
6.1063
3.8251
0.9692
1.0062
1.9565
1.9084
2.8785
3.0000
8
7
6
5
4
3
2
[ppm]
[*1e6]
1.5
1.0
0.5
0.0
52k
1H NMR
400 MHz
CDCl3/
DMSO-d6
Cl
HO
Cl
OH
OH
MeO
52k

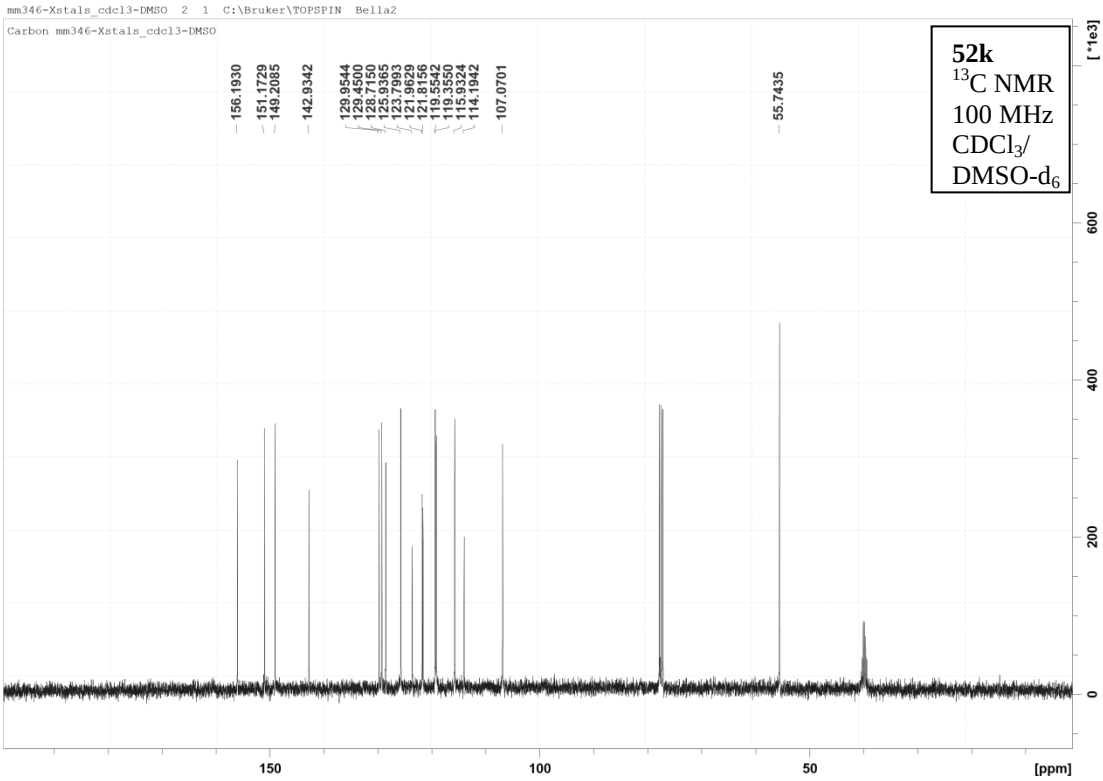
mm346-Xstals_cdcl3-DMSO 2 1 C:\Bruker\TOPSPIN Bella2
Carbon mm346-Xstals_cdcl3-DMSO
156.1930
151.1729
149.2085
142.9342
129.9544
129.4500
128.7156
125.9365
123.7993
121.9629
121.8156
119.5542
119.3550
115.9324
114.1942
107.0701
55.7435
150
100
50
[ppm]
[*1e3]
600
400
200
0
52k
13C NMR
100 MHz
CDCl3/
DMSO-d6

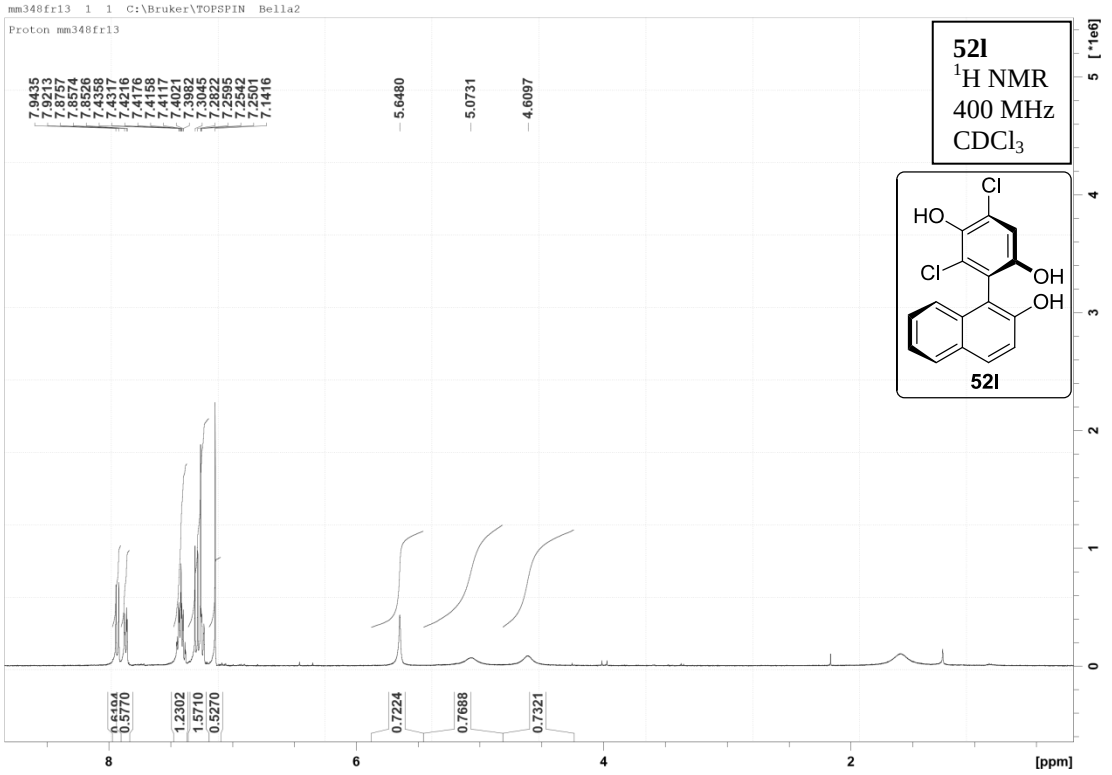
mm348fr13 1 1 C:\Bruker\TOPSPIN Bella2
Proton mm348fr13
7.9435
7.9213
7.8757
7.8574
7.8526
7.4358
7.4317
7.4216
7.4176
7.4158
7.4117
7.4021
7.3982
7.3045
7.2852
7.2695
7.2542
7.2501
7.1416
5.6480
5.0731
4.6097
0.6104
0.5770
1.2302
1.5710
0.5270
0.7224
0.7688
0.7321
8
6
4
2
[ppm]
0
1
2
3
4
5 [*1e6]
52l
1H NMR
400 MHz
CDCl3
Cl
HO
Cl
OH
OH
52l

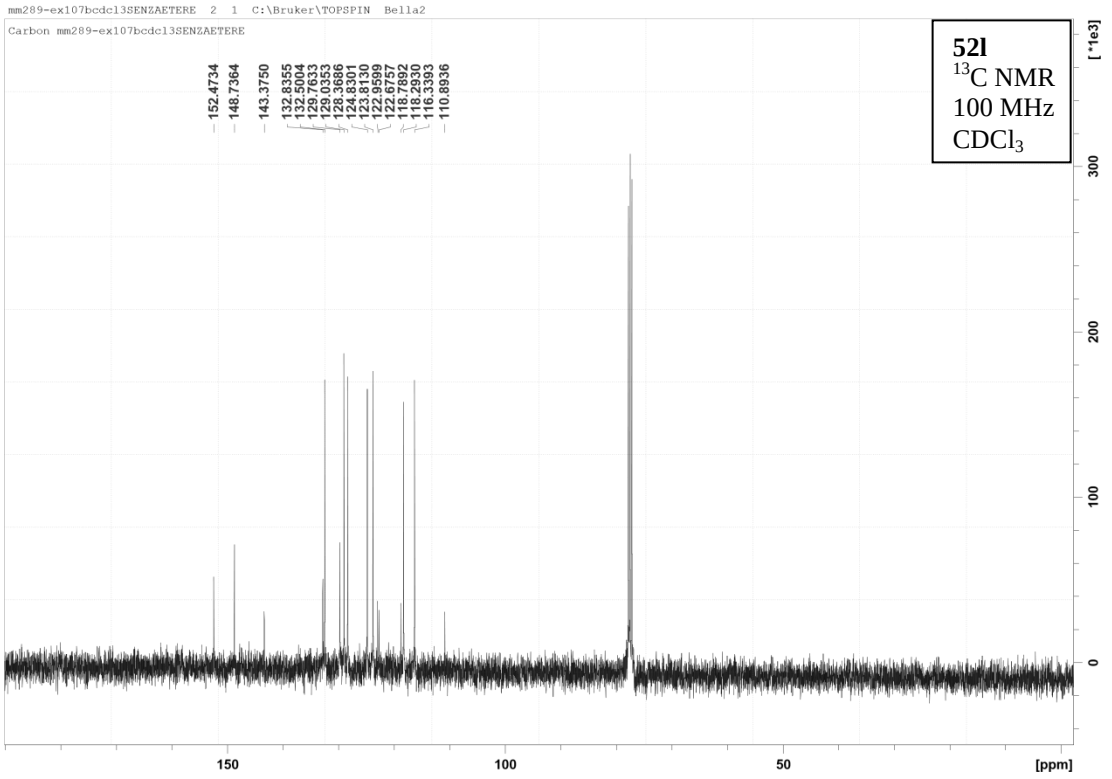
mm289-ex107bcdcl3SENZAETERE 2 1 C:\Bruker\TOPSPIN Bella2
Carbon mm289-ex107bcdcl3SENZAETERE
152.4734
148.7364
143.3750
132.8355
132.5004
129.7033
129.0553
128.3686
124.8301
123.8130
122.9599
122.6757
118.7892
118.2930
116.3393
110.8936
150
100
50
[ppm]
0
100
200
300
[*1e3]
52l
13C NMR
100 MHz
CDCl3

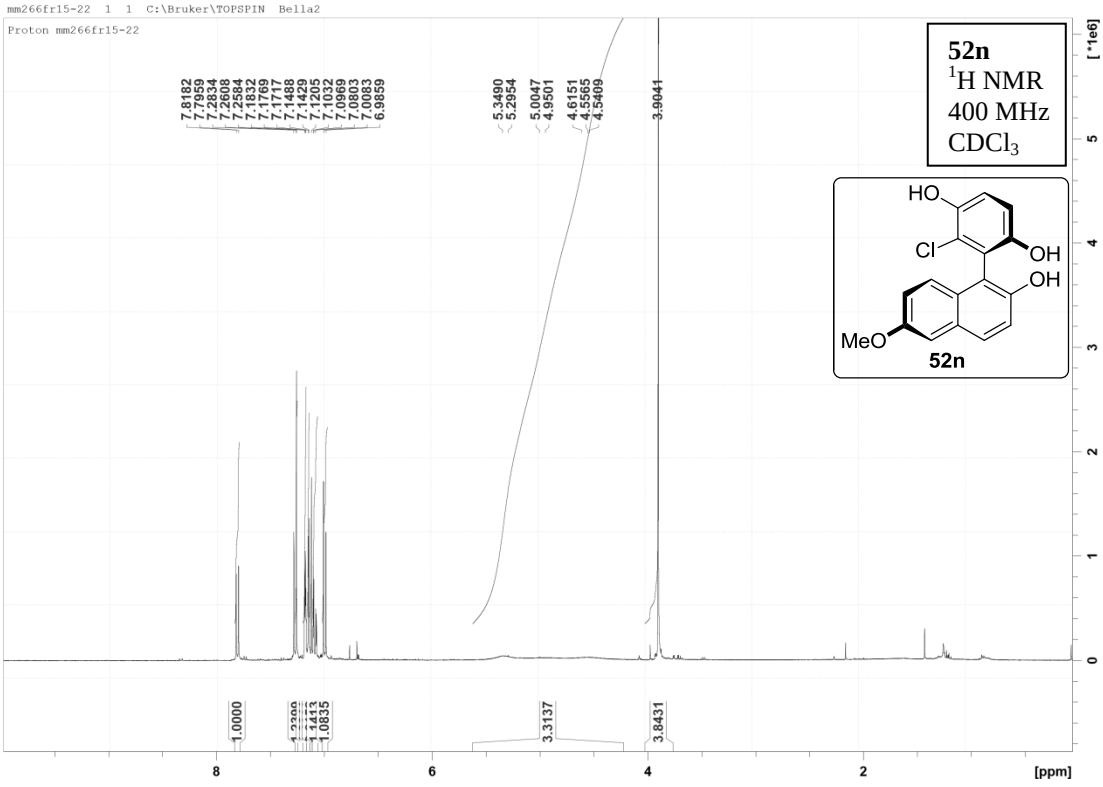
mm266fr15-22 1 1 C:\Bruker\TOPSPIN Bella2
Proton mm266fr15-22
52n
1H NMR
400 MHz
CDCl3
HO
Cl
OH
OH
MeO
52n
7.8182
7.7959
7.2834
7.2608
7.2584
7.1832
7.1769
7.1717
7.1488
7.1429
5.3490
5.2954
5.0047
4.9501
4.6151
4.5565
4.5409
3.9041
1.0000
3.3137
3.8431
[ppm]

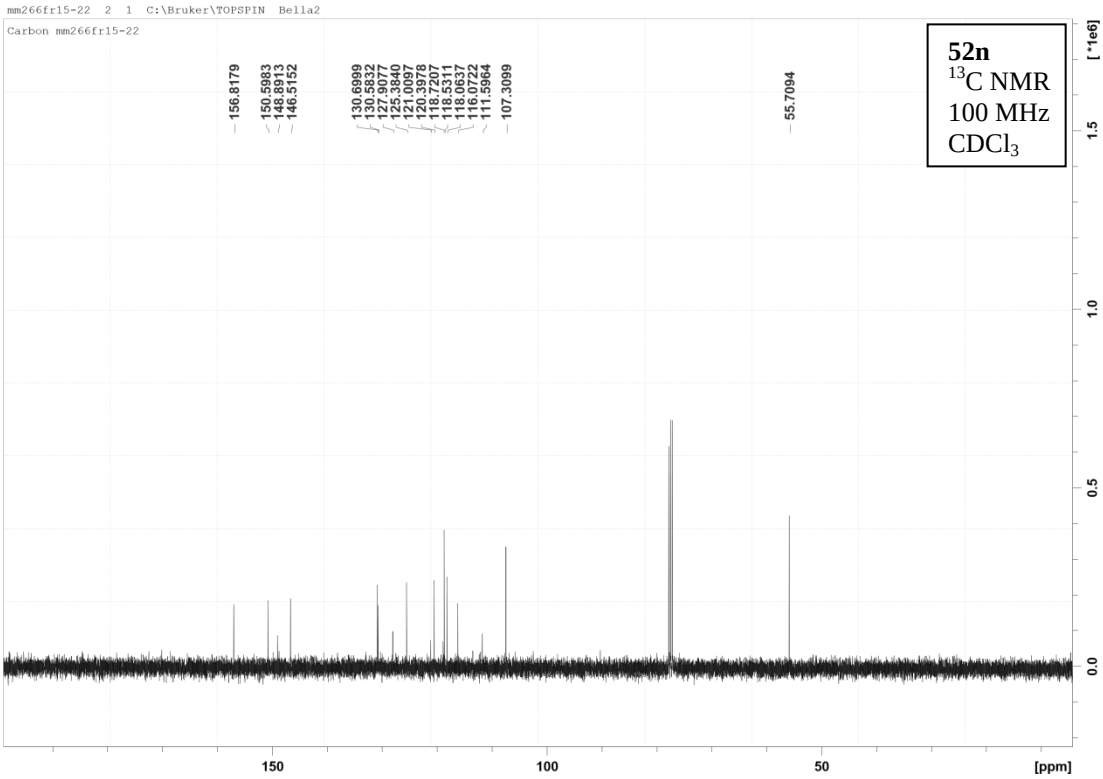
mm266fr15-22 2 1 C:\Bruker\TOPSPIN Bella2
Carbon mm266fr15-22
52n
13C NMR
100 MHz
CDCl3
156.8179
150.5983
148.8913
146.5152
130.6999
130.5832
127.9077
125.3840
121.0097
120.3978
118.7207
118.5311
118.0637
116.0722
111.5964
107.3099
55.7094
[ppm]

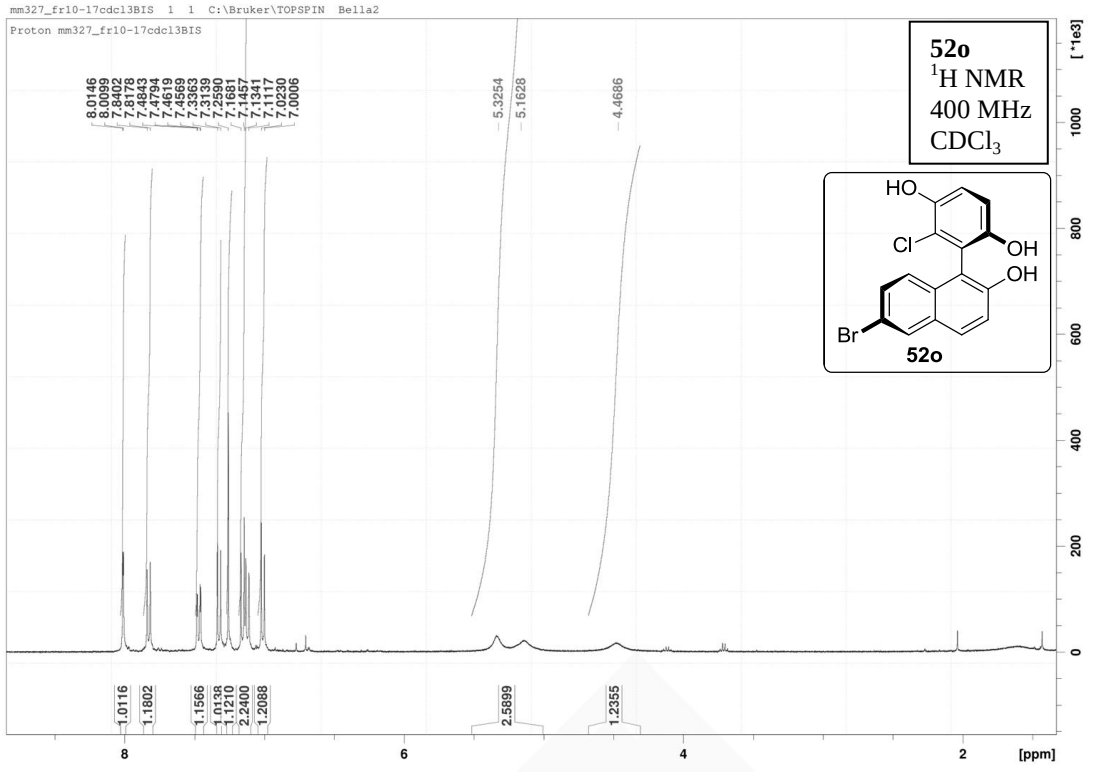
mm327_fr10-17cdcl3BIS 1 1 C:\Bruker\TOPSPIN Bella2
Proton mm327_fr10-17cdcl3BIS
52o
1H NMR
400 MHz
CDCl3
HO
Cl
OH
OH
Br
52o
8.0146
8.0099
7.8402
7.8178
7.4843
7.4794
7.4619
7.4569
7.3363
7.3193
7.2590
7.1681
7.1457
7.1341
7.1117
7.0230
7.0006
5.3254
5.1628
4.4686
1.0116
1.1802
1.1566
1.0138
1.1210
2.2400
1.2068
2.5899
1.2355
8
6
4
2
[ppm]
[*1e3]

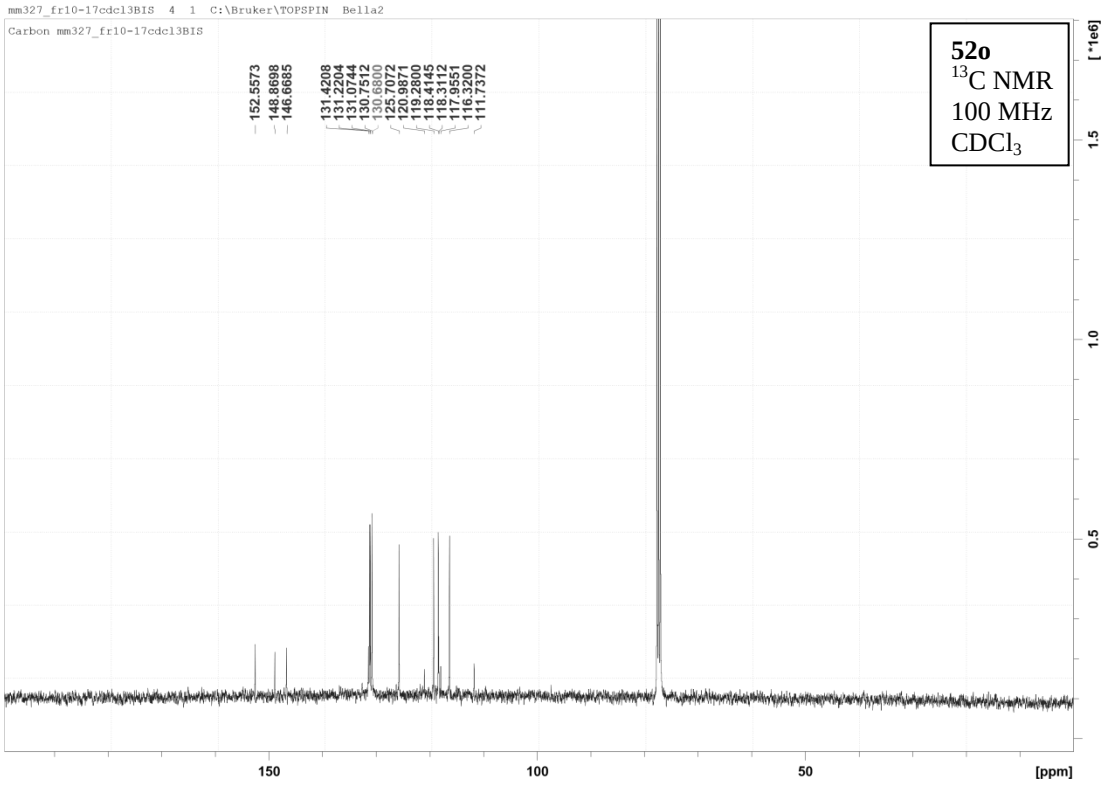
mm327_fr10-17cdcl3BIS 4 1 C:\Bruker\TOPSPIN Bella2
Carbon mm327_fr10-17cdcl3BIS
52o
13C NMR
100 MHz
CDCl3
152.5573
148.8698
146.6685
131.4208
131.2204
131.0744
130.7512
130.6800
125.7072
120.9871
119.2800
118.4145
118.3112
117.9551
116.3200
111.7372
150
100
50
[ppm]
[*1e6]

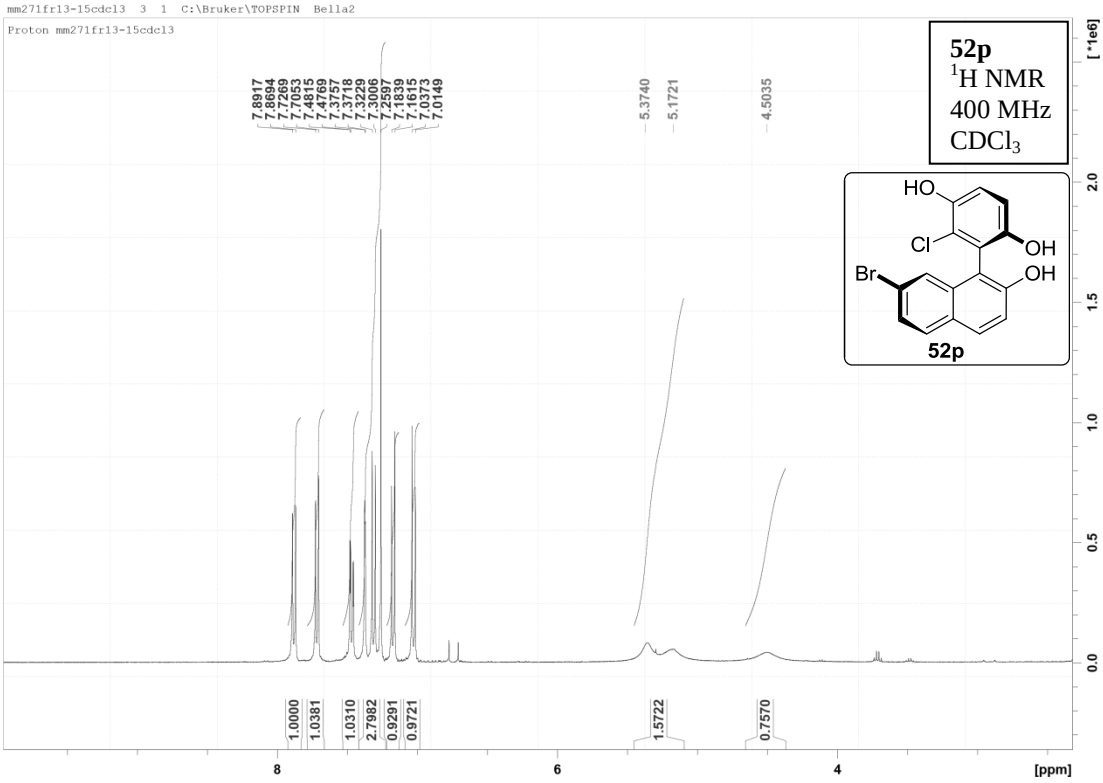
mm271fr13-15cdcl3 3 1 C:\Bruker\TOPSPIN Bella2
Proton mm271fr13-15cdcl3
52p
1H NMR
400 MHz
CDCl3
HO
Cl
OH
Br
OH
52p
7.8917
7.8694
7.7269
7.7053
7.4815
7.4769
7.3757
7.3718
7.3229
7.3006
7.2597
7.2359
7.1615
7.0373
7.0149
5.3740
5.1721
4.5035
1.0000
1.0381
1.0310
2.7982
0.9291
0.9721
1.5722
0.7570
8
6
4
[ppm]
[*1e6]

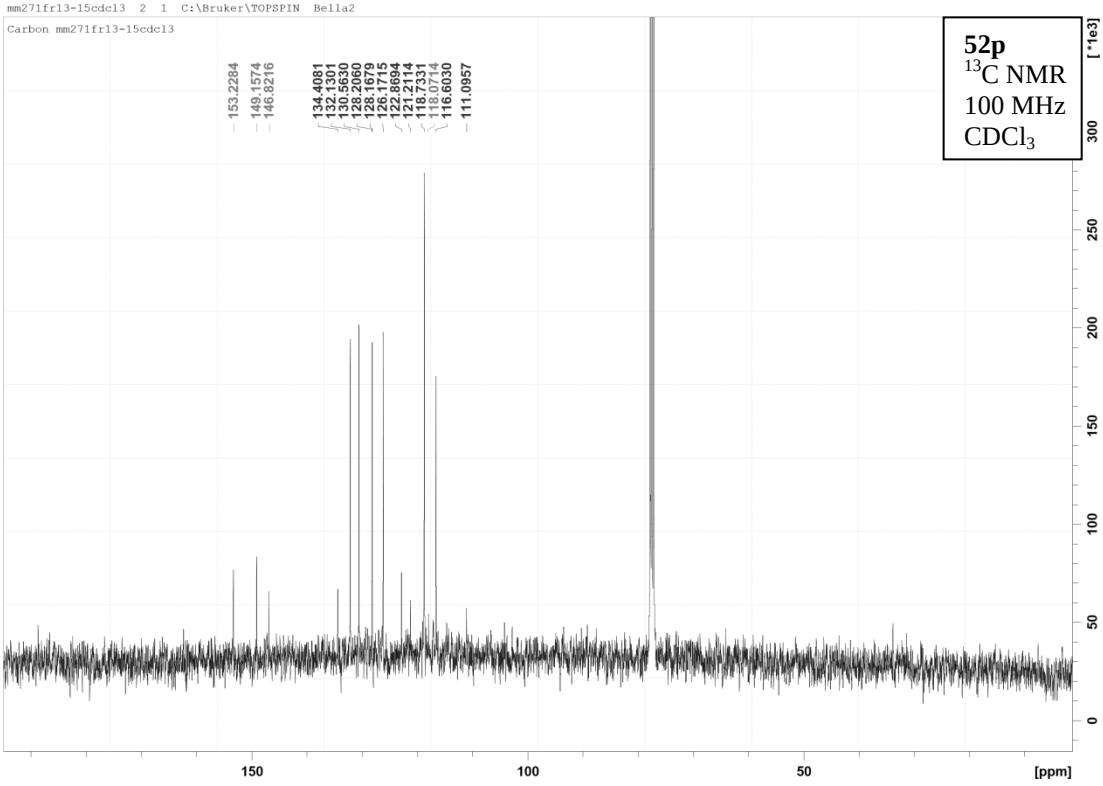
mm271fr13-15cdcl3 2 1 C:\Bruker\TOPSPIN Bella2
Carbon mm271fr13-15cdcl3
52p
13C NMR
100 MHz
CDCl3
153.2284
149.1574
146.8216
134.4081
132.1301
130.5630
130.2060
128.1679
126.1715
122.8694
121.2114
118.7331
118.0714
116.6030
111.0957
150
100
50
[ppm]
[*1e3]

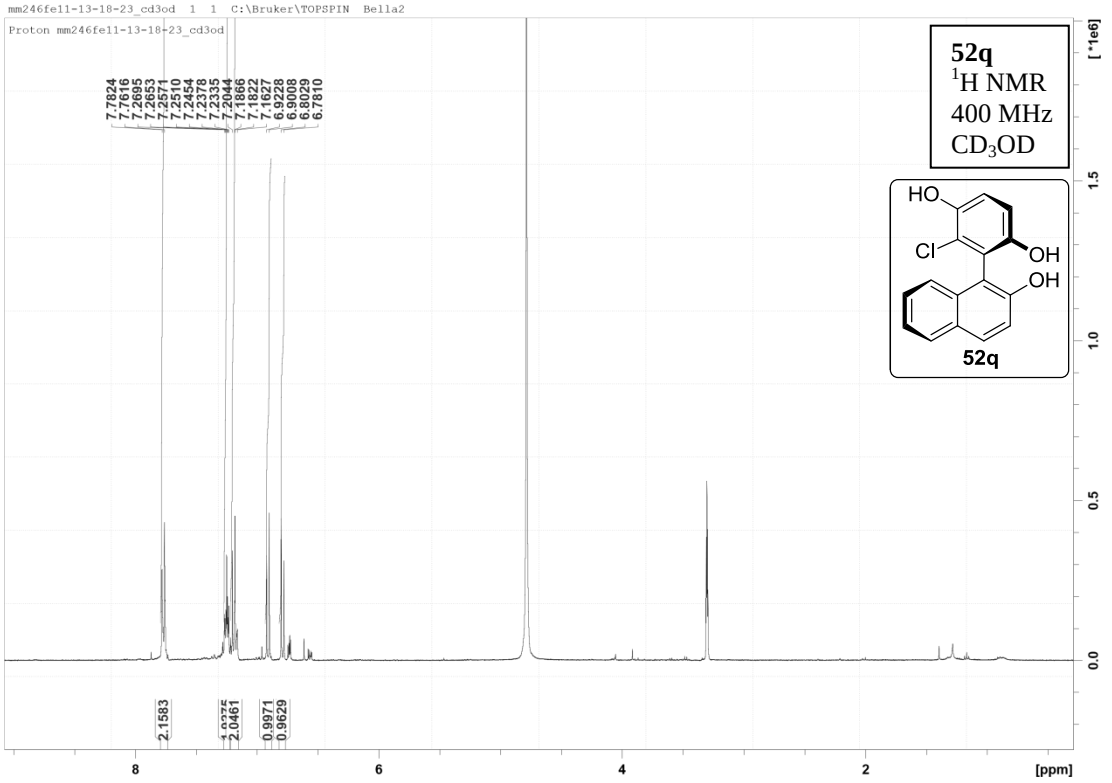
mm246fe11-13-18-23_cd3od 1 1 C:\Bruker\TOPSPIN Bella2
Proton mm246fe11-13-18-23_cd3od
7.7824
7.7616
7.2695
7.2653
7.2571
7.2510
7.2454
7.2378
7.2335
7.2044
7.1866
7.1822
7.1627
6.9228
6.9008
6.8029
6.7810
2.1583
2.0461
0.9971
0.9629
8
6
4
2
[ppm]
[*1e6]
1.5
1.0
0.5
0.0
52q
^{1}H NMR
400 MHz
CD_3OD
HO
Cl
OH
OH
52q

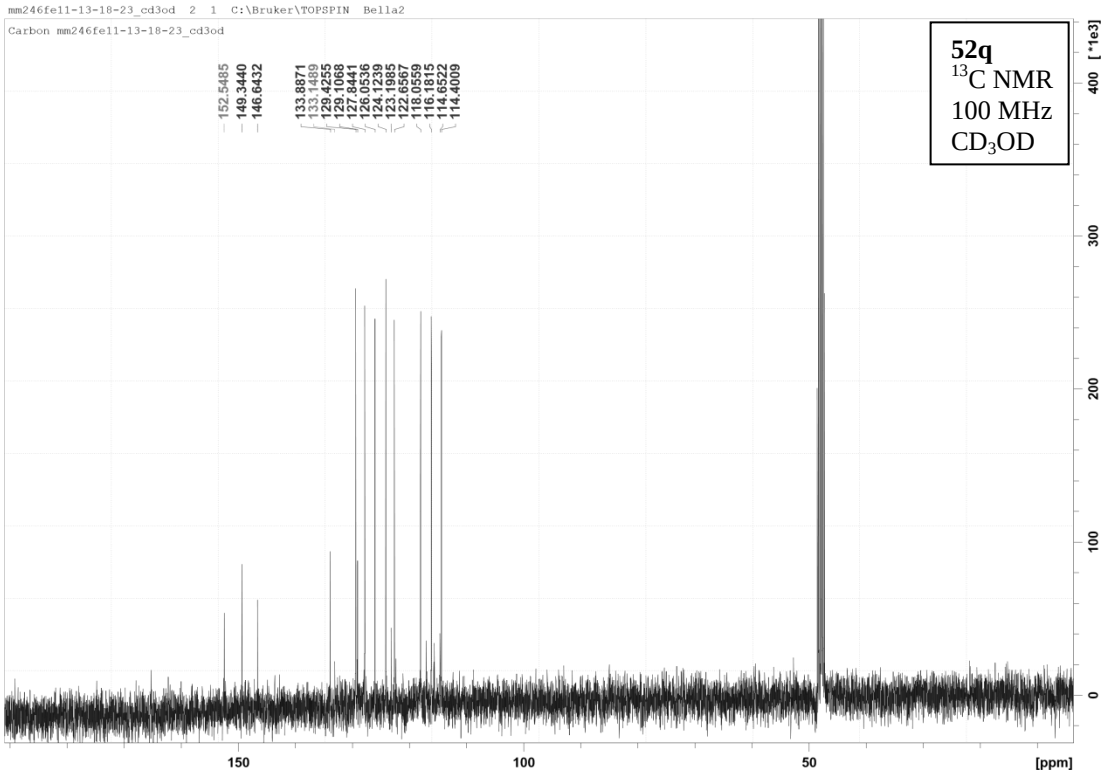
mm246fe11-13-18-23_cd3od 2 1 C:\Bruker\TOPSPIN Bella2
Carbon mm246fe11-13-18-23_cd3od
152.5485
149.3440
146.6432
133.8871
133.1489
129.4655
129.1068
127.8441
126.0536
124.1239
123.1985
122.6567
118.0559
116.1815
114.6522
114.4009
150
100
50
[ppm]
[*1e3]
400
300
200
100
0
52q
^{13}C NMR
100 MHz
CD_3OD

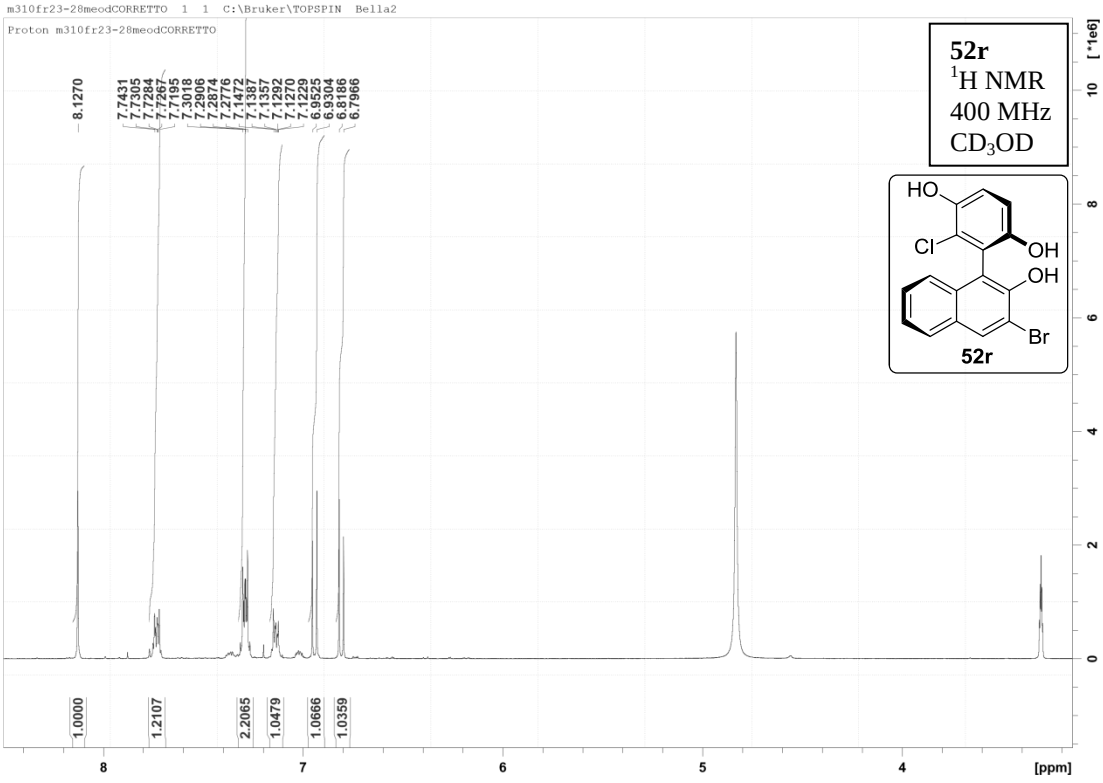
m310fr23-28meodCORRETTO 1 1 C:\Bruker\TOPSPIN Bella2
Proton m310fr23-28meodCORRETTO
8.1270
7.7431
7.7305
7.7284
7.7267
7.7195
7.3018
7.2906
7.2874
7.2776
7.1472
7.1387
7.1357
7.1292
7.1270
7.1229
6.8525
6.8394
6.8186
6.7966
1.0000
1.2107
2.2065
1.0479
1.0666
1.0359
8
7
6
5
4
[ppm]
[*1e6]
52r
1H NMR
400 MHz
CD3OD
HO
Cl
OH
OH
Br
52r

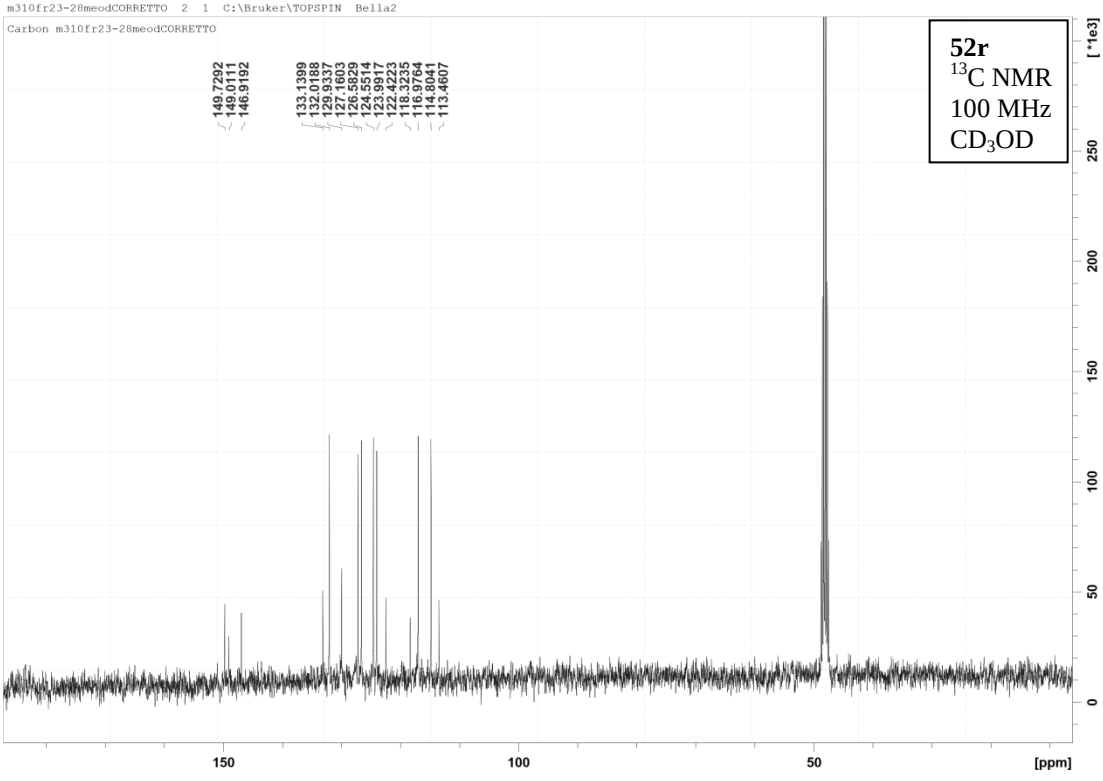
m310fr23-28meodCORRETTO 2 1 C:\Bruker\TOPSPIN Bella2
Carbon m310fr23-28meodCORRETTO
149.7292
149.0111
148.0111
146.9192
133.1399
132.0188
129.9337
127.1603
126.5829
124.5514
123.9917
122.4223
118.3235
116.9764
114.8041
113.4607
150
100
50
[ppm]
[*1e3]
52r
13C NMR
100 MHz
CD3OD

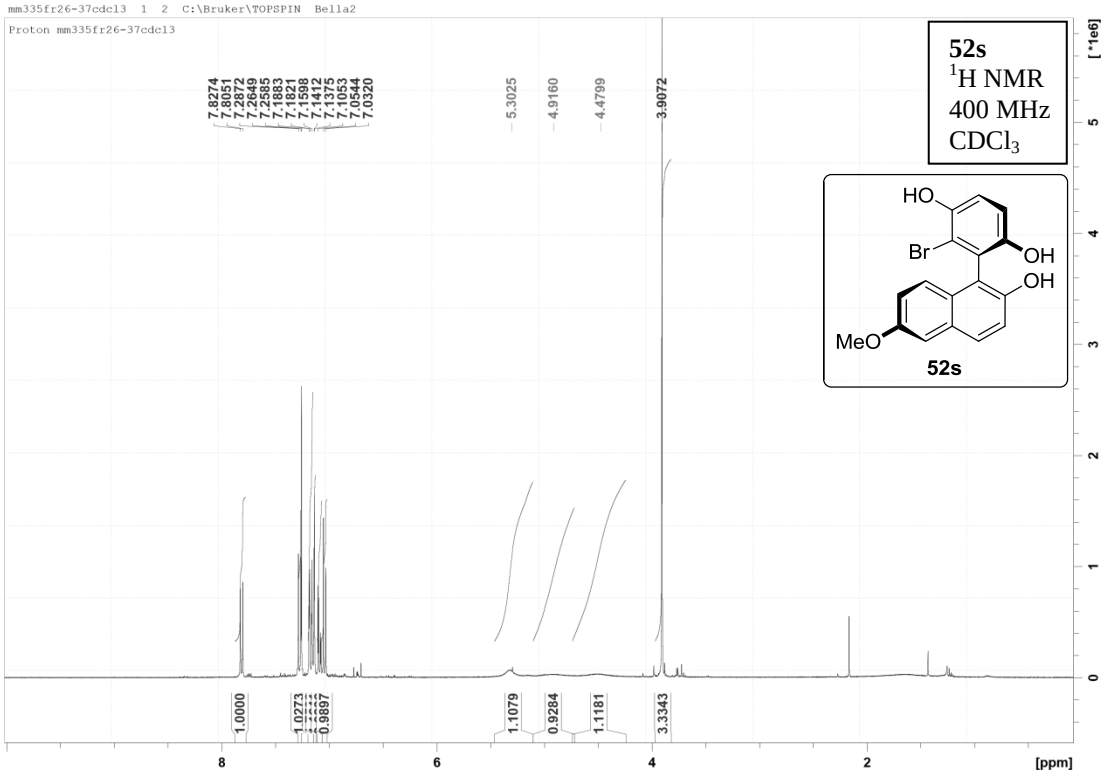
mm335fr26-37cdcl3 1 2 C:\Bruker\TOPSPIN Bella2
Proton mm335fr26-37cdcl3
7.8274
7.8051
7.2872
7.2649
7.2585
7.1883
7.1821
7.1598
7.1412
7.1375
7.1053
7.0544
7.0320
5.3025
4.9160
4.4799
3.9072
1.0000
1.0273
0.9897
1.1079
0.9284
1.1181
3.3343
8
6
4
2
[ppm]
[*1e6]
52s
1H NMR
400 MHz
CDCl3
HO
Br
OH
OH
MeO
52s

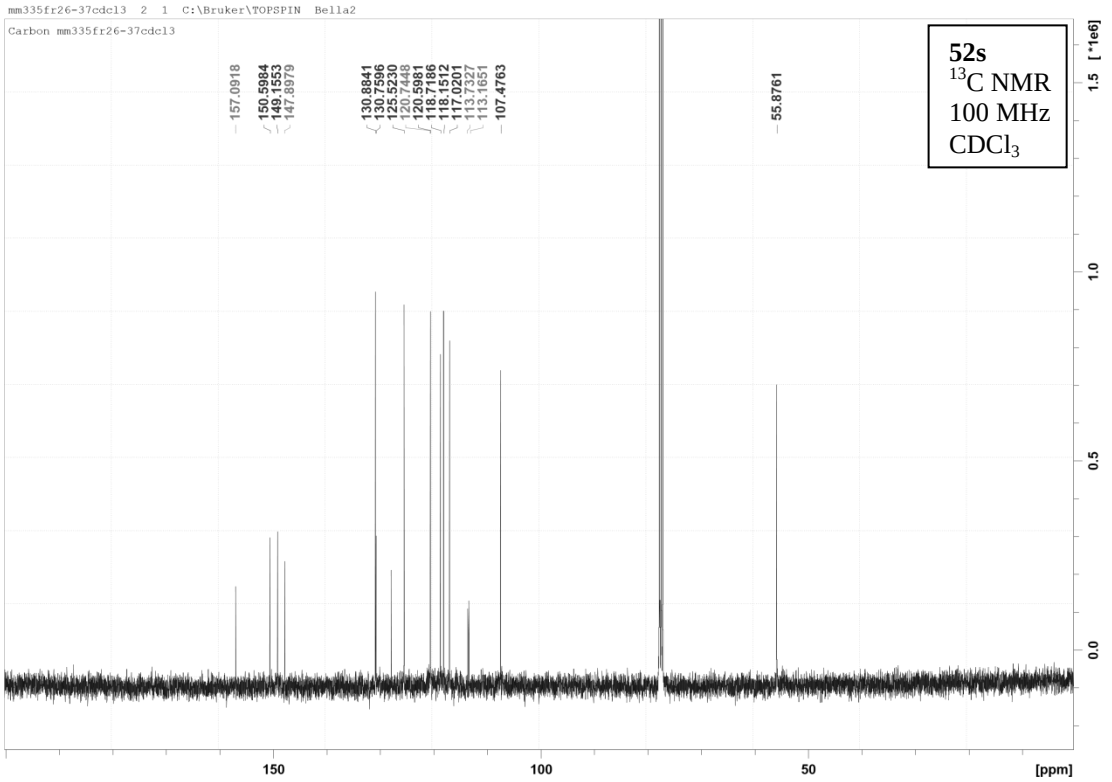
mm335fr26-37cdcl3 2 1 C:\Bruker\TOPSPIN Bella2
Carbon mm335fr26-37cdcl3
157.0918
150.5984
149.1553
147.8979
130.8841
130.7596
125.5230
120.7448
120.5981
118.7186
118.1512
117.0201
113.7327
113.1651
107.4763
55.8761
150
100
50
[ppm]
[*1e6]
52s
13C NMR
100 MHz
CDCl3

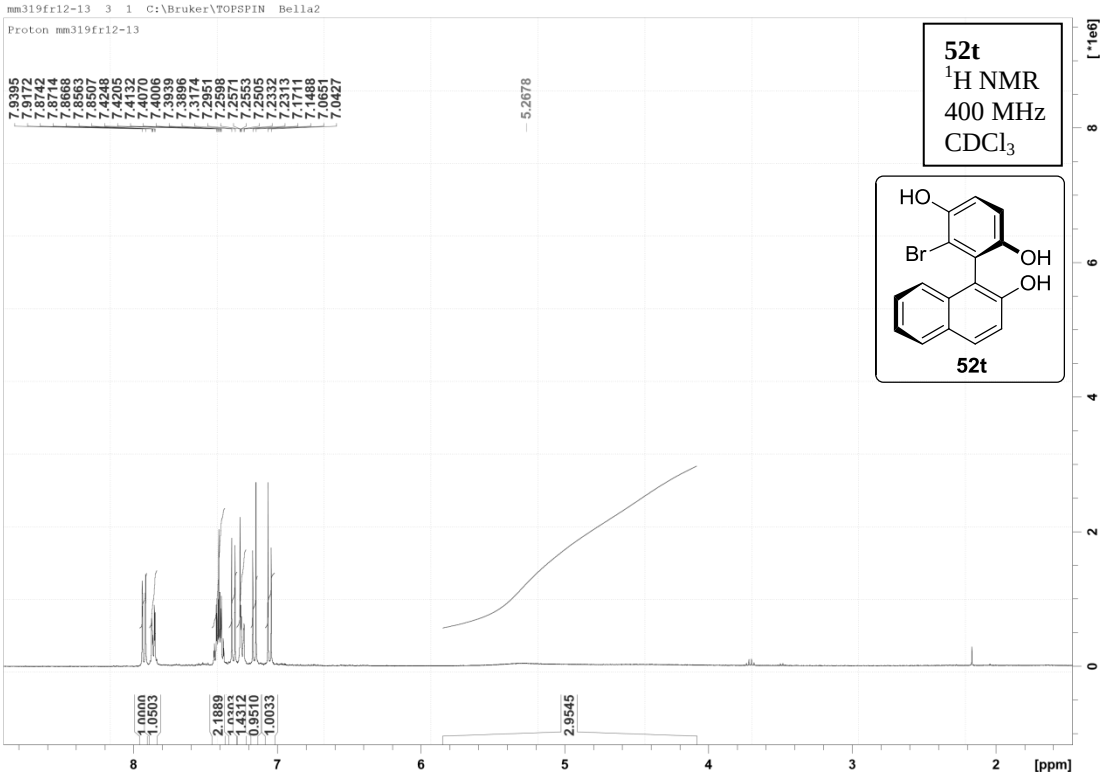
mm319fr12-13 3 1 C:\Bruker\TOPSPIN Bella2
Proton mm319fr12-13
7.9395
7.9172
7.8742
7.8714
7.8668
7.8563
7.8507
7.4248
7.4205
7.4132
7.4070
7.4006
7.3939
7.3896
7.3174
7.2951
7.2598
7.2571
7.2553
7.2535
7.2332
7.2313
7.1711
7.1488
7.0651
7.0427
5.2678
1.0000
1.0503
2.1889
4.0000
1.4312
0.9510
1.0033
2.9545
[*1e6]
[ppm]
52t
1H NMR
400 MHz
CDCl3
HO
Br
OH
OH
52t

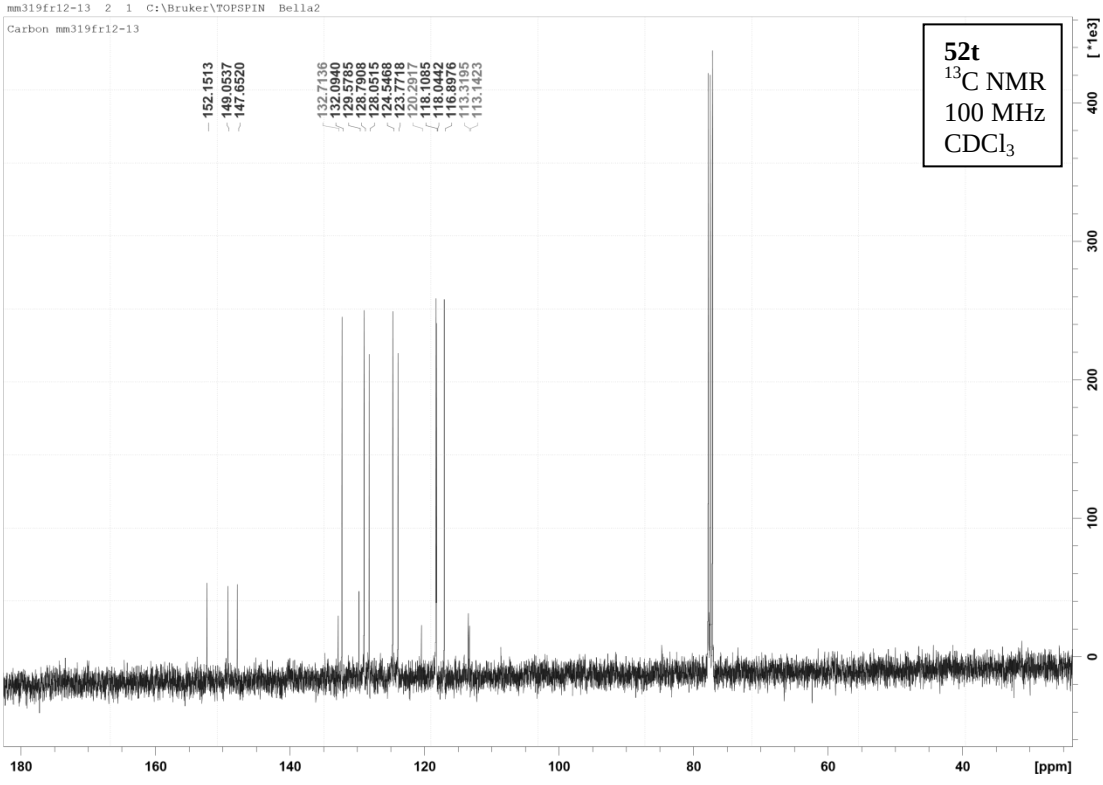
mm319fr12-13 2 1 C:\Bruker\TOPSPIN Bella2
Carbon mm319fr12-13
152.1513
149.0537
147.6520
132.7136
132.0940
129.5785
128.7908
128.0515
124.5468
123.7718
120.2517
118.1085
118.0442
116.8976
113.3195
113.1423
[*1e3]
[ppm]
52t
13C NMR
100 MHz
CDCl3

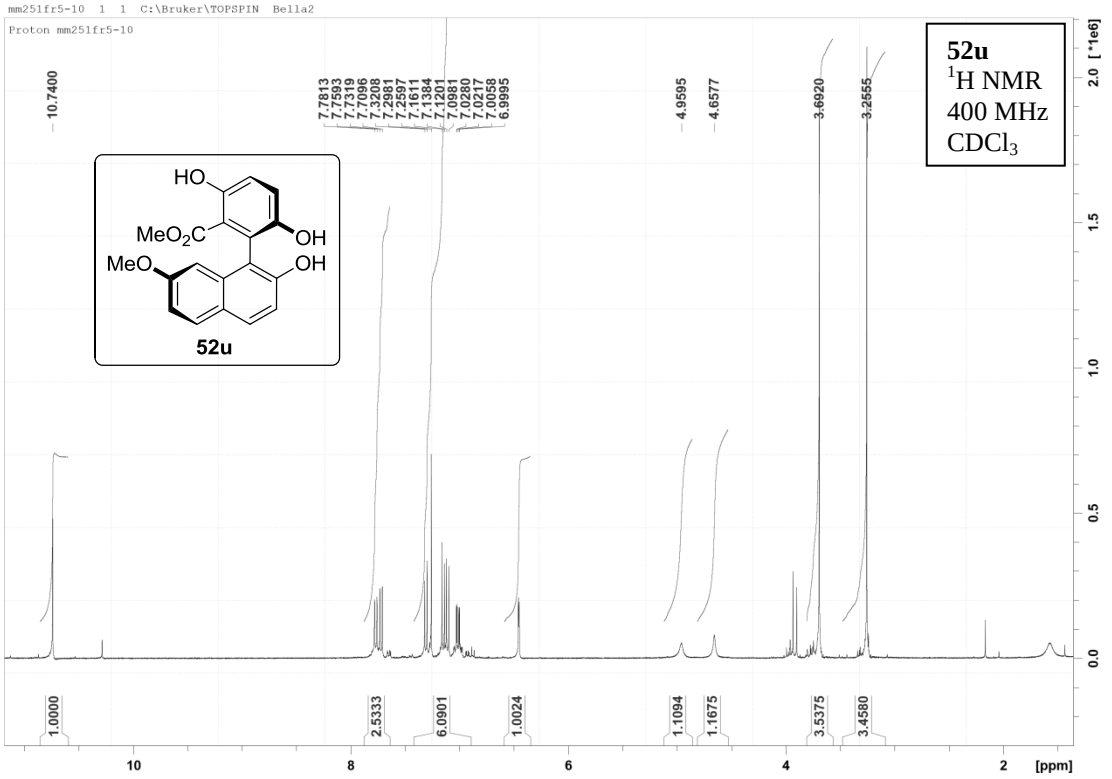
mm251fr5-10 1 1 C:\Bruker\TOPSPIN Bella2
Proton mm251fr5-10
52u
1H NMR
400 MHz
CDCl3
10.7400
7.7813
7.7593
7.7319
7.7096
7.3208
7.2981
7.2597
7.1611
7.1384
7.1201
7.0981
7.0760
7.0217
7.0058
6.9995
4.9595
4.6577
3.6920
3.2555
HO
MeO2C
OH
MeO
OH
52u
1.0000
2.5333
6.0901
1.0024
1.1094
1.1675
3.5375
3.4580
[ppm]

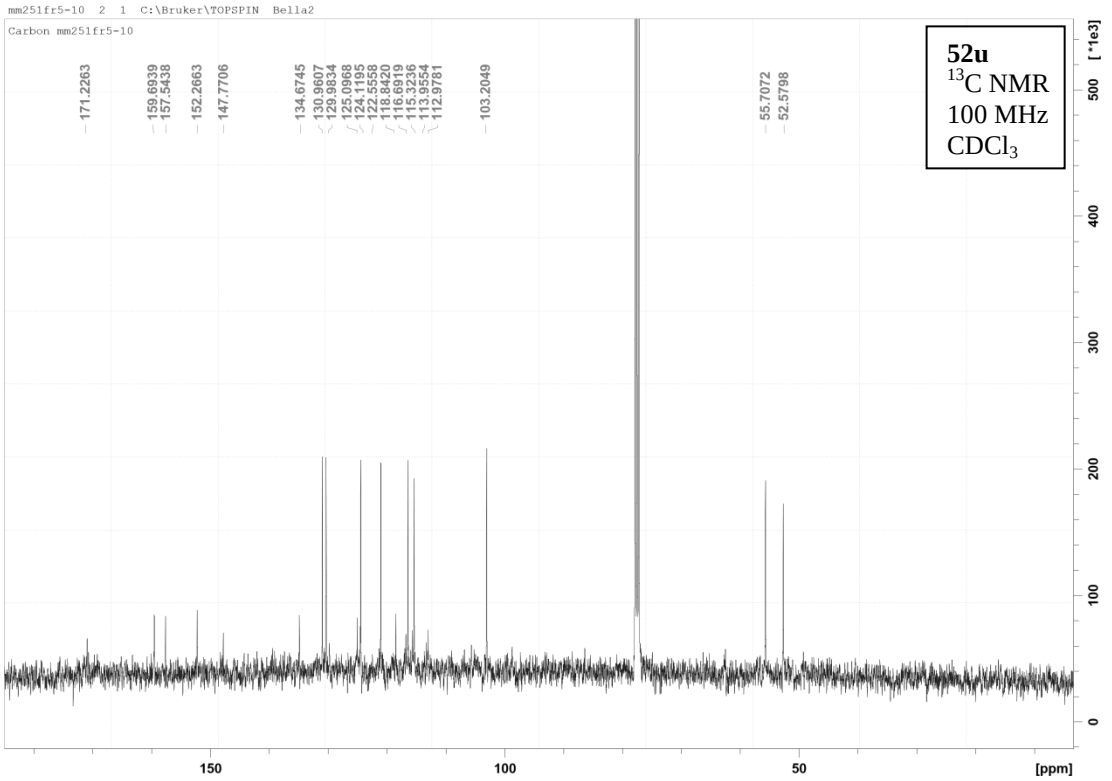
mm251fr5-10 2 1 C:\Bruker\TOPSPIN Bella2
Carbon mm251fr5-10
52u
13C NMR
100 MHz
CDCl3
171.2263
159.6939
157.5438
152.2663
147.7706
134.6745
130.9607
129.9834
125.0968
124.1195
122.5558
118.8420
116.6919
115.3236
113.9554
112.9781
103.2049
55.7072
52.5798
[ppm]

7.3.6. HPLC traces of biaryls 52d-u

Nearly-racemic samples were prepared following the general procedure but employing an equimolar mixture of quinine and quinidine as catalyst.

rac-**52d**

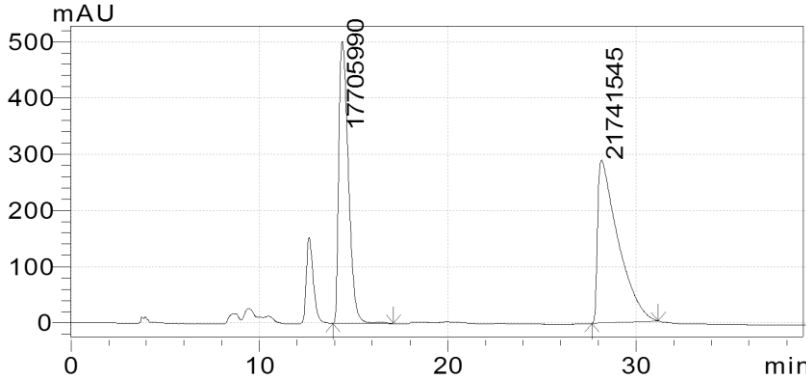

52d (70% *ee*)

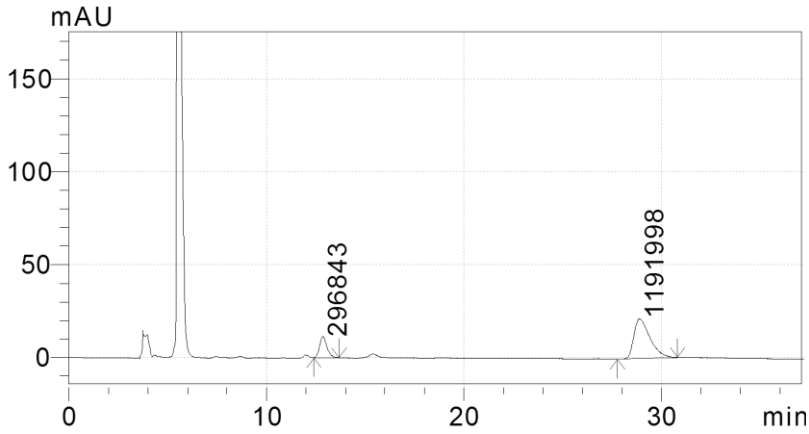

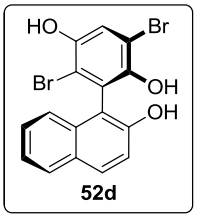

rac-**52e**

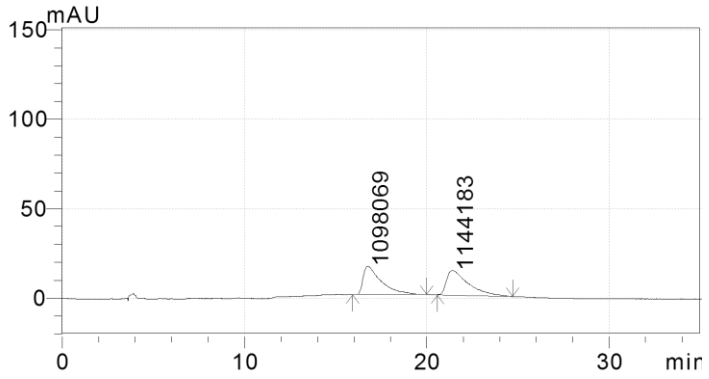

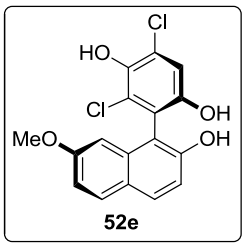

52e (73% *ee*)

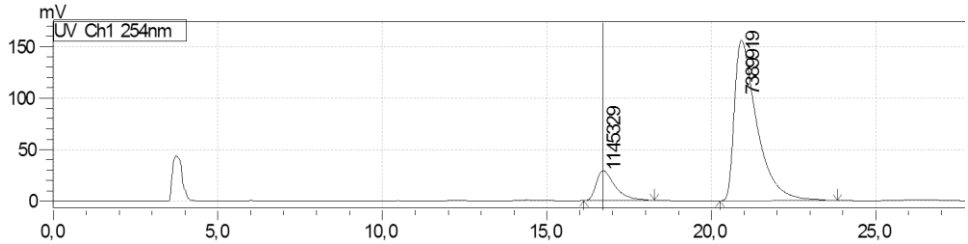

rac-**52f**

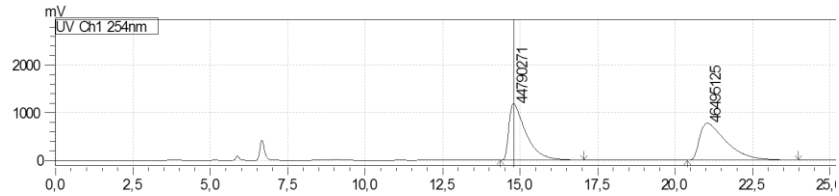

52f (70% *ee*)

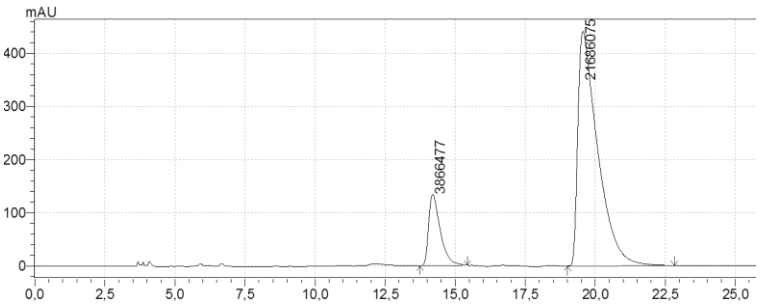

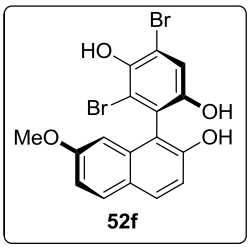

rac-**52g**

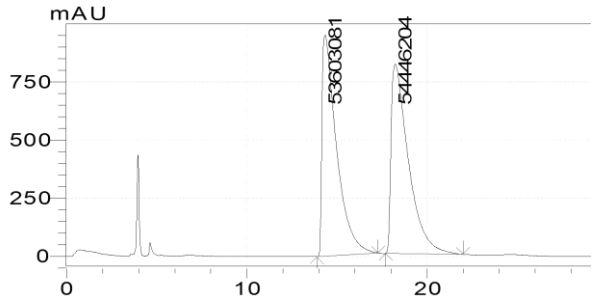

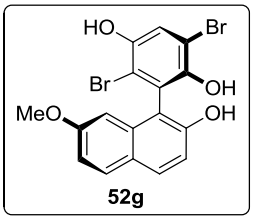

52g

52g (63% *ee*)

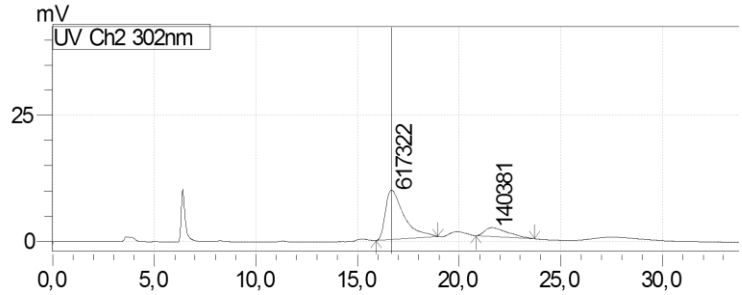

rac-**52h**

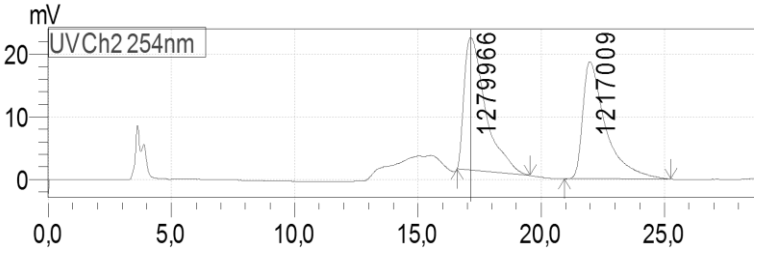

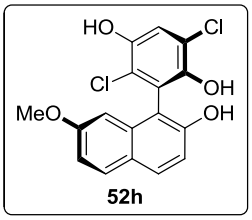

52h

52h (59% *ee*)

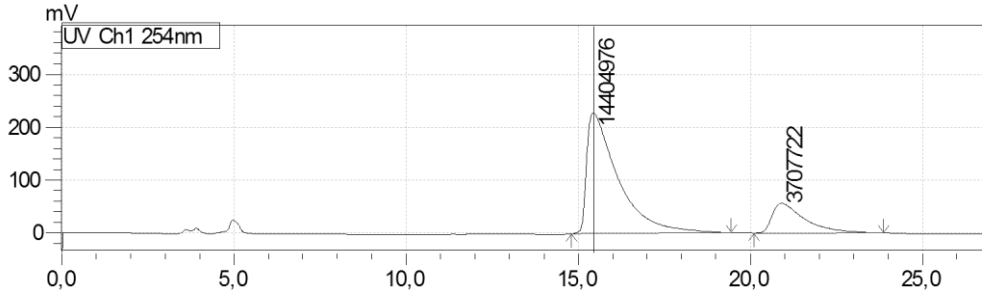

rac-**52i**

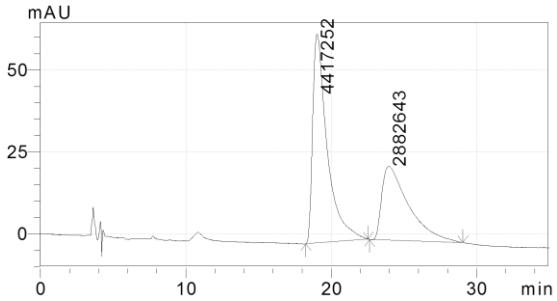

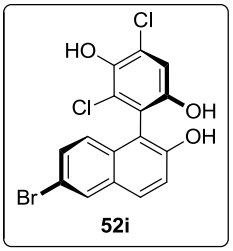

52i

52i (77% *ee*)

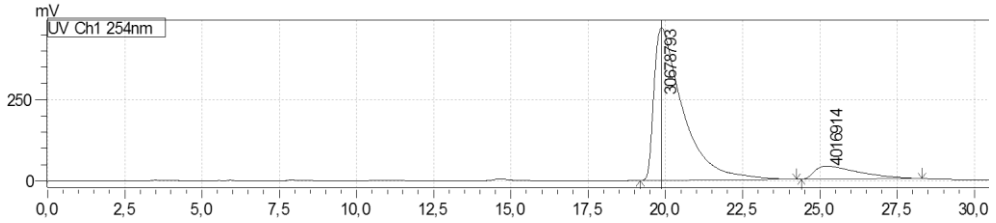

rac-**52j**

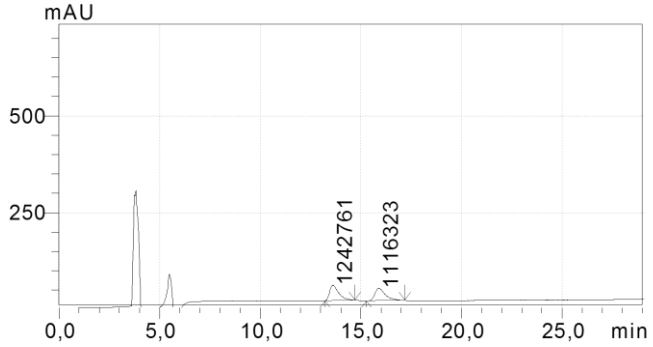

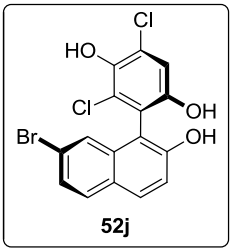

52j

52j (80% *ee*)

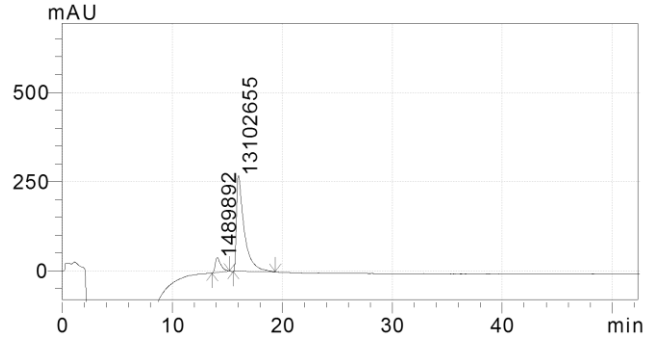

rac-**52k**

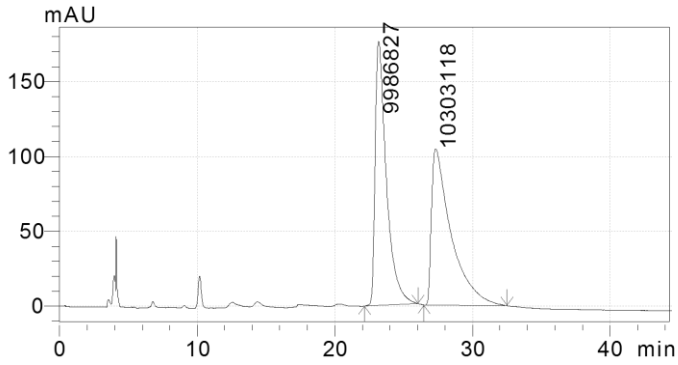

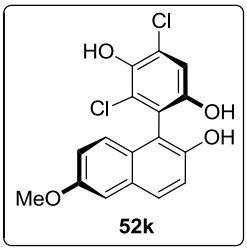

52k (79% *ee*)

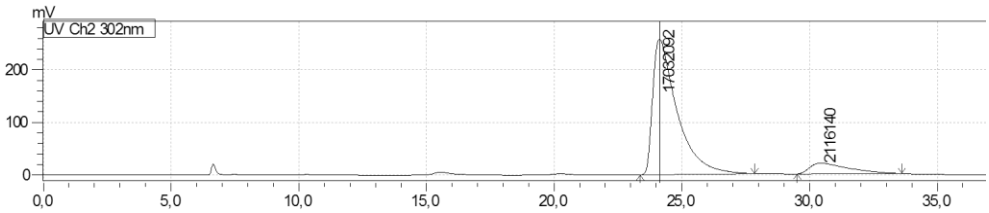

rac-**52l**

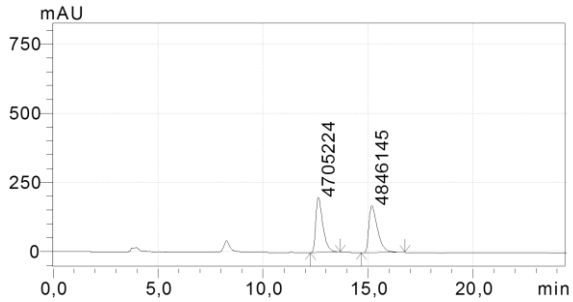

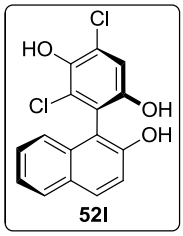

52l (76% *ee*)

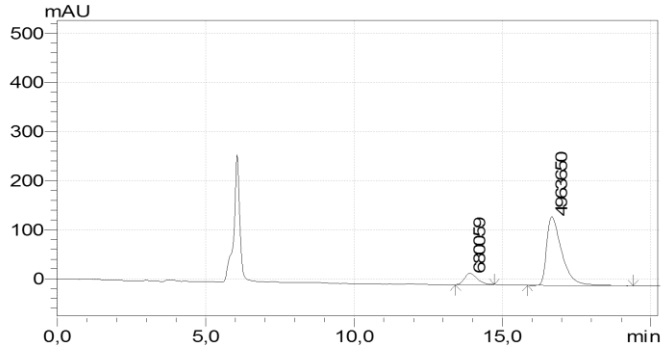

rac-**52m**

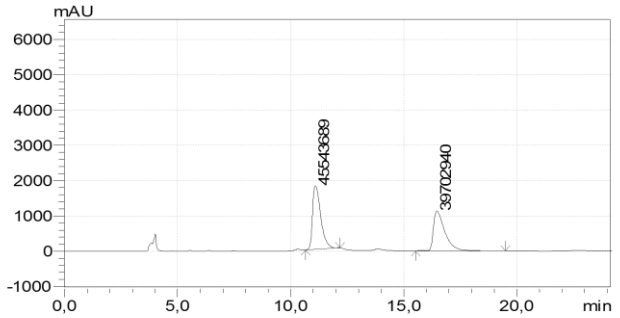

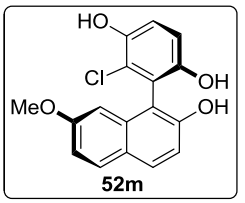

52m (77% *ee*)

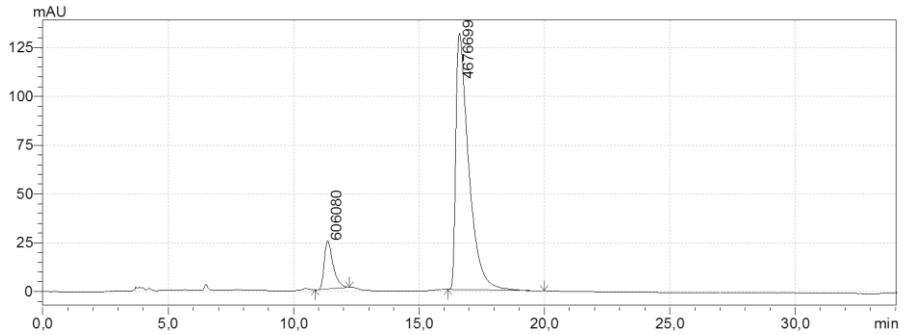

rac-**52n**

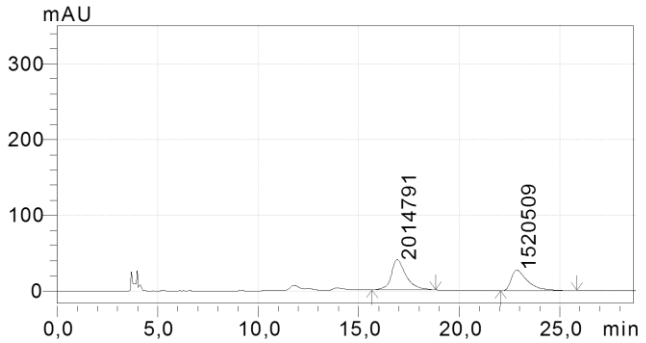

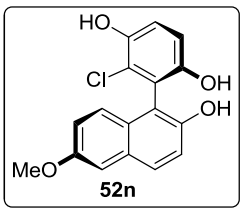

52n (84% *ee*).

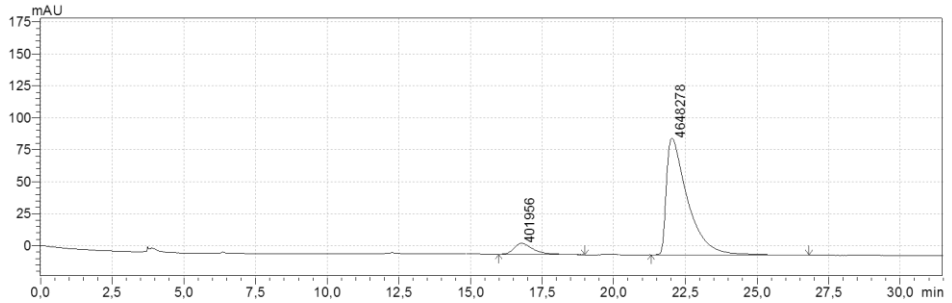

rac-**52o**

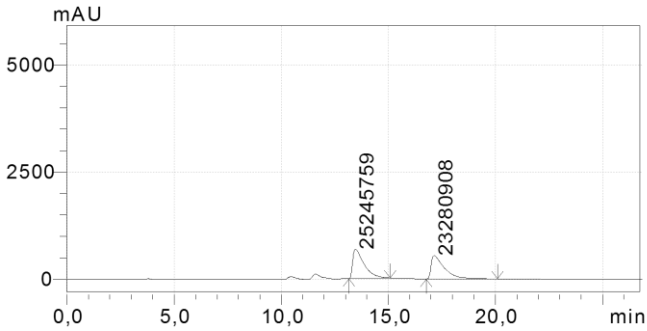

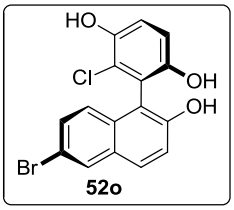

52o (82% *ee*)

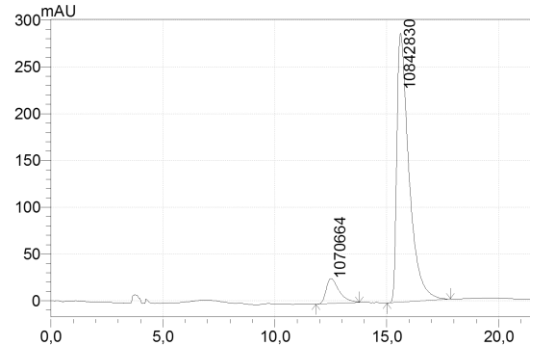

rac-**52p**

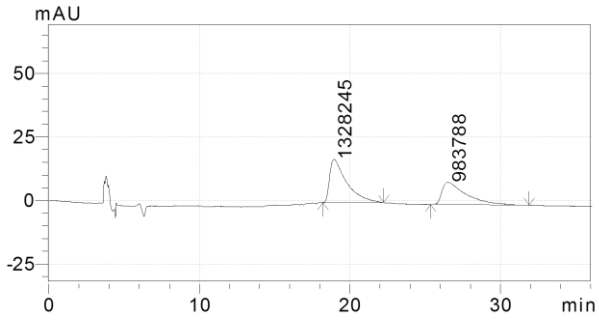

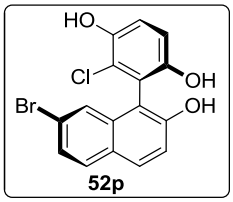

52p (82% *ee*)

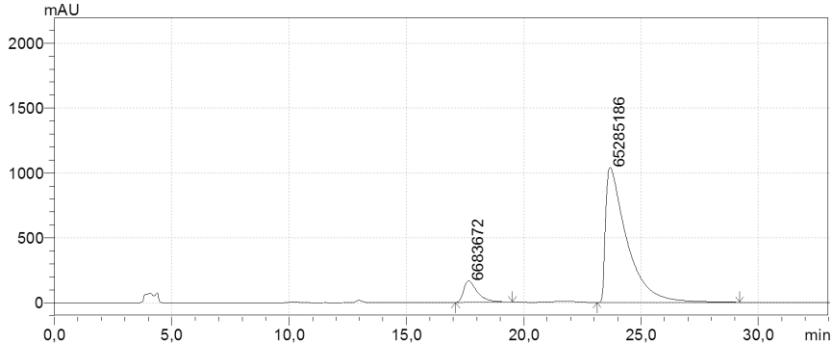

rac-**52q**

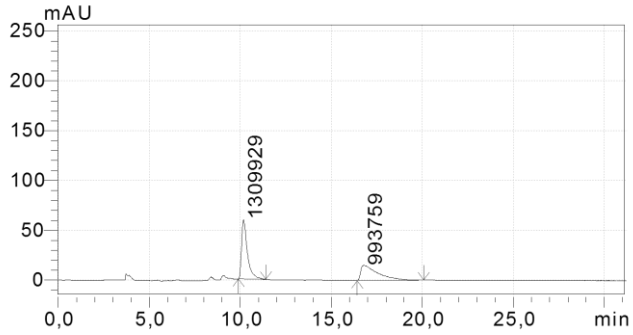

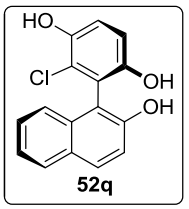

52q (78% *ee*)

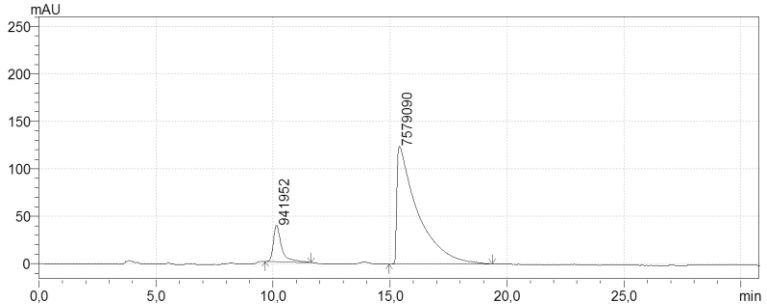

rac-**52r**

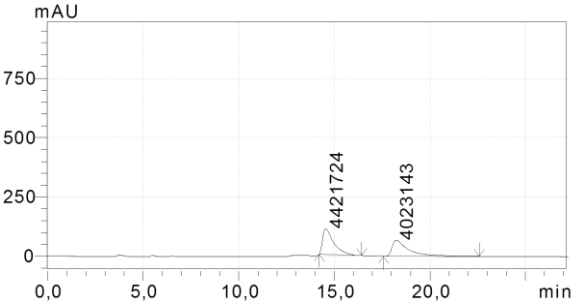

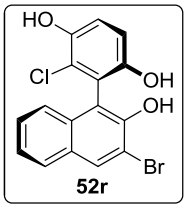

52r (80% *ee*)

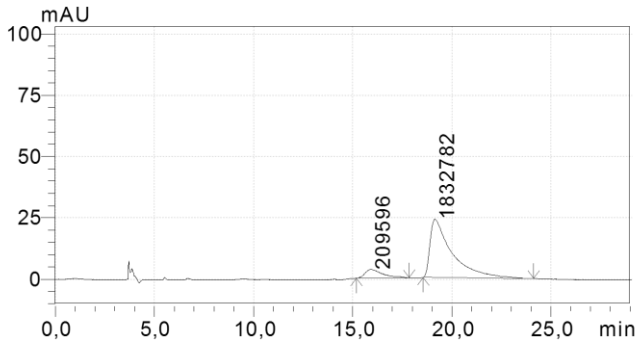

rac-**52s**

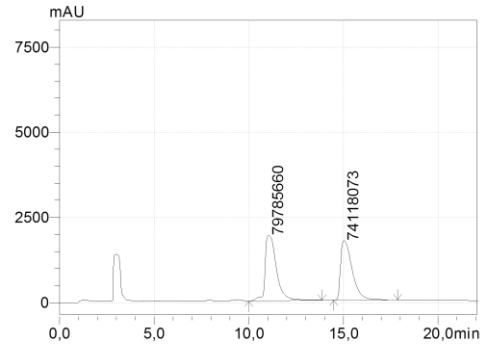

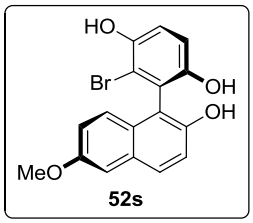

52s (86% *ee*)

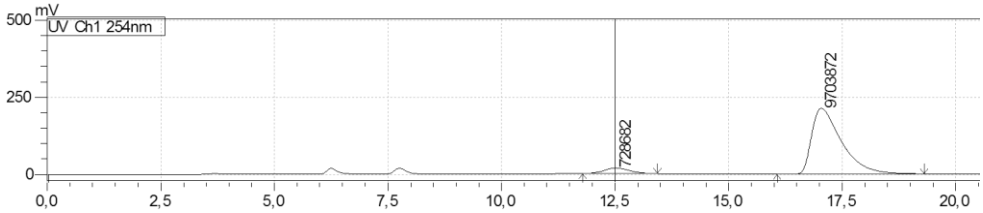

rac-**52t**

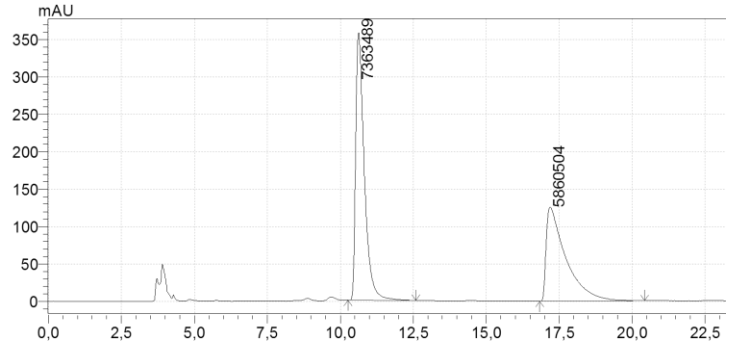

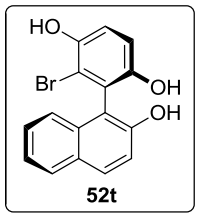

52t (85% *ee*)

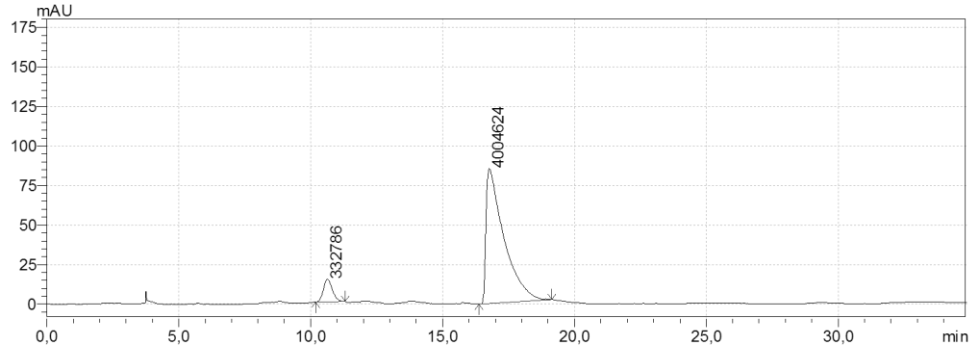

rac-**52u**

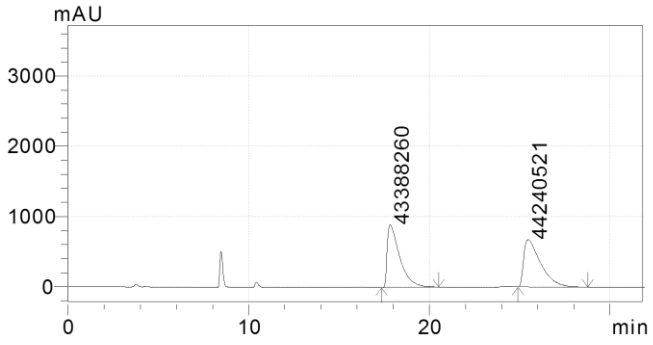

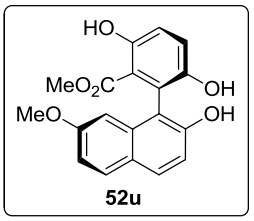

52u

52u (2% *ee*)

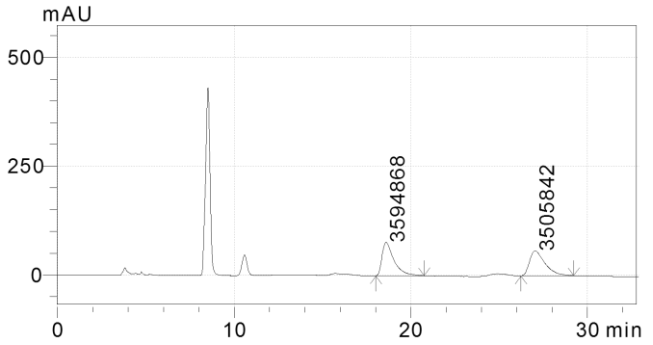

7.4. Experimental Data for the Vinylogous Aldol Reaction

2-(5*H*)-furanones **94a-c** were prepared following the procedure reported by Bella *et al.*.[102] α-Keto esters **95a-g** were prepared following the procedure reported by Smith *et al.*.[103]

7.4.1. General procedure for the diastereoselective synthesis of compounds 96a-i

To a stirred solution of the 2-(5*H*)-furanone **94** (0.64 mmol) in toluene (2.5 mL) was added Et_3N (26 μL, 19 mg, 0.19 mmol) and the resulting mixture was cooled to -20 °C. A cooled (-20 °C) solution of the α-keto ester **95** (0.64 mmol) in toluene (0.5 mL) was then added and the reaction mixture was stirred at -20 °C for 20 h, after which time the crude material was subjected to flash chromatography on silica gel, with petroleum ether/Et_2O gradient elution. The pure product **96** was obtained as a single diastereoisomer.

7.4.2. Characterization of compounds 96a-i

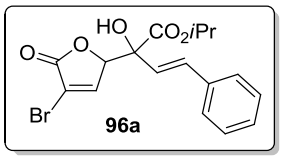

96a. White solid; 88 mg, 39% yield.
^{1}H NMR (400 MHz, $CDCl_3$): δ 1.32-1.36 (m, 6H: $2CH_3$), 3.76 (vbs, 1H: OH), 5.12-5.22 (m, 1H: C<u>H</u>$(CH_3)_2$), 5.29 (d, 1H; *J* = 1.7 Hz: HOC-C<u>H</u>-OCO), 6.34 (d, 1H; *J* = 15.8 Hz: C<u>H</u>=CHPh), 7.01 (d, 1H; *J* = 15.9 Hz: CH=C<u>H</u>Ph), 7.29-7.38 (m, 3H: $3CH_{arom}$), 7.41-7.45 (m, 3H: $2CH_{arom}$, C<u>H</u>=CBr).
^{13}C NMR (100 MHz, CDCl3): δ 21.8 (2C), 72.4, 77.0, 84.5, 115.4, 123.3, 127.1 (2C), 128.9, 128.9 (2C), 134.0, 135.4, 148.1, 168.0, 170.7.
HRMS (ESI): calcd for $C_{17}H_{17}BrO_5Na$ $[M+Na]^+$: 403.0157, found 403.0153.
HPLC: CHIRALPAK IC+IC columns, eluent *n*-hexane/*i*-propanol 85:15, flow 0.9 mL/min, τ_1= 31.5 min, τ_2= 41.0 min.

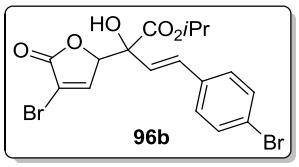

96b. White solid; 153 mg, 52% yield.
^{1}H NMR (300 MHz, $CDCl_3$): δ 1.31-1.34 (m, 6H: $2CH_3$), 3.81 (s, 1H: OH), 5.11-5.20 (m, 1H: C<u>H</u>$(CH_3)_2$), 5.27 (s, 1H: HOC-C<u>H</u>-OCO), 6.34 (d, 1H; *J* = 15.6 Hz: C<u>H</u>=CHPh), 6.94 (d, 1H; *J* = 15.8 Hz: CH=C<u>H</u>Ph), 7.26-7.29 (m, 2H: $2CH_{arom}$), 7.43-7.48 (m, 3H: $2CH_{arom}$, C<u>H</u>=CBr).

^{13}C NMR (75 MHz, CDCl3): δ 21.8 (2C), 72.5, 76.7, 84.7, 115.5, 122.7, 124.2, 128.6 (2C), 132.0 (2C), 132.8, 134.4, 148.0, 167.8, 170.5.
HPLC: CHIRALPAK IC column, eluent *n*-hexane/*i*-propanol 85:15, flow 0.9 mL/min, τ_1= 16.7 min, τ_2= 19.6 min.

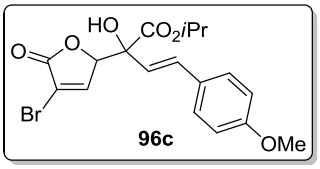

96c

96c. White solid; 118 mg, 45% yield.
^{1}H NMR (400 MHz, $CDCl_3$): δ 1.32-1.35 (m, 6H: $CH(C\underline{H}_3)_2$), 3.74 (s, 1H: OH), 3.82 (s, 3H: OCH_3), 5.16 (hept, 1H: $C\underline{H}(CH_3)_2$), 5.28 (d, 1H; *J* = 1.7 Hz: HOC-C<u>H</u>-OCO), 6.18 (d, 1H; *J* = 15.8 Hz: C<u>H</u>=CHPh), 6.87-6.95 (m, 3H: CH=C<u>H</u>Ph, $2CH_{arom}$), 7.35 (d, 2H; *J* = 8.7 Hz: $2CH_{arom}$), 7.45 (d, 1H; *J* = 1.7 Hz: C<u>H</u>=CBr).
^{13}C NMR (100 MHz, CDCl3): δ 21.8 (2C), 55.5, 72.2, 77.0, 85.0, 114.3 (2C), 115.3, 120.8, 128.1, 128.4 (2C), 133.4, 148.3, 160.2, 168.0, 170.9.
HPLC: CHIRALPAK IC column, eluent *n*-hexane/*i*-propanol 85:15, flow 0.9 mL/min, τ_1= 24.0 min, τ_2= 29.0 min.

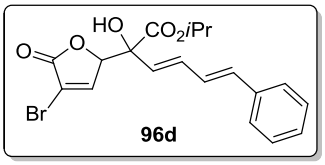

96d

96d. White solid; 26 mg, 10% yield.
^{1}H NMR (300 MHz, $CDCl_3$): δ 1.32-1.35 (m, 6H), 3.69 (s, 1H), 5.12-5.20 (m, 1H), 5.24 (d, 1H; *J* = 1.5 Hz), 6.88-5.97 (m, 1H), 6.64-6.86 (m, 3H), 7.26-7.43 (m, 6H).
^{13}C NMR (100 MHz, CDCl3): δ 21.8, 21.8, 72.3, 76.9, 84.8, 115.4, 126.7, 126.8 (2C), 128.4, 128.9 (2C), 134.2, 135.8, 136.7, 148.2, 167.9, 170.7.
HPLC: CHIRALPAK IC column, eluent *n*-hexane/*i*-propanol 85:15, flow 0.9 mL/min, τ_1= 22.0 min, τ_2= 24.5 min.

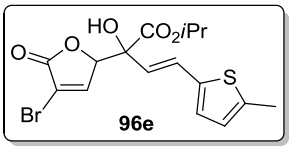

96e

96e. White solid; 82 mg, 32% yield.
^{1}H NMR (300 MHz, $CDCl_3$): δ 1.31-1.35 (m, 6H), 2.47 (s, 3H), 3.71 (s, 1H), 5.09-5.22 (m, 1H), 5.26 (s, 1H), 5.99 (d, 1H; *J* = 15.4 Hz), 6.64 (s, 1H), 6.83 (d, 1H; *J* = 3.0 Hz), 7.01 (d, 1H; *J* = 15.5 Hz), 7.44 (s, 1H).
^{13}C NMR (75 MHz, CDCl3): δ 15.6, 21.6 (2C), 72.2, 76.7, 84.6, 115.1, 120.7, 125.8, 127.3, 128.1, 138.1, 140.8, 148.0, 167.9, 170.5.
HPLC: CHIRALPAK IC column, eluent *n*-hexane/*i*-propanol 85:15, flow 0.9 mL/min, τ_1= 18.5 min, τ_2= 25.0 min.

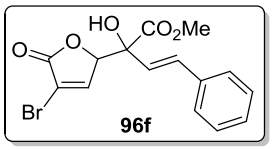

96f. White solid; 93 mg, 41% yield.
^{1}H NMR (300 MHz, $CDCl_3$): δ 3.75 (s, 1H: OH), 3.93 (s, 3H: CH_3), 5.35 (s, 1H: HOC-C<u>H</u>-OCO), 6.33 (d, 1H; *J* = 16.7 Hz: C<u>H</u>=CHPh), 7.01 (d, 1H; *J* = 15.5 Hz: CH=C<u>H</u>Ph), 7.27-7.49 (m, 6H: $5CH_{arom}$, C<u>H</u>=CBr).
^{13}C NMR (75 MHz, CDCl3): δ 54.3, 77.3, 84.7, 115.2, 122.8, 127.1 (2C), 128.8, 128.9 (2C), 134.3, 135.2, 148.0, 167.8, 171.6.
HRMS (ESI): calcd for $C_{15}H_{13}BrO_5Na$ $[M+Na]^+$: 374.9844, found 375.0922.
HPLC: CHIRALPAK IC column, eluent *n*-hexane/*i*-propanol 85:15, flow 0.9 mL/min, τ_1= 28.0 min, τ_2= 35.0 min.

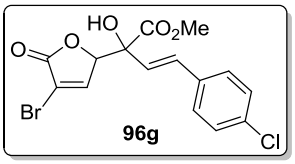

96g. White solid; 221 mg, 89% yield.
^{1}H NMR (400 MHz, $CDCl_3$): δ 3.69 (s, 1H: OH), 3.93 (s, 3H: OCH_3), 5.32 (d, 1H; *J* = 1.8 Hz: HOC-C<u>H</u>-OCO), 6.31 (d, 1H; *J* = 15.7 Hz: C<u>H</u>=CHPh), 6.97 (d, 1H; *J* = 15.8 Hz: CH=C<u>H</u>Ph), 7.31-7.37 (m, 4H: $4CH_{arom}$), 7.41 (d, 1H; *J* = 1.8 Hz: C<u>H</u>=CBr).
^{13}C NMR (100 MHz, CDCl3): δ 54.5, 77.3, 84.6, 115.5, 123.4, 128.4 (2C), 129.2 (2C), 133.2, 133.7, 134.8, 147.8, 167.8, 171.5.
HRMS (ESI): calcd for $C_{15}H_{12}BrClO_5Na$ $[M +Na]^+$: 408.9454, found 409.0049.
HPLC: CHIRALPAK IC column, eluent *n*-hexane/*i*-propanol 90:10, flow 0.9 mL/min, τ_1= 35.0 min, τ_2= 40.0 min.

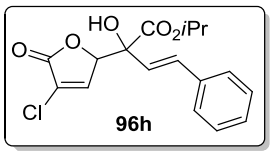

96h. White solid; 84 mg, 39% yield.
^{1}H NMR (300 MHz, $CDCl_3$): δ 1.32-1.36 (m, 6H: $2CH_3$), 3.76 (s, 1H: OH), 5.11-5.23 (m, 1H: C<u>H</u>$(CH_3)_2$), 5.30 (s, 1H: HOC-C<u>H</u>-OCO), 6.34 (d, 1H; *J* = 15.7 Hz: C<u>H</u>=CHPh), 7.01 (d, 1H; *J* = 15.9 Hz: CH=C<u>H</u>Ph), 7.28-7.49 (m, 6H: $5CH_{arom}$, C<u>H</u>=CBr).
^{13}C NMR (75 MHz, CDCl3): δ 21.8 (2C), 72.4, 77.0, 84.5, 115.5, 123.4, 127.1 (2C), 128.9, 128.9 (2C), 134.0, 135.5, 148.1, 167.9, 170.7.
HRMS (ESI): calcd for $C_{17}H_{17}ClO_5Na$ $[M+Na]^+$: 359.0662, found 359.1296.
HPLC: CHIRALPAK IC column, eluent *n*-hexane/*i*-propanol 85:15, flow 0.9 mL/min, τ_1= 17.0 min, τ_2= 22.0 min.

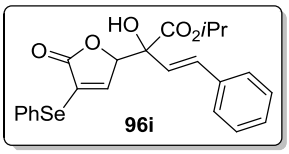

96i. White solid; 158 mg, 54% yield.

^{1}H NMR (400 MHz, $CDCl_3$): δ 1.31 (d, 3H; *J* = 6.2 Hz: CH_3), 1.35 (d, 3H; *J* = 6.2 Hz: CH_3), 3.71 (s, 1H: OH), 5.09-5.17 (m, 1H: C<u>H</u>(CH_3)$_2$), 5.19 (d, 1H; *J* = 1.8 Hz: HOC-C<u>H</u>-OCO), 6.31 (d, 1H; *J* = 15.8 Hz: C<u>H</u>=CHPh), 6.76 (d, 1H; *J* = 1.8 Hz: 1C<u>H</u>=CSe), 6.91 (d, 1H; *J* = 15.8 Hz: CH=C<u>H</u>Ph), 7.28-7.38 (m, 8H: 8CH_{arom}), 7.60-7.63 (m, 2H: 2CH_{arom}).

^{13}C NMR (100 MHz, CDCl3): δ 21.8, 21.8, 72.1, 77.2, 85.9, 124.0, 125.9, 127.0 (2C), 128.6, 128.8 (2C), 129.3, 130.0 (2C), 130.3, 133.3, 135.2, 135.6 (2C), 144.7, 170.7, 171.1.

HRMS (ESI): calcd for $C_{23}H_{22}O_5SeNa$ $[M+Na]^+$: 481.0530, found 481.1588.

HPLC: CHIRALPAK IC column, eluent *n*-hexane/*i*-propanol 85:15, flow 0.9 mL/min, τ_1= 24 min, τ_2= 32 min.

7.4.3. General procedure for the catalyst screening in the asymmetric synthesis of compound 96a

To a stirred solution of the 3-bromo-2-(5*H*)-furanone **94a** (25 mg, 0.15 mmol) and the organocatalyst of interest (0.045 mmol) in toluene (0.3 mL) was added at -20 °C a cooled (-20 °C) solution of the α-keto ester **95a** (34 mg, 0.15 mmol) in toluene (0.1 mL). The reaction mixture was stirred at -20 °C. At the desired time, an aliquote (5 μL) of the reaction mixture was taken and diluted with cold $CHCl_3$ (100 μL). The resulting solution was filtered through a pad of silica gel and analyzed by HPLC (CHIRALPAK IC+IC columns, eluent *n*-hexane/*i*-propanol 85:15, flow 0.9 mL/min. The enantiomeric excess was measured by integration of the peaks of **96a** (τ_1= 31.7 min, τ_2= 41.1 min). The conversion was measured by comparison of the areas of the peaks of **96a** and that of **95a** (τ= 18.9) at λ=272 nm, applying a corrective factor for the difference in absorbance. The corrective factor was calculated by integration of the peaks of **95a** and **96a** at λ=272 nm on a sample containing equimolar quantities of **95a** and **96a**.

7.4.4. NMR spectra of compounds 96a-i

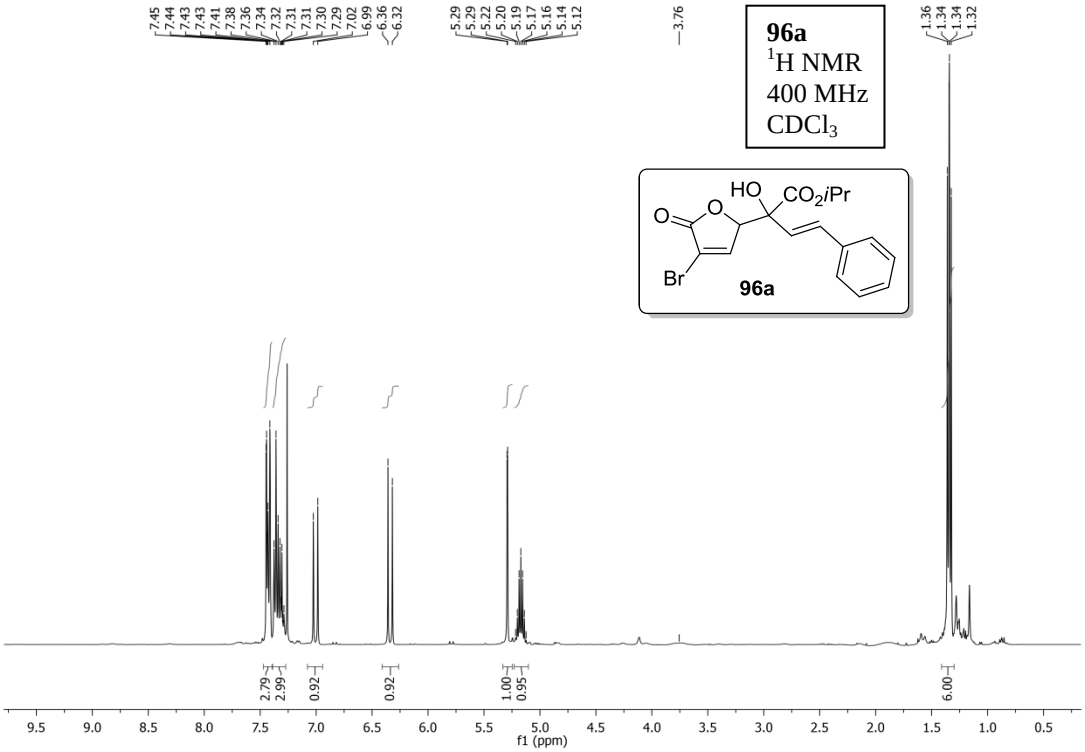

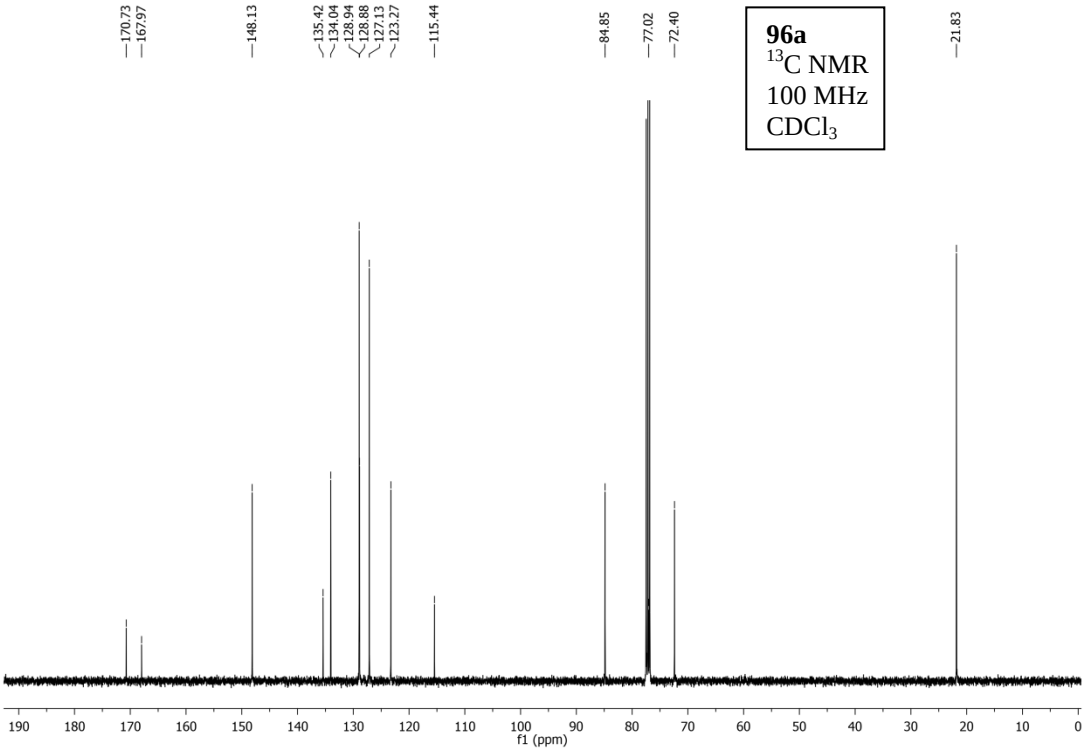

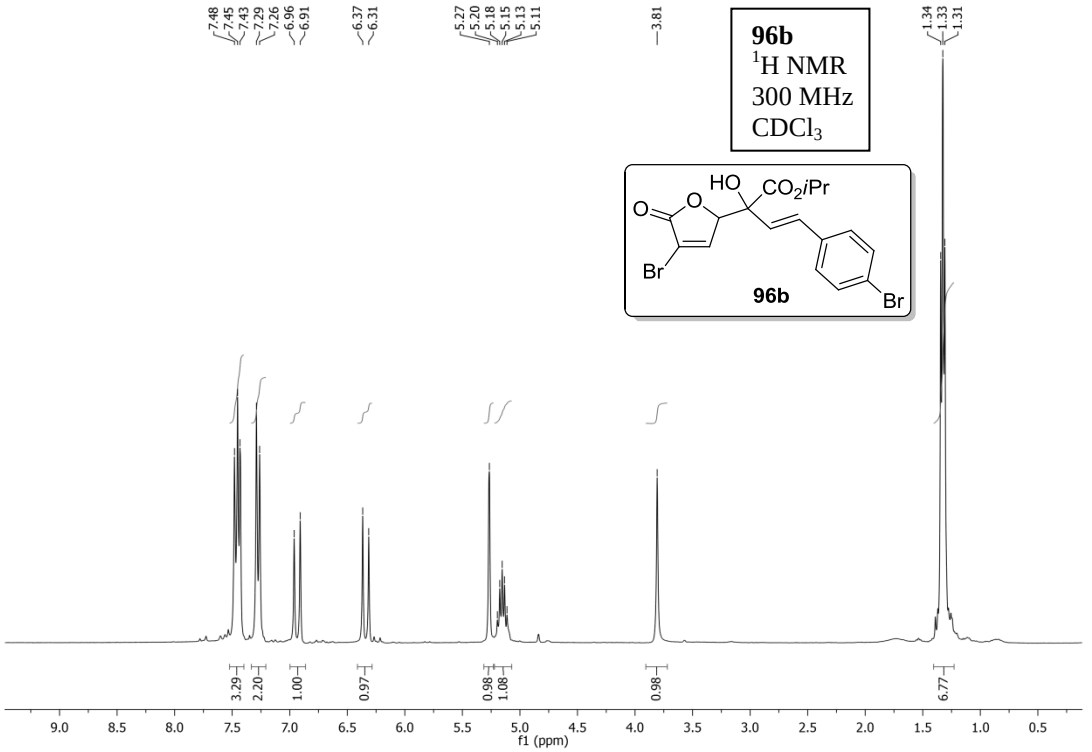
7.48
7.45
7.43
7.29
7.26
6.96
6.91
6.37
6.31
5.27
5.20
5.18
5.15
5.13
5.11
3.81
1.34
1.33
1.31
96b
1H NMR
300 MHz
CDCl3
HO
CO2iPr
O
O
Br
96b
Br
3.29
2.20
1.00
0.97
0.98
1.08
0.98
6.77
9.0
8.5
8.0
7.5
7.0
6.5
6.0
5.5
5.0
4.5
4.0
3.5
3.0
2.5
2.0
1.5
1.0
0.5
f1 (ppm)

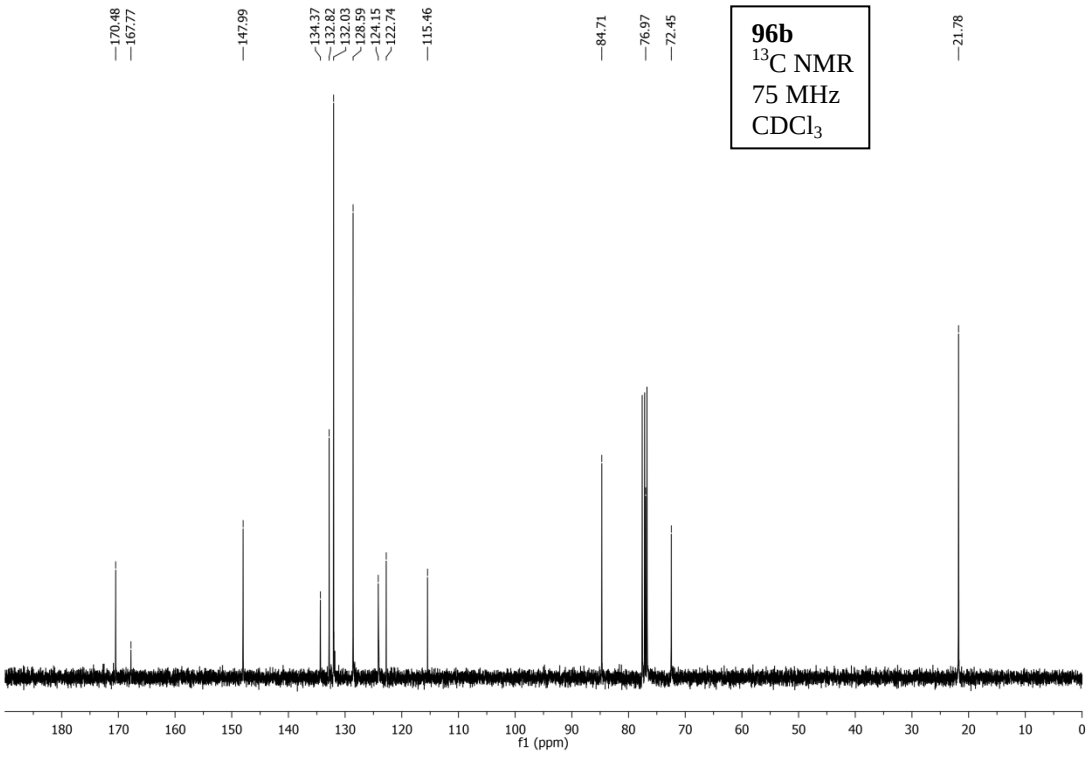
170.48
167.77
147.99
134.37
132.82
132.03
128.59
124.15
122.74
115.46
84.71
76.97
72.45
21.78
96b
13C NMR
75 MHz
CDCl3
180
170
160
150
140
130
120
110
100
90
80
70
60
50
40
30
20
10
0
f1 (ppm)

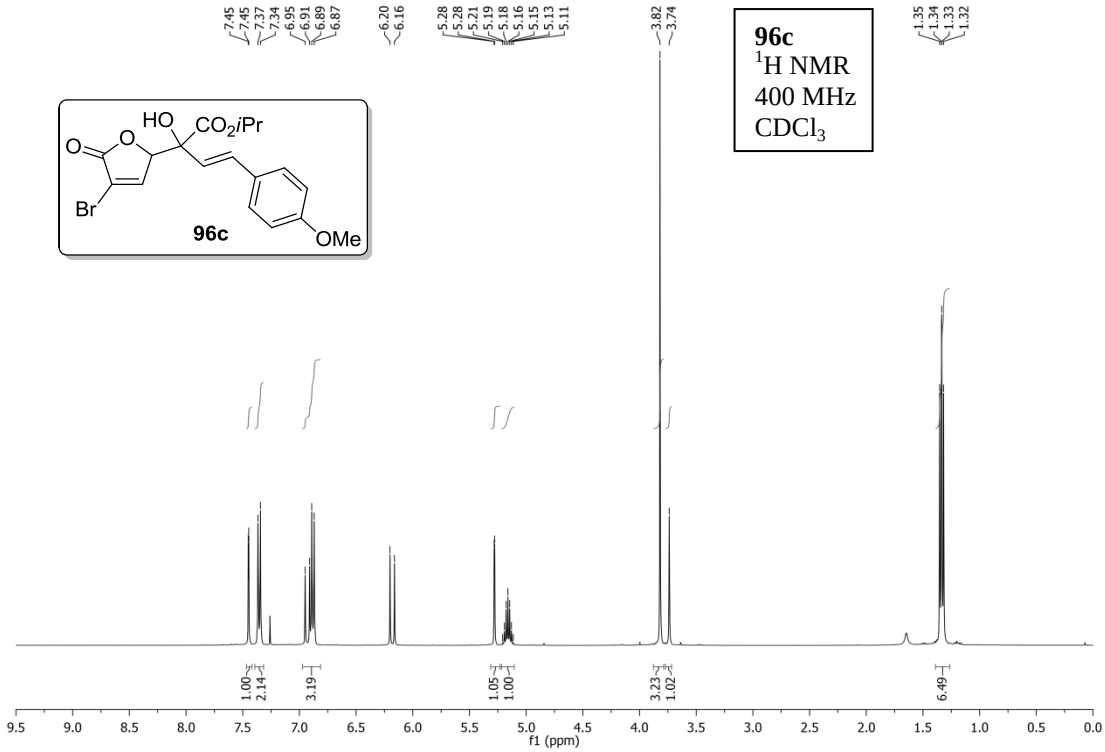
7.45
7.45
7.37
7.34
6.95
6.91
6.89
6.87
6.20
6.16
5.28
5.28
5.21
5.19
5.18
5.16
5.15
5.13
5.11
3.82
3.74
1.35
1.34
1.33
1.32
HO
CO2iPr
O
O
Br
96c
OMe
96c
1H NMR
400 MHz
CDCl3
1.00
2.14
3.19
1.05
1.00
3.23
1.02
6.49
f1 (ppm)

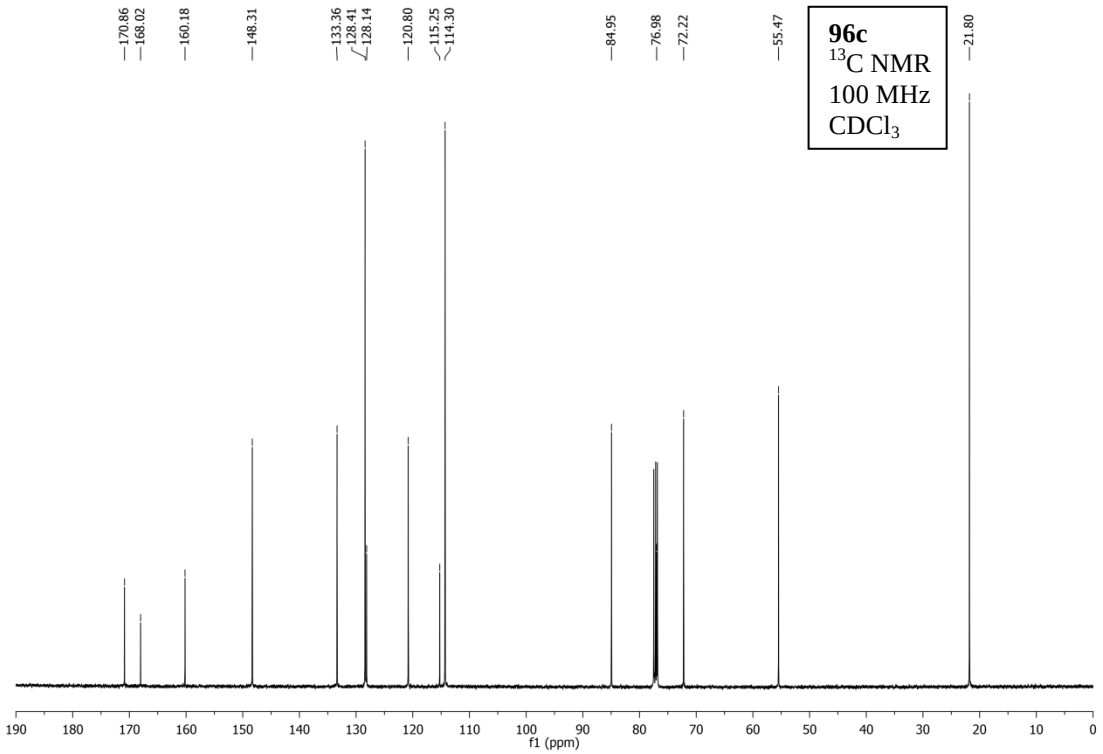
170.86
168.02
160.18
148.31
133.36
128.41
128.14
120.80
115.25
114.30
84.95
76.98
72.22
55.47
21.80
96c
13C NMR
100 MHz
CDCl3
f1 (ppm)

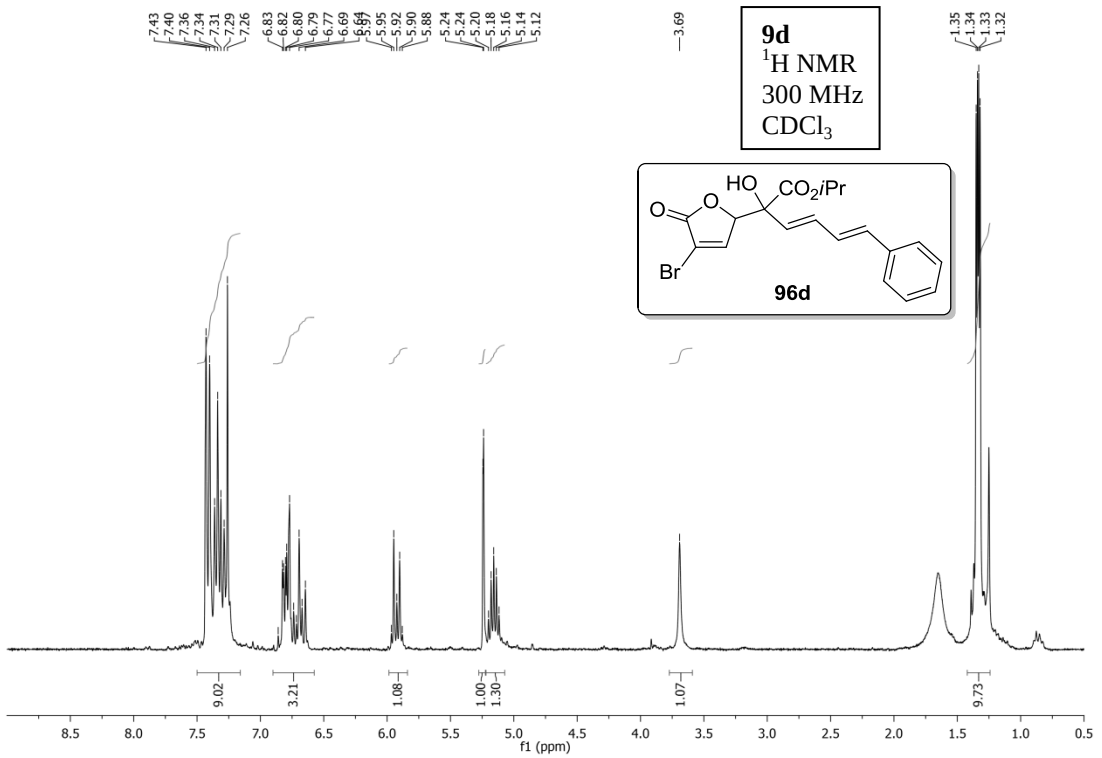
7.43
7.40
7.36
7.34
7.31
7.29
7.26
6.83
6.82
6.80
6.79
6.77
6.69
6.64
5.95
5.92
5.90
5.88
5.24
5.24
5.20
5.18
5.16
5.14
5.12
3.69
1.35
1.34
1.33
1.32
9d
1H NMR
300 MHz
CDCl3
HO
CO2iPr
O
O
Br
96d
9.02
3.21
1.08
1.00
1.30
1.07
9.73
8.5
8.0
7.5
7.0
6.5
6.0
5.5
5.0
4.5
4.0
3.5
3.0
2.5
2.0
1.5
1.0
0.5
f1 (ppm)

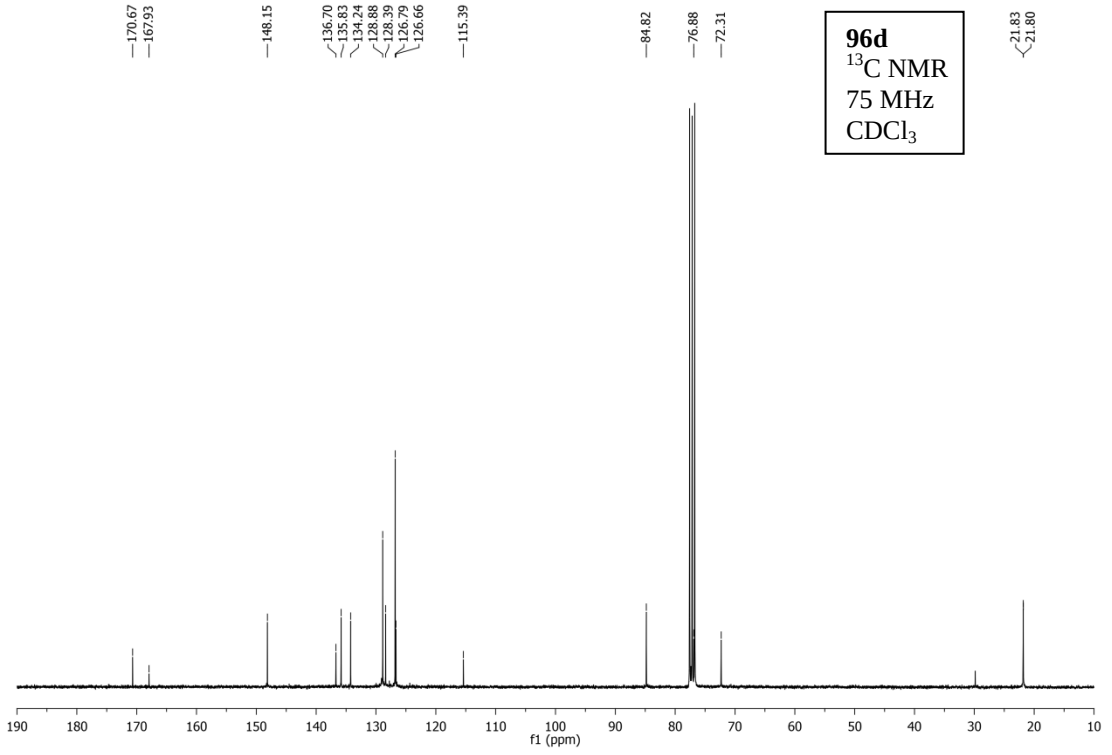
170.67
167.93
148.15
136.70
135.83
134.24
128.88
128.39
126.79
126.66
115.39
84.82
76.88
72.31
21.83
21.80
96d
13C NMR
75 MHz
CDCl3
190
180
170
160
150
140
130
120
110
100
90
80
70
60
50
40
30
20
10
f1 (ppm)

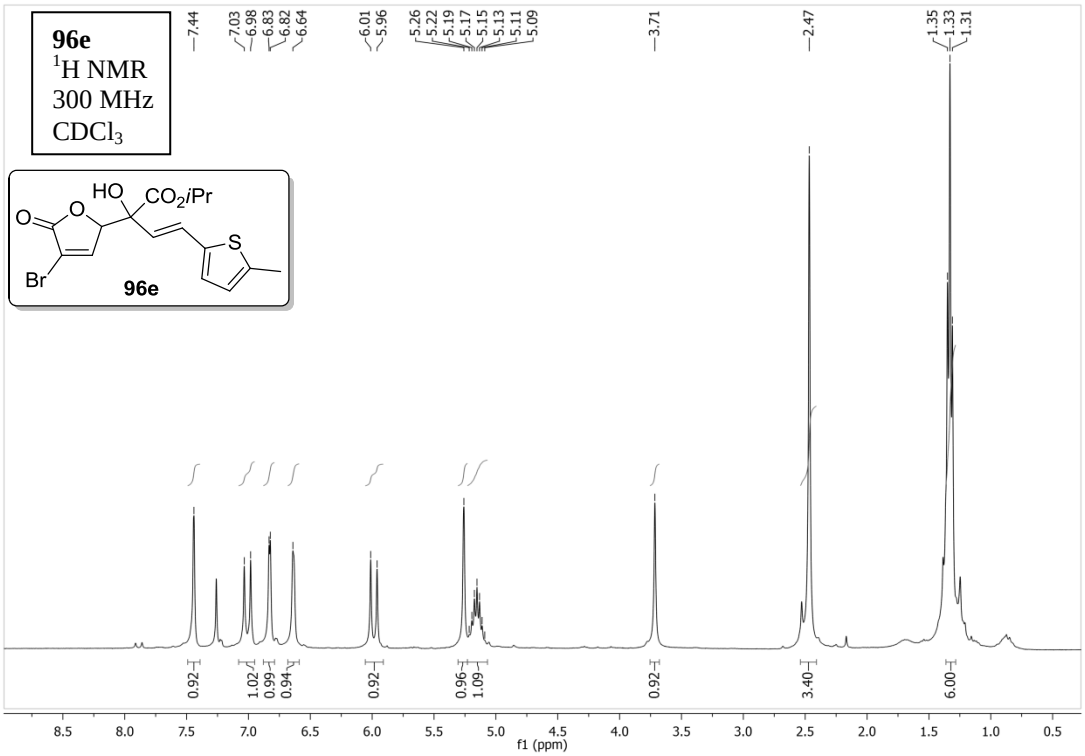
96e
^{1}H NMR
300 MHz
$CDCl_3$
HO
CO_2iPr
O
O
S
Br
96e
7.44
7.03
6.98
6.83
6.82
6.64
6.01
5.96
5.26
5.22
5.19
5.17
5.15
5.13
5.11
5.09
3.71
2.47
1.35
1.33
1.31
0.92
1.02
0.99
0.94
0.92
0.96
1.09
0.92
3.40
6.00
f1 (ppm)

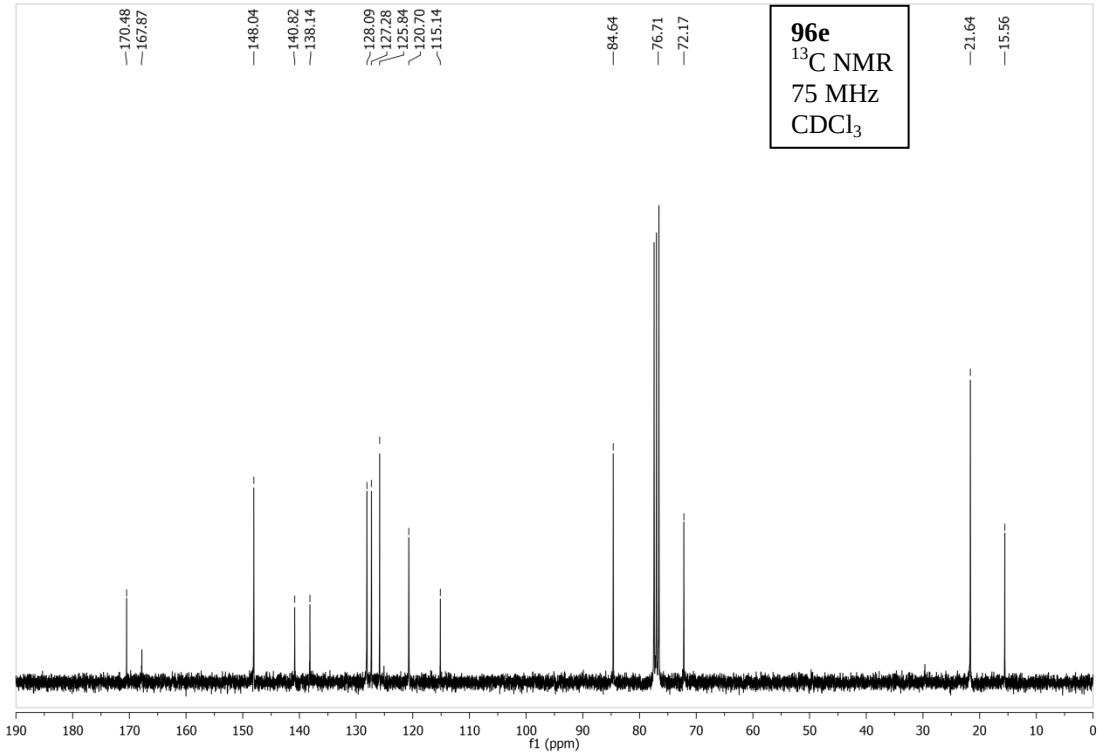
96e
^{13}C NMR
75 MHz
$CDCl_3$
170.48
167.87
148.04
140.82
138.14
128.09
127.28
125.84
120.70
115.14
84.64
76.71
72.17
21.64
15.56
f1 (ppm)

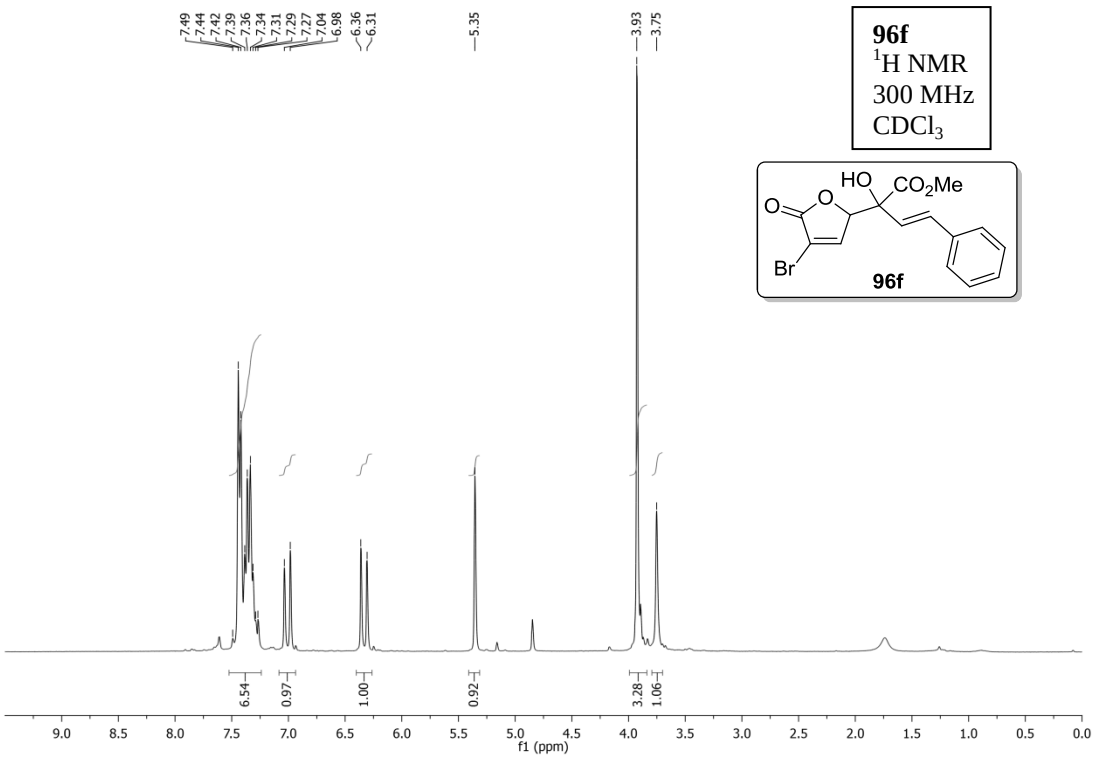

96f
^{1}H NMR
300 MHz
$CDCl_3$

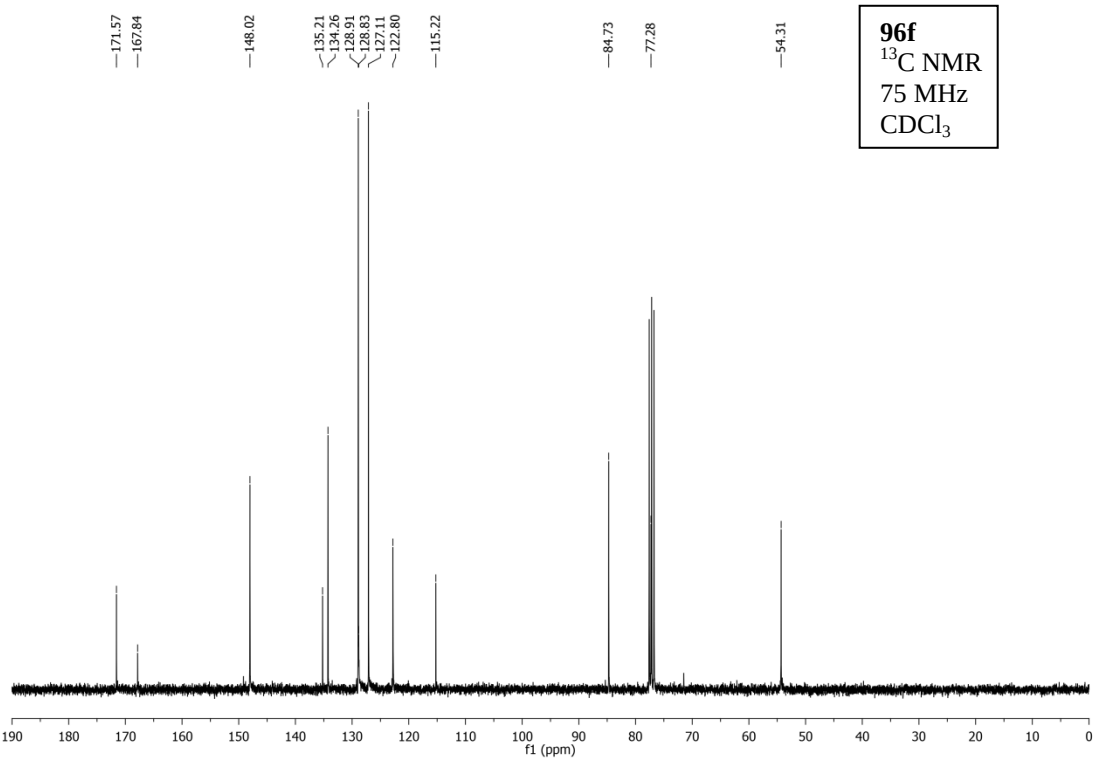

96f
^{13}C NMR
75 MHz
$CDCl_3$

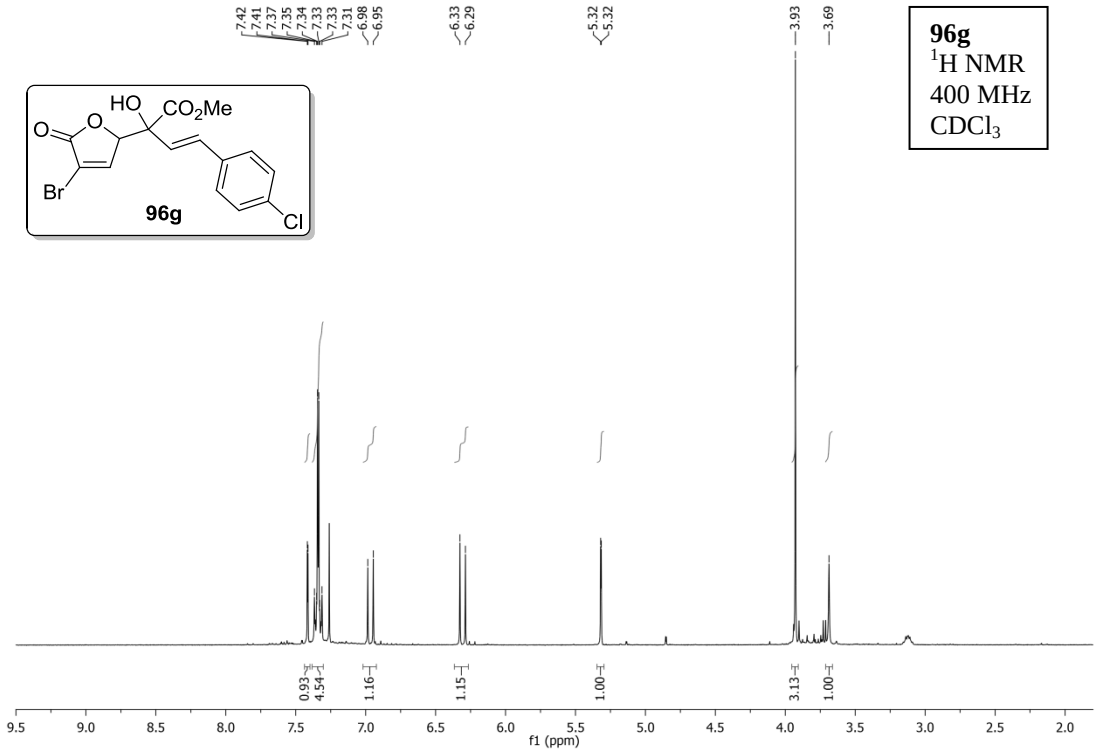
7.42
7.41
7.37
7.35
7.34
7.33
7.33
7.31
6.98
6.95
6.33
6.29
5.32
5.32
3.93
3.69
HO
CO2Me
O
O
Br
Cl
96g
96g
1H NMR
400 MHz
CDCl3
0.93
4.54
1.16
1.15
1.00
3.13
1.00
f1 (ppm)

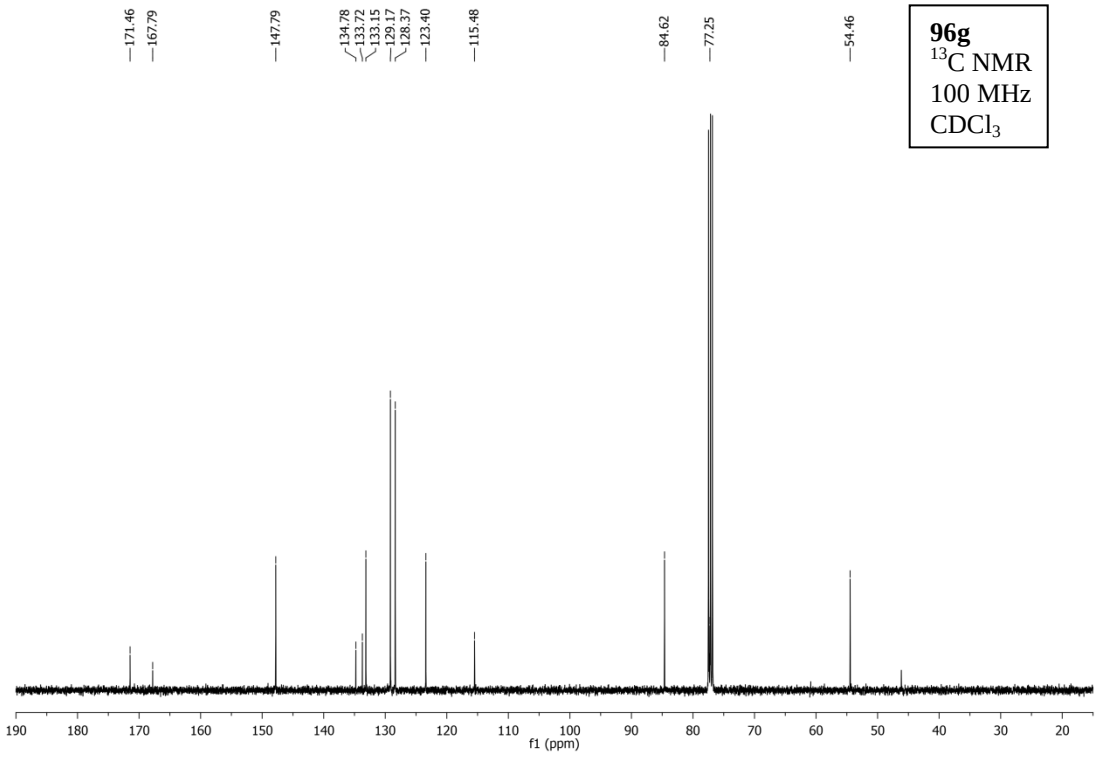
171.46
167.79
147.79
134.78
133.72
133.15
129.17
128.37
123.40
115.48
84.62
77.25
54.46
96g
13C NMR
100 MHz
CDCl3
f1 (ppm)

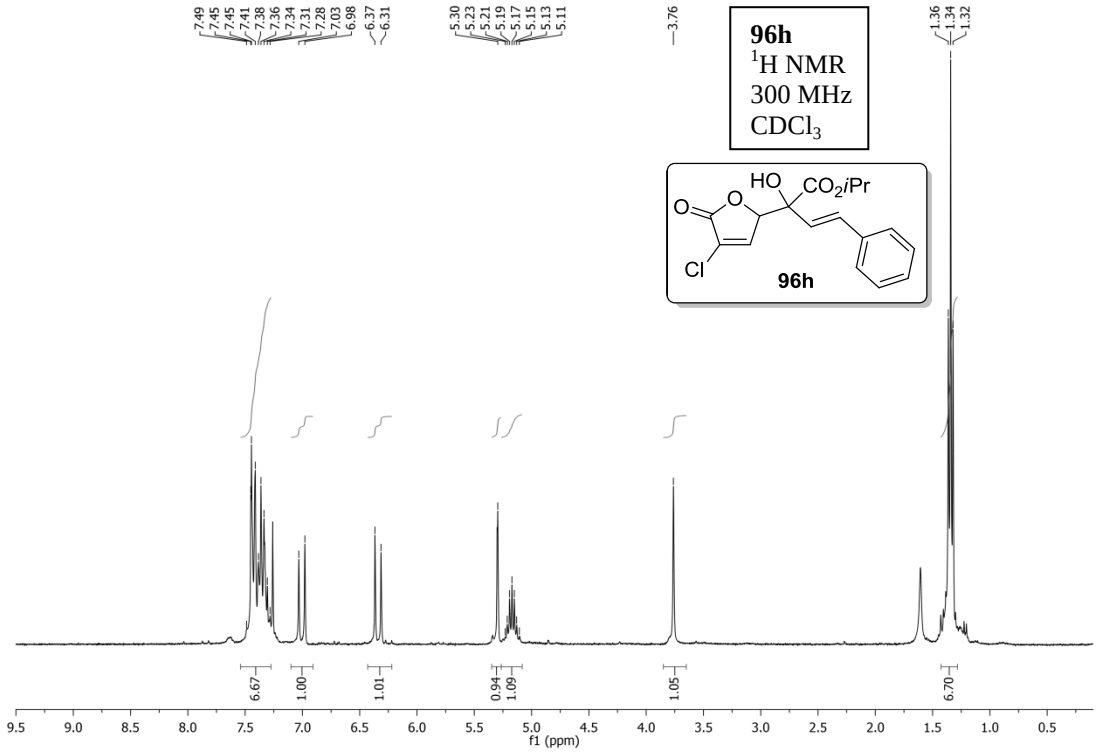
7.49
7.45
7.45
7.41
7.38
7.36
7.34
7.31
7.28
7.03
6.98
6.37
6.31
5.30
5.23
5.21
5.19
5.17
5.15
5.13
5.11
3.76
1.36
1.34
1.32
96h
1H NMR
300 MHz
CDCl3
HO
CO2iPr
O
O
Cl
96h
6.67
1.00
1.01
0.94
1.09
1.05
6.70
9.5 9.0 8.5 8.0 7.5 7.0 6.5 6.0 5.5 5.0 4.5 4.0 3.5 3.0 2.5 2.0 1.5 1.0 0.5
f1 (ppm)

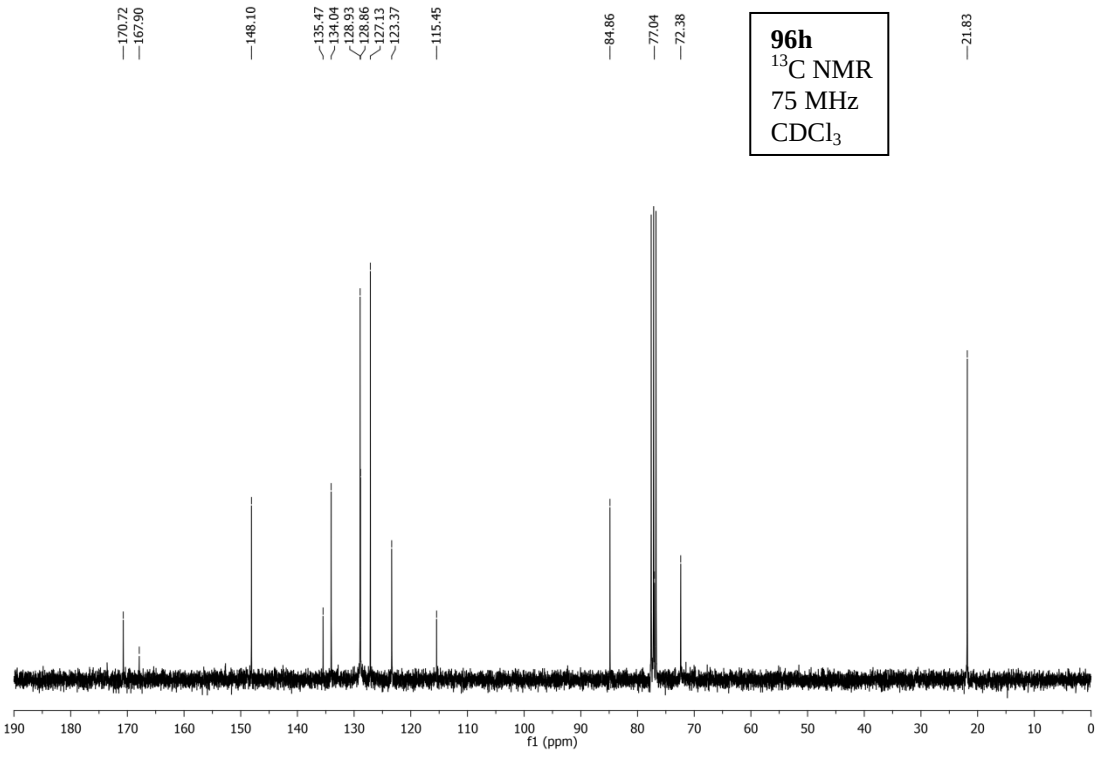
170.72
167.90
148.10
135.47
134.04
128.93
128.86
127.13
123.37
115.45
84.86
77.04
72.38
21.83
96h
13C NMR
75 MHz
CDCl3
190 180 170 160 150 140 130 120 110 100 90 80 70 60 50 40 30 20 10 0
f1 (ppm)

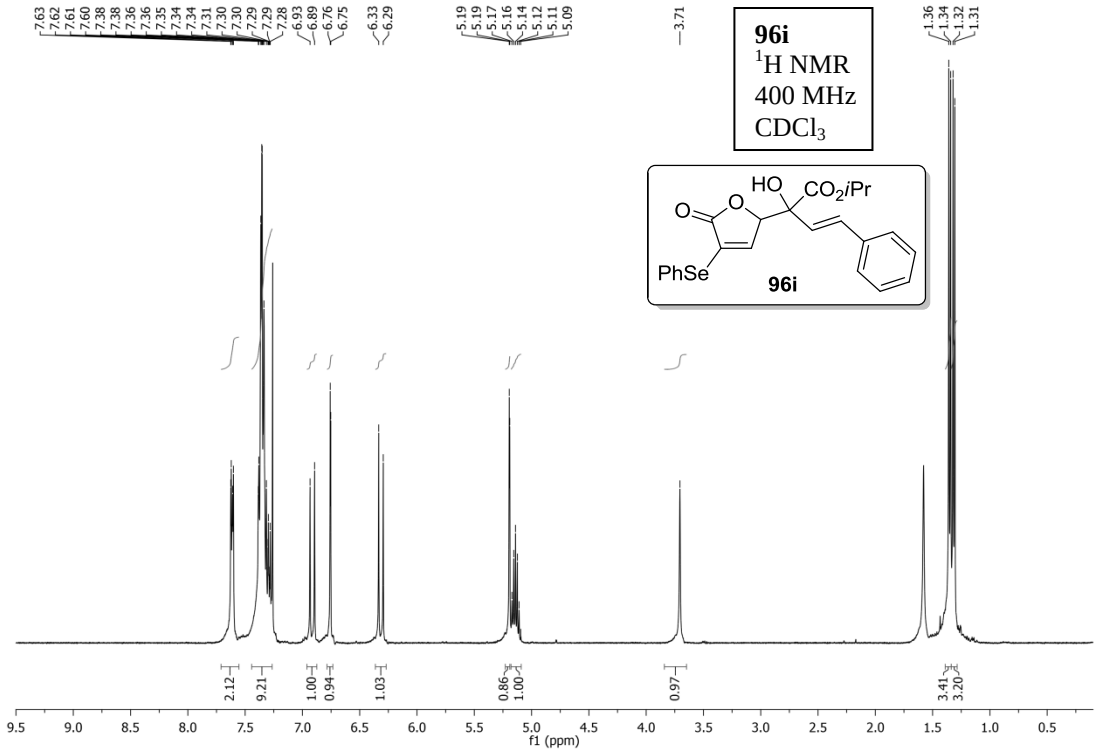
7.63
7.62
7.61
7.60
7.38
7.38
7.36
7.36
7.35
7.34
7.34
7.31
7.30
7.30
7.29
7.29
7.28
6.93
6.89
6.76
6.75
6.33
6.29
5.19
5.19
5.17
5.16
5.14
5.12
5.11
5.09
3.71
1.36
1.34
1.32
1.31
96i
1H NMR
400 MHz
CDCl3
HO
CO2iPr
O
O
PhSe
96i
2.12
9.21
1.00
0.94
1.03
0.86
1.00
0.97
3.41
3.20
f1 (ppm)

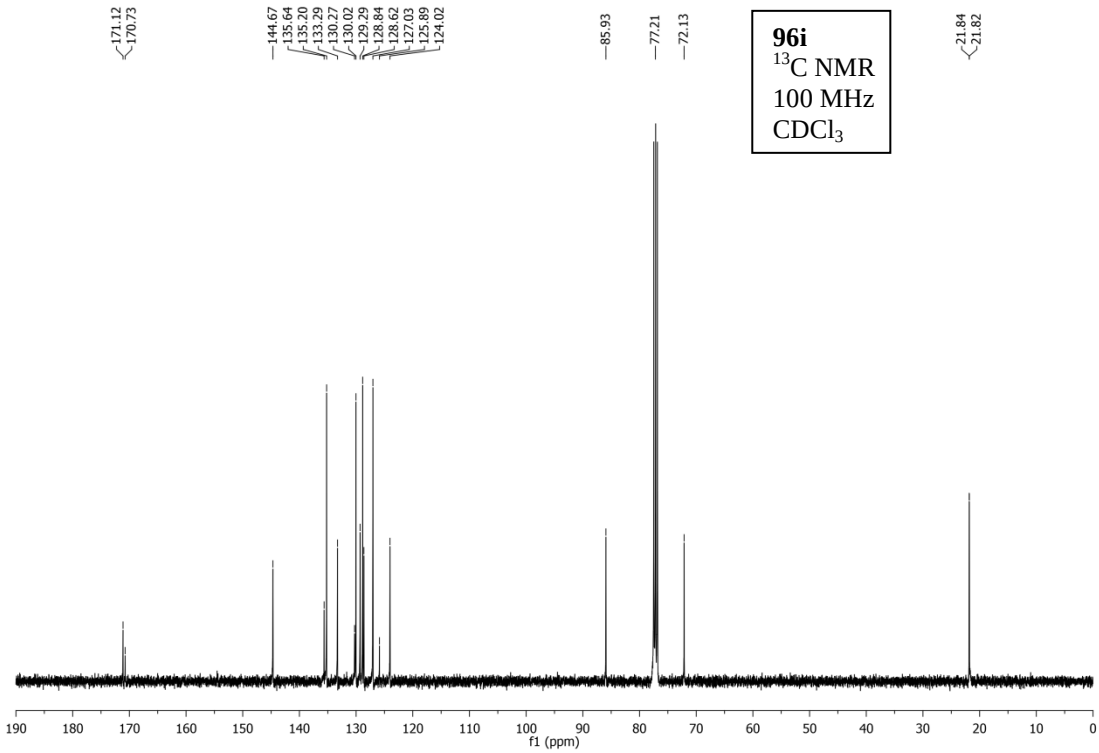
171.12
170.73
144.67
135.64
135.20
133.29
130.27
130.02
129.29
128.84
128.62
127.03
125.89
124.02
85.93
77.21
72.13
21.84
21.82
96i
13C NMR
100 MHz
CDCl3
f1 (ppm)

7.5. Experimental Data for the β-Alkylation of Enals

7.5.1. Preparation of potassium alkyltrifluoroborates 122a-h

Potassium trifluoroborates **122b-c** were used as received from the collection of Prof. Melchiorre. The other trifluoroborates were prepared according to the procedure reported by Fensterbank *et al.*[118]

Typical procedure. To a stirred solution of trimethyl borate (4.68 g, 45 mmol) in THF (30 mL) was added dropwise a 2.0 M THF solution of isopropyl magnesium chloride (15 mL, 30 mmol) over 10 min at -78 °C. The mixture was then stirred for 1 hour at room temperature, after which time it was cooled to 0 °C and KHF_2 (14.1 g, 180 mmol) was added followed by the addition of water (24 mL) over 30 min. The reaction mixture was stirred for 16 hours at room temperature and then the solvent was evaporated under reduced pressure. The solid residue was dried under high vacuum for 4h. The solid was then extracted in hot acetone (3 x 100 mL) and filtered. The filtrate was concentrated under reduced pressure. The resulting solid was treated with Et_2O (40 mL) and the suspension was filtered to afford **122a** as a white solid, which was dried under high vacuum (2.14 g, 48% yield).

Potassium isopropyltrifluoroborate (122a). ^{1}H NMR (400 MHz, CD_3CN): δ 0.10 (br, 1H), 0.92-1.01 (m, 2H), 1.08-1.28 (m, 4H), 1.54-1.63 (m, 4H). **^{13}C NMR** (100 MHz, CD_3OD): δ 19.1 (d, 2C; J = 1.5 Hz). The signal of the C connected to the boron atom is not visible in the spectrum. **^{19}F NMR** (377 MHz, CD_3OD): δ -140.0.

Potassium *tert*-butyltrifluoroborate (122d). White solid. 2.89 g, 59% yield. **^{1}H NMR** (400 MHz, CD_3OD): δ 0.76 (s, 9H). **^{13}C NMR** (100 MHz, CD_3OD): δ 27.6 (3C). The signal of the C connected to the boron atom is not visible in the spectrum. **^{19}F NMR** (377 MHz, CD_3OD): δ -154.6. **^{11}B NMR** (128 MHz, CD_3OD): δ -6.07 (m).

Potassium benzyltrifluoroborate (122e). White solid. 1.51 g, 38% yield. **^{1}H NMR** (400 MHz, CD_3OD): δ 1.70 (br, 2H), 6.92 (tt, 1H; J = 7.2, 1.7 Hz), 7.07-7.12 (m, 4H). **^{13}C NMR** (100 MHz, CD_3OD): δ 123.7, 128.3 (2C), 129.8 (2C), 147.0. The signal of the C connected to the boron atom is not visible in the spectrum. **^{19}F NMR** (377 MHz, CD_3OD): δ -135.1.

Potassium ethyltrifluoroborate (122f). White solid. 1.76 g, 43% yield. **^{1}H NMR** (400 MHz, DMSO-d_6): δ 0.11 (br, 2H), 0.64 (t, 3H; *J* = 7.7 Hz). **^{13}C NMR** (100 MHz, DMSO-d_6): δ 9.8. The signal of the C connected to the boron atom is not visible in the spectrum. **^{19}F NMR** (377 MHz, CD_3OD): δ -131.5.

Potassium vinyltrifluoroborate (122g). White solid. 242 mg, 60% yield. **^{1}H NMR** (400 MHz, CD_3OD): δ 5.29-5.40 (br m, 2H), 5.87 (ddq, 1H; *J* = 21.6, 13.5, 4.0 Hz). **^{13}C NMR** (100 MHz, CD_3OD): δ 121.6. The signal of the C connected to the boron atom is not visible in the spectrum. **^{19}F NMR** (377 MHz, CD_3OD): δ -144.0.

Potassium (phenylethynyl)trifluoroborate (122h). Prepared following the procedure reported by Molander *et al.*[128] White solid. 3.4 g, 82% yield. **^{1}H NMR** (400 MHz, CD_3CN): δ 7.22-7.30 (m, 3H), 7.34-7.37 (m, 2H). **^{13}C NMR** (100 MHz, CD_3OD): δ 127.8, 129.1, 132.2. The signals of the quaternary carbons are not visible in the spectrum, in accordance to reported data. **^{19}F NMR** (377 MHz, CD_3OD): δ -127.5.

7.5.2. Procedure for the photo-organocatalytic asymmetric β-alkylation of 119a

To a solution of catalyst **XXV** (13 mg, 0.020 mmol) in MeCN (100 μL), in a Schlenk tube, were added trifluoroacetic acid (3.1 μL, 0.040 mmol), cinnamaldehyde (**119a**, 38 μL, 0.30 mmol) and the potassium trifluoroborate **122a-h** (0.1 mmol). The tube was closed with a stopper and the reaction mixture was completely deoxygenated by three cycles of freeze-pump-thaw. The reaction vessel was then filled with argon and put at the center of a glass crystallizer (15 cm diameter), around whose walls a 405 nm LEDs strip had been wrapped, equipped with an air-fluxing pipe in order to avoid overheating The light was turned on and the reaction mixture was stirred under irradiation for the time indicated in *Scheme 44*. The LEDs were then turned off and the solvent was removed by rotary evaporation. The crude material was purified by flash chromatography on silica gel, eluting with hexane/DCM 2:1, affording pure product **121a-e**.

[128] Molander, G. A.; Katona, B. W.; Machrouhi, F. *J. Org. Chem.* **2002**, *67*, 8416.

In order to measure the enantiomeric excess of the product, the pure **121a-h** was dissolved in MeOH (1 mL) and treated with $NaBH_4$ (15 mg) at 0 °C for 5 minutes, after which time the solvent was removed under reduced pressure. The residue was taken in DCM (1 mL), filtered through a short pad of silica gel and concentrated again, obtaining the primary alcohol *red*-**121a-h** which was analyzed by HPLC on CSP.

7.5.3. Characterization of β-alkylated compounds 121a-e and 123

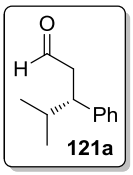

(*S*)-4-Methyl-3-phenylpentanal (121a). 8 mg, 45% yield; 74% *ee*.
^{1}H NMR (500 MHz, $CDCl_3$): δ 0.78 (d, 3H; *J* = 6.7 Hz: CH_3), 0.95 (d, 3H; *J* = 6.7 Hz: CH_3), 1.83-1.92 (m, 1H: C<u>H</u>Me_2), 2.72-2.83 (m, 2H: CH_2), 2.93-2.98 (m, 1H: C<u>H</u>Ph), 7.15 (d, 2H; *J* = 7.3 Hz: $2CH_{arom}$), 7.20 (t, 1H; *J* = 7.3 Hz: $1CH_{arom}$), 7.29 (t, 2H; *J* = 7.5 Hz: $2CH_{arom}$), 9.60 (t, 1H; *J* = 2.1 Hz: HC=O).
^{13}C NMR (125 MHz, $CDCl_3$): δ 20.4, 20.7, 33.6, 47.1, 47.4, 126.7, 128.4 (2C), 128.5 (2C), 142.8, 202.7.
$[\alpha]_D^{23}$ = +11.4° (c 0.1, DCM, 74% *ee*) [lit.[129] $[\alpha]_D^{23}$ +15.8 (c 0.2, DCM, for *S* enantiomer with >99% *ee*)].
HPLC conditions (for reduced **121a**): CHIRALPAK IC column, eluent *n*-hexane/*i*-propanol 97/3, flow 0.8 mL/min, retention times: τ_1(minor)= 14.4 min, τ_2(major)= 16.3 min.

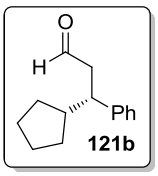

(*S*)-3-Cyclopentyl-3-phenylpropanal (121b). 5 mg, 25% yield; 75% *ee*.
^{1}H NMR (500 MHz, $CDCl_3$): δ 1.00-1.08 (m, 1H), 1.17-1.23 (m, 1H), 1.35-1.49 (m, 2H), 1.56-1.60 (m, 1H), 1.63-1.71 (m, 1H), 1.84-1.90 (m, 1H), 2.02-2.10 (m, 1H), 2.72-2.83 (m, 2H), 2.94 (td, 1H; *J* = 9.7, 5.0 Hz), 7.17-7.21 (m, 3H), 7.27-7.30 (m, 2H), 9.59 (t, 1H; *J* = 2.3 Hz).
^{13}C NMR (125 MHz, $CDCl_3$): δ 25.0, 25.4, 31.5, 31.6, 46.4, 46.6, 49.7, 126.6, 128.0 (2C), 128.6 (2C), 144.0, 202.6.
HRMS (APCI): calcd for $C_{14}H_{17}O$ $[M-H]^+$: 201.1274, found 201.1282.
HPLC conditions (for reduced **121b**): CHIRALPAK IC column, eluent *n*-hexane/*i*-propanol 97/3, flow 0.8 mL/min, retention times: τ_1(minor)= 15.1 min, τ_2(major)= 20.0 min.

[129] Arai, N.; Sato, K.; Azuma, K.; Ohkuma, T. *Angew. Chem. Int. Ed.* **2013**, *52*, 7500.

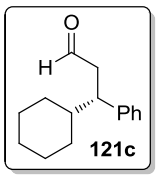

(*S*)-3-Cyclohexyl-3-phenylpropanal (121c). 6 mg, 30% yield; 69% *ee*.

^{1}H NMR (500 MHz, $CDCl_3$): δ 0.80-1.01 (m, 3H), 1.06-1.16 (m, 2H), 1.21-1.27 (m, 1H), 1.46-1.54 (m, 2H), 1.62-1.68 (m, 1H), 1.76-1.84 (m, 2H), 2.74 (ddd, 1H; *J* = 16.4, 9.6, 2.6 Hz), 2.85 (ddd, 1H; *J* = 16.4, 5.4, 1.9 Hz), 3.00 (ddd, 1H; *J* = 9.4, 7.6, 5.5 Hz), 7.15-7.17 (m, 2H), 7.22 (tt, 1H; *J* = 7.5, 1.5 Hz), 7.29-7.32 (m, 2H), 9.63 (t, 1H; *J* = 2.2 Hz).

^{13}C NMR (125 MHz, $CDCl_3$): δ 26.3 (2C), 26.4, 30.7, 31.1, 43.1, 46.2, 47.2, 126.5, 128.3 (2C), 128.4 (2C), 142.8, 202.6.

$[\alpha]_D^{23}$ = -12.9° (c 0.1, DCM, 69% *ee*) [lit.[129] $[\alpha]_D^{23}$ +4.7 (c 0.23, benzene, for *R* enantiomer with >99% *ee*)].

HPLC conditions (for reduced **121c**): CHIRALPAK IC column, eluent *n*-hexane/*i*-propanol 97/3, flow 0.8 mL/min, retention times: τ_1(minor)= 16.9 min, τ_2(major)= 20.6 min.

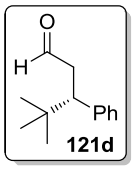

(*S*)-4,4-Dimethyl-3-phenylpentanal (121d). 11 mg, 57% yield; 82% *ee*.

^{1}H NMR (500 MHz, $CDCl_3$): δ 0.90 (s, 9H), 2.79 (ddd, 1H; *J* = 16.4, 4.7, 1.7 Hz), 2.87 (ddd, 1H; *J* = 16.4, 10.7, 2.8 Hz), 3.03 (dd, 1H; *J* = 10.7, 4.7 Hz), 7.15-7.17 (m, 2H), 7.20 (t, 1H; *J* = 7.5, 1.0 Hz), 7.25-7.29 (m, 2H), 9.53 (dd, 1H; *J* = 2.8, 1.7 Hz).

^{13}C NMR (125 MHz, $CDCl_3$): δ 27.9 (3C), 33.7, 44.6, 50.4, 126.6 (2C), 127.9 (2C), 129.4, 141.2, 202.7.

$[\alpha]_D^{23}$ = -40.6° (c 0.1, DCM, 82% *ee*) [lit.[130] $[\alpha]_D$ -37.1 (c 3.0, benzene, for *S* enantiomer with 94% *ee*)].

HPLC conditions: CHIRALPAK IC column, eluent *n*-hexane/*i*-propanol 97/3, flow 0.8 mL/min, retention times: τ_1(minor)= 13.4 min, τ_2(major)= 14.2 min.

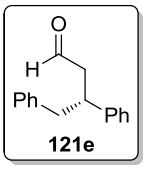

(*R*)-3,4-diphenylpentanal (121e). 12 mg, 52% yield; 68% *ee*.

^{1}H NMR (400 MHz, $CDCl_3$): δ 2.69-2.82 (m, 2H), 2.88 (dd, 1H; *J* = 13.5, 7.8 Hz), 2.96 (dd, 1H; *J* = 13.4, 7.0 Hz), 3.45-3.53 (m, 1H), 7.05-7.07 (m, 2H), 7.15-7.30 (m, 8H), 9.59 (t, 1H; *J* = 1.9 Hz).

^{13}C NMR (100 MHz, $CDCl_3$): δ 42.2, 43.5, 49.1, 126.5, 126.9, 127.7 (2C), 128.5 (2C), 128.8 (2C), 129.4 (2C), 139.4, 143.4, 201.7.

[130] Meyers, A. I.; Shipman, M. *J. Org. Chem.* **1991**, *56*, 7098.

HPLC conditions: CHIRALPAK ID column, eluent *n*-hexane/*i*-propanol 98/2, flow 0.8 mL/min.

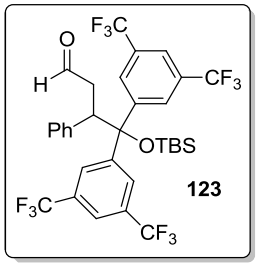

4,4-bis[3,5-bis(trifluoromethyl)phenyl]-4-[(*tert*-butyldimethylsilyl)oxy]-3-phenylbutanal (123). **^{1}H NMR** (400 MHz, $CDCl_3$): δ -0.49 (s, 3H), -0.45 (s, 3H), 0.89 (s, 9H), 2.77 (ddd, 1H; *J* = 17.4, 11.2, 1.7 Hz), 2.98 (dd, 1H; *J* = 17.5, 2.2 Hz), 4.64 (dd, 1H; *J* = 11.2, 2.5 Hz), 6.65 (d, 2H; *J* = 7.2 Hz), 7.10 (t, 2H; *J* = 7.4 Hz), 7.15-7.19 (m, 1H), 7.67 (s, 2H), 7.73 (s, 2H), 7.92 (d, 1H; *J* = 4.9 Hz), 9.62 (d, 1H; *J* = 1.2 Hz).
^{13}C NMR (100 MHz, $CDCl_3$): δ -3.2, -3.0, 19.1, 26.0, 45.6, 48.7, 83.5, 122.5, 128.1, 128.1, 129.5, 129.7, 130.5, 136.6, 144.0, 144.1, 199.2.
^{19}F NMR (377 MHz, CD_3OD): δ -63.2.
GC-MS: m/z 569.2 $[Ar_2COTBS]^+$

7.5.4. HPLC traces of β-alkylated compounds 121a-d

Racemic samples were prepared employing a *rac*-**XXIV** as the catalyst.

rac-**121a**

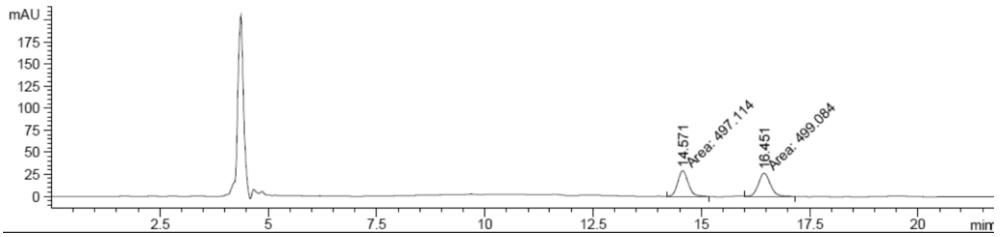

121a (74% *ee*)

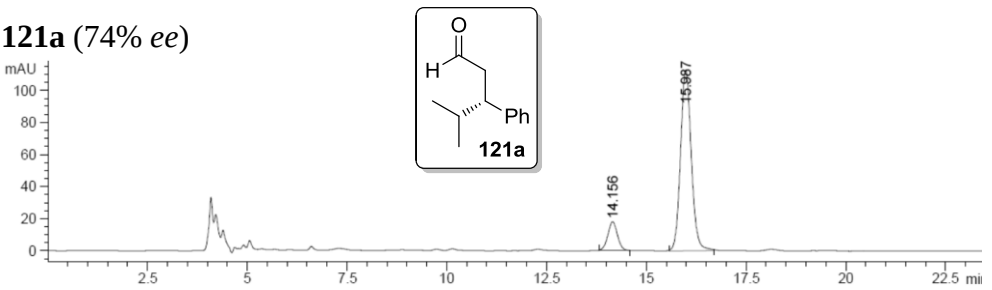

rac-***121b***

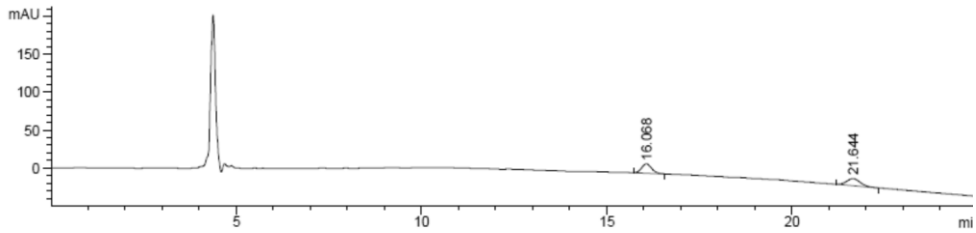

121b (75% *ee*)

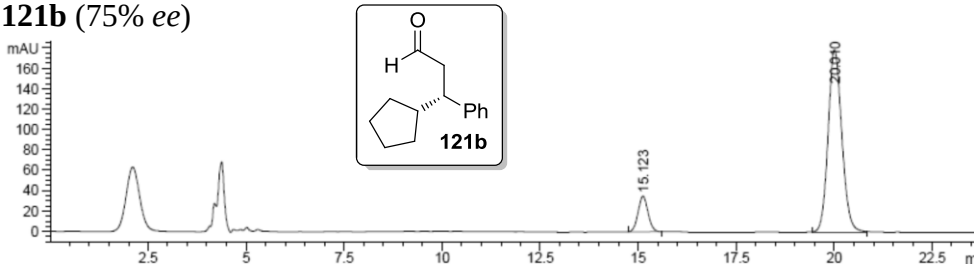

rac-**121c**

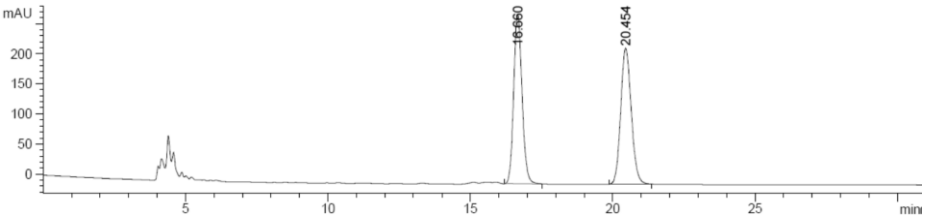

121c (69% *ee*)

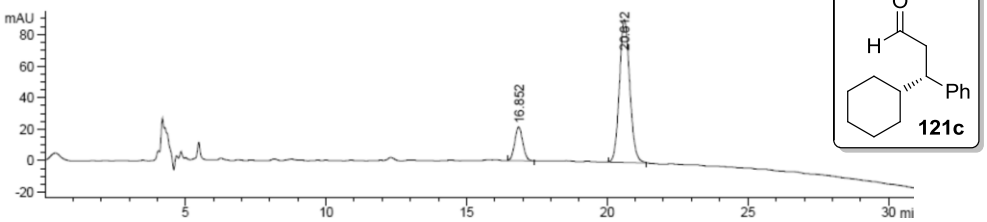

rac-**121d**

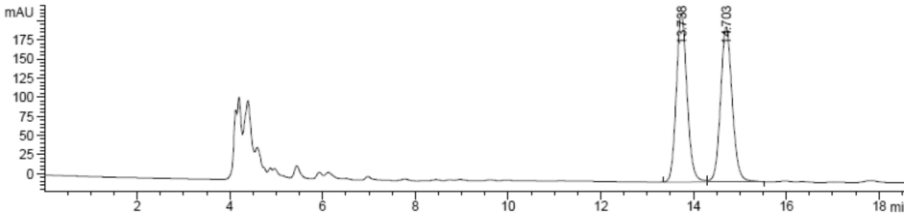

121d (82% *ee*)

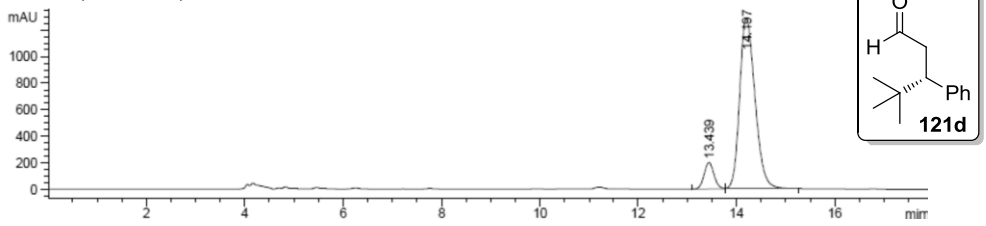

7.5.5. NMR spectra of compounds 121a-e and 123

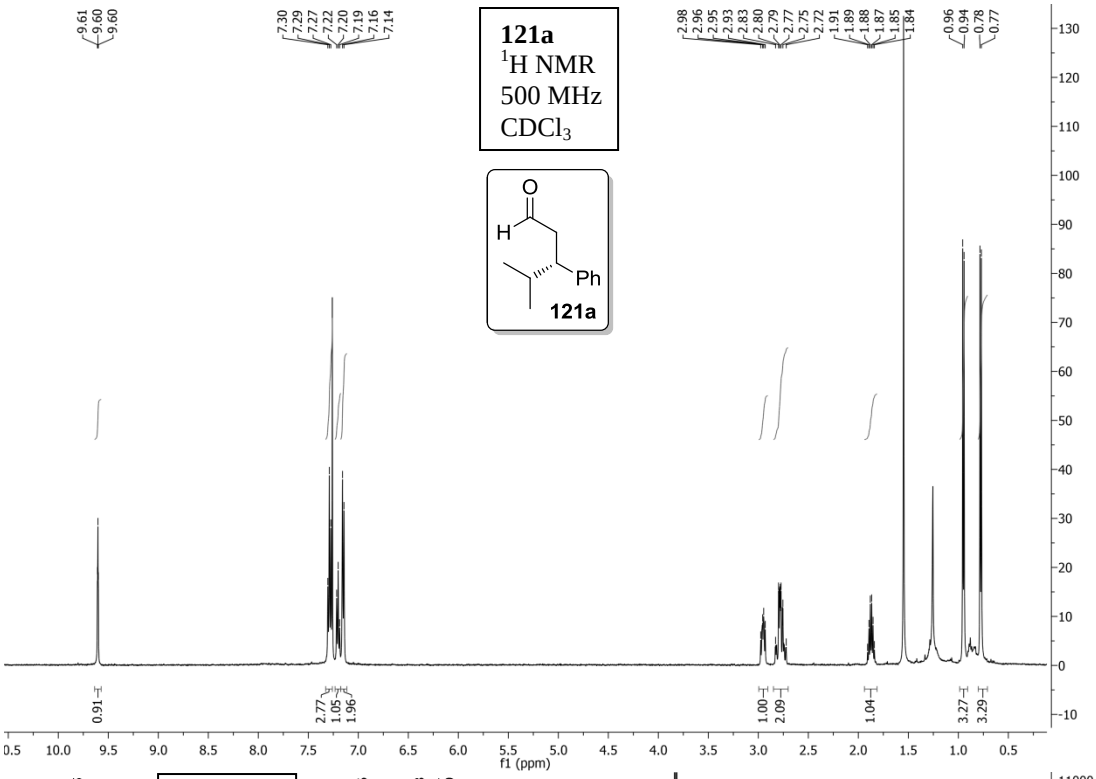

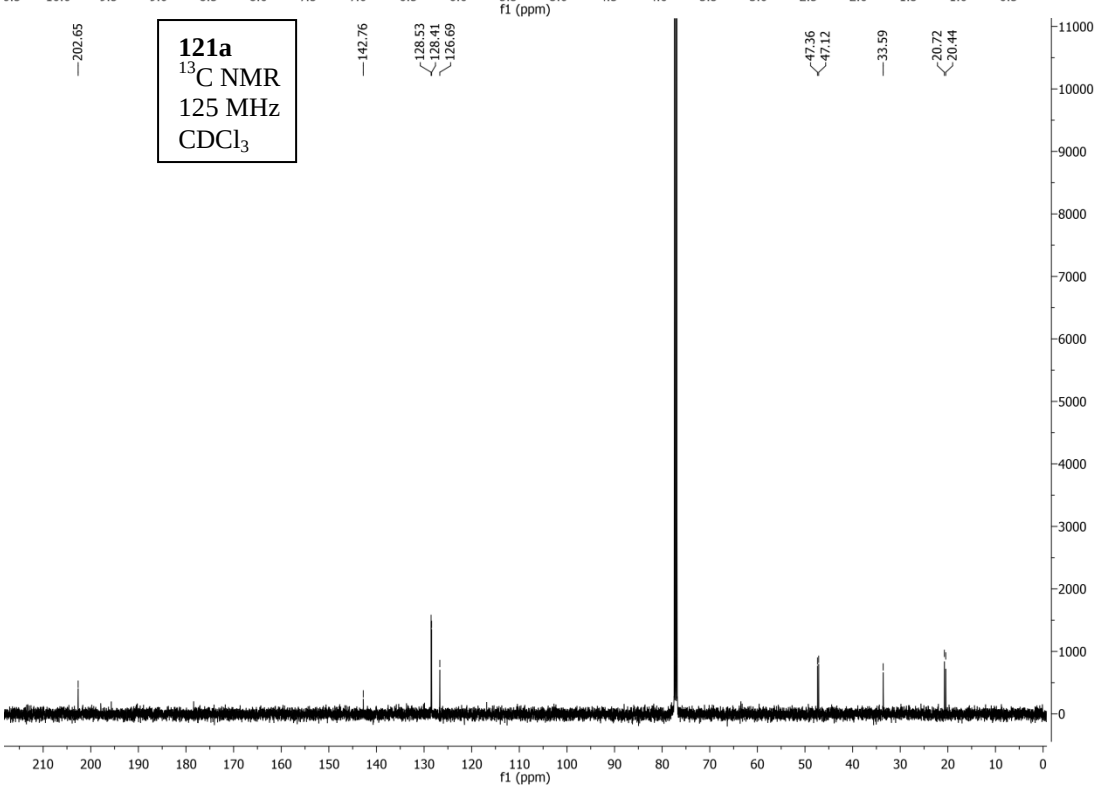

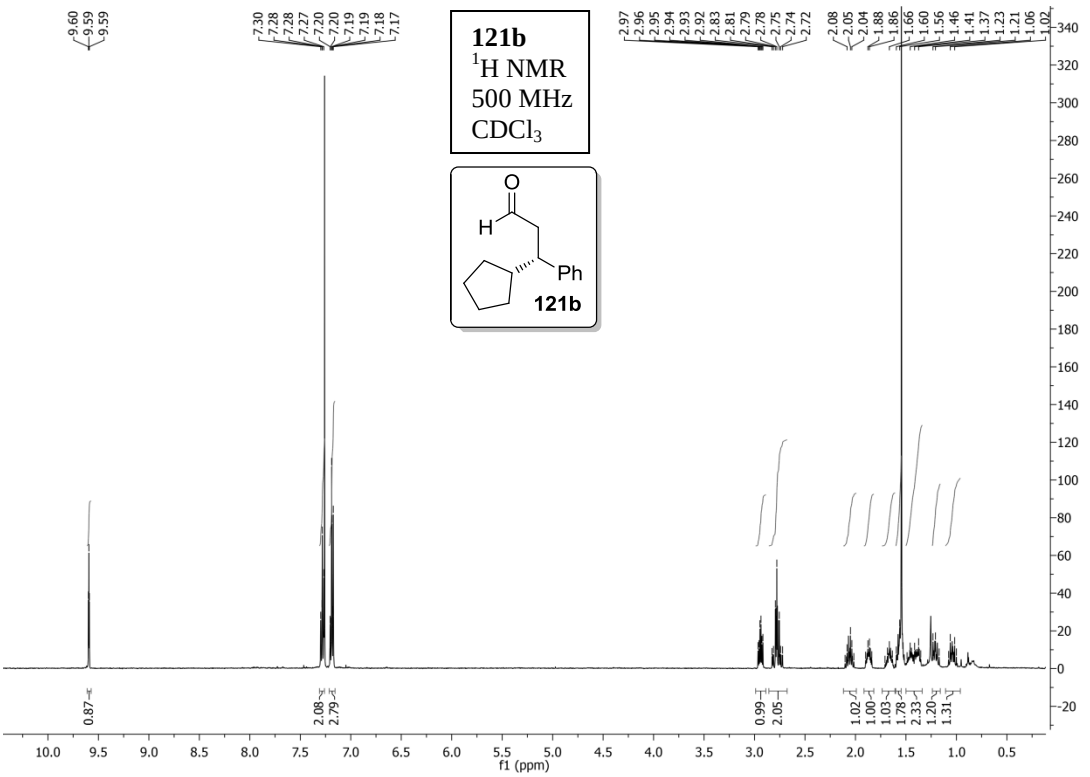
121b
1H NMR
500 MHz
CDCl3
O
H
Ph
121b
9.60
9.59
9.59
7.30
7.28
7.28
7.27
7.20
7.20
7.19
7.19
7.18
7.17
2.97
2.96
2.95
2.94
2.93
2.92
2.83
2.81
2.79
2.78
2.75
2.74
2.72
2.08
2.05
2.04
1.88
1.86
1.66
1.60
1.56
1.46
1.41
1.37
1.23
1.21
1.06
1.02
0.87
2.08
2.79
0.99
2.05
1.02
1.00
1.03
1.78
2.33
1.20
1.31
f1 (ppm)

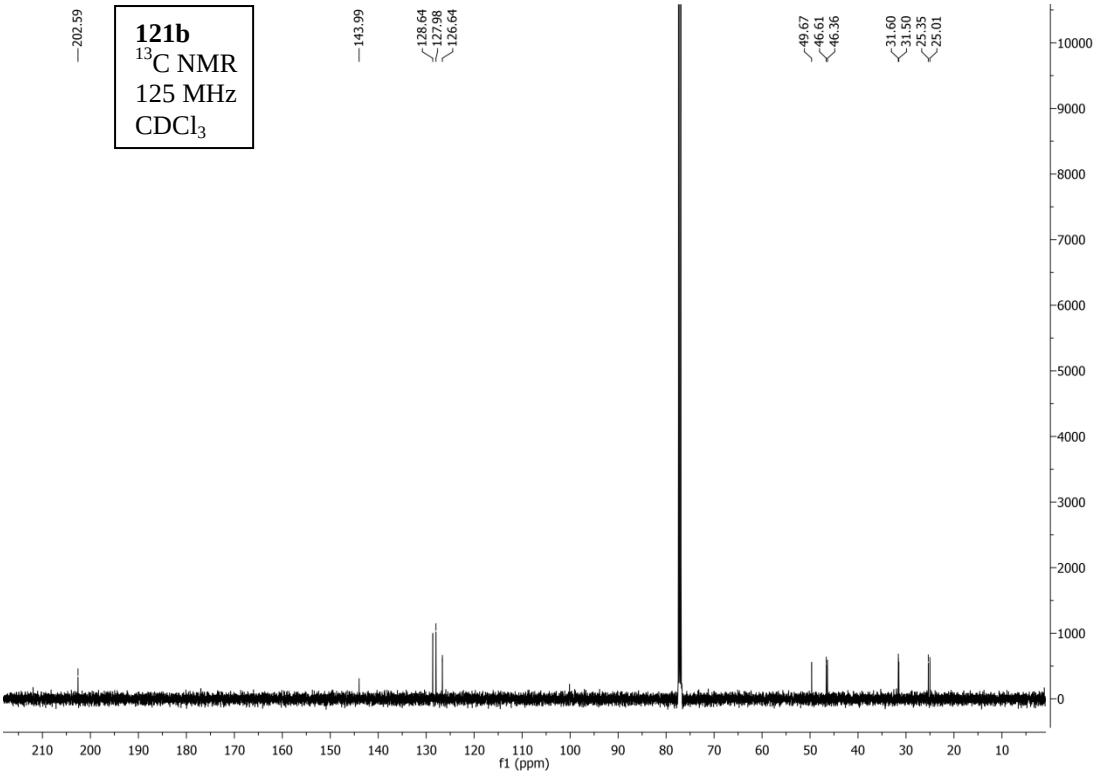
121b
13C NMR
125 MHz
CDCl3
202.59
143.99
128.64
127.98
126.64
49.67
46.61
46.36
31.60
31.50
25.35
25.01
f1 (ppm)

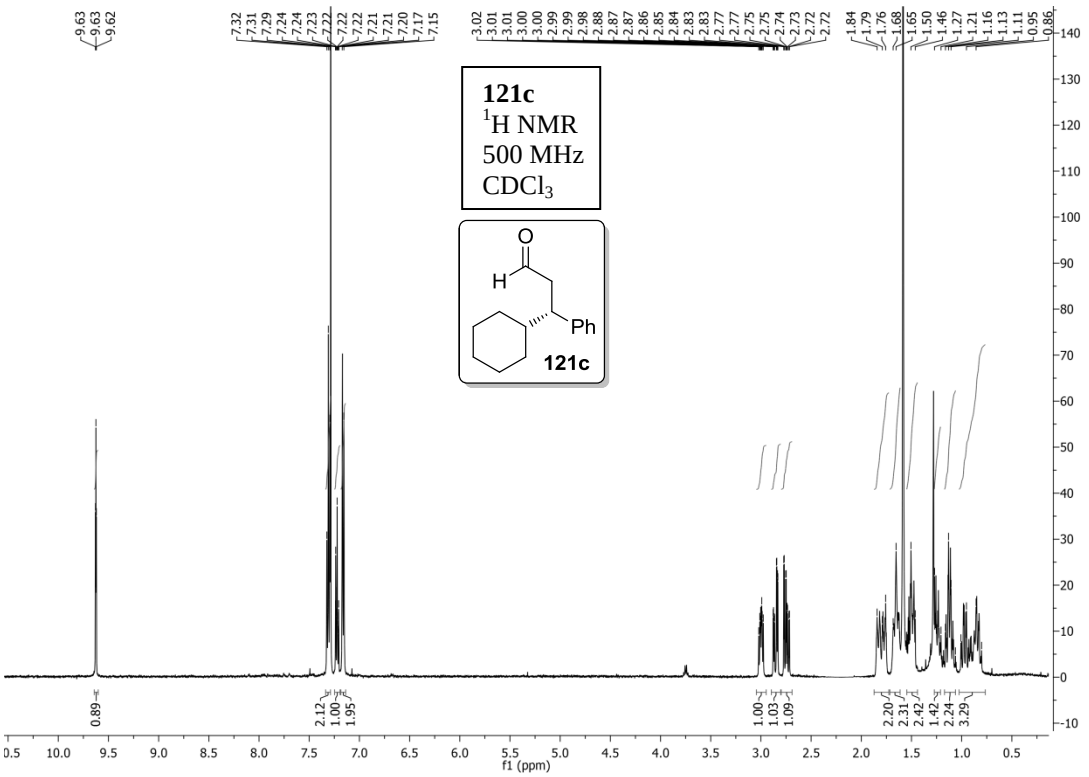
121c
^{1}H NMR
500 MHz
$CDCl_3$
O
H
Ph
121c
f1 (ppm)

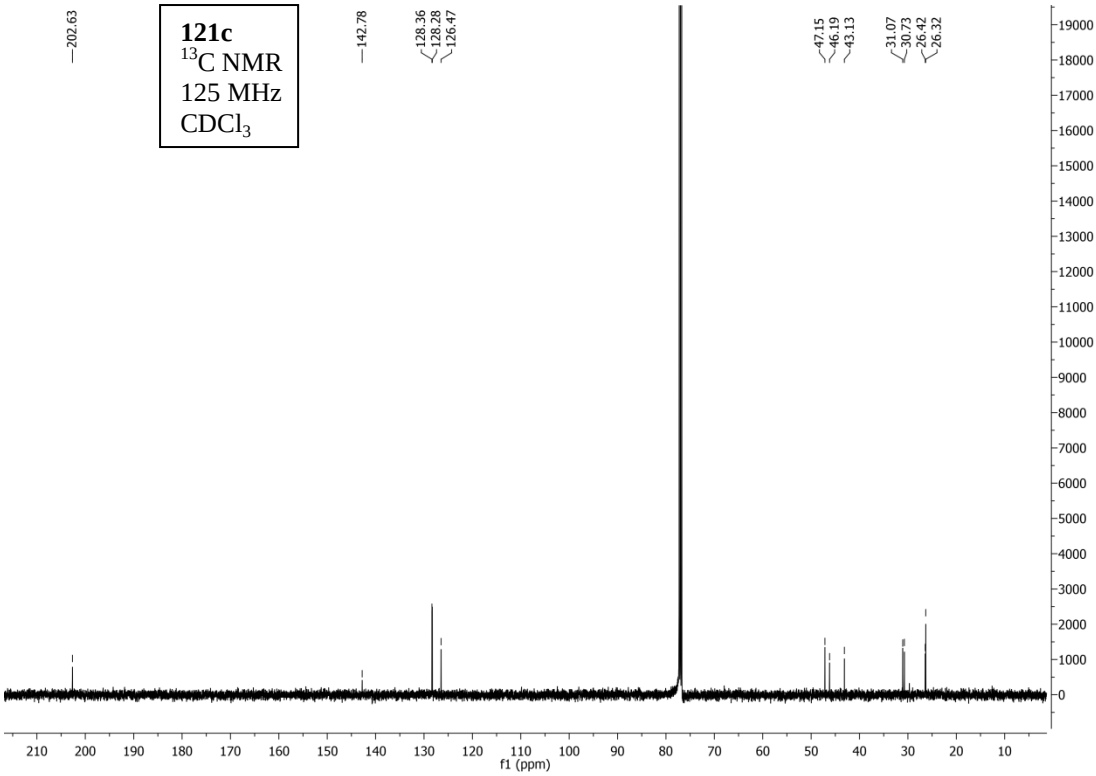
121c
^{13}C NMR
125 MHz
$CDCl_3$
f1 (ppm)

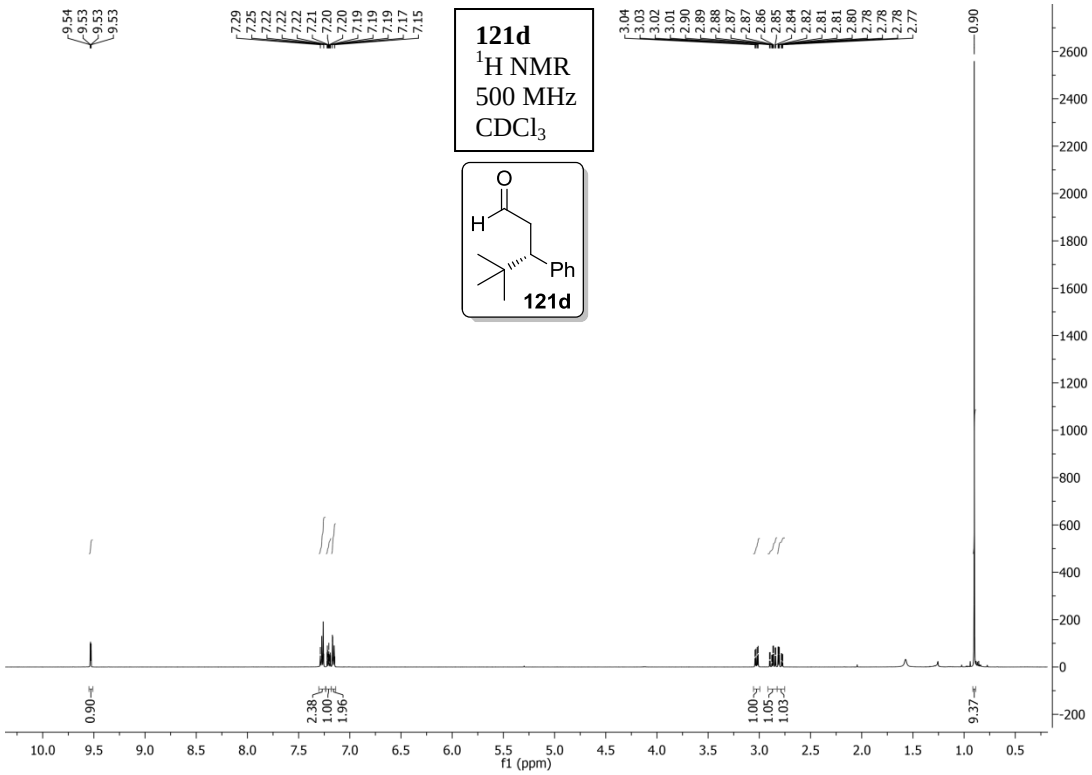
121d
1H NMR
500 MHz
CDCl3
O
H
Ph
121d
9.54
9.53
9.53
9.53
7.29
7.25
7.22
7.22
7.22
7.21
7.20
7.20
7.19
7.19
7.19
7.17
7.15
3.04
3.03
3.02
3.01
2.90
2.89
2.88
2.87
2.87
2.86
2.85
2.84
2.82
2.81
2.81
2.80
2.78
2.78
2.78
2.77
0.90
0.90
2.38
1.00
1.96
1.00
1.05
1.03
9.37
f1 (ppm)

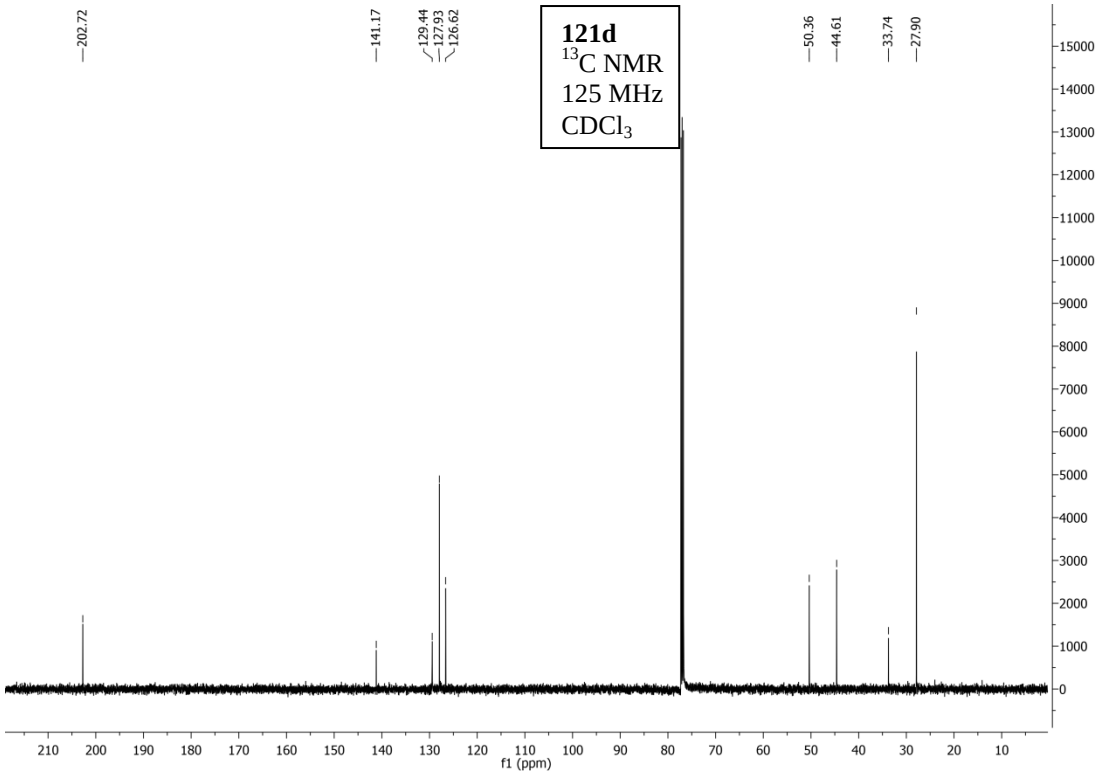
121d
13C NMR
125 MHz
CDCl3
202.72
141.17
129.44
127.93
126.62
50.36
44.61
33.74
27.90
f1 (ppm)

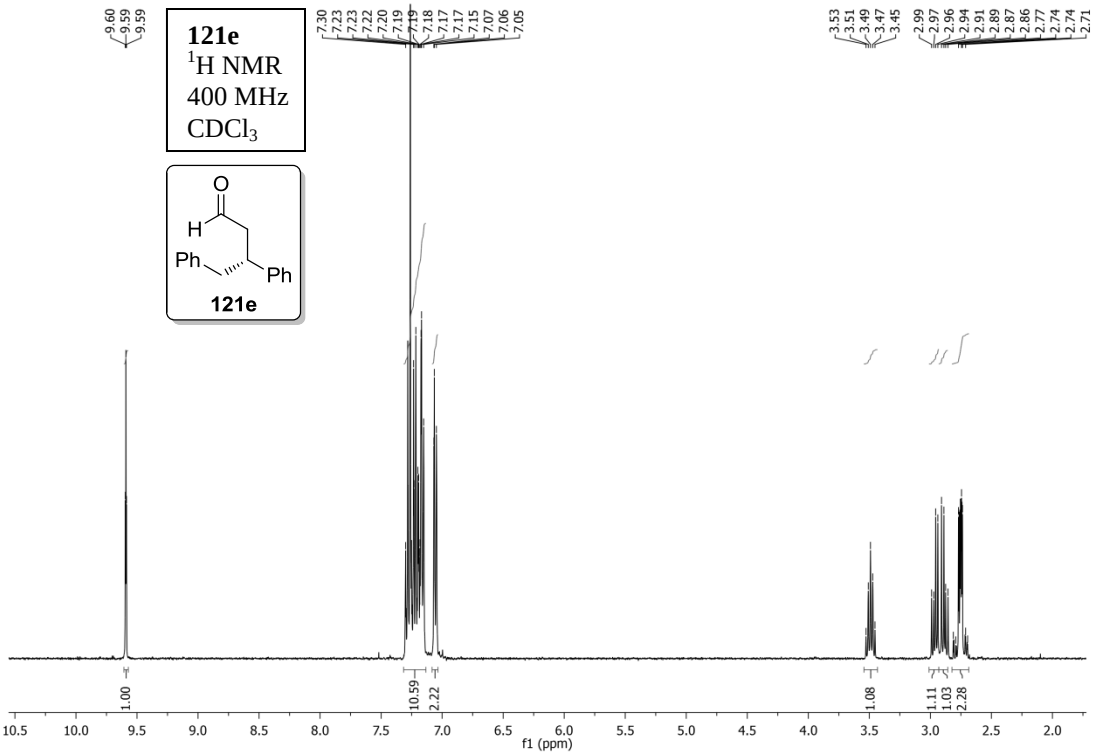
121e
^{1}H NMR
400 MHz
$CDCl_3$
121e
f1 (ppm)

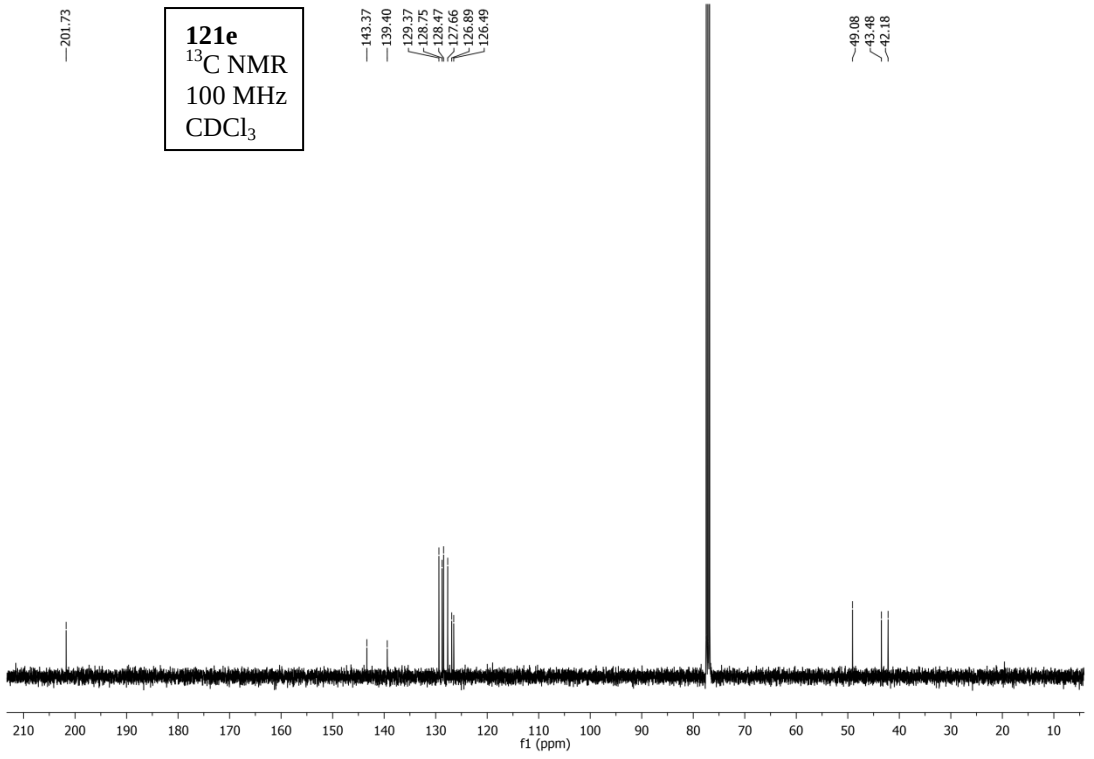
121e
^{13}C NMR
100 MHz
$CDCl_3$
f1 (ppm)

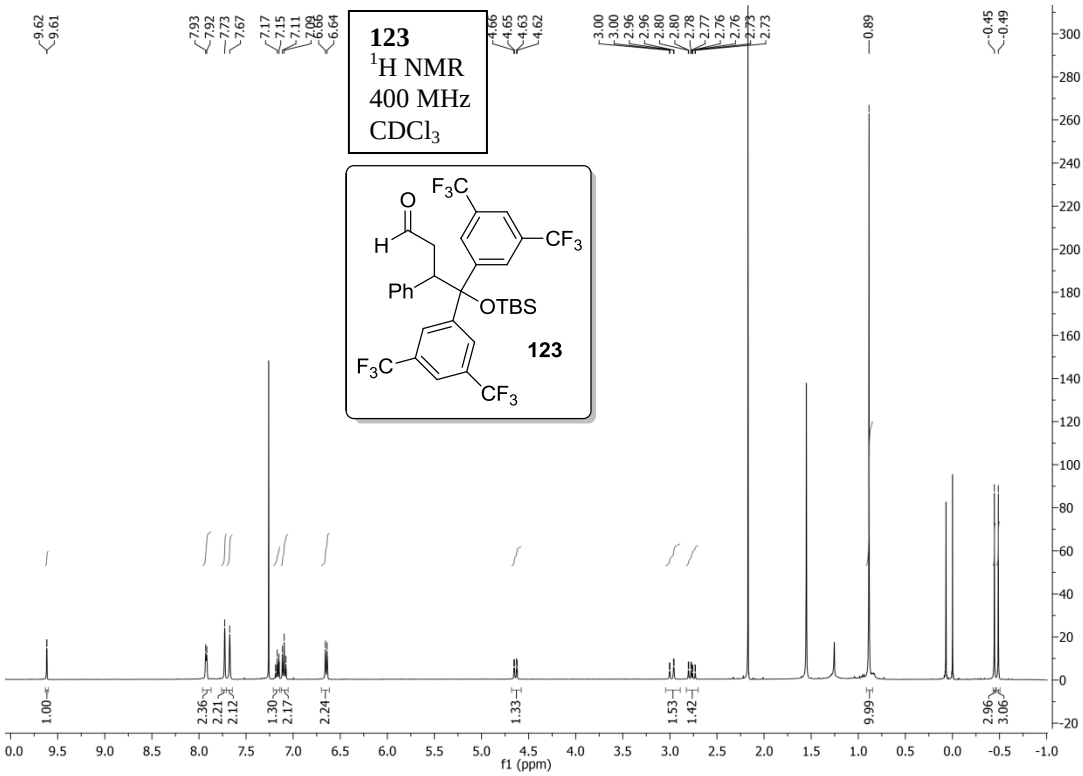
123
1H NMR
400 MHz
CDCl3
F3C
CF3
O
H
Ph
OTBS
123
F3C
CF3
f1 (ppm)

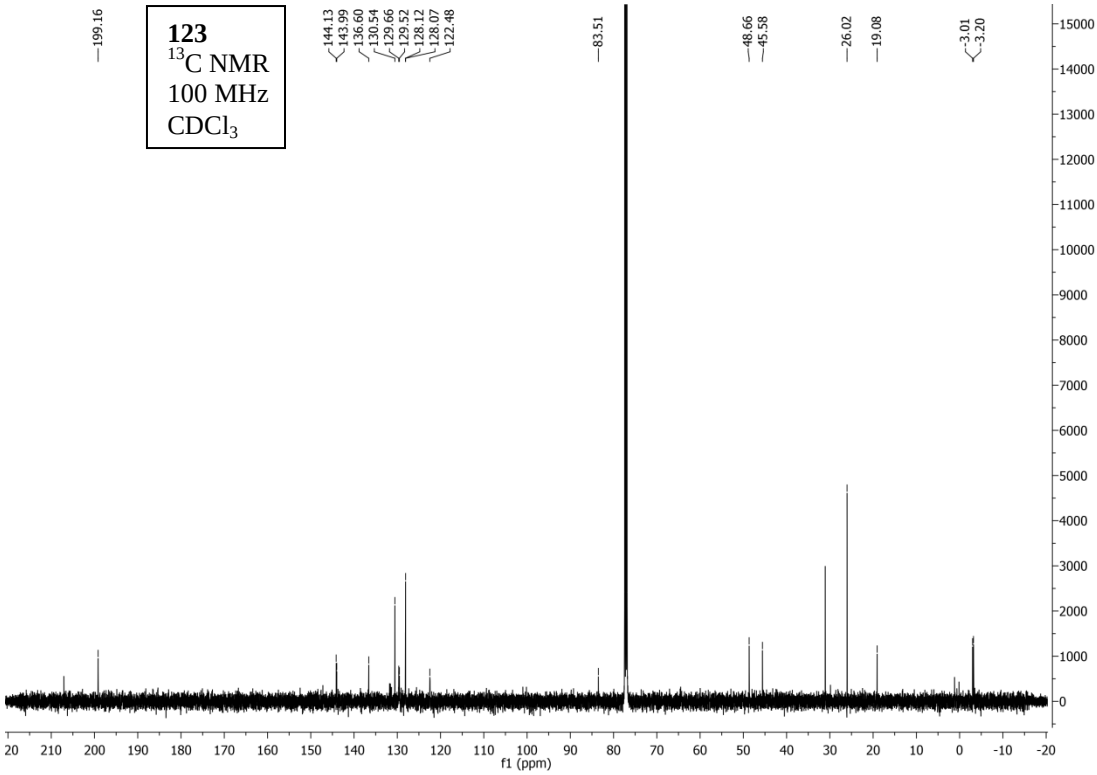
123
13C NMR
100 MHz
CDCl3
f1 (ppm)

8. Articles Reprint

Organocatalysis

International Edition: DOI: 10.1002/anie.201601660
German Edition: DOI: 10.1002/ange.201601660

Quinine-Catalyzed Asymmetric Synthesis of 2,2′-Binaphthol-Type Biaryls under Mild Reaction Conditions

Mauro Moliterno, Riccardo Cari, Antonio Puglisi, Achille Antenucci, Céline Sperandio, Erica Moretti, Antonio Di Sabato, Riccardo Salvio, and Marco Bella**

Abstract: *Simple quinine as an organocatalyst mediates the addition of various naphthols to halogenated quinones to afford non-C_2-symmetrical, axially chiral biaryl products, which are promising compounds as chiral ligands and organocatalysts. The rotational barrier required to have two distinct atropisomers has been evaluated in the products generated from the addition of naphthols to various quinones by means of DFT calculations and HPLC. The use of halogenated quinones as reagents was necessary to have configurationally stable enantiomeric products which can be obtained in good yield and stereoselectivity. These compounds have also been prepared in gram quantities and recrystallized to near enantiopurity.*

Biaryl moieties bearing a chiral axis are present in a number of natural products[1a] and are widely exploited in asymmetric catalysis.[1b–f] A key molecule belonging to this class is 2,2′-binaphthol (BINOL), which is produced on large scale by oxidative coupling and resolved by *Cinchona* alkaloids.[2a,b] Over the years, several chiral ligands and catalysts derived from the privileged BINOL framework have been successfully employed in asymmetric synthesis (Figure 1).[2a–f]

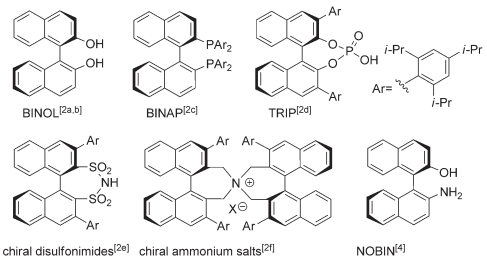

Figure 1. Some widely exploited axially chiral ligands and catalysts.[2]

A C_2-symmetry axis was once considered a key feature for obtaining high enantioselectivity in asymmetric catalysis,[3] but over the years, several authors have also demonstrated the efficiency of non-C_2-symmetrical ligands and catalysts, such as NOBIN.[4] Despite their wide popularity in asymmetric catalysis, the large scale synthesis of these molecules suffers from two critical issues. First, the formation of C–C bonds in an industrial process is a significant challenge, especially $C(sp^2)$–$C(sp^2)$ couplings which are mediated by transition metals and oxidants. The use of metals represents a technical and economic issue for industry.[5a,b] Second, most scalable syntheses only afford racemic products, which need to be resolved by processes having a maximum theoretical yield of 50%.[2,5c] Therefore, an efficient organocatalytic (transition-metal-free) approach to prepare these compounds could represent a major breakthrough. Recently, the groups of Miller[6a,b] and Matsubara[6c] demonstrated the possibility of obtaining axially chiral biaryls through dynamic kinetic resolution by using an organocatalytic bromination reaction. Despite this process being of scientific value within academia, the elaboration of the products into effective ligands and catalysts does not appear straightforward and it has not been demonstrated yet. Moreover, the synthesis of the achiral precursors still requires a transition metal catalyzed reaction. Therefore, a practical synthesis of a structure which closely resembles BINOL, a structure already proven to be highly effective as a chiral ligand and catalyst, might be preferable and open new horizons in the field of asymmetric catalysis.

Prakash and co-workers reported that *Cinchona* alkaloid-derived chiral bases could activate indoles, which would add in an asymmetric way to ethyl trifluoropiruvate.[7a] Jørgensen, Bella, and co-workers described a similar activation mode of the corresponding 2-naphthols, which after addition to azodicarboxylates, produced C–N axially chiral compounds (Figure 2).[7b,c] We thought that this information could be exploited to develop a $C(sp^2)$–$C(sp^2)$ coupling between

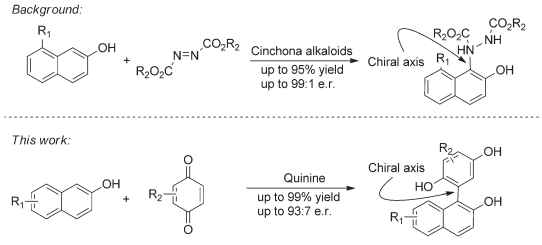

Figure 2. Previous and current work.

[*] M. Moliterno, R. Cari, A. Puglisi, A. Antenucci, C. Sperandio, E. Moretti, A. Di Sabato, Dr. R. Salvio, Prof. M. Bella
Dipartimento di Chimica, Sapienza University of Roma
P. le Aldo Moro 5, 00185 Roma (Italy)
E-mail: marco.bella@uniroma1.it
Dr. R. Salvio
IMC-CNR Sezione Meccanismi di Reazione
Università di Roma—Sapienza
P. le Aldo Moro 5, 00185 Roma (Italy)
E-mail: riccardo.salvio@uniroma1.it
Supporting information and the ORCID identification number(s) for the author(s) of this article can be found under http://dx.doi.org/10.1002/anie.201601660.

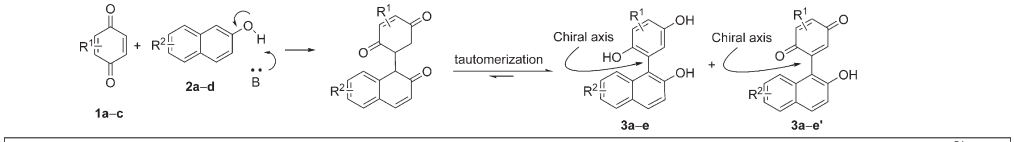

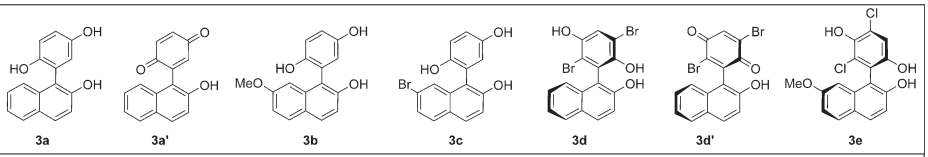

	3a	3a'	3b	3c	3d	3d'	3e
Calculated							
$\Delta G^{\ddagger}$ (kcal/mol)	22.9	11.9	22.1	22.8	45.8	32.4	40.2
$t_{1/2}$ rac (s)	7800	6.3×10^{-5}	2000	6600	5.5×10^{20}	7.6×10^{10}	4.2×10^{16}
Determined							
$\Delta G^{\ddagger}$ (kcal/mol)	22.0 ± 0.1		21.3 ± 0.1	21.9 ±0.1			
$t_{1/2}$ rac (s)	1650 ± 250		510 ± 80	1340 ± 270			

Scheme 1. Base-catalyzed addition of naphthols (**2**) to quinones (**1**) to afford biaryls (**3**) bearing a stereogenic axis (top). Energy of rotational barrier calculated (b3lyp/6-311 + g(d,p)// b3lyp/6-311 + g(d,p)) using Gaussian09[9a] and determined by HPLC[9b] (bottom, see the Supporting Information for details).

activated aromatic compounds and quinones, as electrophiles,[8] to afford C–C axially chiral molecules which closely resemble the skeleton of BINOLs. The configurational stability of BINOLs stems from the hindered rotation along the C–C axis because of the presence of the hydroxy groups (in the 2,2′-positions) and the *peri* protons (in the 8,8′-positions). Since our compounds were missing this feature, a preliminary aspect to be investigated was the substituent pattern allowing a sufficient rotational barrier along the newly formed chiral axis to obtain configurationally stable atropisomers (Scheme 1).

While the rotational barriers of BINOL-like molecules are known, we could not find data in the literature about the specific compounds reported in our paper. The compound **3a** (Scheme 1) was separated into two enantiomers by HPLC using a chiral stationary phase, but the shape of the chromatogram is anomalous because of the appearance of peaks with a plateau between them (this is known as a "Batman" profile).[10] Such peaks can be observed in the case of atropisomers, with hindered rotation, which are interconverting on a time-scale comparable to the retention time of the HPLC run. Indeed, analytical chiral separations can be used to determine the rotational barriers of racemization.[9b] In contrast, we could not get any separation for the enantiomers of **3a′**, thus pointing to a fast interconversion. Accordingly, ab initio calculations indicate a low interconversion barrier for **3a′**, but the calculated energy barrier for the enantiomer interconversion of **3a** (22.9 kcal mol^{-1}) is compatible with a chromatogram of species interconverting on an HPLC time scale and it is in reasonable agreement with that determined by integration of the areas of HPLC peaks (22.0 kcal mol^{-1}).[9] We then prepared **3b** and **3c**, bearing a methoxy and a bromo substituent, respectively, at the 7-position and the rotational barrier still remains similar to that of **3a**. Finally, we tested the same reaction starting from 2,5-dibromo 1,4-benzoquinone (**1b**), thus obtaining a mixture of **3d** and its oxidized form **3d′.** Both in silico and experimental data indicate that the two compounds have a high rotational barrier and consequently are configurationally stable. Also the presence of a chloro substituent on the quinone moiety results in a significant rotational barrier (**3e**), and we find a similar agreement between the calculated and experimental data. Therefore, to obtain configurationally stable enantiomers, it was necessary to employ halogenated quinones such as **1b** and **1c**. The DFT calculations turn out to be useful to predict whether the enantiomers can have an interconversion rate comparable to the HPLC timescale and therefore whether a plateau between the peaks of the enantiomers can be observed.

We then chose as a model the reaction of 7-methoxy 2-naphthol (**2b**) and 2,6-dichloro 1,4-benzoquinone (**1c**), and we investigated which reaction conditions could afford higher yield and stereoselectivity. Previous attempts to run the reaction under argon gave rise anyway to the formation of a mixture of **3e** and its oxidized quinonic form in variable ratios. This oxidation process might be due to the presence of **1c** as it can act as an oxidant. We then added sodium borohydride to the reaction mixture to reduce any oxidized quinone product, and then TFA to reprotonate the naphthol sodium salts. We loaded the crude reaction mixture on a short pad of silica gel and quick filtration afforded a substantially pure sample of **3e**. The combination of THF as the solvent and quinine (**I**) as the catalyst (Table 1, entry 1) afforded **3e** in nearly quantitative yield and with 83:17 e.r. Chloroform or toluene, which are common solvents employed for *Cinchona* alkaloid-derived catalysis, were not as effective (entries 2 and 3). The temperature of 4°C, which can be conveniently achieved, appeared ideal so as to maximize the enantiomeric ratio; the reaction run at −20°C did not increase enantioselectivity (entry 4) and the one conducted at room temperature also produced products in less satisfactory enantioselectivity (entry 5). A minor amount of catalyst and higher dilution were instead beneficial and when we combined these findings we achieved the highest enantioselectivity (entry 6). It is important to stress that simple **I** was the most effective

Table 1: Screening of reaction conditions for the organocatalyzed addition of **2b** to **1c** to afford the axially chiral **3e** (see the Supporting Information for additional screening of reaction conditions and catalysts).

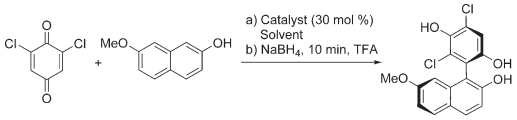

1c **2b** **3e**

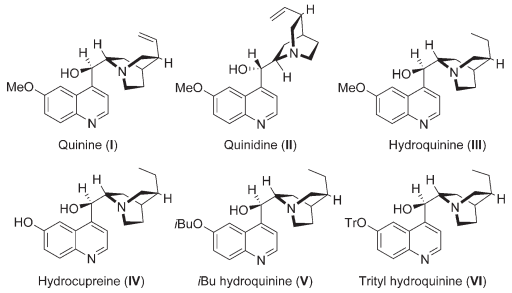

Quinine (**I**) Quinidine (**II**) Hydroquinine (**III**)

Hydrocupreine (**IV**) *i*Bu hydroquinine (**V**) Trityl hydroquinine (**VI**)

Entry[a]	Cat	Solvent	*t* [h]	*T* [°C]	Yield [%][b]	e.r.[c]
1	**I**	THF	24	4	98	83:17
2	**I**	$CHCl_3$	18	4	65	63:37
3	**I**	toluene	18	4	99	63:37
4	**I**	THF	3	−20	50	83:17
5	**I**	THF	24	RT	90	79:21
6[d,e]	**I**	THF	48	4	99	86:14
7	**II**	THF	48	4	99	21:79
8	**III**	THF	4	4	50	83:17
9	**IV**	THF	72	4	< 10	50:50
10	**V**	THF	24	4	99	85:15
11	**VI**	toluene	72	4	99	56:44
12[d,e,f]	**I**	THF	5	4	99	87:13

[a] Reaction performed employing 50 mg (0.28 mmol,1.2 equiv) of **1c** and 40 mg (0.23 mmol, 1 equiv) of **2b** with 4 mL of solvent (concentration: 0.057 M). [b] Yield of isolated product. [c] The e.r. value was determined by HPLC on CSP using Chiralpack ID column and *n*-hexane/isopropyl alcohol (88:12; flow 0.9 mL min). [d] Concentration of 0.0275 M. [e] Used 15 mol% catalyst. [f] Used 2 equiv of **1c**. TFA = trifluoroacetic acid, THF = tetrahydrofuran.

catalyst, at least in our hands. None of the other natural and synthetic *Cinchona* alkaloid derivatives we tested performed better. In particular, the pseudoenantiomer quinidine (**II**) gave rise to the formation of the enantiomer of **3e** with similar stereocontrol (entry 7). The hydroquinine **III** did not perform better (entry 8) and hydrocupreine **IV** afforded essentially racemic material (entry 9). The substitution of the 6-methoxy group with other bulkier groups (**V**; entry 10 and **VI**; entry 11) did not afford better results. The reaction employing 2 equivalents of **1c** was faster (entry 12 versus entry 6). Although the enantioselectivity was not the highest possible, our experience regarding one of our asymmetric reactions,[11a] which became a large-scale industrial process[11b] suggested that for the wide applicability of a novel process this was not a major issue. Specifically, mild reaction conditions (RT or 4°C), high yield (above 95%), cheap and commercially available catalysts (quinine) and reagents, plus the potential to avoid chromatography to purify the products are aspects which are more important than finding a catalyst which would afford a higher enantiomeric ratio.

With our optimized reaction conditions, we explored the scope of our reaction by testing several combinations of halogenated 1,4-benzoquinones (**1**) and naphthols (**2**; Scheme 2). To maximize the enantiomeric ratio, we ran the reactions at high dilution. When compatible with reasonably reaction times, we employed only a small excess of the quinones **1** and ran the reactions at 4°C. At first, we tested carbomethoxy 1,4-benzoquinone (**1d**), which is the most reactive quinone (reaction completed within a day and quantitative yield), but it produced the corresponding biaryl **3f** only as a racemic mixture. The lack of stereocontrol might

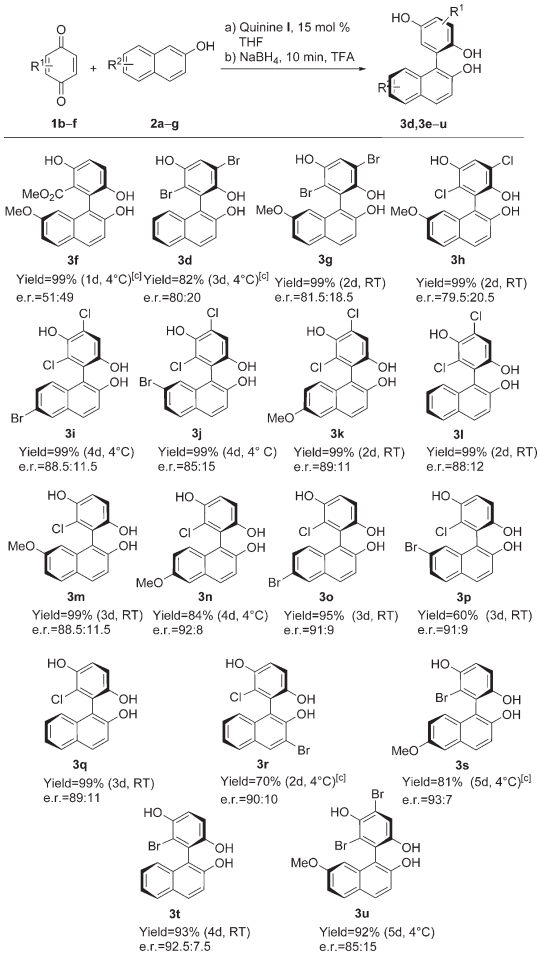

Scheme 2. Scope of the quinine-catalyzed addition reaction of naphthols (**2**) to quinones (**1**) to produce axially chiral compounds (**3**) in enantioenriched form. [a] Reaction performed employing 2.0 equiv of quinones (**1**), 1.0 equiv of naphthol **2b** (0.15 mmol), and with 5.5 mL of solvent (concentration: 0.0275 M). [b] Values within parentheses are reaction time in days. [c] Used 1.2 equiv of **1**. See the Supporting Information for the determination of the absolute configuration.

be due to the fast, nonselective reaction. The use of dihalogenated benzoquinones [**1b**,**c** and **1e** (2,5-dichloro 1,4-benzoquinone)] afforded the biaryls **3d** and **3g**–**l** in good yield and moderate to good enantioselectivity (82–99% yield, 80:20 to 89:11 e.r.). Chloro 1,4-benzoquinone (**1f**) presented a similar reactivity, even if the reactions required a longer reaction time. However, the products **3m**–**r** were formed in better stereoselectivity (60–99% yield, 88.5:11.5 to 92:8 e.r.).

Finally, we tested bromo 1,4-benzoquinone (**1g**) and 2,6-dibromo 1,4-benzoquinone (**1h**), which afforded the products **3s**–**u** after a longer reaction time, but in comparable stereoselectivity with that of the corresponding chloroquinones **1c** and **1f** (81–93% yield, 85:15 to 93:7 e.r.). For a full report of all reaction conditions tested see Schemes S5 and S6 in the Supporting Information.

A possible rationalization regarding the formation of the major enantiomer is depicted in Figure 3. According to this scenario, the deprotonated hydroxy function on the naphthol unit would interact with the protonated quinuclidine unit of quinine and the quinone reagent would be activated by hydrogen bonding at the 9-hydroxy functionality of the

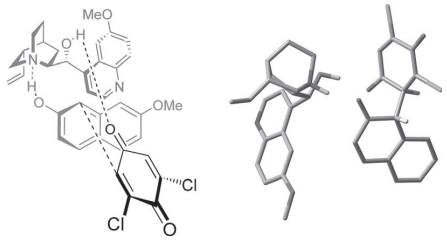

Figure 3. Proposed transition state leading to the major enantiomer and corresponding DFT optimized structure (b3lyp/6-31g*//b3lyp/6-31g*; some atoms are omitted for clarity).

catalyst. The π–π staking between the aromatic moiety of the reagents and the quinoline part of the catalyst does not seem to play any major role. DFT calculations and the inversion of stereoinduction when employing catalysts lacking the free 9-hydroxy group support this hypothesis.

To show the preparative usefulness of our transformation, we performed two reactions on gram scale by employing a higher concentration of reagents. The products **3i** and **3k** were obtained in high yield and with minimal erosion of enantiopurity, and have been recrystallized with high enantiomeric excess (Scheme 3).

In conclusion, we have presented a new organocatalyzed reaction for the synthesis of a class of novel biaryl compounds and we have discussed the features necessary to prepare configurationally stable atropisomers. We believe that the mild reaction conditions of our reaction, coupled with the use of a cheap and commercially available catalyst should render it attractive for the large-scale preparation of these important compounds, at the very least in a research laboratory. Furthermore, the presence of various halogen atoms offers the possibility to functionalize these compounds by using

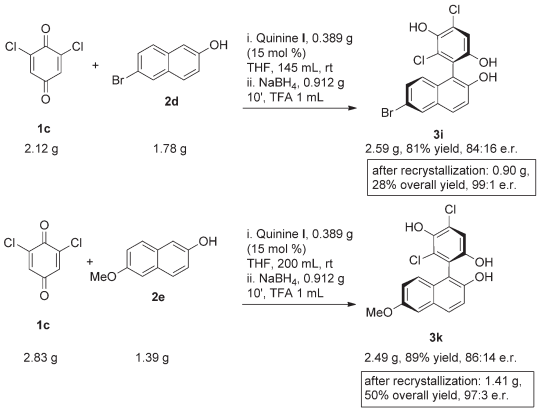

Scheme 3. Preparative large-scale reactions for **3i** and **3k**.

several transformations. Studies are ongoing in our group as well as others[12,13] to apply these compounds as useful ligands and catalysts for highly enantioselective asymmetric reactions.

Experimental Section

Typical experimental procedure: To a cooled (4°C) suspension of the naphthol **2** (0.15 mmol) and quinine **I** (7 mg, 0.0225 mmol, 15 mol %) in THF (4.5 mL) was added a cooled (4°C) solution of the halogenated 1,4 benzoquinone **1** (0.30 mmol, 2 equiv) dissolved in 1 mL of THF. The reaction mixture was stirred at 4°C for 48 h, and then the resulting dark solution was cooled to 0°C (ice bath) and $NaBH_4$ (17 mg, 0.45 mmol) was added, followed by the dropwise addition of 1 mL of MeOH. After 5 min to the solution was added TFA (trifluoroacetic acid, 0.1 mL) and 1 g of silica gel, and the solvent was removed by rotary evaporation. The resulting white solid was loaded on the top of a column, and quickly filtered over a pad of silica gel (20 gr) using diethyl ether/dichloromethane (1:20) as an eluent. The solvent of the fraction containing the desired compound **3** was evaporated, to give chemically pure material.

Acknowledgments

We wish to thank Sapienza Università di Roma for financial support through "Progetto di Ateneo" 2014 and 2015. We are indebted to Prof. Luca Bernardi and Prof. Luigi Mandolini for several useful discussions, to Prof. Ruggero Caminiti for providing computing time on the NARTEN Cluster HPC Facility, to Dr. Antonello Alvino for mass spectra and to Dr. Roberto Cirilli for the HPLC of compound **3m**.

Keywords: atropisomers · biaryls · chirality · density-functional calculations · organocatalysis

How to cite: *Angew. Chem. Int. Ed.* **2016**, *55*, 6525–6529
Angew. Chem. **2016**, *128*, 6635–6639

[1] a) G. Bringmann, T. Gulder, T. A. M. Gulder, M. Breuning, *Chem. Rev.* **2011**, *111*, 563–639; b) E. N. Jacobsen, A. Pfaltz, H. Yamamoto, *Comprehensive Asymmetric Catalysis*, Springer,

New York, **2004**; c) T. Akiyama, *Chem. Rev.* **2007**, *107*, 5744 – 5758; d) I. Ojima, *Catalytic Asymmetric Synthesis, 3rd ed.*, Wiley, **2010**; e) C. A. Busacca, D. R. Fandrick, J. J. Song, C. H. Senanayake, *Adv. Synth. Catal.* **2011**, *353*, 1825 – 1864; f) Q.-L. Zhou, *Privileged Chiral Ligands and Catalysts*, Wiley-VCH, Weinheim, **2011**.

[2] a) Y. Chen, S. Yekta, A. K. Yudin, *Chem. Rev.* **2003**, *103*, 3155 – 3212; b) J. M. Brunel, *Chem. Rev.* **2007**, *107*, PR1 – PR45; c) M. Berthod, G. Mignani, G. Woodward, M. Lemaire, *Chem. Rev.* **2005**, *105*, 1801 – 1836; d) G. Adair, S. Mukherjee, B. List, *Aldrichimica Acta* **2008**, *41*, 31 – 39; e) M. van Gemmeren, F. Lay, B. List, *Aldrichimica Acta* **2014**, *47*, 3 – 13; f) T. Hashimoto, K. Maruoka, *Chem. Rev.* **2007**, *107*, 5656 – 5682.

[3] C. Rosini, L. Franzini, A. Raffaelli, P. Salvadori, *Synthesis* **1992**, 503 – 517.

[4] a) P. Kočovský, Š. Vyskočil, M. Smrčina, *Chem. Rev.* **2003**, *103*, 3213 – 3245; b) D. J. Ramon, M. Yus, *Chem. Rev.* **2006**, *106*, 2126 – 2208; c) M. Shibasaki, S. Matsunaga, *Chem. Soc. Rev.* **2006**, *35*, 269 – 279.

[5] a) H. U. Blaser, H.-J. Federsel, *Asymmetric Catalysis On Industrial Scale*: *Challenges*, *Approaches*, *And Solutions*, 2nd ed., Wiley-VCH, Weinheim, **2010**; b) A. Berkessel, H. Gröger, *Asymmetric Organocatalysis*: *From Biomimetic Concepts to Applications in Asymmetric Synthesis*, Wiley-VCH, Weinheim, **2005**, Chap. 14; c) D. Cai, D. L. Hughes, T. R. Verhoeven, P. J. Reider, *Org. Synth.* **1999**, *76*, 1 – 3.

[6] a) J. L. Gustafson, D. Lim, S. J. Miller, *Science* **2010**, *328*, 1251 – 1255; b) M. E. Diener, A. J. Metrano, S. Kusano, S. J. Miller, *J. Am. Chem. Soc.* **2015**, *137*, 12369 – 12377; c) R. Miyaji, K. Asano, S. Matsubara, *J. Am. Chem. Soc.* **2015**, *137*, 6766 – 6769.

[7] a) B. Török, M. Abid, G. London, J. Esquibel, M. Török, S. C. Mhadgut, P. Yan, G. K. S. Prakash, *Angew. Chem. Int. Ed.* **2005**, *44*, 3086 – 3089; *Angew. Chem.* **2005**, *117*, 3146 – 3149; b) S. Brandes, M. Bella, A. Kjaersgaard, K. A. Jorgensen, *Angew. Chem. Int. Ed.* **2006**, *45*, 1147 – 1151; *Angew. Chem.* **2005**, *118*, 1165 – 1169; c) S. Brandes, B. Niess, M. Bella, A. Prieto, J. Overgaard, K. A. Jorgensen, *Chem. Eur. J.* **2006**, *12*, 6039 – 6052; d) T. Y. Liu, H. L. Cui, Q. Chai, J. Long, B. J. Li, Y. Wu, L. S. Ding, Y. C. Chen, *Chem. Commun.* **2007**, 2228 – 2230; e) X.-S. Wang, C.-W. Zheng, S.-L. Zhao, Z. Chai, G. Zhao, G.-S. Yang, *Tetrahedron: Asymmetry* **2008**, *19*, 2699 – 2704; f) E. Paradisi, P. Righi, A. Mazzanti, S. Ranieri, G. Bencivenni, *Chem. Commun.* **2012**, *48*, 11178 – 11180. For a review see: g) G. Bencivenni, *Synlett* **2015**, *26*, 1915 – 1922.

[8] a) J. Alemán, B. Richter, K. A. Jørgensen, *Angew. Chem. Int. Ed.* **2007**, *46*, 5515 – 5519; *Angew. Chem.* **2007**, *119*, 5611 – 5615; b) J. Alemán, S. Cabrera, E. Maerten, J. Overgaard, K. A. Jørgensen, *Angew. Chem. Int. Ed.* **2007**, *46*, 5520 – 5523; *Angew. Chem.* **2007**, *119*, 5616 – 5619.

[9] a) Gaussian 09 (Revision D.01), > M. J. Frisch, et al., Gaussian, Inc., Wallingford CT, **2010**; b) A. Ciogli, A. D. Cort, F. Gasparrini, L. Lunazzi, L. Mandolini, A. Mazzanti, C. Pasquini, M. Pierini, L. Schiaffino, F. Y. Mihan, *J. Org. Chem.* **2008**, *73*, 6108 – 6118.

[10] "Chiral Separation" in Annual Review of A. M. Stalcup, *Anal. Chem.* **2010**, *3*, 341 – 363.

[11] a) M. Bella, D. M. S. Schietroma, P. P. Cusella, T. Gasperi, V. Visca, *Chem. Commun.* **2009**, 597 – 599; b) S. Abele, R. Inauen, D. Spielvogel, C. Moessner, *J. Org. Chem.* **2012**, *77*, 4765 – 4773.

[12] While this manuscript was in preparation, an important paper by Tan, Liu, and co-workers appeared and described a similar reaction catalyzed by chiral phosphoric acids rather than bases. The authors demonstrated in a preliminary experiment the effectiveness of the aryl diols as chiral ligands in the asymmetric addition of diethyl zinc to aldehydes, and the enantioselectivity achieved by the chiral diols in this reaction was even superior to C_2-symmetrical 2,2′ binaphthol. We believe that the two methodologies can be complementary with regards to the reaction conditions and scope. Y. H. Chen, D. J. Cheng, J. Zhang, Y. Wang, X. Y. Liu, B. Tan, *J. Am. Chem. Soc.* **2015**, *137*, 15062 – 15065.

[13] The preparation of similar chiral diols, albeit in racemic form, has also been very recently published in this journal: H. Gao, Q. L. Xu, C. Keene, M. Yousufuddin, D. H. Ess, L. Kurti, *Angew. Chem. Int. Ed.* **2016**, *55*, 566 – 571; *Angew. Chem.* **2016**, *128*, 576 – 581.

Received: February 16, 2016
Published online: April 20, 2016

Catalysis Science & Technology

PAPER

Cite this: *Catal. Sci. Technol.*, 2016, 6, 2280

Kinetic resolution of phosphoric diester by *Cinchona* alkaloid derivatives provided with a guanidinium unit†

Riccardo Salvio,*[ab] Mauro Moliterno,[a] Dario Caramelli,[a] Luca Pisciottani,[a] Achille Antenucci,[a] Melania D'Amico[a] and Marco Bella[a]

Received 29th July 2015,
Accepted 11th November 2015

DOI: 10.1039/c5cy01208b

www.rsc.org/catalysis

Cinchona alkaloid derivatives featuring a guanidinium group in diverse positions efficiently catalyze the cleavage of the RNA model compound 2-hydroxypropyl *p*-nitrophenyl phosphate (HPNP). Their high catalytic efficiency as phosphodiesterases and the potentiometric and kinetic investigations indicate the existence of a high degree of cooperation between the guanidinium group and the quinuclidine moiety with the operation of a general acid/general base mechanism. The performance of these compounds was investigated and compared in the kinetic resolution of HPNP. These data were also compared with the results of DFT calculations on the transition states of the transesterification reaction that, in part, predict and rationalize the experimental data.

Introduction

The relevance of phosphodiester bonds in biology and chemistry and their reluctance towards hydrolysis[1] have encouraged many scientists to design and synthesize artificial catalysts able to cleave DNA, RNA and their model compounds[2–4] with the idea of using these systems in health-related targets, such as antisense therapy.[4a,5]

Most bifunctional small-molecule enzyme-mimics contain metal cations as catalytically active groups, typically Cu^{II} and Zn^{II}.[2,3] In addition or alternatively to metal ions several artificial catalysts feature other functions as active components. These moieties play the role of anchoring sites, activators and general bases. Among these components the guanidinium group has a noteworthy importance because it has been successfully employed in the design of enzyme mimics.[2b,4] This group can interact, due to its planar and rigid structure and its geometrical complementarity, with the phosphate anion through the formation of a two-point hydrogen bonding chelate motif.[6] In nature this guanidinium–oxanion interaction is frequently observed in enzymes and antibodies.[2b,7]

In artificial phosphodiesterases, as in all supramolecular catalysts, a primary role is played by the molecular scaffold that must be a compromise between preorganization and flexibility, keeping the active functions at the proper distance and in a favourable orientation. Diverse non chiral spacers have been used in the design of these artificial catalysts such as terpyridine,[4i] 2,2′-dipyridyl,[4j] the xylylene unit,[4c,g,h] calix[4]arene[8] and diphenylmethane[4b] derivatives. Another promising and emerging strategy in the preparation of artificial phosphodiesterases is the use of nanostructured supports, *i.e.* gold monolayer protected clusters[2a,9] (Au MPC) and polymer brushes,[10] as spacers for the active units.

In the present study we designed and developed guanidinium-based artificial phosphodiesterases derived from quinine, one of the naturally occurring *Cinchona* alkaloids. These compounds have attracted exceptional attention in the field of asymmetric catalysis[11] because of their ability to efficiently mediate a number of asymmetric reactions together with their commercial availability as enantiopure compounds. In their underivatized form, they can act as chiral Brønsted bases due to their quinuclidine moiety. They can be easily modified in order to improve their catalytic efficiency in enantioselective synthesis. In particular, the most common derivatives are amino derivatives[12] capable of activating carbonyl compounds *via* enamine or iminium ion formation, quaternary ammonium salts acting as phase-transfer catalysts[13] and bifunctional catalysts equipped with an additional H-bond donor moiety.[14]

[a] *Dipartimento di Chimica, Università di Roma – Sapienza, Italy. E-mail: riccardo.salvio@uniroma1.it; Tel: +39 06 4969 3656*
[b] *IMC-CNR Sezione Meccanismi di Reazione, Università di Roma – Sapienza, Italy*

† Electronic supplementary information (ESI) available: ^{1}H and ^{13}C spectra of compounds, distribution diagrams, titrations, kinetic experiments, energies and coordinates of DFT calculations. See DOI: 10.1039/c5cy01208b

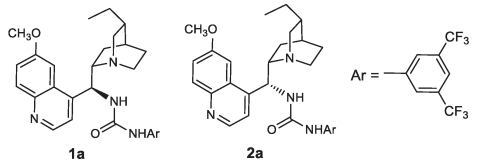

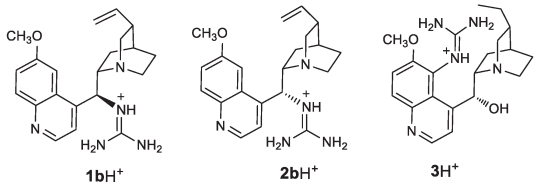

In the present study we have synthesized and investigated compounds **1b**, **2b** and **3**, featuring a guanidinium unit and a tertiary amine in different relative positions and orientations on a *Cinchona* alkaloid scaffold, as catalysts in the transesterification of the RNA model compound 2-hydroxypropyl *p*-nitrophenyl phosphate (HPNP, eqn (1)).

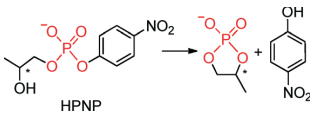

(1)

Compounds **1b** and **2b** differ in the configuration at C9, which can be crucial for catalyst performance as observed by Connon *et al.* with the urea-substituted *Cinchona* alkaloid derivatives **1a** and **2a** which exhibit dramatically different yields and enantioselectivity as bifunctional catalysts in the addition of malonate to nitroalkenes.[15]

Potentiometric and kinetic evidence are presented to evaluate the catalytic efficiency and propose a catalytic mechanism. The different performances of the three catalysts are also compared in the kinetic resolution of HPNP. DFT calculations on the transition states of the transesterification reaction complement kinetic investigation, providing a useful rationalization of the experimental results. In the present paper we have highlighted the importance and the uniqueness of using a chiral spacer such as quinine derivatives for the synthesis of artificial phosphodiesterases, considering the fact that DNA and RNA are chiral molecules.

Results and discussion

Synthesis of the catalysts

The guanidine derivative **1b** was synthesized starting from 9-amino(9-deoxy)*epi* quinine (**4**)[14a] using *N*,*N*′-di-Boc-thiourea and $HgCl_2$,[16] followed by the removal of protecting groups to afford the product as trihydrochloride **1b**·3HCl (Scheme 1).

The preparation of compound **2b** was carried out starting from the 9-epiquinine **6**[17] through steps a–e illustrated in Scheme 2. Direct synthesis of compound **9** from 9-epiquinine through the Mitsunobu reaction afforded the desired

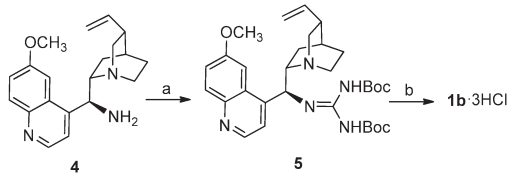

Scheme 1 Synthesis of quinine derivative **1b** starting from 9-amino(9-deoxy)*epi* quinine **4**. Reagents and conditions: (a) BocNHC(*S*)NHBoc, $HgCl_2$, Et_3N, DMF, 12 h, rt, yield: 53%; (b) 0.1 M HCl, 1,4-dioxane, 12 h, rt, yield: 97%.

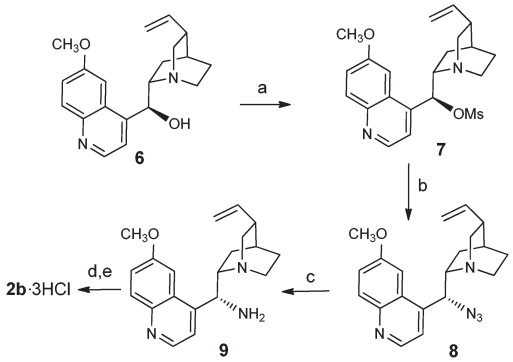

Scheme 2 Synthesis of catalyst **2b** starting from epiquinine **6**. Reagents and conditions: a) MsCl, Et_3N, THF, 3.5 h, rt, yield: 40%; b) NaN_3, DMF, 80 °C, 3 h, yield: 69%; c) PPh_3 in H_2O/THF 80 °C, 3 h, yield 48%; and d, e) as in steps a and b in Scheme 1, yields: 86% and 73%.

compound in low yield. For this reason the synthesis was carried out by converting the alcohol **6** into its mesylate followed by substitution with NaN_3 and reduction with PPh_3 (steps a–c, Scheme 2). The guanidinylation on the 5′ position affording compound **3** was carried out starting from the dihydroquinine derivative **10**[18] with the same guanidinylation method used for the synthesis of **1b** and **2b**.

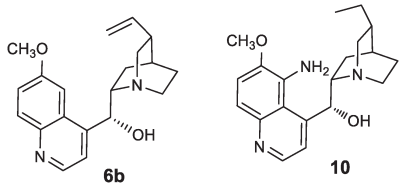

Potentiometric titrations

Determination of the acidity constants of the investigated compounds is a prerequisite for the kinetic study of their catalytic properties. The potentiometric titrations were carried out in 80 : 20 DMSO : H_2O v/v, hereafter referred to as 80% DMSO. In this polar and protic solvent mixture, which is known to be suitable for the investigation of phosphoryl transfer reactions[4b,8,19] and for potentiometric measurements,[20] the autoprotolysis of water is strongly suppressed,

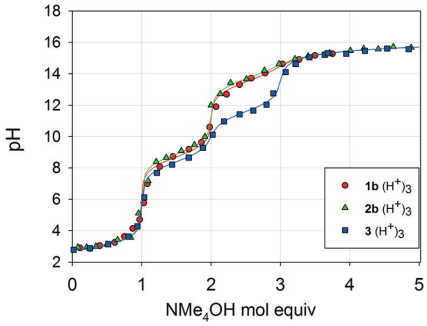

Fig. 1 Potentiometric titrations of trihydrochlorides of **1b**, **2b** and **3** (2 mM) with Me_4NOH in 80% DMSO at 25 °C in the presence of 10 mM NMe_4ClO_4. Data points are experimental and the lines are calculated.

pK_w = 18.4 at 25 °C,[21] and this implies that a neutral solution corresponds to pH 9.2. The results of the elaboration of the titration plots in Fig. 1 are summarized in Table 1, together with the acidity constants of aminoquinines **4** and **9** and the underivatized quinine (**6b**) reported for comparison.

Titrations showed three titratable protons for all the investigated compounds, except for **6b** that features only two acidic groups. **1b** and **2b** show a very similar potentiometric behavior, whereas the curve of the trihydrochloride of **3** significantly differs from that of the other two at higher pH values. The most acidic proton (pK_1 <2) can be attributed to the nitrogen atom of the quinoline unit. Acidity constants in that range cannot be accurately determined for titration carried out at millimolar concentration. This high acidity compared to that of quinolinium ion (pK_a = 4.90)[22] is probably due to the marked electrostatic repulsion between the positively charged units, which facilitates the departure of a proton from the quinoline moiety. pK_2 is similar for compounds **1b**, **2b** and **3**, ranging from 8.4 to 8.7, and can be attributed to the quinuclidine moiety.

The least acidic protons (pK_3) in entries 1–3 belong to the guanidinium unit. The curve relative to the quinine derivative $3(H^+)_3$ reveals a significantly higher acidity constant (pK_3, entry 3, Table 1) compared to the other two guanidine-substituted compounds (**1b** and **2b**) due to the higher acidity of aromatic guanidiniums compared to aliphatic ones.[4g,8,19]

Amino derivatives **4** and **9** show similar acidity constants (entries 4 and 5, Table 1). The least acidic proton (pK_3) can be attributed, in this case, to the quinoline unit. Consequently pK_2 is the constant associated with the deprotonation of the primary amine that is expected to be less basic than a tertiary amine. For comparison the dihydrochloride of quinine was also titrated in this set of experiments showing only two titratable protons with the acidity constants pK_1 and pK_2 indicated in entry 6 of Table 1.

Table 1 Acidity constants of *Cinchona* alkaloid derivatives in 80% DMSO at 25 °C[a]

Entry	Species	pK_1	pK_2	pK_3
1	**1b**$(H^+)_3$	<2	8.7	13.5
2	**2b**$(H^+)_3$	<2	8.9	13.7
3	**3**$(H^+)_3$	<2	8.4	11.6
4	**4**$(H^+)_3$	2.1[b]	7.9	9.0
5	**9**$(H^+)_3$	2.2[b]	8.0	8.9
6	**6b**$(H^+)_2$	3.5	8.6	—

[a] pK_i data measured from potentiometric titration plots in Fig. 1 and 4S–6S in the ESI. The titrations were carried out on 6 mL of 2 mM substrate solutions in the presence of NMe_4ClO_4. Experimental error = ±0.1 p*K* units unless otherwise stated. [b] Experimental error = ±0.3 p*K* units.

Kinetic measurements

The catalytic activity of **1b**, **2b** and **3** in the transesterification of the RNA model compound HPNP (eqn (1)) was investigated in the same solvent mixture and conditions used for the titrations (80% DMSO, 10 mM Me_4NClO_4, 25.0 °C).

A first set of kinetic experiments were carried out to evaluate the best pH value to carry out the measurements. Partial neutralization of 5.0 mM solutions of **1b**·3HCl with different amounts of Me_4NOH afforded a number of buffer solutions with pH values in the range of around 8–12, which were used for catalytic rate measurements of HPNP transesterification using the initial rate method. Pseudo-first-order rate constants (k_{obs}) for the cleavage of HPNP, corrected for background contributions[8] whenever appropriate (pH > 11), are reported in Fig. 2. The pH rate profile shows a maximum of activity around pH 10–12. If we assume that $\mathbf{1bH^+}$, the monoprotonated form of the catalyst, is the only catalytically active species (eqn (2)), k_{obs} can be given by eqn (3), where K_2 and K_3 are the acidity constants as defined in Table 1 and C_{cat} is the total catalyst concentration.

$$v = k_{cat}[1bH^+][HPNP] = k_{obs}[HPNP] \quad (2)$$

$$k_{obs} = \frac{k_{cat}C_{cat}}{\frac{K_3}{[H^+]} + \frac{[H^+]}{K_2} + 1} \quad (3)$$

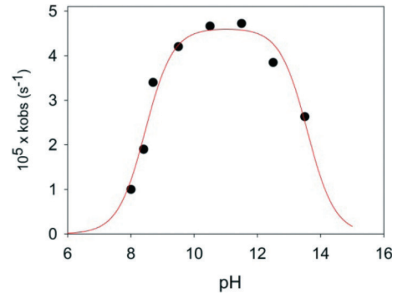

Fig. 2 k_{obs} *versus* pH for the cleavage of 0.10 mM HPNP catalyzed by 5.0 mM **1b** in 80% DMSO, 25.0 °C, 10 mM Me_4NClO_4. The rate constants measured at pH >11 were corrected for background hydrolysis at the given pH.

The data in Fig. 2 can be fitted to a good precision to eqn (3). The acidity constants (K_2, K_3) and k_{cat} were treated as adjustable parameters in a nonlinear least-squares fitting procedure. The following values of best fit parameters were obtained: pK_2 = 8.45 ± 0.12, pK_3 = 13.58 ± 0.13, and k_{cat} = (9.2 ± 0.4) × 10^{-3} M^{-1} s^{-1}.

The nice fit of data points to eqn (3) and the good agreement of the kinetically determined acidity constant values with the potentiometrically determined ones (pK_2 and pK_3 of entry 1 in Table 1) are clearly consistent with the idea that **1b**H^+ is the sole active species and indicate the operation of a bifunctional mechanism in which the guanidinium is acting as an electrophilic activator and the quinuclidine moiety is acting as a general base (Fig. 3).

In a second set of kinetic experiments a number of buffered solutions (pH = 8.7) of catalyst **1b** at different concentrations were used for the transesterification of HPNP. The results of the kinetic experiments are graphically shown in Fig. 7S (pag. 13S, ESI†) as plots of pseudo-first-order rate constants (k_{obs}, s^{-1}) of HPNP cleavage *versus* total catalyst concentration (C_{cat}). Data points could be fitted to a straight line with the following value of best fit parameter: k_2 = (7.6 ± 0.5) × 10^{-3} s^{-1} M^{-1}. This finding indicates that the catalysts do not significantly bind to the substrate in the investigated concentration range. This evidence is in agreement with the fact that the guanidinium–phosphate interaction has a weak binding constant in water and water/DMSO mixtures (K <20 M^{-1}).[2b,19]

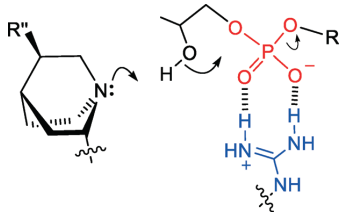

Fig. 3 Proposed bifunctional mechanism for the cleavage of RNA models catalyzed by guanidine-substituted quinine derivatives involving the synergic action of a general base and an electrophilic activator.

Furthermore the straight line resulting from the fitting procedure shows an intercept close to zero, confirming that the contribution of background hydrolysis to the overall rate is negligible.

The phosphodiesterase activity of the other two catalysts (**2b** and **3**) was also investigated and the results of the kinetic experiments are reported in Table 2 together with the results obtained in the presence of the catalysts lacking the guanidinium unit (**4**, **9** and **6b**) that were tested in control experiments. Solutions of trihydrochloride precatalysts were partially neutralized with 1.5 molar equivalents of Me_4NOH. In the resulting buffer solutions the predominant species are the di- and monoprotonated forms of the catalysts (see distribution diagrams calculated using the acidity constants in Table 1 and Fig. 1S–3S, ESI†). These buffer solutions were used for the transesterification of HPNP with the initial rate method.

HPNP transesterification in the presence of 5.0 mM catalysts were in all cases much faster than background transesterification (k_{bg}). The rate enhancements (k_{obs}/k_{bg}) cluster around 5 × 10^3-fold and reach four orders of magnitude in the case of the guanidine derivative **1b** (entries 1–3 in Table 2). The three catalysts also exhibit a different catalytic activity towards the two enantiomers of HPNP. For the general case in which the pseudo-first-order rate constants of the two HPNP enantiomers, k_{obs}^R and k_{obs}^S, are different the integrated kinetic equation for the formation of *p*-nitrophenol is given by (4).[23] For the particular case in which there is no kinetic resolution (k_{obs}^R = k_{obs}^S = k_{obs}) the concentration of *p*-nitrophenol is given by the well-known simpler eqn (5).

$$[p\text{NPhOH}] = [\text{HPNP}]_o\left(1 - \frac{e^{-k_{obs}^R t} + e^{-k_{obs}^S t}}{2}\right) \quad (4)$$

$$[p\text{NPhOH}] = [\text{HPNP}]_o(1 - e^{-k_{obs}t}) \quad (5)$$

The full time-course profile of the HPNP transesterification in the presence of catalyst **1b** significantly deviates from the ordinary first-order behavior of eqn (5) (see Fig.

Table 2 Transesterification of HPNP catalyzed by the listed catalysts (80% DMSO, 25 °C)[a]

Entry	Precatalyst	pH	$10^6 \times k_{obs}(S)$[b] (s^{-1})	$10^6 \times k_{obs}(R)$[b] (s^{-1})	$k_{obs}(S)/k_{obs}(R)$	$10^6 \times k_{obs}$[d] (s^{-1})	$10^{10} \times k_{bg}$[e] (s^{-1})	k_{obs}/k_{bg}
1	**1b**$(H^+)_3$	8.7	62	11.6	5.2	34	32	10 600
2	**2b**$(H^+)_3$	8.9	18.3	6.0	3.0	12	50	2400
3	**3**$(H^+)_3$	8.4	13.5	3.9	2.4	8.7	16	5400
4	**4**$(H^+)_3$	7.9	—[c]	—[c]	—	0.08	5.0	160
5	**9**$(H^+)_3$	8.0	—[c]	—[c]	—	0.12	6.3	190
6	**6b**$(H^+)_2$	8.6	—[c]	—[c]	—	0.10	25	40

[a] 5 mM, $[HPNP]_i$ = 0.1 mM, 10 mM NMe_4ClO_4. [b] Determined by UV-vis measurements using the full time-course method by fitting to eqn (4) and confirmed by HPLC separation with a chiral column (see ref. 23, Experimental section and the ESI for details), error limit = ±12%. [c] Too slow to be measured with the full time-course method. [d] Pseudo-first-order specific rates k_{obs} measured with the initial rate method and calculated as $v_o/[HPNP]$, where v_o is the spectrophotometrically determined rate of *p*-nitrophenol liberation. Error limit = ±5% unless otherwise stated. [e] The spontaneous transesterification rate at the given pH is calculated by the following equation: $k_{bg} = 10^{(pH-17.2)}$, see ref. 8.

8S, ESI†), but it can be fitted to good precision to eqn (4). The values of $k_{obs}{}^{R}$ and $k_{obs}{}^{S}$ were treated in the fitting procedure as adjustable parameters obtaining the values reported in Table 2. The data about the kinetic resolution were confirmed by chiral HPLC chromatography of reaction mixtures quenched with acidic solutions at proper time intervals (see the Experimental section and ESI†).

The compounds which are not provided with the guanidinium unit exhibit a dramatically lower activity in the HPNP transesterification (entries 4–6 of Table 2). This experimental evidence proves that the presence of the guanidinium unit is a key requisite to obtain high catalytic efficiency and confirm the postulated mechanism depicted in Fig. 3. On the basis of kinetic data reported by Yatsimirsky *et al.* on the cleavage of HPNP catalyzed by amines and guanidine derivatives[19] it was possible to evaluate the effectiveness of the investigated catalytic scaffold in terms of effective molarity (EM). The EM values for compounds **1b**, **2b** and **3** are estimated to be in the range 1–5 M.

Ab initio calculations

The mechanism proposed on the basis of the kinetic measurements and schematically depicted in Fig. 3 was also quantitatively investigated by *in silico* experiments. DFT calculations were carried out with the Gaussian 09 package[24] at the b3lyp/6–31 g(d,p)//b3lyp/6–31 g(d,p) level of theory. The Berny optimization using the GEDIIS algorithm was used for the optimization procedure of the transition states of the HPNP transesterification catalyzed by catalysts **1bH**$^+$, **2bH**$^+$ and **3H**$^+$ (see the Experimental section and ESI† for further details and for the coordinates of all the optimized structures). The polarized continuum model was used to take into account the solvent effect, setting a dielectric constant value of 72, that is the experimental value measured in bulk for a DMSO : H_2O 80 : 20 mixture.[19] All the TS structures feature a single imaginary frequency. The animation of the normal mode of vibration with a negative spring constant confirms that the saddle points obtained from the optimization procedure are actually the transition states of the HPNP transesterification. Fig. 4 shows as an example the TS structure of **1bH**$^+$·(*R*)-HPNP. The geometry of the guanidinium-phosphate group and the H_2–O_3 and H_3–O_4 distances (average value = 1.72 Å) indicate the presence of a chelate hydrogen bonding and not only a mere electrostatic interaction. The bond between the hydrogen atom H_1 of the HPNP hydroxyl group and the oxygen atom O_1 is breaking and a new bond is forming between the hydrogen and the quinuclidine nitrogen N_1. The distances of the bonds involved in the proton transfer (O_1–H_1 = 1.42 Å, H_1–N_1 = 1.15 Å) indicate a late transition state. The distances O_1–P (2.08 Å) and O_2–P (1.86 Å), compared with the average P–O distance of phosphodiesters,[2b] indicate the forthcoming formation of a sigma bond and the breaking of the oxygen–phosphorus bond of the leaving group. In addition, the O_3–P–O_4 angle is 121,3°, therefore significantly different from the tetrahedral geometry of the phosphate group of a phosphodiester. These findings suggest the operation of an A_ND_N concerted mechanism rather than an A_N + D_N,[2a,b] also labeled by Kirby as $S_N2(P)$,[25] consistent with the presence of a good leaving group such as the *p*-nitrophenolate.[26]

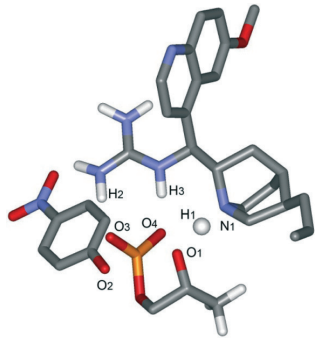

Fig. 4 Transition state structure (DFT calculations) for the transesterification of (*R*)-HPNP catalyzed by **1bH**$^+$. Some of the hydrogen atoms are omitted for clarity.

The results of the calculations on the transition states of HPNP transesterification catalyzed by the investigated compounds are reported in Table 3. The difference in the energies of the transition states for the two enantiomers is significantly higher in the presence of catalyst **1bH**$^+$. In the case of the other two catalysts the energy difference is much lower and does not reach 1 kcal mol^{-1}. On the basis of this energy difference the ratio between the observed rate constants of the two enantiomers was calculated using the Eyring equation. These values are in fair agreement with the experimental data in the last column of Table 2. (*S*)-HPNP turns out to be more reactive than the (*R*) enantiomer in all cases. This is probably due to the repulsive interaction of the (*R*)-HPNP methyl group with the bulky quinine scaffold, specifically with the quinuclidine moiety (see Fig. 4). The largest energy difference is predicted in the presence of **1bH**$^+$, as observed in the kinetic measurements, even though a larger rate constant ratio is calculated for a difference of 2.1 kcal mol^{-1}.

Table 3 Differences in the transition state energies (DFT calculations) for the transesterification of the two HPNP enantiomers catalyzed by the listed species and corresponding calculated ratio of the rate constants of the reactions

Catalyst	$\Delta E^{\neq}$ ($E^{\neq}{}_R - E^{\neq}{}_S$) [a] (kcal mol^{-1})	$k_{obs}(S)/k_{obs}(R)$ calcd[b]
1bH$^+$	2.11	36
2bH$^+$	0.13	1.2
3H$^+$	0.81	3.9

[a] Differences between the energies of the transition states corrected for the zero-point vibrational energy determined by frequency calculation; DFT b3lyp/6 31 g(d,p)//b3lyp/6 31 g(d,p), PCM, ε = 72.0. See the ESI and the Experimental section for further details and for the coordinates of all the optimized structures. [b] Ratio of the transesterification rate constants $k_{obs}(S)$ and $k_{obs}(R)$, calculated with the Eyring equation, on the basis of the energy differences obtained by *ab initio* calculations.

Conclusions

Here we have presented the design, synthesis and investigation on the catalytic activity of quinine-derived guanidines as phosphodiesterases. These compounds feature a guanidinium unit in diverse positions on the molecular scaffold. Potentiometric and kinetic investigations at different pH and catalyst concentrations demonstrate the operation of a general acid/general base mechanism (Fig. 3 and 4). Species **1bH$^+$**, **2bH$^+$** and **3H$^+$** turn out to be very effective catalysts of HPNP transesterification with rate enhancements relative to the background hydrolysis, approaching four orders of magnitude in the case of **1bH$^+$**. These data suggest that the configuration of C9 plays a crucial role in modulating the activity of the catalysts. Interestingly the same compound is slightly stereoselective in the kinetic resolution of HPNP. This experimental evidence is supported by DFT calculations on the transition states of transesterification which confirm the postulated mechanism. The calculations show geometrical complementarity between the catalysts and the substrate and quantitatively predict, with fairly good agreement with experimental data, the ratio between the observed rate constants of the transesterification reaction. These results provide a useful comparison between experimental and *in silico* data which are potentially useful in the design of artificial ribonucleases, and, in general, in catalysis by design.

Experimental section

Instruments and general methods

^{1}H and ^{13}C NMR spectra were recorded on a Bruker 300 MHz spectrometer. Chemical shifts are reported as δ values in ppm. In some cases small amounts of TMS or dioxane were used as an internal standard. High-resolution mass-spectrometric analysis was performed on an electrospray ionization time-of-flight spectrometer. *Ab initio* calculation were carried out with the Gaussian 09 (Revision D.01) package[24] using Narten Cluster – Dipartimento di Chimica - Sapienza. Chiral HPLC separation was performed employing a CHIRALPAK IA column.

Materials

HPNP,[27] 9-amino(9-deoxy)*epi* quinine (**4**,)[14a] 9-epiquinine (**6**),[17] and 5′-aminodihydro quinine (**10**)[18] were prepared as reported in the literature. DMSO was purged for 30 min with argon to eliminate volatile sulphide impurities and mQ water was used in the preparation of 80 : 20 DMSO : H_2O v/v. Anhydrous dichloromethane was obtained by distillation over $CaCl_2$. Triethylamine was distilled over KOH. Anhydrous THF was obtained by distillation over Na. Other reagents and solvents were commercially available and used without any further purification.

9-Bis[4-(*N*,*N*-di(*tert*-butoxycarbonyl)guanidine(9-deoxy)*epi* quinine (5). 507 mg of 9-amino(9-deoxy)*epi* quinine (**4**, 1.57 mmol), *N*,*N*′-di-Boc-thiourea (362 mg, 1.31 mmol) and 0.50 mL of triethylamine were dissolved in dry DMF under an argon atmosphere. The reaction flask was cooled down to 0 °C and $HgCl_2$ (354 mg, 1.31 mmol) was added to the solution. The mixture was stirred for 12 h at room temperature. Then 10 mL of ethyl acetate were added and the HgS was eliminated by filtration through a pad of Celite. A pure sample of **5** was obtained by flash column chromatography (SiO_2, AcOEt/hexane 3 : 2) as a colorless sticky solid (395 mg, 53% yield). ^{1}H NMR (300 MHz, $CDCl_3$): δ 1.39 (s, 9H), 1.44 (s, 9H), 1.55–1.85 (m, 6H), 2.35 (bs, 1H), 2.70–3.05 (m, 2H), 3.21–3.59 (m, 3H), 4.0 (s, 3H), 5.04 (m, 2H), 5.81 (m, 1H), 7.33–7.42 (m. 2H), 7.83 (s, 1H), 8.03 (d, 1H, 12 Hz), 8.75 (s, 1H), 8.77 (s, 1H), 11.32 (s, 1H). ^{13}C NMR (75 MHz, $CDCl_3$): δ 26.9, 27.5, 27.8, 28.1, 28.2, 39.5, 41.3, 55.8, 56.1, 59.3, 78.5, 82.9, 102.1, 114.5, 119.7, 122.3, 128.5, 131.3, 161.6, 144.4, 144.8, 147.4, 152.8, 155.4, 157.9, 163.3. HR ES-MS: *m*/*z* calcd for $C_{31}H_{44}N_5O_5$ $(M+H)^+$: 566.3342, found 566.3336.

9-Guanidine(9-deoxy)*epi* quinine tris-hydrochloride (1b·3HCl). A solution of compound **5** (136 mg, 0.240 mmol) in 20 mL of a 1 : 1 v/v mixture of dioxane and 0.5 M hydrochloric acid was stirred for 12 hours at room temperature. Evaporation of the solvent gave compound **1**·3HCl as a white sticky solid (111 mg, 0.234 mmol, 97% yield). ^{1}H NMR (300 MHz, D_2O): δ 1.26–1.44 (m, 1H), 1.63–1.77 (tr, 1H, J = 12 Hz), 1.97–2.20 (m, 3H), 2.81–2.96 (m, 2H), 3.41–3.56 (m, 2H), 3.67–3.80 (tr, 1H, J = 14 Hz), 3.90–4.02 (m, 1H), 4.08 (s, 3H), 4.13–4.25 (m, 1H), 5.08–5.25 (m, 2H), 5.70–5.88 (m, 1H), 7.79–7.93 (m, 2H), 8.12–8.28 (m, 2H), 9.00 (d, 1H, 6 Hz). ^{13}C NMR (75 MHz, D_2O): δ 23.4, 24.0, 26.1, 30.2, 36.3, 43.0, 54.1, 57.5, 60.7, 103.4, 117.3, 121.7, 124.0, 128.6, 130.1, 134.7, 137.8, 141.4, 150.9, 157.3, 161.8. HR ES-MS: *m*/*z* calcd for $C_{21}H_{28}N_5O$ $(M+H)^+$ 366.2294, found 366.2289.

9-Methanesulfonate(9-deoxy)*epi* quinine (7). 2.71 g of **6** (8.35 mmol) and 4.6 mL of triethylamine were dissolved in dry THF under a nitrogen atmosphere. The reaction flask was cooled down to 0 °C and mesyl chloride (1.33 ml, 17.2 mmol) was added dropwise to the solution. The mixture was stirred for 30 minutes at 0 °C and then 3.5 hours at room temperature. After that the solvent was evaporated under reduced pressure. The residue was dissolved in dichloromethane (400 mL) and washed with a 3.5% $NaHCO_3$ aqueous solution (3 × 200 mL). The organic phase was dried over Na_2SO_4 and evaporated. The crude material was purified by column chromatography (SiO_2; CH_2Cl_2/MeOH 14 : 1) giving a pale yellow amorphous solid (1.351 g, 3.36 mmol, 40% yield). ^{1}H NMR (300 MHz, $CDCl_3$): δ 0.63–0.75 (m, 1H), 1.27–1.48 (m, 1H), 1.49–1.58 (m, 2H), 1.60–1.67 (m, 1H), 2.20–2.32 (bs, 1H), 2.72–2.85 (m, 2H), 2.88–3.07 (bs, 3H), 3.15–3.28 (m, 1H), 3.25–3.50 (br, 2H), 3.94 (s, 3H), 4.90–5.05 (m, 2H), 5.62–5.87 (m, 1H), 6.30 (bs, 1H), 7.37 (d, 1H, J = 3 Hz), 7.40 (d, 1H, J = 3 Hz), 7.46 (m, 1H), 8.03 (d, 1H, 9 Hz), 8.76 (s, 1H). ^{13}C NMR (75 MHz, $CDCl_3$): δ 24.9, 27.2, 27.6, 39.0, 39.2, 41.0, 55.5, 59.6, 76.6, 100.4, 114.5, 119.6, 122.1, 127.2, 131.9, 139.6, 141.2, 144.8, 147.3, 158.3. HR ES-MS: *m*/*z* calcd for $C_{21}H_{27}N_2O_4S$ $(M+H)^+$: 403.1692, found 403.1685.

9-Azido(9-deoxy) quinine (8). 1.35 g of 9-methanesulfonate-(9-deoxy)*epi* quinine (7, 3.36 mmol) were dissolved in DMF

under a nitrogen atmosphere. Sodium azide (0.813 g, 12.5 mmol) was added to the solution. The mixture was stirred for 3 hours at 80 °C and then one night at room temperature. After that the mixture was evaporated under reduced pressure. 400 mL of a 1 M NaOH aqueous solution and dichloromethane (400 mL) were added to the residue. The organic phase was separated, washed with a 1 M NaOH aqueous solution (3 × 200 mL), and dried over Na_2SO_4. The solvent was evaporated and the crude material was purified by column chromatography (SiO_2; CH_2Cl_2/MeOH 100 : 1). Compound **8** was obtained as a white amorphous solid (0.813 g, 2.33 mmol, 69% yield). ^{1}H NMR (300 MHz, $CDCl_3$): δ 1.45–1.80 (m, 3H), 1.80–1.99 (m, 2H), 2.23–2.37 (m, 1H), 2.57–2.75 (m, 2H), 3.01–3.35 (m, 3H), 3.97 (s, 3H), 4.96–5.05 (m, 2H), 5.17–5.37 (bs, 1H), 5.70–5.89 (m, 1H), 7.30–7.36 (m, 1H), 7.36–7.43 (m, 2H), 8.06 (d, 1H, J = 9 Hz), 8.79 (d, 1H, J = 3 Hz). ^{13}C NMR (75 MHz, $CDCl_3$): δ 24.7, 27.2, 27.5, 39.4, 42.1, 55.8, 56.5, 58.4, 65.0, 101.0, 114.7, 119.5, 121.8, 127.0, 132.0, 141.3, 141.7, 144.9, 147.5, 158.2. HR ES-MS: m/z calcd for $C_{20}H_{24}N_5O$ $(M+H)^+$: 350.1981, found 350.1992.

9-Amino(9-deoxy) quinine (9). 2.46 g of 9-azido(9-deoxy)*epi* quinine (**8**, 7.04 mmol) and triphenylphosphine (4.14 mg, 15.8 mmol) were dissolved in dry THF under a nitrogen atmosphere. The mixture was stirred for 3 hours at 80 °C. After cooling 1 mL of water was added and the reaction mixture was stirred for 12 h at room temperature. Afterward the solvent was evaporated under reduced pressure and the residue was dissolved in 10% aqueous HCl (400 mL) and washed with dichloromethane (3 × 200 mL). 1 M NaOH aqueous solution was added to the water phase until alkaline pH was reached. The mixture was extracted with dichloromethane and the organic phase was dried over Na_2SO_4. The crude material was purified by column chromatography (SiO_2, CH_2Cl_2/MeOH 30:1). Compound **9** was obtained as a pale yellow oil (1.10 g, 3.41 mmol; 48% yield). ^{1}H NMR (300 MHz, $CDCl_3$): δ 1.45–1.63 (m, 2H), 1.64–1.78 (m, 2H), 1.83–1.95 (m, 2H), 2.08–2.21 (m, 1H), 2.24–2.35 (m, 1H), 2.47–2.75 (m, 2H), 2.95–3.12 (m, 2H), 3.13–3.26 (m, 1H), 3.96 (s, 3H), 4.65 (d, 1H, J = 9 Hz), 5.00–5.13 (m, 2H), 5.84–6.00 (m, 1H), 7.32–7.39 (m, 2H), 7.43 (d, 1H, J = 3 Hz), 8.02 (d, 1H, J = 12 Hz), 8.73 (d, 1H, J = 3 Hz). ^{13}C NMR (75 MHz, $CDCl_3$): δ 26.3, 27.7, 39.6, 41.9, 53.6, 55.6, 56.1, 60.5, 101.1, 114.4, 118.2, 121.1, 127.6, 131.9, 141.7, 144.7, 147.8, 149.1, 157.7. HR ES-MS: m/z calcd for $C_{20}H_{26}N_3O$ $(M+H)^+$: 324.2076, found 324.2089.

9-Bis[4-(*N*,*N*-di(*tert*-butoxycarbonyl)guanidine(9-deoxy) quinine (9b). 600 mg of 9-amino(9-deoxy) quinine (**9**, 1.86 mmol), *N*,*N*′-di-Boc-thiourea (513 mg, 1.86 mmol) and 0.8 mL of triethylamine were dissolved in dry DMF under a nitrogen atmosphere. The reaction flask was cooled down to 0 °C and $HgCl_2$ (1.25 g, 4.62 mmol) was added portionwise. The mixture was stirred for one night at room temperature and then 50 mL of ethyl acetate were added and the HgS precipitate was eliminated by filtration through Celite. After solvent removal at reduced pressure a pure sample of **9b** was obtained by flash column chromatography (SiO_2, CH_2Cl_2/MeOH/Et_3N 100 : 0.5 : 0.25) as a colorless white solid (904 mg, 86% yield): mp 150–152 °C. ^{1}H NMR (300 MHz, $CDCl_3$): δ 1.10–1.30 (m, 1H), 1.45 (s, 9H), 1.47 (s, 9H), 1.65–2.05 (m, 3H), 2.21–2.41 (m, 1H), 2.55–2.88 (m, 3H), 2.90–3.15 (m, 2H), 3.40–3.58 (m, 1H), 3.99 (s, 3H), 4.98–5.14 (m, 2H), 5.81–6.05 (m, 1H), 6.21–6.35 (m, 1H), 7.32–7.43 (m, 2H), 7.81 (s, 1H), 8.98 (d, 1H, J = 9 Hz), 8.71 (bs, 1H), 8.75 (d, 1H, J = 6 Hz), 11.43 (bs, 1H). ^{13}C NMR (75 MHz, $CDCl_3$): δ 25.1, 27.6, 28.0, 28.2, 39.5, 42.1, 46.1, 51.0, 56.1, 56.4, 58.3, 79.3, 83.7, 101.8, 114.6, 118.8, 122.4, 128.1, 131.5, 141.6, 144.3, 145.0, 147.5, 153.1, 156.3, 158.1, 163.3. HR ES-MS: m/z calcd for $C_{31}H_{44}N_5O_5$ $(M+H)^+$: 566.3342, found 566.3329.

9-Guanidine(9-deoxy) quinine tris-hydrochloride (2b·3HCl). A solution of compound **9b** (100 mg, 0.18 mmol) in 0.41 mL of TFA and 1 mL of dichloromethane was stirred for 2 hours at room temperature. The solution was evaporated, dried under vacuum, and the solid dissolved in 10 mL of 1 M HCl. Evaporation of the solvent gave the compound as a sticky white solid (142 mg, 0.142 mmol, 73% yield). ^{1}H NMR (300 MHz, D_2O): δ 1.91–2.49 (m, 4H), 2.65–2.75 (m, 1H), 2.80–2.98 (m, 1H), 3.05–3.55 (m, 3H), 3.58–3.78 (m, 1H), 4.11 (s, 3H), 4.28–4.48 (m, 1H), 5.15–5.38 (m, 2H), 5.85–5.95 (m, 1H), 5.95–6.10 (m, 1H), 7.83 (d, 1H, J = 12 Hz), 7.90–8.00 (m, 1H), 8.15–8.35 (m, 2H), 9.00–9.15 (m, 1H). ^{13}C NMR (75 MHz, D_2O): δ 23.7, 24.3, 25.9, 36.3, 43.5, 54.8, 57.4, 60.3, 63.1, 67.2, 102.3, 117.8, 121.5, 124.9, 128.7. HR ES-MS: m/z calcd for $C_{21}H_{28}N_5O$ $(M+H)^+$: 366.2294, found 366.2286.

5′-[(*N*,*N*-Di(*tert*-butoxycarbonyl)guanidine dihydroquinine (11). 252 mg of compound **10** (0.74 mmol), *N*,*N*′-di-Boc-thiourea (328 mg, 1.19 mmol) and 0.30 mL of triethylamine were dissolved in dry DMF under a nitrogen atmosphere. The reaction flask was cooled down to 0 °C and $HgCl_2$ (525 mg, 1.93 mmol) was added to the solution. The mixture was stirred for 24 h at room temperature and then 10 mL of ethyl acetate were added and the precipitated HgS was eliminated by filtration through Celite. A pure sample of **11** was obtained by flash column chromatography (SiO_2, AcOEt/MeOH 100 : 1) as a yellow sticky solid (151 mg, 0.26 mmol, 35% yield). ^{1}H NMR (300 MHz, $CDCl_3$): δ 0.87 (tr, 3H, J = 6 Hz), 1.34–1.48 (m, 4H), 1.53 (s, 18H), 1.58–1.75 (m, 2H), 1.77–1.87 (bs, 1H), 2.05–2.21 (m, 1H), 2.41 (d, 1H, J = 15 Hz), 2.57–2.72 (m, 1H), 2.91–3.13 (m, 2H), 3.47–3.67 (m, 1H), 4.08 (s, 3H), 5.49 (d, 1H, J = 9 Hz), 7.39 (d, 1H, J = 3Hz), 7.51 (d, 1H, J = 9Hz), 7.90 (d, 1H, J = 9 Hz), 8.71 (d, 1H, J = 3 Hz), 12.09 (bs, 1H). ^{13}C NMR (75 MHz, $CDCl_3$): δ 12.8, 25.4, 26.2, 28.8, 29.0, 38.1, 42.5, 57.9, 58.1, 58.5, 80.9, 82.6, 116.3, 119.5, 120.6, 121.5, 121.8, 127.0, 142.6, 144.7, 146.1, 149.2. HR ES-MS: m/z calcd for $C_{31}H_{46}N_5O_6^+$ $(M+H)^+$: 584.3448, found 584.3474.

5′-Guanidine dihydroquinine tris-hydrochloride (3·3HCl). A solution of compound **11** (26 mg, 0.044 mmol) in 4 mL of a 1 : 1 v/v mixture of dioxane and 0.1 M hydrochloric acid was stirred for 24 hours at room temperature. Evaporation of the solvent gave compound **3**·3HCl as a sticky white solid (16.1 mg, 0.042 mmol, 96% yield), mp 128–129 °C. ^{1}H NMR (300 MHz,): δ 0.87 (tr, 3H, J = 9 Hz), 1.25–1.43 (m,1H), 1.50–1.78 (m, 3H), 1.95–2.17 (m, 3H), 2.81–2.96 (m, 1H), 3.39–3.64 (m, 3H), 3.65–3.80 (m, 1H), 3.88–4.03 (m, 1H), 4.08 (s, 3H), 5.04

(d, 1H, J = 9 Hz), 7.65 (d, 1H, 9 Hz), 7.83 (d, 1H, 6 Hz), 8.42 (d, 1H, 9Hz), 8.97 (d, 1H, 6 Hz). ^{13}C NMR (75 MHz,): δ 10.8, 22.6 24.1, 26.3, 26.9, 36.1, 41.3, 55.9, 56.7, 58.2, 69.6, 114.0, 117.8, 121.2, 113.3, 133.4, 142.1, 143.9, 148.0, 148.4, 155.1, 157.1. HR ES-MS: m/z calcd for $C_{21}H_{30}N_5O_2$ (MH+): 384.2394, found 384.2403.

Potentiometric titrations

Potentiometric titrations were performed on an automatic titrator equipped with a glass pH microelectrode. Experimental details and procedure for the electrode calibration in 80% DMSO were the same as previously reported.[4b,8]

Potentiometric titrations were carried out under an argon atmosphere, on 6 mL of 2 mM solutions of the investigated compounds, in the presence of 10 mM Me_4NClO_4 (80% DMSO, 25 °C). A 50–70 mM Me_4NOH solution in 80% DMSO was automatically added to the titration vessel in small increments. Analysis of titration plots was carried out by the program HYPERQUAD 2000.[28] Distribution diagrams of the species were calculated using the acidity constants determined by potentiometric titrations.

Kinetic measurements

Kinetic measurements of HPNP cleavage were carried out by UV-vis monitoring of p-nitrophenol liberation at 400 nm on a diode array spectrophotometer. Rate constants reported in Table 2 were obtained by an initial rate method or full time-course experiments, with error limits on the order of ±5% unless otherwise stated. The $k_{obs}(S)/k_{obs}(R)$ ratio and the absolute configuration were confirmed by HPLC separation of the unreacted HPNP enantiomers by quenching the reaction mixture with a solution of $HClO_4$ in 80% DMSO. The following equation was used: $k_{obs}(S)/k_{obs}(R) = \ln[(1 - c)(1 - ee)]/\ln[(1 - c)(1 + ee)]$, see ref. 23 and pag. 15S, ESI† for further details.

Ab initio calculations

DFT calculations were carried out at the b3lyp/6–31 g(d,p)//b3lyp/6–31G(d,p) level of theory (GAUSSIAN-09 package).[24] The Berny algorithm was used to find the transition states of the transesterification reaction (opt = ts). The keywords cartesian, calcfc and noeigentest were used in the optimization of the structure to avoid errors and accelerate the conversion to the optimized structures. All the energy values were corrected for the zero point vibrational energy. Vibrational analysis confirmed all stationary points to be first-order saddle points (one imaginary frequency). The animation of the normal mode of vibration with negative spring constant confirmed that the saddle points resulting from the optimization procedure are actually the transition states of the HPNP transesterification. The polarized continuum model was used to take into account the solvent effect. The solvent parameters were set by using the following keyword and options: scrf = (pcm, read). eps = 72 was used in the separate PCM input section to define the solvent mixture dielectric constant.[19] The command AddSphereonH = N was used in the PCM input section to place an individual sphere on the two guanidinium hydrogen atoms involved in the interaction with the phosphate and on the hydrogen atom of the HPNP hydroxyl. Energies and coordinates of the calculations are reported in the ESI.†

Acknowledgements

The authors thank Chiesa Valdese Italiana and Sapienza University – "Progetti di Ateneo 2014" for financial support. Professor Luigi Mandolini and Dr. Roberta Cacciapaglia are acknowledged for the fruitful discussions. The authors also acknowledge Prof. Ruggero Caminiti for providing computing time on the NARTEN Cluster HPC Facility.

Notes and references

1 R. Wolfenden, *Chem. Rev.*, 2006, **106**, 3379–3396.

2 for review articles see: (*a*) F. Mancin, P. Scrimin and P. Tecilla, *Chem. Commun.*, 2012, **48**, 5545; (*b*) R. Salvio, *Chem. – Eur. J.*, 2015, **21**, 10960; (*c*) M. Raynal, P. Ballester, A. Vidal-Ferran and P. W. van Leeuwen, *Chem. Soc. Rev.*, 2014, **43**, 1734; (*d*) J.-N. Rebilly, B. Colasson, O. Bistri, D. Over and O. Reinaud, *Chem. Soc. Rev.*, 2015, **44**, 467; (*e*) R. Cacciapaglia, S. Di Stefano, L. Mandolini and R. Salvio, *Supramol. Chem.*, 2013, **25**, 537; (*f*) H. Lönnberg, *Org. Biomol. Chem.*, 2011, **9**, 1687; (*g*) Y. Aiba, J. Sumaoka and M. Komiyama, *Chem. Soc. Rev.*, 2011, **40**, 5657; (*h*) T. Niittymäki and H. Lönnberg, *Org. Biomol. Chem.*, 2006, **4**, 15.

3 (*a*) M. Diez-Castellnou, F. Mancin and P. Scrimin, *J. Am. Chem. Soc.*, 2014, **136**, 1158; (*b*) H. Korhonen, T. Koivusalo, S. Toivola and S. Mikkola, *Org. Biomol. Chem.*, 2013, **11**, 8324; (*c*) M. F. Mohamed and R. S. Brown, *J. Org. Chem.*, 2010, **75**, 8471; (*d*) R. Cacciapaglia, A. Casnati, L. Mandolini, D. N. Reinhoudt, R. Salvio, A. Sartori and R. Ungaro, *J. Am. Chem. Soc.*, 2006, **128**, 12322; (*e*) R. Cacciapaglia, A. Casnati, L. Mandolini, D. N. Reinhoudt, R. Salvio, A. Sartori and R. Ungaro, *J. Org. Chem.*, 2005, **70**, 624; (*f*) T.-S. A. Tseng and J. N. Burstyn, *Chem. Commun.*, 2008, 6209; (*g*) K. Nwe, C. M. Andolina and J. R. Morrow, *J. Am. Chem. Soc.*, 2008, **130**, 14861; (*h*) R. Cacciapaglia, A. Casnati, L. Mandolini, A. Peracchi, D. N. Reinhoudt, R. Salvio, A. Sartori and R. Ungaro, *J. Am. Chem. Soc.*, 2007, **129**, 12512; (*i*) A. Scarso, G. Zaupa, F. B. Houillon, L. J. Prins and P. Scrimin, *J. Org. Chem.*, 2007, **72**, 376; (*j*) H. Korhonen, S. Mikkola and N. H. Williams, *Chem. – Eur. J.*, 2012, **18**, 659.

4 for guanidine-based systems see: (*a*) C. Gnaccarini, S. Peter, U. Scheffer, S. Vonhoff, S. Klussmann and M. W. Göbel, *J. Am. Chem. Soc.*, 2006, **128**, 8063; (*b*) R. Salvio, L. Mandolini and C. Savelli, *J. Org. Chem.*, 2013, **78**, 7259; (*c*) L. Tjioe, A. Meininger, T. Joshi, L. Spiccia and B. Graham, *Inorg. Chem.*, 2011, **50**, 4327; (*d*) R. Salvio, S. Volpi, R. Cacciapaglia, A. Casnati, L. Mandolini and F. Sansone, *J. Org. Chem.*, 2015, **80**, 5887; (*e*) S. Ullrich, Z. Nazir, A. Busing, U. Scheffer, D. Wirth, J. W. Bats, G. Durner and M. W. Gobel, *ChemBioChem*, 2011, **12**, 1223; (*f*) X. Sheng, X. Lu, Y. Chen,

G. Lu, J. Zhang, Y. Shao, F. Liu and Q. Xu, *Chem. – Eur. J.*, 2007, **13**, 9703; (*g*) R. Salvio, R. Cacciapaglia and L. Mandolini, *J. Org. Chem.*, 2011, **76**, 5438; (*h*) U. Scheffer, A. Strick, V. Ludwig, S. Peter, E. Kalden and M. W. Göbel, *J. Am. Chem. Soc.*, 2005, **127**, 2211; (*i*) H. Ait-Haddou, J. Sumaoka, S. L. Wiskur, J. F. Folmer-Andersen and E. V. Anslyn, *Angew. Chem., Int. Ed.*, 2002, **41**, 4014; (*j*) J. He, P. Hu, Y. J. Wang, M. L. Tong, H. Sun, Z. W. Mao and L. N. Ji, *Dalton Trans.*, 2008, 3207.

5 (*a*) A. Demesmaeker, R. Haner, P. Martin and H. E. Moser, *Acc. Chem. Res.*, 1995, **28**, 366; (*b*) M. E. Gleave and B. P. Monia, *Nat. Rev. Cancer*, 2005, **5**, 468.

6 D. M. Perreault, L. A. Cabell and E. V. Anslyn, *Bioorg. Med. Chem.*, 1997, **5**, 1209.

7 (*a*) F. A. Cotton, E. E. J. Hazen and M. J. Legg, *Proc. Natl. Acad. Sci. U. S. A.*, 1979, **76**, 2551; (*b*) K. A. Schug and W. Lindner, *Chem. Rev.*, 2005, **105**, 67.

8 L. Baldini, R. Cacciapaglia, A. Casnati, L. Mandolini, R. Salvio, F. Sansone and R. Ungaro, *J. Org. Chem.*, 2012, **77**, 3381.

9 (*a*) G. Zaupa, C. Mora, R. Bonomi, L. J. Prins and P. Scrimin, *Chem. – Eur. J.*, 2011, **17**, 4879; (*b*) R. Salvio and A. Cincotti, *RSC Adv.*, 2014, **4**, 28678.

10 C. Savelli and R. Salvio, *Chem. – Eur. J.*, 2015, **21**, 5856.

11 (*a*) *Cinchona Alkaloids in Synthesis and Catalysis: Ligands, Immobilization and Organocatalysis*, ed. C. E. Song, John Wiley & Sons, Inc., 2009; (*b*) S. J. Connon, *Chem. Commun.*, 2008, 2499; (*c*) R. Salvio, M. Moliterno and M. Bella, *Asian J. Org. Chem.*, 2014, **3**, 340; (*d*) C. Palomo, M. Oiarbide and R. Lopez, *Chem. Soc. Rev.*, 2009, **38**, 632.

12 (*a*) T. Marcelli and H. Hiemstra, *Synthesis*, 2010, **8**, 1229; (*b*) C. Cassani, R. Martin-Rapun, E. Arceo, F. Bravo and P. Melchiorre, *Nat. Protoc.*, 2013, **8**, 325.

13 S. S. Jew and H. G. Park, *Chem. Commun.*, 2009, 7090.

14 (*a*) B. Vakulya, S. Varga, A. Csámpai and T. Soós, *Org. Lett.*, 2005, **7**, 1967; (*b*) B.-J. Li, L. Jiang, M. Liu, Y.-C. Chen, L.-S. Ding and Y. Wu, *Synlett*, 2005, **4**, 603; (*c*) J. Ye, D. J. Dixon and P. S. Hynes, *Chem. Commun.*, 2005, 4481; (*d*) S. J. Connon, *Chem. – Eur. J.*, 2006, **12**, 5418; For the synthesis and use of other guanidine-functionalized Cinchona alkaloids see: (*e*) X. Han, F. Zhong and Y. Lu, *Adv. Synth. Catal.*, 2010, **352**, 2778.

15 S. H. McCooey and S. J. Connon, *Angew. Chem., Int. Ed.*, 2005, **44**, 6367.

16 Y. F. Yong, J. A. Kowalski and M. A. Lipton, *J. Org. Chem.*, 1997, **62**, 1540.

17 A. E. Taggi, A. M. Hafez, H. Wack, B. Young, D. Ferraris and T. Lectka, *J. Am. Chem. Soc.*, 2002, **124**, 6626.

18 C. Palacio and S. J. Connon, *Org. Lett.*, 2011, **13**, 1298.

19 D. O. Corona-Martinez, O. Taran and A. K. Yatsimirsky, *Org. Biomol. Chem.*, 2010, **8**, 873.

20 (*a*) M. Georgieva, *Anal. Chim. Acta*, 1977, **90**, 83; (*b*) R. Wróbel and L. Chmurzyński, *Anal. Chim. Acta*, 2000, **405**, 303.

21 M. M. Kreevoy and E. H. Baughman, *J. Phys. Chem.*, 1974, **78**, 421.

22 *CRC Handbook of Chemistry and Physics*, ed. D. R. Lide, CRC Press, Boca Raton, FL, 90th edn, 2010, Section 8–48, p. 1241.

23 for a review about the quantitative treatment of kinetic resolution see: J. M. Keith, J. F. Larrow and E. N. Jacobsen, *Adv. Synth. Catal.*, 2001, **343**, 5.

24 M. J. Frisch, G. W. Trucks, H. B. Schlegel, G. E. Scuseria, M. A. Robb, J. R. Cheeseman, G. Scalmani, V. Barone, B. Mennucci, G. A. Petersson, H. Nakatsuji, M. Caricato, X. Li, H. P. Hratchian, A. F. Izmaylov, J. Bloino, G. Zheng, J. L. Sonnenberg, M. Hada, M. Ehara, K. Toyota, R. Fukuda, J. Hasegawa, M. Ishida, T. Nakajima, Y. Honda, O. Kitao, H. Nakai, T. Vreven, J. A. Montgomery, Jr., J. E. Peralta, F. Ogliaro, M. Bearpark, J. J. Heyd, E. Brothers, K. N. Kudin, V. N. Staroverov, R. Kobayashi, J. Normand, K. Raghavachari, A. Rendell, J. C. Burant, S. S. Iyengar, J. Tomasi, M. Cossi, N. Rega, J. M. Millam, M. Klene, J. E. Knox, J. B. Cross, V. Bakken, C. Adamo, J. Jaramillo, R. Gomperts, R. E. Stratmann, O. Yazyev, A. J. Austin, R. Cammi, C. Pomelli, J. W. Ochterski, R. L. Martin, K. Morokuma, V. G. Zakrzewski, G. A. Voth, P. Salvador, J. J. Dannenberg, S. Dapprich, A. D. Daniels, Ö. Farkas, J. B. Foresman, J. V. Ortiz, J. Cioslowski and D. J. Fox, *Gaussian 09, Revision D.01*, Gaussian, Inc., Wallingford CT, 2009.

25 A. J. Kirby, M. Medeiros, J. R. Mora, P. S. M. Oliveira, A. Amer, N. H. Williams and F. Nome, *J. Org. Chem.*, 2013, **78**, 1343.

26 W. W. Cleland and A. C. Hengge, *Chem. Rev.*, 2006, **106**, 3252.

27 D. M. Brown and D. A. Usher, *J. Chem. Soc.*, 1965, 6558.

28 L. Alderighi, P. Gans, A. Ienco, D. Peters, A. Sabatini and A. Vacca, *Coord. Chem. Rev.*, 1999, **184**, 311.

DOI: 10.1002/ajoc.201400021

Alkynes in Organocatalysis

Riccardo Salvio,* Mauro Moliterno, and Marco Bella*[a]

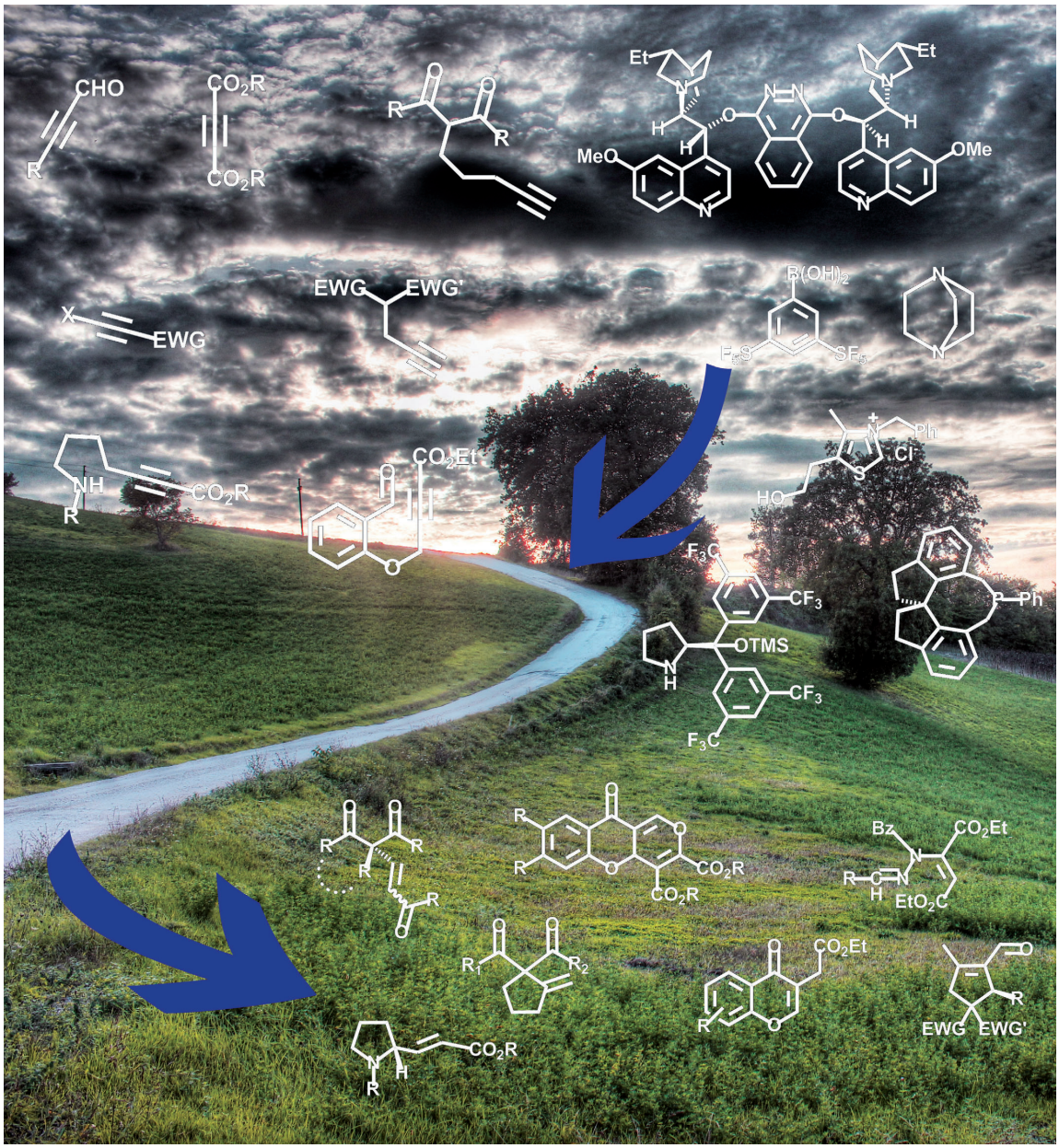

Abstract: In this Focus Review, a selection of organocatalyzed reactions in which alkynes have been used are presented. Catalysis by tertiary and secondary amines, by phase-transfer catalysis, by phosphines and carbenes, as well as bifunctional and multiple catalysis are discussed. Alkynes are versatile intermediates which can open novel synthetic opportunities as their reactivity is enhanced with respect to the corresponding alkenes and further elaboration to develop domino processes is possible.

Keywords: alkynes · asymmetric organocatalysis · bifunctional catalysis · phase-transfer catalysis · phosphines

1. Introduction

Alkynes are versatile molecules which can be used for a number of transformations in organic synthesis.[1] Among these reactions, is the addition of hydrogen, halogens, and related reagents. Alkynes can undergo cycloadditions and oxidation reactions, and terminal alkynes can be easily converted into metal acetylides that can be exploited in several ways in organic synthesis. Alkynes have also a wide importance in nature as in nearly two centuries well over a thousand naturally occurring acetylenes have been discovered and reported.[2]

Most transformations of alkenes can be also performed on the corresponding structures that contain a C–C triple bond. The latter group presents a novel and enhanced reactivity which expands its synthetic utility. The reports in which alkenes are used, however, still outnumber the papers in which the corresponding alkynes are used. The reasons for this can be mainly two: Firstly, few alkynes are currently commercially available. While several carbonyl compounds conjugated with a C–C double bond can be obtained from the main chemical producers and are not expensive, only relatively few molecules bearing a conjugated triple bond can instead be easily ordered from chemical companies. For example, methyl vinyl ketone is cheap and sold in large amounts while alkynyl methyl ketone is quite expensive.[3] Secondly, the highly reactivity of alkynes is a potential issue regarding their stability, use, and storage. For this reason, alkynes have found limited applications as final compounds in medicinal chemistry, even though there are pharmaceuticals containing the carbon-carbon triple bond, such as the contraceptive norethynodrel, the antiretroviral efavirenz, and the antifungal terbinafine. The antitumor calicheamicin, which undergoes Bergman cyclization to generate a highly reactive radical intermediate that attacks DNA within the cancer pathologies,[4] should be also mentioned.

[a] Dr. R. Salvio, M. Moliterno, Dr. M. Bella
Department of Chemistry
"Sapienza" University of Roma
Piazzale Aldo Moro 5, 00185, Roma (Italy)
Fax: (+39) 06-4991-3629
E-mail: riccardo.salvio@uniroma1.it
marco.bella@uniroma1.it

Surely, these issues hampered the widespread usage of alkynes up until today, but it should be considered that if the demand for alkynes increases, their availability will increase and consequently their price will decrease. Furthermore, their high reactivity could be a significant advantage, for example, in asymmetric reactions where the stereoselectivity increases upon lowering the temperature.

Finally, even though the C–C triple bond is a group that is not always desirable in the structure of a drug, alkynes can be convenient key synthetic intermediates for the preparation of several bioactive molecules. We believe that in the future the synthetic potential of alkynes will be successfully and further exploited in a growing number of transformations. Many authors have already reported promising works describing the reactivity of alkynes in many areas.[1] Since the reaction conditions in the emerging field of organocatalysis[5] are often mild, it might be the ideal area in which to develop novel reactions using alkynes as nucleophiles or electrophiles. We are not aware that this specific subject has been critically discussed before in a review paper. Therefore, we feel it could be useful to the scientific community to present a selection of reactions of alkynes in the growing field of organocatalysis, hoping that it might be informative, especially as inspiration for developing novel transformations and new research lines. The classification chosen in this review follows the kind of catalyst used and the possible mechanism that operates in the catalysis.

2. Organocatalysis by Tertiary Amines and Ammonium Salts

Several substrates involved in reactions dealing with alkynes are deprotonated by means of amines or ammonium salts in combination with inorganic bases. Some of them operate through noncovalent interaction with their substrates. These interactions can be van der Waals forces, electrostatic interactions and hydrogen bonding. General base catalytic mechanisms have been proposed in most cases. In other examples, the amine group is catalytically active via nucleophile catalysis. In this section, organocatalysts that can be classified within these categories are discussed.

2.1. Catalysis by Tertiary Amines

The *Cinchona*-alkaloid-catalyzed addition of dicarbonyl compounds and related molecules (β-keto esters, β-diketones and α-cyanoesters) to activated olefins has been one of the milestones of organocatalysis, since the pioneering studies by Wynberg and Helder in the seventies.[6]

Surprisingly, the corresponding reaction of the alkyne compounds was not reported until 2004, when Bella and Jørgensen described the addition of β-diketones **1** to alkynones **2** catalyzed by the *Cinchona*-alkaloid derivative $[DHQ]_2PHAL$ **I** (Scheme 1).[7] The role of the chiral catalyst is to act as a base in the deprotonation of the acidic hydrogen between the two carbonyl groups. The formation of a chiral ion pair is able to induce stereoselectivity that, especially in the case of some substrates, produces a remarkable enantiomeric excess.

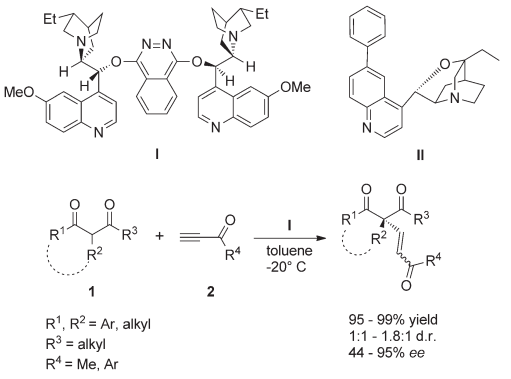

Scheme 1. Enantioselective organocatalyzed addition of β-diketones **1** to alkynones **2**.

Analogous electron-poor acetylenes **4** undergo also a formal [4+2] annulation with 3-formylchromones **3** after activation by a nucleophilic tertiary amine. An asymmetric reaction is possible if the β-isocupreine-derived catalyst **II** is used.[8] It was hypothesized that the alkyne reacts with the catalyst to form an intermediate with enhanced nucleophilicity, which is able to attack the substrate and to afford the product according to the mechanism proposed in Scheme 2. In this case, the tertiary amine group does not

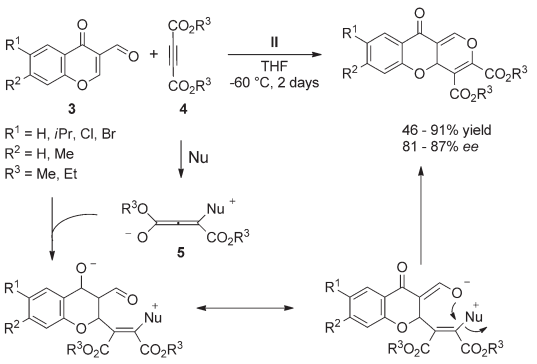

Scheme 2. Reaction of electron-poor acetylenes **4** with 3-formylchromones **3** catalyzed by **II**, and proposed mechanism.

act as a base, but rather as a nucleophilic catalyst that forms a covalent bond with the substrate and generating the reactive species **5**, which triggers the reaction as indicated in Scheme 2.

2.2. Phase-Transfer Catalysts

In the phase-transfer catalysis (PTC) approach, a chiral quaternary ammonium salt is used to transfer reactive anions, generated in situ by an inorganic base, into an organic phase where the reaction occurs. A chiral ionic

Riccardo Salvio was born in 1977 in Rome, Italy. He received his PhD in 2005 from University of Rome La Sapienza in the group of Prof. Luigi Mandolini. He spent the years 2005–2007 as a Research Associate with Prof. Julius Rebek at The Scripps Research Institute, La Jolla, USA. After this experience he moved to The Netherlands and joined the group of Prof. David Reinhoudt as a Postdoc. In 2009, he moved back to Italy and he is currently Research Fellow at La Sapienza University. His research interests include homogeneous catalysis, supramolecular chemistry, and molecular recognition.

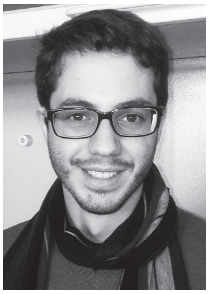

Mauro Moliterno was born in Latina, Italy, in 1989. He studied at Sapienza University of Rome, where he graduated with full marks in Organic Chemistry in 2013. He is currently pursuing his PhD in the same institution under the supervision of Dr. Bella, working in the field of asymmetric organocatalysis.

Marco Bella obtained his PhD from Roma "La Sapienza" University (2000). He then joined the group of K. C. Nicolaou as a Postdoc at The Scripps Research Institute (2000–2003, La Jolla, CA) and after that he moved to Aarhus University to work in the group of K. A. Jørgensen (2003–2005, Aarhus, Denmark). He returned back to his hometown as "Ricercatore" (2005) where he, with the help of several young but bright and motivated students, tries to do his best searching for novel concepts in asymmetric catalysis as well as research funding.

couple with increased solubility in apolar solvent, such as toluene or xylenes, is formed and can react in a stereoselective manner.[9]

PTC has been applied to several asymmetric transformations in which activated alkynes serves as Michael acceptors, to reach the double goal of controlling both the new stereocenter and the double bond (*E*/*Z*) configurations. Maruoka and co-workers[10] achieved excellent stereoselectivity in the addition of α-cyano esters **6** to *tert*-butyl propiolate **7** via phase-transfer catalysis, using a negligible yet effective quantity of a chiral binaphthyl-based quaternary ammonium salt **III** as the catalyst (Scheme 3).

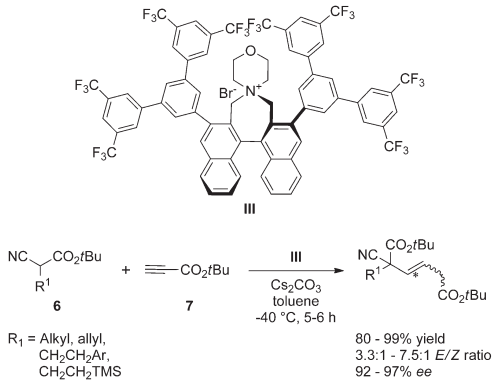

Scheme 3. Addition of α-cyano esters **6** to *tert*-butyl propiolate **7** promoted by **III** via PTC. TMS = trimethylsilyl.

PTC was also exploited by Jørgensen and co-workers[11] for the α-alkynylation of cyclic β-keto esters **8** via acetylenic substitution on activated β-halo alkynes **9** (Scheme 4). Enantioselectivity arises from the tight association of the enolate of β-keto ester and the sterically demanding chiral ammonium cation of catalyst **IV**. Similarly, the cinchonidine-based salt **V** was reported by Veselý and co-workers to catalyze the alkynylation of fluorinated substrates facilitated by hypervalent iodine compounds.[12]

3. Bifunctional Catalysis

Bifunctional catalysts are an emerging class of hybrid molecules in which two functional groups act catalytically in a synergistic way by means of close space relationships.[13] Recently, a few examples reported in the literature illustrate the concept of bifunctional catalysis applied to alkynes.

Catalyst **VI**, shown in Scheme 5, combines a hydrogen-bonding donor motif with a tertiary amine functional group that acts as a base.[14] This compound was reported to promote the isomerization of alkynyl esters and amides **10** to allenes **11** in high enantioselectivity. The presence of the hydrogen-bonding donor moiety in the catalyst makes this

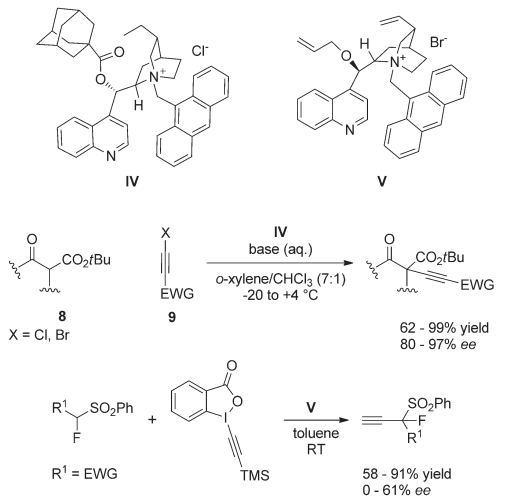

Scheme 4. Alkynylation of two different substrates promoted by chiral quaternary ammonium salts **IV** and **V**. EWG = electron-withdrawing group.

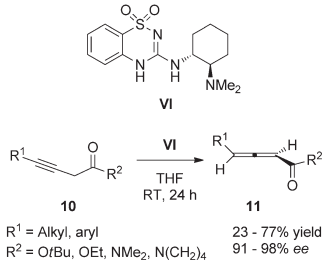

Scheme 5. Conversion of alkynyl esters and amides **10** into allenes **11** in the presence of bifunctional catalyst **VI**.

reaction efficient and versatile with respect to its previous versions,[15] but also reversible, so that the product cannot be resolved from the substrate without using a tandem reaction to trap the allene itself. Adding cyclopentadiene to the reaction mixture to obtain an isolable Diels–Alder adduct is one of the strategies carried out to solve the problem.

Bifunctional catalysis was also used in one of the first examples of highly enantioselective halolactonization involving 1,3-enynes **12** (Scheme 6). The reaction is catalyzed by the bifunctional catalyst **VII**, which promotes the 1,4-*syn*-cyclization and the subsequent formation of enantiomerically enriched bromoallenes **13**.[16] This reaction can be successfully applied to (*Z*)-1,3-enynes bearing either an aliphatic carboxylic acid or a substituted benzoic acid.

A catalyst similar to **VII**, is the quinine-derived urea **VIII**, whose tertiary amine function plays a key role in the conjugated addition of oxindole **14** to super-electrophilic

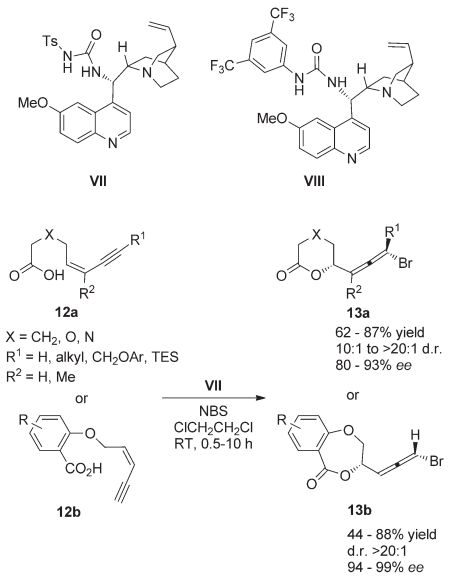

Scheme 6. Catalytic enantioselective halolactonization of enynes **12** in the presence of **VII**. NBS = *N*-bromosuccinimide; TES = triethylsilyl; Ts = tosyl.

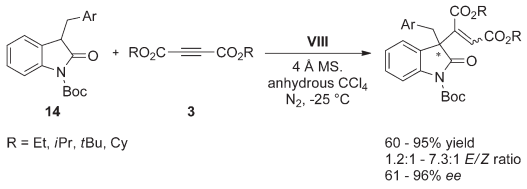

Scheme 7. Addition of acetynenedicarboxylates **3** to oxindoles **14** promoted by **VIII**. Boc = *tert*-butyloxycarbonyl; MS = molecular sieves.

acetylenedicarboxylates **3**, as recently reported by Wu and co-workers (Scheme 7).[17]

4. Non-Asymmetric Organocatalyzed Reactions

While one of the most attractive aspects of organocatalyzed reaction is obtaining chiral nonracemic compounds, the value of producing also achiral or racemic molecules via organocatalysis should not be underestimated. Some organocatalyzed reactions afford products that are difficult to access by different approaches, for example, some aromatics with peculiar substitution patterns. This specific aspect (non-asymmetric organocatalysis) has been recently reviewed.[18] We will briefly highlight some interesting examples with alkynes in non-asymmetric organocatalysis.

An asymmetric bifunctional catalyst was reported by Barbas III and co-workers[19] to effect the diastereoselective dibromination of unsaturated compounds, including prop-2-ynylbenzene **15**, using 1,3-dibromo-5,5-dimethylhydanthoin **16** as the halogen source (Scheme 8).

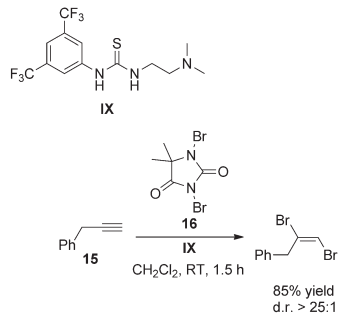

Scheme 8. Diastereoselective dibromination of prop-2-ynylbenzene **15** catalyzed by **IX**.

3,5-Bis(pentafluorosulfanyl)phenylboronic acid **X** was reported as a suitable organocatalyst for the Conia-ene carbocyclization of 1,3-dicarbonyl compounds **17** bearing a terminal C–C triple bond, which leads to cyclopentanes substituted with a methylene moiety adjacent to the newly formed quaternary carbon center (Scheme 9).[20] A variety of 2-alkynic 1,3-dicarbonyl compounds were smoothly converted into ene-carbocyclization products in moderate to good yields.

Another remarkable example of non-asymmetric organocatalysis is the nucleophilic regioselective addition of thiols to propiolic acid esters reported by Truong and Dove,[21] catalyzed by 1,8-diazabicyclo[5.4.0]undec-7-ene (DBU) or 1,5,7-triazabicyclo[4.4.0]dec-5-ene (TBD). The tandem re-

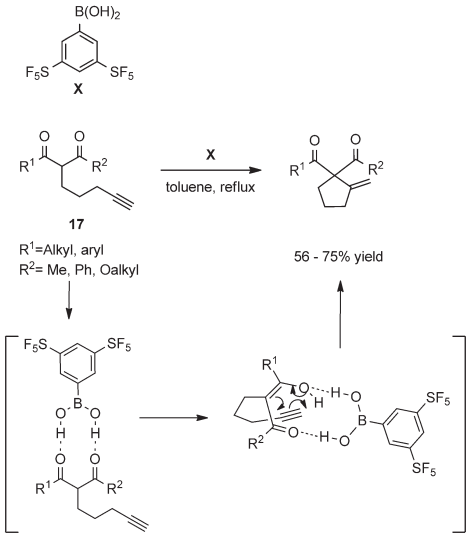

Scheme 9. Carbocyclization of the 1,3-dicarbonyl compounds **17** promoted by phenylboronic acid **X**.

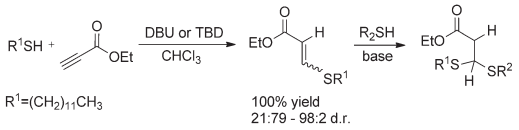

Scheme 10. Diastereoselective "click" addition of thiols to propiolic acid esters.

action depicted in Scheme 10 can be successfully applied to polymer–polymer coupling.

The use of alkynes as Michael acceptors was also explored in the aza-Michael addition reaction of hydrazones **18** with activated alkynes, such as **3a**, catalyzed by nitrogen-containing organic bases like 1,4-diazabicyclo[2.2.2]-octane (DABCO) **XI** as outlined in Scheme 11.[22]

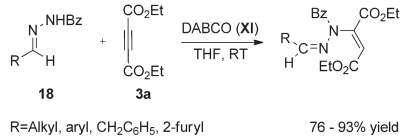

Scheme 11. DABCO-catalyzed Michael-type reactions of hydrazones **18** with electron-poor alkynes **3a**. Bz = benzoyl.

DABCO is also reported to be a good catalyst for the alkyne counterpart of the hetero-Diels–Alder reaction between carbonyl compounds and activated dienes: for example, the [4+2] annulation of but-3-yn-2-one (**2a**) and activated ketones **19** to give the corresponding 2,3-dihydropyran-4-ones **20** as depicted in Scheme 12.[23]

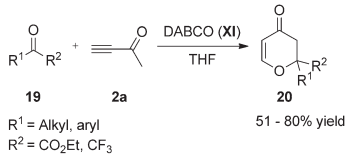

Scheme 12. DABCO-mediated [4+2] annulation for the preparation of 2,3-dihydropyran-4-ones **20**.

5. Alkynes in Reaction Proceeding via Enamine/Iminium Activation

Since the pioneering studies of List et al.[24a] and MacMillan and co-workers,[24b] asymmetric organocatalysis by chiral secondary amines has received tremendous interest from many chemists around the world. So many challenging goals have been reached that asymmetric amino catalysis has been defined as "The gold rush in organic chemistry".[25] In this context, activation of carbonyl-conjugated C–C double bonds through enamine intermediates or through iminium-ion intermediates has been frequently applied in organocatalysis, which is a powerful strategy for the functionalization of the β position with a nucleophile or the γ position with an electrophile, respectively. Recently, this approach was applied to carbonyl-conjugated C–C triple bonds to obtain α,β-unsaturated carbonyl compounds via iminium-allenamine cascade catalysis.[26]

The intramolecular Michael and hetero-Michael addition onto activated double bonds have been elective strategies for the construction of bicyclic systems. The application of this strategy to the corresponding triple bond is significant. 2-Alkynals **21** can be used as substrates for the asymmetric synthesis of 4-amino-4*H*-chromenes **23** carried out by an organocatalytic oxa-Michael/aza-Baylis–Hillman tandem reaction, as reported by Alemán et al.[27] This transformation, most likely occurring via iminium-ion activation (Scheme 13), is a useful strategy to obtain, after reduction,

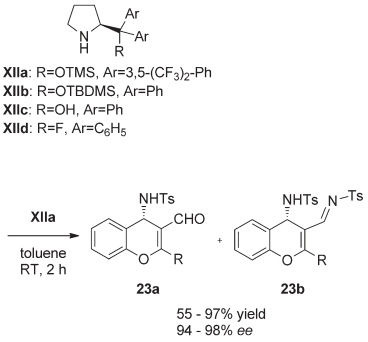

Scheme 13. Synthesis of 4-amino-4*H*-chromenes **23** mediated by prolinol-derivative **XIIa**. TBDMS = *tert*-butyldimethylsilyl.

nonracemic 4-aminochromanes, which are structures present in several natural and bioactive molecules. It is worth noting that the use of an alkyne substrate is necessary because the attempt to prepare 4-aminochromanes directly from α,β-unsaturated aldehydes would lead to 2*H*-chromenes with loss of the stereochemical information associated to the carbon stereocenter in the α position to the nitrogen atom. A similar reaction, reported by Wang and co-workers,[28] starting from 2-alkynals **21** and aromatic nitroalkenes **24** affords chiral 4*H*-chromenes **25**. The proposed mechanism involves an iminium-allenamine cascade reaction, as illustrated in Scheme 14.

The self-condensation of alkynals **21a** was implemented under mild organocatalytic conditions and linked with a domino organocatalytic inverse-electron-demand oxa-Diels–Alder reaction by Sun and co-workers.[29] This approach can be used to produce a variety of polysubstituted chiral 3,4-dihydropyrans **27**. The mechanism of the self-condensation step was investigated (Scheme 15). The iminium-activated C–C triple bond of **28a** is hydrated and the resulting enol **28b** is the active species in the condensation with another molecule of alkynal **21a**. A tentative mecha-

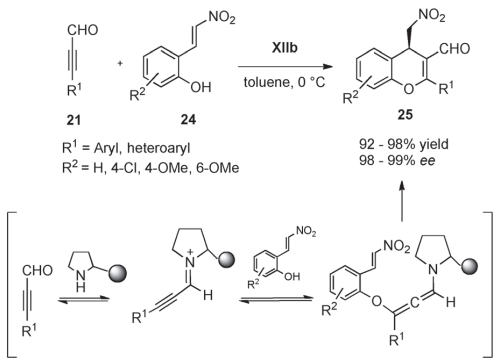

Scheme 14. Enantioselective iminium-allenamine cascade reaction catalyzed by the prolinol-derivative **XIIb**, and postulated mechanism.

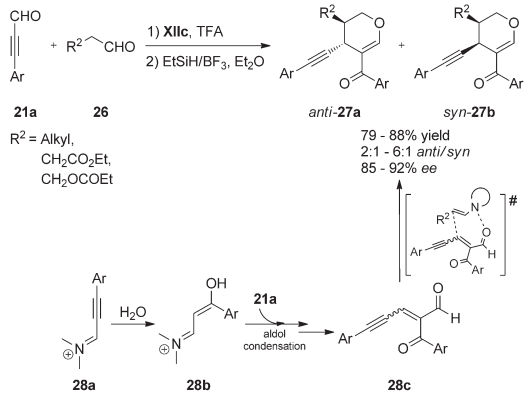

Scheme 15. Synthesis of 3,4-dihydropyrans **27** via a domino sequence starting from alkynals **21a** and promoted by prolinol derivative **XIIc**. TFA = trifluoroacetic acid.

nism for the oxa-Diels–Alder reaction undergone by **28c** is also depicted in Scheme 15.

Amino catalysis was applied in 2012 by Alemán et al.[30] to the enantioselective 1,3-dipolar cycloaddition of nitrones **29** to 2-alkynals **21** for the synthesis of isoxazolidines **30** (Scheme 16). The use of fluorodiphenylmethylpirrolidine **XIId** as the catalyst allows the activation of the dipolarophile via formation of an iminium ion.

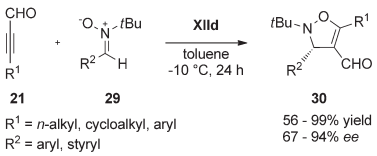

Scheme 16. The first organocatalyzed 1,3-dipolar cycloaddition between 2-alkynals **21** and nitrones **29**.

6. Carbenes

Over the past decades, N-heterocyclic carbenes (NHCs) have played an important role in synthetic organic chemistry. Besides their role as ligands in metal-catalyzed reactions,[31] they are able to catalyze a number of organic reactions (benzoin condensation,[32] transesterification,[33] Stetter reaction,[34] and homoenolate addition[35]).

Efforts in adapting alkene chemistry to the alkyne function have been applied also to NHC catalysis. The Stetter reaction, which is the conjugate addition of aldehydes to α,β-unsaturated esters, was successfully applied to activated alkynes by Liu and co-workers.[36] This organocatalytic intramolecular Stetter-type hydroacylation reaction, illustrated in Scheme 17, starting from salicylaldehyde-derived alkynes **31** and using a catalytic amount of thiazolium-based carbene catalyst **XIII** delivers chromone derivatives **32**.

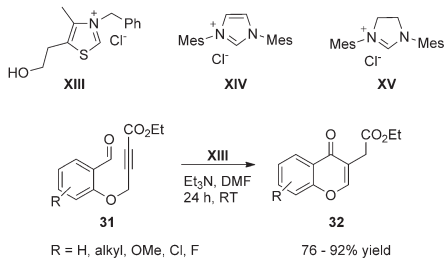

Scheme 17. Intramolecular NHC-catalyzed Stetter-type reaction between aldehydes and alkynyl esters. DMF = *N*,*N*-dimethylformamide; Mes = mesityl.

N-heterocyclic carbenes such as **XIV** can also catalyze the conjugate addition of 1,3-dicarbonyl compounds **33** to 2-alkynals **21**, followed by hydride migration and intramolecular acylation, for the formation of 3,4-dihydropyranones **34** (Scheme 18).[37] This example shows that NHCs can be used in combination with alkynals not only to effect the umpolung of carbonyl group reactivity, but also to activate them towards Michael additions upon protonation of the Breslow intermediate.

The weak nucleophilic nature of the allenolate resulting from the reaction between 2-alkynals and NHCs can be overcome by activating a suitable electrophile with a Lewis acid, as reported by She et al.[38] A formal [3+2] annulation

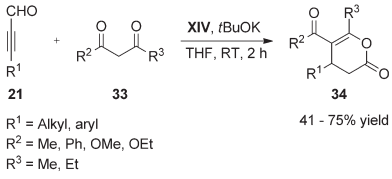

Scheme 18. NHC-catalyzed reaction between 2-alkynals **21** and 1,3-dicarbonyl compounds **33**.

between 2-alkynals **21** and β,γ-unsaturated α-keto esters **35**, leading to furan-2(5*H*)-ones **36** is thus possible by using a NHC-catalyzed/Lewis acid mediated strategy, as outlined in Scheme 19.

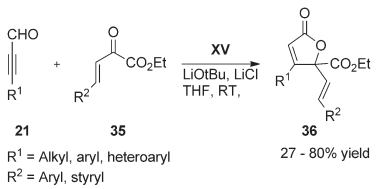

Scheme 19. [3+2] Annulations between 2-alkynals **21** and β,γ-unsaturated α-keto esters **35** catalyzed by **XV**.

7. Phosphines

The use of chiral phosphines as ligands for transition metals in catalytic asymmetric synthesis, is widely documented. Their use as nucleophilic catalysts is an important second aspect of their utility. In Scheme 20 a possible mechanism is proposed, analogous to the one generally accepted for some tertiary amine-catalyzed reactions (see Scheme 2), for phosphine-catalyzed reactions involving activated alkynes.

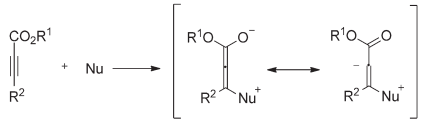

Scheme 20. Activation of a C−C triple bond effected by a nucleophilic phosphine.

Achiral phosphines such as PPh_3 and PBu_3 can be used for the synthesis of tricyclic benzopyrones **38** through a formal [4+2] annulation reaction depicted in Scheme 21.[39] The phosphine catalyst, according to the aforementioned mechanism, transforms electron-poor acetylenes into nucleophilic zwitterions, which can react in a 1,4-addition to 3-formylchromones **37** to give a stabilized oxanion. This species further undergoes a 1,4-addition to the resulting activated alkenes to liberate the catalyst and deliver the cycloaddition adduct **38**. This strategy affords an annulation reaction that was previously reported only with electron-rich olefins as the dienophiles.[40]

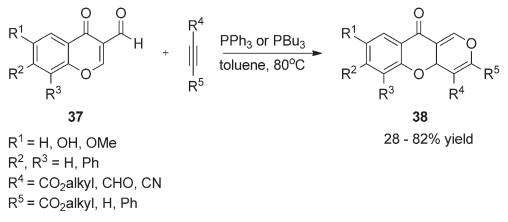

Scheme 21. Phosphine-catalyzed [4+2] annulations of 3-formylchromones **37** and acetylenes.

An additional example is given in Scheme 22, which illustrates the use of the chiral spirophosphine **XVI** as the catalyst in the enantioselective synthesis of pyrrolidines **40a** and indolines **40b** by nucleophilic intramolecular γ-addition to alkynoates **39a** and **39b**.[41]

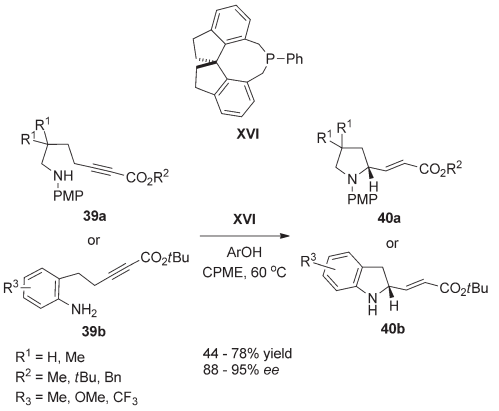

Scheme 22. Intramolecular enantioselective γ-addition in alkynoates **39a** and **39b** catalyzed by phosphine **XVI**. CPME = cyclopentyl methyl ether; PMP = 4-methoxyphenyl.

Yamamoto and co-workers reported that the reaction of activated alkynes **41** with isocyanides **42** bearing an electron-withdrawing group can be catalyzed by phosphines to give the corresponding pyrroles **43** regioselectively in good yields (Scheme 23).[42] The reaction probably proceeds through the 1,4-addition of the nucleophilic phosphine catalyst (see Scheme 20) to the alkyne, followed by a [3+2] cycloaddition between the resulting alkenyl phosphine intermediate and an isocyanide-derived carbanion.

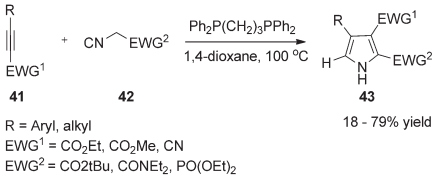

Scheme 23. Phosphine-catalyzed heteroaromatization of activated alkynes **41** and isocyanides **42**.

Hexamethylphosphorous triamide (HMPT) and other phosphites and phosphoramidites have been reported by Grossman et al. to be efficient catalysts for the Michael reaction of alkynone **2b** with malonates, α-cyano esters, β-keto esters, and nitro compounds **44** (Scheme 24).[43] HMPT catalyzes the Michael reaction within seconds at room tem-

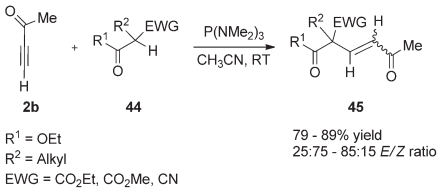

Scheme 24. HMPT-catalyzed Michael addition of dicarbonyl compounds **44** to alkynones **2b**.

perature, and the products **45** are isolated simply by removing the catalyst in vacuo. The Michael reactions of alkynones, unlike those of alkenones, is irreversible.

8. Multicatalysis

Multicatalysis (or cooperative catalysis) is the combination of different catalytic systems, such as metal catalysis and organocatalysis. Multicatalysis has received increasing attention in recent years as it represents a new strategy for the development of reactions not viable by one of the two methods alone.[44]

One example is the asymmetric alkynylation of imines effected by chiral Brønsted acids and a metal catalysts. The former serves as the electrophile activator, supplying a chiral ion pair or an hydrogen-bonded reactive species that can transfer the stereochemical information to the product, while the latter delivers the achiral reactive alkynylide. This system has attractive aspects, such as the use of available chiral Brønsted acids and the simplicity of the metal catalyst, whose achiral ligands can be easily interchanged to modulate its reactivity.[45] Two examples of this catalytic mode of activation are shown in Scheme 25.[46] Imines **46a–b** react enantioselectively with alkynes **47a–b** to afford the alkynylation adducts **48a–b** in the presence of the catalytic systems made up of the chiral binol hydrogen phosphate **XVII** and AgOAc in one case, and of Boc-L-proline and $[CuPF_6(MeCN)_2]/PAr_3$ in the other.

Nishibayashi and co-workers recently reported the enantioselective alkylation of propargylic alcohols **49a** with aldehydes **26a** multicatalyzed by the chiral pyrrolidine **XIIa** and the thiolate-bridge diruthenium complex **XVIII**, as shown in Scheme 26. The metal catalyst generates an alkenylidene complex from the alcohol, which undergoes nucleophilic attack by the enamine formed by reaction between the aldehyde and the secondary amine. Excellent enantioselectivity was achieved, along with a certain diastereoselectivity.[47] This transformation was improved and extended to highly functionalized internal alkynes **49b** and aldehydes **26b** by Cozzi and co-workers, who developed an S_N1-type reaction catalyzed by $In(OTf)_3$ and chiral imidazolinone **XIX** (Scheme 26).[48] A similar method was independently developed by Nishibayashi and co-workers.[49]

As reported by Kirsch and co-workers, carbocyclization of aldehydes and alkynes can be achieved by a combination

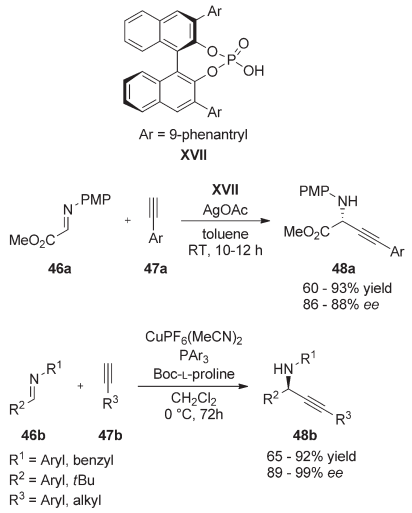

Scheme 25. Asymmetric alkynylation of imines **46** via the combination of chiral Brønsted acid and metal catalysis.

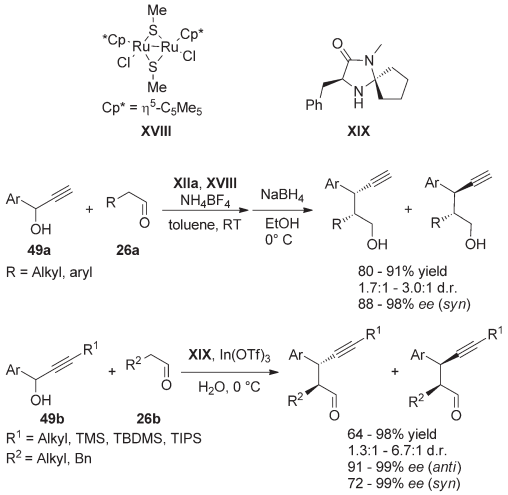

Scheme 26. Multicatalyzed alkylation of propargyl alcohols **49** with aldehydes **26**. Bn = benzyl; Tf = trifluoromethanesulfonyl; TIPS = triisopropylsilyl.

of gold and amino catalysis.[50] Inspired by this and other works,[51] Jørgensen and co-workers developed an enantioselective synthesis of cyclopentene carbaldehydes **52** starting from α,β-unsaturated aldehydes **50** and propargyl malononitriles or cyanoacetates **51**, via iminium ion and metal multicatalysis, as shown in Scheme 27. The chiral organocatalyst **XIIa** accounts for the stereocontrol in the attack of the nucleophile to the iminium ion, while the metal catalysts **XXa-c** are responsible for the 5-*exo-dig* cyclization of

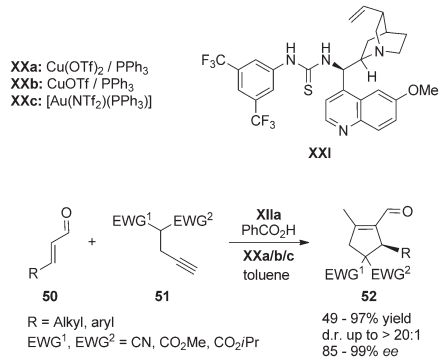

Scheme 27. Carbocyclization of aldehydes **50** with alkynes **51** via iminum-ion/metal catalysis.

the resulting enamine intermediate. Double bond isomerization delivers cyclopentenes **52**.[52]

When the propargyl malononitrile **54** is added to imine **53** via bifunctional catalysis, the resulting adduct can cyclize by intramolecular alkyne hydroamination in the presence of a gold catalyst. Given that the first step is enantioselective, this process leads to enantioenriched dihydropirrole derivatives **55**, as depicted in Scheme 28.[53]

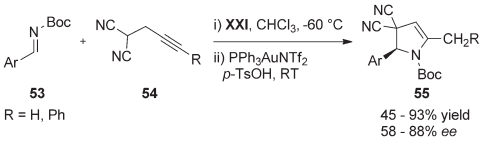

Scheme 28. Dihydropirroles **55** obtained by means of bifunctional organocatalysis and gold catalysis.

An analogous transformation, reported by Dixon and coworkers,[54] starting from imines **53** and nitroalkynes **56** delivers tetrahydropyridines **57** via a nitro-Mannich/hydroamination cascade reaction, with the simultaneous formation of two stereogenic centers (Scheme 29).

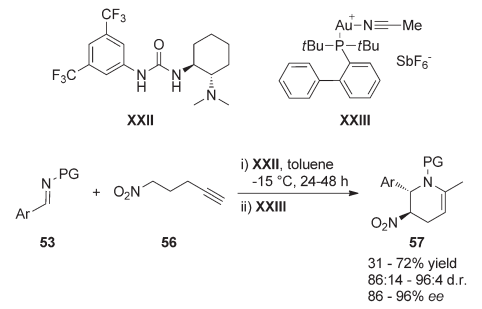

Scheme 29. Tetrahydropyridines **57** obtained by means of bifunctional organocatalysis and gold catalysis. PG = protecting group.

A combination of metal and organocatalysis was also successfully used in a non-asymmetric synthesis. A multicomponent reaction of 2-alkynylbenzaldehydes **58a**, anilines **59a** and ketones **60a** was reported to afford 1,2-dihydroisoquinoline derivatives **61a**, as outlined in Scheme 30.[55] L-Proline promotes the attack of ketone **60a** to the aldimine,

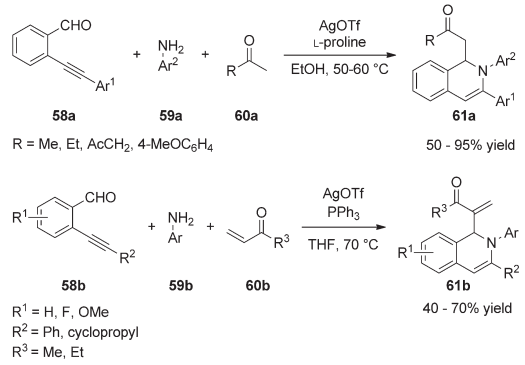

Scheme 30. Multicomponent reaction involving alkynyl benzaldehydes **58a–b**, by means of metal-enamine or metal-phosphine multicatalysis.

which is generated in situ between the aldehyde **58a** and the aniline **59a** (enamine catalysis). On the other hand, the silver catalyst activates the triple bond towards the intramolecular nucleophilic attack that affords the cyclization (Lewis acid catalysis). The same type of process can be applied to α,β-unsaturated ketones **60b** using phosphine catalysis instead of an enamine.[56] This approach was also adapted to a high throughput synthesis for the preparation of a library of isoquinilines.[57]

5. Conclusion

This review has analyzed an emerging aspect in organic synthesis: the combination of alkynes and organocatalysis. While a number of reviews have analyzed the corresponding reactions with alkenes, alkynes have so far received relatively little attention. It is expected that with larger availability of alkynes this review might serve as inspiration for developing novel transformations.

Acknowledgements

M.B. wishes to thank MD Rita Citton, because without the exceptional help of her and all the staff at Ospedale Santa Maria Goretti in Latina, this paper would have never been published. The research of R.S. and M.B. is generously supported by "Finanziamento di Ateneo 2011-2013". M.B. acknowledges crucial support from the "Chiesa Valdese Italiana", through www.ottopermillevaldese.org.

[1] For reviews, see: a) N. E. Schore, *Chem. Rev.* **1988**, *88*, 1081–1119; b) I. Beletskaya, C. Moberg, *Chem. Rev.* **1999**, *99*, 3435–3461; c) T. E. Müller, M. Beller, *Chem. Rev.* **1998**, *98*, 675–703; d) F. Alonso, I. P. Beletskaya, M. Yus, *Chem. Rev.* **2004**, *104*, 3079–3159; e) M. Meldal, C. W. Tornøe, *Chem. Rev.* **2008**, *108*, 2952–3015; f) T. E. Müller, K. C. Hultzsch, M. Yus, F. Foubelo, M. Tada, *Chem. Rev.* **2008**, *108*, 3795–3892; g) F. Amblard, J. H. Cho, R. F. Schinazi, *Chem. Rev.* **2009**, *109*, 4207–4220; h) R. Chinchilla, C. Najera, *Chem. Rev.* **2013**, in press, DOI: 10.1021/cr400133p.

[2] a) F. Bohlmann, H. Burkhardt, C. Zdero, *Naturally Occurring Acetylenes*, Academic Press, New York, **1973**; b) E. R. H. Jones, V. Thaller in *The Chemistry of the Carbon-Carbon Triple Bond*, *Part 2* (Ed.: S. Patai), Wiley, New York, 1978, chap. 14, pp. 621–633.

[3] 100 mL of 3-buten-2-one costs about US$100, while only 10 mL of 3-butyn-2-one costs about US$900, www.sigmaaldrich.com; accessed Jan 21, 2014.

[4] S. Walker, R. Landovitz, W. D. Ding, G. A. Ellestad, D. Kahne, *Proc. Natl. Acad. Sci. USA* **1992**, *89*, 4608–4612.

[5] a) *Asymmetric Organocatalysis* (Eds: A. Berkessel, H. Gröger), Wiley-VCH, Weinheim, **2005**; b) S. Bertelsen, K. A. Jørgensen, *Chem. Soc. Rev.* **2009**, *38*, 2178–2189; c) X. Yua, W. Wang, *Org. Biomol. Chem.* **2008**, *6*, 2037–2046.

[6] H. Wynberg, R. Helder, *Tetrahedron Lett.* **1975**, *16*, 4057–4060.

[7] M. Bella, K. A. Jørgensen, *J. Am. Chem. Soc.* **2004**, *126*, 5672–5673.

[8] H. Waldmann, V. Khedkar, H. Duckert, M. Schurmann, I. M. Oppel, K. Kumar, *Angew. Chem. Int. Ed.* **2008**, *47*, 6869–6872; *Angew. Chem.* **2008**, *120*, 6975–6978.

[9] a) M. Makosza, *Pure Appl. Chem.* **2000**, *72*, 1399–1403; b) T. Ooi, K. Maruoka, *Angew. Chem. Int. Ed.* **2007**, *46*, 4222–4266; *Angew. Chem.* **2007**, *119*, 4300–4345; c) T. Hashimoto, K. Maruoka, *Chem. Rev.* **2007**, *107*, 5656–5682; d) S. Shirakawa, K. Maruoka, *Angew. Chem. Int. Ed.* **2013**, *52*, 4312–4348; *Angew. Chem.* **2013**, *125*, 4408–4445.

[10] H. X. Wang, M. Kitamura, K. Maruoka, *J. Am. Chem. Soc.* **2007**, *129*, 1038–1039.

[11] T. B. Poulsen, L. Bernardi, J. Alemán, J. Overgaard, K. A. Jørgensen, *J. Am. Chem. Soc.* **2007**, *129*, 441–449.

[12] M. Kamlar, P. Putaj, J. Veselý, *Tetrahedron Lett.* **2013**, *54*, 2097–2100.

[13] a) R. Breslow, *J. Mol. Catal.* **1994**, *91*, 161–174; b) W.-Y. Siau, J. Wang, *Catal. Sci. Technol.* **2011**, *1*, 1298–1310.

[14] T. Inokuma, M. Furukawa, T. Uno, Y. Suzuki, K. Yoshida, Y. Yano, K. Matsuzaki, Y. Takemoto, *Chem. Eur. J.* **2011**, *17*, 10470–10477.

[15] a) M. Oku, S. Arai, K. Katayama, T. Shioiri, *Synlett* **2000**, 493–494; b) H. Liu, D. Leow, K. Huang, C. Tan, *J. Am. Chem. Soc.* **2009**, *131*, 7212–7213.

[16] W. Zhang, N. Liu, C. M. Schienebeck, K. Decloux, S. Zheng, J. B. Werness, W. Tang, *Chem. Eur. J.* **2012**, *18*, 7296–7305.

[17] G. Kang, Q. Wu, M. Liu, Q. Xu, Z. Chen, W. Chen, Y. Luo, W. Ye, J. Jiang, H. Wu, *Adv. Synth. Catal.* **2013**, *355*, 315–320.

[18] a) P. Renzi, M. Bella, *Chem. Commun.* **2012**, *48*, 6881–6896; b) Q. Ren, J. Wang, *Asian J. Org. Chem.* **2013**, *2*, 542–557.

[19] G. Hernández-Torres, B. Tan, C. F. Barbas, III., *Org. Lett.* **2012**, *14*, 1858–1861.

[20] Y.-D. Yang, X. Lu, E. Tokunaga, N. Shibata, *J. Fluorine Chem.* **2012**, *143*, 204–209.

[21] V. X. Truong, A. P. Dove, *Angew. Chem. Int. Ed.* **2013**, *52*, 4132–4136; *Angew. Chem.* **2013**, *125*, 4226–4230.

[22] Z.-L. Yuan, Y. Wei, M. Shi, *Eur. J. Org. Chem.* **2010**, 4088–4097.

[23] Z. Lian, Q.-Y. Zhao, Y. Wei, M. Shi, *Eur. J. Org. Chem.* **2012**, 3338–3341.

[24] a) B. List, R. A. Lerner, C. F. Barbas, III., *J. Am. Chem. Soc.* **2000**, *122*, 2395–2396; b) K. A. Ahrendt, C. J. Borths, D. W. C. MacMillan, *J. Am. Chem. Soc.* **2000**, *122*, 4243–4244.

[25] P. Melchiorre, M. Marigo, A. Carlone, G. Bartoli, *Angew. Chem. Int. Ed.* **2008**, *47*, 6138–6171; *Angew. Chem.* **2008**, *120*, 6232–6265.

[26] S. B. Jones, B. Simmons, D. W. C. MacMillan, *J. Am. Chem. Soc.* **2009**, *131*, 13606–13607.

[27] J. Alemán, A. Nunez, L. Marzo, V. Marcos, C. Alvarado, J. L. Garcia Ruano, *Chem. Eur. J.* **2010**, *16*, 9453–9456.

[28] X. Zhang, S. Zhang, W. Wang, *Angew. Chem. Int. Ed.* **2010**, *49*, 1481–1484; *Angew. Chem.* **2010**, *122*, 1523–1526.

[29] L.-J. Dong, T.-T. Fan, C. Wang, J. Sun, *Org. Lett.* **2013**, *15*, 204–207.

[30] J. Alemán, A. Fraile, L. Marzo, J. L. G. Ruano, C. Izquierdo, S. Díaz-Tendero, *Adv. Synth. Catal.* **2012**, *354*, 1665–1671.

[31] a) R. Corberán, E. Mas-Marzá, E. Peris, *Eur. J. Inorg. Chem.* **2009**, 1700–1716; b) N. Marion, R. S. Ramón, S. P. Nolan, *J. Am. Chem. Soc.* **2009**, *131*, 448–449; c) T. W. Hudnall, C. W. Bielawski, *J. Am. Chem. Soc.* **2009**, *131*, 16039–16041.

[32] a) D. Enders, O. Niemeier, T. Balensiefer, *Angew. Chem. Int. Ed.* **2006**, *45*, 1463–1467; *Angew. Chem.* **2006**, *118*, 1491–1495; b) L. Baragwanath, C. A. Rose, K. Zeitler, S. J. Connon, *J. Org. Chem.* **2009**, *74*, 9214–9217.

[33] R. S. A. Grasa, R. Singh, S. P. Nolan, *Synthesis* **2004**, 971–985.

[34] a) A. E. Mattson, A. M. Zuhl, T. E. Reynolds, K. A. Scheidt, *J. Am. Chem. Soc.* **2006**, *128*, 2552–2553; b) S. M. Mennen, J. T. Blank, M. B. Tran-Dubé, J. E. Imbriglio, S. J. Miller, *Chem. Commun.* **2005**, 195–197.

[35] E. M. Phillips, T. E. Reynolds, K. A. Scheidt, *J. Am. Chem. Soc.* **2008**, *130*, 2416–2417.

[36] S. Vedachalam, Q.-L. Wong, B. Maji, J. Zeng, J. Ma, X.-W. Liu, *Adv. Synth. Catal.* **2011**, *353*, 219–225.

[37] a) Z.-Q. Zhu, J.-C. Xiao, *Adv. Synth. Catal.* **2010**, *352*, 2455–2458; b) J. Kaeobamrung, J. Manatthanchai, P. Zheng, J. W. Bode, *J. Am. Chem. Soc.* **2010**, *132*, 8810–8812.

[38] J. Qi, X. Xie, R. Han, D. Ma, J. Yang, X. She, *Chem. Eur. J.* **2013**, *19*, 4146–4150.

[39] H. Dückert, V. Khedkar, H. Waldmann, K. Kumar, *Chem. Eur. J.* **2011**, *17*, 5130–5137.

[40] a) S. J. Coutts, T. W. Wallace, *Tetrahedron* **1994**, *50*, 11755–11780; b) G. Sabitha, *Aldrichimica Acta* **1996**, *29*, 15–29.

[41] R. J. Lundgren, A. Wilsily, N. Marion, C. Ma, Y. K. Chung, G. C. Fu, *Angew. Chem. Int. Ed.* **2013**, *52*, 2525–2528; *Angew. Chem.* **2013**, *125*, 2585–2588.

[42] S. Kamijo, C. Kanazawa, Y. Yamamoto, *Tetrahedron Lett.* **2005**, *46*, 2563–2566.

[43] R. B. Grossman, S. Comesse, R. M. Rasne, K. Hattori, M. N. Delong, *J. Org. Chem.* **2003**, *68*, 871–874.

[44] a) Z. Du, Z. Shao, *Chem. Soc. Rev.* **2013**, *42*, 1337–1378; b) R. C. Wende, P. R. Schreiner, *Green Chem.* **2012**, *14*, 1821–1849; c) C. C. J. Loh, D. Enders, *Chem. Eur. J.* **2012**, *18*, 10212–10225; d) A. E. Allen, D. W. C. MacMillan, *Chem. Sci.* **2012**, *3*, 633–658; e) S. Piovesana, D. M. Scarpino Schietroma, M. Bella, *Angew. Chem. Int. Ed.* **2011**, *50*, 6216–6232; *Angew. Chem.* **2011**, *123*, 6340–6357.

[45] P. de Armas, D. Tejedor, F. Garcia-Tellado, *Angew. Chem. Int. Ed.* **2010**, *49*, 1013–1016; *Angew. Chem.* **2010**, *122*, 1029–1032.

[46] a) M. Rueping, A. P. Antonchick, C. Brinkmann, *Angew. Chem. Int. Ed.* **2007**, *46*, 6903–6906; *Angew. Chem.* **2007**, *119*, 7027–7030; b) Y. Lu, T. C. Johnstone, B. A. Arndtsen, *J. Am. Chem. Soc.* **2009**, *131*, 11284–11285; c) T. Kano, T. Yurino, K. Maruoka, *Angew. Chem. Int. Ed.* **2013**, *52*, 11509–11512; *Angew. Chem.* **2013**, *125*, 11723–11726.

[47] M. Ikeda, Y. Miyake, Y. Nishibayashi, *Angew. Chem. Int. Ed.* **2010**, *49*, 7289–7293; *Angew. Chem.* **2010**, *122*, 7447–7451.

[48] R. Sinisi, M. V. Vita, A. Gualandi, E. Emer, P. G. Cozzi, *Chem. Eur. J.* **2011**, *17*, 7404–7408.

[49] K. Motoyama, M. Ikeda, Y. Miyake, Y. Nishibayashi, *Eur. J. Org. Chem.* **2011**, 2239–2246.

[50] J. T. Binder, B. Crone, T. T. Haug, H. Menz, S. F. Kirsch, *Org. Lett.* **2008**, *10*, 1025–1028.

[51] T. Yang, A. Ferrali, L. Campbell, D. J. Dixon, *Chem. Commun.* **2008**, 2923–2925.

[52] K. L. Jensen, P. T. Franke, C. Arroniz, S. Kobbelgaard, K. A. Jørgensen, *Chem. Eur. J.* **2010**, *16*, 1750–1753.

[53] D. Monge, K. L. Jensen, P. T. Franke, L. Lykke, K. A. Jørgensen, *Chem. Eur. J.* **2010**, *16*, 9478–9484.

[54] D. M. Barber, H. J. Sanganee, D. J. Dixon, *Org. Lett.* **2012**, *14*, 5290–5293.
[55] a) Q. Ding, J. Wu, *Org. Lett.* **2007**, *9*, 4959–4962; b) A. K. Verma, S. K. Kotla, D. Choudhary, M. Patel, R. K. Tiwari, *J. Org. Chem.* **2013**, *78*, 4386–4401.
[56] S. Ye, J. Wu, *Tetrahedron Lett.* **2009**, *50*, 6273–6275.
[57] N. A. Markina, R. Mancuso, B. Neuenswander, G. H. Lushington, R. C. Larock, *ACS Comb. Sci.* **2011**, *13*, 265–271.

Received: January 28, 2014
Published online: March 12, 2014

